DOCTOR OF PHILOSOPHY

Phytochemical Investigation of Trichilia emetica (Natal mahogany)

Usman, Abdullahi

Award date:
2015

Awarding institution:
Bangor University

Phytochemical Investigation of *Trichilia emetica* (Natal mahogany)

Abdullahi Usman

A thesis submitted for the degree of

Doctor of Philosophy

in the School of Chemistry

PRIFYSGOL
BANGOR
UNIVERSITY

Prifysgol Bangor University

Dedication

To my wife Halima for her endurance, prayers and unwavering support
and
my children Hauwa (4) and Usman (2). May this inspire them to continue learning.

Acknowledgements

I wish to express my deepest gratitude to my supervisor Dr Vera Thoss for her encouragement, endless support and constructive criticism and Dr Mohammed Nur-e-Alam for his guidance and comments in the lab. I must thank them both for their kind tutelage, patience and guidance throughout the period of these studies.

Furthermore, I am indebted to the following people who have assisted me in various ways in the completion of these studies:

- My research committee members; Prof Mark Baird and Dr Lorrie Murphy for their valuable suggestions.
- Nigerian tertiary education trust fund (TETFUND) for the sponsorship. Without this, the study would not have been possible.
- The Management of Nasarawa State University Keffi, for giving me these life-changing opportunities.
- Plant chemistry group members in the 1st and 6th floor lab, the university technicians and the ladies in the general office.
- Dr Graham Tizzard, UK National Crystallography Service, School of Chemistry, University of Southampton for helping with the x-ray crystallography of some compounds.
- Dr Rainer Ebel from Marine Bio discovery Centre, Department of Chemistry, University of Aberdeen, for assisting with high resolution mass of some of my compounds.
- Dr Ahmed Tawfike from the Strathclyde Institute of Pharmacy and Biomedical Sciences, Glasgow, for assisting with high resolution mass of some of my compounds.
- Dr Carol Clements from Strathclyde Institute of Pharmacy and Biomedical Sciences, Glasgow, for assisting with antibacterial and antitrypanosomal assay.
- Prof Steve Kelly from Centre for P450 Biodiversity, College of Medicine, Swansea University for assisting with antifungal assay.
- Dr Simon J. Cameron from Institute of Biological, Environmental and Rural Sciences, Aberystwyth University, for assisting with antimicrobial assay.
- Stephania Christou from Manchester University for assisting with the optical rotation of some compounds.

- Dr Radek Braganca from BioComposite Centre, Bangor University for assisting with collection of *T. emetica* seeds from Mozambique.
- Dr Godfred Darko from Kwame Nkruma University of Science and Technology, Kumasi Ghana (KNUST) for assisting with the collection of *T. emetica* seeds and stem in Ghana.
- Prof Bala Sidi of Bayero University Kano, Nigeria for assisting with the identification of *Azadirachta indica*.
- Mr Martin A Akoh from KNUST botanical garden for assisting with the identification of *T. emetica* seed samples.
- Mr Nigel Brown from Treborth Botanical Garden and Umar Shehu Galla from Ahmadu Bello University Botanical Garden, Zaria Nigeria for permitting the collection of Voucher specimens of the seeds of *T. emetica* and *Azadirachta indica*.
- My families, colleagues and friends.
- Last, but not the least, my wife Halima, for her prayers and unwavering support throughout this study.

ABSTRACT

Trichilia emetica seeds have already been utilised for oil extraction. This project investigated the chemistry of by-products, especially water after boiling the seeds and the defatted residue. The first part of the study was to subject the seed oils to physicochemical analysis using standard methods of food analysis. The data obtained were acid (0.4±0.0 and 0.4±0.1 mg KOH/g), iodine (69.2±2.1 and 64.6±2.8 gI_2/100g), peroxide (10.3±0.5 and 9.2±0.4 %) and saponifiable value (195.4±5.4 and 197.3±4.6) for *T. emetica* seeds from Ghana and Mozambique and were comparable to those of other edible oils. The fatty acid composition of the seeds and shell oils was determined using different analytical methods. The result obtained using ^{1}H and ^{13}C NMR and GC-MS of fatty acid methyl esters are 56-65% saturated (C14:0, C16:0, C18:0), 27-34% monounsaturated (C18:1, ω-9) and 4-10% polyunsaturated (C18:2 ω-6, 9 and C18:3 ω-6, 9, and 12) are in good agreement between the different methods of analysis for the proportion of individual fatty acids. Linolenic acid methyl ester was not detected in the seed oil. Phytochemical investigation of the unsaponifiable fraction of *T. emetica* seed oil resulted in the isolation of two sterols, β-sitosterol and stigmasterol.

The second part of the study was the phytochemical examination of the boiled water extract of the seed. This resulted in the isolation of one new flavanol glycoside, catechin-3-O-α-L-rhamnopyranosyl (1→4) β-D-glucopyranoside and eight known compounds; catechin, epicatechin, taxifolin, elephantorrhizol, catechin 3-O-β-D-glucopyranoside, taxifolin 4'-O-β-D-glucopyranoside and eriodictyol 4'-O-β-D-glucopyranoside. Similarly, three known compounds Naringenin, Quercetin and Quercetin 3-O-β-D-glucopyranoside were isolated from the stem. To the best of our knowledge, this is the first report on the phenolic content of *T. emetica*.

The third part of the study was the use of *Azadirachta indica* seeds and the seeds oil of *Millettia pinnata* as a model to check the various methods used in the unsuccessful attempt to isolate a limonoids from the seeds of *T. emetica*. These resulted in the isolation of two known limonoids and three furanoflavonoids: azadirachtin, nimbin, karanjin, pongapin and lanceolatin. The structures of these compounds were determined on the basis of spectroscopic methods and by comparison of the data obtained with literature. Some compounds were confirmed with X-ray crystallography.

Table of Contents

List of Figures

List of Tables

Abbreviations

CC	Column chromatography
COSY	Correlation spectroscopy
dd	Doublet of doublet
DEPT	Distortionless enhancement by polarization transfer
ESI	Electron spray ionisation
FAME	Fatty acid methyl esters
FC	Flash chromatography
GC	Gas chromatography
HSQC	Heteronuclear single quantum coherence
HMBC	Heteronuclear multiple bond correlation
HPLC	High performance liquid chromatography
HR	High resolution
Hz	Hertz
IR	Infrared
NMR	Nuclear magnetic resonance spectroscopy
m	Multiplet
MS	Mass spectrometry
MUFA	Monounsaturated fatty acid
ODS	Octadecylsilane
PTLC	Preparative thin layer chromatography
PUFA	Polyunsaturated fatty acid
RP	Reverse phase
s	Singlet
SFA	Saturated fatty acid
TLC	Thin layer chromatography
ToF	Time-of-flight
UV	Ultraviolet

CHAPTER 1

1.0 Introduction

Plants have always been an indispensable companion of mankind by providing the basic necessities of life such as food, shelter, clothing and fuel. Furthermore, after fulfilling these basic needs they also serve humanity in the cure or prevention of different diseases (Gasparetto et al., 2011). The use of plants to cure diseases and relieve physical suffering predates written human history (Hill, 1989). Evidence from different archaeological studies indicates that humans were using medicinal plants during the Paleolithic Era. Example of such findings were the plant samples collected from the prehistoric burial sites "Shanidar IV" in northern Iraq, where seven out of the eight pollens from different plant species are currently used as plant drugs (Solecki, 1975). Similarly, a bracket fungus, *Piptoporus betulinus* discovered among the personal effects of the preserved human dating of "*Ötzi the iceman"* (3300-3255 BC), which is believed to have antimicrobial activities (Capasso, 1998). Apart from humans, other non-human primates are also known to ingest medicinal herbs to treat diseases (Sumner, 2000a). This was observed by the occasional consumption of *Vernonia amygdalina* (DEL.), a wild chimpanzee when they are exhibiting signs of lethargy, lack of appetite, and irregularity of body excretions (Huffman and Seifu, 1989).

The earliest written records on plant uses were mostly on the medicinal values documented in herbals by the Sumerians, who documented the uses of hundreds of plants such as myrrh and opium on clay tablets (Sumner, 2000a). Similarly, the Ancient Egyptians (1500 B.C.) produced the Ebers Papyrus, a medical handbook documenting therapeutic treatments and pharmaceutical plant preparations of about 850 medicinal herbs, including garlic, juniper, cannabis, castor bean, aloe and mandrake (Heinrich et al., 2004; Sumner, 2000a). The Ayurveda system was developed by the Indians in the 1900 BC, and to the use of about 700 medicinal plants in Ayurveda medicine was described by an ancient Indian herbalist Sushruta Samhita in the 6th century (Aggarwal et al., 2007; "Turmeric," 2012). In the 7th century, the mythological Chinese emperor Shennong is said to have written the first Chinese pharmacopoeia, the "Shennong Ben Cao Jing" where the use of 365 medicinal plants including ephedra, hemp and chaulmoogra were discussed (Sumner, 2000b; Wu, 2005).

The Greeks and Romans equally play a significant role in documenting the use of medicinal plants, as seen in *De herbis et curis*, the preserved writing of Hippocrates (460 BC-375 BC), which provided the pattern for later western medicine. Hence, Hippocrates is described as the father of western medicine. Pedanius Dioscorides (1 BC), in his encyclopaedic *De Materia*

Medica, highlighted the use of more than 600 medicinal plants, 35 animal products, and ninety minerals. This work has remained the authoritative reference of herbalism in the modern day pharmacopoeias (Loudon, 2002).

The holy Quran and the hadith offer an explanation on the uses of approximately 32 medicinal floras (Ahmad et al., 2009), while the holy Bible gave an account of about 30 healing plants with frankincense (*Boswellia spp*) and myrrh (*Commiphora spp*) the most noteworthy. The uses of these plants most recognized among the Greeks, Romans, Babylonians, Persians and Hebrews were frankincense used for treating wounds, skin diseases, urinary tract infections and gynecological disorders while myrrh was used for embalming and also in the treatment of topical conditions (Cowan, 1999; Dharmananda, 2003; Marshall, 2004).

The age of exploration and the Columbian Exchange introduced new medicinal plants to Europe. It is at this period that herbal documentation became available in English and other languages and this has become a motivating force in the modern day phototherapy (Gimmel, 2008).

In 1630, the bark of Cinchona tree (*Cinchona officinalis* and related species) was found to be useful in the treatment of fever, the World's most devastating disease by then. Cinchona had become so popular by the eighteenth century that several species of these trees were becoming extinct. In 1820, two French chemists, Pierre Pelletier and Joseph Caventou, isolated the alkaloids quinine and cinchonine from the cinchona bark. Within a year, several French physicians were successfully using pure quinine to treat patients with intermittent fever.

In the 18th century, Reverend Edward Stone used the bark of the white willow (*Salix alba*) which has a bitter taste like Cinchona for the treatment of fever and, in 1829, the active principle in willow bark, salicin was isolated (Fig. 1.1). Although, naturally occurring salicin in willow bark was not present in high amount, as high doses a required to achieved pain relief. Herman Kolbe in 1859, synthesised salicylic acid, and this was found to be irritant to the stomach and was not useful because of its severe side effect. In 1897, Felix Hoffman's research efforts led to the synthesis of O-acetyl salicyclic acid, which is commonly known as aspirin, Bayer, developed a process for synthesising the drug in large quantities and in 1899 the drug was patented (Collier, 1984; Meshnick and Dobson, 2001).

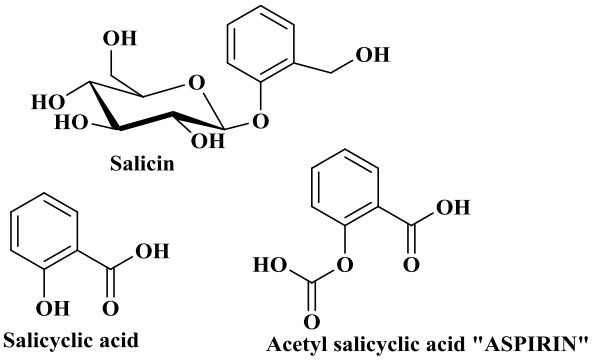

Fig. 1.1. The structures of salicin, salicyclic acid and acetyl salicyclic acid.

The concept of "privileged structures" was first suggested by Evans et al., (1988) and it was in relation to the benzodiazepines. Peptides are the best recognized of privileged structures, followed by purine, pyrimidine bases and their corresponding nucleosides (Wiley and Rich, 1993). Newman, (2008) included majority of secondary metabolites with known bioactivities into this concept, and was extended to the natural product structures such as indoles (Mason et al., 1999). The current use of natural product-based privileged structures as leads to novel bioactive compounds, resulted in a data showing over 10 000 structures with this base structures (either benzopyran or a partially reduced benzopyran) in the natural product literature. A series of iterative molecules based on combinatorial syntheses were tested against a wide series of biological assay, and a novel biological activities have been reported from this relatively small series of compounds (Newman, 2008).

1.1 The Role of Secondary Metabolites in Plants

Flowering plants (angiosperms) were the original source of most plant medicines because of their ability to undergo photosynthesis, thus maintaining atmospheric oxygen levels and supplies of all the organic compounds and most of the energy necessary for life on earth (Bryant and Frigaard, 2006). Their biosynthetic potential is not confined to the production of sugars and proteins; they also synthesize a wide variety of chemical compounds or secondary metabolites that are not necessarily involved in cell metabolism (Harbone, 1993). Plant secondary metabolites mediate their effects on other ecosystem components, including the human body and also on pests. Many of these compounds have been used to treat a wide range of diseases (Newman and Cragg, 2012), while others have been used for a more sinister reason like murder using plant toxins from plants such as hemlock and nightshade (Muller, 1998). Several studies have supported the view that secondary metabolites are adaptive traits that have been diversified during evolution by natural selection (Harbone, 1993; Wink, 1993, 1988).

Plants can easily be attacked by bacteria, fungi, viruses, snails, insects or herbivores because they are sessile organisms. Hence, these metabolites have evolved to perform important biological functions such as to ward off, inhibit or kill their natural predators. They also play an important role in plant reproduction (signals for attracting pollinators, e.g. fragrant monoterpenes, coloured anthocyanin or carotenoids) and for seed dispersal. Research has shown that many of these secondary metabolites like alkaloids, cyanogenics, glycosides, glucosinolates, terpenes, saponins, anthraquinones, tannins and polyacetylenes are allelochemicals. Some carry out physiological roles such as serving as mobile transport or storage compounds or UV-protectants (Wink and Mohamed, 2003; Wink, 2003).

Table 1.1. Structural diversity of plant secondary metabolites (Wink, 2003)

Natural products	Number
Alkaloids[x]	12,000
Sesquiterpenes[y]	5,000
Triterpenes, Saponins, Steriods[y]	5,000
Flavonoids[y]	4,000
Monoterpenes[y]	2,500
Diterpenes[y]	2,500
Phenylpropanoids, Coumarin, Lignans[y]	2,000
Polyacetylenes, Fatty acids, Waxes[y]	1,000
Polyketides[y]	750
Non-protein amino acids[x]	700
Tetraterpenes[y]	500
Carbohydrates[y]	>200
Alkamides[x]	150
Glucosinolates[x]	100
Amines[x]	100
Cyanogenic glucosides[x]	60

Where, [x]with nitrogen [y]without nitrogen

Higher plants are a store house of secondary metabolites, with each containing high structural diversity (Table 1.1) above. Most of the time, a given taxon is usually dominated by a single group of secondary metabolites accompanied by several derivatives and minor components. The pattern of secondary metabolites in a given plant is complex and changes depending on the plant part where they are stored. They are generally concentrated in one particular region of a plant such as the root, bark, leaves, fruits, seeds or glandular hairs (Wink, 2003). In cases where they occur in different organs of the same plant, they frequently have different chemical

profiles (Araujo et al., 2003). The difference in concentration and composition of secondary metabolites can be seen between different developmental stages (e.g. organs important for survival and reproduction have the highest and most potent SM), between individuals and also between populations. These metabolites can be present in a plant in an active state or as a 'prodrug' that becomes activated upon wounding, infection or in the body of a herbivore (Wink, 2003). For thousands of years, these compounds have been used by herbal practitioners to treat different diseases in man, and chemical studies of these herbal drugs were the basis of most early medicine such as aspirin and quinine (Butler, 2004). These natural compounds are formed from diverse precursors such as acetyl-CoA or amino acids, through enzymatic reactions (Harbone, 1993).

1.2 Herbal medicines

In developing countries, the use of herbs to treat diseases is common practice. About 75- 80% of the population in the developing countries uses herbal medicine for their primary health care (Kamboj, 2000). The reliance on herbal medicines could be attributed to the absence of modern health care facilities, economic factors, cultural acceptability, better compatibility with the human body, and lesser side effects (Kamboj, 2000; Matu and van Staden, 2003). The high cost of imported pharmaceuticals are beyond the reach of the populace in these nations, unlike the herbal drugs that are grown from seeds or gathered from nature at little or no cost (Matu and van Staden, 2003). In these areas, even when the modern health care facilities are present they normally exist side by side (Sindiga, 1994). The use and preparation of herbal drugs are conveyed orally from one generation to the next, a process that involved the risk of losing essential details (Atindehou et al., 2004). Some of these plants used by herbal practitioners are either collected at a specific time of the day or at a different period of the year and it may be a specific part of the plant or the whole plant.

The study of traditional human uses of plants by native cultures (ethnobotany) is recognized as an effective way to discover future medicines. The World Health Organisation (WHO) noted that out of 122 plant–derived pharmaceuticals, about 80% are used in modern medicine in ways correlated directly with their traditional uses. Today, about 25% of pharmaceuticals currently available to physicians are derived from trees, shrubs or herbs. Some drugs are obtained directly from plants extracts, while others are synthesized to mimic a plant-derived compound. If the therapeutic importance of plant-derived drugs like morphine, quinine, digitalis, atropine, reserpine, taxol, vincristine and artemisinin are considered, the contribution of plant-derived

drugs to medicine can hardly be over emphasized (Fabricant and Farnsworth, 2001; Newman and Cragg, 2012).

Recently, there is an increasing demand for plant-derived chemicals for drugs and food supplements. Hence, researchers are combing the Earth for phytochemicals for new therapeutic agents or leads that could be developed for treatment of various diseases. This has led to the isolation of taxol, an important anticancer drug from the stem bark of *Taxus brevifolia*, and "artemisinin" a powerful antimalarial drug from the Chinese plant *Artemisia annua* (Kingston, 2000; Miller and Su, 2011). Further screening of large numbers of unexamined plants are ongoing. The work presented in this thesis relates to the isolation, structure elucidation and biological activity studies of secondary metabolites from African traditional plant *Trichilia emetica*.

1.3 Azadirachta indica (neem)

The neem (*Azadirachta indica* A. JUSS), is a tree belonging to the Meliaceae (mahogany) family (Fig. 1.2). It is a native of Myanmar (Burma) and India. Currently, A. indica is widely distributed in tropical and subtropical areas of Africa, America, and Australia. During the last 50 years neem has been introduced in many countries of the world for shade, afforestation, fuelwood production, and as a producer of natural pesticides. The neem tree is an evergreen, or deciduous, fast-growing tree that can reach a height of 30 meters. The trunk is stout and the branches are wide and spreading, in severe drought may shed most or nearly all of its leaves. The flowers and fruits are borne in axillary clusters and when ripe the smooth ellipsoidal drupes are greenish yellow and comprise a sweet pulp enclosing a seed. The seeds consist of a shell and 1-3 kernels which contain azadirachtin and its homologues (Mordue and Nisbet, 2000). In India, the annual fruit yield of a mature tree may be up to 50 kg, while in Nigeria about 21 kg/tree was obtained, but this depends on a number of environmental factors like rainfall and soil conditions (Schmutterer, 1990). Both the bark and leaves also contain biologically active molecules but with low levels of azadirachtin which is mainly found in the seed kernels (Mordue and Nisbet, 2000). Neem seeds contain several azadirachtin analogs, but the major form is azadirachtin and the remaining minor analogs like nimbin, salannin, and marrangin contribute little to overall efficacy of the extract. Additionally, azadirachtin was first isolated based on its exceptional antifeedant activity in the desert locust, and this substances remains the most potent locust antifeedant discovered to date (Isman, 2006; Mordue and Nisbet, 2000). The properties of azadirachtin and its minor analogs were also investigated in the management

of other insects' pest such as acarina, crustacea, nematodes, bacteria, fungi, viruses and soil fertility (Hummel et al., 2014; Schmutterer, 1990). Generally, these compounds are nontoxic to humans, compatible with beneficial insects, pollinators and are eco-friendly (Hummel et al., 2014).

Fig. 1.2. Indian neem tree (*A. indica*) and seeds (Ref.: http://www.atacora.com -259 × 194)

1.3.1 Plant derived insecticides

The use of plant derived insecticides in agriculture practices dates back to 2000 years in ancient China, Egypt, Greece, and India (Thacker, 2002). In Europe and North America the use of botanical insecticides date back to more than 150 years, existing before the discovery of synthetic chemical insecticides such as organochlorides, organophosphates, carbamates, and dichlorodiphenyltrichloroethane (DDT) in the mid-1930s to 1950s. The introduction of these synthetic insecticides has reduced the role of botanicals in agriculture to insignificant positions in marketplace among crop protectants. Nonetheless, the use of these insecticides has led to numerous problems like acute and chronic poisoning of applicators, farmworkers and even consumers; destruction of fish, birds and other wildlife; disruption of natural biological control and pollination; extensive ground water contamination, potentially threatening human and environmental health; and the evolution of resistance to pesticides in pest population that were never thought of at inception (Isman, 2006).

In the early 1980s, the problems posed by the used of synthetic insecticides led the United State Government to respond with regulatory action in banning the most damaging products, and creating policies to replace chemicals of concern with those demonstrated to have fewer risks to human health and environment. These government policies appeared to be the driving force

for the discovery and development of alternative pest management products, including plant-derived insecticides such as azadirachtin which have already been proven to have an antifeedant and growth regulating activities on target organisms (Isman, 2006).

The isolation of azadirachtin from the neem seeds has prompted researchers to screened plant species belonging to the Meliaceae family, and has found the genus *Trichilia* to have a potential that can be developed into a plant-based insecticides. Several limonoids have been isolated from different *Trichilia species* and their biological activities such as feeding deterrents, growth inhibitors, growth regulators, repellents or ovipositor inhibitors against a variety of insect species have been tested (Mikolajczak and Reed, 1987; Mikolajczak et al., 1989; Nakatani et al., 1985, 1981). Limonoids isolated from *T. hirta, T. glabra, T. americana and T. connaroides* have shown to inhibit larval growth of *Spodoptera litura, Peridroma saucia* (Wheeler et al., 2001; Xie et al., 1994), while limonoids from *T. roka*, the trichilins are antifeedants to *Spodoptera eridania* and the *Epilachna varivestis* (Nakatani et al., 1985, 1981).

1.4 Review of Literature

T. emetica is a coveted multipurpose tree that has long history of use in Africa's traditional medicine. The extensive use of these plants species to a treat wide range of diseases has encouraged researchers to explore several biological activities including antiplasmodial, antischistosomal, anti-inflammatory, anti-oxidant, and antimutagenic properties. Several limonoids have been isolated from the root and stem bark of this plant, together with the sesquiterpenoid "kurubasch aldehyde" from the root. These phytochemicals were reported to exert antimicrobial, antifeedant and growth regulating properties. Anecdotal evidence suggests that the presence of seeds reduces the incident of insect attack on stored natural materials. A very powerful limonoid, *azadirachtin* isolated from the seeds of *Azadirachta indica*, a cousin has been the subject of intense research because it is eco-friendly, nontoxic to humans, and highly toxic to agricultural pest insect. These properties of azadirachtin have prompted us to search for the same compound in the seeds of *T. emetica*, which has been considered in West Africa as a waste product, due to the bitter taste of the seeds. This bitterness is remove by boiling the seeds in water for ten to twenty minutes before oil extraction. The availability of alternative vegetable oils and the labour involved in the oil extraction has relegated these seeds to the background.

1.4.1 Plant profile

Trichilia emetica Vahl., is an evergreen tree belonging to the Family Meliaceae. The genus Trichilia has the following taxonomic classification:

Kingdom : Plantae
Subkingdom : Tracheobionta- Vascular plants
Super division : Spermatophyta- Seed plants
Division : Angiosperm- Flowering plants
Class : Magnoliopsida
Subclass : Magnoliidae
Order : Rutales
Family : Meliaceae
Subfamily : Melioideae
Genus : *Trichilia*
Species : *T. emetica* Vahl

The generic name '*Trichilia*' is derived from the Greek "tricho" referring to the 3-lobed fruits and "emetica" relating to the emetic properties of the tree. It has a synonyms including *Trichilia roka* Chiov, *Trichilia somalensis* Chiov., *Trichilia grotei* Harms., *Trichilia jubensis* Chiov., *Trichilia umbrifera* Swynn (Iwu, 2014). *T. emetica* has two subspecies: subsp. e*metica* occurring from Senegal to Uganda, and subsp. *superosa* from Eritrea to South Africa. Subsp. *superosa* tends to be smaller, shrub like and has twigs (Grundy and Campbell, 1993; Van der Vossen and Mkamilo, 2007). *T. emetica* is commonly known as Natal mahogany, woodland mahogany, Christmas bells, red ash, thunder tree, Ethiopian mahogany or Cape mahogany (Orwa et al., 2009). Other vernacular names include Mafura (France), Mafurreira (Poland), Mkungwina, mafura, mti maji, muwamaji, musikily, mgolimazi (South Africa), gor-mas (Somali), jan saiwa, ashapa (Nigeria), umshara, um hagi, safsafa (Arabic) (Iwu, 2014; Mashungwa and Mmolotsi, 2007; Orwa et al., 2009; Van der Vossen and Mkamilo, 2007). This species is native to Africa and it grows widely throughout sub-Saharan African extending from Ghana to the Red Sea, throughout East and Central Africa to Zambia and KwaZulu-Natal in South Africa. It also grows naturally in Yemen and have been introduced as an ornamental tree in Cape Verde (Iwu, 2014; Orwa et al., 2009; Van der Vossen and Mkamilo, 2007).

T. emetica is regarded as an indication of an area with palatable grass species and it grows naturally in low altitude areas of up to 1300 m, with mean annual temperatures of 19-31 ^{O}C

and rainfall ranging from 600-2300 mm, respectively. It prefers a well-drained, rich alluvial or sandy soils (Orwa et al., 2009).

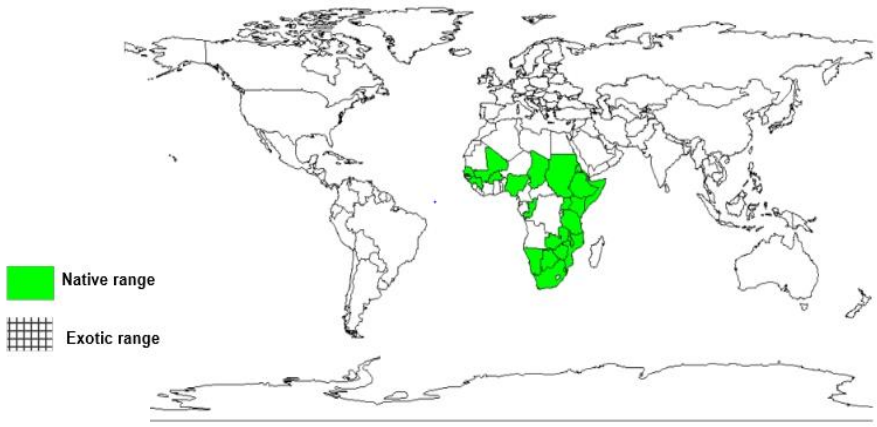

Fig. 1.3. Geographical distribution range of *T. emetica* (Orwa et al., 2009)

1.4.2 Botanical description of *T. emetica* Vahl.

T. emetica is an evergreen shrub or tree that sometimes reaches up to 35 m in height. The tree has a non-aggressive root system and the trunk is swollen at the base (Fig. 1.4). The bark is grey-brown with shallow striations and smallish scales (Orwa et al., 2009). The leaves are alternate; imparipinnately compound with 3 to 5 pairs of leafs, the upper surface is dark glossy green while the lower surface is covered with short brownish hairs. Inflorescences are either terminal or produced on short congested axillaries, and the flowers are unisexual (Fig. 1.5) (Van der Vossen and Mkamilo, 2007). The fruit is pear-shaped with a long stipe about 2-4 cm with three valve capsules, which are split into three or four parts to reveal 3-6 shiny black seeds which are almost completely concealed in a scarlet sarcotesta (Fig. 1.6 and 1.7) (Orwa et al., 2009; Van der Vossen and Mkamilo, 2007). They are propagated by cuttings and regenerate naturally by root suckers, and seeds (Orwa et al., 2009). Plant maturity depends on the location where the tree is planted, with thirteen years for those planted in the open, and twenty four for those in the shade (Grundy and Campbell, 1993). Flowering occurs between spring and summer with fruiting January to May. Fruits are harvested when the capsules open up. They are dried in the shade and the seeds are shaken out (Orwa et al., 2009).

Fig. 1.4. *T. emetica* tree

Fig. 1.5. *T. emetica* leaves and flowers

Fig. 1.6. *T. emetica* fruit

Fig. 1.7. Dehulled T.emetica seeds

(Fig. 1.4 to 1.6: Ref.: http://www.westafricanplants.senckenberg.de- 800 × 600)

1.4.3 Nutritive value

T. emetica seeds have a seed weight between 0.35-1.0 g. The seed is made up of 21 – 29% oily shell like husk called sarcotesta and 71 – 79% kernel. The kernel also contain 55-65 % of a brownish fat that melts between 35-41 ^{O}C (Fupi and Mork, 1982). The seeds, when pressed, give two kinds of oil: 'mafura oil' from the seed coat (sarcotesta) and 'mafura butter', from the kernel. These oils may be separately extracted in traditional extraction or combined as a single product as in commercial extraction. The mafura oil is edible, but mafura butter is not suitable for consumption because of its bitter taste (Saka and Msonthi, 1994; Komane et al., 2011; Van der Vossen and Mkamilo, 2007).

The nutritional value of *T. emetica* seeds per 100 g dry matter (approximately 58% of fresh weight), had an energy value of 1897 kJ (453 kcal). The proximate composition was reported to be crude protein 17 g, fat/lipid 23 g, crude fibre 8 g and carbohydrate 48 g. Also, minerals such as Na, P, K, Mg, Fe were reported to be 146, 3164, 13017, 1129 and 43µg/g (Fupi and Mork, 1982; Orwa et al., 2009; Saka and Msonthi, 1994). The fatty acid composition of *T. emetica* has also been reported, the most abundant ones being palmitic and oleic acid, while linoleic, stearic, myristic, and linolenic acid are the minor fatty acids present. The multivitamin juice produced from a mixture of *T. emetica* seeds and other edible indigenous plants is used to control malnutrition, a major challenge faced by children and mothers in rural areas in Africa (Komane et al., 2011; Saka and Msonthi, 1994). The seeds are bitter and emetic, thus for the oil to be used for edible purposes the whole nuts are boiled in water for 10-20 minutes, dried in the sun and then milled for oil extraction upon which, a yellow edible oil is obtained (Fupi and Mork, 1982; Grundy and Campbell, 1993). The liquid resulting from soaking seeds without testas may be used when making porridge, and the crushed seeds may be mixed with maize meal or vegetable relishes during cooking (Grundy and Campbell, 1993; Tredgold, 1986; Williamson, 1974). The seed arils are cooked as vegetables or crushed to yield a milky juice that is added to spinach for flavour (Coates-Palgrave, 1972; van Wyk, B., van Wyk, P., van Wyke, 2000).

1.4.4 Non-medicinal uses of *T. emetica*

T. emetica tree bark is used for carving ornaments, furniture and household implements. The wood is used as firewood and to construct the frame of an African traditional musical instrument called "mbila", and the oil extracted from the seeds is rubbed on "mbilas" and it is also used to soften animal skin (Palmer and Pitman, 1972). The trees are planted to assist in soil conservation and as a windbreak. In urban areas, they are planted as ornamental trees, ideal

for car parking. *T. emetica* seeds and flower nectar are consumed by birds while the fruit and flower buds are enjoyed by monkeys and baboons, and the leaves are consumed by domestic animals (Orwa et al., 2009; Palmer and Pitman, 1972). The mafura butter is used in soap and candle making, as a body ointment, wood-oil and for medicinal purposes (Komane et al., 2011; Saka and Msonthi, 1994; Van der Vossen and Mkamilo, 2007). The *T. emetica* seed oil is used as starting material in lipase catalysis for the production of cocoa butter equivalents (Khumalo et al., 2002). The crushed seed is used in protecting cowpea seed from storage pest and seed cake for fertilizer (Van der Vossen and Mkamilo, 2007).

1.4.5 Traditional medicinal uses of *T. emetica* seeds

In African traditional medicine, different parts of *T. emetica* tree are used alone, mixed or in combination with other plant parts in treating different diseases. The seed oil is rubbed into cuts made on a fractured limb in order to hasten healing, and it is also taken internally to treat rheumatism (Grundy and Campbell, 1993). The seed oil is used in combination with *Cyathula natalensis* Sond to treat leprosy (Cunningham, 1996). The oil is sometimes combined with coconut oil to provide an emollient and moisturising effect on the skin (Vermaak et al., 2011). In South Africa, the decoction of the root and bark is used as an emetic, purgative and also as a remedy for colds, pneumonia, and intestinal disorders such as hepatitis. In Mali, the powdered root is given to treat river blindness and ascaris, while its decoction is supposed to cure jaundice, infertility, induce labour in women, and to relief stomach and chest pain (Van der Vossen and Mkamilo, 2007). Also, a decoction of the leaves is used against scabies, fever, cough, bronchial trouble, gonorrhoea, syphilis and chronic wounds (Diallo et al., 2003). In Senegal, the macerated root bark is used for epilepsy and leprosy while the leaves are taken against blennorrhoea. In Zimbabwe, the bark is used to induce abortion, while in Nigeria the leaves are used for treating syphilis. The fruit is used in Tanzania for treating eczema (Orwa et al., 2009; Van der Vossen and Mkamilo, 2007). The traditional medicinal uses and its methods of preparations are summarised in Table 1.2.

Table 1.2: Preparation methods and uses of *T. emetica* (Diallo et al., 2003; Komane et al., 2011).

Condition/diseases	Part Used	Preparation and administration
Abdominal pain	Leaf, root	Decoction for bathing or mixed with salt and lemon for drinking, twice a day.
Breast pain	Leaf	Decoction for bathing
Backache	Bark, leaf	Infusion for drinking
Cough	Leaf	Infussion for drinking
	Root	Decoction for drinking
Constipation	Leaf, root or stem Leaf	Decoction for drinking, three to seven days Decoction mixed with *Opilia celtidifolia* leaf for drinking
Chest pain	Leaf	Decoction for steam bath or massage.
Dermatitis	Leaf, bark	Leaf decoction, steam bath or powdered leaves applied on the lesion and powdered bark for cleansing
Digestive infections	Root	Decoction mixed with coffee or *Cassia sieberiana* root and honey for drinking for three to five days.
Dysmenorrhoea	Leaf	Decoction mixed with *Tamarindus indica* or *Citrulus limonene* for drinking for seven days.
Eye infection	Leaf, bark	Decoction for drinking for two days.
Infertility	Leaf	Decoction mixed with *Combretum molle* for drinking
Sterility	Root	Powder mixed with ginger and salt added to porridge for drinking.
Flatulence	Root	Infusion mixed with *Acacia nilotica* seed for drinking.
Gastric ulcer	Bark	Powdered mixed with salt and ginger are added to porridge for consumption, twice a day.
Hernia	Root	Powdered added to porridge for consumption
Inflammation	Root	Powder root mixed with potash in water to drink
Headaches	Leaf	Decoction for drinking or bathing
Hemorrhoids	Root	Powdered root mixed with black pepper are added to the fruit of *Xylopia aethiopica* taken orally every day untill healing occurs.
Jaundice	Root	Decoction taking orally for 15 days or crushed roots mixed with honey and water in a bath.
Leprosy	Root, leaf	Decoction drink or bath
Malaria	Leaf Stem Root	Decoction mixed with lemon used for bathing or drinking. Decoction mixed with honey for drinking Infusion mixed with *Pseudocedrala kotschii, Nauclea latifolia* and honey for drinking. All are taken five to ten days.
Paralyses	Root	Powdered roots mixed with porridge for eaten
Pneumonia	Root, leaf	Decoction, drink or bath for twelve days.
Tiredness	Leaf	Decoction for bathing and root powder ointment has a relaxing effect.
Teniasis	Stem	Powdered bark mix with root of *Securidaca longependonculata* and drink for three days.
Urinary infection	Leaf	Decoction mixed with fruits of *Sticnos spinosa and* Drink.
Weight loss	Leaf	Decoction mixed with sugar is taking orally
Wound healing	Root Leaf	Roasted root powdered is applied on the incision of the broken limb. Leaf decoction used for cleansing.
Poison antidote	Root	Powder of the ground root mixed with milk is taken orally.
Asthma	Root	Powdered ground root mixed with honey for drinking

1.4.6 Pharmacological studies

A literature search showed that *T. emetica* has a long history of use in African traditional medicine. The solvent extracts from different parts of the tree and the compound kurubasch aldehyde (**1**) isolated from the root displayed a wide range of biological activities such as antibacterial, anticandidal, anti-inflammatory, antischistosomal, antiplasmodial, antitrypanosomal, anti-oxidant and anticancer. The presence of limonoids in these extracts is speculated to be responsible for the bioactivities (Komane et al., 2011). The solvent extract, part of the plant and the assay used are as discussed below.

1.4.6.1 Antimicrobial activity

The aqueous and ethyl acetate extract of *T. emetica* root were screened against these bacterial species: *Staphylococcus aureus, Streptococcus Pyogenes, Streptococcus pneumoniae, Moraxella catarrhalis,* and *Haemophilus influenza* using the disc diffusion and epsilometer test methods. The aqueous extract showed low activity at MIC values greater than 500 µg/ml against all the tested pathogens. The ethyl acetate extract exhibited good activity at MIC values less than 125.00 µg/ml against all the tested pathogens, while MIC values of less than 62.50 µg/ml were recorded for *S. aureus* and *S. pyogenes* (Germanò et al., 2005). Shai et al., (2008) *tested* acetone, dichloromethane and hexane extracts of *T. emetica* leaves against four bacterial species: *Enterococcus faecalis, Staphylococcus aureus, Pseudomonas aeruginosa and Escherichia coli***.** The acetone extract showed higher activity with an average MIC value of 0.42 mg/ml, followed by dichloromethane with MIC value range of 0.08 to 1.3 mg/ml and hexane extract with an average MIC value of 1.64 mg/ml. The antifungal activity of these extracts were also studied against *Candida albicans, Cryptococcus neoformans, Aspergillus favus, Sporathris schenckii and Micrococcus canis* using the microdilution assay (Geyid et al., 2005). The acetone extract also showed good activity against these species with an average MIC value of 0.33 mg/ml compared to the dichloromethane extract with 0.81 mg/ml, while the hexane extract exhibit moderate antifungal activity against *M. canis* with an MIC value of 0.15 mg/ml.

The methanol extract of *T. emetica* fruits, screened against *Candida albicans*, *Cryptococcus neoformans, Aspergillus flavus, Trichophyton mentagrophytes* and *Trichophyton violaceum,* showed low activity at 500 µg/ml (Geyid et al., 2005). In another study, (Kolaczkowski et al., 2010) showed that the hexane extract of *T. emetica* leaves screened against *C. albicans* and *C.*

glabrata, inhibit the growth of these fungal species at an MIC value of 0.8 mg/ml and 0.1 mg/ml respectively.

1.4.6.2 Anti-inflammatory activity

Inflammation is a complex biological response of body tissue to harmful stimuli such as pathogens, damaged cells or irritants. McGaw et al., (1997) tested the ethanol and aqueous extracts of *T. emetica* leaves for anti-inflammatory activity. Using the concentration of 5 µg/ml, the percentage inhibition of prostaglandin synthesis for ethanol and aqueous leaf extracts were 22% and 89% respectively. Frum and Viljoen, (2006) using the 5-lipoxygenase assay, reported that methanol and aqueous extracts of *T. emetica* leaves exhibited low activity at an IC_{50} value greater than 100 µg/ml.

1.4.6.3 Antischistosomal activity

Schistosomiasis (also known as bilharzia, snail or Katayama fever) is a disease caused by different species of parasitic flatworms. These worms are found in water and are released by freshwater snail hosts and may affect the urinary tract or the intestines. The aqueous extract of *T. emtica* root harvested from KwaZulu-Natal in South Africa was tested for antischistosomal activity, and showed low activity with an MIC value of 6.25 mg/ml (Sparg et al., 2000). Conversely, Ndamba et al., (1994) reported that the root aqueous extract of *T. emetica* harvested from Zimbabwe showed no antischistosomal activity at the same concentration.

1.4.6.4 Antiplasmodial activity

Malaria is an infectious disease caused by protozoan parasites which are usually transmitted by the bite of the anopheles mosquito. It is a major health challenge with highest rate of complication and death. And 90% of malaria-related deaths occur in sub-Saharan Africa. The methanolic extract of *T. emetica* leaves was tested against two strains of *Plasmodium falciparum* (3D7 and Dd2) using the radiometric assay. Moderate activity was obtained for 3D7 and Dd2 with an IC_{50} value of 17.5 µg/ml and 2.5 µg/ml, respectively (El Tahir et al., 1999). Bah et al., (2007) screened three solvent extracts (dichloromethane, methanol and water) of *T. emetica* leaves against Plasmodium parasites, and reported the dichloromethane extract to have moderate antiplasmodial activity with an IC_{50} value of 12 µg/ml, while the methanol extract had low activity with an IC_{50} value of 48 µg/ml, and no activity for the aqueous leaf extract at a concentration greater than 100 µg/ml. In another study, Bero et al., (2009), using a dichloromethane extract of *T. emetica* leaves, reported poor antiplasmodial activity with an IC_{50} value of 59.2 µg/ml. Atindehou et al., (2004), also tested the dichloromethane extract of

root bark of *T. emetica* against strain K1 of *P. falciparum* and they reported a good activity with an IC_{50} value of 3.6 µg/ml.

1.4.6.5 Anticonvulsant activity

Epilepsy is a neurological disorder of the brain and it is characterised by repeated seizures. Bah et al., (2007) tested dichloromethane and methanol extracts of *T. emetica* leaves at different concentrations of 10 mg/ml, 1 mg/ml and 0.1 mg/ml using the $GABA_A$-flumazenil assay. The results showed that there were no activity for 1 mg/ml and 0.1 mg/ml, while the dichloromethane and methanol extracts exhibited activity of 21% and 64% at 10 mg/ml.

1.4.6.6 Antitrypanosomal *activity*

This is a vector-borne disease transmitted by the bite of the tse-tse fly, causing a fatal human disease called sleeping sickness (Hoet et al., 2004). Hoet et al., (2004) investigated the dichloromethane extracts of five different plants, including *T. emetica* used traditionally in Benin to fight trypanosoma infection. The study was conducted using a long incubation low inoculation test (LILIT). The investigations revealed that the leaf extract of *T. emetica* exhibited moderate activity with an IC_{50} value of 14.9 µg/ml and 8.6 µg/ml against T*rypanosoma brucei brucei* (Tbb) and *Trypanosoma brucei rhodesiense* (Tbr), respectively. Another study, Atindehou et al., (2004) reported the antitrypanosomal activity of 56 plants including *T. emetica.* They reported that the methanol extract of *T. emetica* stem bark had strong activity against Trypanosoma brucei rhodesiense with an IC_{50} value of 0.04 µg/ml.

1.4.6.7 Anti-oxidant activity

The antioxidant activity of *T. emetica* was also assessed. The methanol extract of the leaves was screened using the 2,2-diphenyl-1-pircrylhydrazyl (DPPH) assay, and showed good activity with an IC_{50} value of 18 µg/ml compared to 44 µg/ml reported for the aqueous leaf extract by (Frum and Viljoen, 2006). Germanò et al., (2006) also tested the aqueous extract of the root using the auto-oxidation of methyl linoleate (MeLo) expressed as hydroperoxide production and ascorbate/Fe^{2+}-induced lipid peroxidation in rat liver microsomes. The result indicated that MeLo auto-oxidation was strongly inhibited after 72 hours incubations, and the IC_{50} values obtained were 0.013 and 0.12 µg/ml for the hydroperoxide production and ascorbate/Fe^{2+}-induced lipid peroxidation, respectively.

1.4.6.8 Anticancer activity

The search for new anticancer agents is ongoing and more than 7500 plants extracts have been screened, including *T. emetica* with the sole aim of identifying new anticancer drugs. The methanol and dichloromethane extract of *T. emetica* did not exhibit potent antimutagenic properties compared to the positive control (Verschaeve and Van Staden, 2008). Traore et al., (2007) tested Kurubasch aldehyde **(1)**, a sesquiterpenoid isolated from *T. emetica* root bark against different cell lines using the Ames assay. The compound reduced the proliferation of breast cancer cells MCF-7 with an IC_{50} value of 78 µM and inhibited the proliferation of murine sarcoma S180 cancer cells with an IC_{50} value of 7.4 µM.

1.4.7 Phytochemistry

A sesquiterpenoid and several limonoids have been isolated from the root and stem bark of *T. emetica.*

Traore et al., (2007) isolated a sesquiterpenoid, named Kurubasch aldehyde **(1)** from the root bark of *T. emetica*.

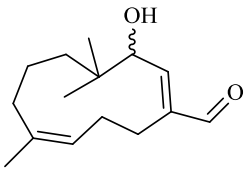

1

Nakatani et al., (1981) reported the isolation of trichilin A **(2)**, trichilin C **(3)**, trichilin D **(4)** and aphanastatin **(5)** from the root bark of *T. roka*. These limonoid exhibited considerable antifeedant activity when tested against *Spodeptera eridania* and *Epilachna varivestis* using an army worm assay.

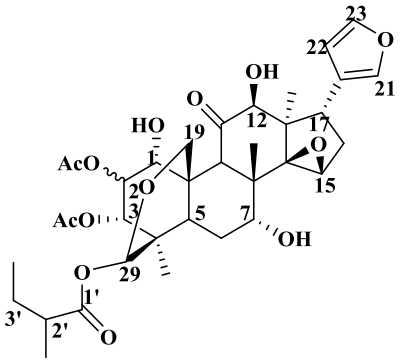

2

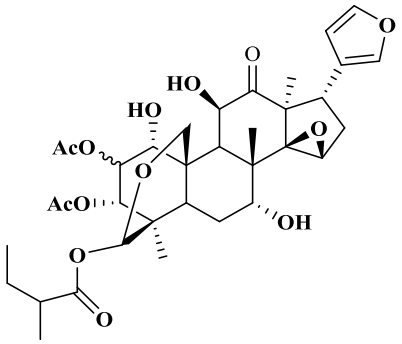

3

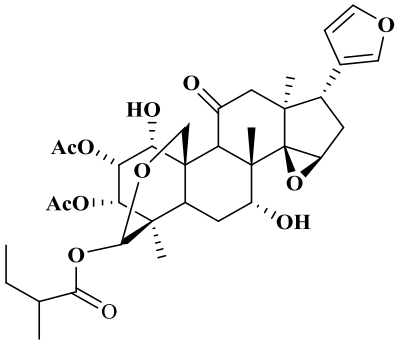

4

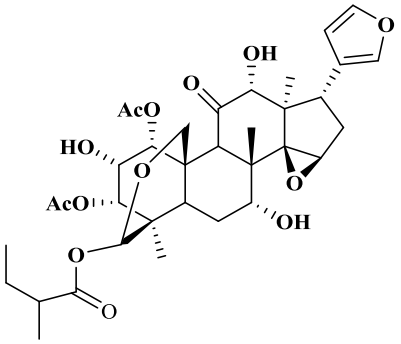

5

Nakatani et al., (1985) reported the isolation of a new limonoids, named 7-acetyltrichilin A **(7)** from the root bark of *T. roka*. The limonoids were also screened against *S. eridonia*, *E. varivestis* and a Japanese plant, *Spodoptera littoralis* Boisd using an antifeedant assay. The result indicated that they possess good antifeedant activity.

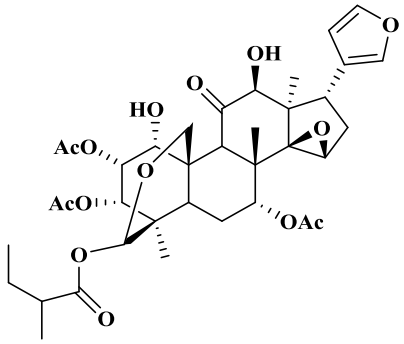

6

Gunatilaka et al., (1998) also isolated five known limonoids; trichilin A **(2)**, rohituka 3 **(8)**, nymania 1 **(9)**, Tr-B **(10)**, drageana 4 **(11)**, and the novel seco-A-protolimonoid **(12)** from the stem bark of *T. emetica*. Nymania 1 and Tr B showed selective inhibitory activity toward DNA repair-deficient yeast mutants.

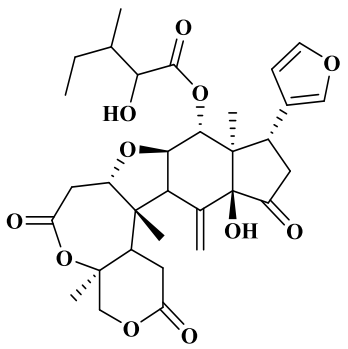

7

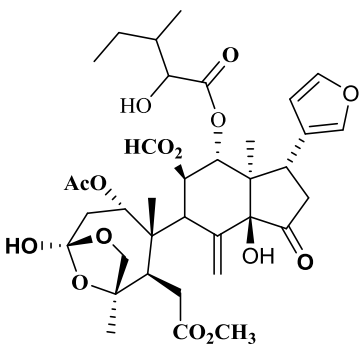

8

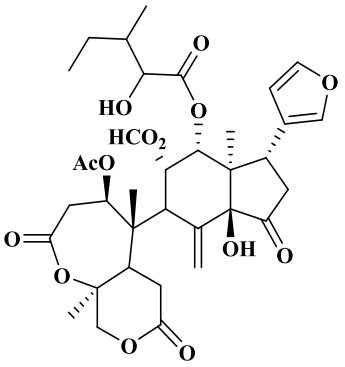

9

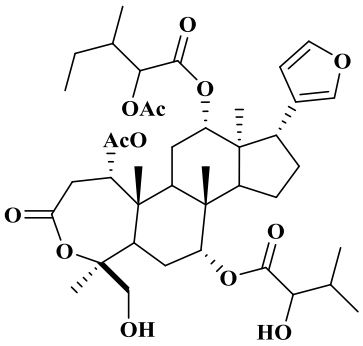

10

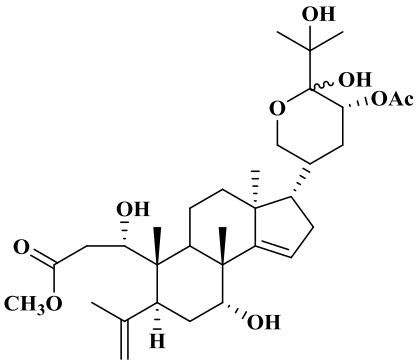

11

Komane et al., (2011) reported that limonoids: trichilin A **(2)**, trichilin B **(3)**, trichilin C **(4)**, trichilin D **(5)**, rohituka 3 **(8)**, nymania 1 **(9)**, Tr-B **(10)**, drageana 4 **(11)**, seco-A-protolimonoids **(12)**, rohituka-**7 (13)**, rohituka-5 **(14)**, Tr-A **(15)**, Tr-C **(16)**, trichilinin **(17)**, trichilin E **(18)**, and sendanin **(19)** are present in the bark of *T. emetica.*

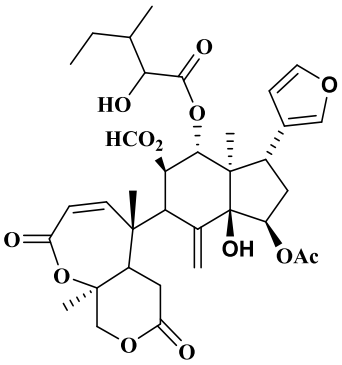

12

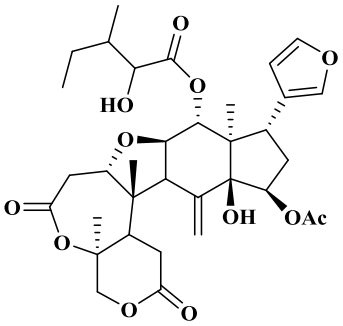

13

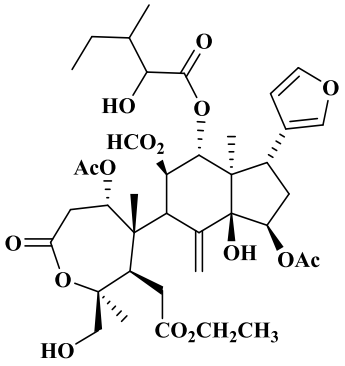

14

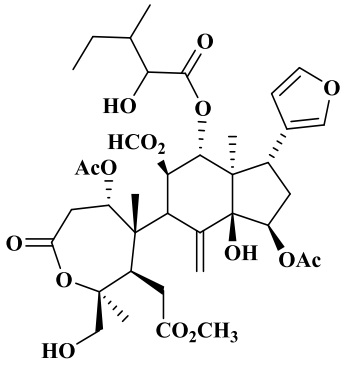

15

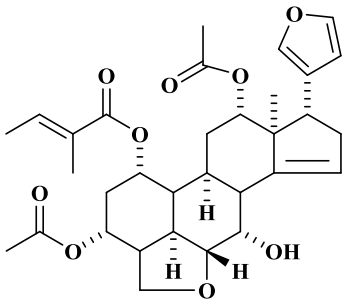

16

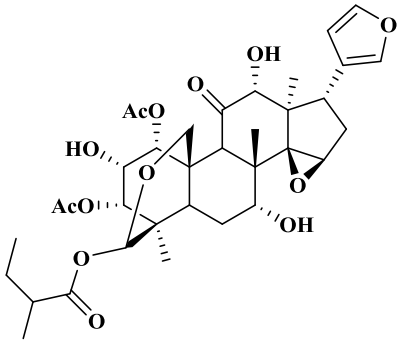

17

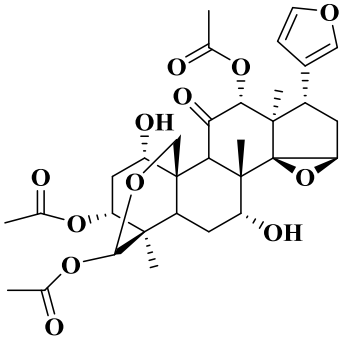

18

1.4.8 Flavonoids

Flavonoids are one of the most diverse and widespread, constituting over 50% of the naturally occurring phenolic compounds. Flavonoids are groups of compounds consisting of fifteen carbon atoms, arranged in a C_6-C_3-C_6 configuration. Basically, the structure consists of two phenyl ring A and B linked through an oxygen-containing pyran or pyrone ring C (Fig. 1.8)

(Balasundram et al., 2006; Merken and Beecher, 2000). This structure is common to all family members, and changes in substitution patterns to ring C result in the major flavonoid classes, such as flavanols, flavones, flavanones, flavonols and anthocyanidins (Hollman and Katan, 1999). Of these flavonoids, flavonols and flavones are the most widely distributed and structurally diverse (Harborne et al., 1999). Similarly, substitutions such as oxygenation, alkylation, glycosylation, acylation, and sulfation to rings A and B may give rise to different compounds within each class of flavonoids. Furthermore, individual differences within each group result from the variation in number and arrangement of the hydroxyl groups as well as from the nature and extent of alkylation and /or glycosylation of these groups (Hollman and Katan, 1999; Pietta, 2000). The most commonly occurring flavonoids are those with dihydroxylation in the 3' and 4' position of the B ring, and to a lesser extent, are those with trihydroxylation in the 3', 4' and 5' positions.

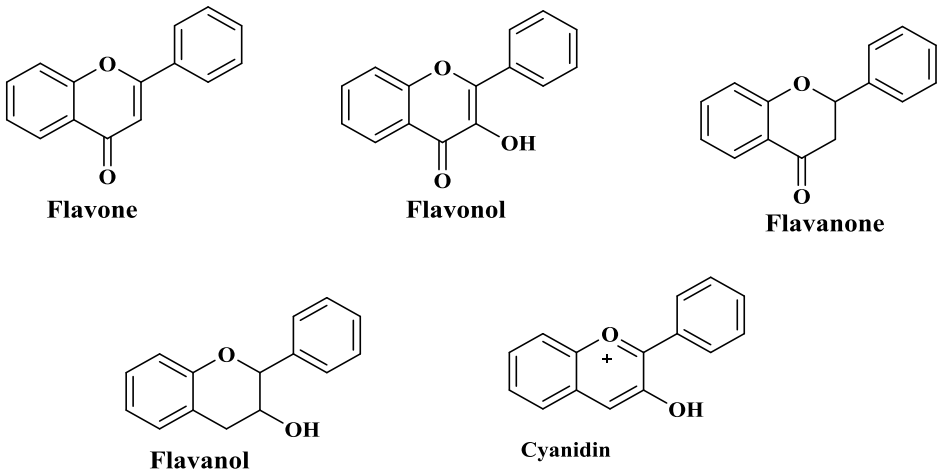

Figure 1.8. Structure of major classes of flavonoids

A large number of flavonoids occur as *O*-glycosides in which one or more of the hydroxyl groups of the flavonoids nucleus are bound to a sugar or sugars via an acid labile hemiacetal bond. Similarly, C-glycosylation also occurs, so that the sugar is *C*-linked and this linkage is acid resistant. Glycosylation make the flavonoids less reactive and more water soluble (Harborne et al., 1999). The D-glucose is the most common sugar residue of the flavonoids, and other sugars are D-galactose, L-rhamnose, L-arabinose and D-xylose. The preferred glycosylation site for the sugars is C3 and less frequently the C7 position (Harborne et al., 1999; Herrmann, 1988, 1976). The wide range of colours and shades in flowers and leaves in many higher plants are mainly due to the presence of flavonoids particularly anthocyanidins (Monitto, 1981).

1.4.9 The function of flavonoids

1.4.9.1 Anti-oxidant activity

The discovery of flavonoids to have anti-oxidant activity has generated considerable interest in the scientific community and in the functional food industry. This activity is due to their ability to scavenge free radicals, donate hydrogen atom or electrons, or chelate metal cations. Furthermore, the anti-oxidant activity depends on the number and positions of the hydroxyl groups, and the presence of a double bond between C2 and C3 in ring C (van Acker et al., 1996). The antioxidant activity of the flavonoids is enhanced with the presence of hydroxyl groups at 3', 4' and 5' positions of the ring B, while those with free hydroxyl groups at position C5 and C7 have a pro-oxidant effect (Seeram and Nair, 2002). Furthermore, the replacement of hydroxyl groups in ring B by methoxyl groups reduces the radical scavenging capacity of the flavonoids (Pietta, 2000; Seeram and Nair, 2002).

1.4.9.2 Plant pigments

Insect-pollinated plants such as rose sweet pea have petals that are large and brightly coloured, while wind-pollinated plants like maize have no petals or small petals which are often brown or dull green. The wide range of colours in flowers are principally due to the presence of certain flavonoids, and the pigments responsible for these colourations are the anthocyanins (red or purple colours), aurones and chalcones (yellow colours) (Koes et al., 1994; Martin and Gerats, 1993). Many flowers are known to accumulate colourless flavonols and flavanones in their petals and these flavonoids form complexes with anthocyanins and metal ions, thus altering the colour of the flowers. The result of these co-pigmentation is the appearance of strong blue colours in flowers (Kondo et al., 1992). These flower pigments usually act as a visual signal to attract pollinating animals, informing them of the presence of nectar. And this was achieved as a result of the presence of anthocyanin in the inner epidermis of the petal, the transcriptional activity of the structural genes and the rate of anthocyanin biosynthesis will reach a maximum just prior to opening of the flower bud (Koes et al., 1994a; Martin and Gerats, 1993).

1.4.9.3 Plant sexual reproduction

Many plant species store flavonoids in the male (anthers) and female (pistil) reproductive organs of the plant. Flavonoids such as anthocyanins, flavonols and chalcones are found in anthers. The flavonoids biosynthetic genes and enzymes are active in the tapetum and connectivum at the early stage, and become disintegrated at the later development stage where the cell contents are discharged into the pollen locule (Beerhues et al., 1989; Koes et al., 1990;

Van der Meer et al., 1992). The flavonoid biosynthetic genes are active in the. The ovules being the primary site for gene expression, the stored flavonols form a gradient along which the growing pollen tubes are guided to their target (Koes et al., 1994).

1.4.9.4 Symbiotic plant-microbe interactions

The rhizobia bacteria (*Rhizobium, Bradyrhizobium and Azorhizobium*) live in a symbiosis association with leguminous plants. These bacteria can infect the roots of a specific plant host and induced the formation of a root nodules, which is a complex development process that requires the action of both bacterial and plant genes (Koes et al., 1994). In legumes, flavonoid biosynthetic genes are active in young root cap cells and in the zones where root hairs emerge (Yang et al., 1992). These flavonoids are released into soil, the nodD gene is constitutively expressed in rhizobia that live in the soil while the other nod genes are induced by the flavonoids released from the host plant. Genetic evidence indicates that the NodD protein functions as the receptor for the flavonoids signal. NodD proteins from different bacteria differ in their response to distinct flavonoids and generally respond optimally to the flavonoids excreted by their corresponding host plant. Unusually, flavonoids can also act as an inhibitor of the nod gene expression. For instance, daidzein induces nod gene expression in *Bradyrhizobium japonicum* (nodules on soybean), but is an inhibitor in *Rhizobium leguminosarum* (nodulates peas) (Fisher and Long, 1992; Schlaman et al., 1992).

1.4.9.5 UV protection

Sunlight apart from driving photosynthesis in plants, it also activates the flavonoid biosynthetic genes via phenylalanine ammonialyase, resulting in the synthesis of flavonoids especially anthocyanin and flavones (Britton, 1983; Dixon and Paiva, 1995). In plants, the flavonoids are stored in the epidermal cells and help to reduce the amount of light reaching the photosynthetic cells (Beggs et al., 1985). The UV irradiation of Petunia and Arabidopsis was also shown to induce the synthesis of flavonols with higher hydroxylation levels (Ryan et al., 2002, 2001). The isolation of an Arabidopsis mutant that is tolerant of very high UV-B levels further indicates the role of flavonoids in UV protections (Bieza and Lois, 2001).

The effects of wounding or infection by microorganisms or herbivores will increase the synthesis of flavonoids and other polyphenolic compounds in plants (Bennet and Wallsgrove, 1994; Dixon and Paiva, 1995; Strack, 1997). Research has shown that the accumulation of flavonols such as kaempferol and its glycosides is induced by wounding and these flavonoids

can serve to prevent microbial infection in the stigma of *Petunia* in nutrient- rich environment (Mo et al., 1992; Vogt et al., 1994).

1.4.10 Aims of the study

The search for plant-derived phytochemicals have long been a subject of research in an effort to find a suitable replacements for conventional insecticides with less impact to human health and the environment. Researchers have reported that most biopesticides, with few exceptions, are more ecologically friendly and less toxic to humans while still possessing anti-insect properties which are either purely insecticidal or act as feeding deterrents, growth inhibitors, growth regulators, repellents or ovipositor inhibitors against a variety of species (Akhtar et al., 2007; Copping and Menn, 2000; Schmutterer, 1990). According to the recent studies of plants with insecticidal properties, species of the families *Meliaceae, Rutaceae, Asteraceae, Annoaceae, Labiatae and Canellaceae* have proven themselves to be plants for the future (Arnason et al., 1987). The Meliaceae, belongs to the mahogany family and it contains approximately 50 genera and over 500 species (Pennington and Styles, 1975). The chemical investigation of this plant family, revealed that it is characterized by a diverse variety of limonoids, many of which are known to possess insecticidal properties. This has resulted to the system investigation of this plant family for bioactivity against insects (Isman, 2006). In this family, most research has been focused on azadirachtin, a limonoids isolated from the seeds of the Indian neem tree, *Azadirachta indica* which acts both as potent antifeedant and insect growth regulator. It is also reported that neem seeds extract containing 10-25% of azadirachtin, act both as potent antifeedants and insect growth regulators (Akhtar et al., 2007; Kraus, 2002), this has resulted in the registering of neem extracts as commercial insecticide products in the United States of America (Isman, 1997). The outstanding bioactivity exhibited by azadirachtin from the *A. indica* led to the search for other natural insecticides in the closely related genus (Akhtar et al., 2007).

Screening of plant species belonging to the *Meliaceae* family has found the genus *Trichilia* to have a potential that can be developed into plant-based insecticides. Several limonoids such as sendanin, trichilinin, trichilin A, trichilin B, trichilin C, trichilin D, trichilin E, dregeana 4, nymania 1, rohituka 3, rohituka 5, rohituka 7, trichilia substance Tr-A, trichilia substance Tr-B, trichilia substance Tr-C and seco-A-protolimonoid has been reported from the root and stem bark of *Trichilia emetica* but no such report from the seeds. These limonoids have demonstrated potent insecticidal properties. Therefore, the aims of these research are;

- To investigate the phytochemistry of the seeds of *T. emetica*

- In chapter 2, the oil content was assessed for physicochemical analysis and fatty acid profiles.
- In chapter 3, the individual compounds of the "phenolic content" are isolated and identified and their biological activity assessed.
- In chapter 4, the seeds as a source of limonoids are investigated.

CHAPTER 2

Fatty acid profiles and some minor components of *T. emetica* seed oils: Result and Discussion

2.0 Introduction

In this chapter, the objectives were to establish the fatty acid composition of the seed and shell oil samples, and this relies on high temperature GC-MS, ^{1}H NMR and ^{13}C NMR data of crude oil, and GC-MS of fatty acid methyl esters (FAMEs). The yields of the oil is expressed on a dry matter, and compared with other seed oils. The physico-chemical characteristics of crude oil samples were determined. The data obtained for the iodine value, saponification value, acid value and peroxide were compared to the recommended standard for some edible oils (FAO/WHO, 1994).

2.1 Extraction of *T. emetica* seed and shell oil

Flaked *T. emetica* seed and shell was extracted using hexane at room temperature. The crude extract was used to evaluate the fatty acid and physicochemical analysis. The minor component was determined from the unsaponifiables fraction of the oil. The seeds were from Ghana and Mozambique and were prepared as described in 6.3 and a portion of this crude oil was used to evaluate the fatty acid content and for physico-chemical analysis as shown in 6.4.1 to 6.4.6. The minor components were separated according to 6.4.7.

2.2 RESULTS AND DISCUSSION

2.2.1 Moisture and ash content of *Trichilia emetica* seed and shell

The percentage moisture contents of *T. emetica* seed and shell were 14 and 19%. This is lower when compared to that reported previously (Saka and Msonthi, 1994). The low moisture contents could be attributed to the extent of drying of the seed sample during harvest or prolonged storage.

The ash contents of the seed and shell samples were 5 and 7% respectively, this result is higher than that reported for seed sample (Saka and Msonthi, 1994). Hence, since the mineral contents of food are contained in the ash, the value obtained will be useful in assessing the quality of edible materials.

2.2.2 Chemical Characteristics of *T. emetica* Seed and Shell Oil

T. emetica seeds have an average seed length between 8.08 – 18.14 mm and a weight between 0.10 − 0.71 g. The seed samples consisted of 21 – 29% oily shell like husk and 71 – 79% kernel. These seeds were very hard and to extract oil from them, they were flaked to physically break them down. However, the shell was not very hard but it was also flaked. The extracted oils were both golden yellow brown. The oil yield was 23% and 60% for shells and seeds, respectively.

The seed length and weight reported in this studies agrees with 14 to 18mm and 0.35 to 1.0 g reported for similar analysis (Fupi and Mork, 1982; Vermaak et al., 2011). The oil contents of the seed samples determined in this study were similar to 55-68% but higher than 22.90% reported by other researchers (Fupi and Mork, 1982; Orwa et al., 2009; Saka and Msonthi, 1994). Similarly, the result obtained for the shell is within 14 – 51% but lower than 35 – 45% respectively (Fupi and Mork, 1982; Orwa et al., 2009). The emission of greenhouse gasses from fossil fuel and the dwindling of the world reserves has resulted in the search for an alternative eco-friendly and renewable fuel. The result obtained in this studies is above 23.70 – 46.60% reported for *Jatropha curcas L* which has been a good candidate for biodiesel production (Mazumdar et al., 2012). Therefore, *T. emetica* seeds can also be an alternative feedstock for biodiesel production since its bitter taste has limited it use for food or feedstock.

2.2.3 Analysis of NMR Data for Crude *T. emetica* Seed Oil

The use of NMR to study lipids, especially triacylglycerol (TAG) in edible oils is increasing in recent years (Ng and Gee, 2001; Vlahov et al., 2002). Apart from using NMR for structural characterisation, both the ^{1}H and ^{13}C NMR spectra have been used for authentication and quality assessment (Jie and Mustafa, 1997; Vlahov et al., 2001). The major disadvantage of ^{1}H spectrum of TAG is the signal overlap in the aliphatic region while small chemical shift differences observed for some carbons may lead to incomplete assignment of the ^{13}C NMR spectrum (Lie Ken Jie and Lam, 1995). The concentration dependence of the ^{13}C chemical shift may be another setback, but some researchers have applied additivity rules and/ or relaxation times to assist in the assignment (Mannina et al., 2000). The 2D NMR spectra (^{1}H-^{1}H COSY, HMBC, HMQC, HSQC, HSQC - TOCSY) are mainly used to established the position and configuration of unsaturated fragments in the alkyl chain (Vatele et al., 1998; Mannina et al 1999).

The analysis of the ^{1}H and ^{13}C NMR spectrum of crude *T. emetica* seed oils is as shown in (Table 2.1, 2.2, and Fig. 2.2) and the results were consistent with reported values for other seed oils (Mannina et al., 1999; Tariq et al., 2011; Thoss et al., 2012).

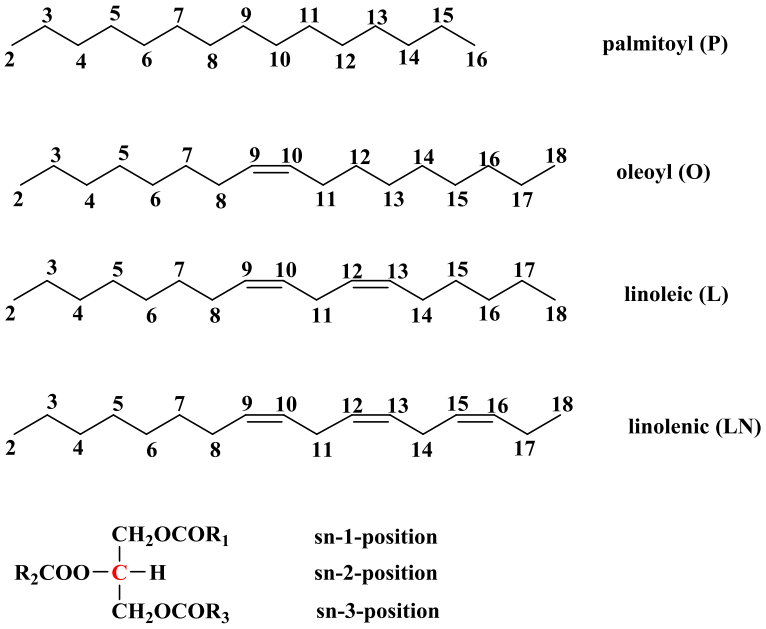

Fig. 2.1. The structure of the model triacylglycerols

The ^{1}H NMR resonances appearing between δ_H 4.10 - 4.28 ppm and 5.25 ppm were assigned for glycerol, which is one of the main components of the triacylglycerol fraction and it serve as a backbone to which fatty acid chains are attached (Fig. 2.1). Protons on *sn*-1, 2, and 3 on the glycerol have different environments depending on the nature of the fatty acid composition of the oil. The 2 protons of the *sn*-1 and 3, assigned α-position are each split by a single proton of *sn*-2 assigned β-position thus creating a multiplet at δ_H 4.10 and 4.25. The single proton of the *sn*-2, was split by four protons of the *sn*-1 and 3 yielding a multiplet at δ_H 5.25.

The spectrum showed signals at δ_H 0.86 which is assigned to the terminal methyl group of the fatty acid chain. The absence of methyl signals at δ_H 0.93, indicated the absence of linolenic acid (Hidalgo and Zamora, 2003). The signals of the CH_{2n} chain resonate at δ_H 1.22. Other significant resonance is that found at δ_H 5.32 which is attributed to CH=CH found within all unsaturated fatty acids such as oleic and linoleic acid (Table 2.1).

The ^{13}C NMR spectrum show a characteristic peaks at 172.77 and 173.22 ppm, which were assigned to ester carbonyl (-CO-) and is the observed difference in chemical shift of α/β splitting's in carbon atoms of glycerol backbone (Simova et al., 2003; Tariq et al., 2011). The

Table 2.1. Chemical shifts and assignments of the characteristic resonance in the ^{1}H NMR spectrum of crude *T. emetica* seed oil

δ (ppm)	Proton	Assignment
0.86	$-CH_3$	Terminal methyl
1.24	$(CH_2)_n$	Methylene
1.59	-CH2-COO	All acyl chains
1.99	-CH=CH	All unsaturated fatty acids
2.29	$-CH_2-COO$	All acyl chains
2.75	$C=C-CH_2C=C$	Proton attached to bis allylic carbon
4.10-4.28	CH_2O (α)	Glycerol (triglycerides)
5.25	CHO (β)	Glycerol (triglycerides)
5.32	CH=CH	Olefinic (all unsaturated fatty acids)

acyl distribution measurement is believed to occur in the carbonyl region (Sacchi et al., 1996). In the distribution of the major fatty acid components between the *sn* 1,3 (α) and 2 (β) position of glycerol as it occur from the carbonyl region, saturated fatty acid are distributed over the α-position while only trace amount (< 0.5%) are found in β-positions. On the other hand, unsaturated fatty acids are more abundant in position 2 (β). Linoleic acid has a higher preference for this position than oleic and other unsaturated fatty acids. And the concentration of the linoleic/oleic ratio in position 2 is about twice as large as that in position 1,3 (Mannina et al., 1999).

The unsaturated region within the fatty acid methyl esters is indicated with a peak around 127.84 and 130.13 ppm, this is a frequency range within which alkene carbons resonate (Table 2.2 and Fig. 2.2). Since C18:1 is the most abundant unsaturated fatty acid present in the oil samples, signals at α/β position is readily seen for both alkene carbons; C9 at α- = 129.65 ppm and β- = 129.67 ppm. Other important peaks are those ranging from 62.06 - 68.86 ppm were assigned to glycerol, 22 – 34.17 ppm were for methylene carbons of long chain in fatty methyl esters (FAMEs) and 14.08 ppm are for terminal carbons of the triglycerides (Simova et al., 2003; Tariq et al., 2011; Thoss et al., 2012).

Table 2.2. Chemical shifts and assignments of the characteristic resonance in the ^{13}C spectrum of crude *T. emetica* seeds.

δ (ppm)	Carbon	Assignment
14.08	-CH3	All acyl chains
22.55	-(CH_2)n	All acyl chains
24.82	C3	All acyl chains
25.60	C11	Diallylic
27.14	C8-11 (oleyl)	Allylic
	C8-14 (linoleyl)	
29.02-29.74	CH_2n	All acyl chains
31.50	αβ-C16	Linoleyl
31.90	αβ-C16	Oleyl
34.02	α-C2	All acyl chains
34.17	β-C2	All acyl chains
62.06	α-CH_2O	Glycerol (triacylglycerols)
68.86	β-CH_2O	Glycerol (triacylglycerols)
127.86	β-C12	Linoleyl
127.88	α-C12	Linoleyl
128.04	α-C10	Linoleyl
128.06	β-C10	Linoleyl
128.17	α-C12	Linolenic
128.34	β-C12	Linolenic
129.65	β-C9	Oleyl
129.67	α-C9	Oleyl
129.94	β-C9	Linoleyl
129.99	α-C9	Oleyl
130.18	α-C13	Linoleyl
172.82	α-C1	Glycerol (triacylglycerol)
173.26	β-C1	Glycerol (triacylglycerol)

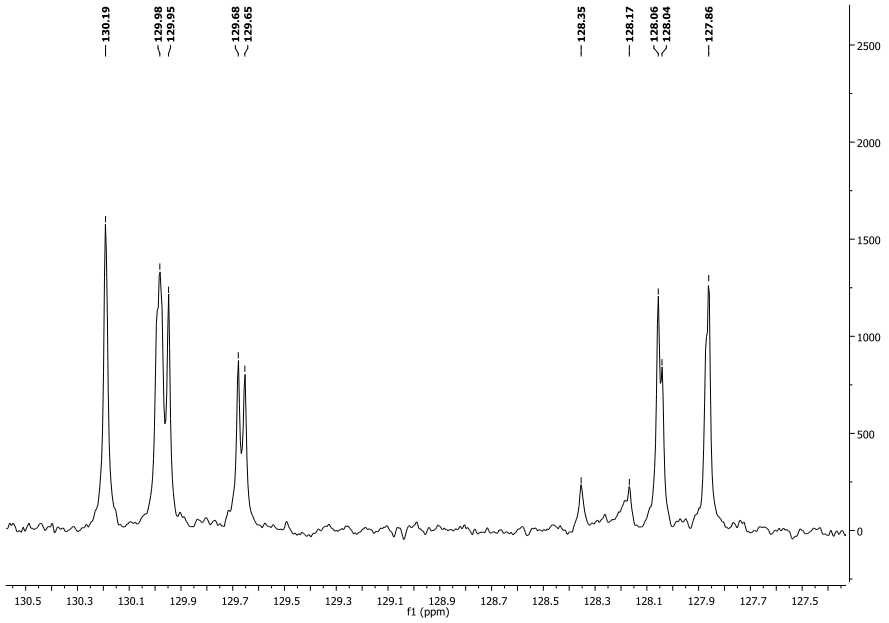

Fig. 2.2. The ^{13}C NMR olefinic region (127-130.19 ppm) of crude *T. emetica* seed oil

The signals in the ^{1}H NMR spectrum (Fig. 2.3) was used to calculate the relative percentage of saturated fatty acid (SFA), monounsaturated (MUFA) and polyunsaturated fatty acids (PUFA) in the *T. emetica* seed and shell oils. This was achieved by integrating different proton environment at X, Y and Z (Table 2.3) (Thoss et al., 2012). This method does not identified individual fatty acids presents, it only provide information on the degree of saturation and unsaturation of the oil.

Table 2.3. Integrations of ^{1}H NMR assignment used for determination of saturation vs unsaturation.

Peak	δ (ppm)	Seed oil (G)	Shell oil (G)	Seed oil (M)	Shell oil (M)
X	2.02	9.23	3.88	9.13	4.86
Y	2.29	10.52	4.95	11.05	6.15
Z	2.75	1.00	0.41	1.00	0.43

Where, G – Ghana M − Mozambique

The relative amount of PUFA was calculated by using the integrations of the acyl group at δ_H 2.29 ppm (Y) and δ_H 2.75 ppm for protons attached to bis-allylic carbons (Z) which is only present in polyunsaturated fatty acids within the *T. emetica* seed oil. The relative amount of PUFA was calculated using equation 1.

PUFA = {Z/Y} eq. 1

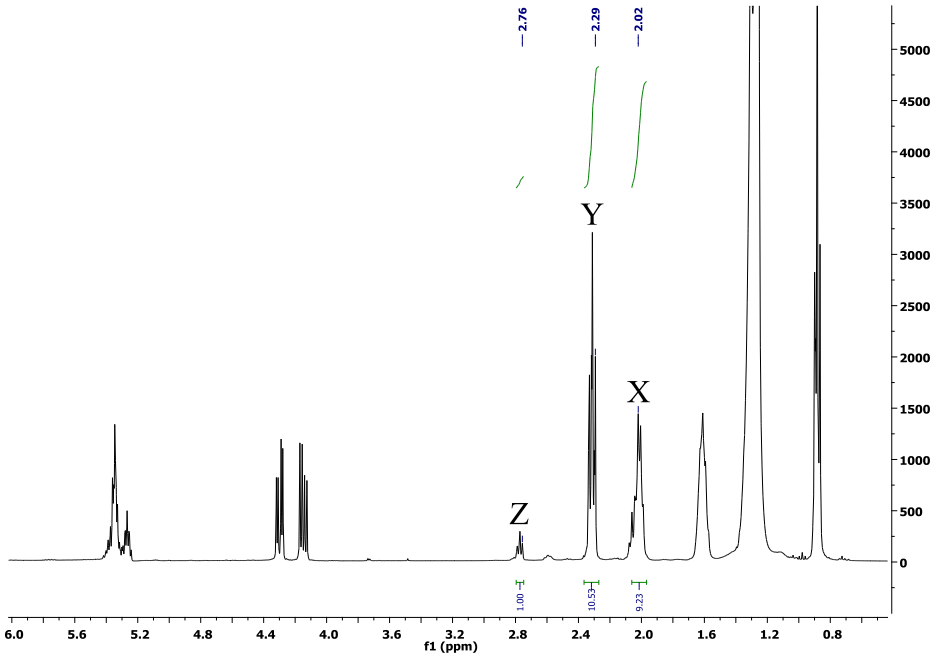

Fig. 2.3. ^{1}H NMR spectrum of crude *T. emetica* seed oil from Ghana

The relative amount of MUFA was calculated by integrating the acyl group (Y) and α-allylic region at δ_H 2.02 ppm (X) which is present in all unsaturated fatty acid. The relative amount of the total unsaturation present in the seed sample is given by the fraction (X/2Y). Hence, relative MUFA content was calculated using equation 2:

$$MUFA = [(X/2Y)] - PUFA \quad \text{eq. 2}$$

The relative percentage of saturated fatty acid (SFA) was determined by subtracting the relative amount of the total unsaturation from the total amount of fatty acid as shown in equation 3:

$$SFA = 1- (X/2Y) \quad \text{eq. 3}$$

This result (Table 2.4) show that saturated fatty acid is dominant in the *T. emetica* seed and shell oils, agreeing with earlier findings (Khumalo et al., 2002; Vermaak et al., 2011).

Table 2.4. Relative percentage of PUFA, MUFA, and SFA for *T. emetica* seeds and shell oils.

T. emetica oil	PUFA	MUFA	SFA
Seed oil (M)	9	32	59
Shell oil (M)	7	33	60
Seed oil (G)	10	34	56
Shell oil (G)	8	31	61

G – Ghana M – Mozambique

2.2.4 Transesterification of *T. emetica* Oils

The ^{1}H NMR spectrum of transesterified oil sample was also studied (Fig. 2.4). Two characteristic peaks were seen which were absent in the crude oil sample, a singlet peak

observed at B (δ_H 3.65 ppm) and a triplet of α- carbonyl methylene protons at A (2.28 ppm). The presence of these distinct peaks at position A and B was use to confirm the presence of methyl esters present in the oil sample (Tariq et al., 2011). Other observed peaks in the spectrum were the same with that of ^{1}H NMR of the crude sample (Tariq et al., 2011; Thoss et al., 2012).

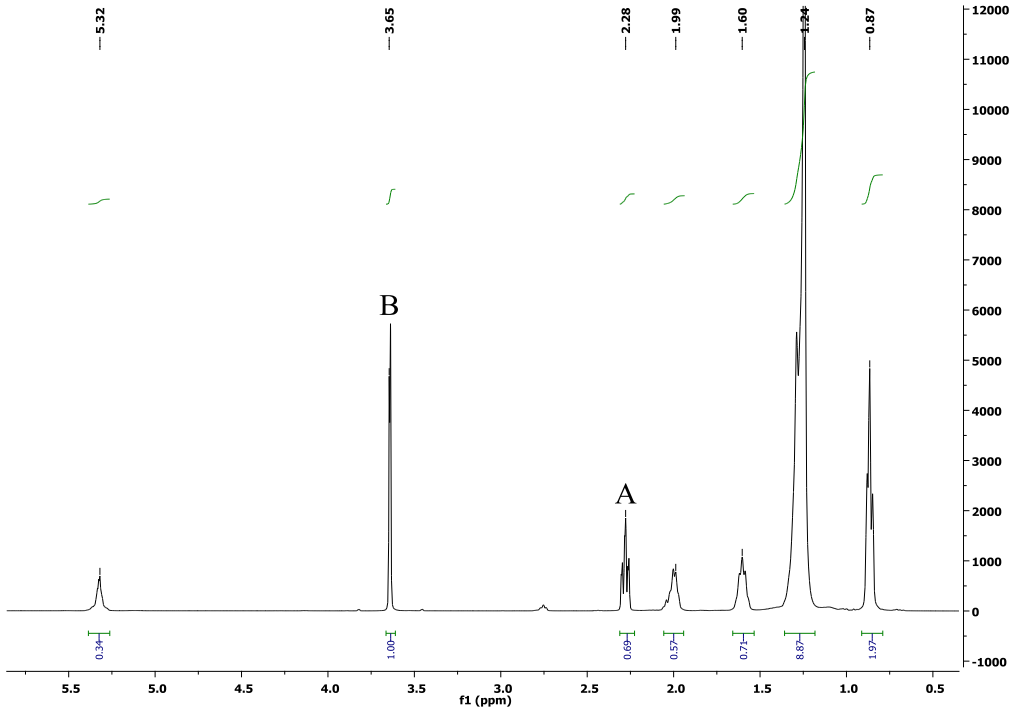

Fig. 2.4. ^{1}H NMR spectrum of transesterified *T. emetica* seed oil

The transesterification of crude oil to methyl esters can be quantified using ^{1}H NMR and this is done by integrating these two distinct peaks at δ_H 3.65 and 2.01 ppm. (Tariq et al., 2011), the yield of transesterification reaction was quantified using equation 4:

$$H\ (\%) = 100 \times 2B / 3A \qquad \text{eq. 4}$$

Where:

H = Percentage conversion of triacylglyceride to methyl esters

A = Integration value of α-methylene protons

B = Integration value of the methoxy protons of the methyl esters and

The percentage conversion of triacylglycerides to its corresponding methyl esters was 97 %. This is a very good yield.

2.3 GC/MS analysis

GC–MS was used to analyse the fatty acid methyl ester composition of *Trichilia emetica* seed and shell oils (Table 2.5). Two major peaks and other minor ones were observed in the total ion chromatogram of the shell and seed oil samples. Each of this peaks correspond to FAMEs content of the oil samples and was identified from the NIST library match software. FAMEs have characteristic fragmentation patterns due to the specific way in which the fatty acid breaks down, and also how it undergoes McLafferty rearrangement to produce new ions. The parent ion is the molecular ion, which is equal to the molecular mass and this peak is used as a reference to further characterize other peaks (Fig. 2.6). The base peak of all saturated FAMEs is observed at *m/z* 74 and it is due to a McLerffaty rearrangement (Fig. 2.5) (McLerffaty, 1959; Tariq et al., 2011). Other peaks are those observed at *m/z* 239, which is produced due to α – cleavage of methoxy group [M –31]$^+$, and at *m/z* 227 due to a loss of a propyl radical [M – 43]$^+$ and a hydrogen atom within the chains (Gunawan et al., 2013; McLerffaty, 1959; Tariq et al., 2011). The other distinct peaks observed for saturated fatty acid were those at *m/z* 87, 101 and 115 and so on with a difference of 14 *amu*., these ions were abundant in the lower mass region and were formed due to β-cleavage of carbomethoxy ion $[CH_3O_2C(CH_2)_n]^+$, where n is a positive integer and it is equal or greater than 1 (Tariq et al., 2011). Similarly, palmitic acid methyl ester could be identified with peaks at *m/z* 270, 227 and 199 (Table 2.6).

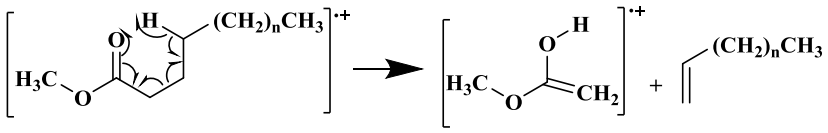

Fig. 2.5. McLafferty Rearrangement of a Fatty Acid

The monounsaturated FAME identified in these oil samples is to oleic acid (C18:1) with a relative percentage of 27.7 - 35.8 % in both *T. emetica* seeds and shell oils. The base peak for this FAMEs is at *m/z* 55, other peaks at [M – 32]$^+$ due to loss of methoxy group plus hydrogen atom and those occurring due to loss of McLafferty ion [M – 74] (Gunawan et al., 2013). These three distinct peaks also help to identify oleic acid methyl esters in the oil. The polyunsaturated fatty acid found to be present in the oil samples is linoleic acid [C18:2] with relative proportion of 0.7 and 7.5% respectively. This is confirmed by the characteristics base peak at *m/z* 67 with other prominent peaks at m/z 263 [M – 31]$^+$ and 220 [M – 74]$^+$ which is due to loss of methoxy group and McLafferty ion. At the lower mass range, peaks were also observed at m/z 67, 81,

95, 109 (Gunawan et al., 2013; Tariq et al., 2011). Linolenic acid [C18:3] was only found to be present in trace amounts in the shell oil samples.

From this analysis, the presence of fatty acids containing 14, 16 and 18 carbon chain length in the seed and shell oils was confirmed (Table 2.5). The saturated fatty acids found to be present were C14:0, C16:0 and C18:0, the only monounsaturated fatty acid was C18:1 while polyunsaturated fatty acid were C18:2 and C18:3, respectively. Palmitic acid methyl ester (C16:0) was the most abundant FAME with a relative percentage of 59.1 to 63.6%, followed by oleic acid methyl ester with relative percentage of 27.7 to 35.8 % in the seed and shell oil samples.

Table 2.5. Relative percentage (%) of fatty acid methyl esters present in *T. emetica* oil samples.

Fatty acid methyl ester/ molecular weight	Characteristics MS ions	Seed (m)	Shell (m)	Seed (g)	Shell (g)
Myristic (242, C14:0)	242, 199, 143	0.2±0.0	1.1±0.3	0.6±0.2	0.7±0.2
Palmitic (270, C16:0)	270, 227, 199	63.6±3.6	59.1±4.2	60.7±4.1	62.9±3.3
Stearic (298, C18:0)	298, 227, 199	0.4±0.1	3.2±0.4	2.1±0.2	1.3±0.2
Oleic (296, C18:1(ω_9))	296, 264, 222	27.7±2.3	31.8±1.9	30.4±1.3	29.3±1.2
Linoleic (294, C18:2 ($\omega_{6,9}$))	294, 263, 220	7.2±0.9	4.6±0.7	4.3±0.3	5.8±0.8
Linolenic (292, C 18:3 ($\omega_{6,9,12}$))	292, 236, 173	0.9±0.2	n.d.	1.9±0.5	n.d.

Where, M - Mozambique G – Ghana n.d – not detected,

This result differs from those reported by (Engelter and Wehmeyer, 1957; Grundy and Campbell, 1993), but is similar to the reported composition of the *T. emetica* seed oil (Khumalo et al., 2002; Vermaak et al., 2011). The relative percentage of SFA and MUFA determined in the oil samples using GC-MS is in agreement with the calculated values using ^{1}H NMR of the oil samples.

From this study, *T. emetica* oil is rich in palmitic and oleic acid making it a potentially useful raw material in soap, candle and cosmetic industries, and also as wood oil use in upholstery (Fupi and Mork, 1982; Grundy and Campbell, 1993; Orwa et al., 2009; Van der Vossen and Mkamilo, 2007). This explains why this oil is used as a starting material in cocoa butter production (Vermaak et al., 2011). Furthermore, the development of an efficient method to remove its bitter taste could increase it potential as food oil (Grundy and Campbell, 1993).

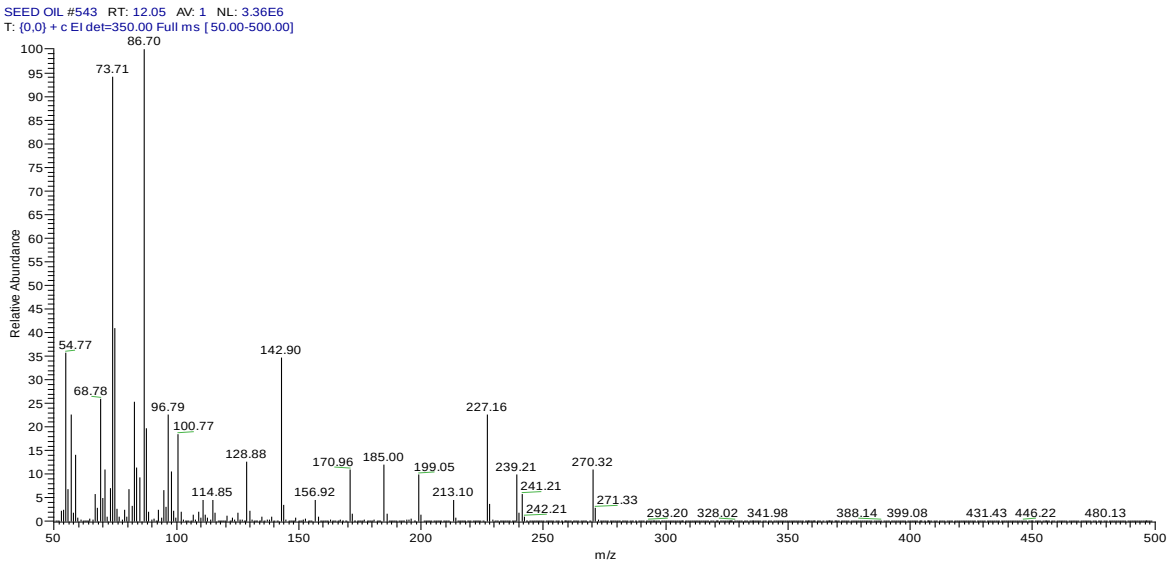

Fig. 2.6. Mass spectrum of palmitic acid in *T. emetica* seed oil

2.4. Physico-chemical analysis

The physico-chemical analysis of *T. emetica* seeds oils from Ghana and Mozambique is presented in Table 2.7. The Food and Agricultural Organization/ World Health Organization (FAO/WHO) reference standard of some notable edible oil is as shown in Table 2.6.

2.4.1 Iodine value

This is the measure of the degree of unsaturation of an oil. The iodine values for crude *T. emetica* seeds oils from Mozambique and Ghana were 64.6 and 69.1 g I_2/100g. These values are within 60.0-80.0 reported for similar analysis (Grundy and Campbell, 1993; Vermaak et al., 2011) and are also comparable to 64.2-100.3 reported for *Sclerocarya birrea*, (Mariod et al., 2004; Ogbobe, 1992) but lower than 119.8-125.0 for *Citrullus lanatus* (Nyam et al., 2009).

Table 2.6. Recommended standard for physicochemical characteristics of some edible oils as given by FAO/WHO (1994).

Oil type	Saponification value	Iodine value	Acid value	Peroxide value
Sun flower	188-194	110-143	≤ 0.6	≤ 10
Cotton seed	189-198	99-119	≤ 0.6	≤ 10
Corn oils	187-193	103-128	≤ 0.6	≤ 10
Palm oils	190-209	50-55	≤ 0.6	≤ 10

The result obtained in this research is comparable to recommended standard for palm oil (FAO/WHO, 1994) but lower than other vegetable oils (Table 2.6). The low iodine values of these oil samples signified that they have a high oxidative storage stability (Perkins, 1992)

(Ngassapa and Othman, 2001). The low iodine value of these oil samples indicate that it is a non-drying oil, and an excellent raw materials in personal care industry (Fernando and Akujobi, 1987). Furthermore, these oils will not be an attractive raw material in the paint and coating industry (Abayeh and Okoughae, 1998).

Table 2.7. Physicochemical analysis of crude *T. emetica* seed oils

Parameters	Ghana seeds oil	Mozambique seeds oil
Acid value (mg KOH/g)	0.4 ± 0.0	0.4 ± 0.1
Peroxide value (%)	10.3 ± 0.5	9.2 ± 0.4
Iodine value (g I_2/100g)	69.2 ± 2.1	64.6 ± 2.8
Saponification value (mg KOH/g)	195.4 ± 5.4	197.3 ± 4.6
Unsaponifiable matter (%)	1.3 ± 0.1	1.0 ± 0.1

2.4.2 Saponification value

The saponification values of *T. emetica* oil from Ghana and Mozambique were 195.4 and 197.3 (mg KOH/g) and are comparable (Grundy and Campbell, 1993; Vermaak et al., 2011). They also compare favourably to the literature (165-182) for *Ximenia americana* (Eromosele and Paschal, 2003). These results are within the range of recommended standard (FAO/WHO, 1994) for edible oils (Table 2.6) The high saponification value is an indication of the dominance of fatty acids of low molecular weight (Vermaak et al., 2011).

2.4.3 Peroxide value

The rancidity of the crude *T. emetica* seed oils was measured in terms of its peroxide value (Table 2.7). The values are lower than 12.85 reported for similar analysis (Vermaak et al., 2011) and are within the values of standards for edible oils (FAO/WHO, 1994). Oxidative rancidity is the oxygenation of the unsaturated fatty acids in the presence of an enzyme, resulting in the liberation of short chain carboxylic acids and aldehydes as odours and flavours (Ekpa and Epka, 1996). The values obtained in this research tally with the maximum acceptable value of 10 (FAO/WHO, 1994). Hence, this indicates that they are less liable to oxidative rancidity when stored at room temperature (Anyasor et al., 2009).

2.4.4 Acid value

Acid value is the number of mg of KOH required for neutralization of fatty acid present in oils and fats. It is a common parameter in the specification of oils and fats, and it is used for quality control.

The acid value, the index of free fatty acid contents, was found to be 0.44 and 0.37 mg $KOHg^{-1}$. This is higher than 0.008 (Grundy and Campbell, 1993) but lower than 3.82 mg $KOHg^{-1}$ (Vermaak et al., 2011). The low acid value suggests that the oil is good for human consumption as the value is below the maximum acceptable value of 0.6 mg KOH/g (FAO/WHO, 1994).

2.4.5 Unsaponifiable Contents

The output weight of extracted unsaponifiable matter in these seeds oils were 1.03 and 1.27% for Mozambique and Ghana respectively. These values compare favourably with 1.4% reported for *Ximenia americana* (Eromosele and Paschal, 2003). The low values obtained for unsaponifiables matter in this study justified the use of the *T. emetica* oils as a starting material for soap production. The chromatogram of the unsaponifiables fraction of *T. emetica* showing individual component is as shown below.

Figure 2.7. GC chromatogram of trichilia seed oil; (1) Squalene, (2) Cholesterol, (3) campoesterol, (4) stigmasterol, (5) β-sitosterol, (6) sitostanol, (7) botulin

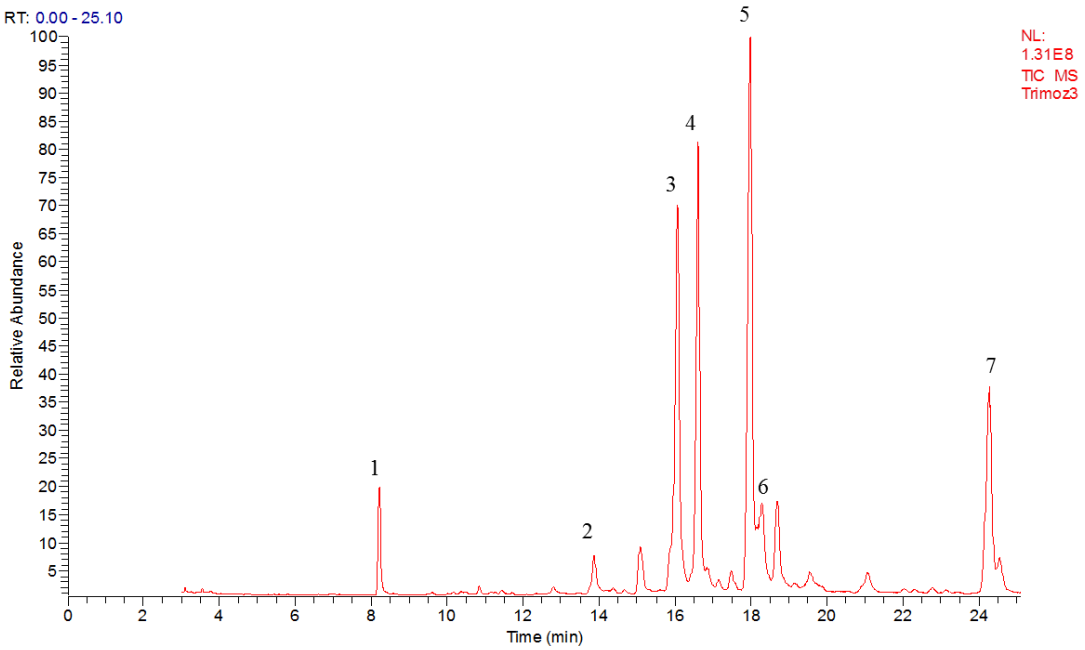

2.5 Sterols isolated from unsaponifiable *T. emetica* seed oil

Table 2.8. Compound AU 1 (β-sitosterol)

17-(5-Ethyl-6-methylheptan-2-yl)-10,13-dimethyl-2,3,4,7,8,9,11,12,14,15,16,17-dodecahydro-1*H*-cyclopenta[*a*]phenanthren-3-ol	
Synonyms	β-Sitosterol
Sample codes	AU 1
Sample amount	17 mg
Physical Description	White crystalline powder
Molecular formula	$C_{29}H_{50}O$
Molecular Weight	414 g/mol
Melting Point	136-138 °C
IR:($CHCl_3$)	3395, 2960, 1667, 1464, 1376, 1061, 757 cm^{-1}

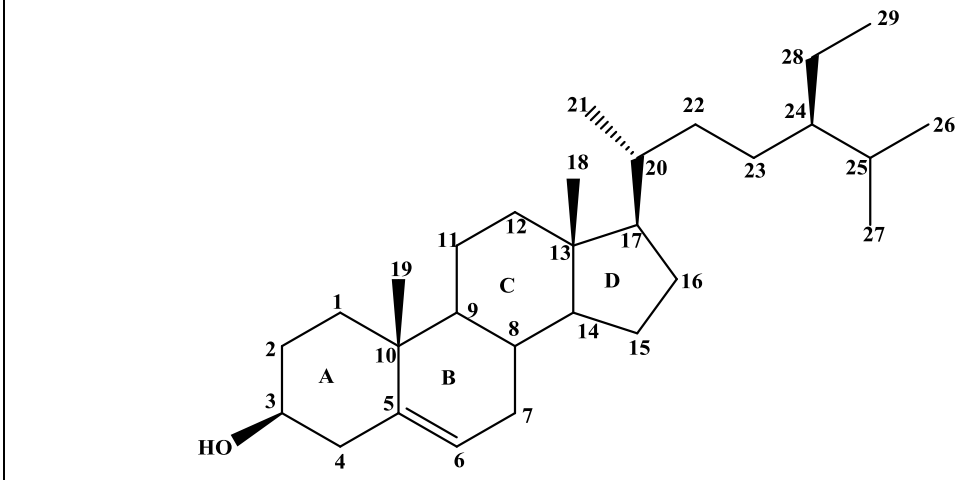

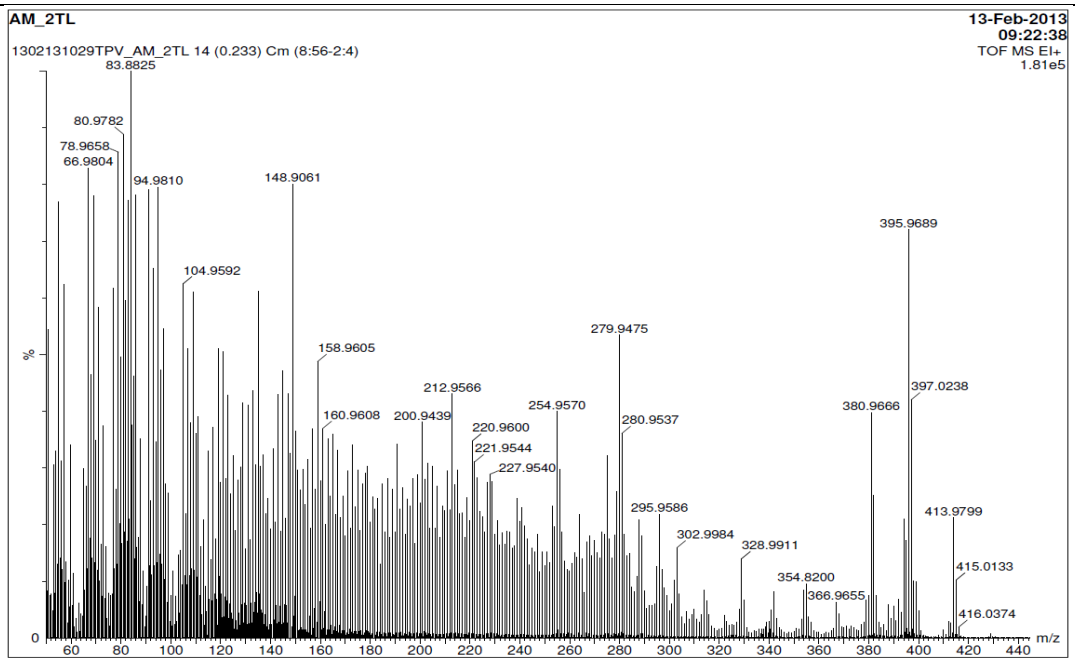

Compound AU 1 (17 mg) was isolated as a white crystalline powder and recrystallized from MeOH. It has a molecular formula of $C_{29}H_{50}O$ which was established on the basis of TOF-MS at *m/z* 415.0133 $[M + H]^+$ (Calcd for 415.3941). The optical rotation was not measured as this

was deemed unnecessary for a steroid. The IR spectrum of this compound has a broad band at 3395 cm^{-1} corresponding to O-H stretching. Other absorption frequencies were at 2935 and 2868 cm^{-1} are due to SP^3 C-H stretching, weak band at 1667 cm^{-1} is due to C=C stretching, 1464 cm^{-1} is a bending frequency for C-H deformation and 1376 cm^{-1} for methyl group symmetrical deformation, 1061 cm^{-1} signifies C-O stretching and 757 cm^{-1} was a result of C-H out of plane deformation, see appendix I. The DEPT spectrum (Fig. 2.9) showed twenty nine carbon signals, which consist of six methyl, eleven methylene, nine methane and three quaternary carbons. The ^1H NMR spectrum (Fig. 2.8) has a proton signals at δ_H 3.51 (m) which is a carbinolic proton on ring A and is assigned position 3. The carbinolic proton coupled with two methylene groups at position 2 and 4 as observed in COSY spectrum (Fig. 2.12). The direct correlation between carbons and hydrogens is exhibited in the HSQC spectrum (Fig. 2.13), and it shows the correlation between methyl protons (δ_H 0.66) to carbon (δc 11.9) assigned position 18, methylene protons (δ_H 2.22) to carbon (δc 42.3) assigned position 4, methine protons at (δ_H 3.51, δ_H 5.37) to carbon (δc 71.8 and 121.7) assigned to position 3 and 6 respectively. The triplet on the ring B structure was confirmed by the COSY correlations between the olefinic proton at δ_H 5.37 (t, 5.4 Hz) for H-6 and a methylene protons at H-7. These correlations were further confirmed by long-range coupling observed in HMBC. The HMBC coupling of ring B shows that H-6 correlated with C-4, C-5, C-7 and C-10 (F). Ring A and B were sustained by the HMBC correlation of the Me-19 singlet (δ_H 1.03) to C-1 (δc 37.3), C-5 (δc 140.8), C-9 (δc 50.1) and C-10 (δc 36.2) (Fig. 2.10 and 2.11). Similarly, ring C and D were sustained by singlet methyl Me-18 (δ_H 0.67) which was correlated with C-12 (δc 39.8), C-13 (δc 42.3), C-14 (δc 56.8) and C-17 (δc 56.0). The attachment of the 3-ethyl-2-methylheptane side chain to the ring was confirmed from the HMBC correlation of Me-21 (δ_H 0.93, d) with C-17.

This compound has been reported from the leaves of *Mamordica charantia* and was tested to have good antimicrobial activity (Sen et al., 2012), it has also been reported from the rhizomes of *Etlingera sphaerocephala* Var. *Grandiflora* (Yahya *et al.*, 2011) and from the leaves of *Rubus suavissimus* S. Lee (Chaturvedula and Prakash, 2012). The NMR data (Table 2.9) showed signals typical of sterols, which led to its identification as β- sitosterol and is the most abundant sterols in most vegetable oils. This was confirmed by MS, IR spectroscopy and comparison of its ^1H and ^{13}C NMR data with those reported in the literature.

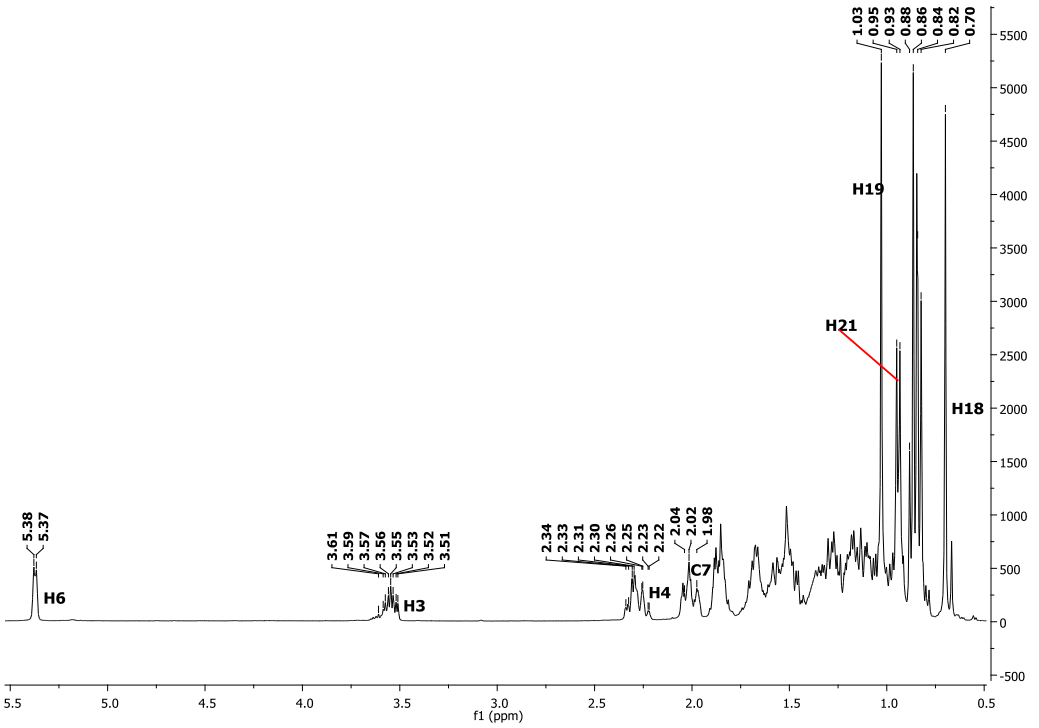

Fig. 2.8. [1]H NMR spectrum of compound AU 1

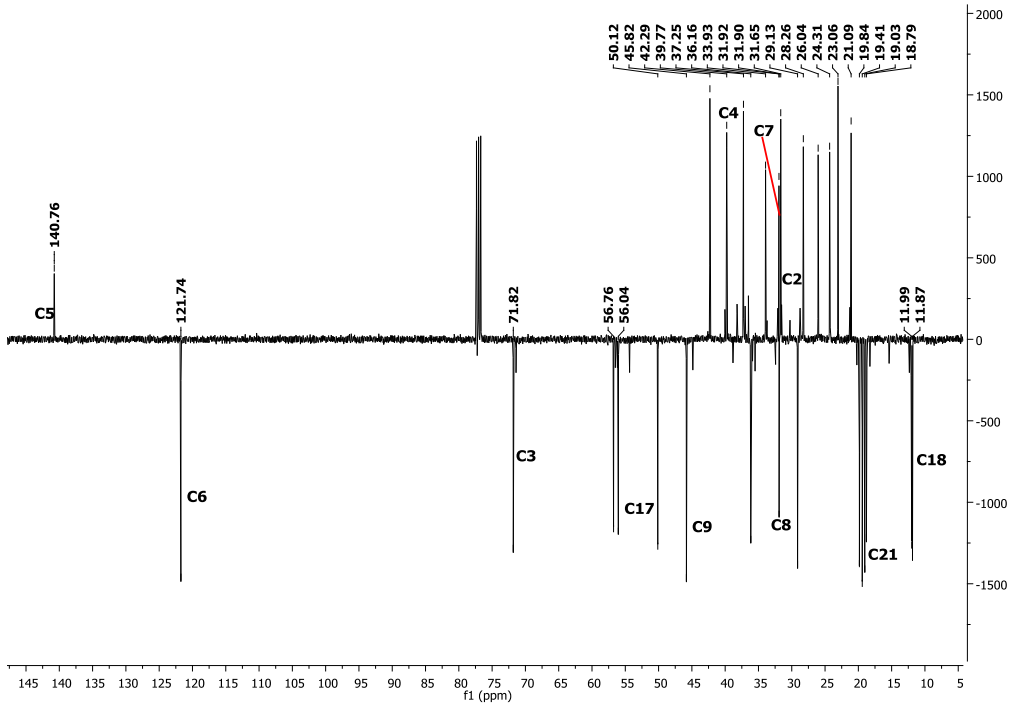

Fig. 2.9. DEPT spectrum of compound AU 1

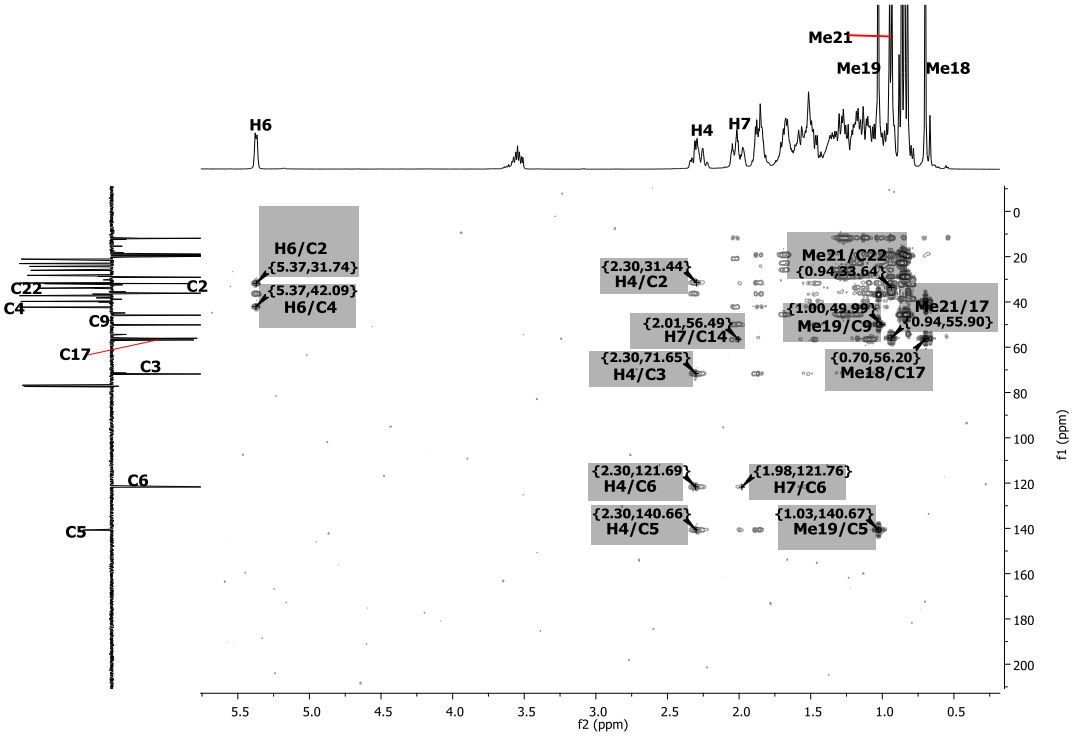

Fig. 2.10. HMBC spectrum of compound AU 1

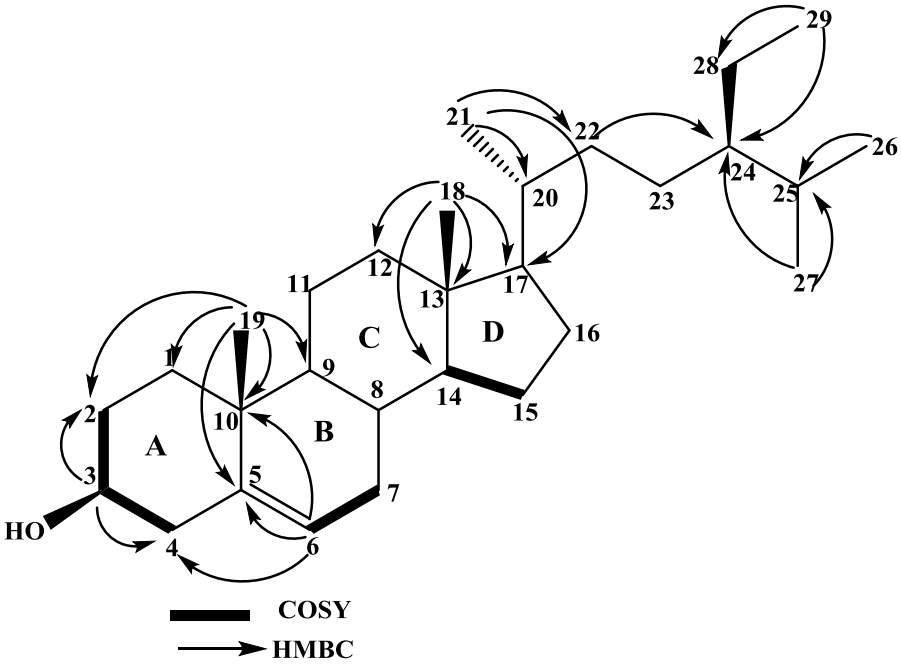

Fig. 2.11. HMBC and COSY correlations of compound AU 1

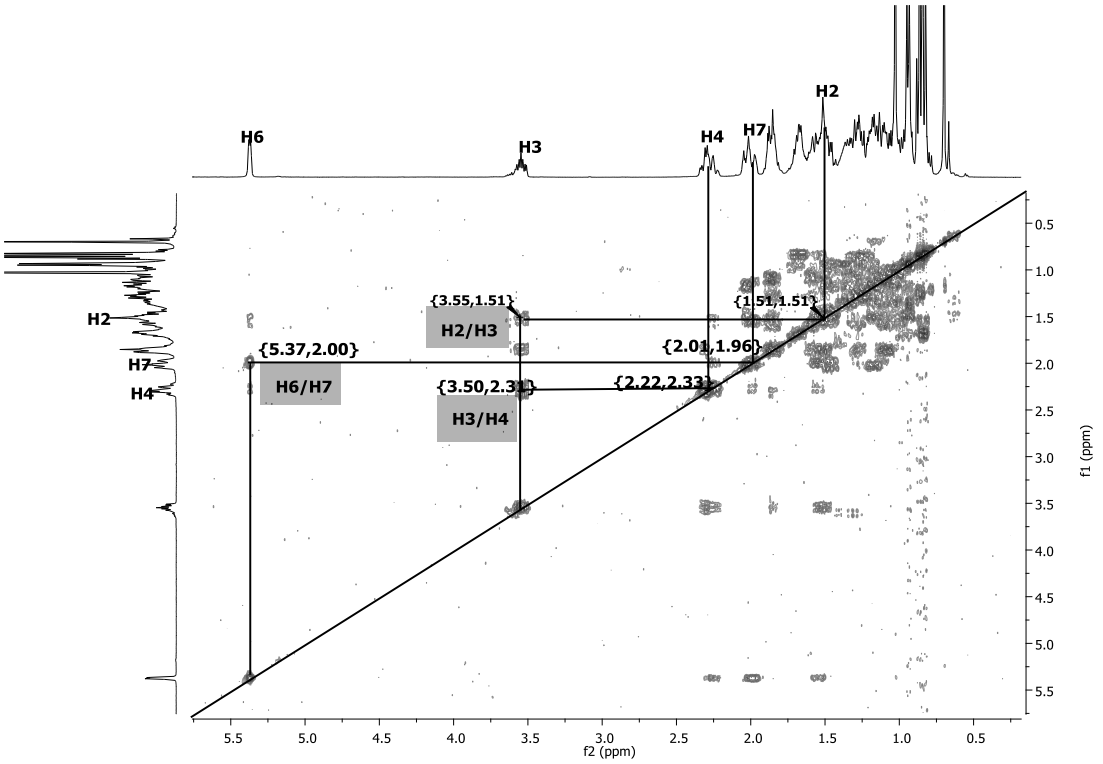

Fig. 2.12. COSY spectrum of compound AU 1

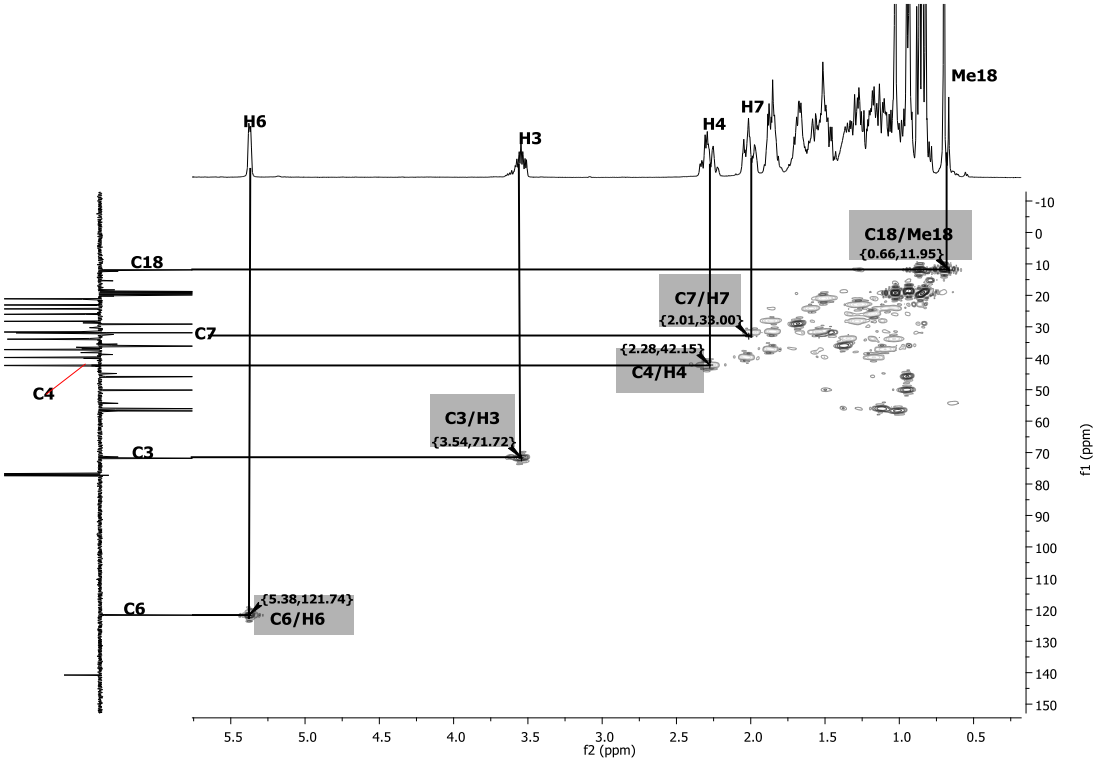

Fig. 2.13. HSQC spectrum of compound AU 1

Table 2.9. ^{13}C and ^{1}H NMR data of compound AU 1

Atom No.	Yahya 2011	Chaturvedula and Prakash, 2012	AU 1	-AU 1	-Yahya 2011	-Chaturvedula and Prakash, 2012
	$CDCl_3$ δ_C	$CDCl_3$ δc	$CDCl_3$ δc (m)	$CDCl_3$ δ_H (m, *J* in Hz)	$CDCl_3$ δ_H (m, *J* in Hz)	$CDCl_3$ δ_H (m, *J* in Hz)
1	37.5	37.5	37.3 (CH_2)			
2	31.9	31.9	31.7(CH_2)			
3	72.0	72.0	71.8(CH_2)	3.51 (m)	3.53 (m)	3.53 (tdd,4.5, 4.2, 3.8)
4	42.6	42.5	42.3(CH_2)	2.22 (m)		
5	141.0	140.9	140.8(C)			
6	121.9	121.9	121.7(CH)	5.37 (t, 5.4)	5.36 (d, 5.1)	5.36 (t, 6.4)
7	32.1	32.1	32.2(CH_2)			
8	32.2	32.1	31.9(CH)			
9	50.4	50.3	50.1(CH)			
10	36.7	36.7	36.2(C)			
11	21.3	21.3	21.1(CH_2)			
12	40.0	39.9	39.8(CH_2)			
13	42.3	42.6	42.3(C)			
14	57.0	56.9	56.8(CH)			
15	24.5	26.3	24.3(CH_2)			
16	28.5	28.5	28.3(CH_2)			
17	56.3	56.3	56.0(CH)			
18	12.1	36.3	11.9(CH_3)	0.67 (s)	0.69 (s)	
19	19.6	19.2	19.4(CH_3)	1.03 (s)	1.02 (s)	0.93 (d, 6.5)
20	36.4	34.2	36.5(CH)			
21	19.0	26.3	19.0(CH)	0.95 (d, 6.6)	0.93 (d, 6.6)	
22	34.2	46.1	33.9(CH)			
23	26.3	23.3	26.0(CH_2)			
24	46.1	12.2	45.8(CH_3)			
25	29.4	29.4	29.1(CH)			
26	19.3	20.1	19.8(CH_3)	0.85 (d, 7.1)	0.85 (d, 7.0)	0.83 (d, 6.4)
27	20.1	19.6	18.8(CH_3)	0.83 (d, 7.1)	0.83 (d, 7.0)	0.81 (d, 6.4)
28	23.3	19.0	23.1(CH_3)			0.68 (s)
29	12.2	12.0	12.0(CH_3)	0.89 (d, 7.6)	0.87 (t, 7.7)	1.01 (s)

Table 2.10. Compound AU 2 (Stigmasterol)

(3*S*,8*S*,9*S*,10*R*,13*R*,14*S*,17*R*)-17-[(*E*,2*R*,5*S*)-5-ethyl-6-methylhept-3-en-2-yl]-10,13-dimethyl-2,3,4,7,8,9,11,12,14,15,16,17-dodecahydro-1*H*-cyclopenta[*a*]phenanthren-3-ol	
Synonyms	Stigmasterol
Sample codes	AU 2
Sample amount	6 mg
Physical Description	White crystalline powder
Molecular formula	$C_{29}H_{48}O$
Molecular Weight	412 g/mol
Melting Point	164 -165 ºC
IR:($CHCl_3$)	3368, 2934, 2852, 1654, 1456, 1377, 1114, 1030, 760 cm^{-1}

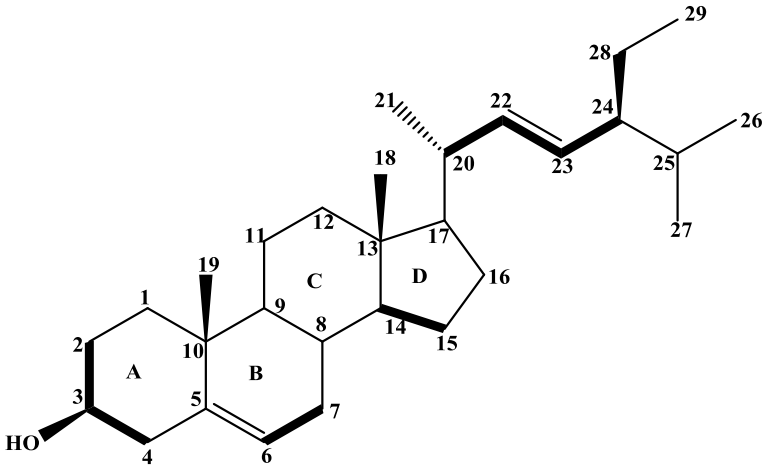

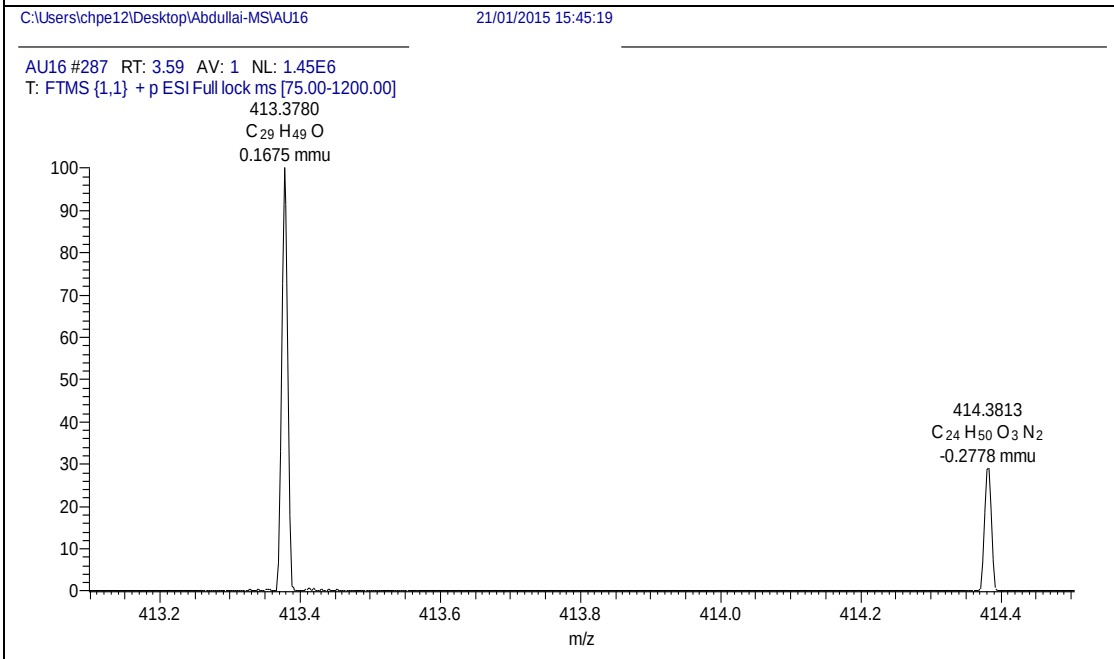

Compound AU 2 (6 mg) was isolated as a white crystalline powder and recrystallized from methanol. It has a molecular formula of $C_{29}H_{48}O$ which was established on the basis of ESI-HRMS at *m/z* 413.3780$[M + H]^+$ (Calcd for 413.3784). No optical rotation was measured as

this was deemed unnecessary for a steroid. The IR spectrum of this compound showed a band at 3368 (broad, O-H stretching), 2934 and 2852 (C-H stretching), 1654 (weak, C=C stretching), 1456 (C-H deformation), 1377 (methyl group symmetrical deformation), 1114, 1030 (C-O stretching) and 760 (C-H out of plane deformation) cm^{-1}, see appendix I. The DEPT spectrum (Fig. 2.15) of AU 2 showed twenty nine carbon signals, which consist of six methyls, nine methylenes, eleven methines and three quaternary carbon. The ^{1}H and ^{13}C NMR spectra of this compound are comparable to that of AU 1 except the presence of a double bond at C-22 and C-23. In the ^{1}H NMR spectrum (Fig. 2.14), Proton H-22 was split by proton H-20 and H-23 resulting in a doublet of doublet at 5.15 (dd, 15.5, 8.6 Hz), proton H-23 was also split by H-24 and H-22 resulting in a doublet of doublet at 5.01 (dd, 15.5, 8.6 Hz).These proton signals coupled with each other in the COSY spectrum (Fig 2.18). The HSQC spectrum (Fig 2.19) showed the direct correlation between H-22 to C-22 and H-23 to C-23 (δc 129.3). The side chain occurring at C-17 was identified as 5- ethyl-6-methylhept-3-ene and was confirmed from the HMBC (Fig. 2.16) correlation of Me-21 (δ_H 0.92, d) with C-17 (δc 56.0). The structure of the side chain was obtained from the correlation of Me-21 to C-20 and olefinic C-22. Also, the olefinic proton H-22 correlated with C-20 and C-17. Similarly, the olefinic proton H-23 correlated with C-24 while Me-29 correlated with C-28 and C-24. The two methyl doublets, Me-26 (δ_H 0.85, δc 21.1) and Me-27 (δ_H 0.81, δc 19.0) were found to correlate with each other and with C-25 (Fig. 2.17).

This compounds has been reported from the leaves of an endemic plants *Glyptopetalum calocarpum* and it showed anti-leptospiral activity. The minimum inhibitory concentrations when tested against pathogenic leptospiral strains belonging to 10 serovars were in the range of 100-200 µg/mL (Chander et al., 2015). Similarly, it has been reported in the rhizomes of *Etlingera sphaerocephala* Var. *Grandiflora* (Yahaya et al., 2011) and also from the leaves of *Rubus suavissimus* S. Lee (Chaturvedula and Prakash, 2012). The NMR data (Table 2.11) are comparable with those reported in the literature.

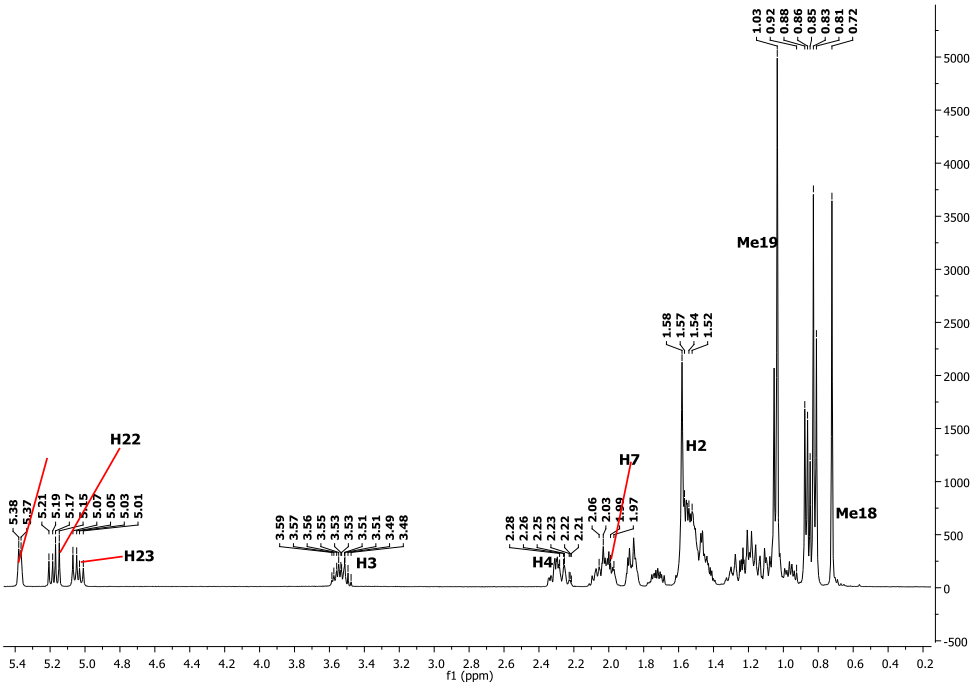

Fig. 2.14. [1]H NMR spectrum of compound AU2

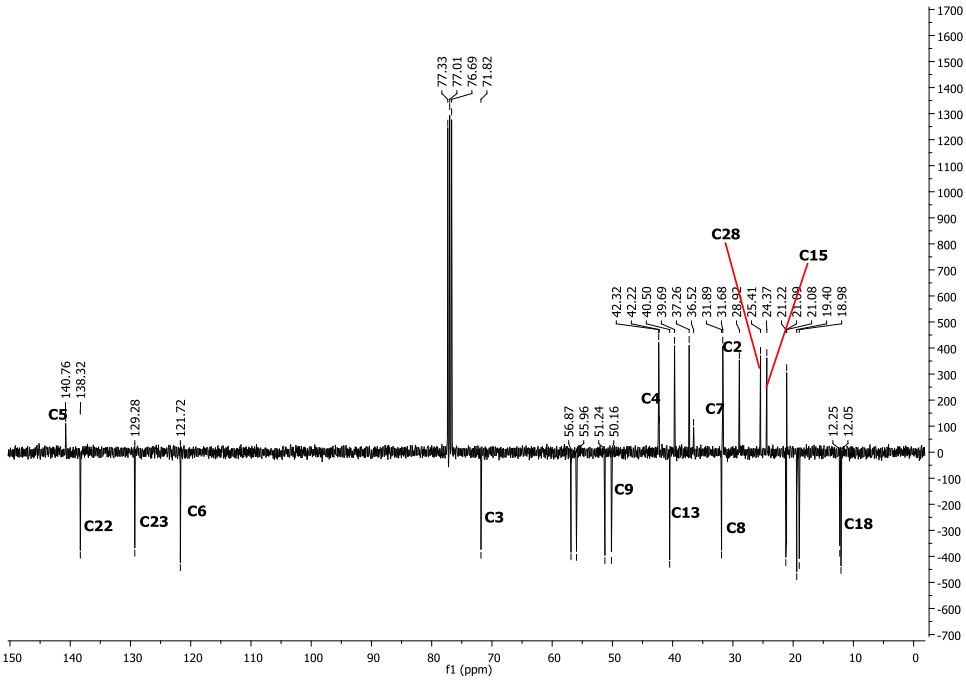

Fig. 2.15. DEPT spectrum of compound AU 2

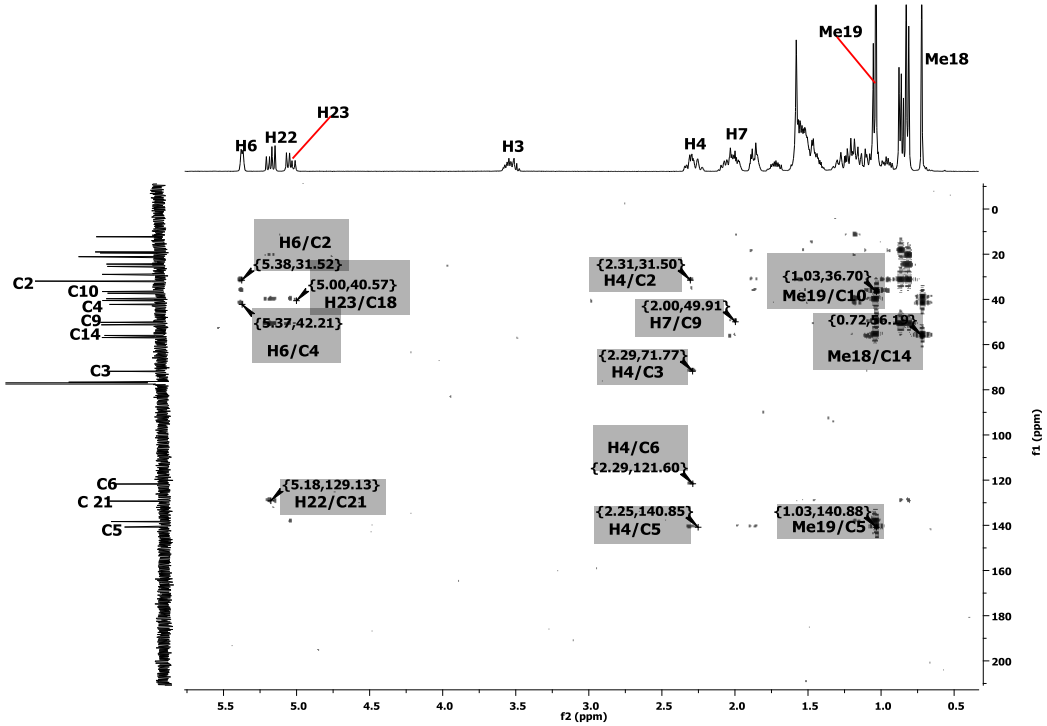

Fig. 2.16. HMBC spectrum of compound AU2

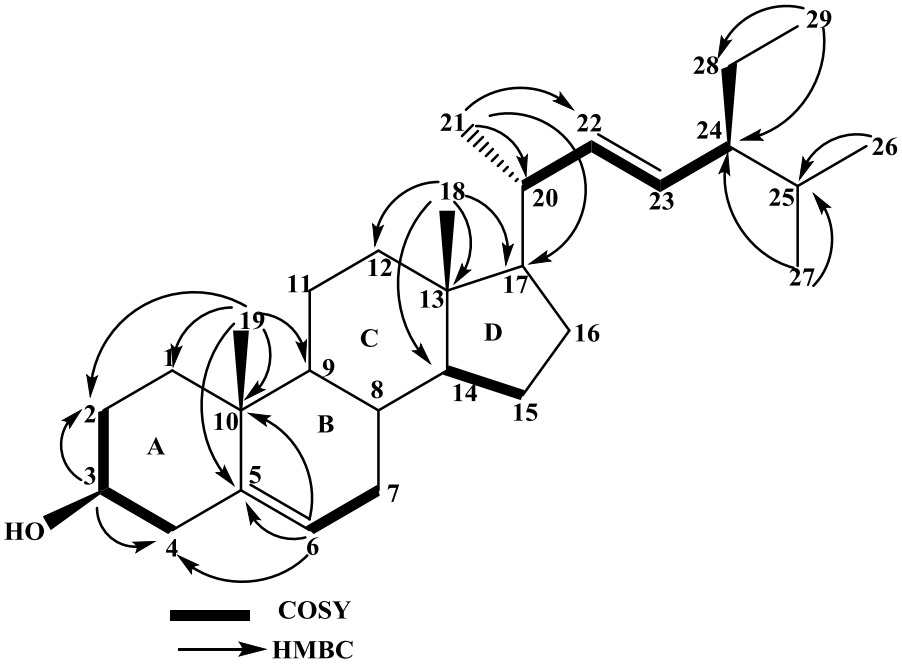

Fig. 2.17. HMBC and COSY correlations of compound AU 2

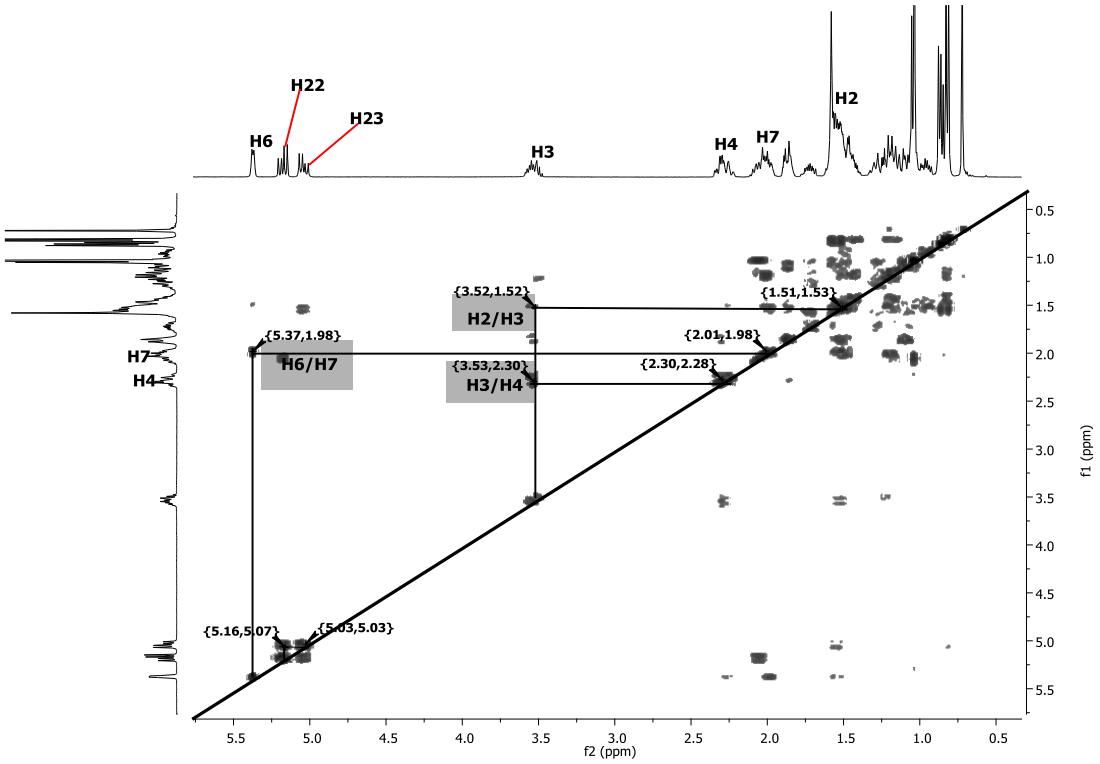

Fig. 2.18. COSY spectrum of compound AU 2

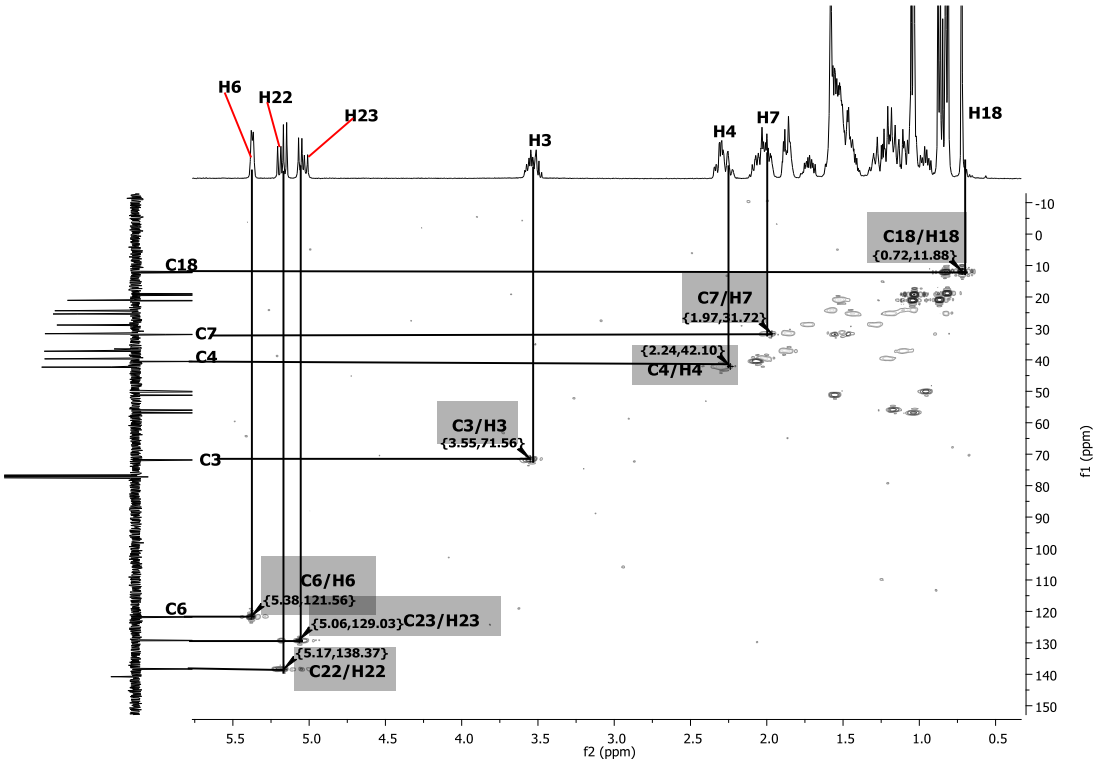

Fig. 2.19. HSQC spectrum of compound AU 2

Table 2.11. ^{13}C and ^{1}H NMR data of compound AU 2

Atom No.	Yahya 2011 $CDCl_3$ δc	Chaturvedula & Prakash, 2012 $CDCl_3$ δc	AU 2 $CDCl_3$ δc	AU 2 $CDCl_3$ δ_H (m, *J* in Hz)	.Chaturvedula & Prakash, 2012 $CDCl_3$ δ_H (m, *J* in Hz)	-Yahya 2011 $CDCl_3$ δ_H (m, *J* in Hz)
1	37.5	37.6	37.3 (CH_2)			
2	31.7	32.1	31.7(CH_2)	1.52 (m)		
3	72.0	72.1	71.8(CH)	3.48 (m)	3.51 (tdd, 4.5, 4.2, 3.8)	3.53 (m)
4	42.6	42.4	42.3(CH_2)	2.30 (m)		
5	141.0	141.1	140.8 (CH_2)			
6	121.9	121.8	121.7(CH)	5.37 (t, 5.4)	5.31 (t, 6.1)	5.36 (d, 7.3)
7	31.9	31.8	31.9 (CH_2)	2.01 (m)		
8	32.1	31.8	31.9 (CH)			
9	50.3	50.2	50.2 (CH)			
10	36.7	36.6	36.5 (C)			
11	21.3	21.5	21.1 (CH_2)			
12	40.0	39.9	39.7 (CH_2)			
13	42.3	42.4	42.2 (C)			
14	57.1	56.8	56.9 (CH)			
15	24.5	24.4	24.4 (CH_2)			
16	29.3	29.3	28.9 (CH_2)			
17	56.3	56.2	56.0 (CH)			
18	12.1	40.6	12.1 (CH)	0.72 (s)		0.69 (s)
19	19.6	21.7	19.4 (CH_3)	1.03 (s)	0.91 (d, 6.2)	1.02 (s)
20	40.7	138.7	40.5 (CH)			
21	21.3	129.6	21.2 (CH)	0.92 (m)	5.14 (m)	0.93 (d, 6.2)
22	138.5	46.1	138.3 (CH)	5.15 (dd, 15.49, 8.61)		5.16 (dd, 15.5, 8.4)
23	129.5	25.4	129.3 (CH_2)	5.01 (dd, 15.49, 8.61)		5.02 (dd, 15.6, 9.2)
24	51.5	12.1	51.3 (CH_3)			
25	31.9	29.6	28.9 (CH)			
26	21.4	20.2	21.1 (CH_3)	0.85 (d, 7.1)	0.82 (d, 6.6)	0.85 (d, 7.0)
27	19.0	19.8	19.0(CH_3)	0.81 (d, 7.1)	0.80 (d, 6.6)	0.81 (d, 7.0)
28	25.6	18.9	25.4 (CH_3)			
29	12.2	12.2	12.3(CH_3)	0.85 (d, 6.5)	1.03 (s)	0.83 (t, 6.8)

CHAPTER 3

Phytochemical investigation of *T. emetica* stem and boiled seed water extract: Results and Discussion

3.0 Introduction

As the seeds of *T. emetica* are bitter and emetic, for the oil to be used for edible purpose the whole nuts are boiled in water for 10-20 minutes and then dried in the sun. The phytochemical investigation of the water extract resulted in the isolation of twelve compounds, and the structure of nine of these compounds were successfully elucidated using MS, IR and NMR spectroscopy. The methanol extract of *T. emetica* stem was also phytochemically screened.

3.1 Extraction of *T. emetica* seeds and stems

A series of extractions was carried under various conditions and using different solvents to isolate the minor components in *T. emetica* seed and stem samples. The seed and stem samples were prepared as described in experiment 6.5 to 6.7, portions of these materials were extracted in a series of experiments 6.5.1 to 6.5.5 for seed and 6.7.1 for stem. The phytochemicals isolated from these samples are as itemized and discussed in 3.2.

3.2 Isolated compounds

Table 3.1. Compound AU 3 (2,6-Di-*tert*-butyl-4-methylphenol)

Synonyms	Butylated hydroxytoluene (BHT)
Sample codes	AU3
Sample amount	1.31 g
Physical Description	Pale yellow needle
Molecular formula	$C_{15}H_{24}O$
Molecular Weight	220 g/mol
Optical Rotation $[\alpha]_D^{24.4}$	-8.59 (c 0.33 in MeOH)
IR:($CHCl_3$)	3647, 2958, 1431, 1231, 860 cm^{-1}

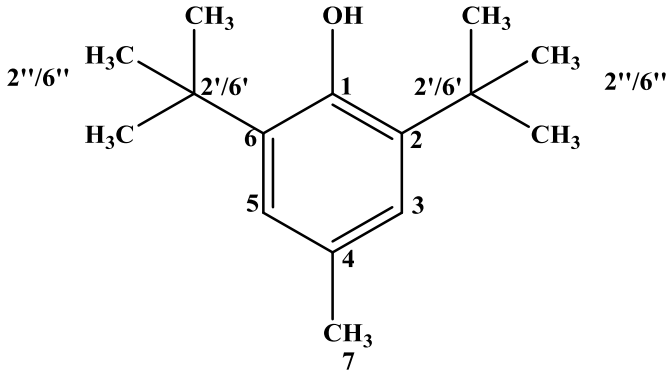

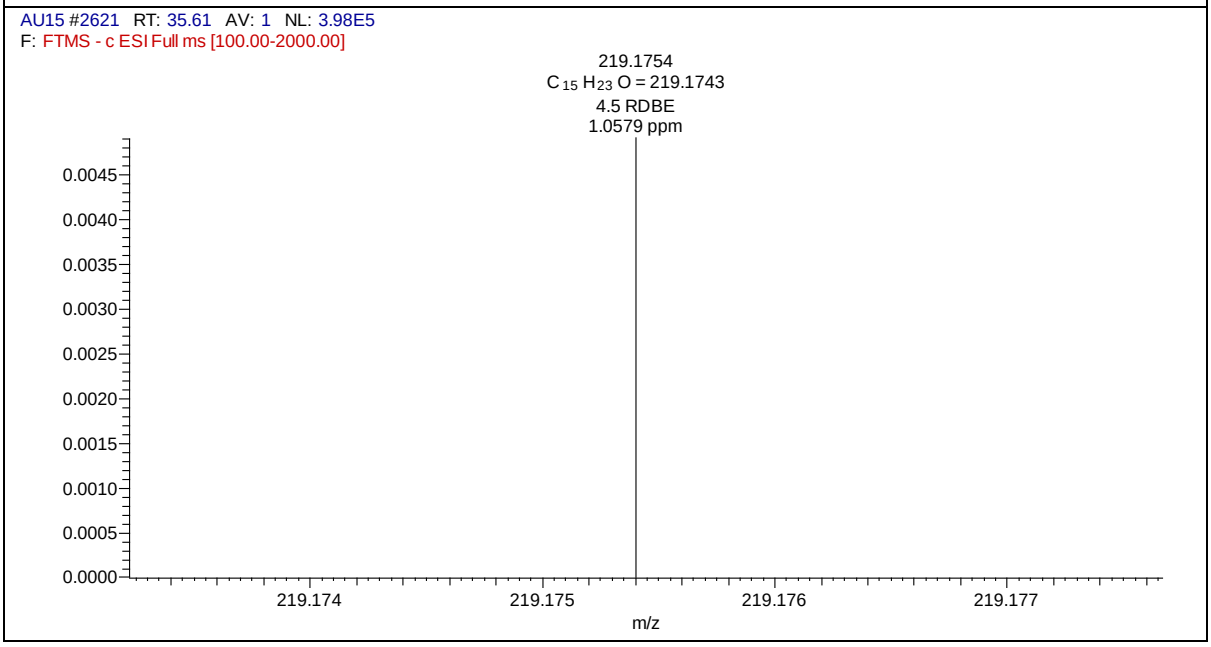

Compound AU 3 (1.31 g) was obtained as pale yellow needles. The optical rotation of this compound is supposed to be zero because there is no chirality in the compound but $[\alpha]_D^{24.4}$ -8.59 (MeOH: c 0.33) was recorded, this is due to the presence of optically active impurities.

The compound has a molecular formula of $C_{15}H_{24}O$ which was established on the basis of ESI-HRMS/MS at *m/z* 219.1754 $[M - H]^-$, (Calcd for 219.1748). The IR spectrum of this compound has a band at 3647 (O-H stretching), 2958 (C-H stretching), 1431(C-H deformation) and 860 (C-H out of plane deformation) cm^{-1}, see appendix I. The DEPT spectrum (Fig. 3.2) showed seven carbon signals, which consist of two methyl, one methine, four quaternary carbons. In the ^1H NMR spectrum (Fig. 3.1), the methine protons signals on the ring appeared at δ_H 7.03 (2H, s) assigned to positions 3/5 are magnetically equivalent and have no spin-spin interaction. The OH-signal lies at δ_H 5.05 (s) and the signals at δ_H 2.31 is attributable to aromatic CH_3 on account of the ring effect while the signal at δ_H 1.48 is assigned to 18 equivalent protons in the two tert-butyl substituents. The ^{13}C NMR spectral data were assigned through the assistance of HSQC spectrum (Fig. 3.6), where the carbon resonances of the ring at δ_C 21.2 (C-7) correlate with proton at δ_H 2.31 (H-7) and the side chains (tert-butyl methyl) C (2/6) at δ_C 31.3 correlated with protons at δ_H 1.47 (H-2/6). The COSY spectrum (Fig. 3.5) displayed correlations between δ_H 7.02 (H-3/5) and δ_H 2.31 (H-7); and also between δ_H 7.02 (H-3/5) and δ_H 1.47 assigned to position (H-2''/6''). These correlations were further confirmed by long-range couplings observed in the HMBC spectrum (Fig. 3.3) and (Fig. 3.4), where the methine protons at H-3/ 5 (δ_H 4.55) correlate with C-1, C-2/6, and C(2'/6') (δc 34.3); and H(2''/6'') (δ_H 1.47) correlate with C(2'/6'), C(2/6) and C(3/5), while the methyl protons at H-7 (δ_H 21.2) correlate with C-1, C-3/5 and C-2/6 (δc 135.5) respectively.

The structure was therefore deduced as 2,6-di-t-butyl-4-methylphenol. The ^1H and ^{13}C NMR data of this compound were consistent with those reported in the literature (Benjamin et al., 1978; Pliev, 1970). Finally, the structure of the compound was confirmed by X-ray crystallography and it is identical to a known crystal structure (CSD: MBPHOL).

The United State Food and Drug Administration (US FDA) in 1954, approved the use of this compound in low concentrations in foods and food packaging (Hilton, 1989). The data obtained from US FDA, indicated that the industrial usage of BHT in 1984 was at a concentration of 1% while in 1999 was between 0.0002% – 0.5% (Lanigan and Yamarik, 2002). Presently, BHT is one of the antioxidants extensively used in food industry to manufactured food containing fats (Yehye et al., 2015), petroleum products and rubber (Dacre, 1961). It is also use as food preservatives (Chan and Kan, 1999). This compound, though not a natural compound, it presence in large amount in this plant may be as a result of contamination from the bag used for the storage.

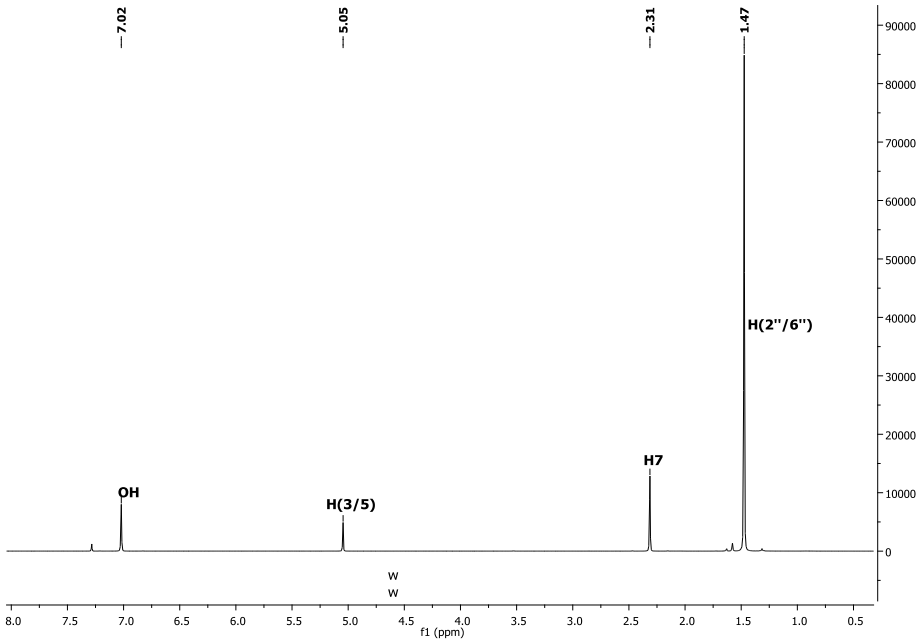

Fig. 3.1. [1]H NMR spectrum of compound AU 3

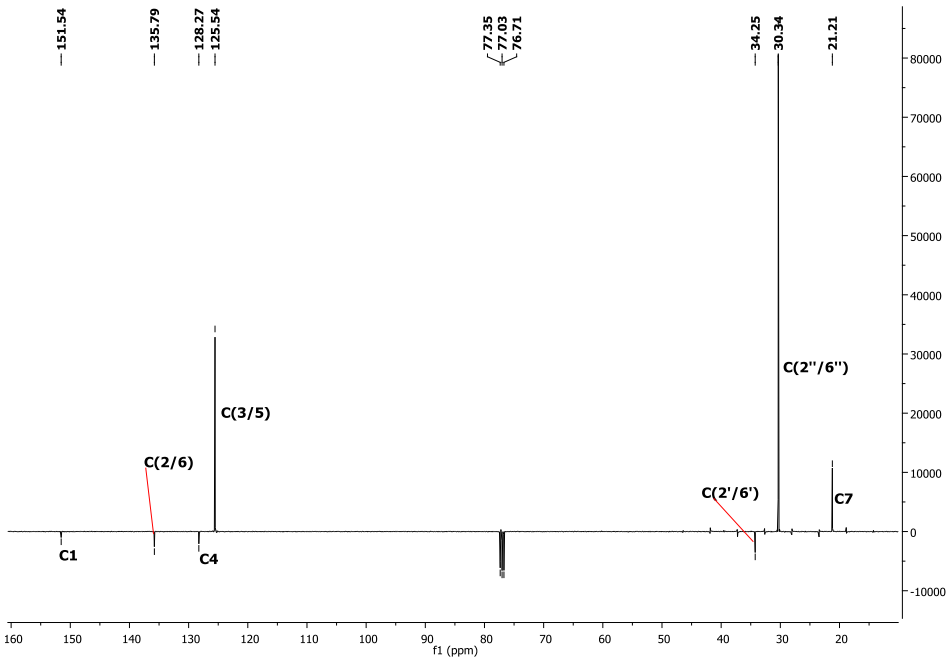

Fig. 3.2. DEPT spectrum of compound AU 3

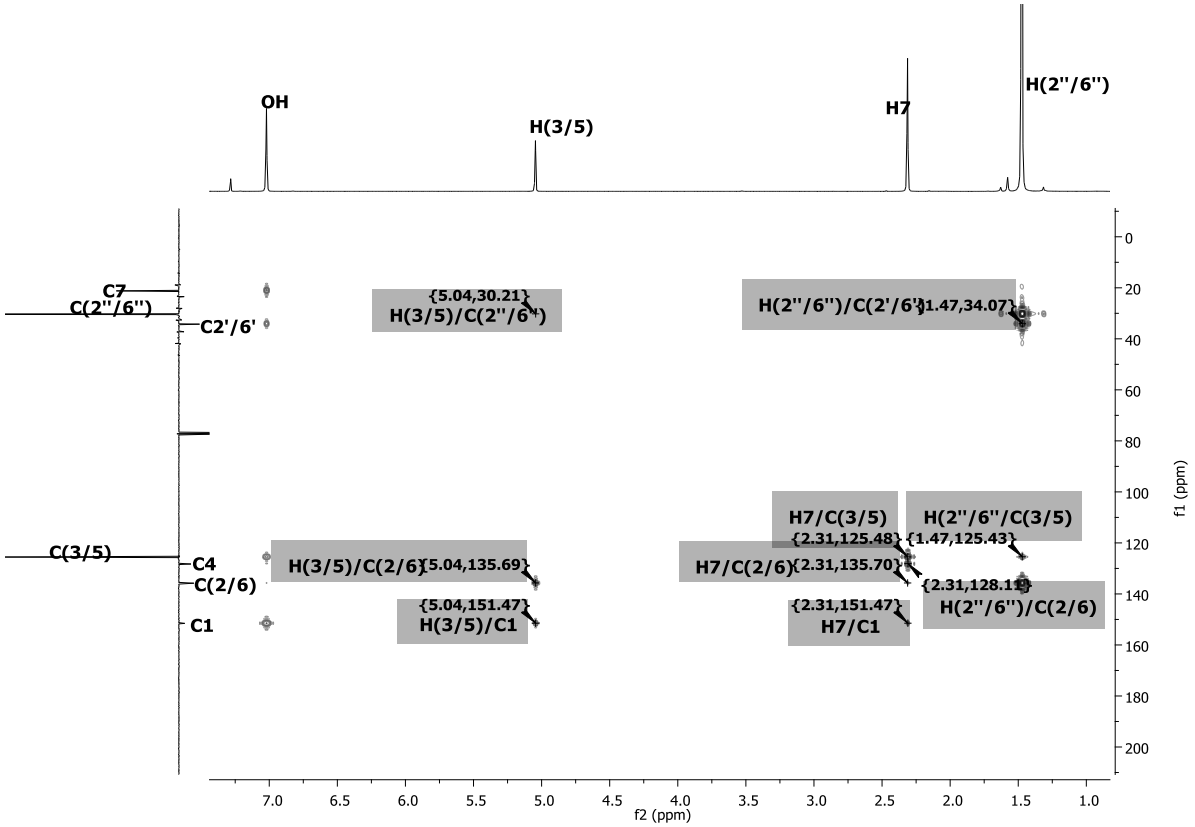

Fig.3.3. HMBC spectrum of compound AU 3

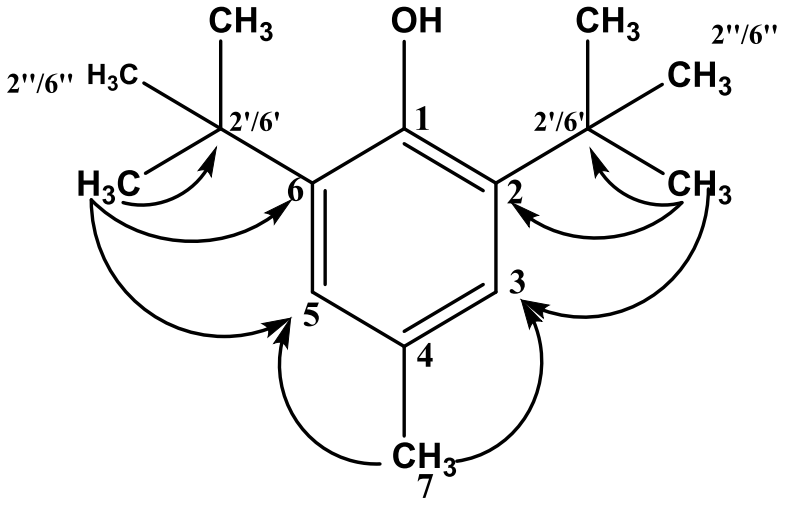

Fig. 3.4. HMBC correlations of compound AU 3

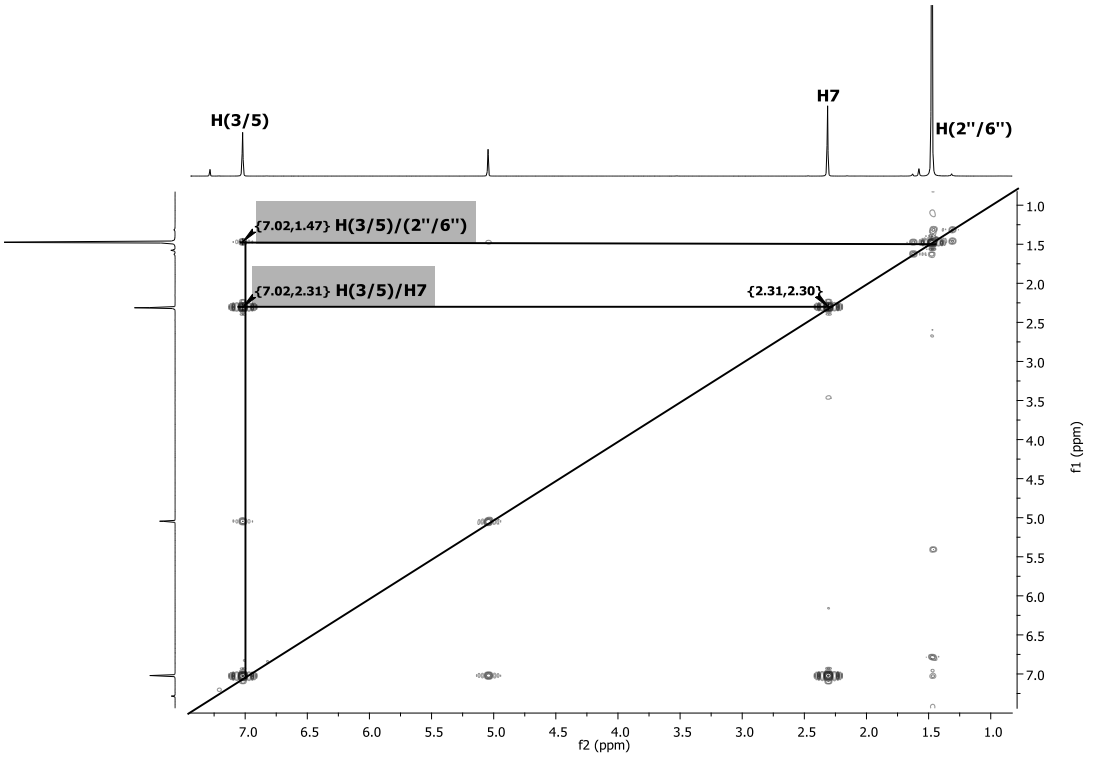

Fig.3.5. COSY spectrum of compound AU 3

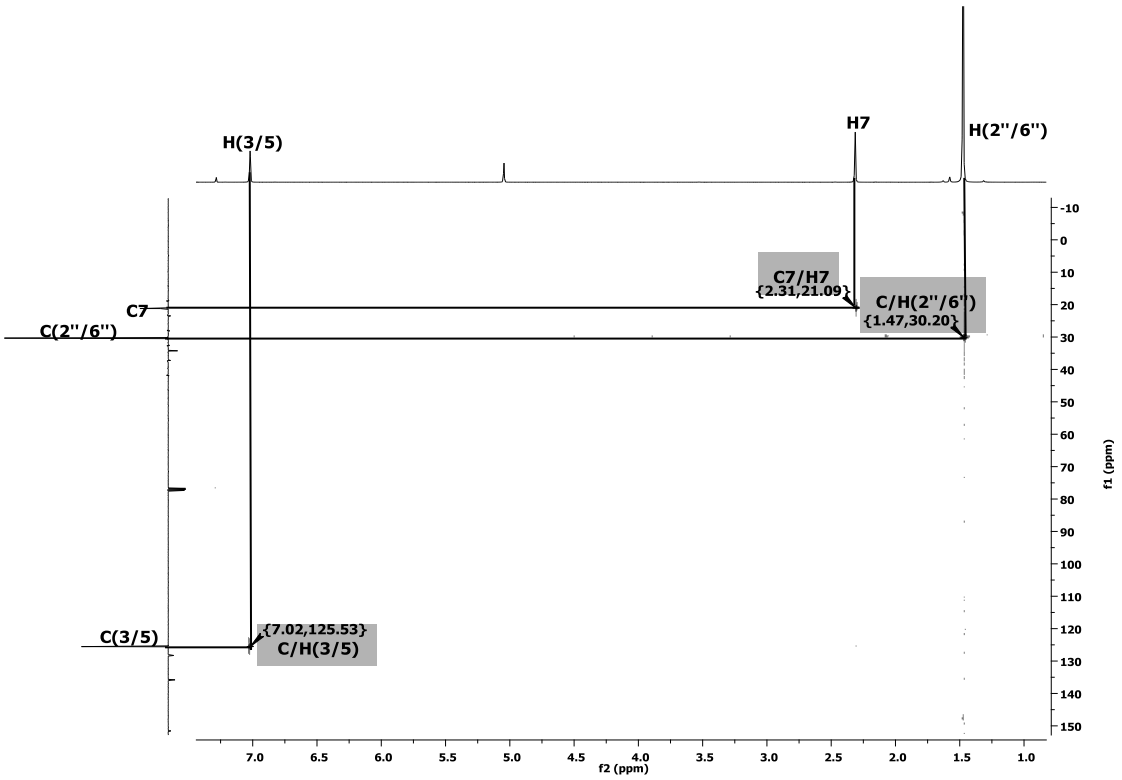

Fig.3.6. HSQC spectrum of compound AU 3

Fig. 3.7. The X - ray crystal structure of BHT

Table 3.2. ^{1}H and ^{13}C NMR data of compound AU 3

Atom No.	Benjamin 1978 $CDCl_3$ δc	AU 3 $CDCl_3$ δc	AU 3 $CDCl_3$ δ_H (m, *J* in Hz)	Pliev 1970 $CDCl_3$ δ_H (m, *J* in Hz)	HMBC [H→C]
1	151.3	151.5			
2/6	135.5	135.8			
3/5	125.3	125.5	7.02 (s)	6.85 (s)	C-1, C-4, C-7, C-t, C-2&6, C-A
4	128.0	128.3			
7	21.2	21.2	2.31 (s)	2.22 (s)	C-4, C-2&6, C-3&5
t-butyl [2'/6' (2''/6'')]	30.4 (34.2)	30.3 (34.33)	1.47 (s)	1.41 (s)	C-A, C-2&6, C-3&5

Table 3.3. Compound AU 4 (Catechin)

(2R,3S)-2-(3,4-dihydroxyphenyl)-3,4-dihydro-2H-chromene-3,5,7-triol	
Synonyms	Catechin
Sample codes	AU 4
Sample amount	17 mg
Physical Description	Yellow needles
Molecular formula	$C_{15}H_{14}O_6$
Molecular Weight	290 g/mol
Melting Point	175-176 ^{O}C
Optical Rotation $[\alpha]_D^{24.7}$	+15.7 (c 0.5 in MeOH)
UV (λ_{max} methanol)	230 and 279 nm
IR:($CHCl_3$)	3306, 2930, 1608, 1519, 1467, 1141, 1032, 819 cm^{-1}

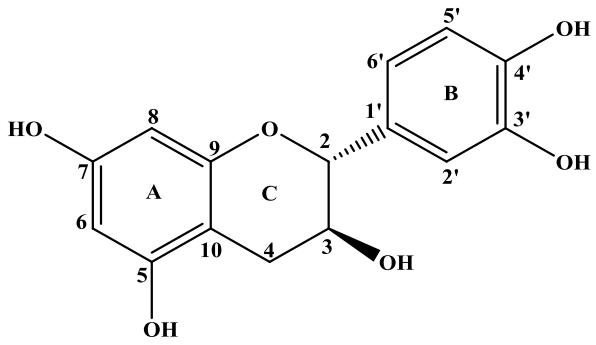

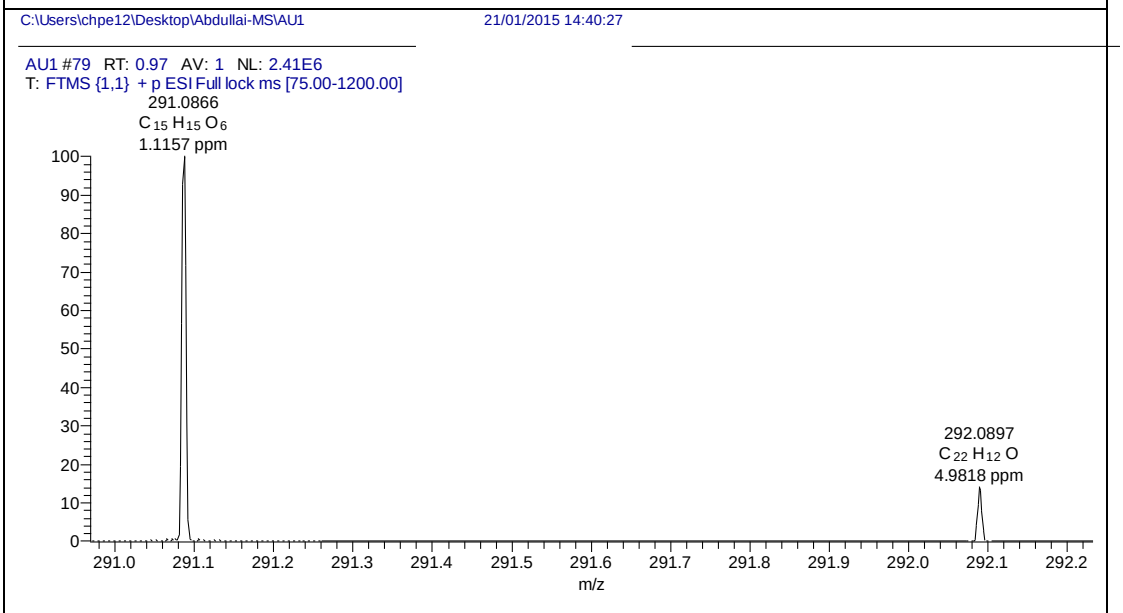

Compound AU 4 (17 mg) was obtained as a yellow needles. $[\alpha]_D^{24.7}$ +15.7 (MeOH: c 0.5) and literature was +15.5 (Seto et al., 1997). It has a molecular formula of $C_{15}H_{14}O_6$ which was established on the basis of ESI-HRMS at *m/z* 291.0866[M + H]$^+$ (Calcd for 291.0869). The

mass at *m/z* 291 corresponded to the protonated molecule $[M + H]^+$ of catechin whose exact mass is 290.0790. The spectrum also shows the main fragment ions at *m/z* 273 $[M - H_2O]^+$ which is due to water loss and 139 $[M – C_8H_7O_3]^+$ due to retro Diels Alder reaction (Fig. 3.8) (Shen et al., 2006; Wu et al., 2003). The compound showed absorption band at 230 and 279 nm in the ultraviolet spectrum. The IR spectrum showed a band at 3306 (broad, O-H stretching), 2930 (saturated C-H stretching), 1608 (C=C stretching), 1519 (C-H deformation), 1141, 1032 (C-O stretching) and 819 (C-H out of plane deformation) cm^{-1}, see appendix I.

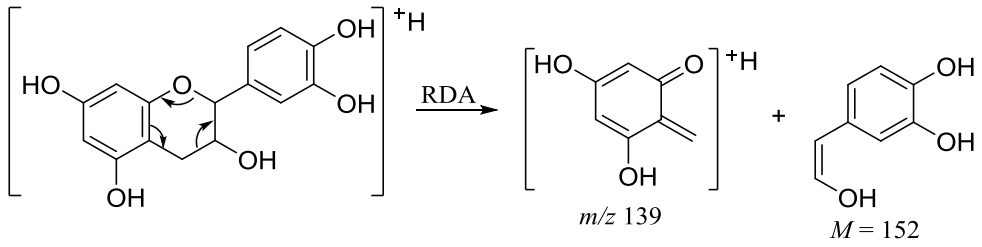

Fig. 3.8. Retro Diels-Alder (RDA) fission

The DEPT spectrum (Fig. 3.10) of AU 4 showed fifteen carbon signals, which consist of one methylene, seven methine and seven quaternary carbons. The carbinolic proton H-3 on ring C was split by H-2 and H-$4_{a\&b}$, resulting in a multiplet at δ_H 3.95. Protons H-$4_{a\&b}$ was split by H-3 resulting in a doublet of doublet at δ_H 2.48 (dd, 8.3, 16.2 Hz) and δ_H 2.84 (dd, 5.6, 16.2 Hz), and H-2 was split by H-3 resulting in a doublet at δ_H 4.56 (d, 7.5 Hz). The COSY spectrum (Fig. 3.13) showed H-3 coupled to H-4 and to H-2. The characteristic signals due to B-ring aromatic protons is of the ABX- type and indicated the presence of a 1,2,4-substituted aromatic ring, it compossed δ_H 6.84 (d, 2.2 Hz) assigned to position 2', and it meta-coupled with δ_H 6.71 (dd, 2.2, 8.2 Hz) assigned to position 6', which also undergo ortho coupling with δ_H 6.76 (d, 8.2 Hz) assigned to position 5'. Similarly, the meta-coupled aromatic proton signals at δ_H 5.86 (d, 2.3 Hz) and δ_H 5.93 (d, 2.3 Hz) were assigned to position H-6 and H-8 and it corresponded to the A-ring.

The down field position of the C-2 chemical shifts (δ_C 82.9) observed in the DEPT and ^{13}C spectra and the appearance of a doublet at 4.57 (d, 7.5 Hz) attributed to position 2, indicated that the flavan moieties possessed the 2,3-trans stereochemistry (Foo and Karchesy, 1989; Ishimaru et al., 1987; Takahama et al., 2013). These positions were further confirmed by long-range coupling observed in HMBC (Fig. 3.11 and 3.12), where the ring C methine protons H-2 correlate with C-3, C-4, C-1' and C-2', and H-3 correlate with C-2, C-10, C-1' and C-6', while methylene protons H-4 correlate with C-2, C-3 and C-10 (δc 100.8). Ring B was

confirmed by the HMBC correlations of H-2’ to C-2, C-1’, C-3’ and C-6’ (δc 120.0), H-5’ to C-2, C-1’ and C-3’ (δc 82.7), and H-6’ to C-2, C-1’ and C-2’ (δc 115.1). The HMBC spectrum further displayed correlations of H-6 to C-7, C-8 and C-10 (δc 100.6), while H-8 correlated with C-6, C-7 and C-10 respectively. The NMR data (Table 3.4) thus showed signals typical of catechin, and this was confirmed by comparison of its ^{1}H and ^{13}C NMR data with those reported in the literature (Lin et al., 2009; Oh et al., 2014).

Catechin are known flavonoids that has been isolated from the leaves and wood of *Acacia catechu* (Hye et al., 2009; Shen et al., 2006), bark of *Quercus marilandica* Muenchh (Bae et al., 1994) and the leaves of green tea (Dalluge and Nelson, 2000; Si et al., 2006). This compound has been reported to showed various pharmacological activities, such as antioxidant (Gadow et al., 1997), anti-inflammatory (Monga et al., 2014) and antimicrobial (Kumar et al., 2015).

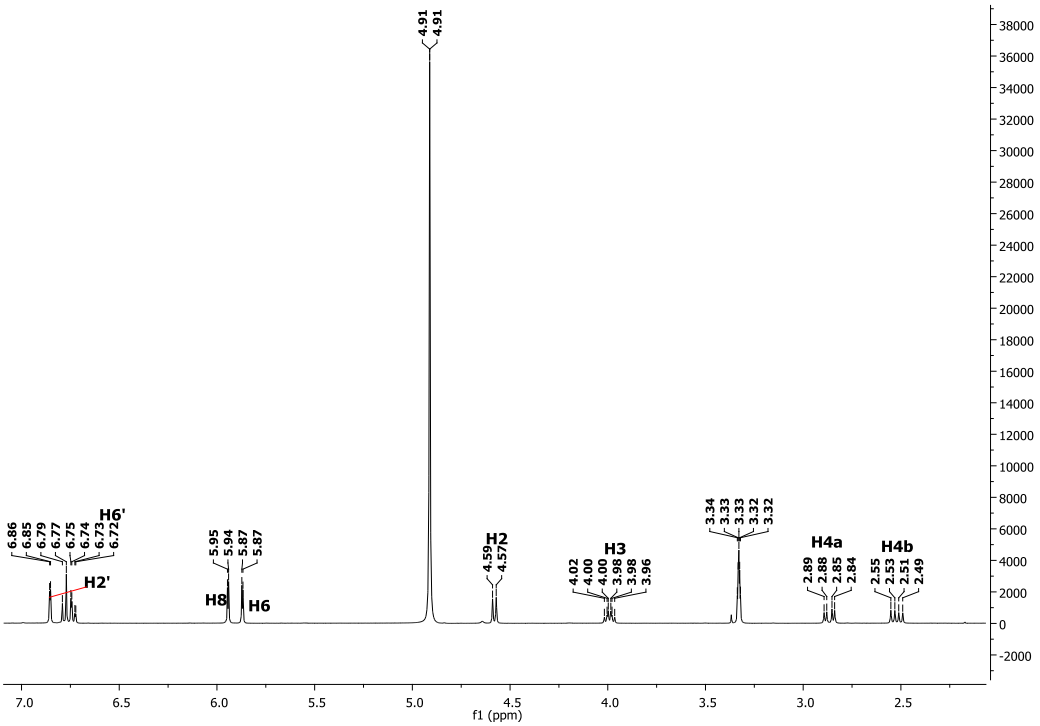

Fig. 3.9. ^{1}H NMR spectrum of compound AU 4

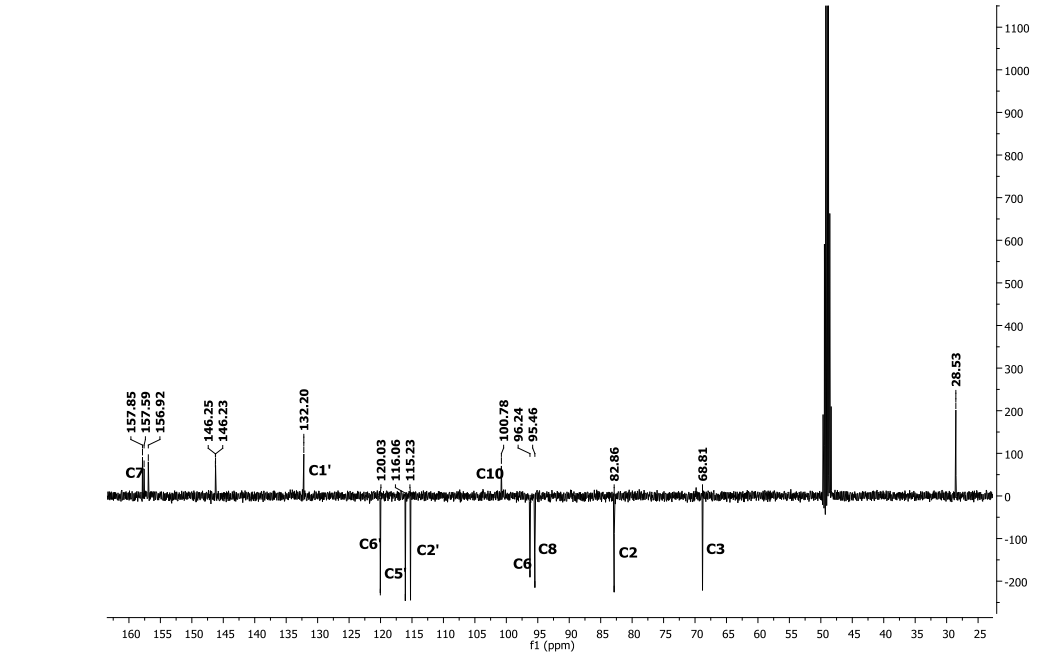

Fig. 3.10. DEPT spectrum of compound AU 4

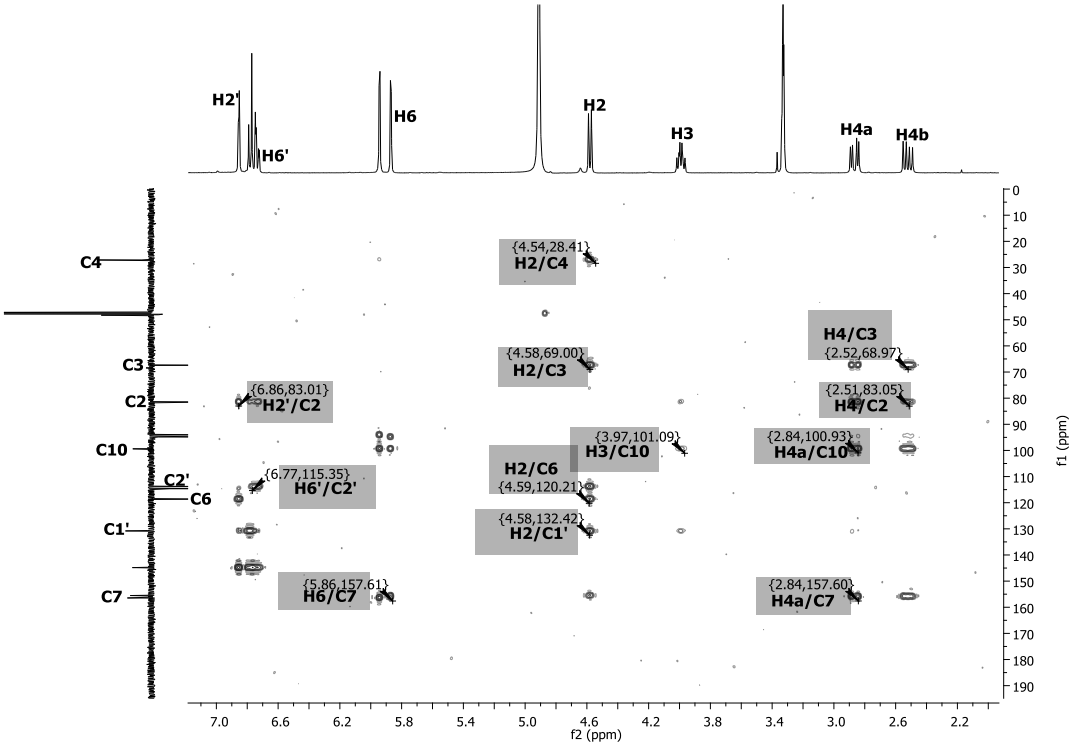

Fig. 3.11. HMBC spectrum of compound AU 4

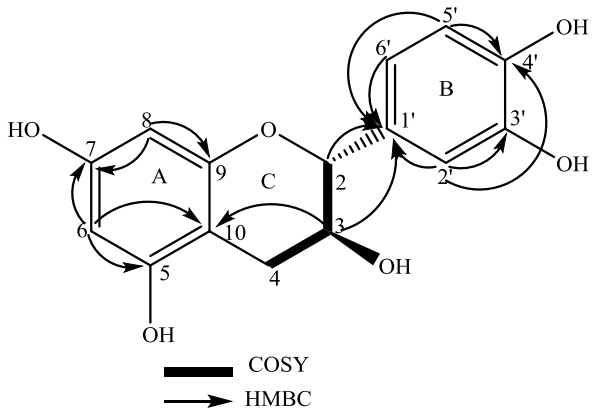

Fig. 3.12. HMBC and COSY correlations of compound AU 4

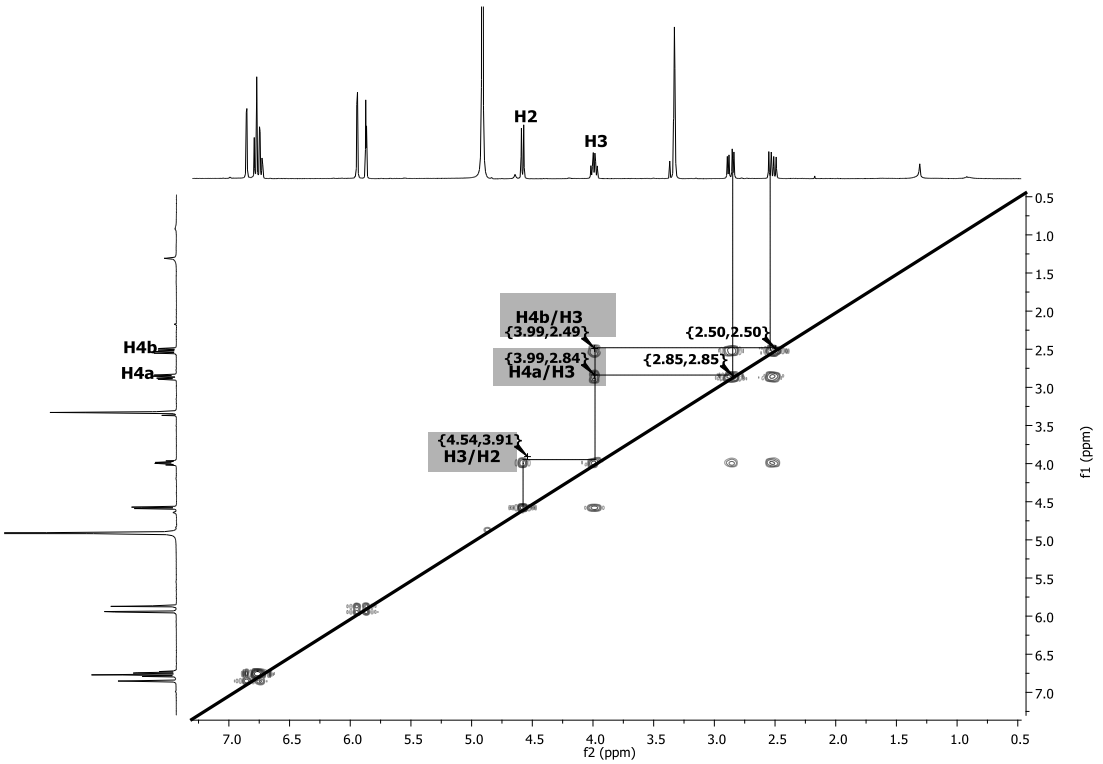

Fig. 3.13. COSY spectrum of compound AU 4

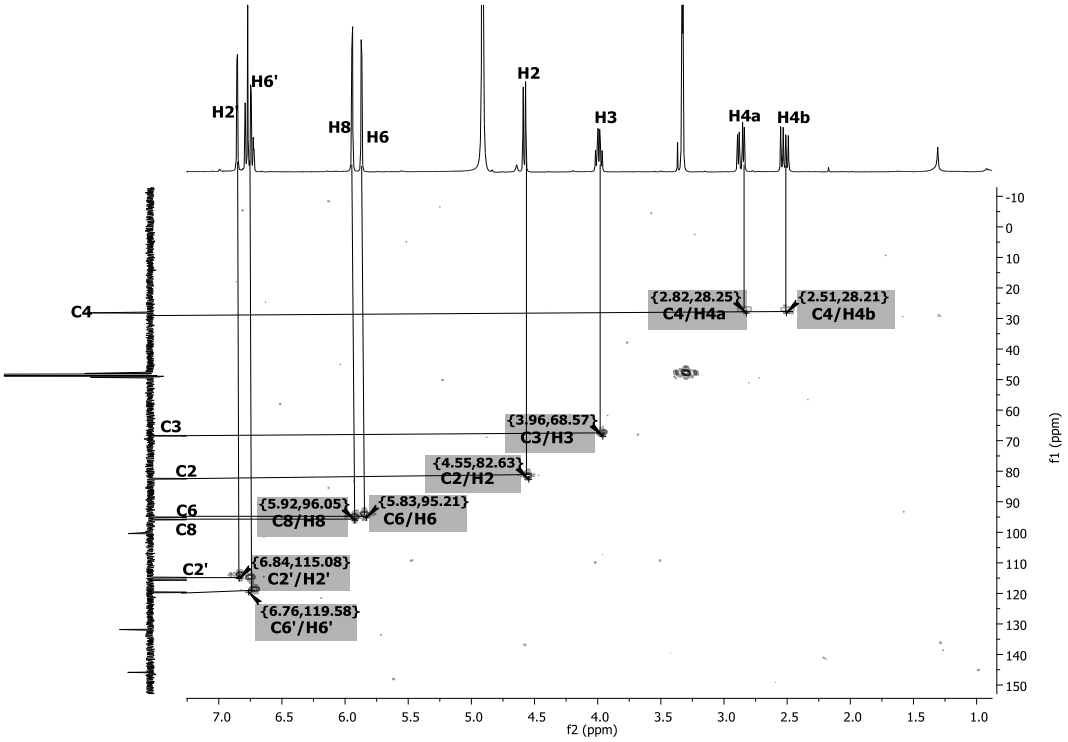

Fig. 3.14. HSQC spectrum of compound AU 4

Table 3.4. ^{1}H and ^{13}C NMR data of compound AU 4

Atom No.	Oh 2014 CD3OD + D_2O δc	Lin 2009 CD3OD δc	AU 4 CD3OD δc (m)	-AU 4 CD3OD δ_H (m, *J* in Hz)	- Lin 2009 CD3OD δ_H (m, *J* in Hz)	-Oh 2014 CD3OD + D_2O δ_H (m,*J* in Hz)
2	82.9	82.8	82.9 (CH)	4.57 (d, 7.5)	4.46 (d, 7.8)	4.55 (d, 7.5)
3	68.8	68.8	68.8 (CH)	3.96 (m)	3.87 (m)	3.97 (m)
4a	28.5	28.4	28.5 (CH_2)	2.84 (dd, 5.8, 16.2)	2.75 (dd, 6.4, 16.0)	2.84 (dd, 5.7, 16.0)
4b	28.5	28.4	28.5 (CH_2)	2.49 (dd, 8.3, 16.2)	2.40 (dd, 8.0, 16.1)	2.50 (dd, 8.4, 16.0)
5	157.8	156.8	156.9 (C)			
6	96.3	96.3	96.2 (CH)	5.87 (d, 2.3)	5.75 (d, 2.4)	5.85 (d, 2.1)
7	157.9	157.5	157.9 (C)			
8	95.5	82.8	95.5 (CH)	5.94 (d, 2.3)	5.82 (d, 2.4)	5.92 (d, 2.1)
9	157.6	157.8	157.6 (C)			
10	100.8	100.8	100.8 (C)			
1’	132.2	132.2	132.2 (C)			
2’	115.3	115.2	115.2 (CH)	6.85 (d, 2.0)	6.89 d (1.95)	6.83 (d, 1.6)
3’	146.3	146.2	146.2 (C)			

4’	146.3	146.2	146.3 (C)			
5’	116.1	116.1	116.1 (CH)	6.77 (d, 8.2)	6.79 (8.07)	6.76 (d, 8.1)
6’	120.1	120.0	120.0 (CH)	6.72 (dd, 2.0, 8.2)	6.73 (dd, 1.94, 8.19)	6.71 (dd, 1.6, 8.1)

Table 3.5. Compound AU 5 (Epicatechin)

(2*R*,3*R*)-2-(3,4-dihydroxyphenyl)-3,4-dihydro-2*H*-chromene-3,5,7-triol	
Synonyms	Epicatechin
Sample codes	AU 5
Sample amount	9 mg
Physical Description	White amorphous powder
Molecular formula	$C_{15}H_{14}O_6$
Molecular Weight	290 g/mol
Melting Point	234-240 ^{O}C
Optical Rotation $[\alpha]_D^{24.4}$	-47.5 (c 0.33 in MeOH)
UV (λ_{max})	230 and 279 nm
IR:($CHCl_3$)	3293, 1628, 1519, 1468, 1359, 1281, 1143, 822 cm^{-1}

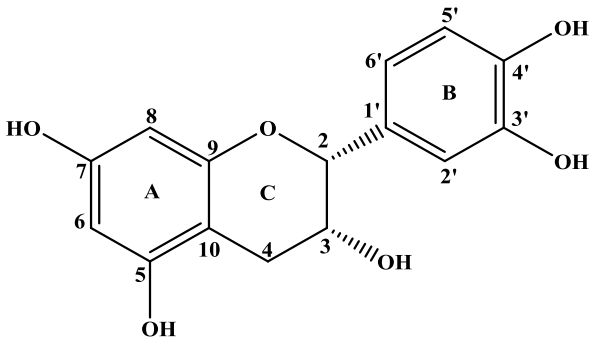

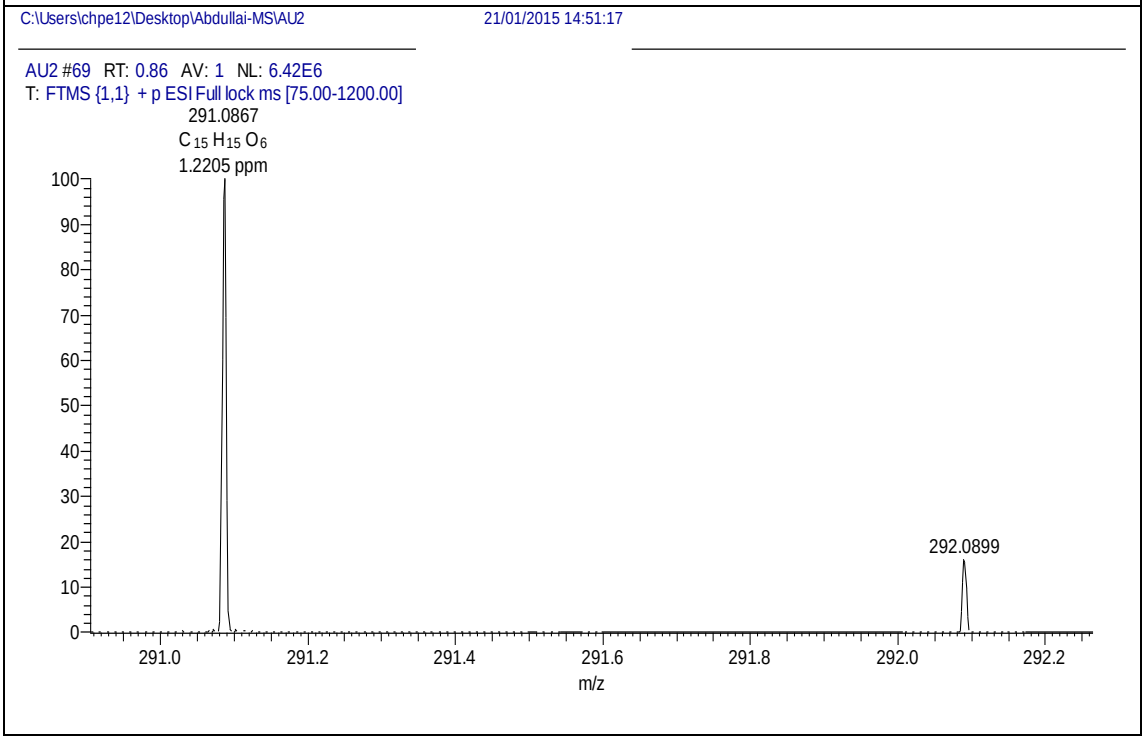

Compound AU 5 (9 mg) was obtained as a white amorphous powder, $[\alpha]_D^{24.4}$ -47.5 (MeOH: c 0.33) and literature is −55.7 (Seto et al., 1997). The MS, UV, IR and NMR spectra of AU 5 is similar to AU 4, the major difference is in their stereochemistry. In ring C, the up field position

of the C-2 chemical shift (δ_C 79.9) suggested that the flavan possessed the 2,3 stereochemistry, this was supported by the minimum couplings (< 1 Hz) between the H-2 and H-3 protons, thus appearing as broad singlet at H-2 (δ_H 4.84) (Fan et al., 2004; Foo and Karchesy, 1989; Pizzolatti et al., 2002). The carbinolic proton on ring C appeared in its ^{1}H NMR spectrum (Fig. 3.15) at δ_H 4.19 (m) attributable to position 3 which in the COSY (Fig. 3.19), coupled with methylene protons at δ_H 2.73 (dd, 3.0, 16.8 Hz) and δ_H 2.86 (dd, 4.75, 16.8 Hz) assigned to position 4 and also to δ_H 4.84 (br s) assigned to position 2. The HSQC spectrum (Fig. 3.20), show the correlations between methylene protons at δ_H (2.73 and 2.86) to δc (29.3) assigned to position 4. These positions were further confirmed by long-range coupling observed in HMBC (Fig. 3.17) and (Fig. 3.18), where the ring C methine protons H-2 (δ_H 4.84) correlate with C-3 C-4, C-1' and C-2' (δc 115.3), and H-3 (δ_H 4.19) correlate with C-2, C-10, C-1' and C-6' (δc 119.4), while methylene protons H-4 (δ_H 2.73 and δ_H 2.86) correlate with C-2, C-3 and C-10 (δc 100.1). The NMR data (Table 3.6) thus showed signals typical of epicatechin, and it is comparable to the ^{1}H and ^{13}C NMR data reported in the literature (Oh et al., 2014; Sun et al., 2006).

Epicatechin has been isolated from the leaves and wood of *Acacia catechu* (Shen et al., 2006), root and stem bark of *Acacia karoo* (Nyila et al., 2012), bark of blackjack oak (*Quercus marilandica* Muenchh) (Bae et al., 1994) and the leaves of green tea (Dalluge and Nelson, 2000; Si et al., 2006). This compound has been reported to showed antioxidant activity (Gadow et al., 1997). And Nyila et al., (2012) reported epicatechin to showed good antilisterial activity at IC_{50} greater than 200 µg/mg, and antimicrobial activity at MIC value greater than 500 µg/ml.

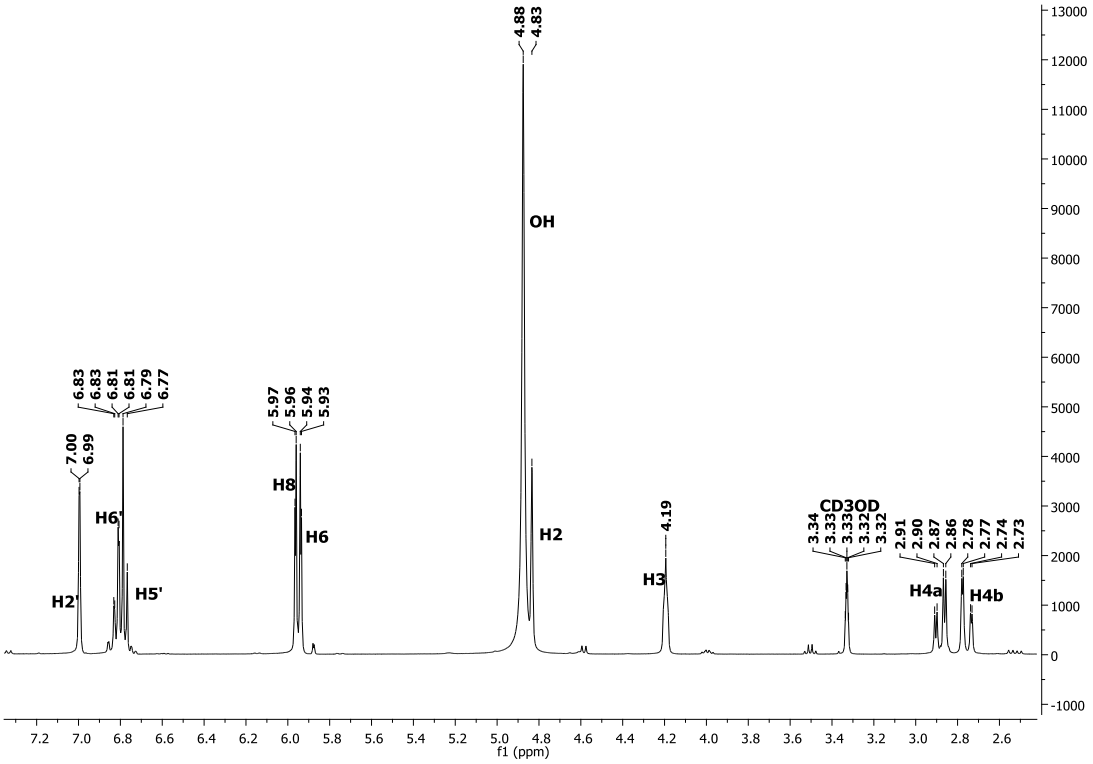

Fig. 3.15. [1]HNMR spectrum of compound AU5

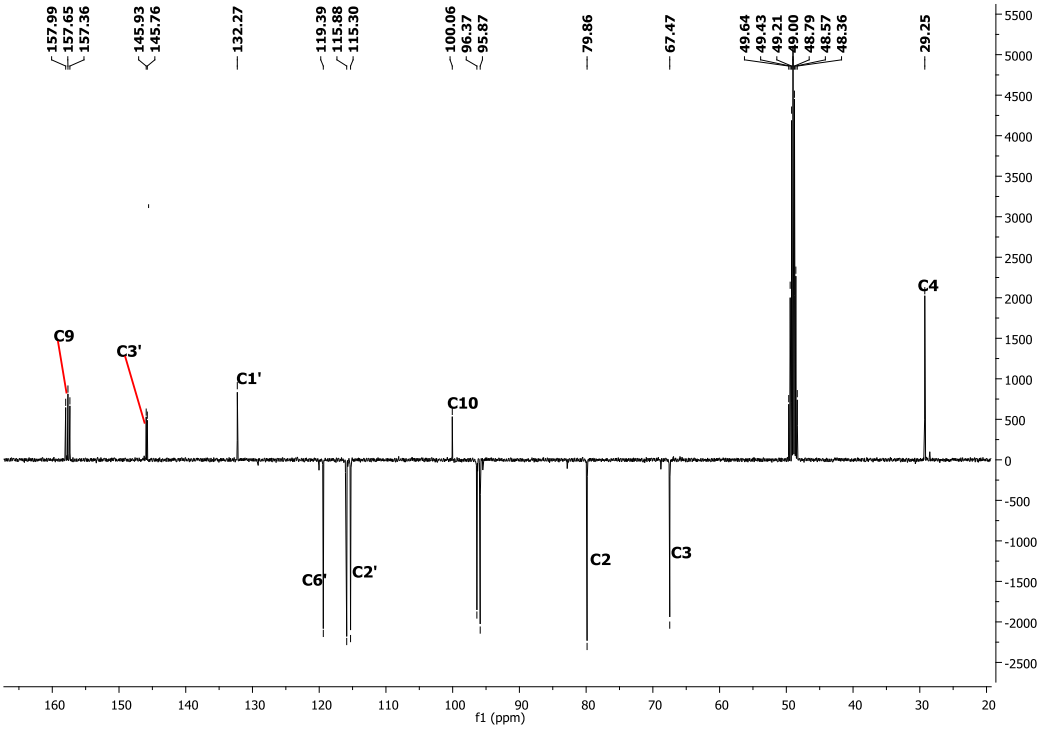

Fig. 3.16. DEPT spectrum of compound AU5

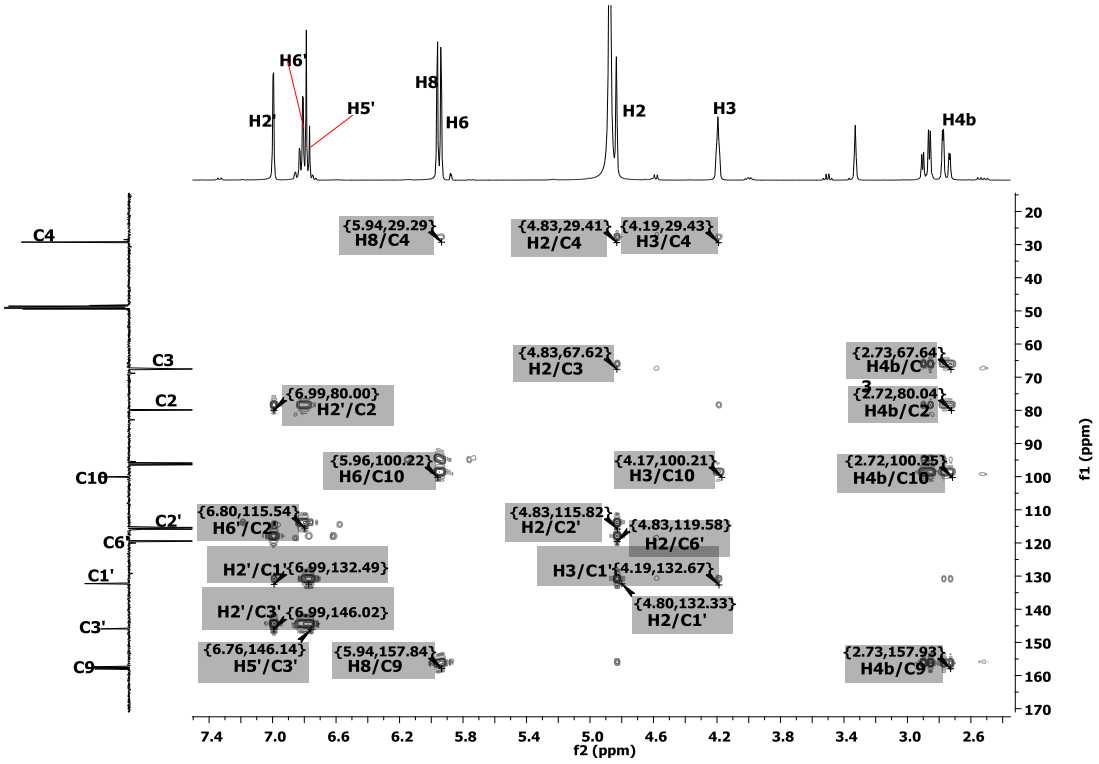

Fig. 3.17. HMBC spectrum of compound AU5

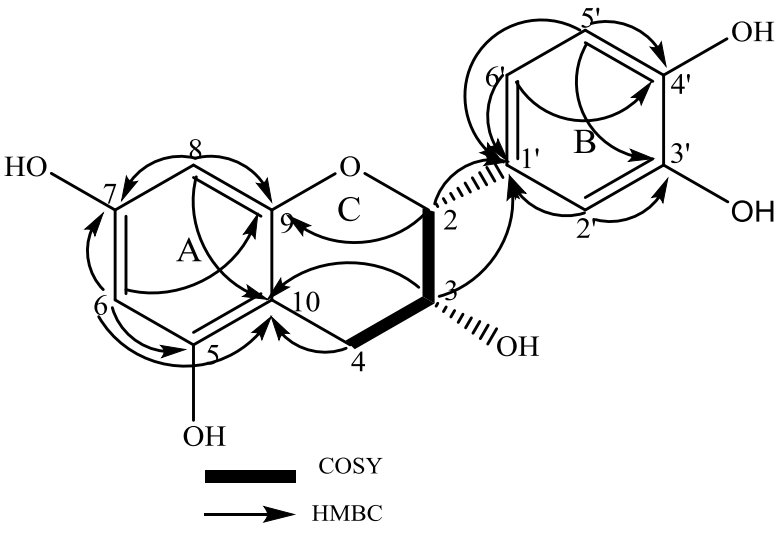

Fig. 3.18. HMBC and COSY correlations of AU 5

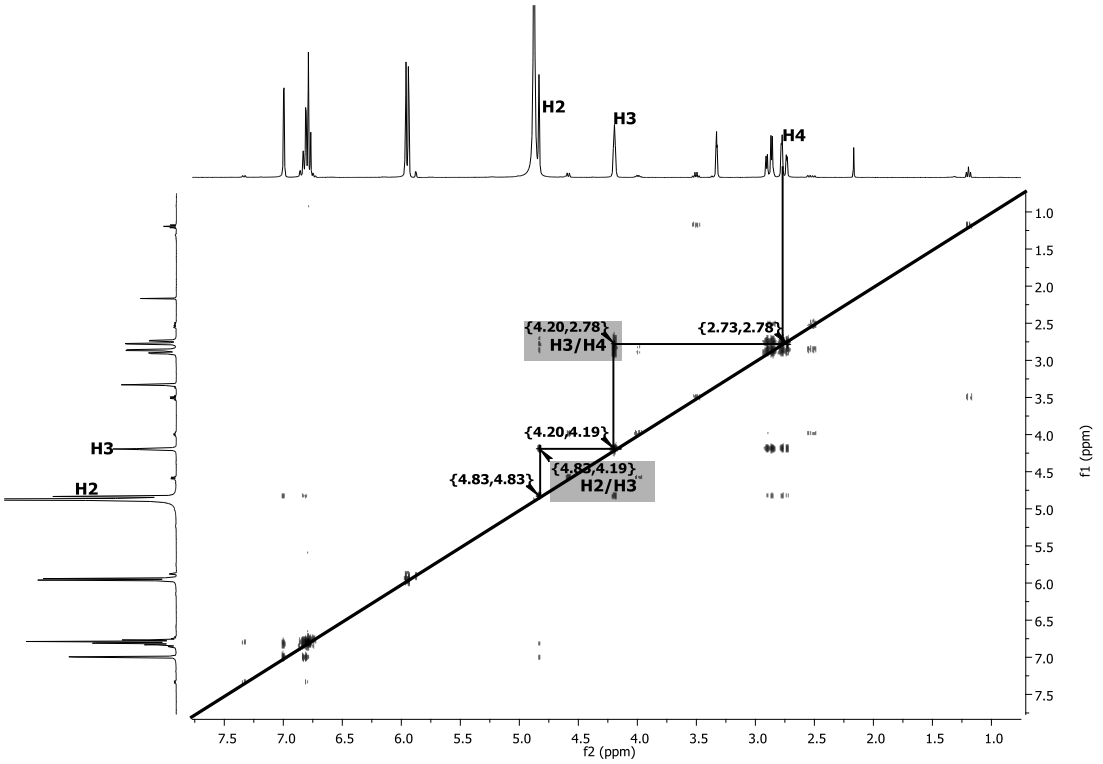

Fig. 3.19. COSY spectrum of compound AU 5

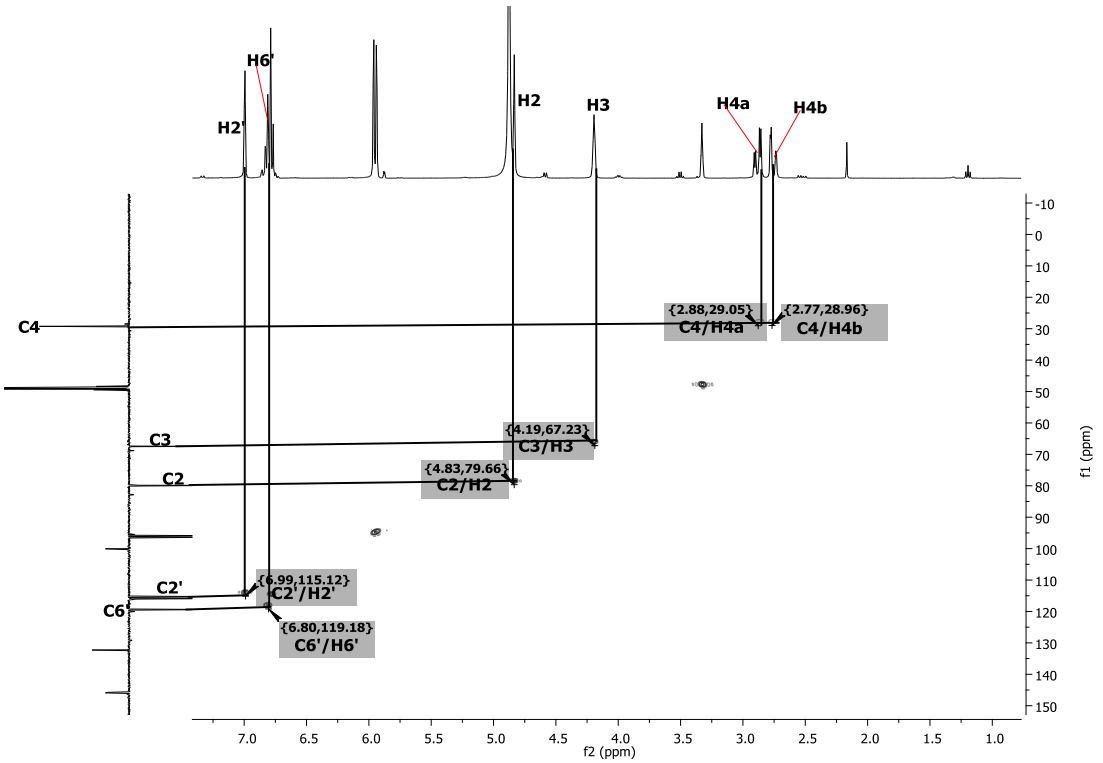

Fig. 3.20. HSQC spectrum of compound AU 5

Table 3.6. ^{1}H and ^{13}C NMR data of compound AU5

Atom No.	-Oh 2014 CD3OD + D_2O	Sun 2006 CD3OD	AU 5 CD3OD	AU 5 CD3OD	Sun 2006 CD3OD	-Oh 2014 CD3OD + D_2O
	δc	δc	δc	δ_H (m, *J* in Hz)	δ_H (m, *J* in Hz)	δ_H (m, *J* in Hz)
2	79.9	79.8	79.89 (CH)	4.83 (br s)	4.82 (br s)	4.81 (br s)
3	67.5	67.4	67.50 (CH)	4.19 (m)	4.17 (m)	4.17 (br s)
4a	29.3	29.2	29.27 (CH_2)	2.86 (dd, 4.8, 16.80)	2.85 (dd, 4.8, 16.8)	2.86 (dd, 4.8, 16.8)
4b	29.3	29.2	29.27 (CH_2)	2.73 (dd, 2.7, 16.8)	2.72 (dd, 2.8, 16.8)	2.73 (dd, 2.7, 16.8)
5	158.0	157.5	157.38 (C)			
6	96.4	96.4	96.39 (CH)	5.93 (d, 2.3)	5.93 (d, 2.4)	5.92 (d, 2.4)
7	158.0	157.9	158.02 (C)			
8	96.4	95.9	95.88 (CH)	5.96 (d, 2.3)	5.91 (d, 2.4)	5.94 (d, 2.4)
9	157.6	157.3	157.70 (C)			
10	100.1	100.1	100.07 (C)			
1’	132.3	132.3	132.30 (C)			
2’	115.3	115.3	115.33 (CH)	6.99 (d, 1.7)	6.96 (d, 1.6)	6.97 (d, 1.5)
3’	145.8	145.9	145.96 (C)			
4’	145.8	145.7	145.80 (C)			
5’	115.9	115.9	115.88 (CH)	6.77 (d, 8.2)	6.74 (d, 8.0)	6.75 (d, 8.1)
6’	119.4	119.4	119.39 (CH)	6.81 (dd, 1.7, 8.2)	6.79 (dd, 2.0, 8.4)	6.80 (dd 1.5, 8.1)

Table 3.7. Compound AU 6 (Elephantorrhizol)

3,3′,4′,5,6,7,8-heptahydroxyflavan	
Synonyms	Elephantorrhizol
Sample codes	AU 6
Sample amount	1.6 mg
Physical Description	Yellow powder
Molecular formula	$C_{15}H_{14}O_8$
Molecular Weight	322 g/mol
IR:($CHCl_3$)	3307, 2930, 1628, 1468, 1359,1142, 1091, 1013, 822 cm^{-1}

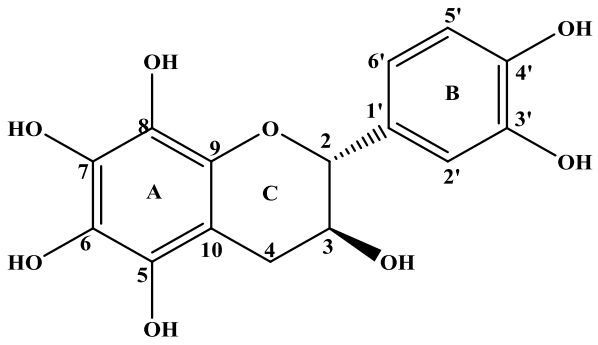

Compound AU 6 (1.6 mg) was isolated as a yellow powder. The structure was elucidated based on its ^{1}H NMR analysis (Fig 3.21). The mass, optical rotation, UV, ^{13}C NMR, 2D NMR analyses was not possible because of the insufficient amount (1.6 mg). IR spectra of this compound has a broad band at 3307 cm^{-1} region corresponding to phenolic and alcoholic O-H stretching. Another band at 1606.93 cm^{-1} is due to aromatic C=C stretching, see appendix I. The aliphatic signals of the C-ring protons was observed at δ_H 4.55 (d, 7.55 Hz), 3.94 (ddd, 5.46, 8.27, 7.75 Hz), 2.47 (dd, 8.34, 16.24 Hz) and 2.82 (dd, 5.51, 16.24 Hz). The ABX- type aromatic signals was also observed indicating the presence of a 1,2,3-trisubstituted aromatic ring at δ_H 6.83 (H-2', d, 1.98 Hz), 6.75, (H-5', d, 8.10 Hz), 6.70 (H-6', dd, 1.98, 8.27 Hz) equivalent to B-ring was recognized. The basic structure was therefore deduced as 3, 3', 4', 5, 6, 7, 8-heptahydroxyflavan. This compound also exhibit 2,3-trans configuration, see AU 4. The ^{1}H NMR data (Table 3.8) of this compound were consistent with those reported in the literature (Moyo et al., 1999).

This compound has been isolated from the roots of *Elephantorrhiza goetzei* (Moyo et al., 1999) and *Nelumbo nucifera* leaves (Ahn et al., 2013). And when tested for antibacterial and antifungal activity using the TLC bio autography technique, there was no activity at 100 µg/ml (Moyo et al., 1999).

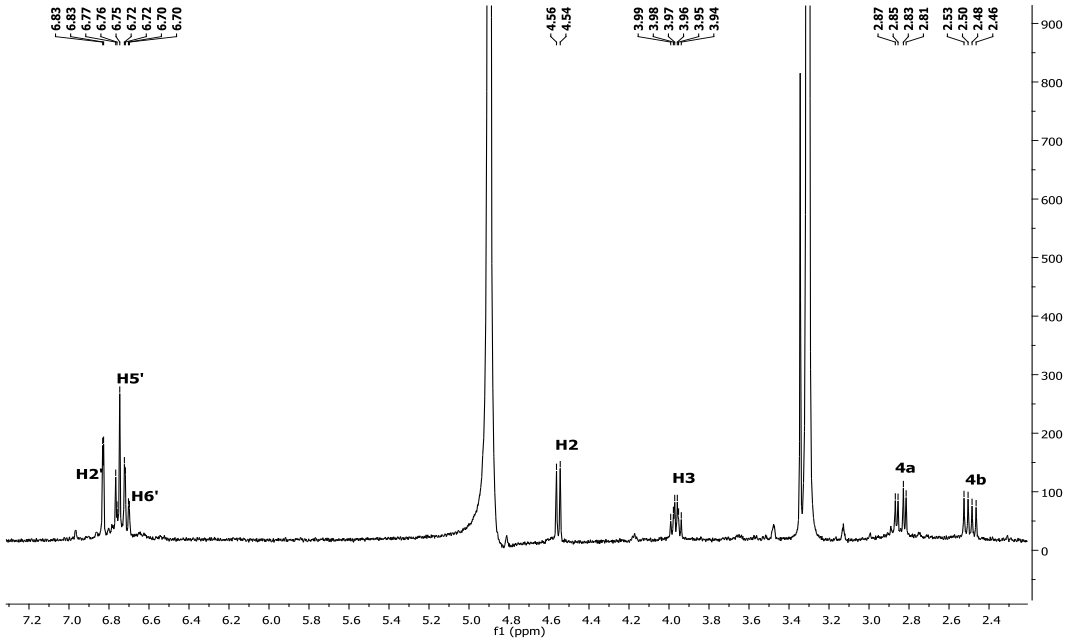

Fig. 3.21. [1]HNMR spectrum of compound AU 6

Table 3.8. [1]H and [13]C NMR spectrum data of AU 6

Atom No.	AU 6	Moyo 1999 CD3OD δc	AU 6 CD3OD δ_H (m, *J* in Hz)	Moyo 1999 CD3OD δ_H (m, *J* in Hz)
2	-	82.8	4.55 (d, 7.5)	4.56 (d, 7.1)
3	-	68.8	3.94 (m)	3.97 (m)
4b	-	28.5	2.47 (dd, 8.3, 16.2)	2.53 (dd, 8.4, 16.1)
4a	-	28.5	2.82 (dd, 5.5, 16.2)	2.82 (dd, 5.5, 16.1)
5	-	148.6		
6	-	138.6		
7	-	151.8		
8	-	132.7		
9	-	147.6		
10	-	100.9		
1’	-	132.2		
2’	-	116.1	6.83 (d, 2.0)	6.83 (d, 2.0)
3’	-	146.2		
4’	-	146.4		
5’	-	115.3	6.75 (d, 8.1)	6.76 (d, 8.2)
6’	-	120.1	6.70 (dd, 2.0, 8.1)	6.72 (dd, 2.0, 8.2)

Table 3.9. Compound AU 7 (Catechin 3-*O*-β-D-glucopyranoside)

Synonyms	(+)-Catechin 3-*O*-β-D-glucopyranoside
Sample codes	AU 7
Sample amount	43 mg
Physical Description	Yellow needles
Molecular formula	$C_{21}H_{24}O_{11}$
Molecular Weight	452 g/mol
Optical Rotation $[\alpha]_D^{24.4}$	-11.73 (c 0.33 in MeOH)
UV (λ_{max})	232 and 279 nm
IR:($CHCl_3$)	3339, 2923, 1609, 1520, 1464, 1373, 1142, 1028, 821 cm^{-1}

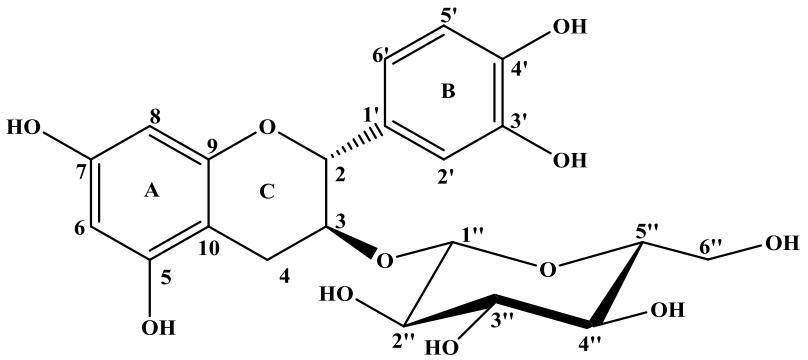

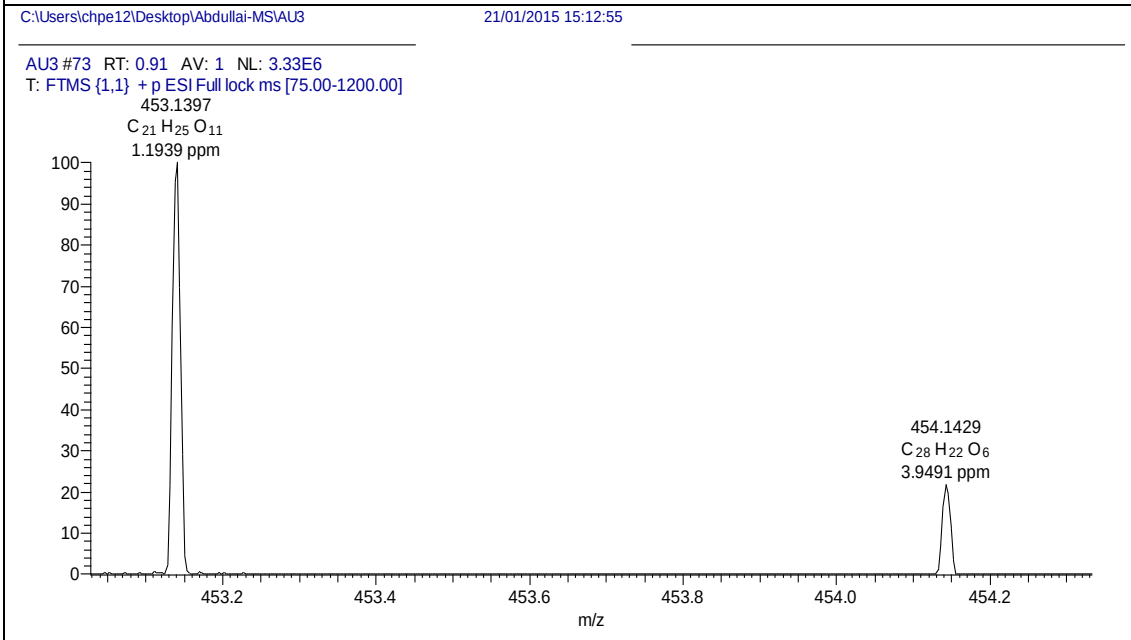

Compound AU 7 (43 mg) was obtained as a yellow needles, $[\alpha]_D^{24.4}$ −11.73 (MeOH: c 0.33) and literature value is –13.2 (Me_2CO: c 0.4). It has a molecular formula of $C_{21}H_{24}O_{11}$, which was established on the basis of ESI-HRMS at *m/z* 453.1397 $[M + H]^+$ (Calcd for 453.1398). The IR spectrum of this compound is similar to that of AU 4, see appendix I. Similarly, when

comparing the ^{1}H NMR spectra of this compound with that of AU 4, the presence of all the proton signals of AU 4 can be observed with the exception of the signals for a glucose moiety. Hence, this observation suggests that the aglycone is a catechin. The spectrum also shows one anomeric proton at δ_H 4.20 (d, 7.5 Hz, H-1''), based on this coupling constant, the configuration of the sugar moiety is determined to be β-oriented indicating a β-glucosyl moiety. The COSY spectrum (Fig. 3.26), also show the coupling of H-2 with H-3 (δ_H 4.25) and H-3 with H-4 (δ_H 2.74).

The DEPT spectrum (Fig. 3.23) revealed twenty one signals equivalent to two methylene, twelve methine and seven quaternary carbons. The spectrum also show one anomeric carbon at 103.89 (C-1'') and other signals for glucose were observed at δ_H 75.2 (C-2''), 77.8 (C-3''), 71.6 (C-4''), 78.1 (C-5'') and 62.9 (C-6''). Additionally, the C-3 site of glycosides resonated at higher field δ_C 76.10, thus exhibiting a shielding effect and this indicated that the attachment of the sugar was at C-3 via a C-O-C linkage. Similarly, the HMBC (Fig. 3.24 and 3.25) experiment, showed the anomeric proton signal at 4.20 (H-1'', d, 7.5 Hz) coupling with 76.1 (C-3) confirming the above mentioned linkage. The ^{1}H and ^{13}C NMR data (Table 3.10) of this compound is consistent with the reported literature values for catechin 3-*O*-β-D-glucopyranoside (Ishimaru et al., 1987; Raab et al., 2010).

Compound AU 7 has been isolated from the leaves and bark of Quercus miyagii (Ishimaru et al., 1987), bark of blackjack oak (Bae et al., 1994) and the fern of *Davallia divaricate* (Hwang et al., 1989). This compound has been reported to be potent antioxidant at an IC_{50} value of 39 µg/ml (Khallouki et al., 2007).

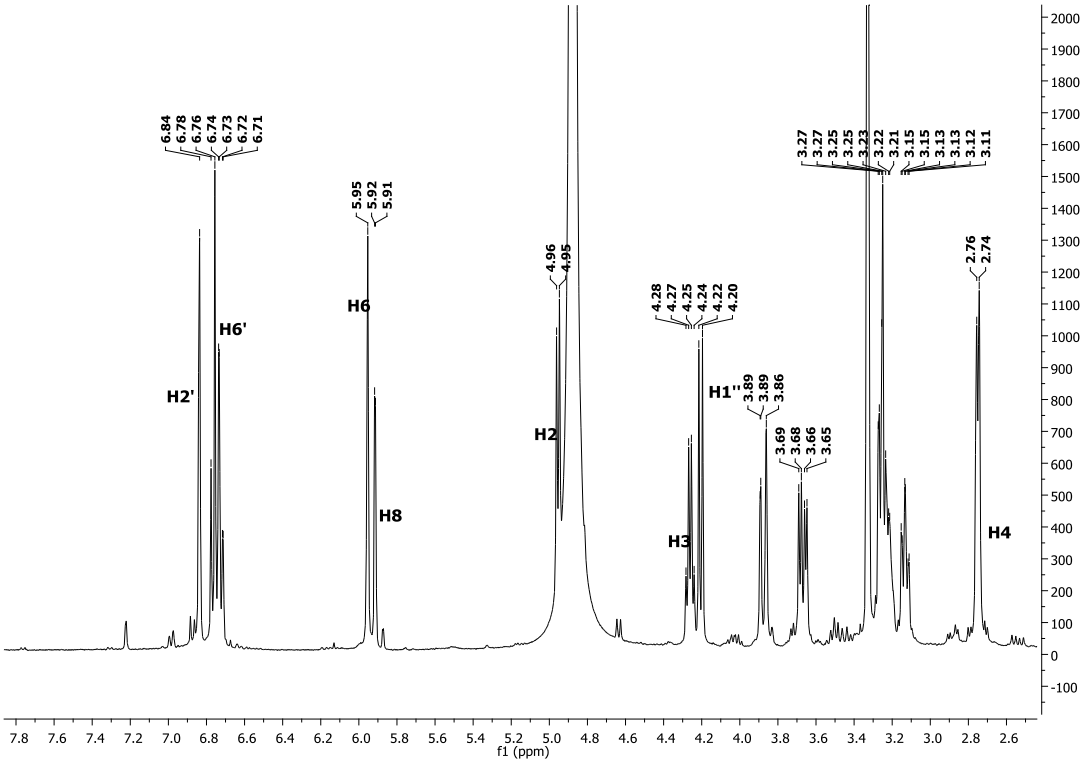

Fig. 3.22. [1]H NMR spectrum of compound AU 7

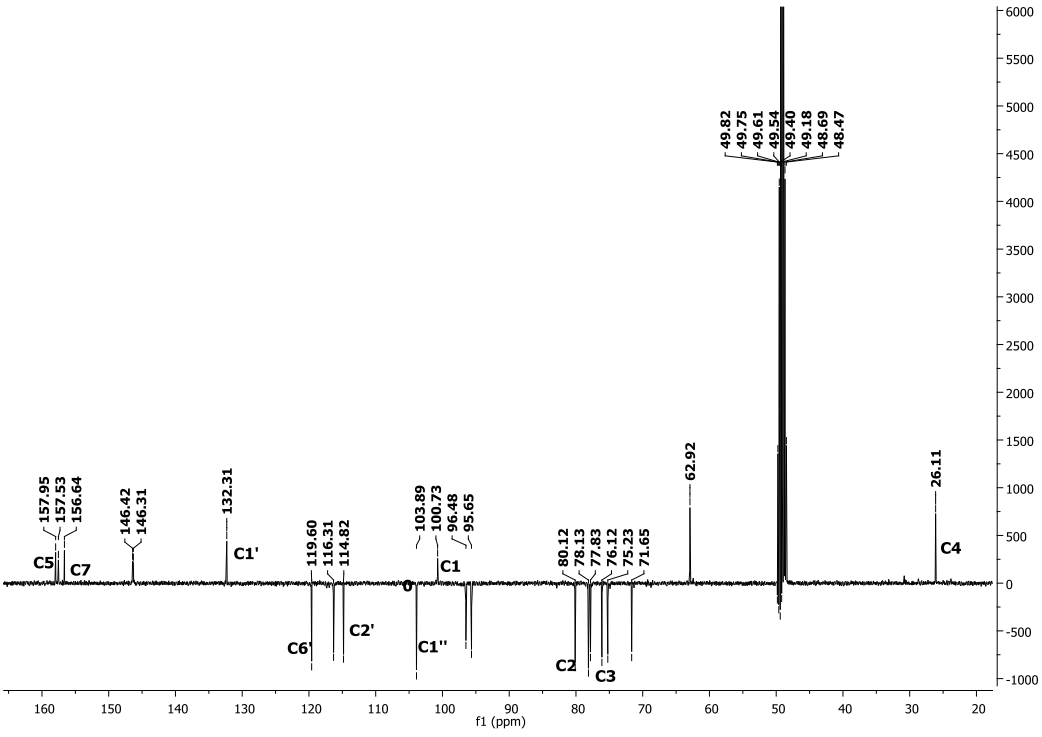

Fig. 3.23. DEPT spectrum of compound AU7

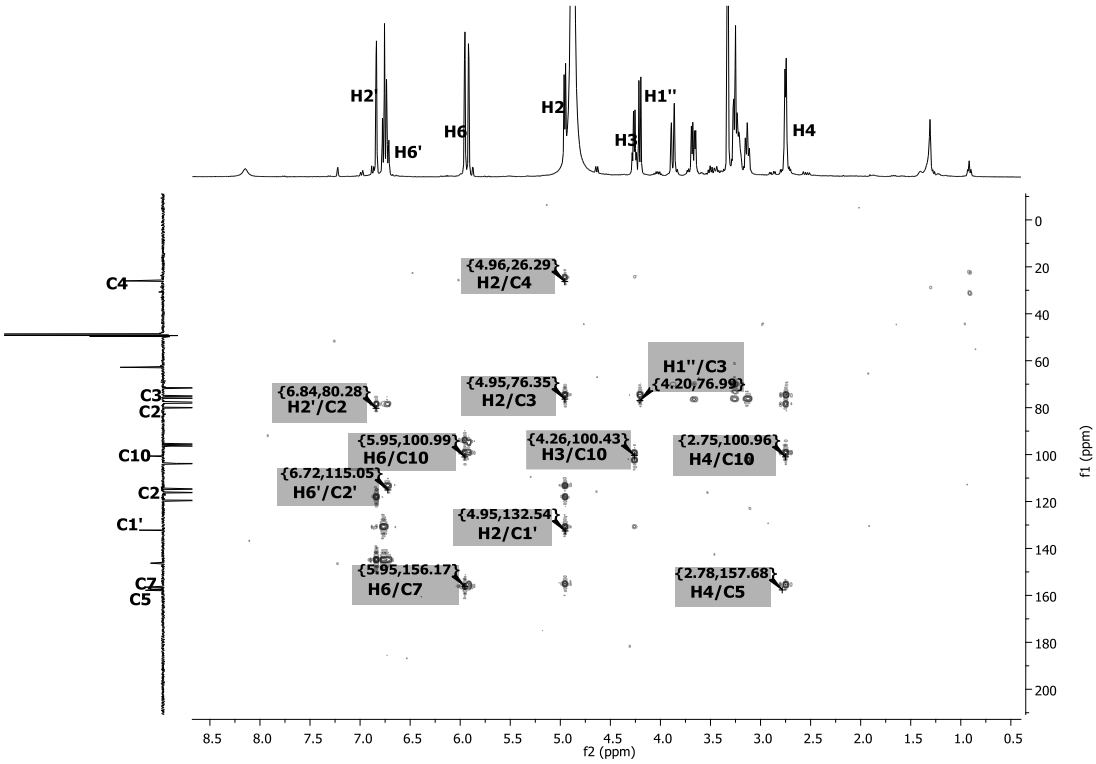

Fig. 3.24. HMBC spectrum of compound AU 7

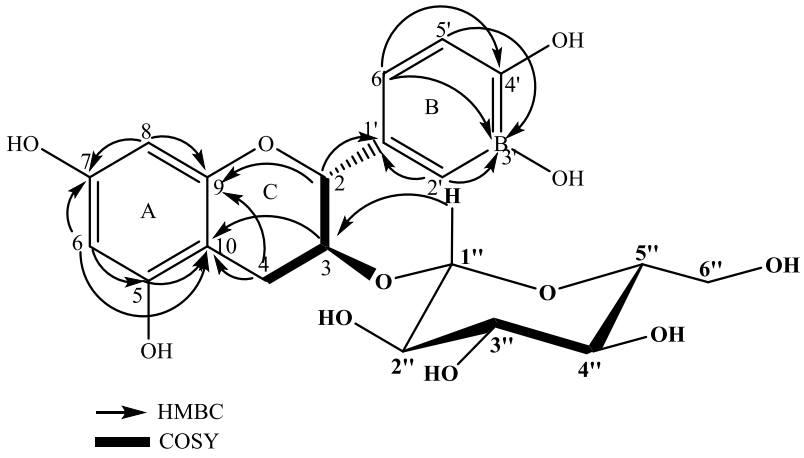

Fig. 3.25. HMBC and COSY correlation of compound AU 7

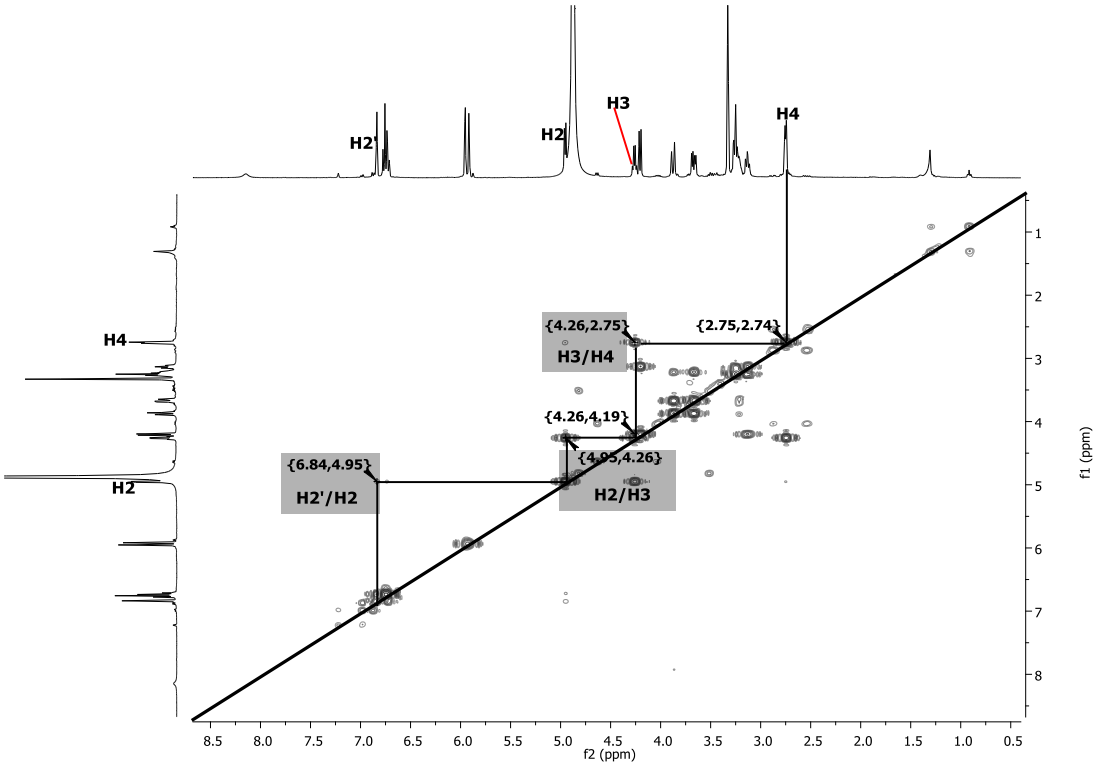

Fig. 3.26. COSY spectrum of compound AU 7

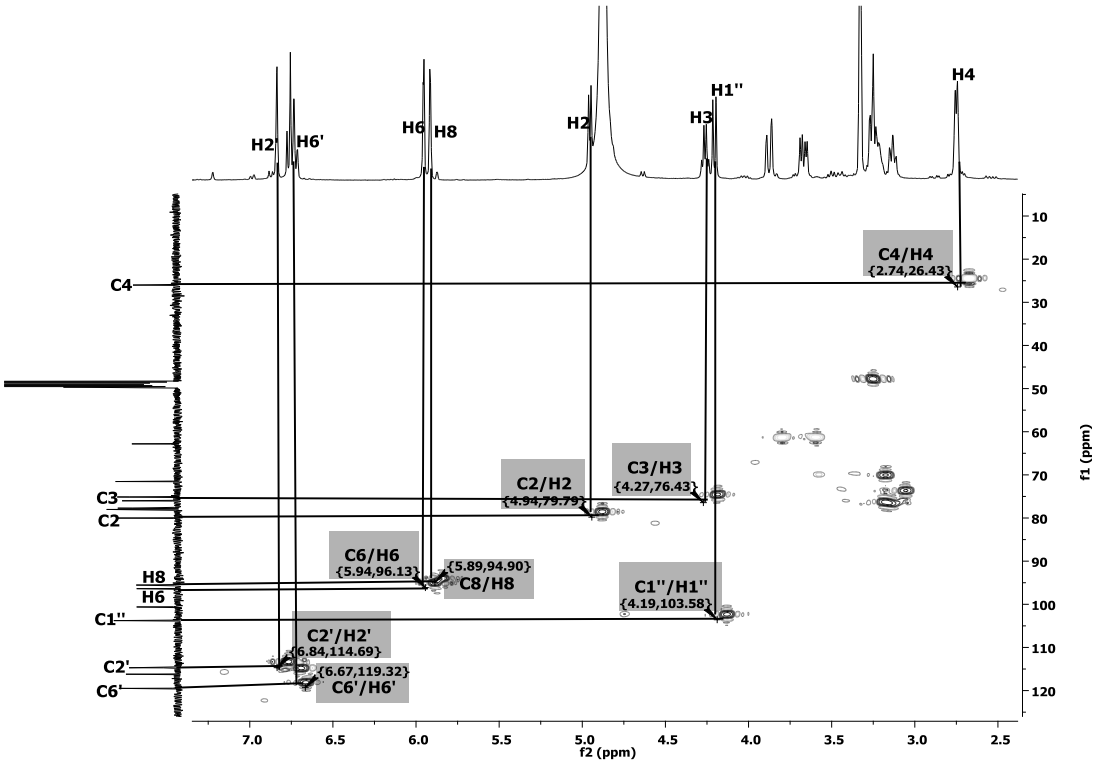

Fig. 3.27. HSQC spectrum of compound AU 7

Table 3.10. ^{1}H and ^{13}C NMR data of compound AU 7

Atom No.	Ishimaru 1987 (CD3)2CO + D_2O δc	Raab 2010 CD3OD δc	AU 7 CD30D δc (m)	AU 7 CD3OD δ_H (*J* in Hz)	Raab 2010 δ_H (*J* in Hz)	Ishimaru 1987 (CD3)2CO + D_2O δ_H (*J* in Hz)
2	79.3	80.0	80.1 (CH)	4.95 (d, 5.85)	4.94 (d, 5.9)	4.93 (d, 6.0)
3	75.6	76.1	76.1 (CH)	4.25 (m)	4.24 (dd, 11.4, 5.9)	4.24 (dd, 6.0, 8.0)
4	28.4	26.0	26.1 (CH2)	2.74 (m)	2.74 (m)	2.6-2.9 (m)
5	156.9	157.8	157.9 (C)			
6	95.3	96.4	96.4 (CH)	5.95 (d, 1.90)	5.94 (d, 2.3)	5.92 (d, 2.0)
7	157.4	157.4	157.5 (C)			
8	96.4	95.6	95.6 (CH)	5.91 (d, 1.90)	5.90 (d, 2.3)	6.04 (d, 2.0)
9	156.5	156.6	156.6 (C)			
10	100.0	100.7	100.7 (C)			
1’	131.7	132.2	132.3 (C)			
2’	114.6	114.8	114.8 (CH)	6.84 (d, 1.65)	6.82 (d 1.9)	
3’	145.6	146.3	146.4 (C)			
4’	145.7	146.3	146.3(C)			
5’	116.0	116.3	116.1(CH)	6.76 (d, 8.15)	6.75 (d, 8.1)	
6’	119.1	119.5	119.6 (CH)	6.71 (dd 1.65, 8.17)	6.70 (dd, 8.1, 1.9)	
1’’	103.5	103.8	103.8 (CH)	4.20 (d 7.43)	4.19 (d, 7.7)	4.28 (d, 8.0)
2’’	74.6	75.1	75.2(CH)	3.13 (m)	3.12 (m)	
3’’	77.3	77.7	77.8 (CH)	3.27 (m)	3.21-3.27 (m)	
4’’	71.1	71.6	71.6(CH)	3.25 (m)	3.21-3.27 (m)	
5’’	77.1	78.0	78.1(CH)	3.11 (m)	3.18-3.20 (m)	
6’’	62.5	62.8	62.9 (CH)	3.65 (dd, 5.3, 11.7) 3.85 (dd, 1.8, 11.7)	3.66 (dd, 11.8, 5.4) 3.86 (dd, 11.8, 2.1)	

Table 3.11. Compound AU 8 (New compound)

Synonyms	Catechin-3-*O*-α-L-rhamnopyranosyl (1→4) β-D-glucopyranoside
Sample code	AU 8
Sample amount	23 mg
Physical description	Brown needles
Molecular formula	$C_{27}H_{34}O_{15}$
Molecular weight	598 g/mol
Optical rotation $[\alpha]_D^{24.4}$	-9.34 (c 0.33 in MeOH)
UV (λ_{max})	241 and 273 nm
IR: ($CHCl_3$)	3368, 2933, 1610, 1520, 1452, 1362, 1286, 1141, 1069, 818 cm^{-1}

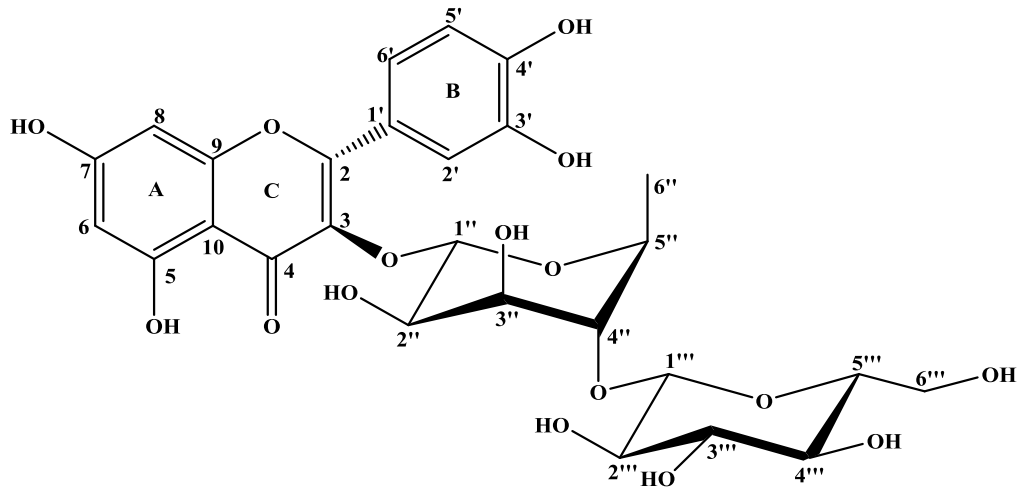

LC-HRFTMS spectrum [M+H]+ 599.1979

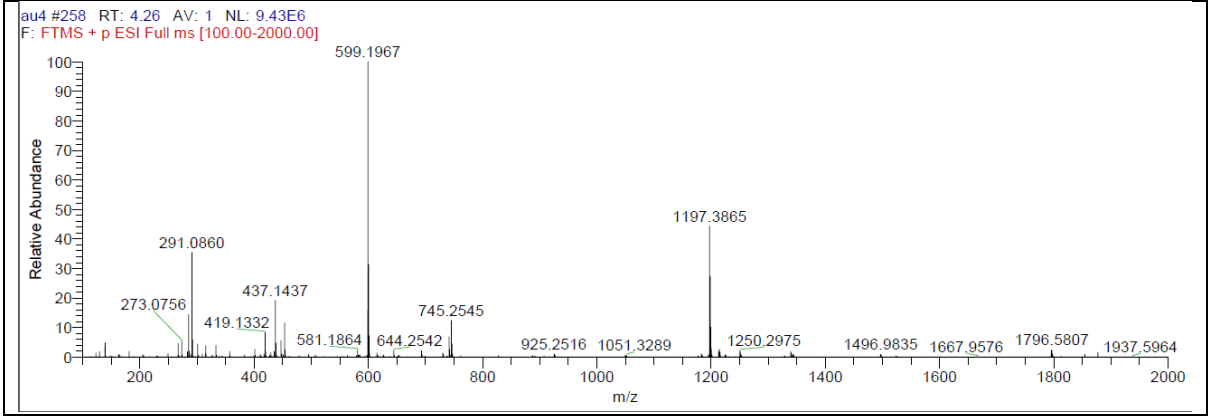

Compound AU 8 (23 mg) was obtained as brown needles, $[\alpha]_D^{24.4}$ -9.34 (MeOH: c 0.33), and it molecular formula was established as $C_{27}H_{34}O_{15}$ by HR-FT-MS as *m/z* 599.1967 ([M + H]$^+$(Calcd for 599.1977) and confirmed by ^{13}C NMR spectrum. The positive ESI-MS gave a fragment at m/z 437 ([M+H-162]$^+$ and 291 [M+H-162-146]$^+$ indicating the presence of a pentose unit and a terminal hexose. The IR spectrum of this compound has absorptions at 3368 and 1610 cm^{-1} corresponding to hydroxyl and a conjugated system, see appendix I. The ^{1}H NMR data of AU 8 resembles that of AU 4, except that AU 8 has two more sugar units. Hence,

this observation suggests that the aglycone is a catechin. The ^{1}H NMR spectrum (Fig. 3.28) shows two aromatic doublets at δ_H 5.88, 5.94 (each, d, 2.0 Hz) assignable to the A-ring and three aromatic proton signals at δ_H 6.88 (d, 1.7 Hz), 6.77 (d, 8.1 Hz), and 6.80 (dd, 1.7, 8.1 Hz) attributable to a 1,3,4-trisubstitued B-ring. Additionally, the spectrum showed a singlet at δ_H 5.14 and methyl protons at δ_H 1.22 (d, 6.2 Hz, H-6'') indicative of the anomeric proton (H-1'') and the methyl group of *α-L*-rhamnose; and another anomeric proton at δ_H 3.97 (d, 7.5 Hz, H-1''') assignable to *β-D*-glucopyranose as judged by the coupling constant. Both are linked via an *O*-glycosidic bond. On acid hydrolysis, the compound gave D-glucose and L-rhamnose. The COSY spectrum (Fig. 3.32) displayed correlations between δ_H 4.80 (H-2) and 4.34 (H-3), and also between δ_H 4.34 (H-3) and δ_H 2.64 and δ_H 2.75 assigned to position H-4. The DEPT spectrum (Fig. 3.29) resolved twenty seven carbon signals, corresponding to one methyl, two methylene, seventeen methine, seven quaternary. The anomeric carbons of glucose and rhamnose appeared at δ_C 101.11 (C-1'') and 101.85 (C-1''') respectively. Other signals for sugars appeared at δ_C 72.05 (C-2''), 72.15 (C-3''), 79.17 (C-4''), 69.62 (C-5''), 17.97 (C-6'') for rhamnose and 73.99 (C-2'''), 77.64 (C-3'''), 71.69 (C-4'''), 78.67 (5''') and 62.71 (C-6''') for glucose moiety. The GC analysis of the TMS derivatives of AU 8 hydrolysates showed that this compound contains D-glucose and L-rhamnose. The obtained values for sugars were comparable with their reported values except for a 6.1 ppm downfield shift of C-4'' due to interglycosidic bond between C-4'' and C-1''' that established a 1→4 linkage between rhamnose and glucose. The ^{13}C spectral data were assigned through the assistance of the HSQC spectrum (Fig. 3.33), where the carbon resonances of the A-ring at δ_C 95.81 (C-6) and δ_C 96.54 (C-8) correlated with meta-coupled (1.98 Hz) protons at δ_H 5.94 (H-6) and δ_H 5.88 (H-8), thus showing that the C-rhamnosylation did not occur in the A-ring. In the C-ring, the HSQC assignment was more important in the C-2, C-3 and the two sugar units. The C-2 signal of the C-ring appeared at δ_C 81.03 and it coupled with the proton doublet at δ_H 4.80 (6.7 Hz) assigned to position H-2. The down field position of the C-2 chemical shifts (δ_C 80.80) observed in the DEPT spectrum and the appearance of a doublet at 4.80 (d, 6.7 Hz) attributed to position 2, indicate that the flavan moieties possessed the 2,3-trans configuration (Foo and Karchesy, 1989; Ishimaru et al., 1987; Takahama et al., 2013). The attachment of the sugar units at C-3 is evident from the downfield shift 5.8 ppm of the C-3 signal to δ_C 74.1 that was coupled with the proton multiplet at (δ_H 4.34) assigned to the proton at C-3 of the C-ring. This attachment was confirmed by HMBC spectrum (Fig. 3.30) and (Fig. 3.31), as correlations from H-1''' (5.14) to C-4'' (δ_C 79.17) and H-1'' (3.99) to C-3 (δ_C 76.22) were observed confirming the above mentioned link. Based on this evidences, the structure of the compound was elucidated

as catechin-3-*O*-α-L-rhamnopyranosyl (1→4) β-D-glucopyranoside. The isolation and characterization of this compound has been reported for the first time.

Bae et al., (1994) has isolated 3-*O*-[α-L-rhamnopyranosyl (1→6) β-D-glucopyranosyl]-Catechin from the bark of blackjack oak, the inter glycosidic linkage of this compound is between a terminal rhamnose and inner glucose.

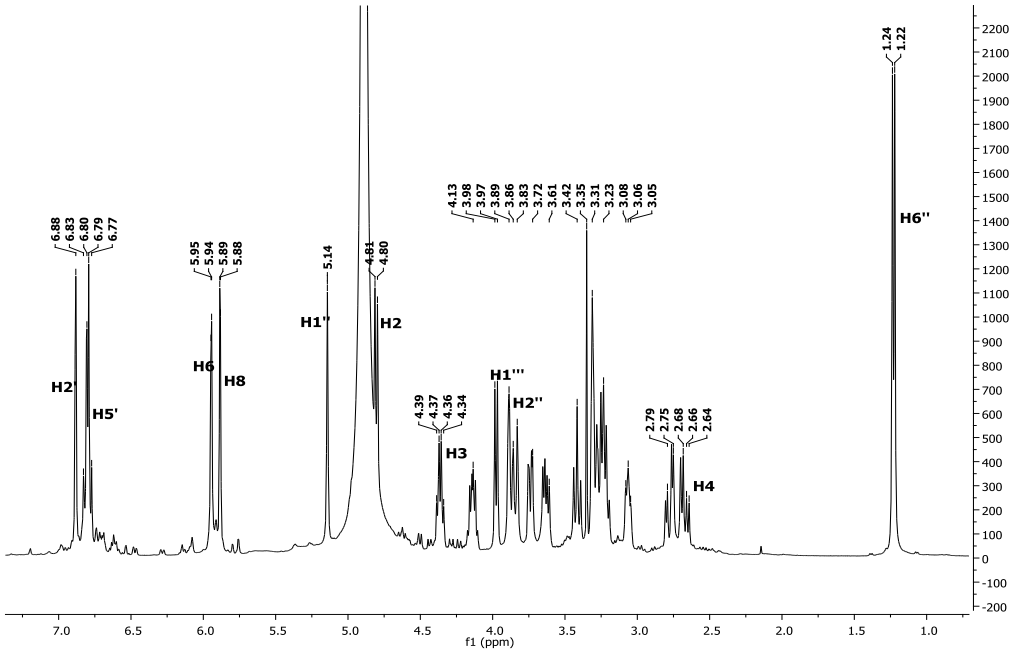

Fig. 3.28. ^{1}H NMR spectrum of compound AU 8

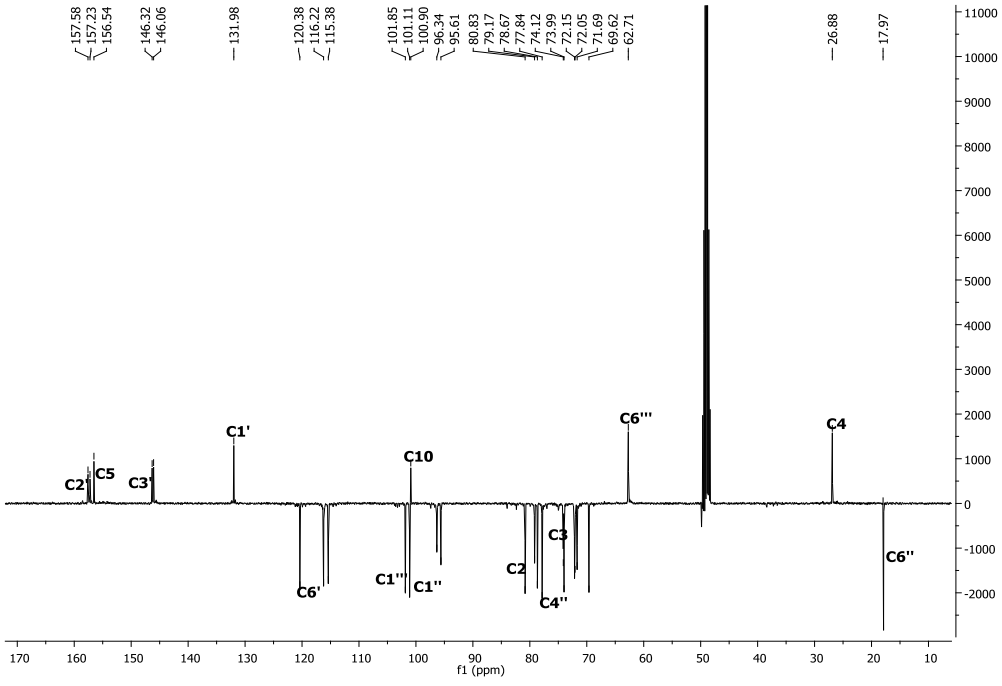

Fig. 3.29. DEPT spectrum of compound AU 8

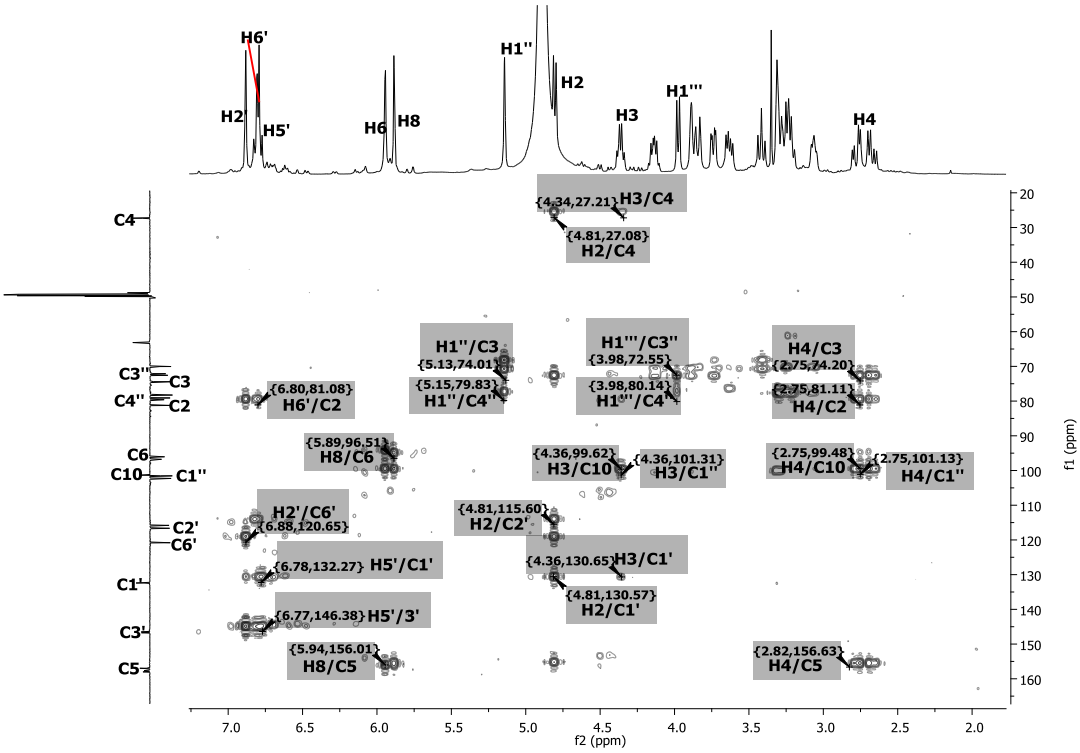

Fig. 3.30. HMBC spectrum of compound AU 8

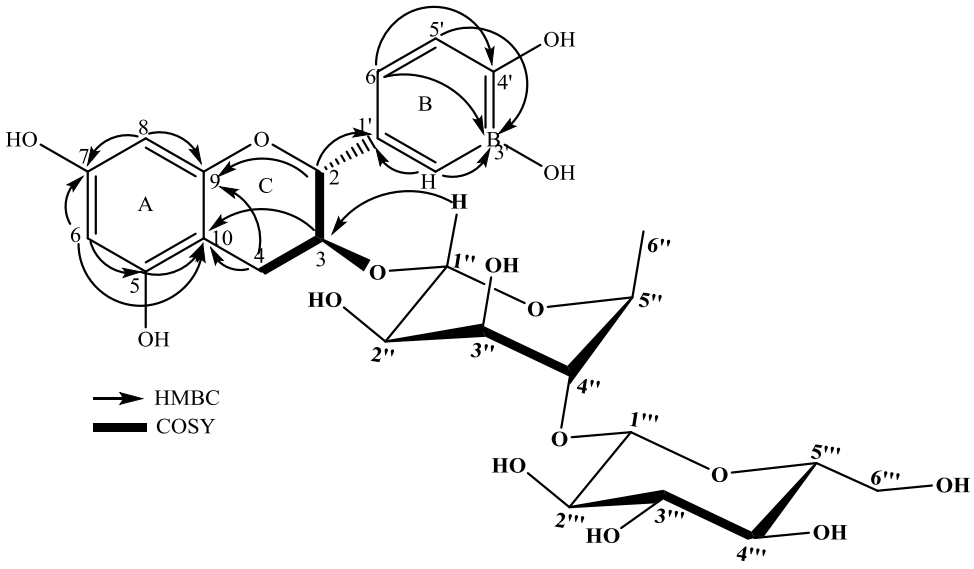

Fig. 3.31. HMBC and COSY correlations of compound AU 8

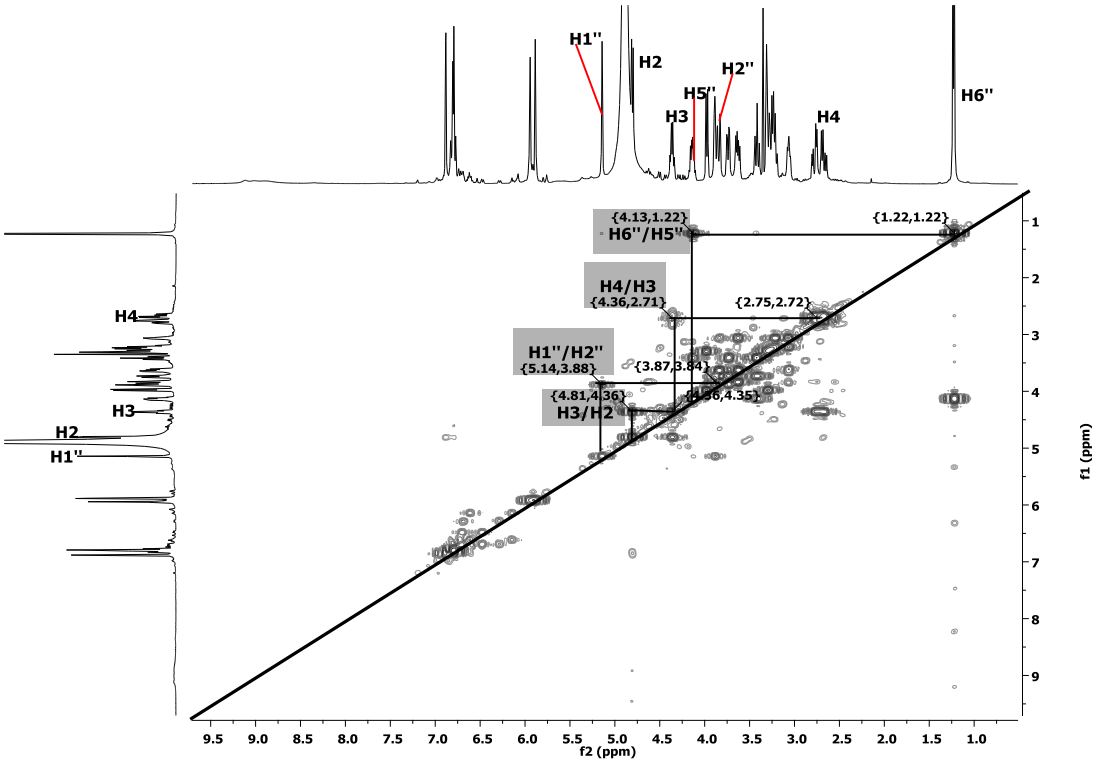

Fig. 3.32. COSY spectrum of compound AU 8

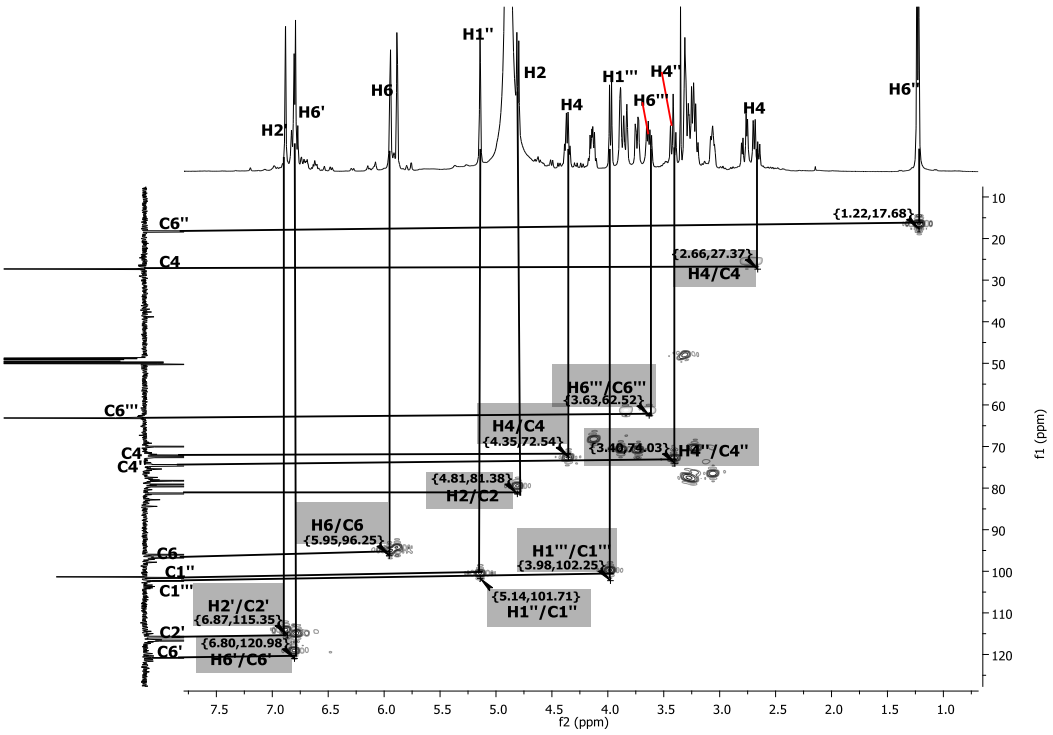

Fig. 3.33. HSQC spectrum of compound AU 8

Table 3.12. ^{13}C and ^{1}H NMR data of compound AU 8

Atom No.	AU 8 CD30D δc (m)	AU 8 CD3OD δ_H (*J* in Hz)	HMBC [H→C]
2	80.8	4.80 (d, 6.7)	C-3, C-4, C-9, C-1', C-2', C-6'
3	74.1	4.34 (m)	C-2, C-4, C-10, C-1', C-1''
4	26.8	2.64 (dd, 5.2, 16.3)	C-2, C-3, C-5, C-10, C-1''
		2.75 (dd, 7.2, 16.3)	
5	156.5		
6	96.3	5.94 (d, 2.0)	C-5, C-7, C-8, C-10
7	157.2		
8	95.6	5.88 (d, 2.0)	C-5, C-7, C-8, C-9, C-10
9	157.6		
10	100.9		
1'	132.0		
2'	115.4	6.88 (d, 1.7)	C-2, C-1', H-3', C-6'
3'	146.3		
4'	146.1		
5'	116.2	6.77 (d, 8.1)	C-2, C-1', C-2', C-4', C-6'
6'	120.4	6.80 (dd, 1.7, 8.1)	C-2, C-1', C-2', C-3'
Rhamnose			
1''	101.1	5.14 (br s)	C-3, C-3'', C-4'', C-5''
2''	72.1	3.89 (m)	
3''	72.2	3.72 (m)	
4''	79.2	3.42 (m)	
5''	69.6	4.13 (m)	
6''	17.9	1.22 d (6.21)	
Glucose			
1'''	101.9	3.97 (d, 7.4)	C-3'', C-4'', 5'', 5'''
2'''	73.9	3.35 (m)	
3'''	77.6	3.31 (m)	
4'''	71.7	3.23 (m)	
5'''	78.7	3.05 (m)	
6'''	62.7	3.61 (dd, 6.1, 11.9)	
		3.83 (dd, 1.7, 11.9)	

Table 3.13. Compound AU 9 (taxifolin)

(2*R*,3*R*)-2-(3,4-Dihydroxyphenyl)-3,5,7-trihydroxy-2,3-dihydrochromen-4-one	
Synonyms	Taxifolin
Sample codes	AU 9
Sample amount	3 mg
Physical Description	Yellow needles
Molecular formula	$C_{15}H_{12}O_7$
Molecular Weight	304 g/mol
IR:($CHCl_3$)	3369, 1638, 1459, 1282, 1169, 1089 cm^{-1}

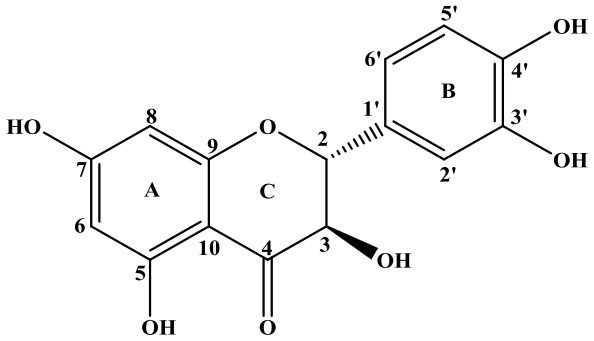

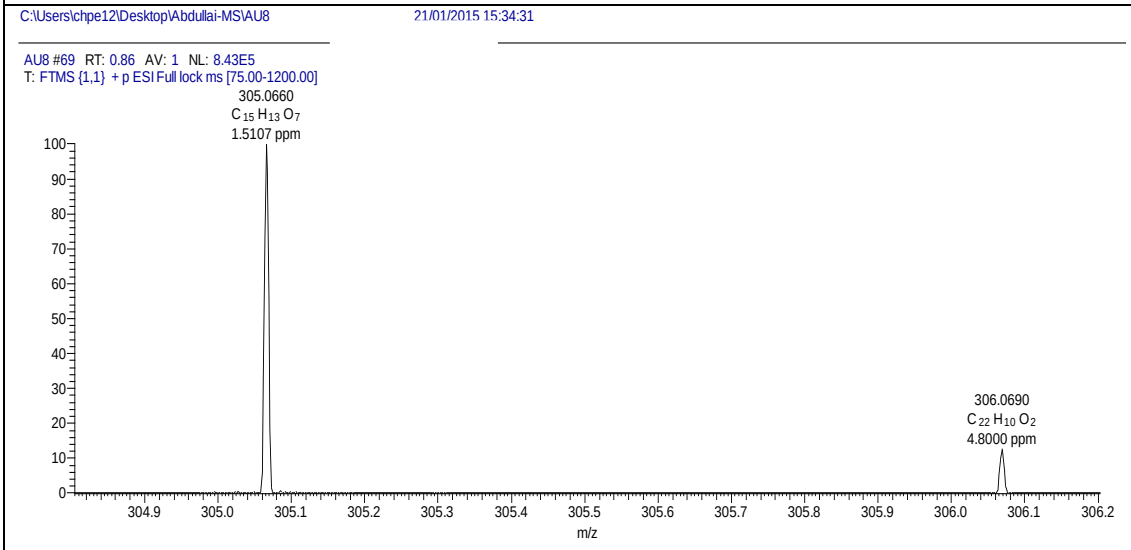

Compound AU 9 (3 mg) was obtained as yellow needles. It has a molecular formula of $C_{15}H_{12}O_7$ which was established on the basis of ESI-HRMS at *m/z* 305.0660 $[M + H]^+$ (Calcd for 305.0662). The IR spectra of this compound has a broad band at 3369 cm^{-1} region corresponding to phenolic and alcoholic O-H stretching. Another band at 1638 cm^{-1} is due to carbonyl and aromatic C=C stretching, see appendix 1. The DEPT spectrum (Fig. 3.34) showed fifteen carbon signals, which consist of seven methine and eight quaternary carbon.

In ring C, the ^1H NMR spectrum (Fig. 3.33) showed that the resonance of proton H-2 had been split by proton H-3 resulting in a doublet at δ_H 4.91 (d, 11.5 Hz), while proton H-3 was split by

proton H-2 yielding a doublet at δ_H 4.51 (d, 11.5 Hz). These protons signals were seen to couple to each other in COSY spectrum (Fig. 3.37). The DEPT spectrum showed resonances for the keto group at C-4 (δc 198.4). The down field position of the C-2 chemical shifts (δ_C 885.1) observed in the DEPT spectrum and the appearance of a doublet at 4.91 (d, 11.1 Hz) attributed to position 2, indicate that the flavan moieties possessed the 2,3-trans configuration (Foo and Karchesy, 1989; Ishimaru et al., 1987; Takahama et al., 2013).

In ring B, proton H-2' was split by proton H-6' (meta position) resulting in a doublet at δ_H 6.98 (d, 1.3 Hz), proton H-5' was split by proton H-6' yielding a doublet at δ_H 6.81(d, 8.2 Hz) while proton H-6' was split by proton H-5' and H-2' resulting in a doublet of doublet at δ_H 6.87 (dd, 1.8, 8.2 Hz) indicating a 1,2,3-trisubstituted aromatic ring system.

In ring A, proton H-6 and H-8 split each other in a meta position and each yielding a doublet at δ_H 5.90 and 5.94 (d, 1.3 Hz, each). The structure was further confirmed by long-range coupling observed in HMBC (Fig. 3.35), where the ring C methine protons H-2 (δ_H 4.91) correlated with C-3, C-4, C-1', C-2'and C-6' (δc 116.1); and H-3 (δ_H 4.51) correlated with C-2, C-4, C-1' (δc 129.8). Ring B showed HMBC correlation of H-2' to C-2, C-4', and C-6' (δc 116.1); H-5' to C-2, C-1' and C-3' (δc 144.9); and H-6' to C-2, C-1' and C-3' (δc 146.2). The comparison of the NMR data (Table 3.14) with those reported in the literature (Oh et al., 2014; Wang et al., 2012) showed that the isolated compound is taxifolin.

Compound AU 9 has been isolated from the stem of *Quercus acuta* Thunberg (Oh et al., 2014), whole plant and fruit of *Cayratia japonica* and it is also reported to show weak monoamine oxidase (MAO) activity at an IC_{50} value of 154.7 µg/ml (Han et al., 2007).

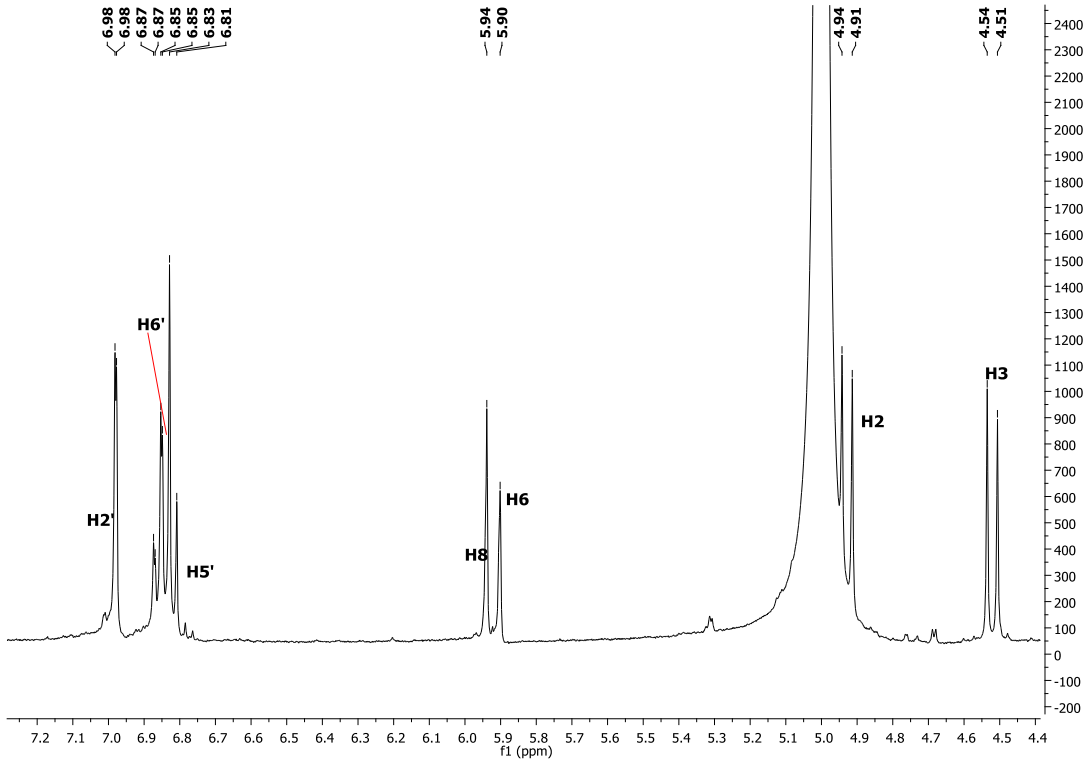

Fig. 3.34. ^{1}H NMR spectrum of compound AU 9

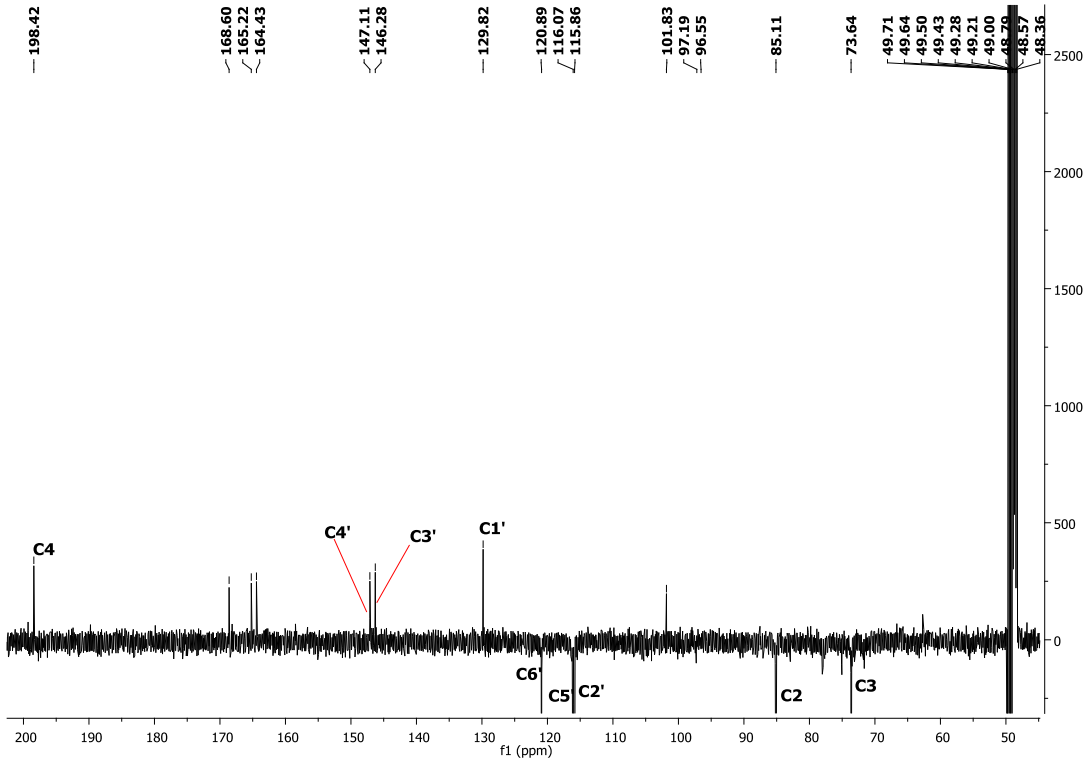

Fig. 3.35. DEPT spectrum of compound AU 9

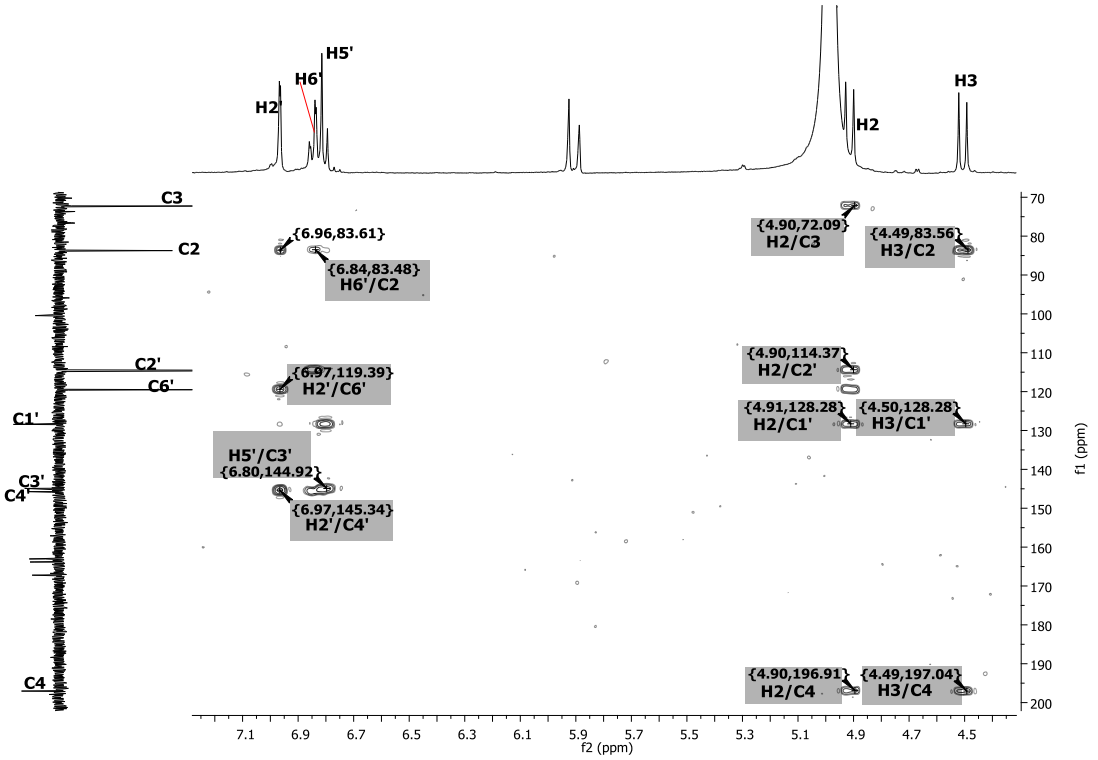

Fig. 3.36. HMBC spectrum of compound AU 9

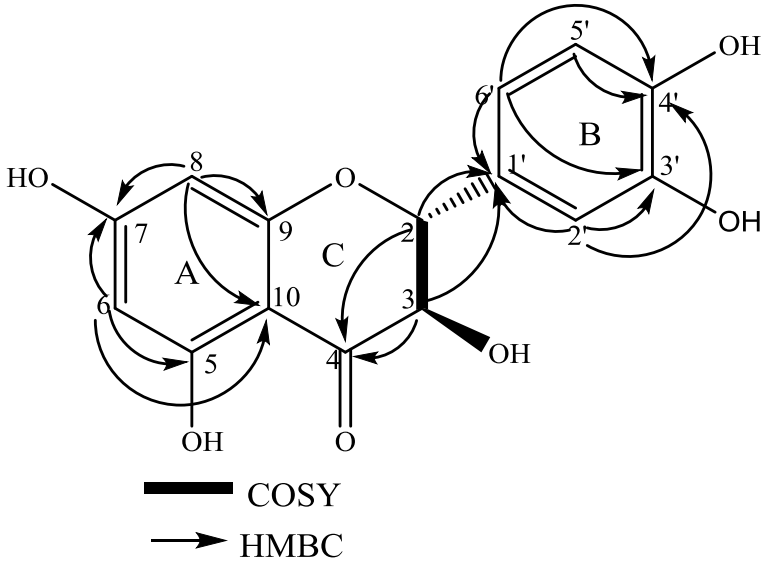

Fig. 3.37. HMBC and COSY correlations of compound AU 9

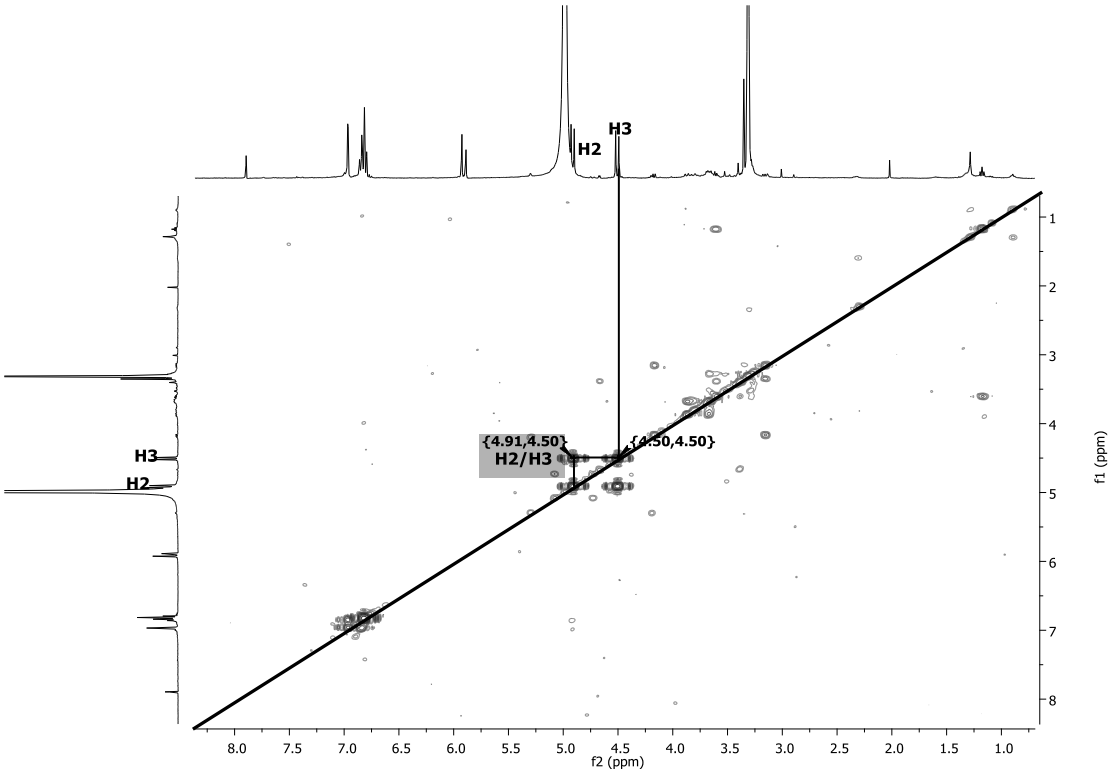

Fig. 3.38. COSY spectrum of compound AU 9

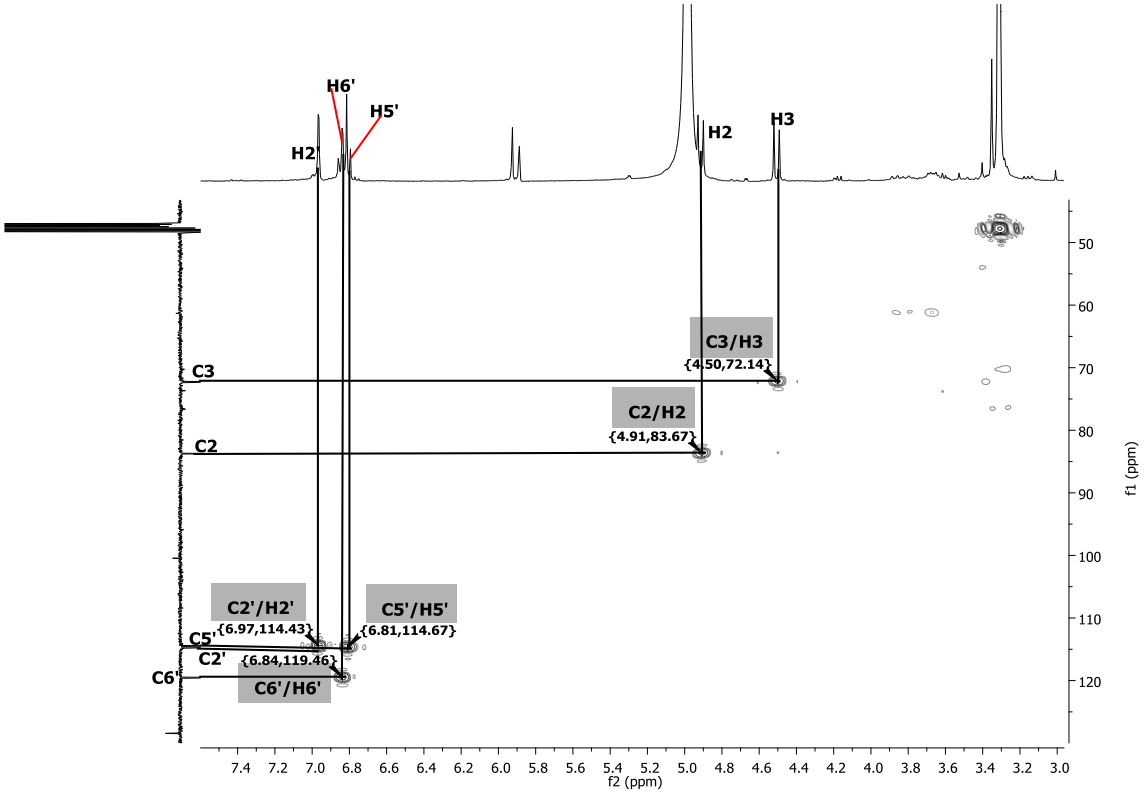

Fig. 3.39. HSQC spectrum of compound AU 9

Table 3.14. ^{1}H and ^{13}C NMR data of compound AU 9

Atom No.	Oh 2014 DMSO + D_2O δc	Wang 2012 CD3OD δc	AU 9 CD3OD δc (m)	AU 9 CD3OD δ_H (m, *J* in Hz)	Oh 2014 DMSO + D_2O δ_H (m, *J* in Hz)	Wang 2012 CD3OD δ_H (m, *J* in Hz)
2	83.4	84.9	85.1 (CH)	4.91 (d, 11.5)	4.93 (d, 11.1)	4.90 (d, 11.7)
3	71.8	73.5	73.6 (CH)	4.51 (d, 11.5)	4.45 (d, 11.1)	4.52 (d, 11.7)
4	197.8	198.4	198.4 (C)			
5	162.9	165.0	165.2 (C)			
6	96.4	97.4	97.2 (CH)	5.90 (s)	5.82 (d, 2.1)	5.88 (s)
7	167.4	168.7	168.6 (C)			
8	95.4	96.4	96.5 (CH)	5.94 (s)	5.87 (d, 2.1)	5.92 (s)
9	162.9	164.4	164.4 (C)			
10	100.6	101.7	101.8 (C)			
1’	128.4	129.7	129.8 (C)			
2’	115.5	121.0	120.9 (CH)	6.98 (d, 1.8)	6.85 (d, 2.1)	6.98 (d, 1.8)
3’	145.1	146.1	146.2 (C)			
4’	146.0	146.9	147.1 (C)			
5’	115.6	115.9	115.9 (CH)	6.81 (dd, 1.8, 8.2)	6.72 (m)	6.82 (d, 8.1)
6’	119.9	116.1	116.1 (CH)	6.87 (d, 8.2)	6.72 (m)	7.00 (s)

Table 3.15. Compound AU 10 (Taxifolin 4-*O*-β-D-glucopyranoside)

Synonyms	Taxifolin 4'-*O*-β-D-glucopyranoside
Sample codes	AU 10
Sample amount	4 mg
Physical Description	yellow needle
Molecular formula	$C_{21}H_{22}O_{12}$
Molecular Weight	466 g/mol
Optical Rotatio $[\alpha]_D^{24.4}$	-8.53 (c 0.33 in MeOH)
IR:($CHCl_3$)	3368, 2927, 1640, 1518, 1448, 1361, 1166, 1076, 828 cm^{-1}

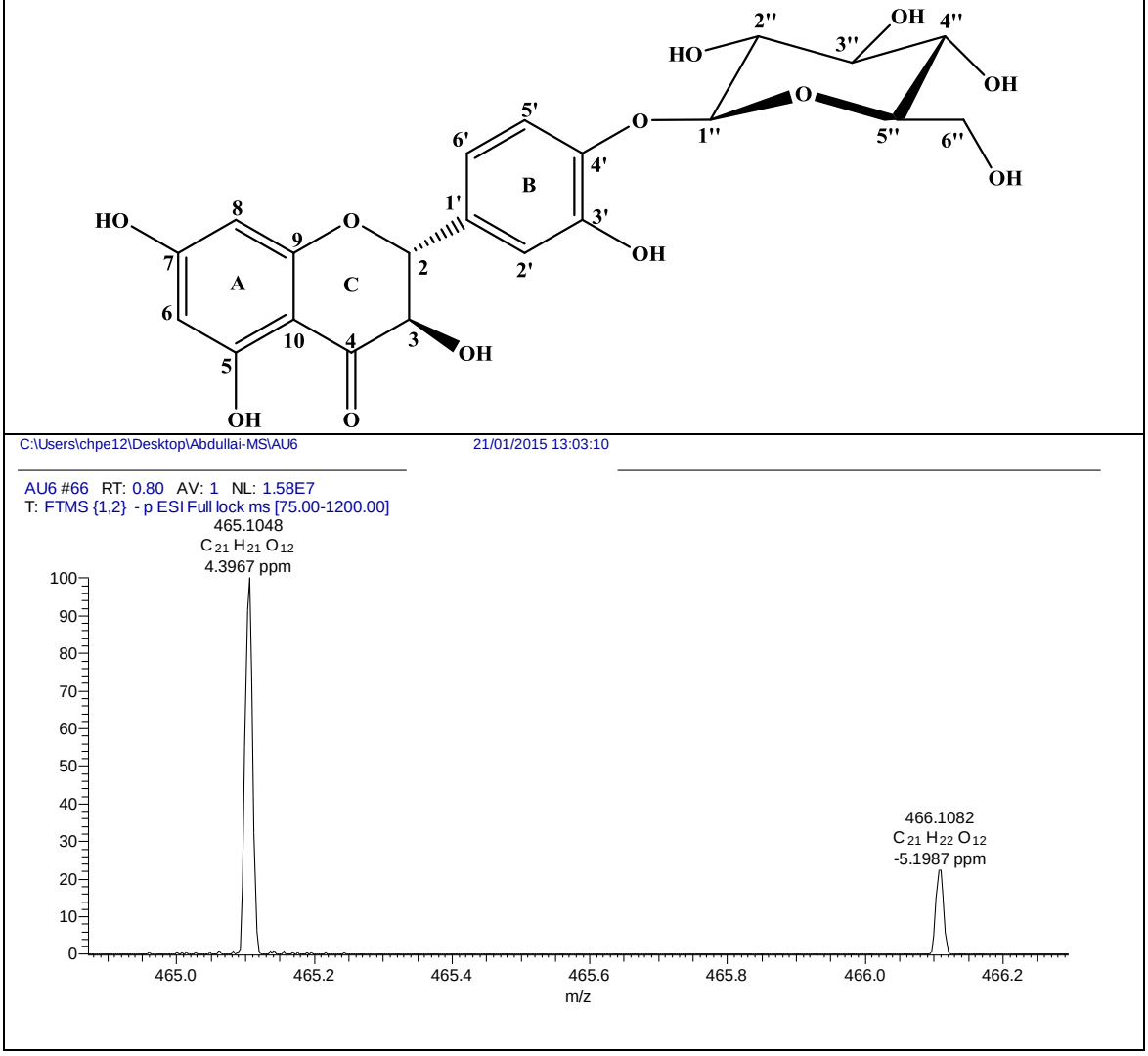

Compound AU 10 (4 mg) was obtained as yellow needles, $[\alpha]_D^{24.4}$ -9.34 (MeOH: c 0.33). It has a molecular formula of $C_{21}H_{22}O_{12}$ which was established on the basis of ESI-HRMS at *m/z* 465.1048 $[M-H]^-$ (Calcd for 465.1032). The IR spectrum of this compound is similar to AU 9, see appendix I. The DEPT spectrum (Fig. 3.41) showed twenty one carbon signals, which comprised of one methylene, twelve methine and eight quaternary carbons. The ^1H and ^{13}C NMR spectra of this compound showed signals that are similar to that of AU 9 with the

exception of signals for the glucose moiety and the downfield shift of the resonance at C-4' (δc 149.0), suggesting it to be the site of glycosylation. The spectrum also showed one anomeric proton at δ_H 4.85 (H-1'', d, J=7.5 Hz), and based on this coupling constant, the configuration of the sugar moiety was determined to be β-oriented indicating a β-glycosyl moiety. The anomeric carbons appeared at δc 104.1 and other signals for the glucose occurred at δc 73.50 (C-2''), 77.62 (C-3''), 71.69 (C-4''), 78.37 (C-5'') and 62.55 (C-6'') which are typical signals for the glucose. The GC analysis of the TMS derivatives of AU 10 hydrolysates showed that this compound contains D-glucose.

In the analysis of COSY spectrum (Fig. 3.44), the coupling of the anomeric proton signal H-1'' with H-2'' (δ_H 3.51) and H-2 with H-3 (δ_H 4.57) was observed. In the HMBC spectrum (Fig. 3.42), the H-1'' was linked to C-4' (δ_C 149.01), signifying that the β-D-glucose moiety was located at C-4' of the taxifolin skeleton. The ^{1}H and ^{13}C NMR data (Table 3.16) of this compound are consistent with the reported literature values (Oh et al., 2014; Xu et al., 2011).

Compound AU 10 has been isolated from the stem of *Quercus acuta* Thunberg (Oh et al., 2014), and seeds of *Litchi chinensis*, when tested against human cancer, A549; human pulmonary carcinoma, LAC; human hepatoma, Hep-G2; and human cervical carcinoma Hela cell lines using the 3-(4,5-dimethylthiazol-2-yl)-2,5-diphenyltetrazolium bromide (MTT) colorimetric assay, it demonstrate moderate activity at an IC_{50} values of 17.50, 11.58, 4.22, and 1.82 µg/ml, respectively (Xu et al., 2011).

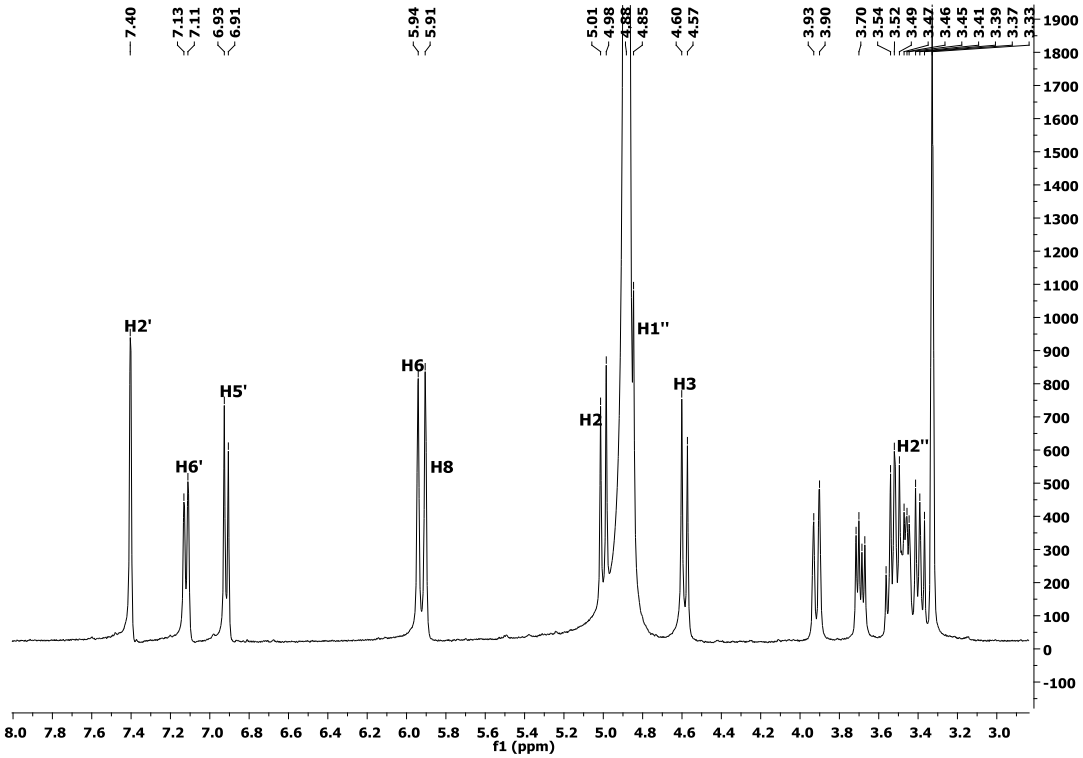

Fig. 3.40. ^{1}H NMR spectrum of compound AU 10

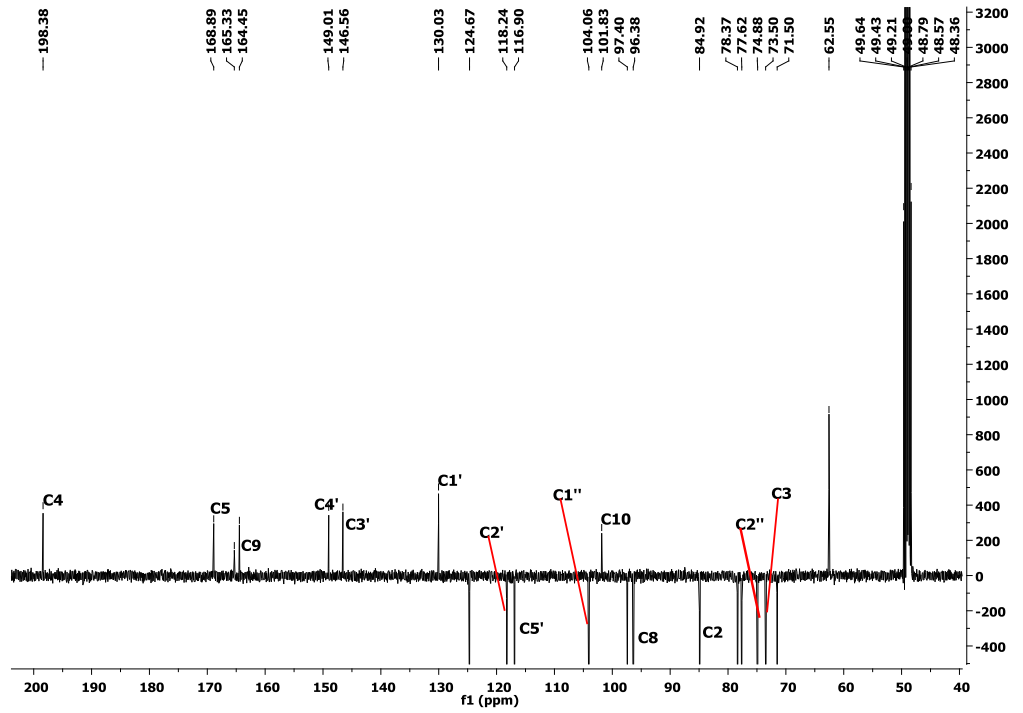

Fig. 3.41 DEPT spectrum of compound AU 10

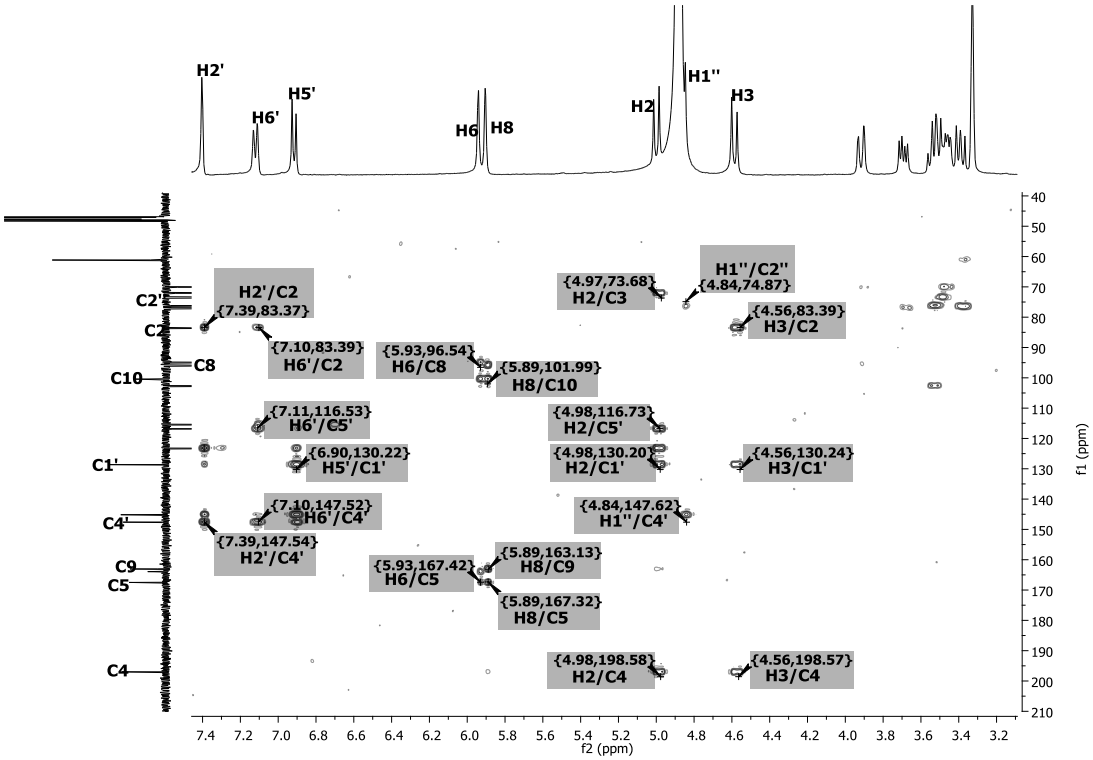

Fig. 3.42. HMBC spectrum of compound AU 10

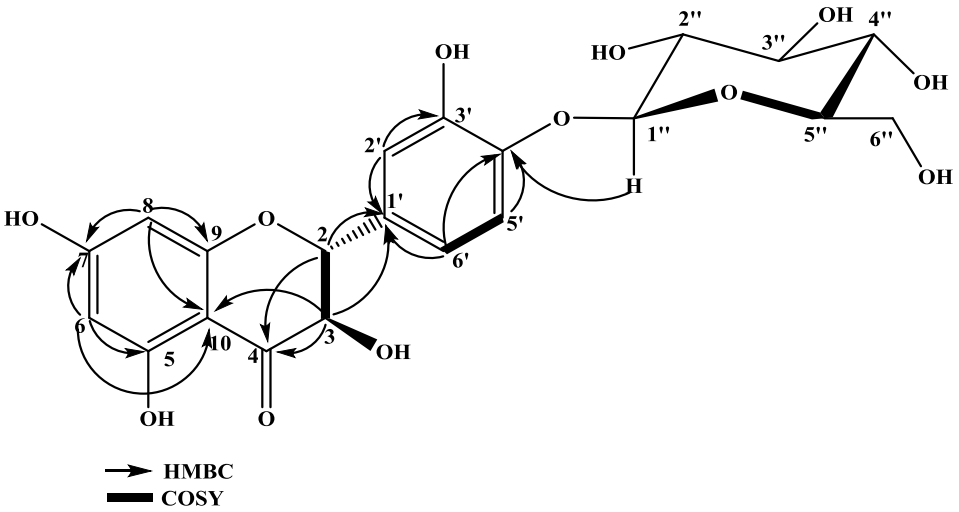

Fig. 3.43. HMBC and COSY correlations of compound AU 10

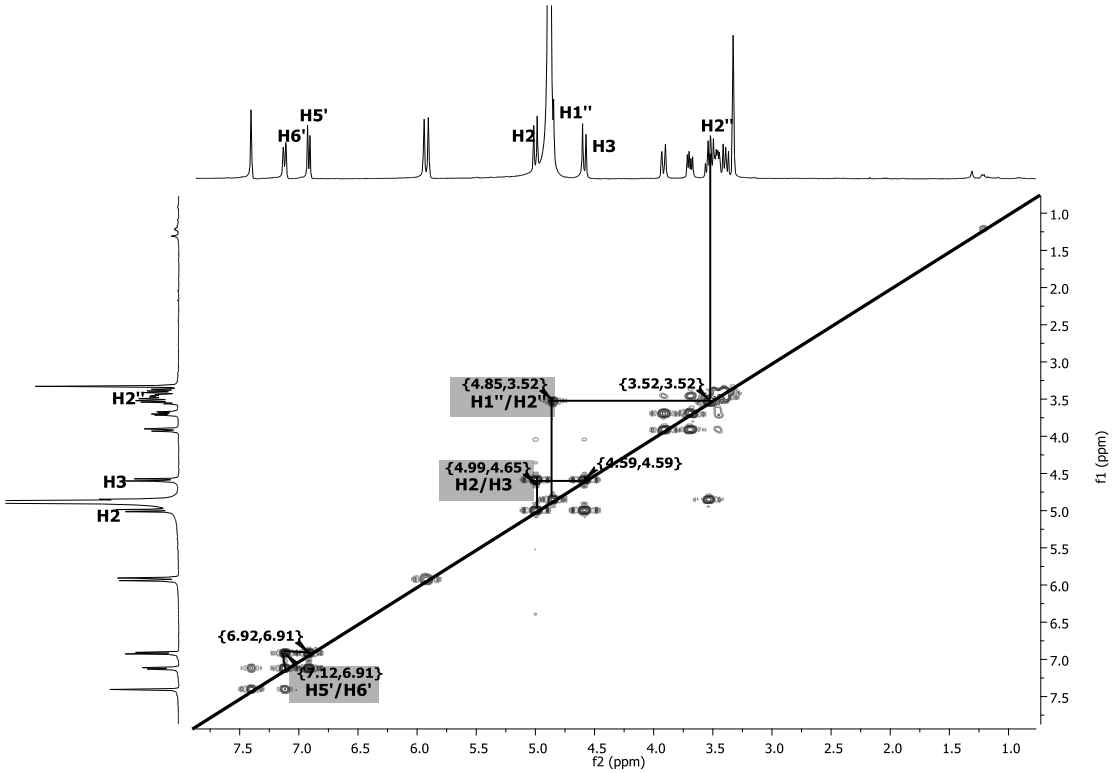

Fig. 3.44. COSY spectrum of compound AU 10

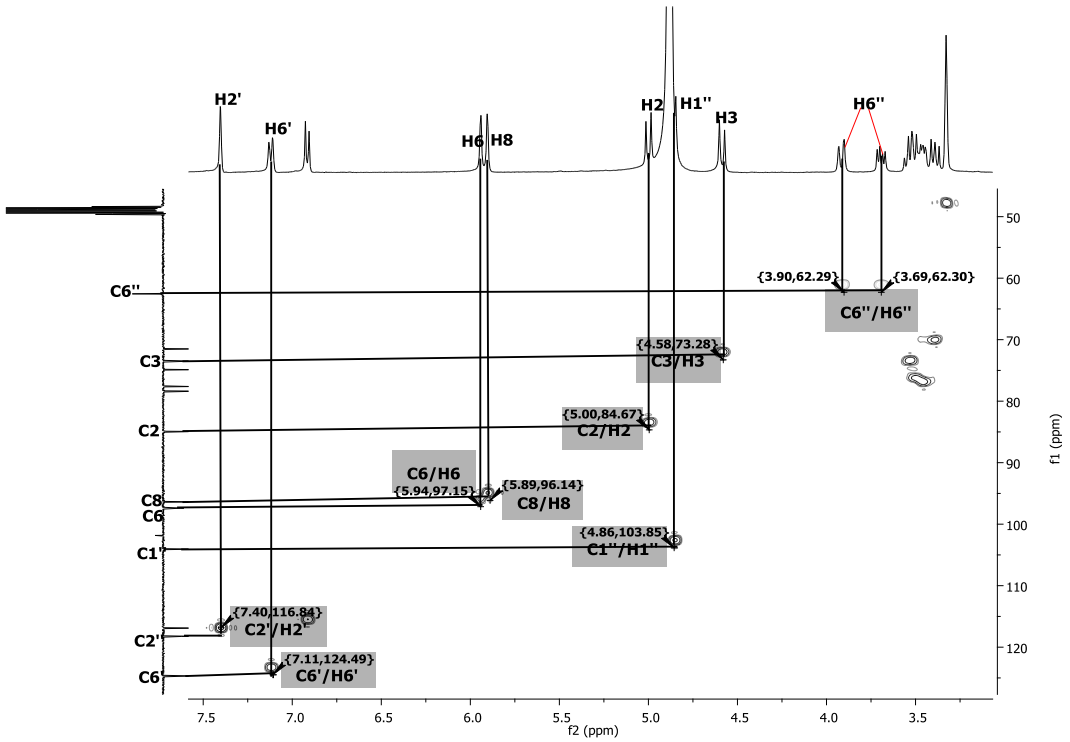

Fig. 3.45. HSQC spectrum of compound AU 10

Table 3.16. ^{1}H and ^{13}C NMR data of compound AU 10

Atom No.	Oh 2014 DMSO + D_2O δc	Xu 2011 DMSO δc	AU 10 CD3OD δc (m)	AU 10 CD3OD δ_H (*J* in Hz)	Xu 2011 DMSO δ_H (*J* in Hz)	Oh 2014 CD3OD + D_2O δ_H (*J* in Hz)
2	83.4	82.68	84.9 (CH)	4.98 d (11.4)	5.82 (d, 11.2)	5.24 d (9.0)
3	72.4	71.51	73.5 (CH)	4.57 d (11.4)	5.04 (d, 11.2)	4.88 d (9.0)
4	196.2	197.67	198.4 (C)			
5	169.1	166.92	168.9 (C)			
6	97.3	96.11	97.4 (CH)	5.94 (s)	5.86 (d, 1.8)	5.89 (s)
7	165.6	163.35	165.3 (C)			
8	95.4	95.08	96.3 (CH)	5.91 (s)	5.90 (d, 1.8)	5.89 (s)
9	164.1	162.48	164.4 (C)			
10	102.4	100.48	101.8 (C)			
1’	128.9	131.83	130.0 (C)			
2’	116.0	115.64	118.2 (CH)	7.40 (d, 1.4)	6.96 (d, 1.8)	6.96 (d, 1.8)
3’	146.0	146.55	146.5 (C)			
4’	147.0	145.61	149.0 (C)			
5’	116.3	116.36	116.9 (CH)	6.91 (d, 8.4 Hz)	7.12 (d, 8.4)	6.75 (d, 8.1)
6’	121.2	119.33	124.6 (CH)	7.11 (dd, 1.4, 8.4 Hz)	6.87 (dd, 8.4, 1.8)	6.80 (dd, 1.8, 8.1)
1’’	104.6	104.24	104.1 (CH)	4.85 d (7.58)	4.91 d (7.1)	4.67 (d, 7.8)
2’’	75.4	74.87	74.9 (CH)	3.51 (m)	3.60 (m)	3.10-3.21(m)
3’’	77.7	77.63	77.6(CH)	3.49 (m)	3.52 (m)	3.10-3.21(m)
4’’	71.5	71.33	71.5 (CH)	3.26 (m)	3.50 (m)	3.10-3.21(m)
5’’	78.0	78.37	78.4 (CH)	3.37 (m)	3.56 (m)	3.10-3.21(m)
6’’	62.9	62.01	62.6 (CH_2)	3.90 dd (1.50, 11.76) 3.67 dd (5.91, 11.76)	3.82 (dd, 11.8, 2.1) 3.99 (dd, 11.8, 5.4)	3.80 (dd, 1.2, 11.7) 3.57 (dd, 3.9, 11.7)

Table 3.17. Compound AU 11(eriodictyol 4'-*O*-β-D-glucopyranoside)

(2S)-5,7,3'-trihydroxyflavanone-4'-O-β-D-glucopyranoside	
Synonyms	Eriodictyol 4'-*O*-β-D-glucopyranoside
Sample codes	AU 11
Sample amount	6 mg
Physical Description	Yellow needles
Molecular formula	$C_{21}H_{22}O_{11}$
Molecular Weight	450 mg/mol
Optical Rotation $[\alpha]_D^{24.4}$	-12.11 (c 0.33 in MeOH)
IR:($CHCl_3$)	3349, 1643, 1523, 1468, 1286, 1173, 1082, 801 cm^{-1}

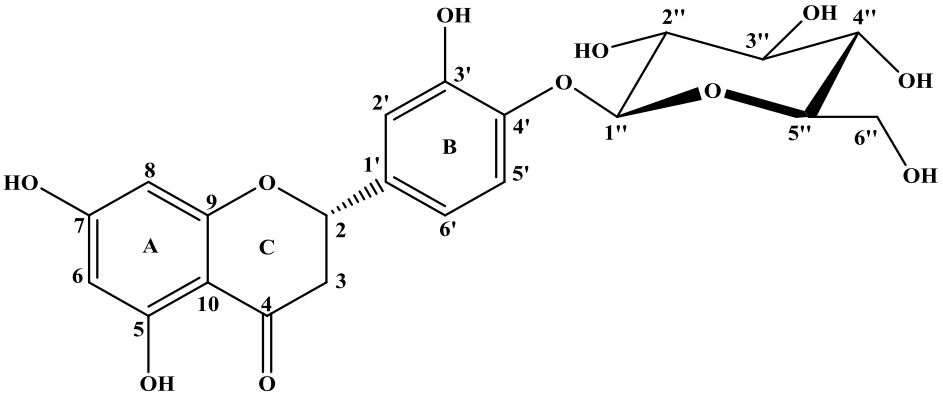

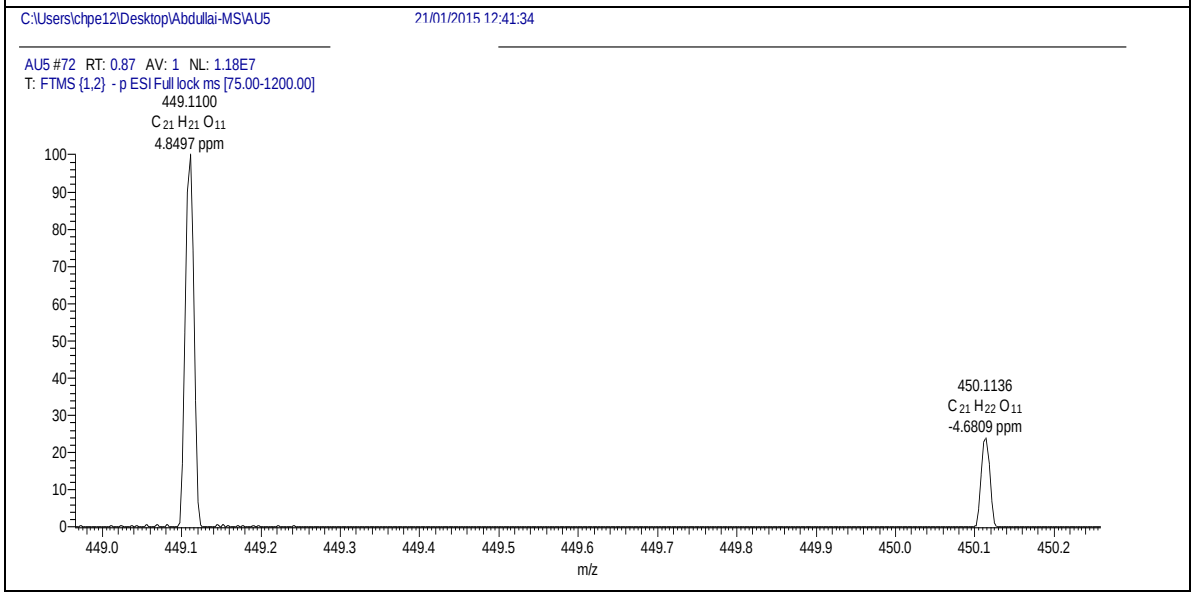

Compound AU 11 was obtained as yellow needles, $[\alpha]_D^{24.4}$ -12.11 (MeOH: c 0.33). It showed a quasimolecular ion peak due to $[M - H]^-$ in the negative ESI-HRMS at *m/z* 449.1100 (Calcd for 449.1083). The ^{13}C NMR spectrum (Fig. 3.46) showed twenty one carbon signals, and the DEPT spectrum showed that these comprised of two methylene, eleven methine and eight quaternary carbon. The IR spectrum of this compound showed bands at 3349 (broad, O-H stretching), 1643 (C=C stretching), 1468 (C-H deformation), 1173, 1082 (C-O stretching) and 801 (C-H out of plane deformation) cm^{-1}, see appendix I. The methylenic protons of position 3

on ring C appeared in the ^{1}H NMR spectrum (Fig. 3.46) at δ_H 2.72 and δ_H 3.14 which in the COSY spectrum (Fig. 3.49), coupled with H-2 δ_H 5.35 (dd, 2.54, 12.69 Hz). The spectrum also showed two meta-coupled aromatic doublets at δ_H 5.90 (d, 1.61 Hz) and 5.92 (d, 1.61 Hz) allotted to the A-ring and the three aromatic proton signals at δ_H 7.35 (d, 1.95 Hz, H-2'), 6.89 (d, 8.40 Hz, H-5') and 7.09 (dd, 1.95, 8.40 Hz, H-6') assigned to B-ring indicating a 1,2,4-trisubstituted aromatic ring. In addition, one anomeric proton δ_H 4.82 (d, 7.18 Hz, H-1'') was also observed and based on this coupling constant, the configuration of the sugar moiety was determined to be β-oriented indicating a β-glycosyl moiety. The GC analysis of the TMS derivatives of AU 11 hydrolysates showed that this compound contains D-glucose. In the HMBC spectrum, the proton at δ_H 4.82 (H-1'', d, J=7.18 Hz) was linked to C-4' (δ_C 145.27), signifying that the β-D-glucose moiety was located at C-4'. Comparison of the NMR values (Table 3.18) with those published, confirmed eriodictyol 4'-*O*-β-D-glucopyranoside as the compound isolated.

This compound has been isolated from the flowers of *Carthamus tinctorius* (Lie et al 2014), leaves of *Viscum coloratum* and the antioxidant activities of this compound based on their scavenging effects on hydroxyl radicals and superoxide anion radicals was reported to be 0.18 and 0.53 µg/ml, respectively (Yao et al., 2006).

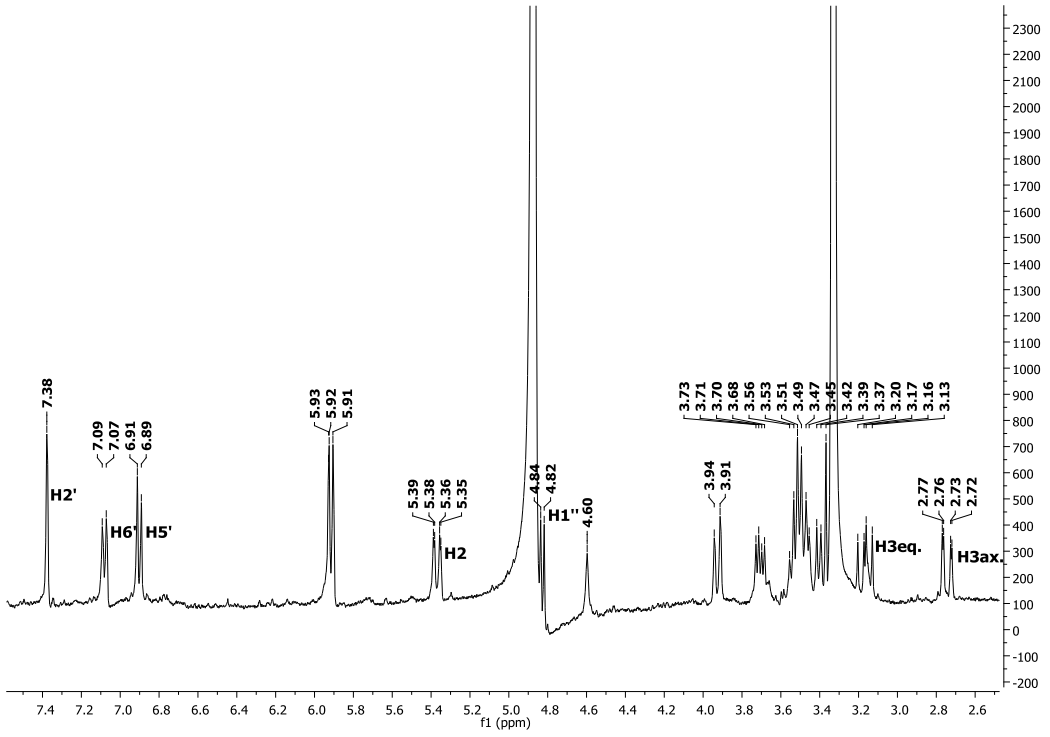

Fig. 3.46. ^{1}H NMR spectrum of AU 11

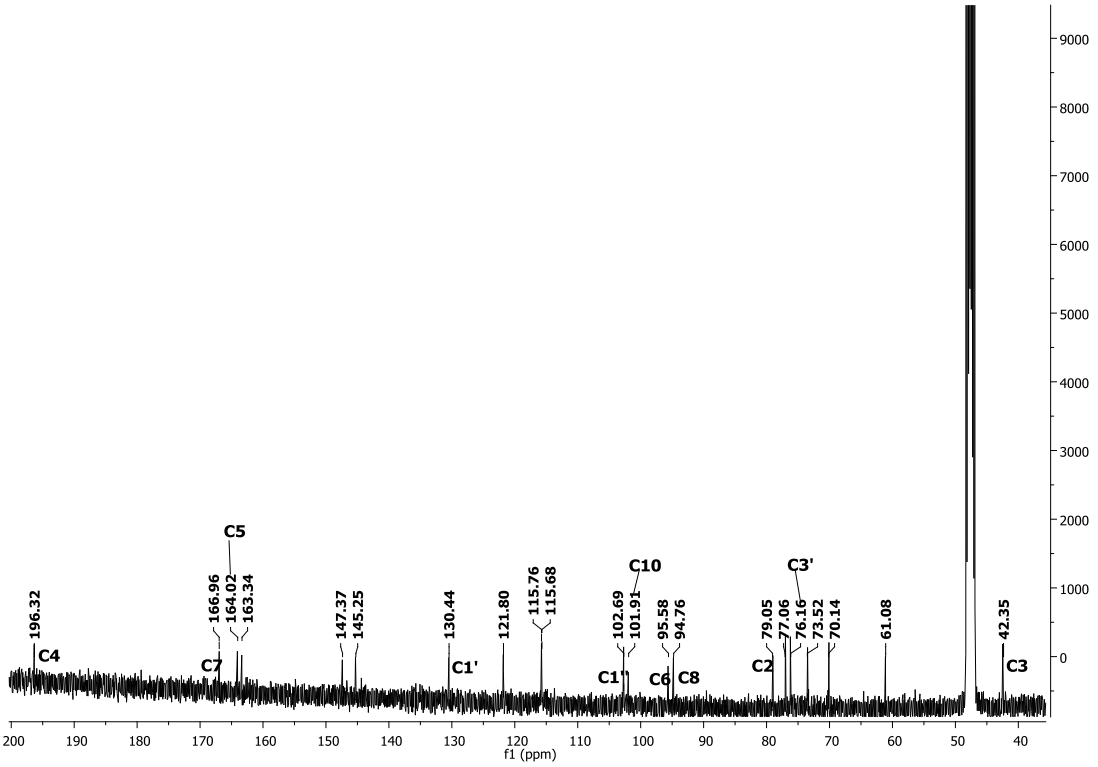

Fig. 3.47. ^{13}C NMR spectrum of compound AU 11

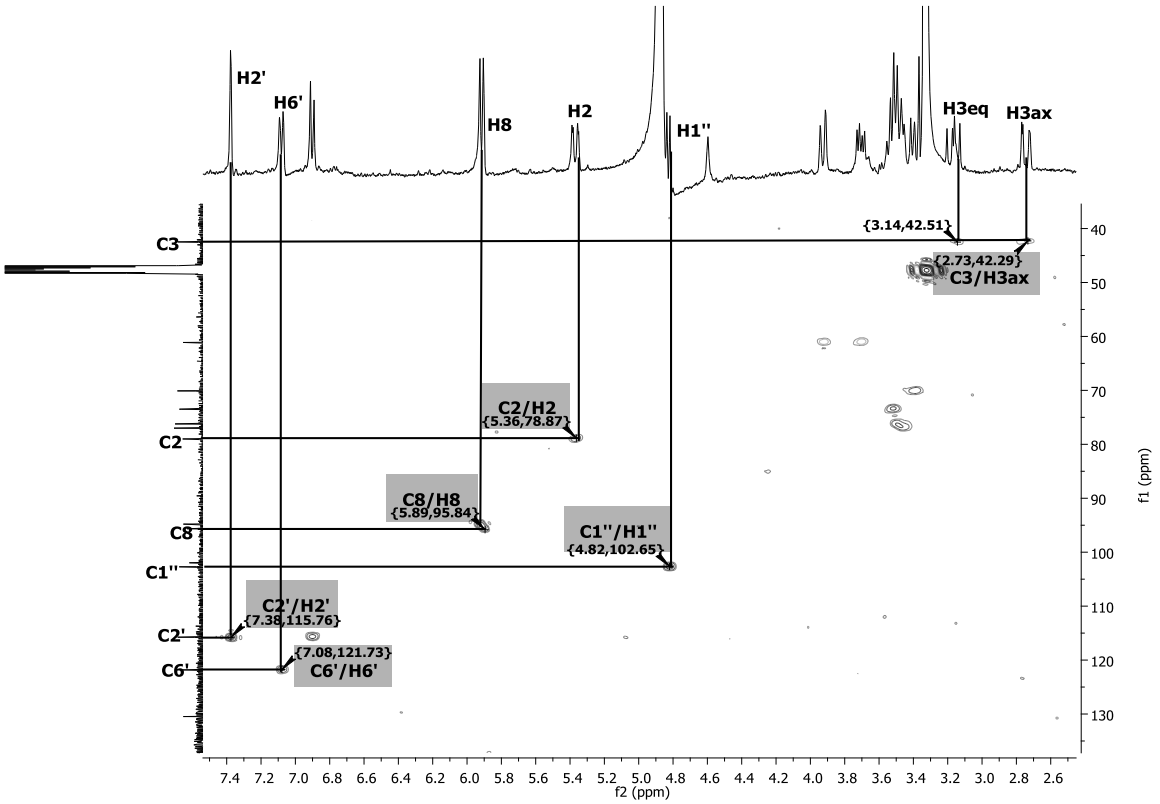

Fig. 3.48. HSQC spectrum of compound AU 11

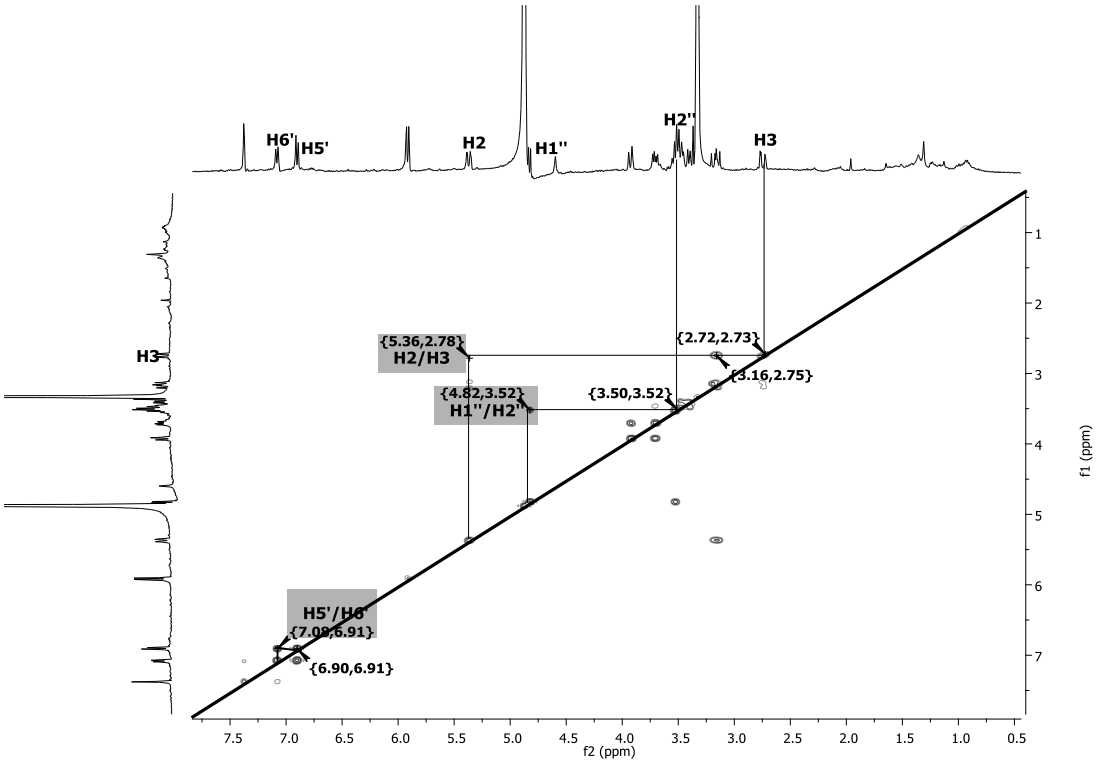

Fig. 3.49. COSY spectrum of compound AU 11

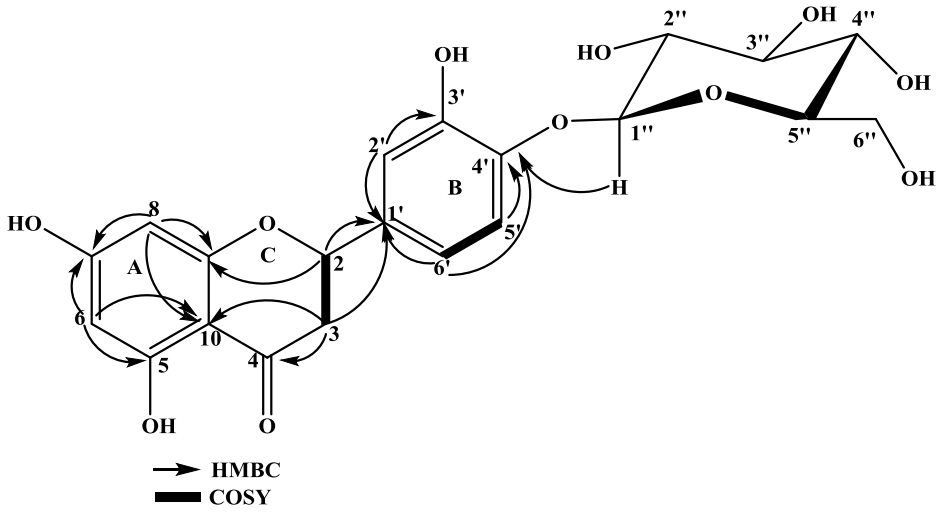

Fig. 3.50. HMBC and COSY correlation of compound AU 11

Table 3.18. ^{1}H and ^{13}C NMR data of compound AU 11

Atom No.	Liu 2014 DMSO δc	AU 11 CD_3OD δc (m)	AU 11 CD_3OD δ_H (m, *J* in Hz)	Liu 2014 DMSO δ_H (m, *J* in Hz)
2	78.1	79.1 (CH)	5.35 (dd, 2.54, 12.69)	5.44 (dd, 3.42, 12.36)
3	42.0	42.4 (CH_2)	2.72 (dd, 2.54, 17.09)	2.71 (dd, 3.42, 17.16)
3	42.0	42.5 (CH_2)	3.14 (dd, 12.65, 17.09)	3.21 (dd, 12.36, 17.16)
4	196.1	196.3 (C)		
5	163.4	164.0 (C)		
6	95.8	96.8 (CH)	5.92 (d, 1.61)	5.80 (d, 2.10)
7	166.6	167.1 (C)		
8	95.0	96.0 (CH)	5.90 (d, 1.61)	5.89 (d, 2.10)
9	162.7	163.3 (C)		
10	101.8	101.9 (C)		
1’	133.2	130.4 (C)		
2’	114.4	115.8 (CH)	7.35 (d, 1.95)	6.95 (d, 2.04)
3’	146.7	147.3 (C)		
4’	145.4	145.3 (C)		
5’	116.6	115.7 (CH)	6.89 (d, 8.40)	7.12 (d, 8.22)
6’	117.7	121.8 (CH)	7.09 (dd, 1.95, 8.40)	6.85 (dd, 2.04, 8.22)
1’’	102.2	102.7 (CH)	4.82 (d, 7.18)	4.69 (d, 7.56)
2’’	73.3	73.5 (CH)	3.53 (m)	3.46 (m)
3’’	75.8	76.2 (CH)	3.50 (m)	3.46 (m)
4’’	79.8	70.1 (CH)	3.45 (m)	3.40 (m)
5’’	77.2	77.1 (CH)	3.39 (m)	3.40 (m)
6’’	60.7	61.1 (CH_2)	3.68 (dd, 1.95, 12.01)	3.71 (dd, 3.42, 11.7)
			3.91 (dd, 5.91, 12.01)	

Table 3.19. Compound AU 12 (Quercetin)

2-(3,4-dihydroxyphenyl)-3,5,7-trihydroxy-4*H*-chromen-4-one	
Synonyms	Quercetin
Sample codes	AU 12
Sample amount	13 mg
Physical Description	Yellow needles
Molecular formula	$C_{15}H_{10}O_7$
Molecular Weight	302 g/mol
Optical Rotation $[\alpha]_D^{24.4}$	-8.15 (c 0.33 in MeOH)
IR:($CHCl_3$)	3376, 1659, 1562, 1513, 1463, 1317, 1209, 1163, 807 cm^{-1}

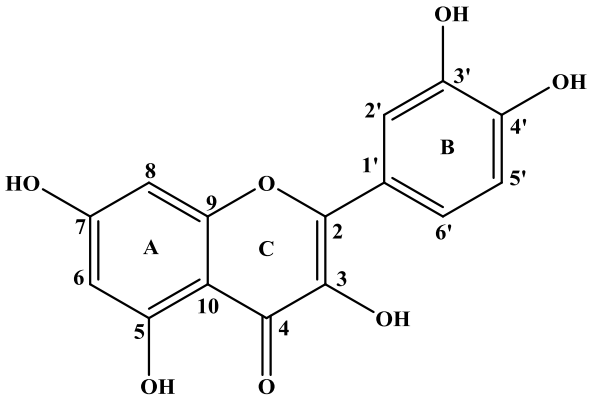

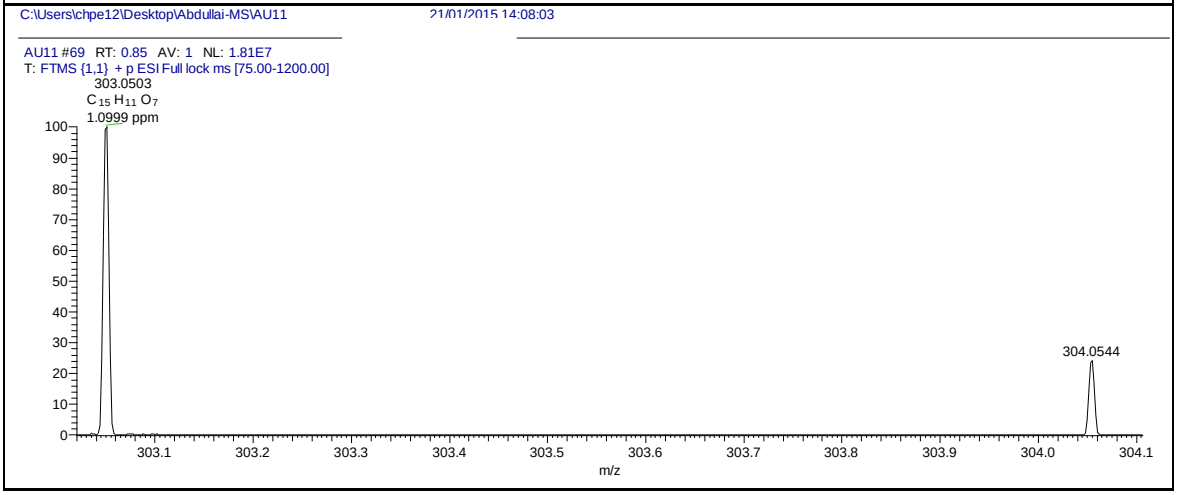

Compound AU 12 (13 mg) was obtained as yellow needles $[\alpha]_D^{24.4}$ -8.15 (MeOH: c 0.33). It has a molecular formula of $C_{15}H_{10}O_7$ which was established on the basis of ESI-HRMS at *m/z* 303.0503 $[M + H]^+$ (Calcd for 303.0506). The IR spectrum of this compound showed bands at 3376 (broad, O-H stretching), 1659 (C=C stretching), 1463 (C-H deformation), 1163 (C-O stretching) and 807 (C-H out of plane deformation) cm^{-1}, see appendix I. The DEPT spectrum (Fig. 3.52) showed fifteen carbon signals, which consisted of five methine and ten quaternary carbons.

For ring B, the ^{1}H NMR spectrum (Fig. 3.51) showed three aromatic protons signals at δ_H 7.75 (d, 2.2 Hz, H-2'), δ_H 6.89 (d, 8.6 Hz, H-5') and δ_H 7.63 (dd, 2.2, 8.5 Hz, H-6') indicating a 1,2,3-trisubstituted aromatic ring in the form of an ABX spin-system. In the COSY spectrum (Fig. 3.55) these signals δ_H 7.63 (H-6') and δ_H 6.89 (d, 8.6 Hz, H-5') were mutually coupled, and similarly, the meta-coupled aromatic proton signals at δ_H 6.20 (d, 2.1 Hz) and δ_H 6.40 (d, 2.1 Hz) were assigned to H-6 and H-8 in the A-ring.

For ring C, the ^{13}C NMR spectrum showed resonances for the keto group at C-4 (δc 175.91) and its nature was further confirmed by long-range coupling observed in HMBC (Fig. 3.53), where the ring A methine protons H-6 (δ_H 6.20) correlated with C-5, C-7, C-8 and C-10 (δc 103.11); and H-8 (δ_H 6.40) correlated with C-4, C-6, C-7, C-9 and C-10 (δc 103.11).

Ring B was confirmed by the HMBC correlations of H-2' to C-1', C-3', C-4' and C-6' (δc 120.27); H-5' to C-1', C-2', C-3' and C-4' (δc 147.35); and H-6' to C-2', C-3' and C-4' (δc 147.35) (Fig. 3.54). On the basis of NMR data (Table 3.20), AU 12 was identified as quercetin and this was confirmed by comparison of its ^{1}H and ^{13}C NMR data with those reported in the literature (Kim et al., 2011; Wei et al., 2013).

This compound has been reported from the aerial part of *Achyrocline satureioides* (Lam) (Carini et al., 2015), and the whole plant and fruit of *Cayratia japonica*, it is reported to showed potent inhibitory effect against monoamine oxidase (MAO) activity at an IC_{50} value of 31.6 µg/ml (Han et al., 2007).

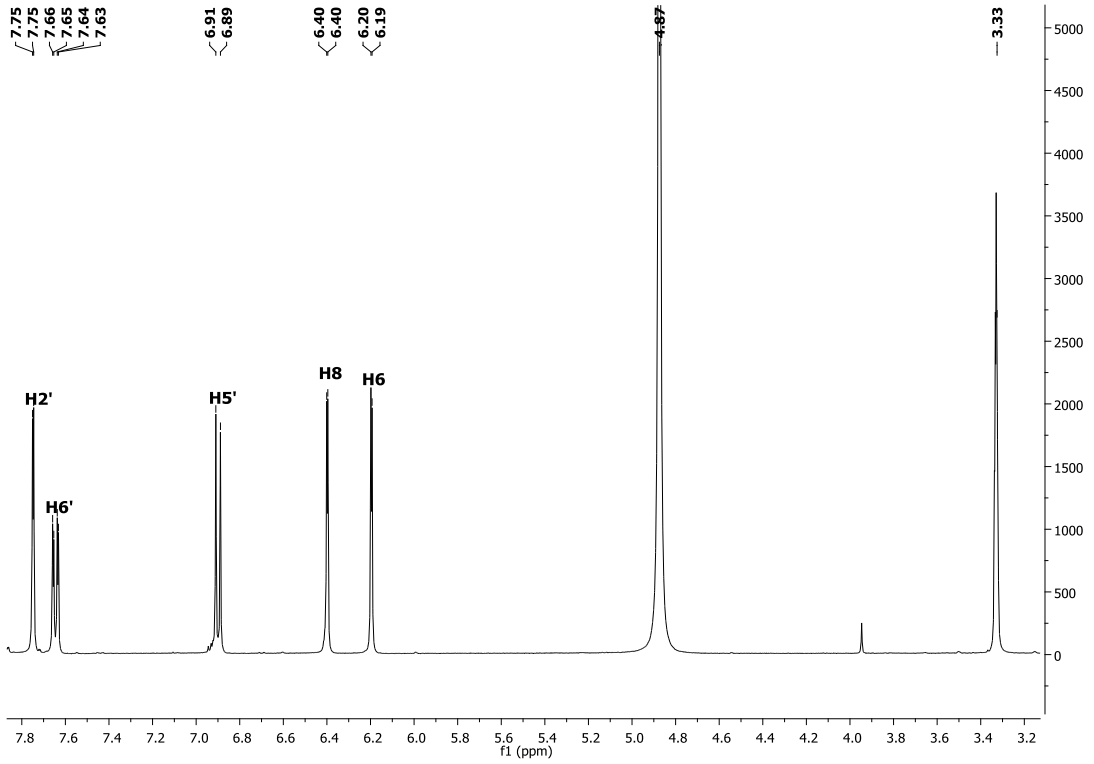

Fig. 3.51. [1]H NMR spectrum of compound AU 12

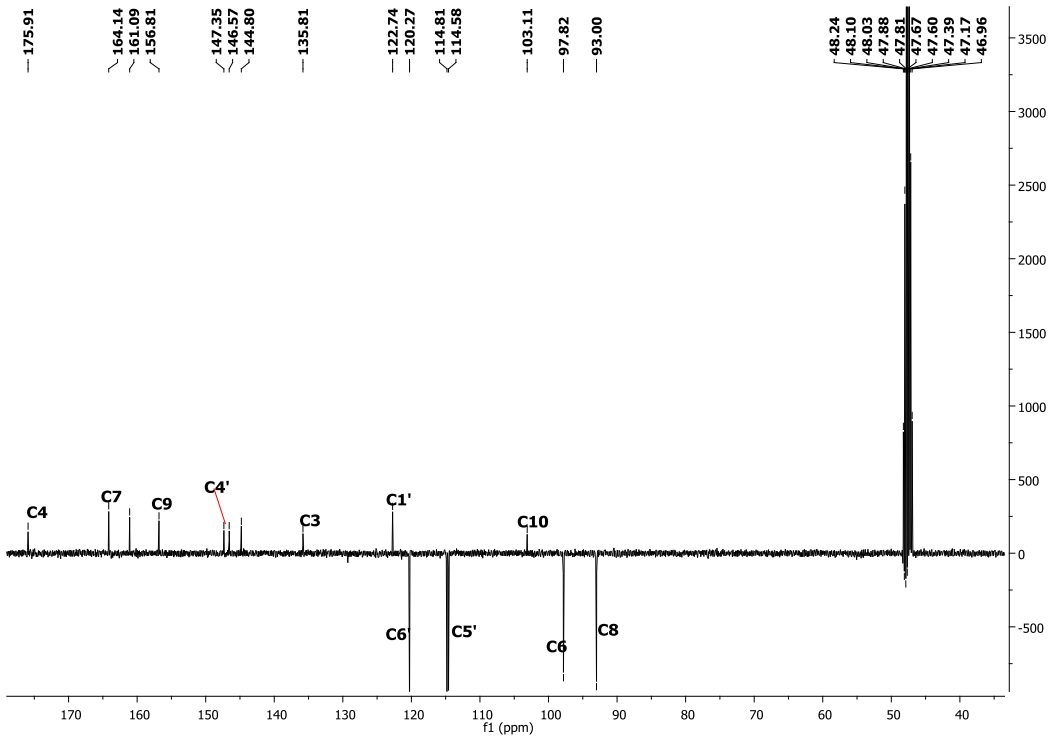

Fig. 3.52. DEPT spectrum of compound AU 12

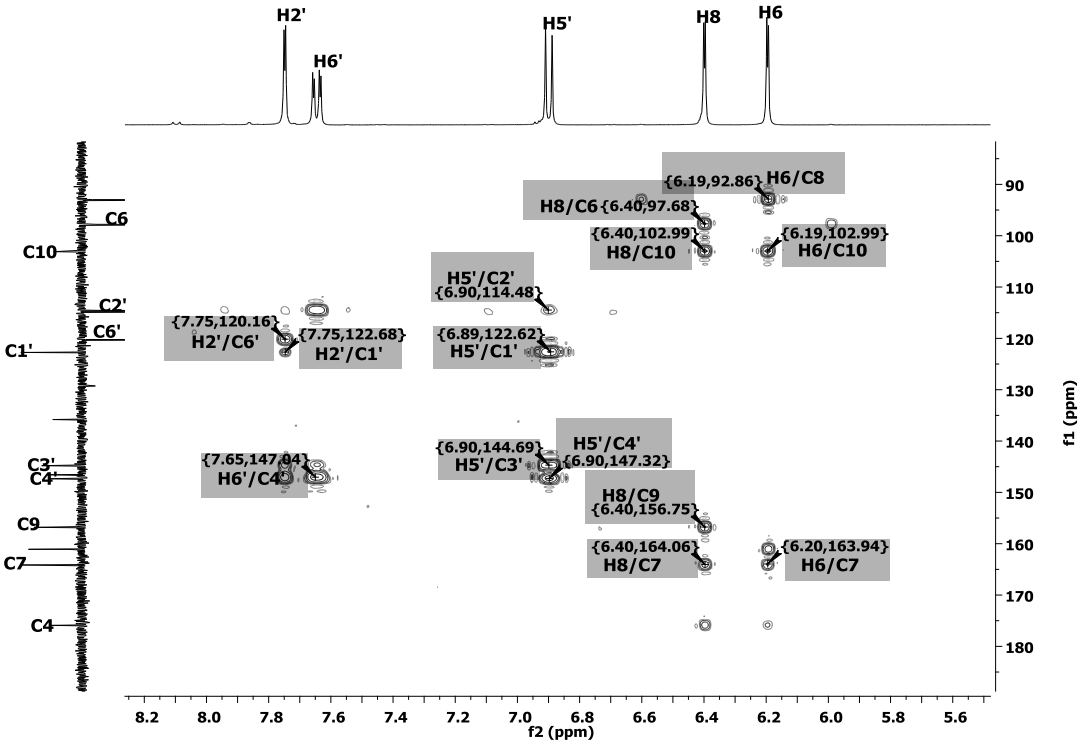

Fig. 3.53. HMBC spectrum of compound AU 12

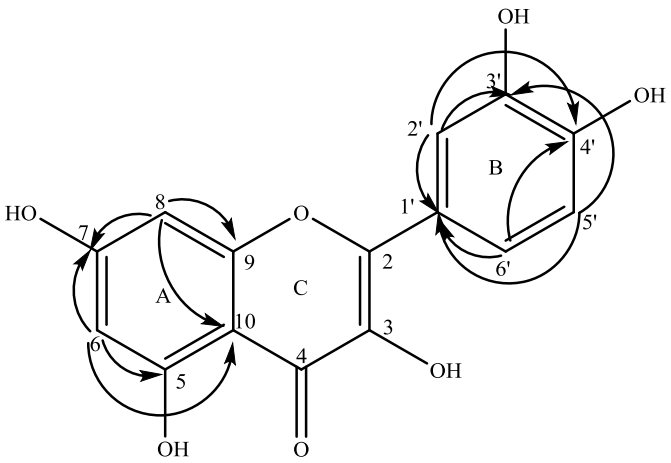

Fig. 3.54. HMBC correlations of compound AU 12

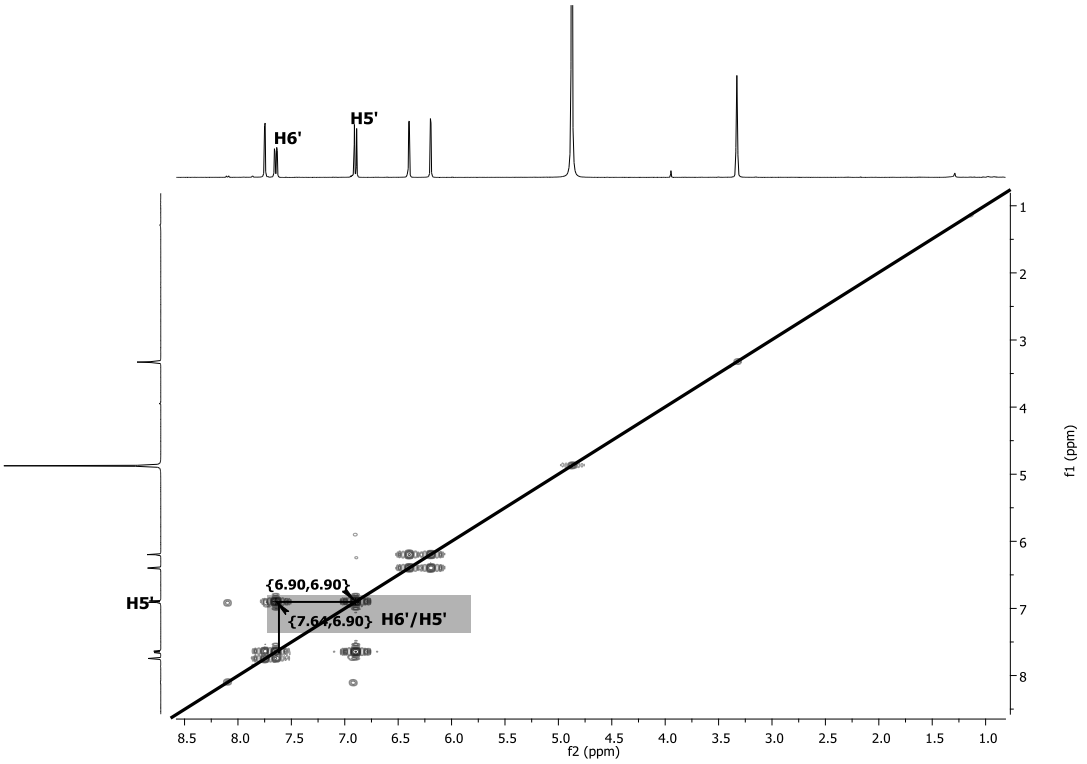

Fig. 3.55. COSY spectrum of compound AU 12

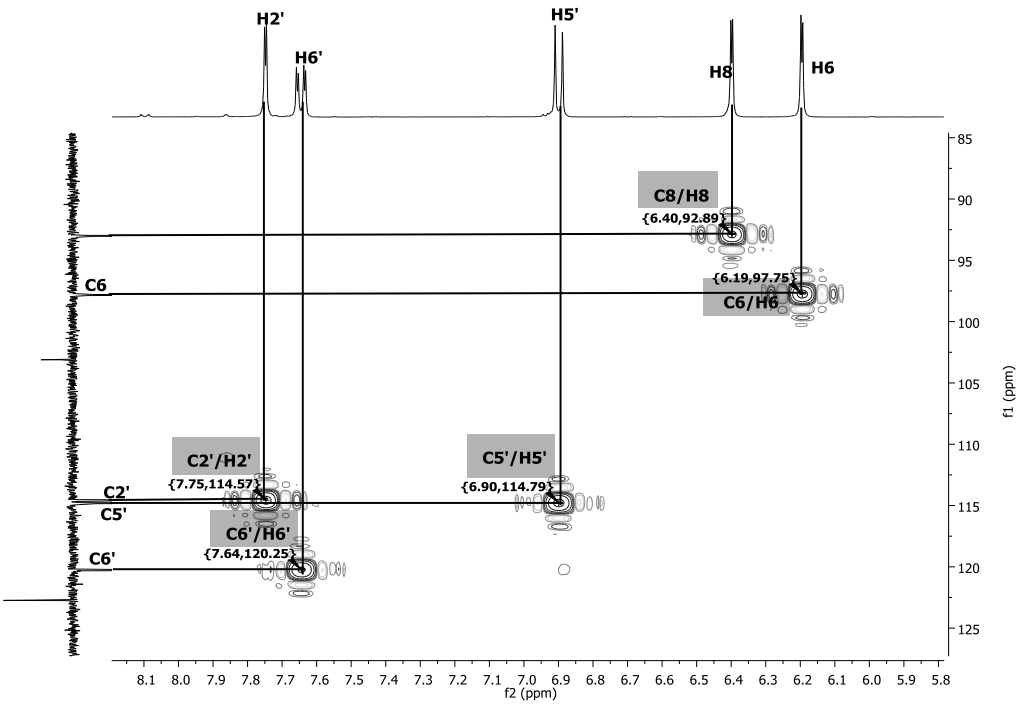

Fig. 3.56. HSQC spectrum of compound AU 12

Table 3.20. ^{1}H and ^{13}C NMR data of compound AU 12

Atom No.	Wei 2013 CD_3OD δ_C	Kim 2011 CD_3OD δ_C	AU 12 CD_3OD δ_C (m)	AU 12 CD_3OD δ_H (m, *J* in Hz)	Wei 2013 CD_3OD δ_H (m, *J* in Hz)	Kim 2011 CD_3OD δ_H (m, *J* in Hz)
2	146.7	146.99	146.57 (C)			
3	135.9	135.95	135.81 (C)			
4	176.0	176.05	175.91 (C)			
5	161.2	160.92	161.09 (C)			
6	97.9	98.38	97.82 (CH)	6.20 (d, 2.06)	6.16 (d, 2.3)	6.19 (d, 1.8)
7	164.3	164.09	164.14 (C)			
8	93.1	93.55	93.0 (CH)	6.40 (d, 2.06)	6.37 (d, 2.3)	6.41 (d, 2.4)
9	156.9	156.32	156.81 (C)			
10	103.2	103.21	103.11 (C)			
1’	120.3	122.15	122.74 (C)			
2’	114.6	115.80	114.58 (CH)	7.75 (d, 2.2)	7.71 (d,1.7)	7.68 (d, 2.4)
3’	144.9	145.26	144.80 (C)			
4’	146.0	147.91	147.35 (C)			
5’	114.9	116.39	114.81 (CH)	6.89 (d, 8.6)	6.86 (d, 8.5)	6.82 (d, 8.1)
6’	122.8	120.17	120.27 (CH)	7.63 (dd, 2.2, 8.5)	7.61 (dd, 1.7, 8.5)	7.55 (q, 2.4, 8.4)

Table 3.21. Compound AU 13 (Quercetin 3-*O*-β-D-glucopyranoside)

3',4'-dihydroxyphenyl-3,5,7-trihydroxyflavanone-3'- *O*-β-D-glucopyranoside	
Synonyms	Quercetin 3-*O*-β-D-glucopyranoside
Sample codes	AU 13
Sample amount	6 mg
Physical Description	Yellow needle
Molecular formula	$C_{21}H_{20}O_{12}$
Molecular Weight	464 g/mol
Melting Point	226-242 °C
Optical Rotation $[\alpha]_D^{24.4}$	-11.31 (c 0.33 in MeOH)
IR:($CHCl_3$)	3392, 1627, 1521, 1466, 1286, 1197,1023,760,669 cm^{-1}

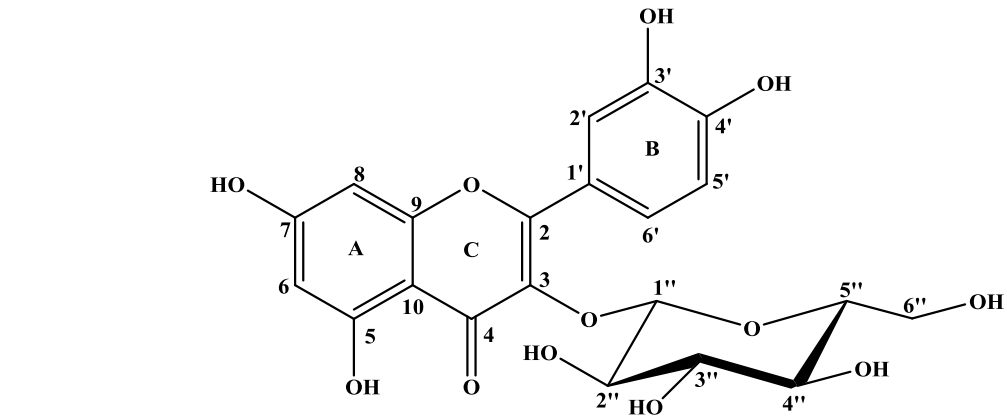

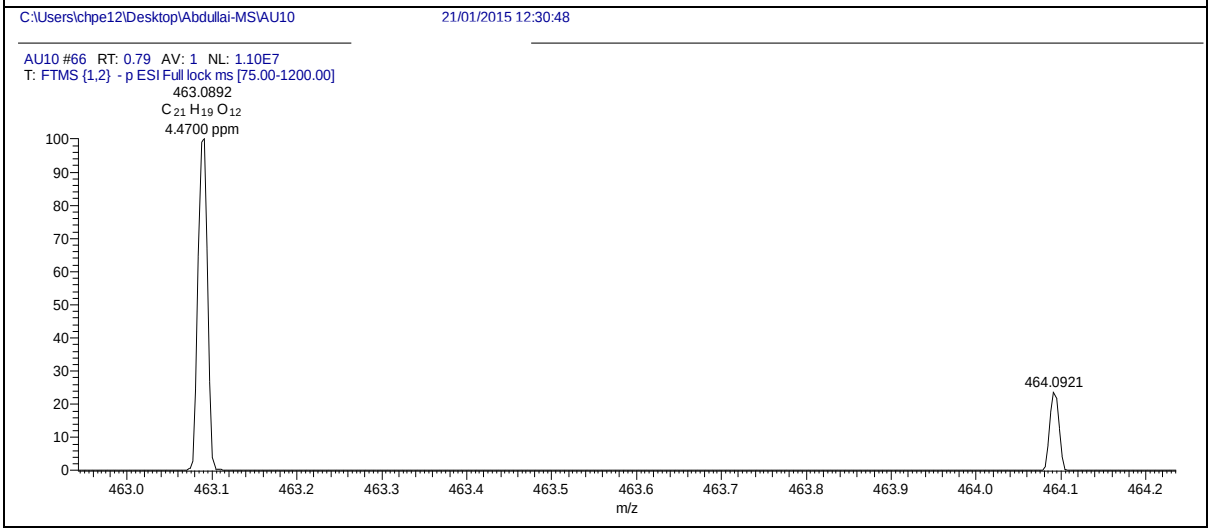

Compound AU 13 (6 mg) was obtained as yellow needles, $[\alpha]_D^{24.4}$ -11.31 (c 0.33 in MeOH). It has a molecular formula of $C_{21}H_{20}O_{12}$ which was established on the basis of ESI-HRMS at m/z 463.0892 $[M-H]^-$ (Calcd for 463.0876). The IR spectrum of this compound is similar to AU 12, see appendix I. The DEPT spectrum (Fig. 3.58) showed twenty one carbon signals, which consist of one methylene, ten methine and ten quaternary carbon atoms. The comparison of the ^1H and ^{13}C NMR data (Table 3.22) with that of AU 12 revealed close similarity except for the presence of signals for glucose moiety. Hence, the aglycone is suggested to be a quercetin. The

spectrum showed one anomeric proton at δ_H 5.27 (d, 7.5 Hz, H-1’’), indicating a β-glycosyl moiety based on the coupling constant.

In the COSY spectrum (Fig. 3.61), the correlation between the anomeric proton signal δ_H 5.27 (d, 7.5 Hz, H-1’’) with δ_H 3.50 (m) assigned to position 2’’ was observed. The remaining ^{13}C NMR data for glucose moiety are consistent with those of glucose. The attachment of the glucose unit at C-3 (δc 135.62) was apparent from the H-1’’ to C-3 HMBC connectivity (Fig. 3.59 and 3.60). The NMR data (Table 3.22) were thus consistent with quercetin-3-*O*-β-D-glucoside, and this was confirmed by comparison of its ^1H and ^{13}C NMR data with those reported in the literature.

This compound has been reported from the fruit of *Vitis accessions* (Hilbert et al., 2015), bark of *Acer barbinerve* (Kwom and Bae, 2011), and whole plants of *Euphorbia humifusa* (Kang et al., 2012). The antioxidant activities of this compound based on their free radical scavenging effects on 2,2-diphenyl-1-picrylhydrazyl-hydrate (DPPH) and ABTS [2,2’-azinobis(3-ethylene benzothiazolin-6-sulfonic acid)] colorimetric assays was assessed, and was reported to displayed strong activity at IC_{50} value of 4.10 and 5.00 µg/ml, respectively (Conqueiro et al., 2013).

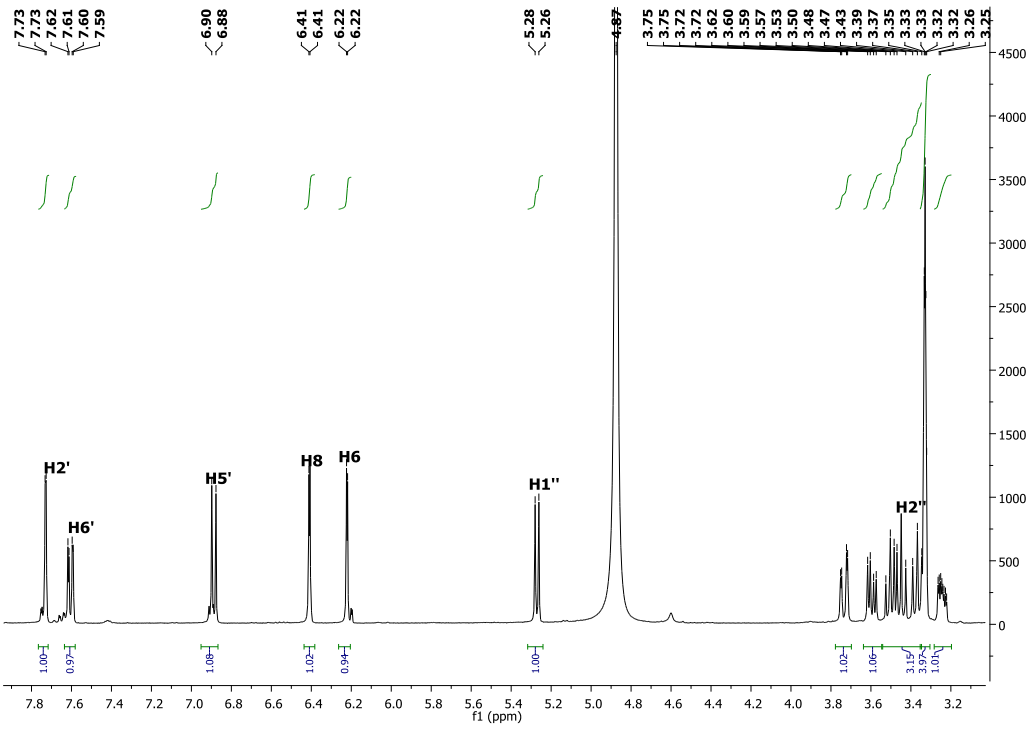

Fig. 3.57. ^1H NMR spectrum of compound AU 13

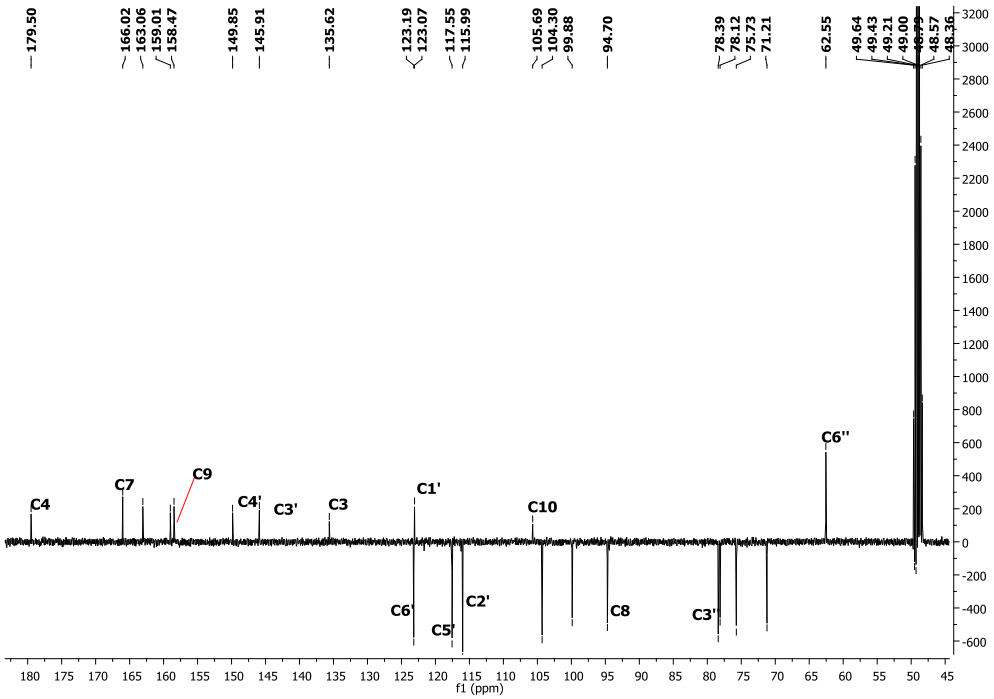

Fig. 3.58. DEPT spectrum of compound AU 13

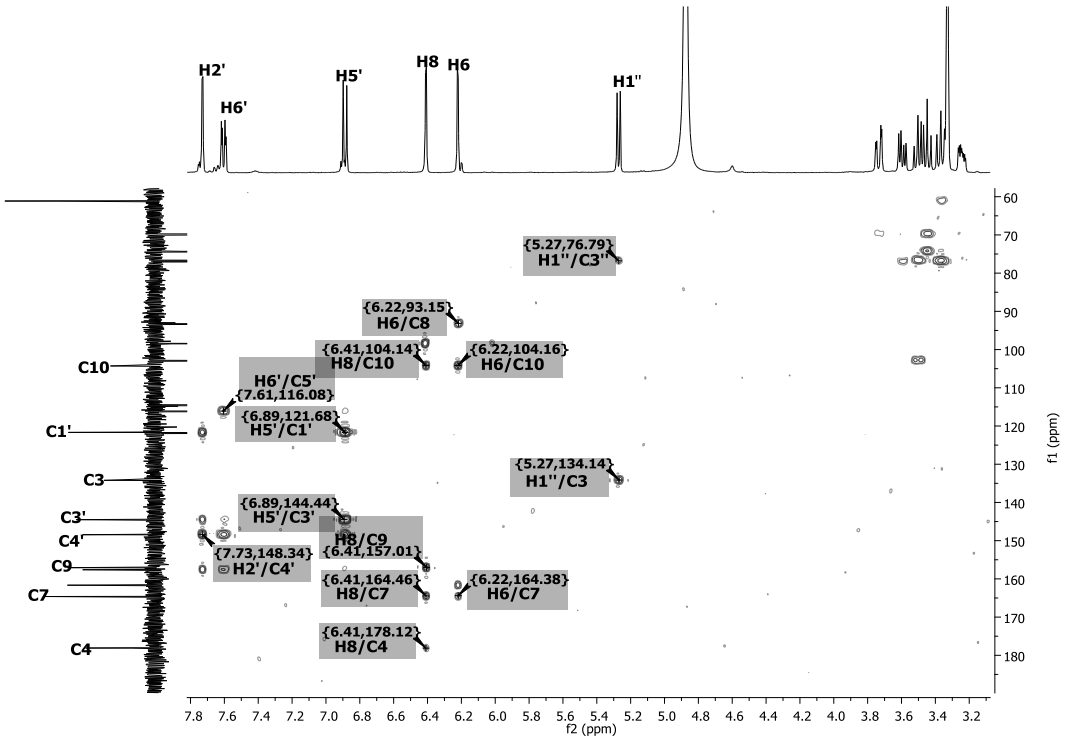

Fig. 3.59. HMBC spectrum of compound AU 13

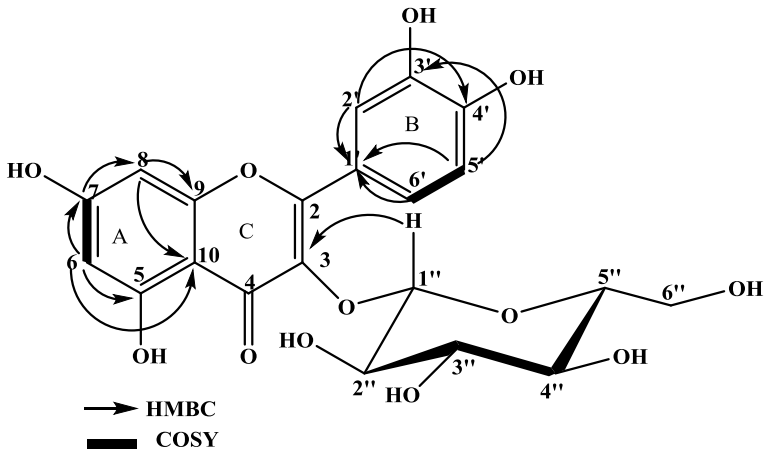

Fig. 3.60. HMBC and COSY correlations of compound AU 13

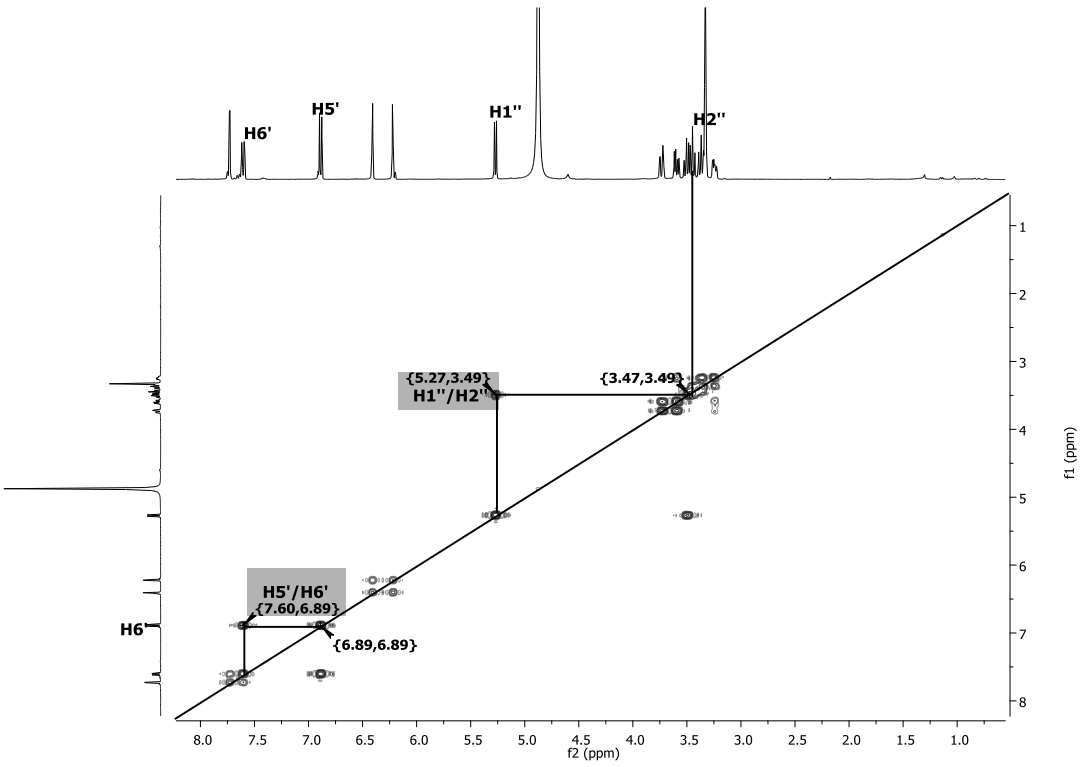

Fig. 3.61. COSY spectrum of compound AU 13

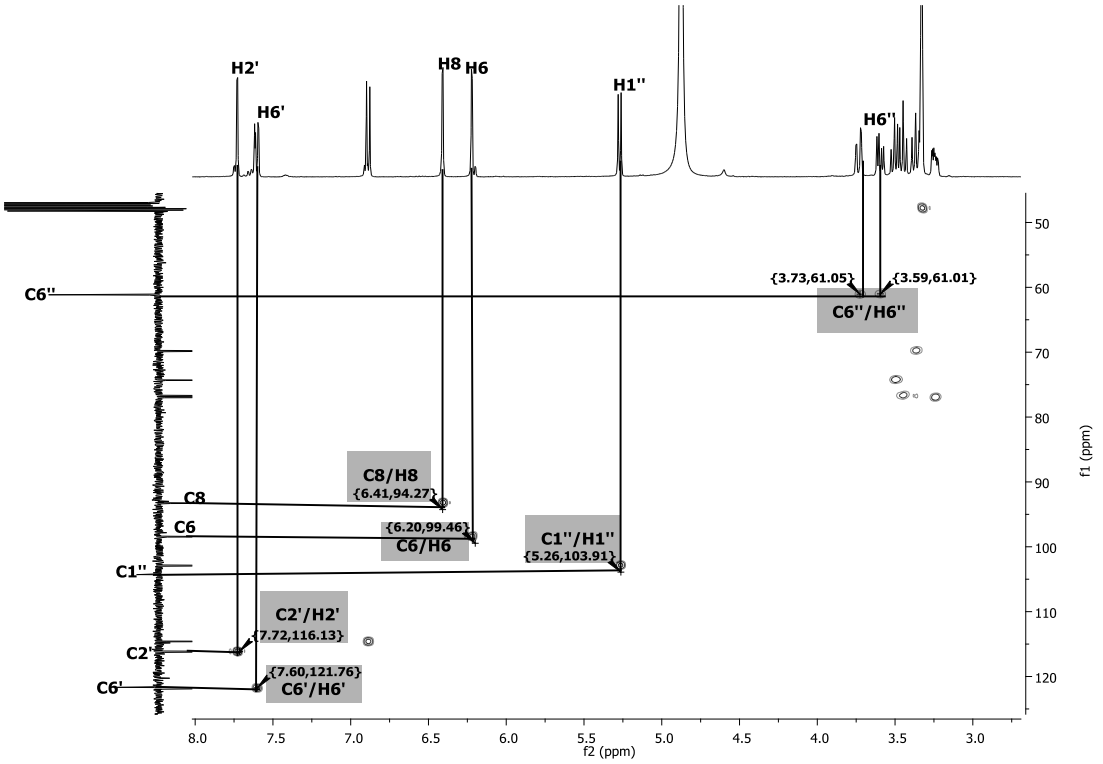

Fig. 3.62. HSQC spectrum of compound AU 13

Table 3.22. ^{1}H and ^{13}C NMR data of compound AU 13

Atom No.	Kwom and Bae, 2011 CD_3OD δ_C	AU 13 CD_3OD δ_C (m)	AU 13 CD_3OD δ_H (m, *J* in Hz)	Hilbert 2015 CD_3OD δ_H (m, *J* in Hz)	Kwom and Bae 2011 CD_3OD δ_H (m, *J* in Hz)
2	159.04	159.01 (C)			
3	135.66	135.62 (C)			
4	179.52	179.50 (C)			
5	163.06	163.06 (C)			
6	99.91	99.60 (CH)	6.22 (d, 2.1)	6.21 (d, 2.1)	6.20 (d, 1.2)
7	166.02	166.02 (C)			
8	94.75	94.42 (CH)	6.41 (d, 2.1)	6.40 (d, 2.1)	6.40 (d, 1.2)
9	158.48	158.47 (C)			
10	105.75	105.42 (C)			
1’	123.10	123.07 (C)			
2’	116.03	115.99 (CH)	7.73 (d, 2.1)	7.71 (d, 2.1)	7.52 (d, 1.9)
3’	145.93	145.91 (C)			
4’	149.88	149.85(C)			
5’	117.60	117.55 (CH)	6.88 (d, 8.5)	6.87 (d, 8.5)	6.82 (d, 8.5)
6’	123.24	123.19 (CH)	7.59 (dd, 2.1, 8.5)	7.59 (dd, 2.1, 8.5)	7.67 (dd, 1.9, 8.5)

1''	104.35	104.30 (CH)	5.26 (d, 7.5)	5.25 (d, 7.5)	5.25 (d, 7.4)
2''	75.76	75.73 (CH)	3.50 (m)	3.50-3.20 (m)	3.22-3.71 (m)
3''	78.41	78.39(CH)	3.34 (m)	3.50-3.20 (m)	3.22-3.71 (m)
4''	71.24	71.21 (CH)	3.23 (m)	3.50-3.20 (m)	3.22-3.71 (m)
5''	78.14	78.12 (CH)	3.58 (m)	3.50-3.20 (m)	3.22-3.71 (m)
6''	62.58	62.55 (CH_2)	3.72 (dd, 2.3, 11.8)	3.71 (dd, 2.5, 11.9)	3.22-3.71 (m)
			3.57 (dd, 5.3, 11.8)	3.57 (dd 5.3, 11.9)	

Table 3.23. Compound AU 14 (naringenin).

5,7-dihydroxy-2-(4-hydroxyphenyl)chroman-4-one	
Synonyms	Naringenin
Sample codes	AU 14
Sample amount	13 mg
Physical Description	White needles
Molecular formula	$C_{15}H_{12}O_5$
Molecular Weight	272 g/mol
Melting Point	247-251
Optical Rotation $[\alpha]_D^{24.4}$	-6.51 (c 0.33 in MeOH)
IR:($CHCl_3$)	3433, 1638, 1518, 1464, 1160, 830 cm^{-1}

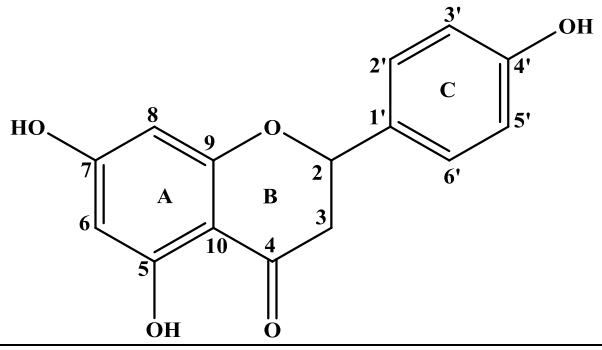

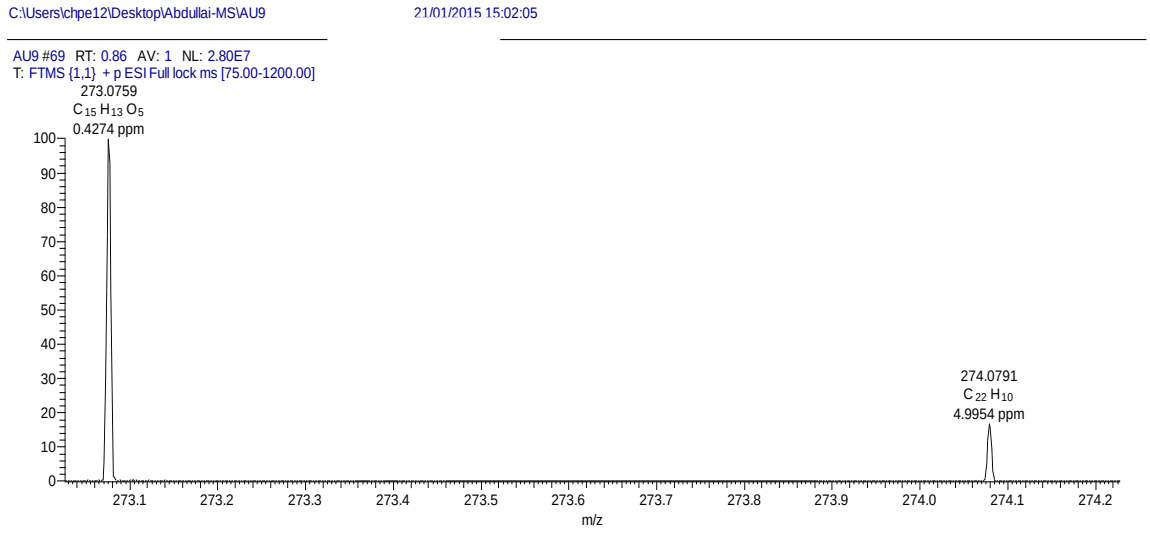

Compound AU 14 (13 mg) was obtained as white needles, $[\alpha]_D^{24.4}$ -6.51 (c 0.33 in MeOH). The molecular formula was deduced as $C_{15}H_{12}O_5$ from its quasimolecular ion peak which was established on the basis of ESI-HRMS at *m/z* 273.0759 $[M + H]^+$ (Calcd for 273.0764). The IR spectrum showed important bands at 3433, 1638, 1518 and 1160 cm^{-1} corresponding to the presence of O-H, C=C, C=O and C-O functional groups, see appendix I. The DEPT spectrum (Fig. 3.64) exhibited fifteen carbon signals, corresponding to one methylene, seven methine, seven quaternary carbon, of which were six olefinics and five oxygen bound carbon.

For ring C, the ^{1}H NMR spectrum (Fig. 3.63) showed that proton H-2 was split by H-$3_{a\&b}$ resulting in a doublet of doublet at δ_H 5.34 (dd, 3.0, 12.9 Hz), and H-3 was split by H-2 yielding doublet of doublet at δ_H 2.70 (dd, 2.9, 17.1 Hz) and δ_H 3.12 (dd, 12.4, 17.1 Hz), indicating the characteristic of a flavanone. In the COSY spectrum (Fig. 3.67), the methylene protons of ring C, H-3 coupled with H-2.

In ring B, the ^{1}H NMR signals is a characteristic set of two "doublets" (d, 8.5 Hz) integrating for 2H each, indicative of the AA'BB' spin system of 1,4-disubstituted aromatic ring'. Similarly, the meta-coupled aromatic proton signals at δ_H 5.96 (br s) and δ_H 5.93 (br s) assigned position H-6 and H-8 correspond to A-ring. These positions were further confirmed by long-range couplings observed in HMBC spectrum (Fig. 3.65), where the ring C methine protons H-2 (δ_H 5.34) correlated with C-4 and C-10 (δc 101.95) while methylene protons at H-3 correlated with C-2, C-4, C-10 and C-6' (δc 129.68) respectively. Ring B was confirmed by the HMBC correlation of H-2' to C-2, C-4', C-5' and C-6' (δc 129.68); H-3' to C-4', C-5' and C-6' (δc 129.68). The HMBC correlation of H-6 to C-7, C-8 and C-9 (δc 163.48); and H-8 to C-6, C-7 and C-9 confirmed ring C (Fig. 3.66). The NMR data (Table 3.24) thus showed signals typical of naringenin and this was confirmed by comparison of its ^{1}H and ^{13}C NMR data with those reported in the literature.

Compound AU 14 has been isolated from the whole plant of *Eucalyptus globulus* Labill (Ibrahim et al., 2014), and the leaves of *Mentha aquatica* L. (Olsen et al., 2008). Olsen et al., (2008) also tested the compound in a photometric peroxidase linked MAO bioassay, the result showed that the IC_{50} values for MAO inhibition were 342 µg/ml for the rat liver mitochondrial fraction, 955 µg/ml for MAO-A and 288 µg/ml for MAO-B.

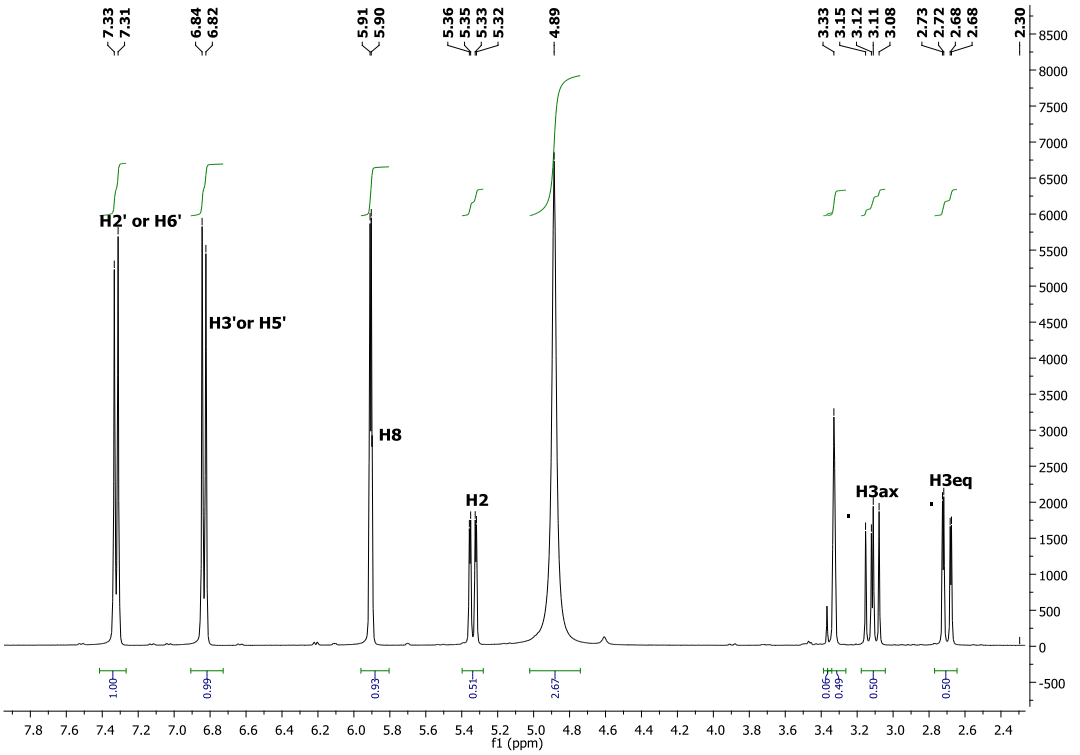

Fig. 3.63. ^{1}H NMR spectrum of compound AU 14.

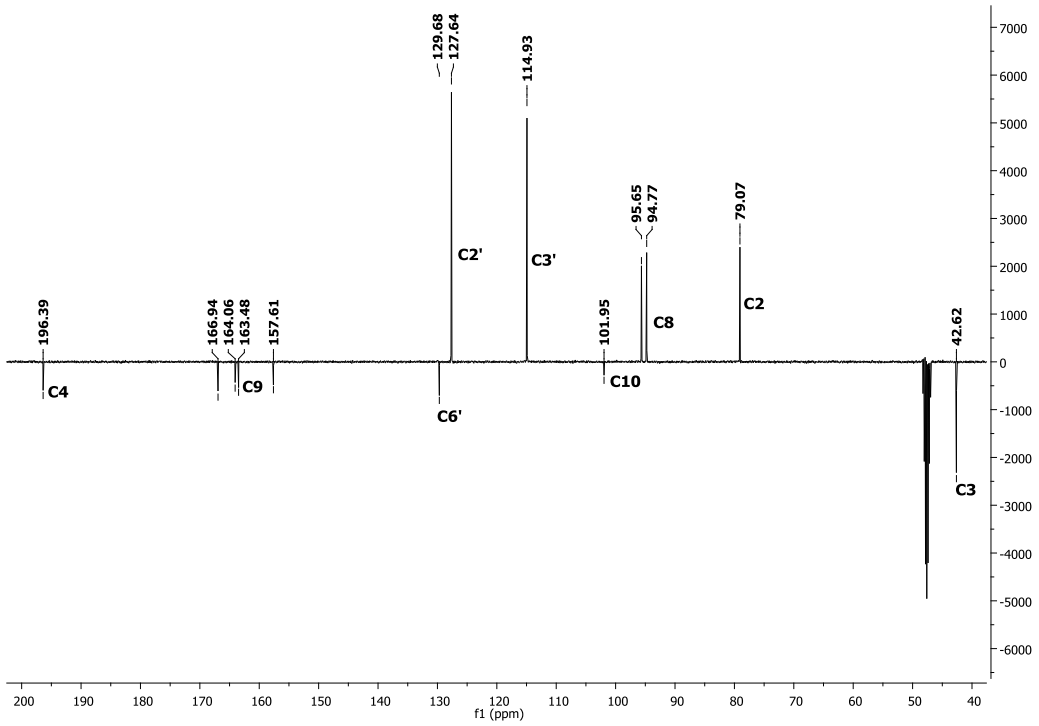

Fig. 3.64. DEPT spectrum of compound AU 14.

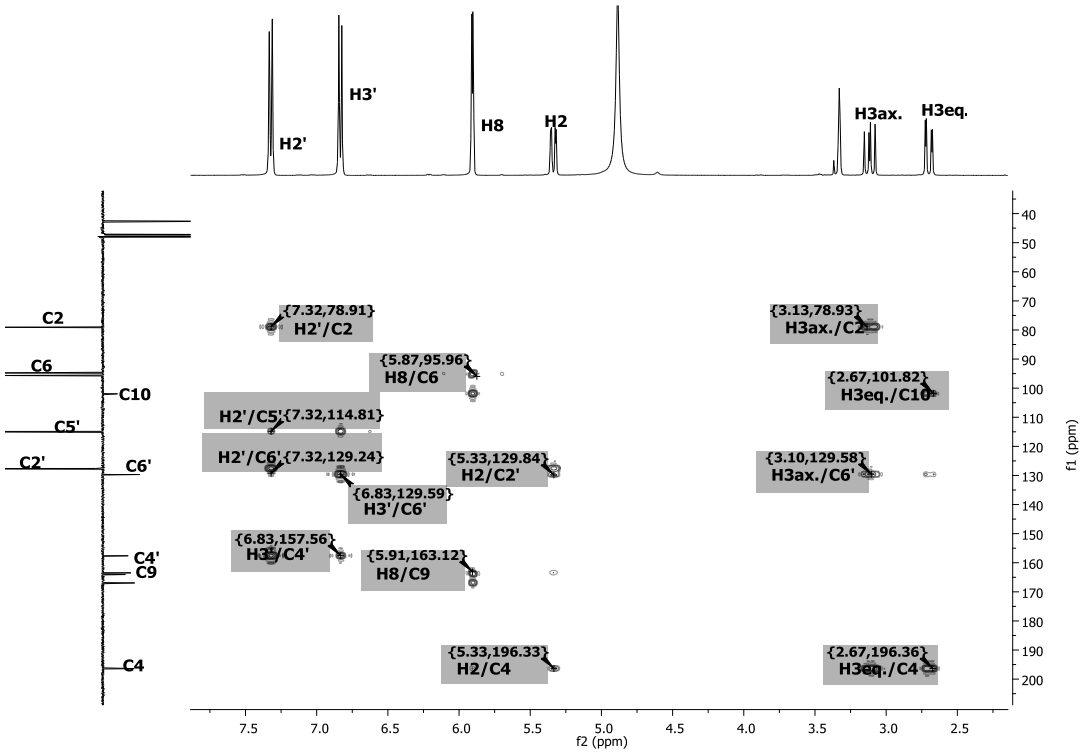

Fig. 3.65. HMBC spectrum of compound AU 14.

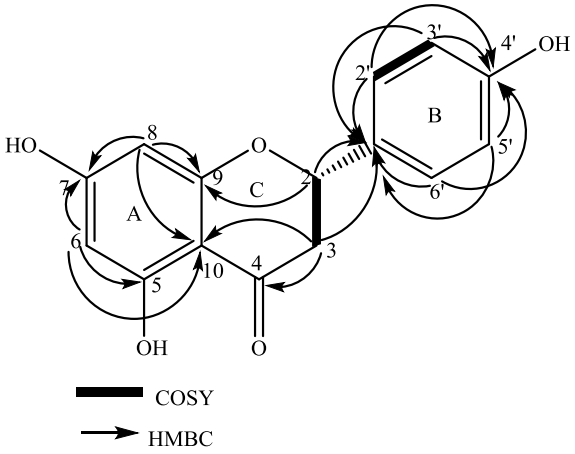

Fig. 3.66. HMBC and COSY correlations of compound AU 14.

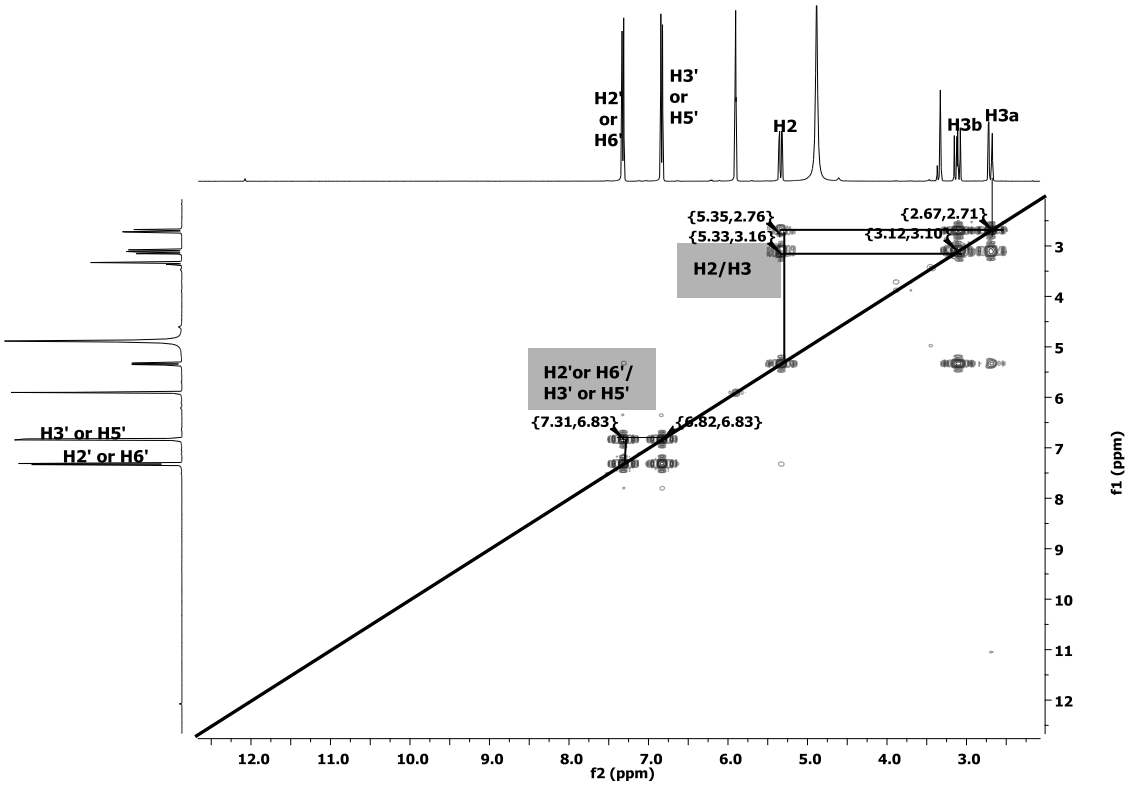

Fig. 3.67. COSY spectrum of compound AU 14.

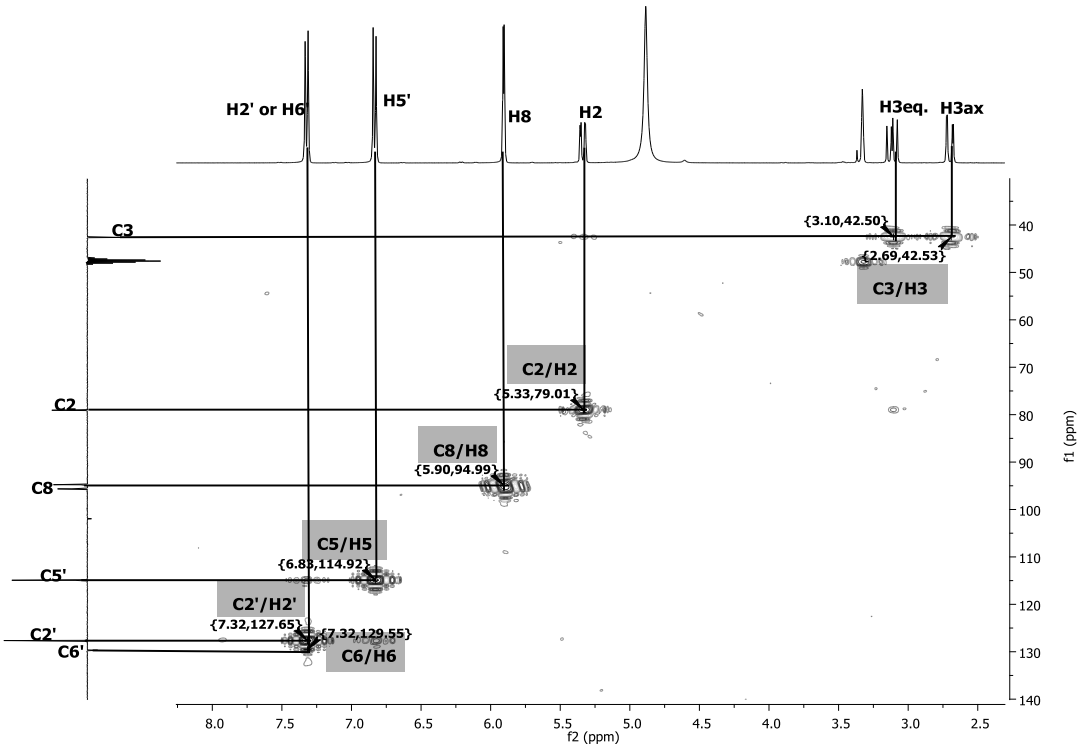

Fig. 3.68. HSQC spectrum of compound AU 14.

Table 3.24. ^{1}H and ^{13}C NMR data of compound AU 14.

Atom No	Olsen 2008 CD3OD δ_C	Ibrahim 2014 DMSO δ_C	AU 14 CD3OD δ_C	AU 14 CD3OD δ_H (m, *J* in Hz)	Olsen 2008 CD3OD δ_H (m, *J* in Hz)	Ibrahim 2014 DMSO δ_H (m, *J* in Hz)
2	80.2	78.41	79.07 (CH)	5.34 (dd, 3.01, 12.93)	5.27 (dd, 3, 12)	5.42 (dd, 2.8, 12.6)
3a	43.8	41.95	42.62 (CH_2)	3.12 (dd, 12.4, 17.06)	3.06 (dd, 12, 18)	3.26 (dd, 12.9, 17.0)
3b			42.62 (CH_2)	2.70 (dd, 2.91, 17.06)	2.64 (dd, 3, 18)	2.67 (dd, 2.8, 17.0)
4	197.5	196.40	196.39 (C)			
5	165.2	163.47	164.06 (C)			
6	96.8	95.76	95.65 (CH)	5.91 (br s)	5.88 (s)	5.86 (br s)
7	168.0	166.62	166.94 (C)			
8	96.0	94.94	94.77 (CH)	5.91 (br s)	5.88 (s)	5.86 (br s)
9	164.9	162.93	163.48 (C)			
10	103.1	101.75	101.95 (C)			
1’	131.8	128.83	131.01 (C)			
2’/6’	128.9	128.34	127.64 (CH)	7.32 (d, 8.50)	7.28 (m)	7.30 (d, 8.5)
3’/5’	116.1	115.14	114.93 (CH)	6.83 (d, 8.45)	6.81 (m)	6.78 (d, 8.5)
4’	158.7	157.71	157.61 (C)			

3.3 Biological activity of isolated compounds

The compounds tested for biological activities are flavonoids, isolated from *T. emetica* seeds. These phytochemicals are thought to be synthesized by plants in response to microbial infections and may play a role as a plant self-defensive system, as they have been found to be effective for example as antimicrobial substances against a wide range of microorganisms (Mori et al., 1987; O’Neill and Mansfiel, 1982; Puupponen-Pimia et al., 2001; Rauha et al., 2000).

3.3.1 Antifungal activity

This was conducted by Professor Steve Kelly’s group. These flavonoids tested against five strains of *Candida albicans* did not inhibit the growth of any of the strains at 20 and 40 µg/ml (Table 3.25). This agrees with (Rauha et al., 2000) who reported inactivity against *Candida albicans* at 500 µg/ml. In contrast, (O’Neill and Mansfiel, 1982) reported naringenin a

flavanone to be a very active antifungal compound against *Botrytis cinerea* at 50 µg/ml. They also concluded that the presence of hydroxyl and a keto groups at different position of the flavanone ring to be responsible for their antifungal activity.

Table 3.25. Antifungal effect of isolated (phenolic) compounds. Sample amount is 20 µg/mL, 40 µg/mL (n = 3).

Isolated compounds	*C. albicans* SC514	*C. albicans* CA12	*C. albicans* CA488	*C. albicans* CA490	*C. albicans* CA1008
Catechin	–	–	–	–	–
Catechin 3-*O*-β-D-glucopyranoside	–	–	–	–	–
Catechin-3-*O*-α-L-rhamnopyranosyl (1→4) β-D-glucopyranoside	–	–	–	–	–
Taxifolin 4'-*O*-β-D glucopyranoside	–	–	–	–	–
Eriodictyol 4'-*O*-β-D-glucopyranoside	–	–	–	–	–
Naringenin	–	–	–	–	–
Epicatechin	–	–	–	–	–

–: No antimicrobial activity

3.3.2 Antitrypanosoma activity

This was conducted by Dr Carol Clements. The antitrypanosoma activity of seven pure flavonoids compounds tested against *T. brucei* brucei is presented in (Table 3.26). All the compounds tested did not show any inhibition at a concentration of 20 µg/ml. This is contrary to the moderate activity reported for *T. brucei rhodesiense* at IC_{50} value for catechin, epicatechin, taxifolin, eriodictyol and naringenin to be 14.5, 16.8, 14.6, 24.3 and 46.1 µg/ml. These flavonoids show weak activity when tested against *T. cruzi* with the exception of eriodictyol that showed some inhibition at IC_{50} value of 14.5 µg/ml, although they lack a double bond between C2 and C3 (Tasdemir et al., 2006). They proposed that this activity was due to the presence of a free hydroxyl group, keto group at C-4 and a double bond at position C-2 and C-3 (3.32).

3.3.3 Antibacterial activity

This was conducted by Drs Simon J. Cameron and Carol Clements. Catechin and catechin 3-*O*-β-D-glucopyranoside did not show any antibacterial activity against gram-positive (*B. cereus and S. aureus*) and gram negative (*E. coli and P. aureginosa*) bacteria at 10 µg/ml (Table 3.26). These and other pure compounds, when tested against methicillin-resistant *staphylococcus aureus* (strain 16 and 106), *K. pneumonia* (strains ATCC13883 and BAA-2146 NDM) and *M. marinum* at 100 µg/ml (MIC) did not show any activity except for *K. pneumonia*

(strains ATCC13883) that showed moderate antibacterial activity. The results for flavonoids against *Staphylococcus aureus* are in agreement with those reported in the literature (Mori et al., 1987). Additionally, the flavanone naringenin only inhibited the growth of MRSA at a concentration of 200 – 400 µg/ml, which was found to be due to the absence of the 2'-hydroxyl group in the B-ring (Tsuchiya et al., 1996). This result was confirmed by (Rauha et al., 2000) who showed naringenin to have moderate activity with a MIC value of 500 µg/ml against gram-positive and negative bacteria, while catechin did not show any activity. In contrast, the catechins isolated from tea leaves showed anti-staphylococcal activity at 50 µg/ml (Toda et al., 1991). The result obtained for glycosides in this study disagree with other researchers that reported flavonoid glycosides to have no activity against most microbial strains (Rauha et al., 2000; Waage and Hedin, 1985). Illustrating the relationship between the chemical structure of flavonoids and *Klebsiella pneumonia* (Table 3.26). The activity of catechin and its glycosides against *K. pneumonia* (strain ATCC13883) may be due to the presence of a 3', 4'-dihydroxylation of the B-ring combined with 3-OH. Also, the trans-substitution at position 2 and 3 of catechin and flavanonols may also play an important role for the activity while the trans-substituted compound are inactive. In addition to catechin skeleton, the presence of a keto group and a double bond between C-2 and C-3 as observed in flavanones are also known to enhance activities (Mori et al., 1987).

The lipid content of the cell wall of Gram-negative bacteria is greater than the Gram-positive bacteria. The flavonoids tested for bioactivity in this study are relatively hydrophilic and may permeate the cell walls of *Klebsiella pneumonia* at different rates, which may account for the discrepancy in the inhibitory effect (Mori et al., 1987; O'Neill and Mansfiel, 1982).

Table 3.26. Antibacterial and antitrypanosoma activity of isolated compounds.

Isolated compounds	Bacillus cereus ATCC 14579	*Escherichia coli* K12	*Staphylococcus aureus* RN 42420	*Pseudomonas aureginosa* PA 01	*Klebsiella pneumonia* BAA 2146 NDM	*MRSA* 16	*MRSA* 106	*Mycobacterium marinum*	*Trypanosoma brucei*	*Klebsiella pneumonia* ATCC 13883	(%) Inhibition
Catechin	−	−	−	−	−	−	−	−	−	+	51
Catechin 3-*O*-β-D-gluco pyranoside	−	−	−	−	−	−	−	−	−	+	53
Catechin-3-*O*-α-*L*-rhamnopyranosyl (1→4) *β-D*-glucopyranoside					−	−	−	−	−	+	49
Taxifolin 4'-*O*-β-D-glucopyra noside					−	−	−	−	−	+	56
Eriodictyol 4'-*O*-*β-D*-glucopy ranoside					−	−	−	−	−	+	61
Naringenin					−	−	−	−	−	+	56
Epicatechin					−	−	−	−	−	+	57

Methicillin resistant staphylococcus aureus (MRSA), No antimicrobial activity (−), Moderate antimicrobial activity (+)

CHAPTER 4

Isolation of limonoids from neem seeds (Azadirachta indica) and furanoflavonoids from the seed oil of karanja tree (*Milettia pinnata*). Several-failed attempt to isolate limonoids from the seed of *T. emetica*: Result and Discussion

4.0 Introduction

Several limonoids have been reported from the root and stem bark of *T. emetica,* but no such report from the seeds. This chapter report some of the failed efforts made to isolate limonoids from the seeds of *T. emetica*. Hence, neem seed and seed oil of karanji (sold as neem oil) was used as a model to check the workability of the methods used. At each stage, the process of isolation was monitored with TLC and ^{1}H NMR spectroscopy.

4.1 Extraction of *T. emetica* and *A. indica* seeds and the seed oil of *M. pinnata*

The seeds and oil samples were extracted at different conditions and the extract purified with a series of solvents of increasing polarity in a liquid-liquid partitioning or column chromatography or both. The seeds of *T. emetica* was prepared as described in experiment 6.6 and the extract purified in a series of experiments 6.6.1 to 6.6.6. The *M. pinnata* oil was also prepared as described in 6.8 and the extract purified as in 6.8.1. The seeds of *A. indica* was prepared as described in 6.9 and purified as shown in 6.9.1 and 6.9.2.

4.2 Isolation of limonoids from *T. emetica* seed. The approaches:

The first to the fifth approaches were monitored using ^{1}HNMR spectroscopy. The spectrum did not show any limonoid signals in all the cases, see appendix X to Z.

4.3 Isolated compounds from *M. pinnata* oil

The compounds isolated from M. pinnata oil are as shown in Table 4.1 to 4.6.

4.4 Isolated compounds from *A. indica*

The compound isolated from A. indica oil is as shown in Table 4.7 and 4.8 while that from the defatted flour is in Table 4.9 and 4.10.

Table 4.1. Compound AU 15 (Karanjin)

3-methoxy-2-phenylfuro[2,3-h]chromen-4-one	
Synonyms	Karanjin
Sample codes	AU 15
Sample amount	29 mg
Physical Description	white crystals
Molecular formula	$C_{18}H_{12}O_4$
Molecular Weight	292 g/mol
Melting Point	156-157 ^{O}C
IR:($CHCl_3$)	2929, 1637, 1461, 1371, 1285, 1164, 1035, 756 cm^{-1}

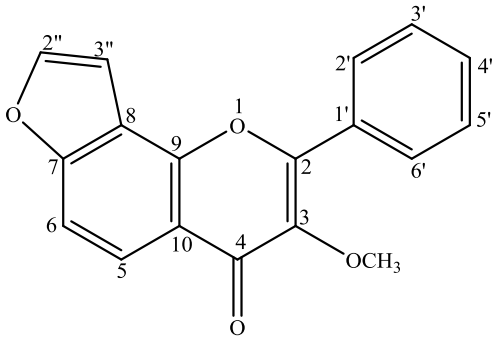

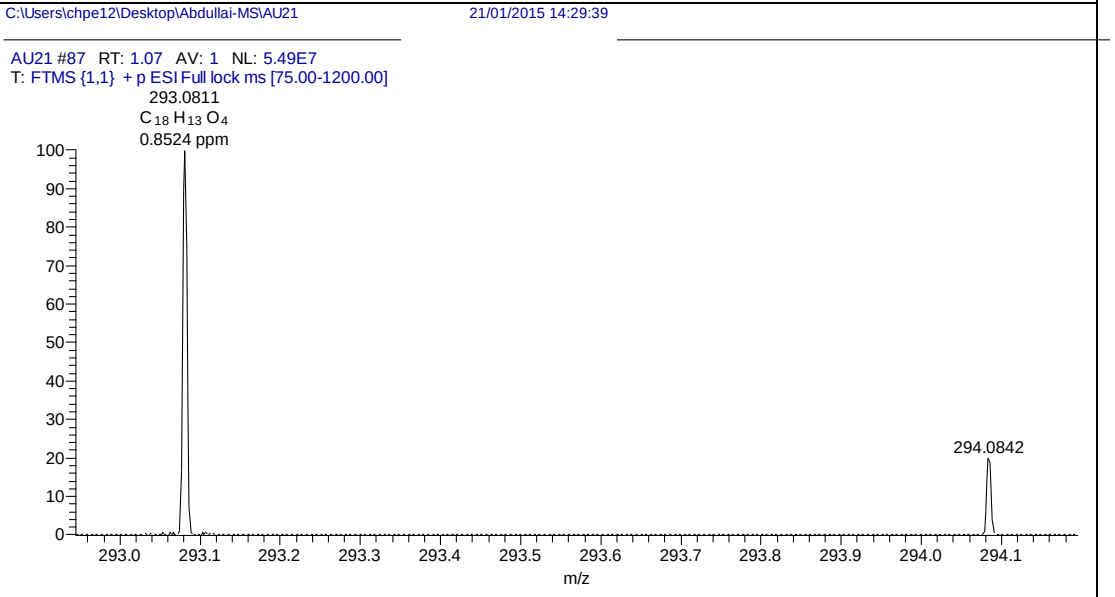

Compound AU 15 (29 mg) was isolated as white crystalline solid. It has a molecular formula of $C_{18}H_{12}O_4$ which was established on the basis of ESI-HRMS at *m/z* 293.0811$[M + H]^+$ (Calcd for 293.0805). Its IR spectrum showed peaks at 2929, 1637, 1461 and 1164 cm^{-1} signifying the presence of C-H, C=O, C=C and C-O groups, see appendix I. The ^{13}C NMR spectrum (Fig. 4.2) showed sixteen carbon signals, and DEPT spectrum defined it to consist of seven methine, eight quaternary carbons and a methoxy

group. Four of these aromatic carbons δc (145.72, 158.19, 149.97, and 154.86) were assigned to positions 2", 7, 9, and 2, are linked to oxygen in a furano-flavonoid molecule. Also, a mono-substituted aromatic ring is shown by signals at δc (130.67, 128.65 and 128.40) assigned to positions 4', 3'/5' and 2'/6'; and other aromatic signals are δc (141.85, 121.92, 110.01, 117.02 and 119.72) assigned to positions 3, 5, 6, 8 and 1'. The characteristic signals for furan ring protons appeared in its ^{1}H NMR spectrum (Fig. 4.1) at δ_H 7.79 (d, 2.1 Hz) and δ_H 7.21 (d, 2.2) attributable to position 2" and 3". The mono substituted aromatic ring signals appeared at δ_H 8.16 (2H, m) assigned to positions H-2'/6'; and δ_H 7.59 (3H, m) assigned to position 3'/4'/5'. In the COSY (Fig. 4.5), the methine protons of furan ring δ_H 7.79 (d, 2.1 Hz) assigned to position 2'' coupled with δ_H 7.21 (d, 2.2 Hz) of position 3'' while the aromatic proton δ_H 8.22 (d, 8.7) assigned to position 5 coupled with δ_H 7.57 (d, 8.7) of position 6. The spectrum of HSQC (Fig. 4.6), showed the direct correlations between a methoxy proton δ_H 3.96 (s) to a methoxy carbon δc (42.62); and also a methine protons at δ_H [8.22, 7.57, 8.16, 7.59, 7.59, 7.59, 8.16, 7.79 and 7.21(2.2 Hz)] to δc (121.92, 110.01, 128.40, 128.65, 130.67, 128.65, 128.40, 145.72 and 104.26) assigned to positions 5, 6, 2', 3', 4', 5', 6', 2" and 3". These positions were further confirmed by long-range coupling observed in HMBC (Fig. 4.3), where the methine proton of the furano ring H-2" (δ_H 7.79) correlated with C-3", C-7 and C-8 (δc 117.02); and H-3" (δ_H 7.21) correlated with C-2", C-7, C-8 and C-9 (δc 149.97). The ^{1}H and ^{13}C NMR data (Table 4.2) were virtually identical with those reported in the literature for karanjin (Katekhaye et al., 2012; Vismaya et al., 2010). The identity of compound AU 15 was confirmed by X-ray crystallography. This is similar to a known X-ray crystal structure CSD: SEMVAH.

Compound AU 15 has been reported from the *Pongamia pinnata* seed oil (Katekhaye et al., 2012; Vismaya et al., 2010), root extract of *Deris indica* (Ranga Rao et al., 2009), roots of *Lonchocarpus latifolius* (Magalhaes et al., 2000) and roots of *Dahlstedtia pinnata* and *D. pentaphylla* (Garcez et al., 1988). This compound was tested in vitro for intestinal α-glucosidase inhibitory activity and it was reported that the compound displayed 26.3 μg/ml α-glucosidase inhibitory activity (Ranga Rao et al., 2009).

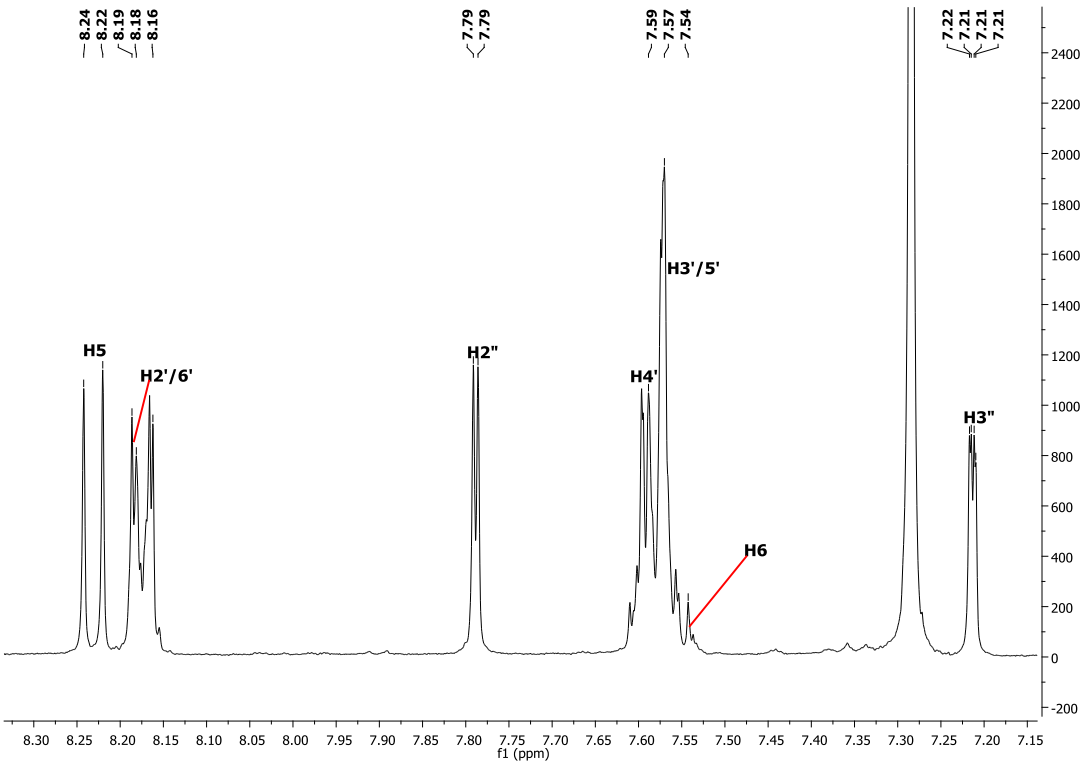

Fig. 4.1. ^{1}H NMR spectrum of compound AU 15 (δ 7.10 – 8.35)

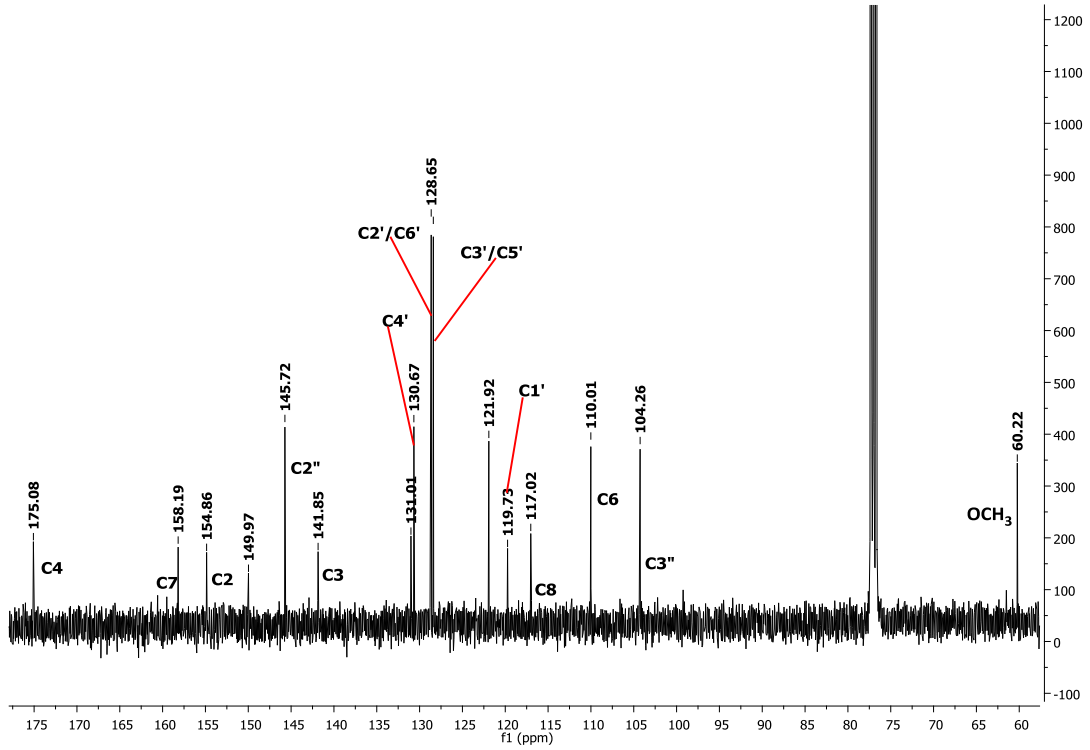

Fig. 4.2. ^{13}C NMR spectrum of compound AU 15

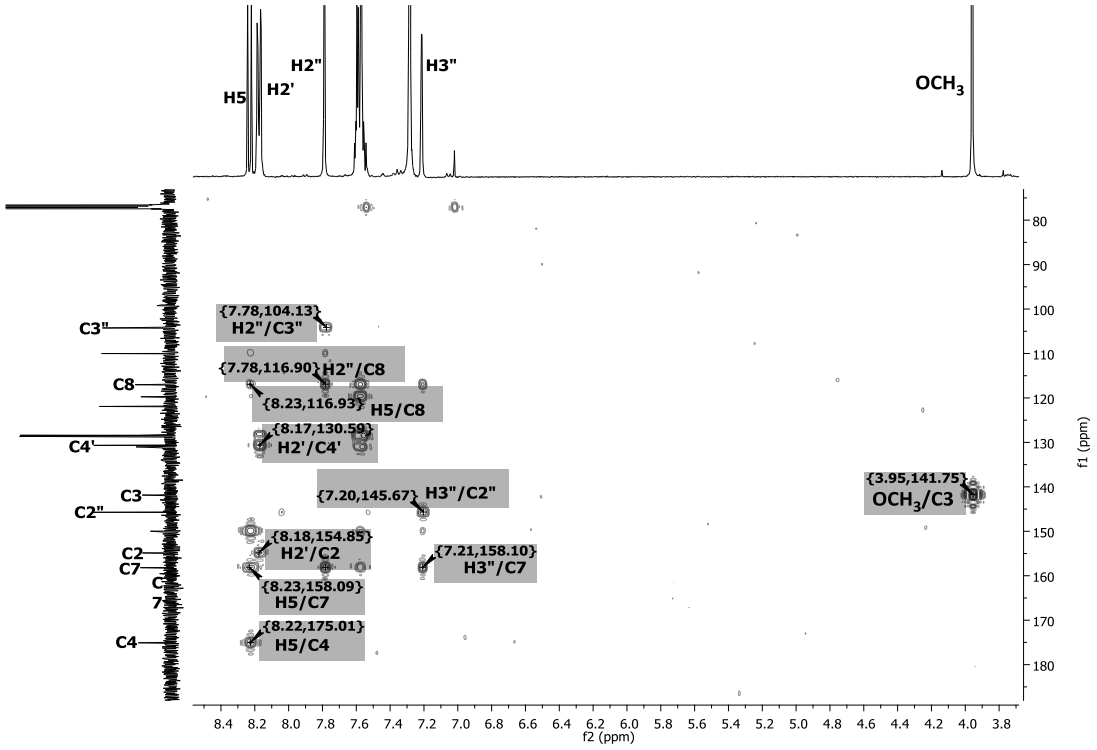

Fig. 4.3. HMBC spectrum of compound AU 15.

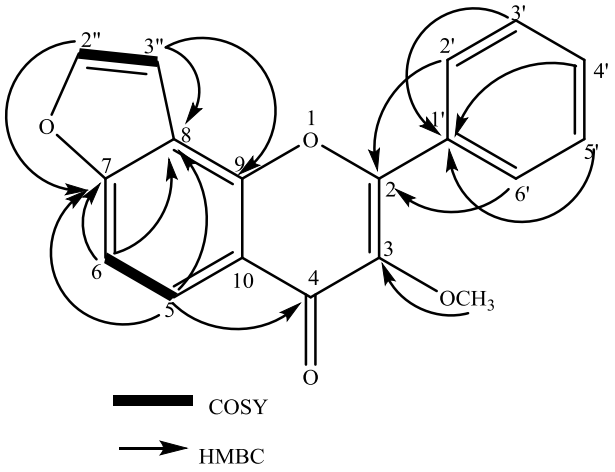

Fig. 4.4. HMBC and COSY correlations of compound AU 15.

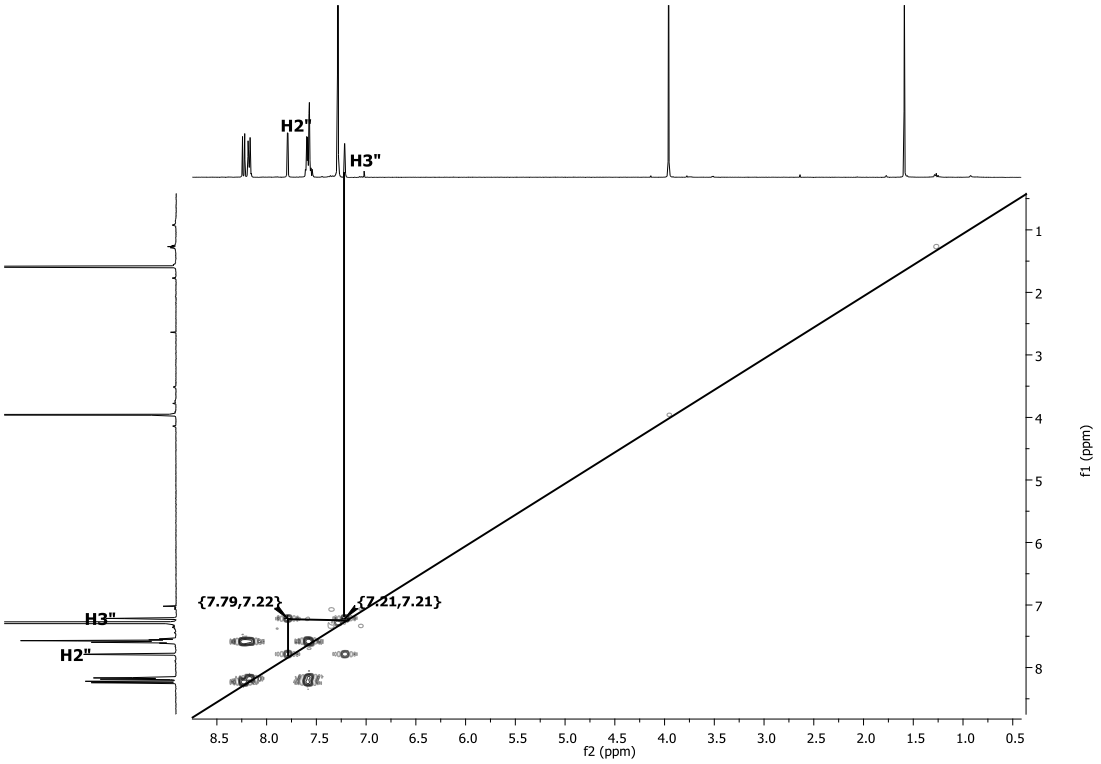

Fig. 4.5. COSY spectrum of compound AU 15.

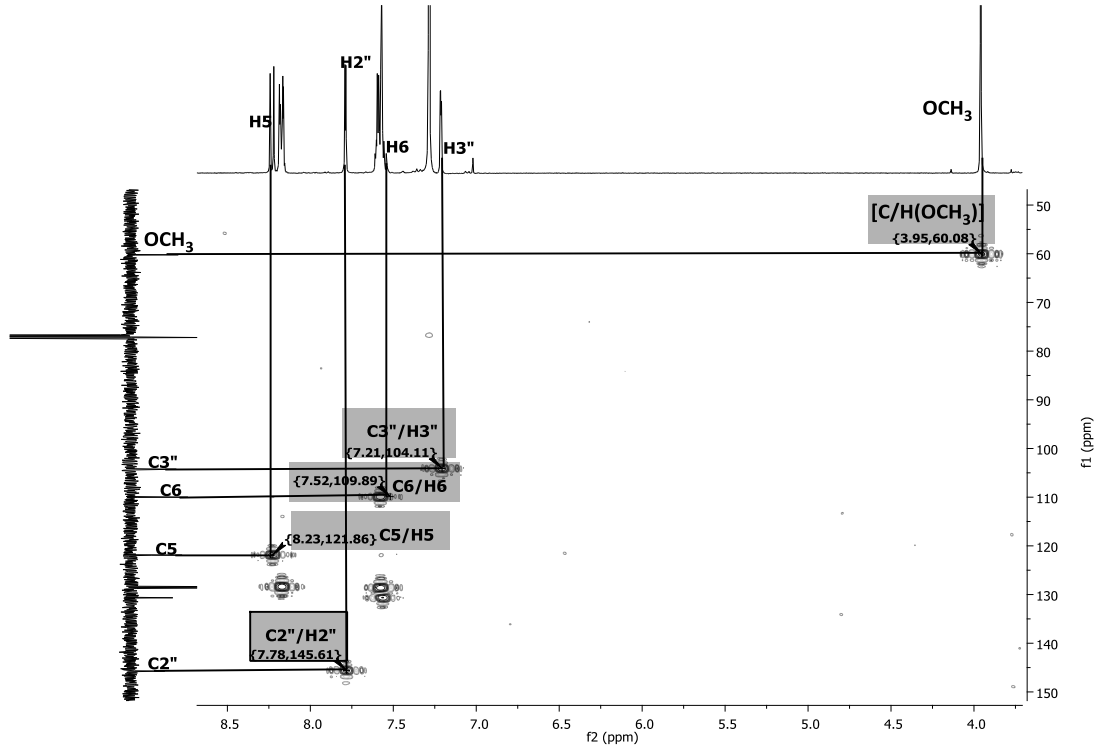

Fig. 4.6. HSQC spectrum of compound AU 15.

Figure 4.7. The X-ray crystal structure of karanjin.

Table 4.2. ^{1}H and ^{13}C NMR data of compound AU 15.

Atom No.	Katekh-aye 2012 DMSO δ_C	Visamaya 2010 DMSO δ_C	AU 15 $CDCl_3$ δ_C	AU 15 $CDCl_3$ δ_H (m, *J* in Hz)	Katekhaye 2012 $CDCl_3$ δ_H (m, *J* in Hz)	Visamaya 2010 DMSO δ_H (m, *J* in Hz)
2	154.84	154.5	154.86 (C)			
3	141.81	141.5	141.85 (C)			
4	175.07	174.7	175.08 (C)			
5	121.86	121.6	121.92 (CH)	8.22 (d, 8.7)	8.20 (d,4.0)	8.22 (d, 8.5)
6	109.99	109.7	110.01 (CH)	7.54 (d, 8.7)	7.54 (d,4.0)	7.57 (d, 8.5)
7	158.15	157.8	158.19 (C)			
8	116.99	116.7	117.02 (C)			
9	149.93	149.6	149.97 (C)			
10	130.96	130.7	131.01 (C)			
1’	119.68	119.4	119.72 (C)			
2’/6’	128.37	128.0	128.40 (CH)	8.16 (m, 2H)	8.15 (m)	8.17 (m)
3’/5’	128.63	128.3	128.65 (CH)	7.59 (m, 2H)	7.57 (m)	7.60 (m)
4’	130.67	130.3	130.67 (CH)	7.59 (m)	7.58 (m)	7.60 (m)
2”	145.72	145.4	145.72 (CH)	7.79 (d. 2.1)	7.57 (d, 1.0)	7.78 (d, 2.0)
3”	104.23	103.9	104.26 (CH)	7.21 (d, 2.1)	7.18 (d, 1.0)	7.20 (d, 2.0)
3-OCH_3	60.20	59.9	60.22 (OCH_3)	3.96 (s)	3.93 (s)	3.85 (s)

Table 4.3. Compound AU 16 (Pongapin).

3-methoxy-3',4'-methylenedioxy-furo[8,7:4'',5'']flavone	
Synonyms	Pongapin
Sample codes	AU 16
Sample amount	13 mg
Physical Description	white crystals
Molecular formula	$C_{19}H_{12}O_6$
Molecular Weight	336 g/mol
IR:($CHCl_3$)	3004, 1625, 1489, 1372, 1256, 1036, 759 cm^{-1}

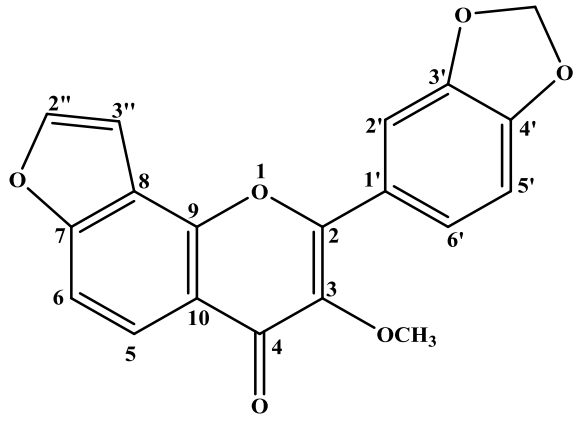

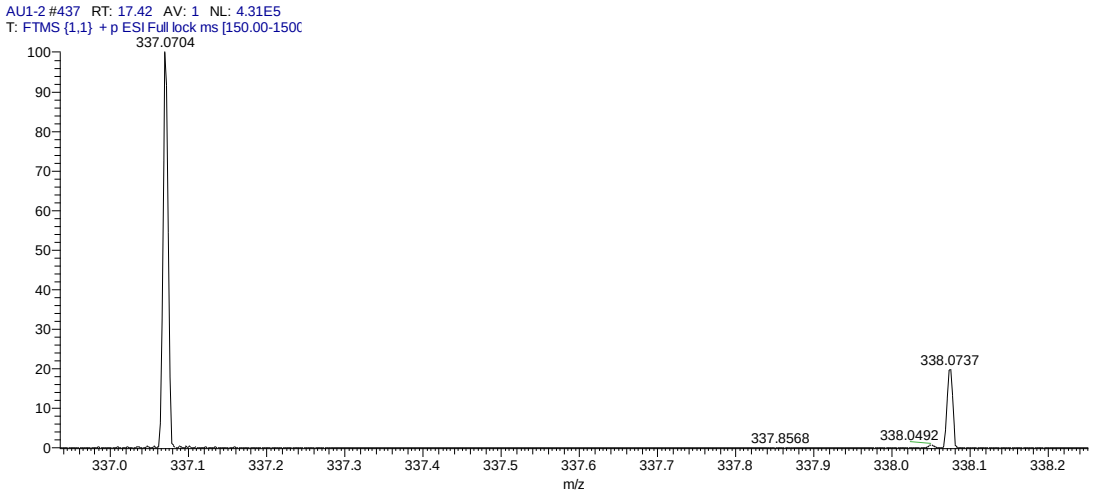

Compound AU 16 (13 mg) was isolated as white crystalline solid. It has a molecular formula of $C_{19}H_{12}O_6$ which was established on the basis of ESI-HRMS *m/z* 337.0704 $[M + H]^+$ (Calcd for 337.0713) together with its ^1H and ^{13}C NMR spectroscopic data (Table 4.4). The IR spectrum showed band at 3004, 1625 and 1036 cm^{-1} corresponding to C-H, C=C and C-O stretching, respectively, see appendix I. The ^{13}C NMR spectrum (Fig. 4.9) showed 19 signals. The ^1H NMR spectrum (Fig. 4.8) showed two singlets at δ_H 3.96 and δ_H 6.12 which were equivalent to three and two protons confirming the

presence of a methoxy and a methylenedioxy group. The spectrum showed two furan ring proton signals at δ_H 7.58 (d, 1.7 Hz, H-2'') and δ_H 7.20 (dd, 0.8, 2.1 Hz, H-3'') and two ortho coupled aromatic doublets at the lowest field δ_H 8.20 (d, 8.8 Hz, H-5) and δ_H 7.56 (dd, 0.7, 8.8 Hz, H-6). The ring B aromatic signals at H- 6' and H- 2' (δ_H 7.70 and 7.78) are also shifted down field from the usual aromatic region by their neighbouring oxygen functions. The two proton signals at H-6' resonates at δ_H 7.78, and the furan doublet at H=2'' superimposed on the H-6' resulting in a doublet of doublet at H-6'. The HSQC spectrum (Fig. 4.13), showed direct correlations between the methoxy protons δ_H 3.95 (s) to the methoxy carbon δc (60.03), methylenedioxy proton resonating at δ_H 7.78 to methylenedioxy carbon at δc 101.68 and also the two furan protons at H-2'' and H-3'' to C=2'' and C=3''. The spin system was further exhibited in the COSY spectrum (Fig. 4.12), where the methine proton of the furan ring δ_H 7.80 (d, 1.7 Hz) assigned to position H-2'' coupled with H-3'' while the aromatic proton at H-5 coupled with H-6 and H-5' coupled to H-6'. The heteronuclear multiple bond connectivity (HMBC) correlations observed from H-2'' (δ_H 7.80) to C-3'', C-7 and C-8 (δc 116.90); and also from H-3'' to C-2'', C-7 and C-8 (Fig. 4.10 & 4.11) supported the structure of the benzofuran moiety. Furthermore, the correlation between methylenedioxy protons with C-3' and C-4' confirmed it presence on the B ring. The NMR data agreed with the literature values (Magalhaes et al., 2000; Mukerjee et al., 1969). Further confirmation was done using X-ray crystallography. See appendix IV for the Table with the crystal data.

Pongapin has been isolated from the fruit of *Pongamia pinnata* (Minakawa et al., 2010), stem bark of *P. glabra* (Mukerjee et al., 1969) and the root of *Lanchocarpus latifolius* (Magalhaes et al., 2000). This compound did not produce any inhibition on TRAIL-rsistance in human gastric adenocarcinoma (AGS) cell lines when tested at concentration of 30 and 40 µg/ml using the fluorometric microculture cytotoxicity assay (FMCA) method (Minakawa et al., 2010).

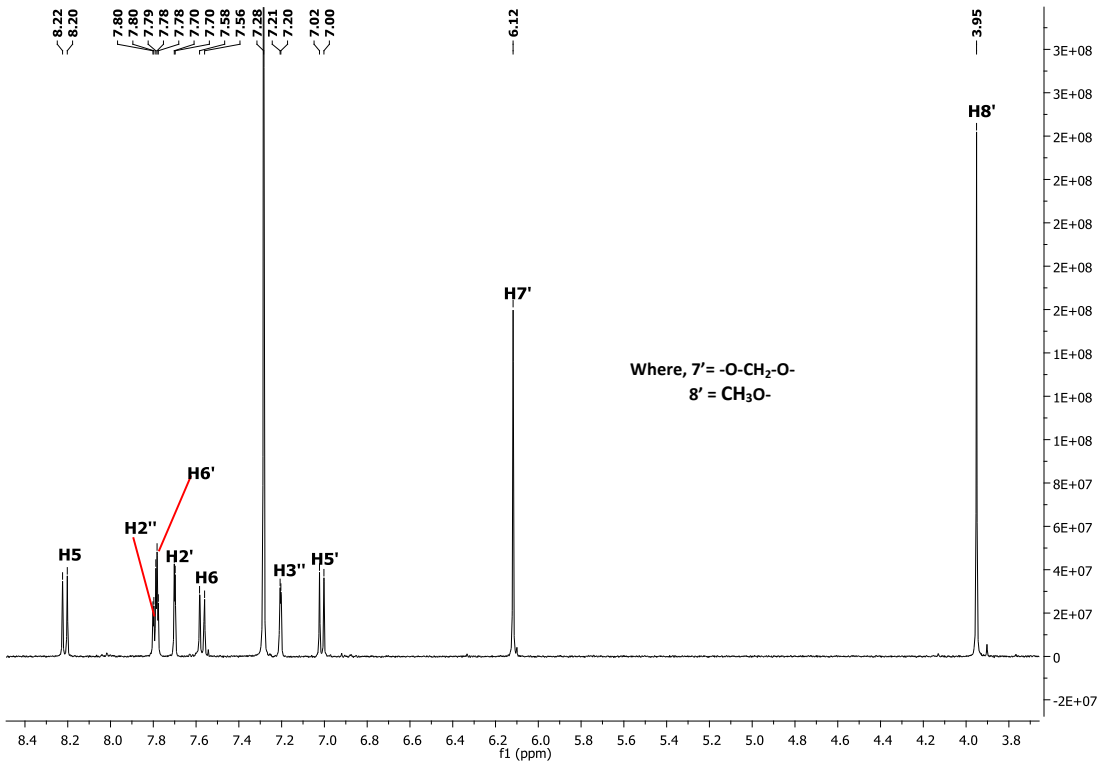

Fig. 4.8. ^{1}H NMR spectrum of compound AU 16.

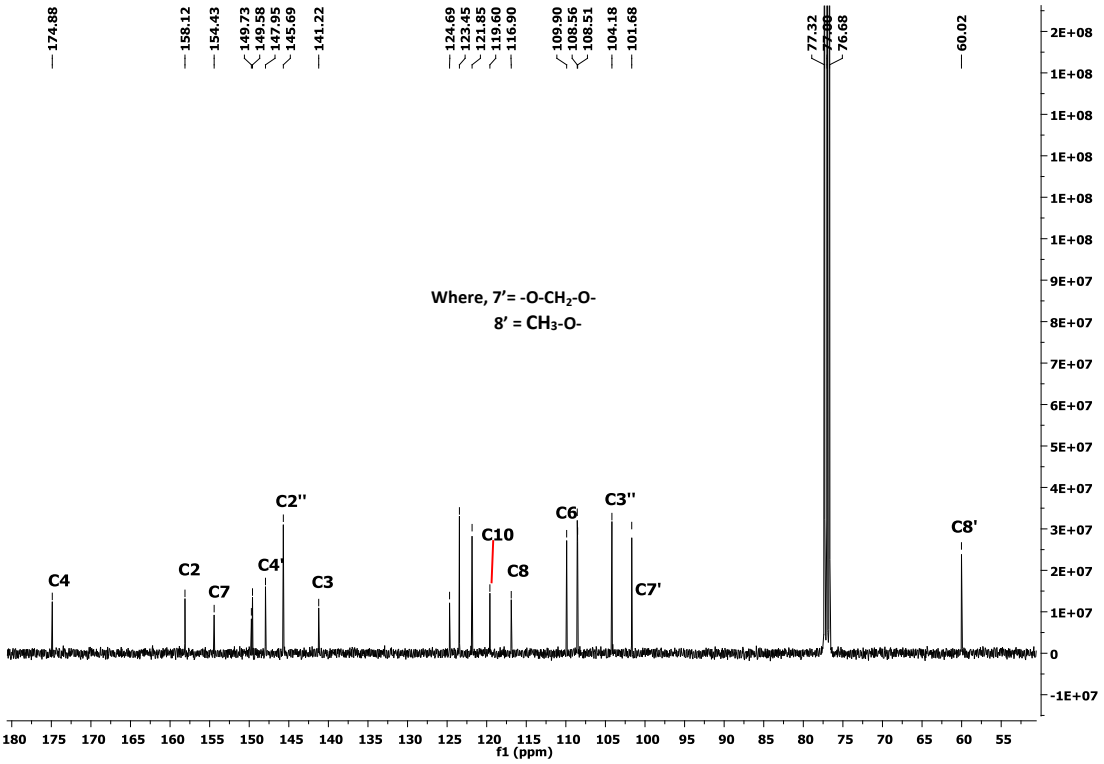

Fig. 4.9. ^{13}C NMR spectrum of compound AU 16.

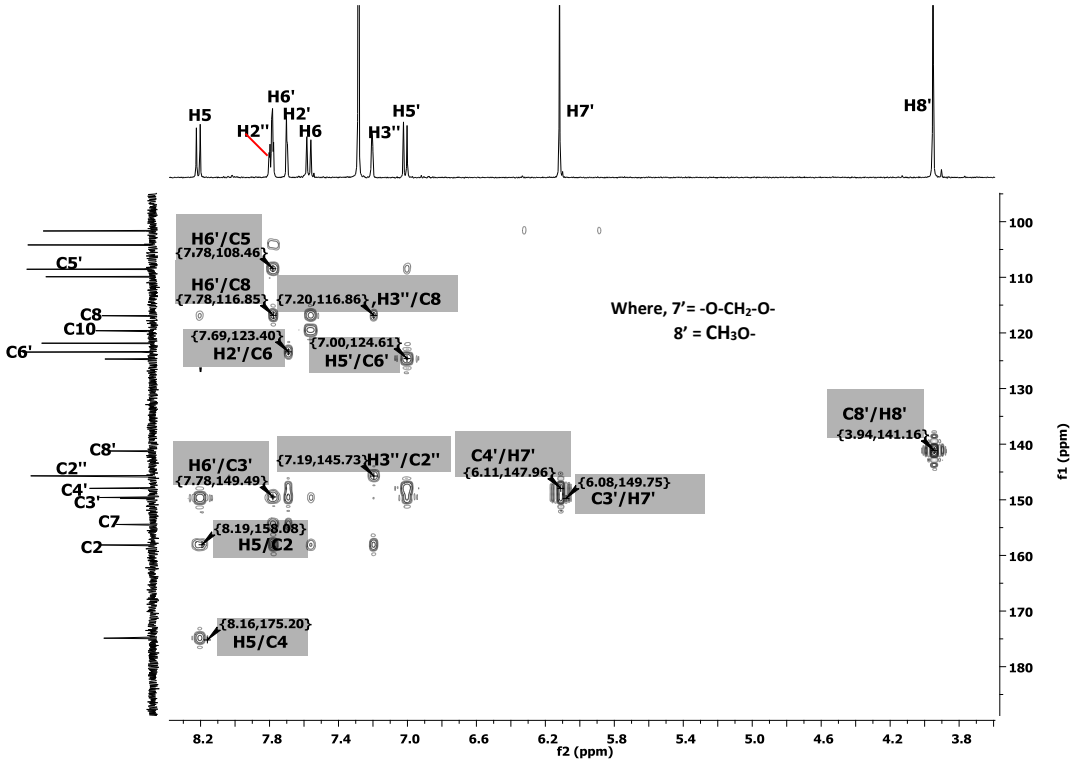

Fig. 4.10. HMBC spectrum of compound AU 16.

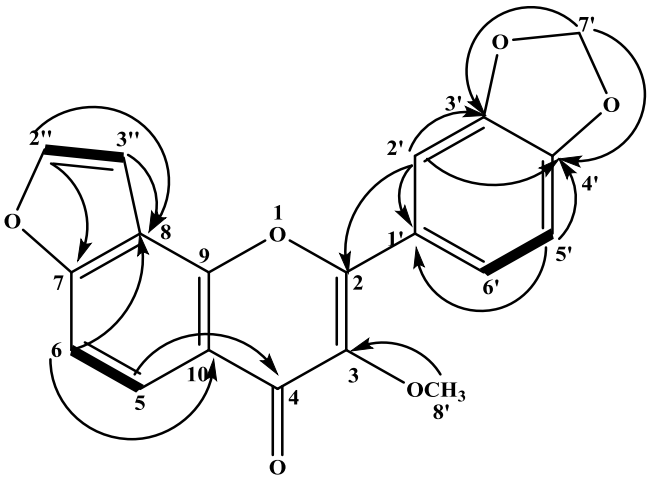

Fig. 4.11. HMBC and COSY correlations of compound AU 16.

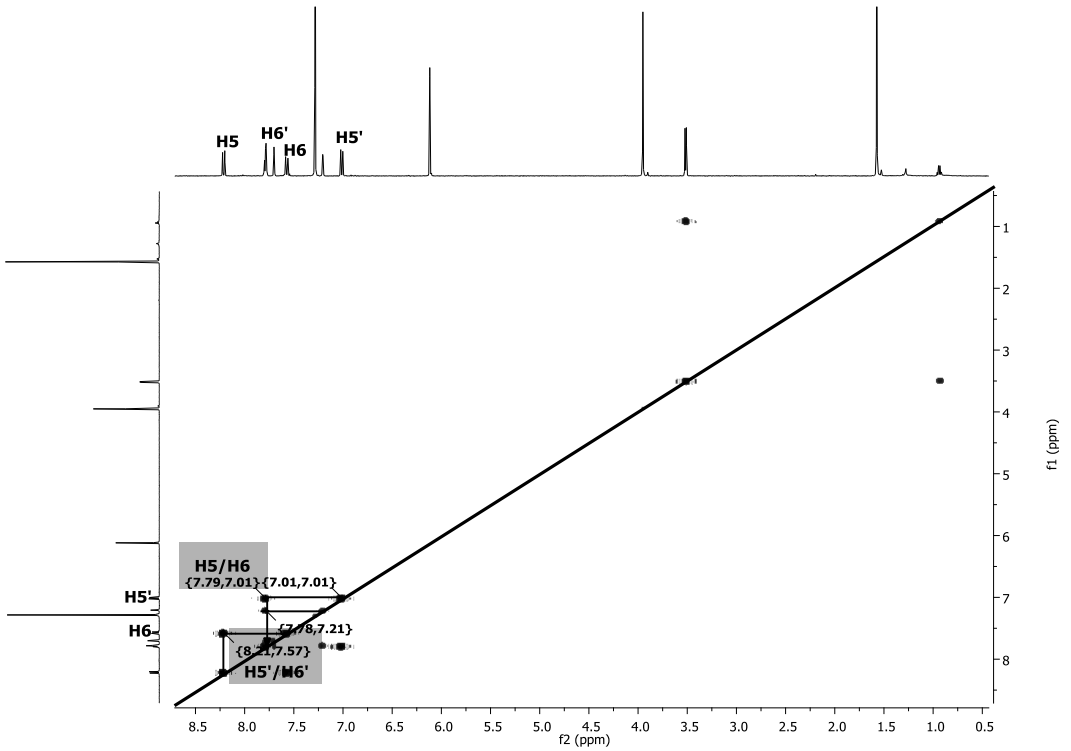

Fig. 4.12. COSY spectrum of compound AU 16.

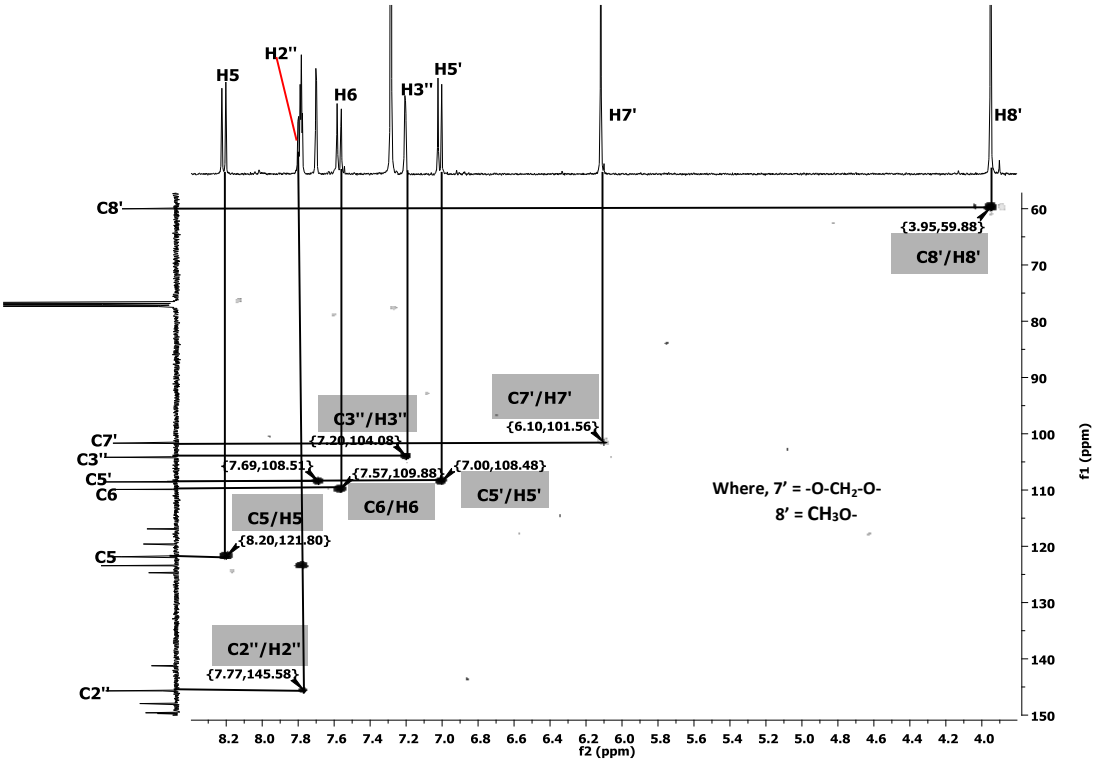

Fig. 4.13. HSQC spectrum of compound AU 16.

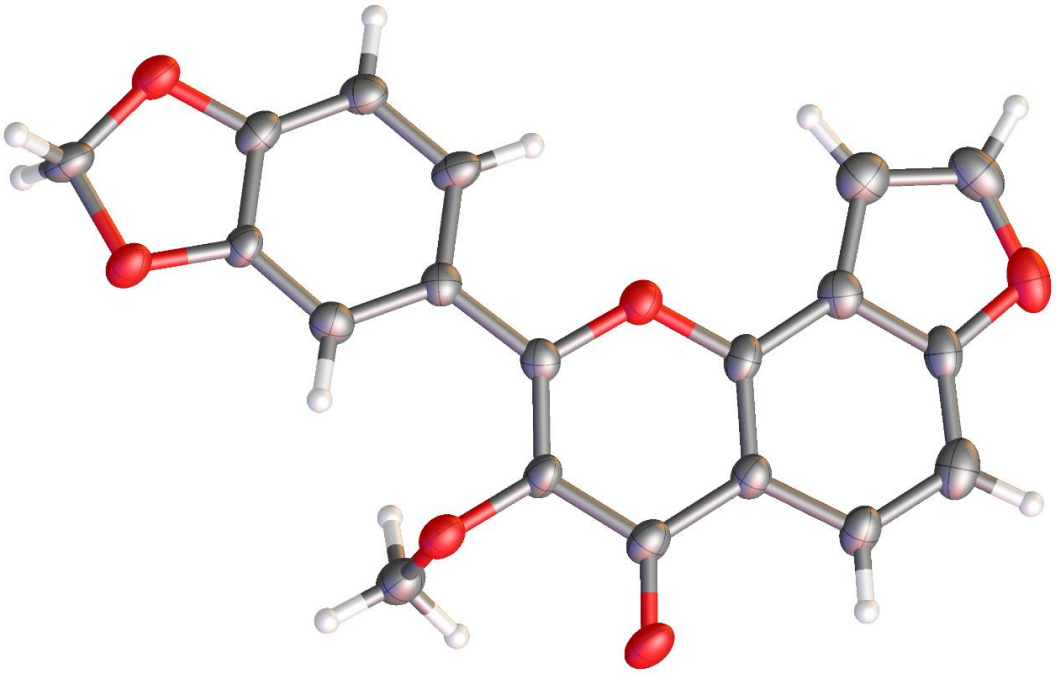

Figure 4.14. The X-ray crystal structure of pongapin.

Table 4.4. ^{1}H and ^{13}C NMR data of compound AU 16.

Atom No.	AU 16 CD_3OD δc (m)	AU 16 CD_3OD δ_H (*J* in Hz)	HMBC [H→C]
2	158.12(C)		
3	141.27(C)		
4	174.88(C)		
5	121.85	8.20 (d, 8.8)	C-4, C-6, C-8, C-10
6	109.90	7.56 (dd, 0.7, 8.8)	C-5, C-7, C-8, C-10
7	154.43		
8	116.90		
9	149.58		
10	119.60		
1’	124.7		
2’	108.51	7.70 (d, 1.8)	C-3’, C-4’, C-6’
3’	149.73		
4’	147.95		
5’	108.56	7.00 (d, 8.3)	C-1’, C-2’, C-4’, C-6’
6’	123.45	7.78 (dd, 0.8, 8.5)	C-2, C-1’, C-2’, C-3’
2’’ 3’’	145.69 104.18	7.80 (d, 1.7) 7.20 (dd, 1.7)	C-3’’, C-7, C-8, C-2’’, C-7, C-8
8’ (-OCH_3)	60.02	3.95 s	C-1’, C2, C4, C10
7’ (OCH_2O)	101.68	6.12 s	C-3’, C-4’

Table 4.5. Compound AU 17 (Lanceolatin).

(1'',2'':7,8)-Furanoflavone	
Synonyms	Lanceolatin
Sample codes	AU 17
Sample amount	9 mg
Physical Description	white crystals
Molecular formula	$C_{17}H_{10}O_3$
Molecular Weight	262 g/mol
Melting Point	135-136 ºC
IR:($CHCl_3$)	2926, 1642, 1604, 1449, 1361, 1253, 1140, 1070, 1035, 686 cm^{-1}

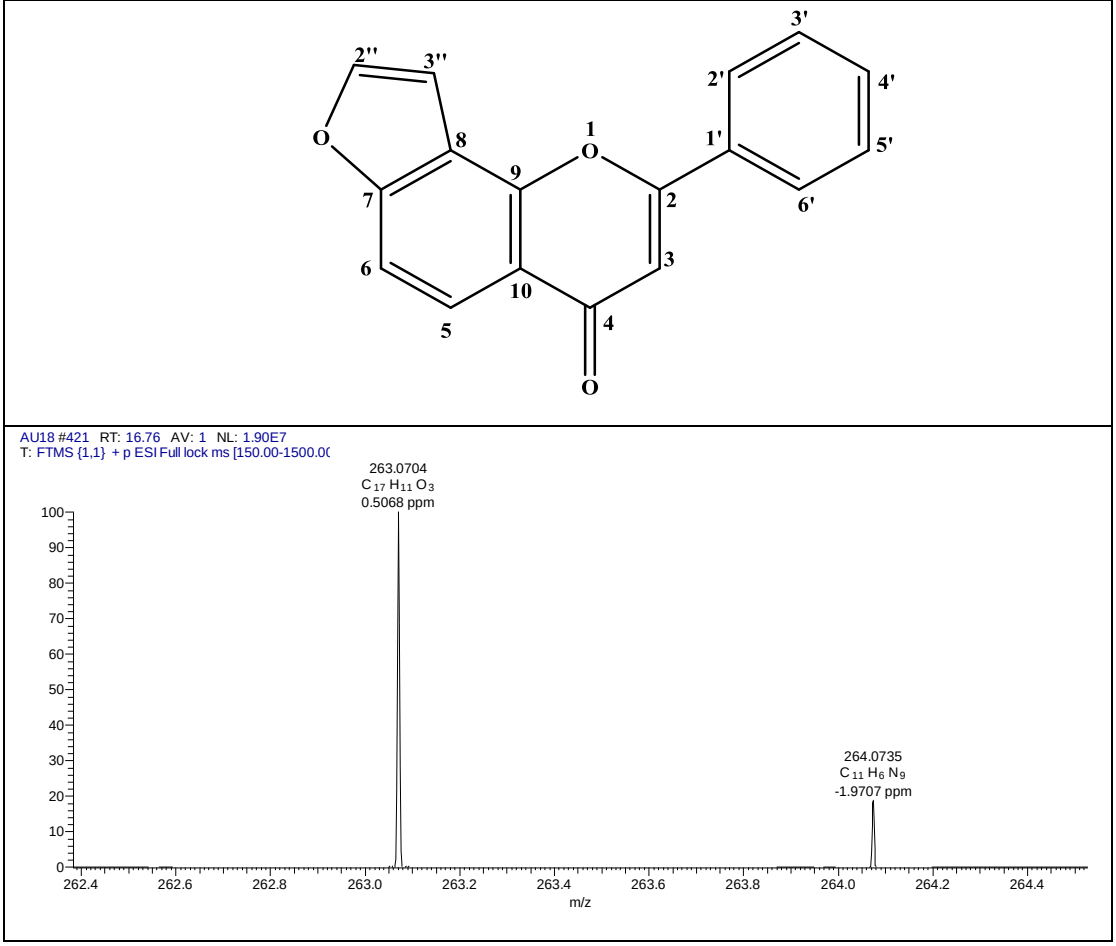

Compound AU 17 (9 mg) was isolated as white crystalline solid. It has a molecular formula of $C_{17}H_{10}O_3$ which was established on the basis of ESI-HRMS at m/z 263.0704 $[M + H]^+$ (Calcd for 263.0709) together with its ^1H and ^{13}C NMR spectroscopic data (Table 4.6). The ^{13}C NMR spectrum (Fig. 4.16) showed fifteen carbon signals. The IR spectrum is similar to AU 15, see appendix I. The spectrum also showed signal for the carbon atom of the keto group at (δc 178.3) assigned to (C-4).

The ^1H NMR spectrum (Fig. 4.15) revealed the presence of a one-proton singlet at δ_H 6.90 for H-3. Two characteristic one-proton doublets at δ_H 7.23 and 7.79 (d, 2.2 Hz,)

assignable to position H-3'' and H-2'', are due to the furan ring and two ortho coupled aromatic doublets at the lowest field δ_H 8.18 (d, 8.8 Hz, H-5) and δ_H 7.59 (m, H-6). Additionally, a two-proton multiplet resonating at δ_H 7.98 assigned to position H-2' and H-6', and a three-proton multiplet centred at δ_H 7.57 assigned to H-3', H-4' and H-5' suggested that the ring was unsubstituted. The HSQC spectrum (Fig. 4.20), showed direct correlations between C-1'' to H-1'', C-2'' to H-2'' and C-3 (δc 108.1) to H-3 (δ_H 6.90). The spin system was further exhibited in the COSY spectrum (Fig. 4.19), where the furan ring proton H-2'' coupled with H-3'' and the aromatic proton at H-5 coupled to H-6. The location of the furan ring on ring A was determined on the basis of the HMBC spectrum (Fig. 4.17), which showed a long range correlation between H-2'' to C-3'', C-7 and C-8, and H-3'' to C-2'', C-7 and C-8 respectively. These correlations confirmed that the furan ring was fused in an angular form on ring A at position 7 and 8 (Fig. 4.18). The NMR data (Table 4.6) are virtually identical to literature values (Lee and Morehead, 1995; Mbafor et al., 1995).

This compound has been isolated from *Pongamia pinnata* fruits (Minakawa et al., 2010; Yadav et al., 2004), roots of *Dahlstedtia pinnata* and *D. pentaphylla* (Garcez et al., 1988), root bark of *Millettia sanagana* (Mbafor et al., 1995) and *Lonchocarpus latifolius* roots (Magalhaes et al., 2000). This compound did not produce any inhibition on TRAIL-rsistance in human gastric adenocarcinoma (AGS) cell lines when tested at concentration of 30 and 40 µg/ml using the fluorometric microculture cytotoxicity assay (FMCA) method (Minakawa et al., 2010).

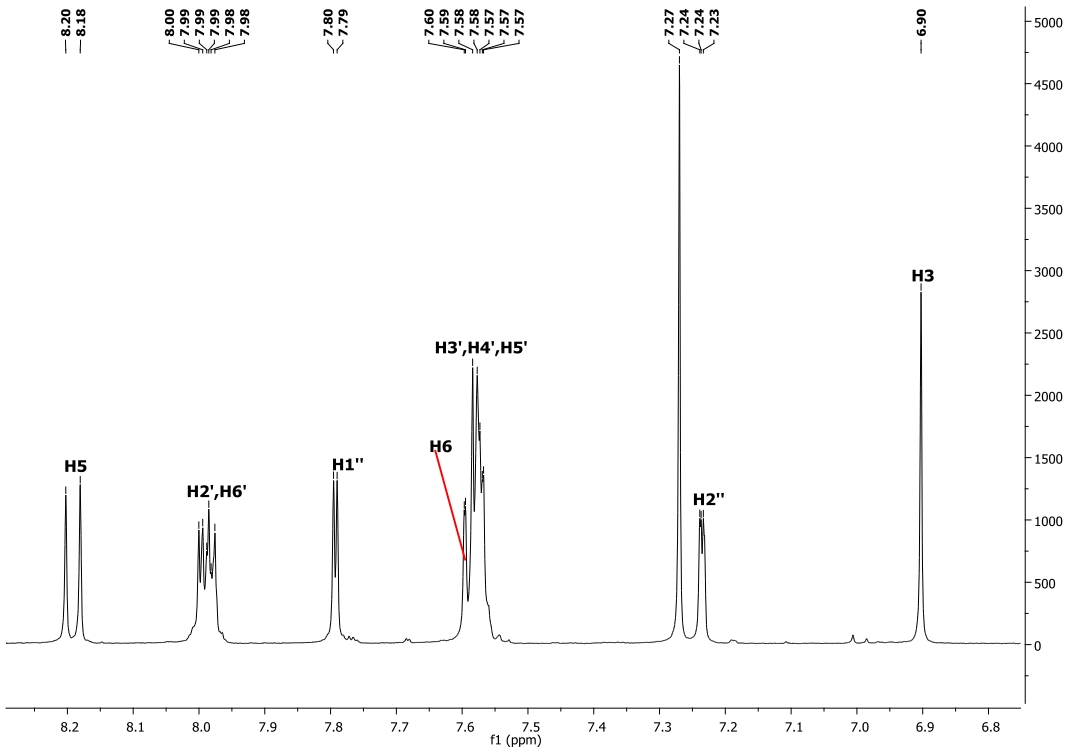

Fig. 4.15. ^{1}H NMR spectrum of compound AU 17.

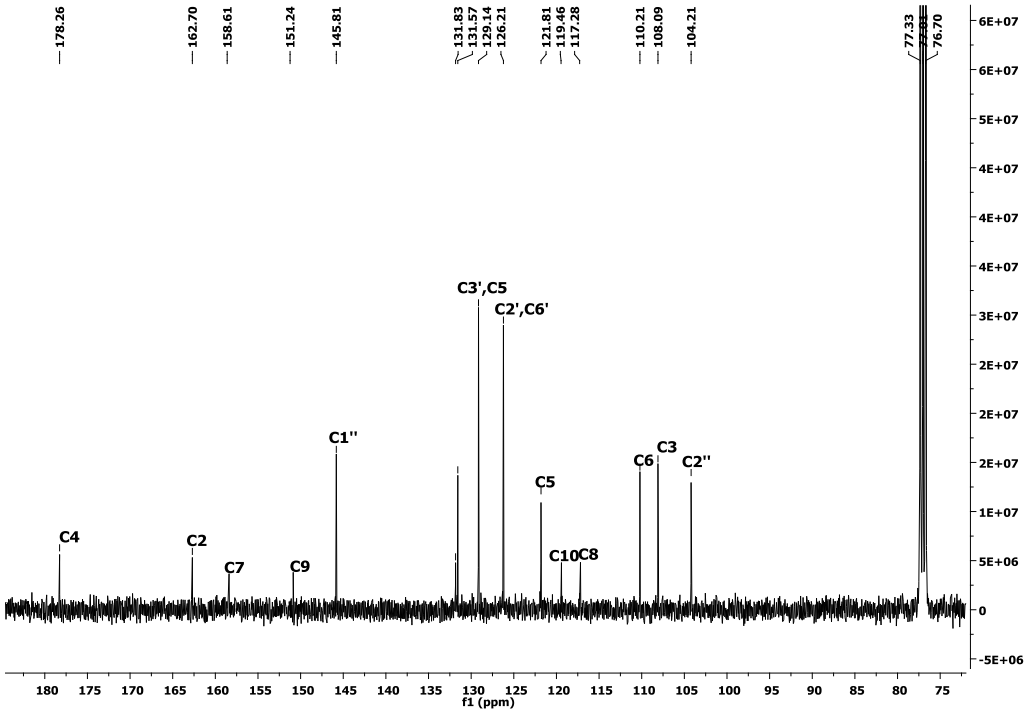

Fig. 4.16. ^{13}C NMR spectrum of compound AU 17.

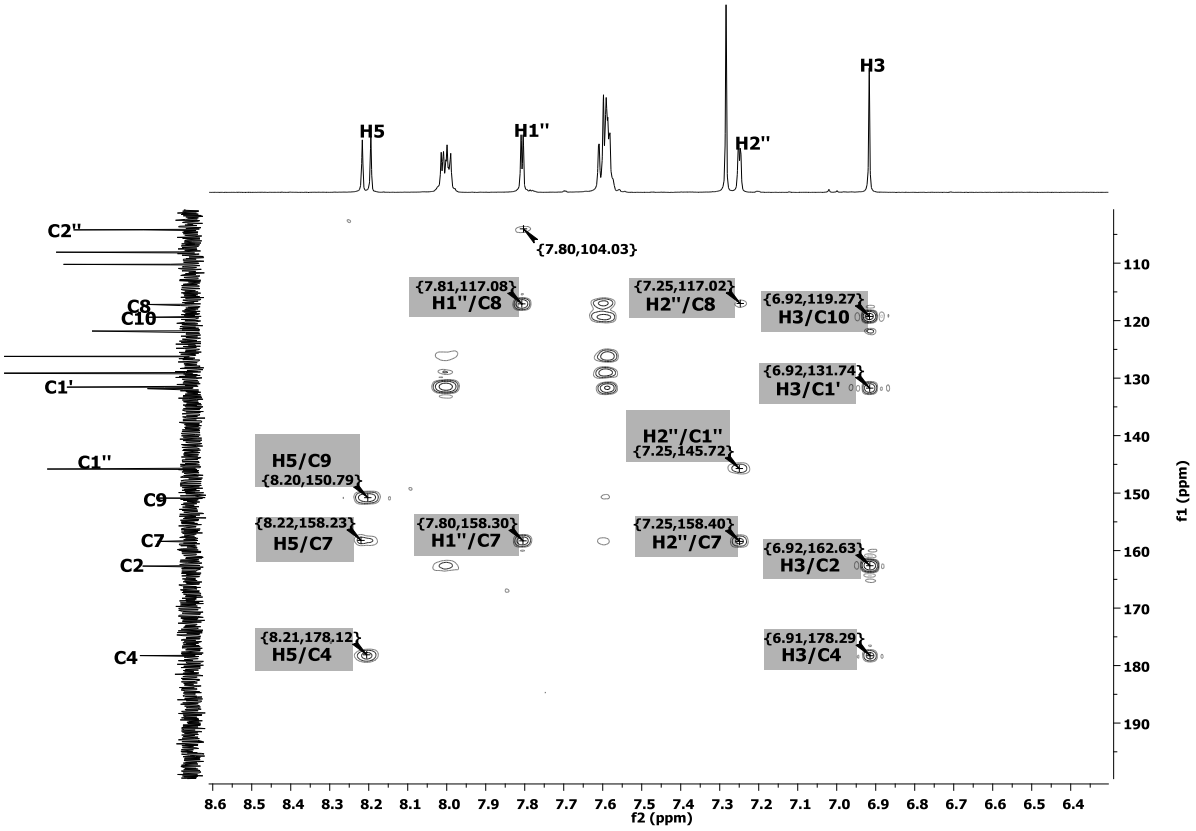

Fig. 4.17. HMBC spectrum of compound AU 17.

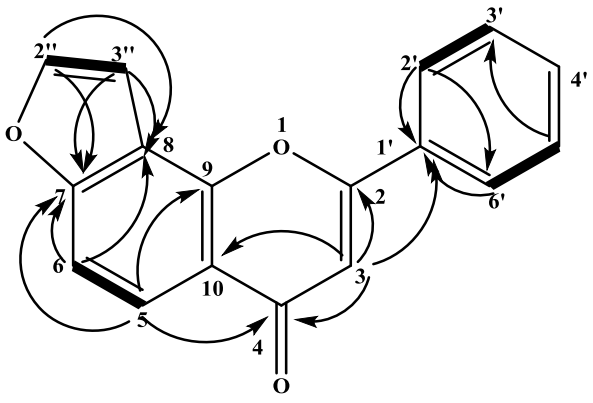

Fig. 4.18. HMBC and COSY correlations of compound AU 17.

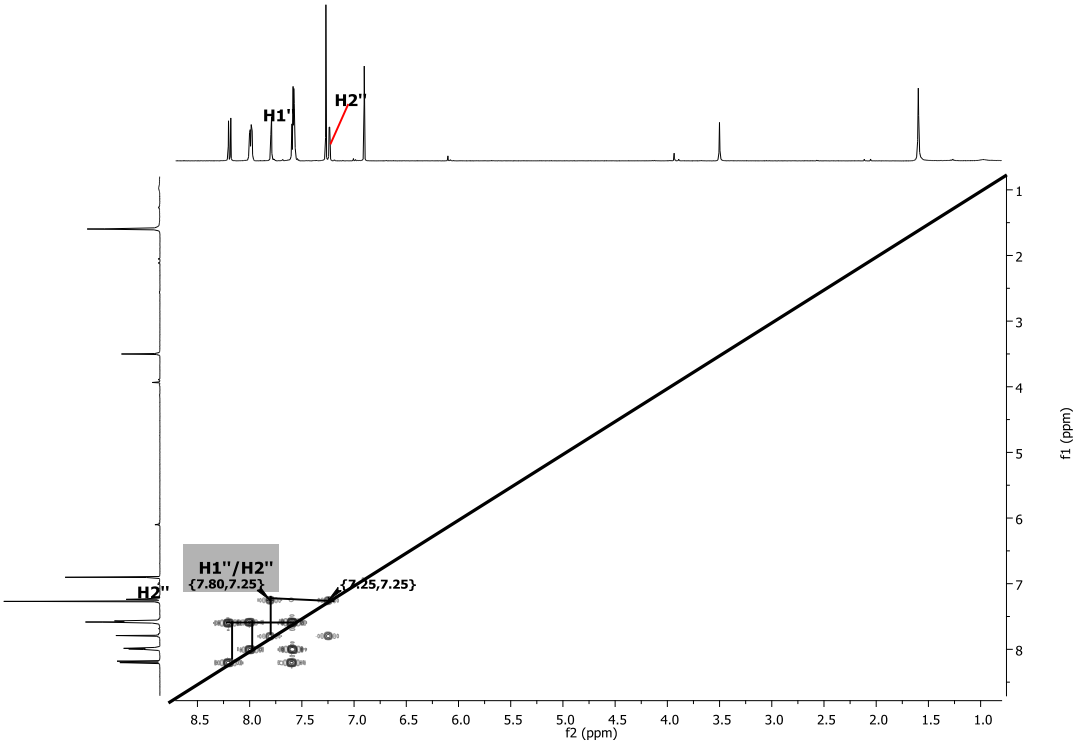

Fig. 4.19. COSY spectrum of compound AU 17.

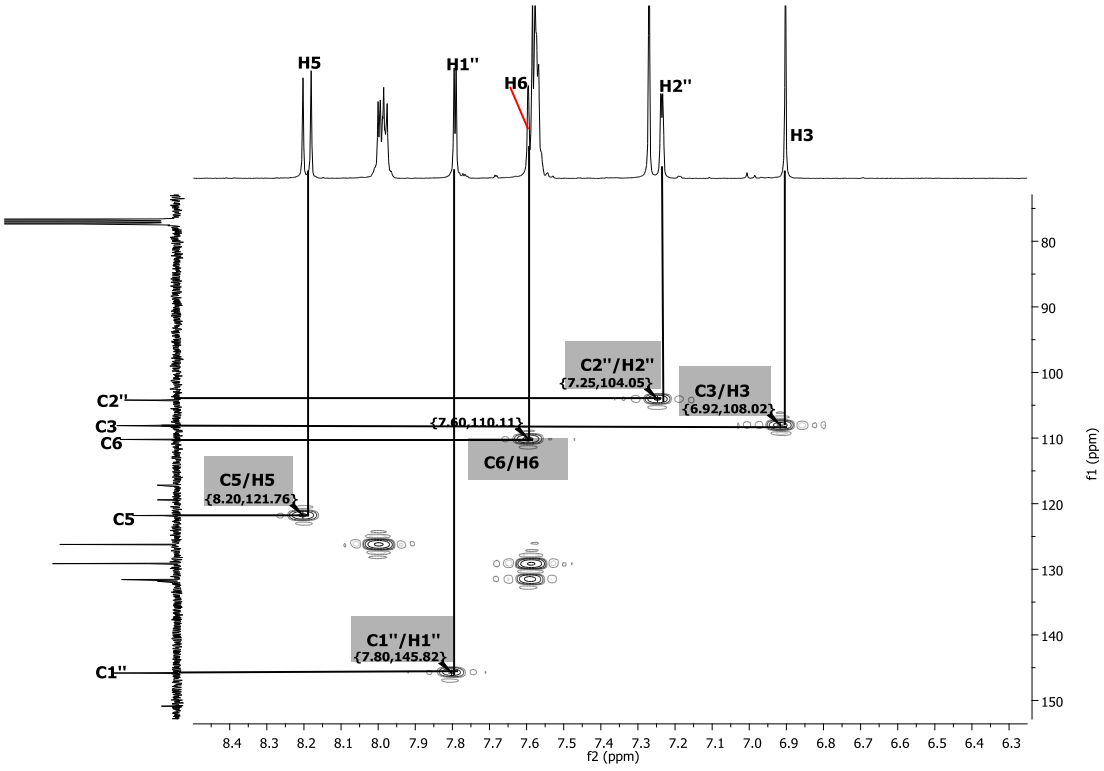

Fig. 4.20. HSQC spectrum of compound AU 17.

Table 4.6. ^{1}H and ^{13}C NMR data of compound AU 17.

Atom No.	Lee 1995 $CDCl_3$ δ_C	Mbafor 1995 DMSO δ_C	AU 17 $CDCl_3$ δ_C (m)	AU 18 $CDCl_3$ δ_H (m, *J* in Hz)	Lee 1995 $CDCl_3$ δ_H (m, *J* in Hz)	Mbafor 1995 DMSO δ_H (m, *J* in Hz)
2	162.6	162.7	162.7 (C)	–	–	–
3	108.1	108.1	108.1 (C)	6.90 (s)	6.90 (s)	6.74 (s)
4	178.2	178.2	178.3 (C)			
5	121.8	121.8	121.8 (CH)	8.18 (d, 8.8)	8.17 (d, 8.8)	–
6	110.1	110.2	110.2 (CH)	7.59 (m)	7.62 (m)	–
7	158.3	158.4	158.6 (C)			
8	117.1	117.2	117.3 (C)			
9	150.8	150.9	151.2 (C)			
10	119.3	119.4	119.5 (C)			
1’	131.6	131.8	131.8 (C)			
2’	126.1	126.2	126.2 (CH)	7.98 (m)	7.97 (m)	7.88 (m)
3’	129.0	129.1	129.1 (CH)	7.57 (m)	7.56 (m)	7.50 (m)
4’	131.6	131.5	131.6 (CH)	7.57 (m)	7.56 (m)	7.50 (m)
5’	129.0	129.1	129.1 (CH)	7.57 (m)	7.56 (m)	7.50 (m)
6’	126.1	126.2	126.2 (CH)	7.98 (m)	7.97 (m)	7.88 (m)
2’’	145.8	145.8	145.8 (CH)	7.79 (d, 2.2)	7.78 (d, 2.1)	7.70 (d, 1.8)
3’’	104.2	104.2	104.2 (CH)	7.23 (d, 2.2)	7.24 (d, 2.1)	7.12 (d, 1.8)

Table 4.7. Compound AU 18 (nimbin).

Methyl (2*R*,3a*R*,4a*S*,5*R*,5a*R*,6*R*,9a*R*,10*S*,10a*R*)-5-(acetyloxy)-2-(furan-3-yl)-10-(2-methoxy-2-oxoethyl)-1,6,9a,10a-tetramethyl-9-oxo-3,3a,4a,5,5a,6,9,9a,10,10a-decahydro-2*H*-cyclopenta[*b*]naphtho[2,3-d]furan-6-carboxylate	
Synonyms	Nimbin
Sample codes	AU 18
Sample amount	41 mg
Physical Description	White crystalline solid
Molecular formula	$C_{30}H_{36}O_9$
Molecular Weight	540 g/mol
Melting Point	214 - 216 ºC
IR:($CHCl_3$)	2953, 1735, 1685, 1435, 1376, 1234, 1030, 758 cm^{-1}

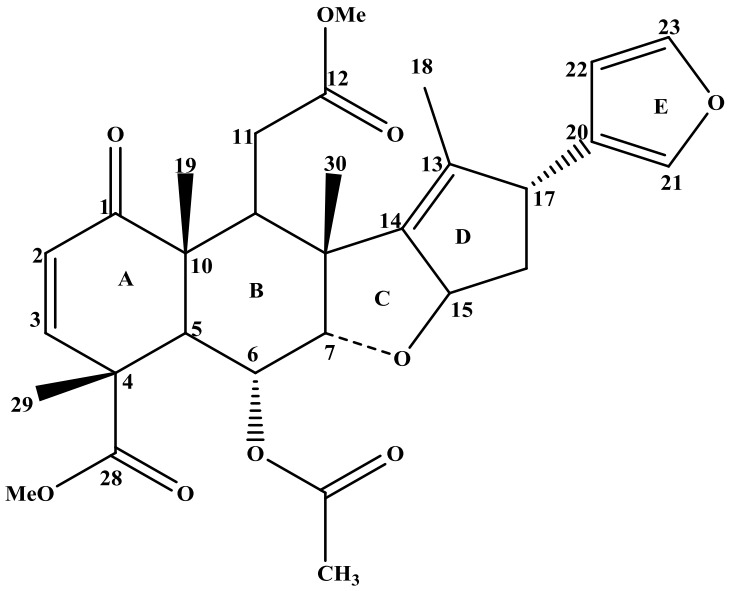

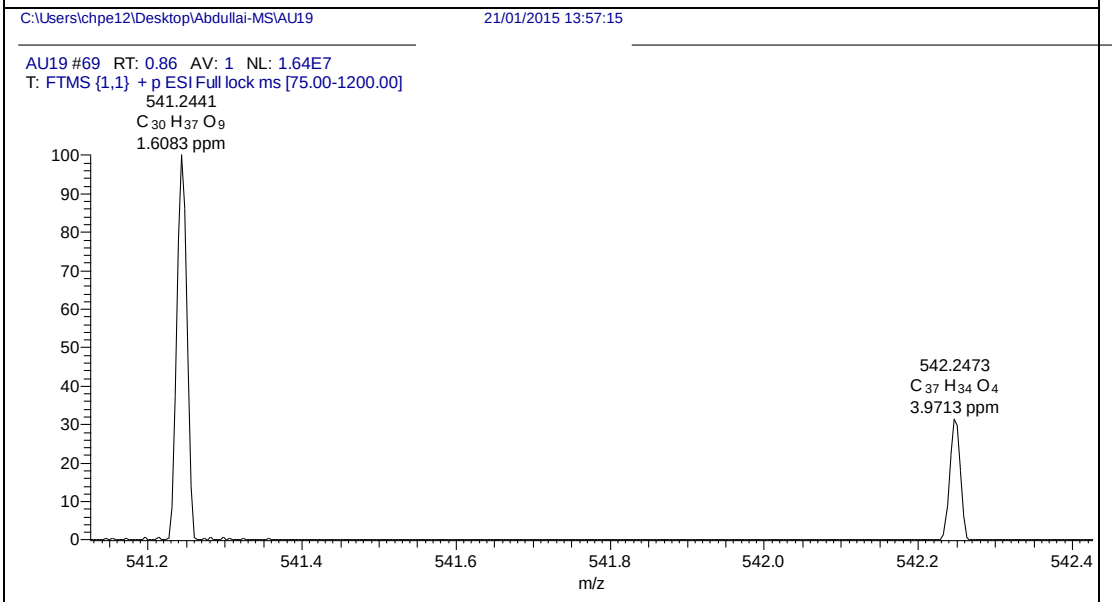

Compound AU 18 (41 mg) was isolated as white crystalline solid. It has a molecular formula of $C_{30}H_{36}O_9$ which was established on the basis of ESI-HRMS at m/z 541.2441 $[M + H]^+$ (Calcd for 541.2438). The IR spectrum showed a band at 2953 cm^{-1} (saturated C-H stretching), 1735 (C=O stretching), 1685 (C=C stretching), 1435 (C-H deformation), 1234 and 1030 (C-O stretching) and 754 (C-H out of plane deformation) cm^{-1}, see appendix I. The DEPT spectrum (Fig. 4.22) showed thirty carbon signals, which consisted of ten quaternary, eleven methine, two methylene, seven methyl group. Although this has been counted in the DEPT spectrum, also showed signals for the carbon atoms of the keto group (C-1) at (δc 201.62), two methyl esters carbonyl carbon atoms C-12 and 28 (δc 173.66 and 174.64), the acetate carbon atom at C-6 (δc 170.58), the β-substituted furan ring resonates at C-21 (δc 139.01), C-22 (δc 110.49) and C-23 (δc 143.02), and the carbon atoms in the tetrahydrofuran ring linked to oxygen occured at C-7 (δc 84.58) and C-15 (δc 87.12).

The ^1H NMR spectrum (Fig 4.21) revealed the characteristic signals due to a β-substituted furan ring (ring E) protons at δ_H 7.34 (m, H-21), 6.35 (m, H-22) and 7.25 (m, H-23). These protons signals were seen to be coupled to each other in the COSY spectrum (Fig. 4.25). The HSQC spectrum (Fig 4.26) correlated the proton signals at δ_H 7.34, 6.35 and 7.25 to the carbon resonance at δc 139.01, 110.49 and 143.02 attributable to position (C-21), C-22) and (C-23) respectively. The quaternary carbons atom resonance at δc 126.82 were assigned to C-20.

In ring A, the ^1H NMR spectrum displayed resonances ascribable to enone protons at (H-2) and (H-3). These vinylic protons split each other resulting in a doublet at δ_H 5.86 and 6.34 (d, 10.1 Hz, each) assigned to position H-2 and H-3. The COSY spectrum showed these protons to be coupled to each other. The HSQC spectrum correlate H-2 to C-2 (δc 125.98) and H-3 to C-3 (δc 147.59). The keto and methyl ester carbonyl carbon atom occured at C-1 and C-28, while the quaternary carbon atom resonance at δc 47.77 was assigned to C-4.

In ring B, ^1H NMR, H-5 was split by H-6 resulting in a doublet at δ_H 3.71 (d, 3.3 Hz) in the spectrum. Proton H-6 was split by H-5 and H-7 resulting in a doublet of doublet at δ_H 5.21 (dd, 3.0, 12.2 Hz) and H-9 was split by H-$11_{a\&b}$ resulting in a multiplet at δ_H 2.85. The COSY spectrum showed H-6 coupled to H-5. The HSQC spectrum correlated H-5 to the carbon atom resonance at δc 41.52 and H-6 to the carbon atom at δc 68.69.

The C-10 quaternary carbon atom resonance occurred at δc 48.03.

In ring C, Proton H-7 was split by proton H-6 resulting in a doublet at 4.06 (d, 2.9 Hz). The COSY spectrum also showed H-7 to be coupled to H-6. The HSQC spectrum correlated H-7 to the carbon atom resonance at δc 84.58 (CHO) which was indicative of a carbon atom linked to an oxygen atom. The C-8 quaternary carbon atom resonance occured at δc 47.09.

In ring D, proton H-15 was split by protons H-$16_{a\&b}$ and yielded a multiplet at δ_H 5.56. The protons H-$16_{a\&b}$ were split by the H-15 and H-17 δ_H 3.64 resulted in a multiplet at δ_H 2.01 and δ_H 2.19. H-17 was equally split by H-$16_{a\&b}$ and occurred as a multiplet at δ_H 3.64. The COSY spectrum confirmed the coupling between H-16 and H-17. The spectrum of HSQC, also show the coupling of proton resonances H-15, H-$16_{a\&b}$ and H-17 to the carbon resonance at δc 87.12 (CHO), δc 41.60 and δc 49.49 (CH). The quaternary carbon atom resonance for C-13 and C-14 occurred at δc 135.11 and δc 146.15.

The four-methyl proton resonances; H-18, H-19, H-29 and H-30 were assigned to carbon atom resonances at δc 12.85, δc 16.67, δc 17.21 and δc 16.72. Finally, the rings were sustained by long range coupling of quaternary carbon to protons as observed in the HMBC (Fig 4.23 and 4.24), where C-4 correlate with H-5 and H-29; C-8 correlate with H-7, H-9, H-11 and H-30; C-10 correlate with H-5, H-9 and H-19; C-13 correlate with H-17 and H-18; C-14 correlate with H-15 while C-20 correlate with H-17 and H-22 (6.35 m) respectively. Comparison of the, ^{1}H and ^{13}C NMR data with those published by (Johnson and Morgan, 1997; Narasimhan et al., 2011) confirmed nimbin as the compound isolated. Finally, the X-ray crystallography (Fig. 4.27) of this compound also confirmed it to be nimbin.

This compound was previously reported from the seed oil of *Azadirachta indica* (Johnson and Morgan, 1997; Silva et al., 2007). The antifeedant and insect growth-regulating activity of nimbin was studied against S*podoptera litura*, *Pericallia ricini* and *Oxya fuscovittata* at a concentration of 5 µg/cm^2 leaf area. It was reported that nimbin is more effective in *Oxya fuscovittata* followed by *Pericallia ricini* and then *Spodoptera litura* (Govindanchari et al., 1996).

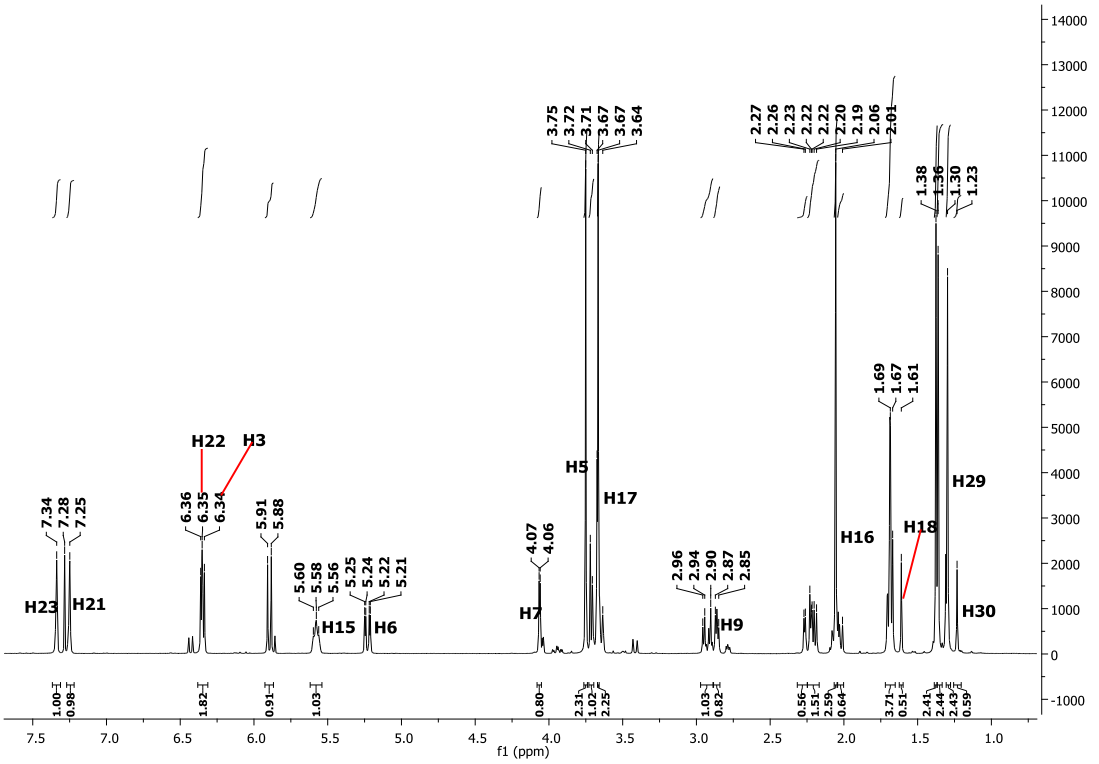

Fig. 4.21. [1]HNMR spectrum of compound 18.

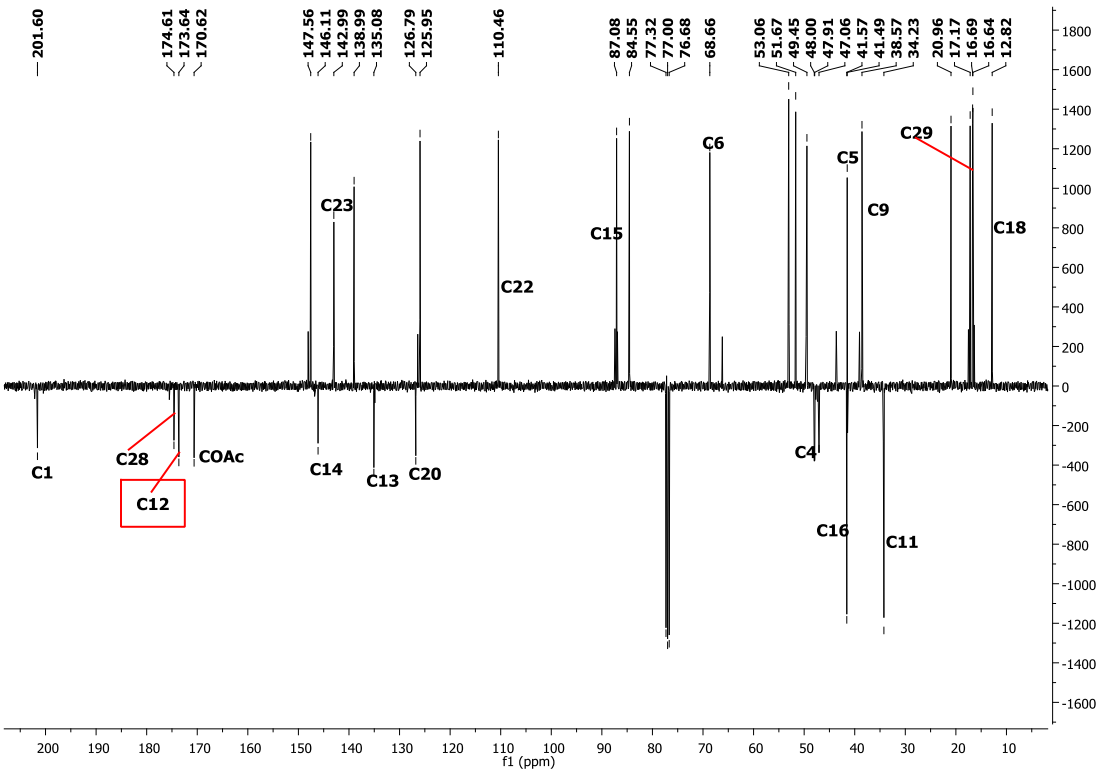

Fig. 4.22. DEPT spectrum of compound AU 18.

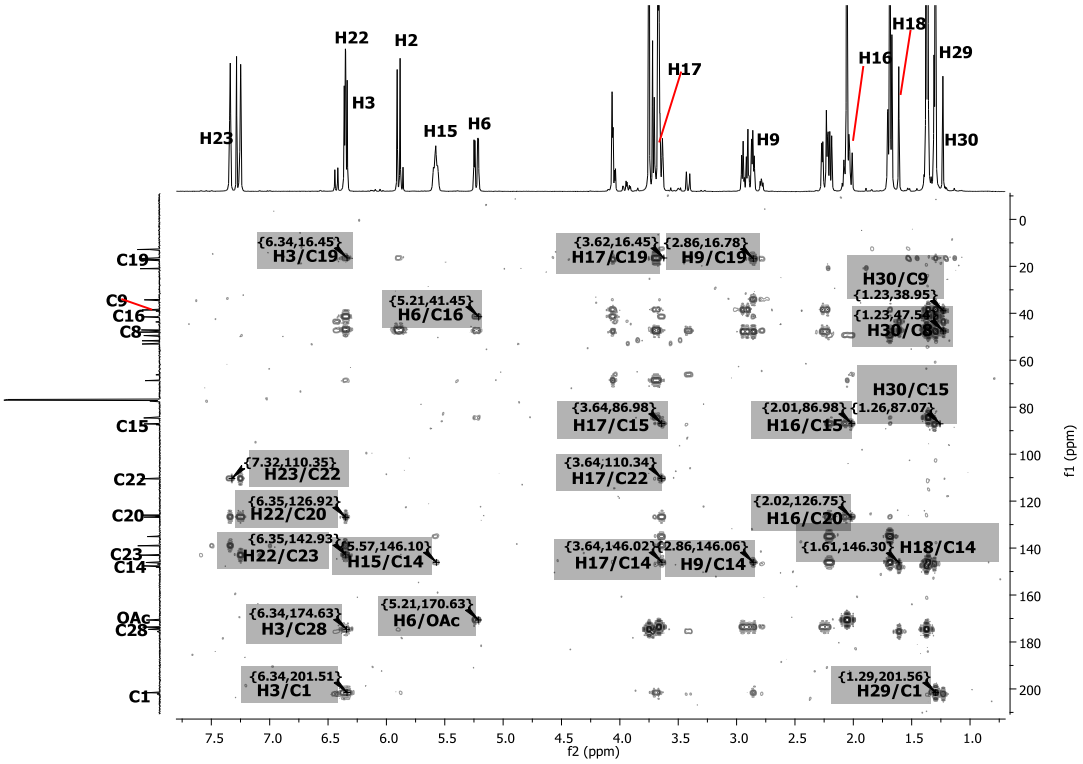

Fig. 4.23. HMBC spectrum of compound AU 18.

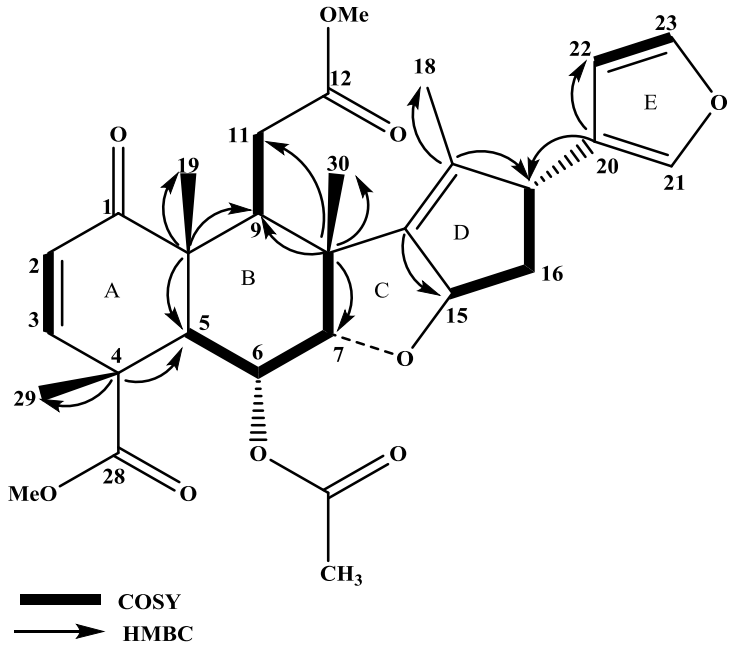

Fig. 4.24. HMBC and COSY correlations of compound AU 18.

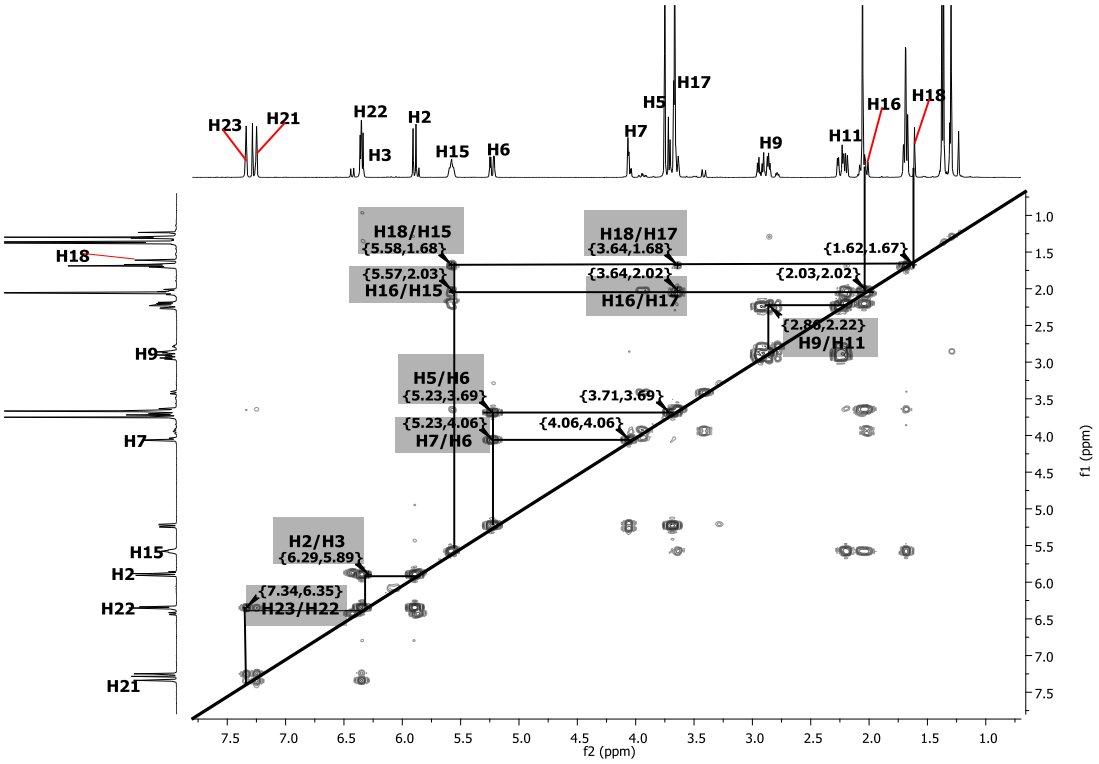

Fig. 4.25. COSY spectrum of compound AU 18.

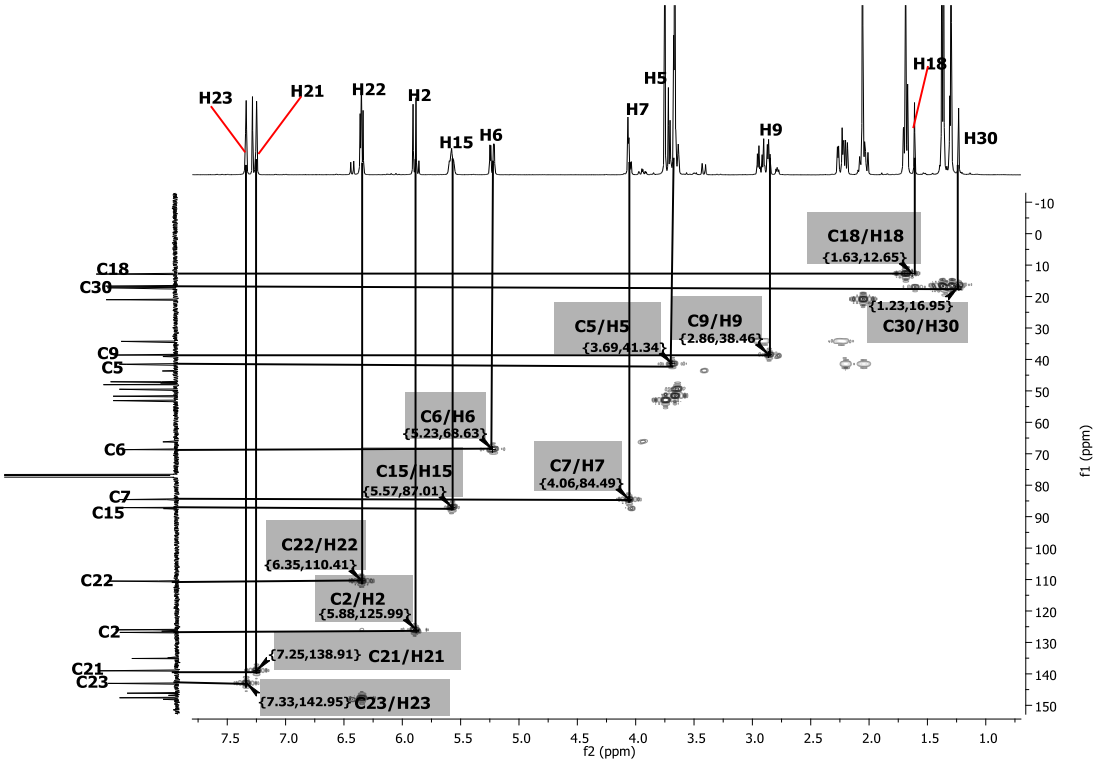

Fig. 4.26. HSQC spectrum of compound AU 18.

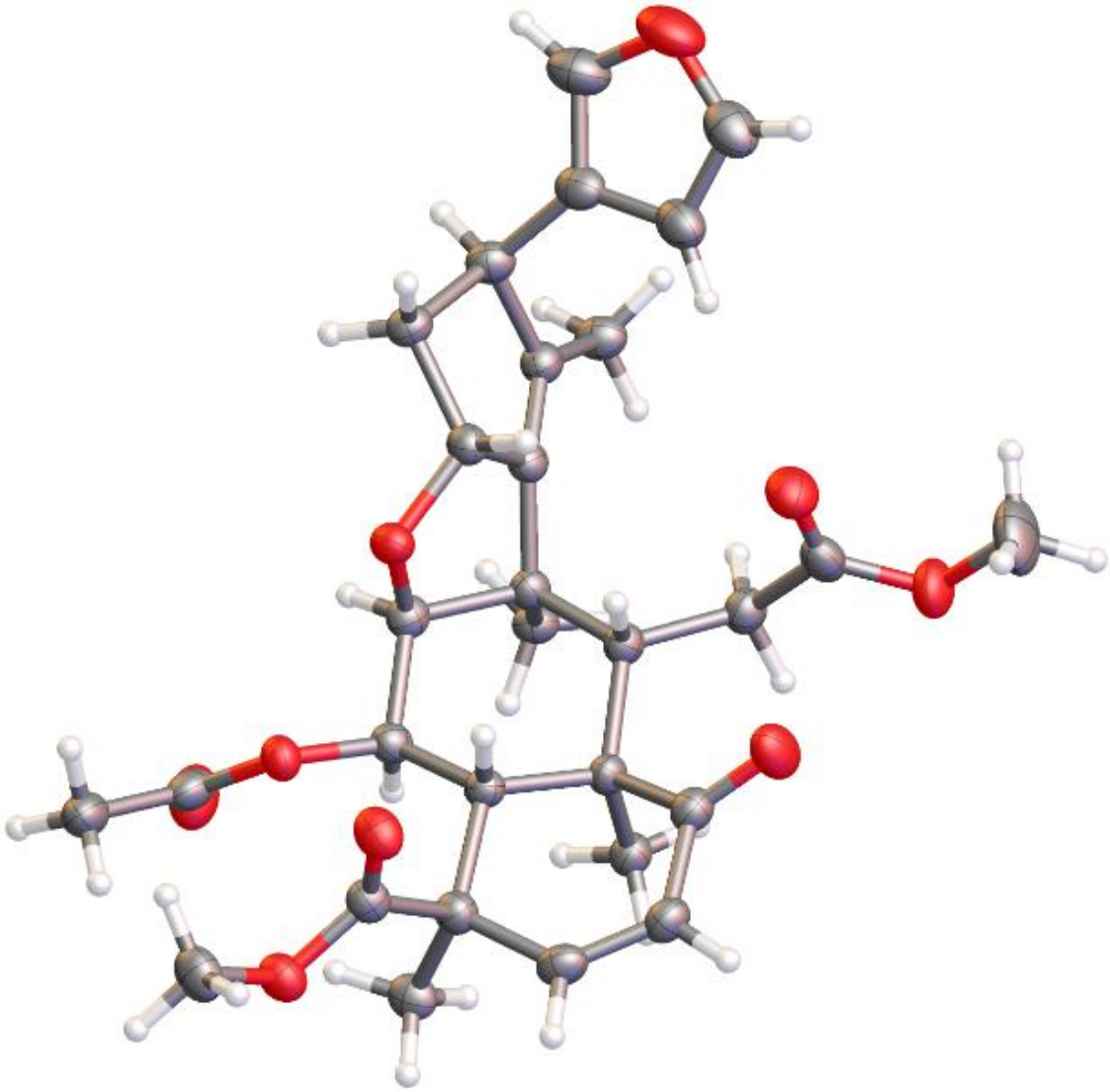

Figure 4.27. The X-ray crystal structure of nimbin.

Table 4.8. ^{1}H and ^{13}C NMR data of compound AU 18.

Atom No.	Narasimh-an, 2011 $CDCl_3$ δ_C	Johnson and Morgan, 1997 $CDCl_3$ δ_C	AU 18 $CDCl_3$ δ_C (m)	AU 18 $CDCl_3$ δ_H (m, *J* in Hz)	Narasimhan 2011 $CDCl_3$ δ_H (m, *J* in Hz)	Johnson and Morgan, 1997 $CDCl_3$ δ_H (m, *J* in Hz)
1	201.8	201.73	201.62 (C)			
2	126.0	125.96	125.98 (CH)	5.86 (d, 10.2)	5.85 (d, 10.5)	5.58 (d)
3	147.6	147.58	147.59 (CH)	6.34 (d, 10.2)	6.34 (d, 10.4)	6.34 (d)
4	47.0	47.77	47.77 (C)			
5	42.3	41.53	41.52 (CH)	3.71 (d, 3.3)	3.50 (d, 3.0)	3.70 (d)
6	68.3	68.66	68.69 (CH)	5.21 (dd, 3.0, 12.3)	5.19 (dd, 3.0, 12.3)	5.22 (dd)
7	84.55	84.53	84.58 (CH)	4.06 (d, 2.9)	3.80 (d, 2.3)	4.05 (d)
8	49.9	47.08	47.09 (C)			
9	41.3	38.59	38.60 (CH)	2.85 (m)	2.70 (m)	2.87 (m)
10	48.9	47.93	48.03 (C)			
11A	33.2	34.23	34.26 (CH_2)	2.19 (m)	2.13 (m)	2.25 (m)
11B				2.90 (m)	2.70 (m)	2.94 (m)
12	174.9	173.64	173.66 (C)			
13	135.07	135.08	135.11 (C)			
14	146.12	146.16	146.15 (C)			
15	87.08	87.10	87.12 (CH)	5.56 (m)	2.34 (m)	5.57 (m)
16A	41.50	41.59	41.60 (CH_2)	2.01 (m)	5.74 (m)	2.02 (m)
16B				2.19 (m)		2.19 (m)
17	49.46	49.47	49.49 (CH)	3.64 (m)		3.61 (m)
18	12.81	12.83	12.85 (CH_3)	1.61 (s)	1.66 (s)	1.69 (d)
19	16.96	16.66	16.67 (CH_3)	1.36 (d, 5.8)	1.34 (s)	
20	119.2	126.81	126.82 (C)			
21	139.5	139.01	139.01 (CH)	7.34 (m)	7.32 (m)	7.32 (m)
22	109.4	110.48	110.49 (CH)	6.35 (m)	6.45 (m)	6.33 (m)
23	142.5	143.01	143.02 (CH)	7.25 (m)	7.59 (m)	7.23 (m)
28	174.9	174.59	174.64 (C)			
29	17.1	17.19	17.21 (CH_3)	1.30 (s)	1.29 (s)	1.36 (s)
30	16.67	16.70	16.72 (CH_3)	1.23 (s)	0.96 (s)	1.34 (s)
12-OCH3	51.8	51.66	51.70	3.67 (s)	3.76 (s)	3.65 (s)
28-OCH3	52.7	53.05	53.09	3.75 (s)	3.81 (s)	3.73 (s)
OAc	170.3 20.62	170.58 20.96	170.65 20.99	2.06 (s)	1.90 (s)	2.04 (s)

Table 4.9. Compound AU 19 (Azadirachtin).

dimethyl (2a*R*,3*S*,4*S*,*R*,*S*,7a*S*,8*S*,10*R*,10a*S*,10b*R*)- 10-(acetyloxy)- 3,5-dihydroxy- 4-[(1*S*,2*S*,6*S*,8*S*,9*R*,11*S*)- 2-hydroxy- 11-methyl- 5,7,10-trioxatetracyclo [6.3.1.$0^{2,6}$.$0^{9,11}$]dodec- 3-en- 9-yl]- 4-methyl- 8-{[(2*E*)- 2-methylbut- 2-enoyl]oxy}octahydro- 1*H*-furo[3',4':4,4a]naphtho[1,8-*bc*]furan- 5,10a(8*H*)-dicarboxylate	
Synonyms	Azadirachtin
Sample codes	AU 19
Sample amount	2.3 mg
Physical Description	Reddish needle
Molecular formula	$C_{35}H_{44}O_{16}$
Molecular Weight	720 g/mole

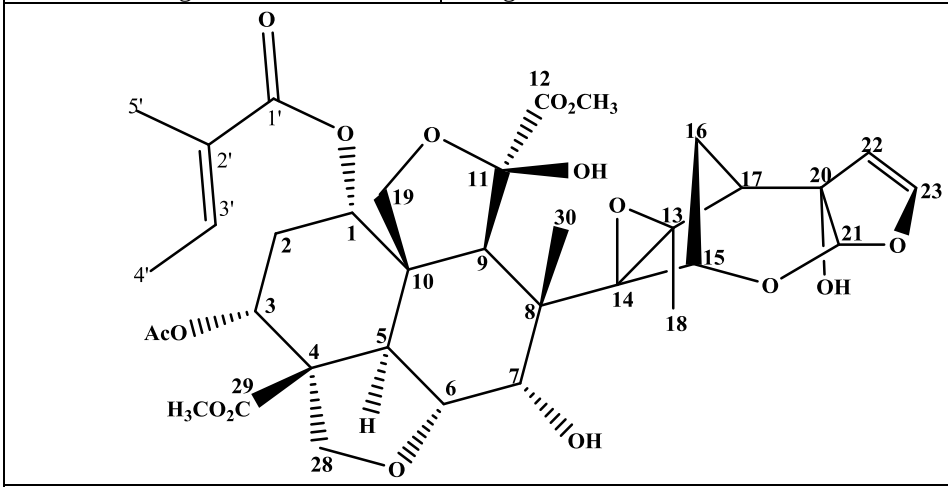

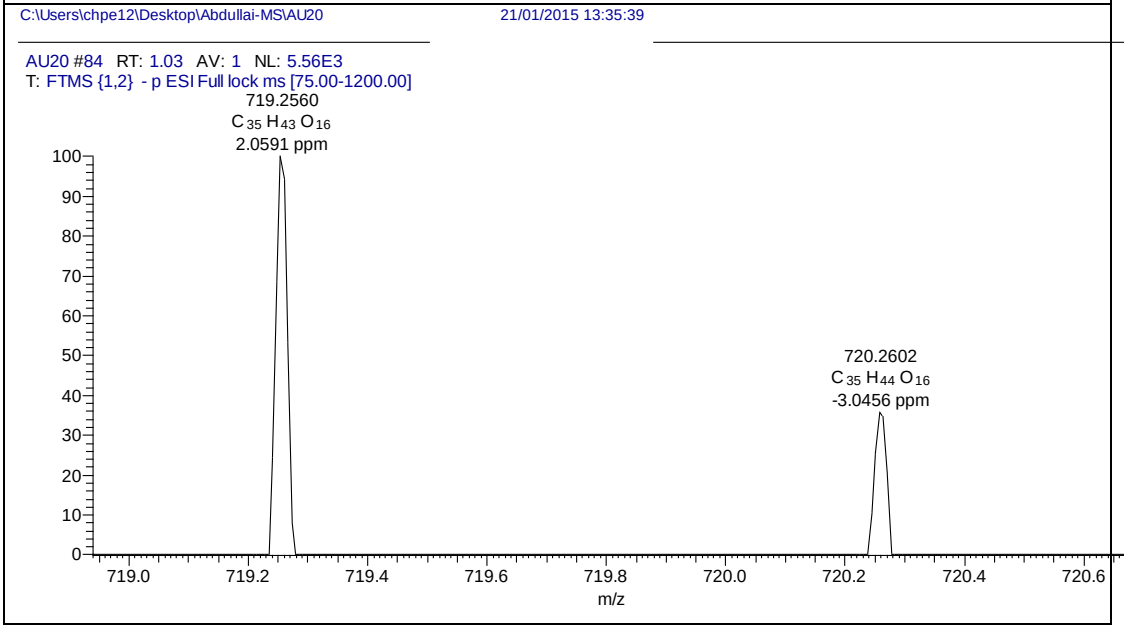

Compound AU 19 (2.3 mg) was isolated as reddish needles. It has a molecular formula of $C_{35}H_{44}O_{16}$ which was established on the basis of ESI-HRMS at m/z 719.2560 $[M - H]^-$ (Calcd for 719.2550). The ^1H NMR spectrum (Fig. 4.28) showed a pair of coupled doublets at δ_H 5.05 and δ_H 6.46 (d, 2.8 Hz, each) assigned to H-22 and H-23 with a methine proton at 5.64 (s, H-21), indicating the presence of 2,3-dihydrofuran ring. The protons for annulated tetrahydrofuranacetal were observed at δ_H 3.34 (s), δ_H 3.61 and

δ_H 4.14 (d, 9.7 Hz, each) attributable to H-9 and H-19. The spectrum also showed two methyl groups at δ_H 2.01 and δ_H 1.75 assigned to H-18 and H-30.

The NMR data (Table 17) showed signals typical of azadirachtin and this was confirmed by high resolution MS, and comparison of its ^{1}H MR data with those reported in the literature (Johnson and Morgan et al 1997 and Kraus 1987). Due to the low amount obtained, no further ^{13}C or 2D NMR spectra were acquired.

This compound was previously reported from the seed oil of *Azadirachta indica* (Johnson and Morgan, 1997; Kraus, 2002; Kraus et al., 1981; Silva et al., 2007). The antifeedant and insect growth-regulating activity of azadirachtin was compared to that of nimbin using a concentration of 5 µg/cm^2 leaf area for S*podoptera litura*, *Pericallia ricini* and *Oxya fuscovittata*. Azadirachtin was reported to be as twice as effective as nimbin and was most effective on *O. fuscovittata* followed by *P. ricini* and then *S. litura* (Govindanchari et al., 1996).

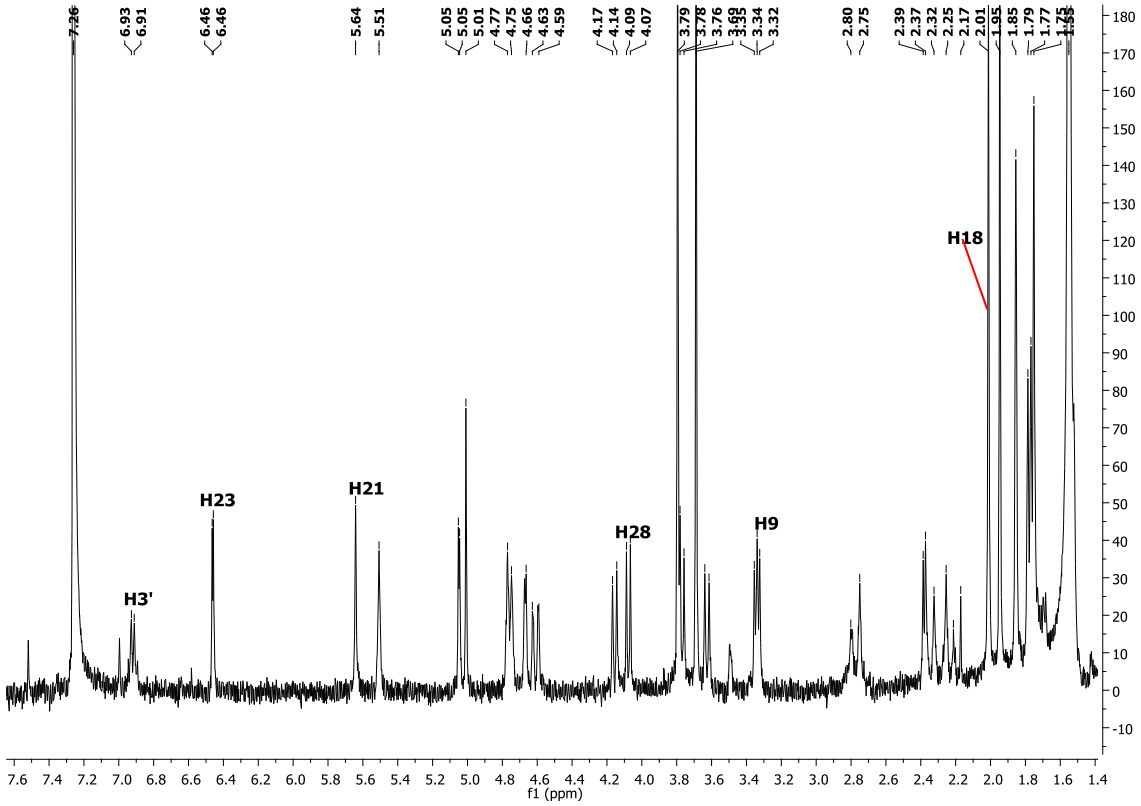

Fig. 4.28. ^{1}H NMR spectrum of compound AU 19.

Table 4.10. ^{1}H and ^{13}C NMR data of compound AU 19.

Atom No.	Johnson and Morgan 1997 $CDCl_3$ δ_C	Kraus 1987 $CDCl_3$ δ_C	Johnson and Morgan 1997 $CDCl_3$ δ_H (m, *J* in Hz)	Kraus 1987 $CDCl_3$ δ_H (m, *J* in Hz)	AU 19 $CDCl_3$ δ_H (m, *J* in Hz)
1	70.58	70.88	4.77 (m)	4.75 (dd, 2.9, 3.1)	4.75 (m)
2A	29.73	29.37	2.32 (m)	2.34 (ddd, 16.7, 2.9 2.7)	2.32 (m)
2B			2.26 (m)	2.13 (ddd, 16.7, 3.1, 2.9)	2.25 (m)
3	67.00	66.99	5.51 (br t)	5.50 (dd, 2.7, 2.9)	5.51 (m)
4	52.76	52.52			
5	36.96	37.06	3.34 (d)	3.35 (d, 12.5)	3.34 (m)
6	73.95	73.79	4.62 (dd)	4.60 (dd, 12.5, 2.7)	4.59 (dd, 12.3, 2.6)
7	74.28	74.37	4.77 (m)	4.75 (d, 2.7)	4.76 (m)
8	45.56	45.41			
9	44.69	44.69	3.34 (s)	3.34 (s)	3.34 (m)
10	50.24	50.19			
11	104.20	104.10			
12	171.83	171.70			
13	68.70	68.53			
14	70.04	69.69			
15	76.70	76.43	4.67 (d)	4.67 (d, 3.4)	4.66 (d, 3.56)
16A	25.07	25.06	e	1.73 (ddd, 13.0, 3.4, 5.1)	a
16B			1.31 (d)	1.31 (d, 13.0)	1.25 (d, 12.5)
17	48.63	48.67	2.38 (d)	2.38 (d, 5.1)	2.37 (d, 5.2)
18	18.47	18.49	2.01 (s)	2.01 (s)	2.01 (s)
19A	69.02	69.07	3.63 (d)	3.63 (d, 9.6)	3.61 (d, 9.7)
19B			4.15 (d)	4.15 (d, 9.6)	4.14 (d, 9.7)
20	-	83.55			
21	108.55	108.70	5.65 (s)	5.65 (s)	5.64 (s)
22	107.56	107.30	5.05 (d)	5.05 (d, 2.9)	5.05 (d, 2.8)
23	146.88	147.00	6.46 (d)	6.46 (d, 2.9)	6.46 (d, 2.75)
28A	72.92		3.75 (d)	4.08 (d, 9.0)	4.07 (d, 8.9)
28B			4.08 (d)	3.76 (d, 9.0)	3.77 (d, 8.9)
29	173.63	173.20			
30	21.40	21.33	1.75 (s)	1.74 (s)	1.75 (s)
7-OH			2.83 (br s)	2.89 (br s)	2.75 (br s)
11-OH	53.05	53.52	5.03 (d)	5.05 (s)	5.01 (s)
20-OH			2.89 (br s)	2.92 (br s)	2.80 (br s)
12-OCH_3	52.76	52.52	3.69 (s)	3.68 (s)	3.69 (s)
29-OCH_3	53.24	52.72	3.80 (s)	3.76 (s)	3.79 (s)
CH_3COO	169.79	169.50	1.95 (s)	1.95 (s)	1.95 (s)
CH_3COO	20.80	20.88			
Tigloyl'	166.30	166.22			
2'	128.56	128.60			
3'	137.89	137.50	6.92 (m)	6.93 (qq, 7.0, 1.5)	6.92 (m)
4'	14.34	14.29	1.78 (dd)	1.78 (dq, 7.0, 1.1)	1.77 (dd, 1.1, 7.1)
5'	11.94	11.94	1.86 (s)	1.85 (dq, 1.5, 1.1)	1.85 s

[e] Masked by signal at δ 1.75 **[a] Not recorded in spectrum**

CHAPTER 5
Conclusions and proposals for further work

T. emetica is a coveted multipurpose tree, which has been in use throughout Africa for medicinal and non-medicinal purposes. Sadly, this plant has not been well phytochemically studied as there are only few reviews available (Gunatilaka et al., 1998; Komane et al., 2011; Nakatani et al., 1985, 1981; Traore et al., 2007), unlike its cousin *Azadirachta indica*.

5.1 Fatty acid profiles

The crude oil content of both the seed and shell reported in this study has been established at around 60 and 23 % respectively, of the dry matter. The fatty acid composition of the seeds and shell oils from Ghana and Mozambique were determined using different analytical methods. The result obtained using ^{1}H and ^{13}C NMR and GC-MS of fatty acid methyl esters for the oil samples were palmitic (59.1-64 %), oleic 27.7-31.8 %), linoleic (4.3-7.2 %), stearic (0.4-3.2 %), myristic (0.2-1.1%) and linolenic acid (0.9-1.9 %). This result agrees with the findings of other researchers (Khumalo et al., 2002; Vermaak et al., 2011). The high percentage of saturated fatty acid in these oil samples indicated why it is a good raw material in body care industries.

The physicochemical parameters of the seeds oil samples from Ghana and Mozambique were also studied using standard methods of food analysis. From the results obtained, the acid (0.4±0.0 and 0.4±0.1 mg KOH/g), iodine (69.2±2.1 and 64.6±2.8 gI_2/100g), peroxide 10.3±0.5 and 9.2±0.4 %), saponifiable (195.4±5.4 and 197.3±4.6 mg KOH/g) and unsaponifiable value (1.3±0.1 and 1.0±0.1 %), respectively. The high saponification value in this oil samples, confirm the presence of low molecular weight fatty acid, while the low acid value suggested that in principle, the oil will be suitable for human consumptions. Because the oil is bitter and other alternative vegetable oils are available, its use for human consumption is limited, while it could be used as feedstock. In Eastern and Southern Africa, the oil is utilized in personal care industries while in West Africa the seeds are treated as waste product.

GC-MS was used to determine the individual components of the unsaponifiables fractions of *T. emetica* seed oil. Several peaks were observed with some identified from the NIST library. Two minor components was isolated and the structures elucidated to be β-sitosterol and stigmasterol. These compounds have been reported to exhibit good antimicrobial (Sen et al., 2012) and anti-leptospiral activity (Chander et al., 2015). Further screening of the

unsaponifiables matter will be necessary in order to identify compounds corresponding to unknown peaks, which may be of biological importance.

5.2 Phytochemicals from *T. emetica*

Trichilia emetica root and stem has been known to be rich in limonoids, with more than sixteen structures being identified. These limonoids were proven to have antifeedant property against some pest insects (Gunatilaka et al., 1998; Komane et al., 2011; Nakatani et al., 1985, 1981**).**

In the present study, the phytochemical investigation of the stems and seeds of *T. emetica* resulted in the isolation of eighteen pure compounds from the boiled water and methanol extracts of *T. emetica* seeds and stem bark. The structures of fourteen compounds were successfully elucidated using spectroscopic methods, two of which were sterols, and the rest flavonoids. These flavonoids could be classified according to their basic skeleton as flavonols (AU 12 and 13), flavanols (AU 4, 5, 6, 7 and 8), flavanonols (AU 9 and 10) and flavanones (AU 11 and 14). This study has proven that there is insufficient quantities of limonoids in the seed sample (less than 0.1 mg/kg), with some unresolved NMR spectra which could be alkaloids.

These isolated compounds were inactive when tested against *Trypanosoma brucei* and several other strains of bacterial and fungal species, except *K. pneumonia* (strains ATCC 13883) against which they were moderately active. Generally, flavonoids have been reported to have good antioxidant properties (Khallouki et al., 2007), they showed moderate activity at IC_{50} value greater than 500 and 200 µg/ml for antimicrobial and antilisterial activity (Nyila et al., 2012).

Similarly, three of the four pure compounds isolated from the methanol extract of *T. emetica* stem were structurally elucidated and were also found to be flavonoids.

Fig. 5.1. Hypothetic biosynthetic scheme leading to compounds AU 4 to AU 14

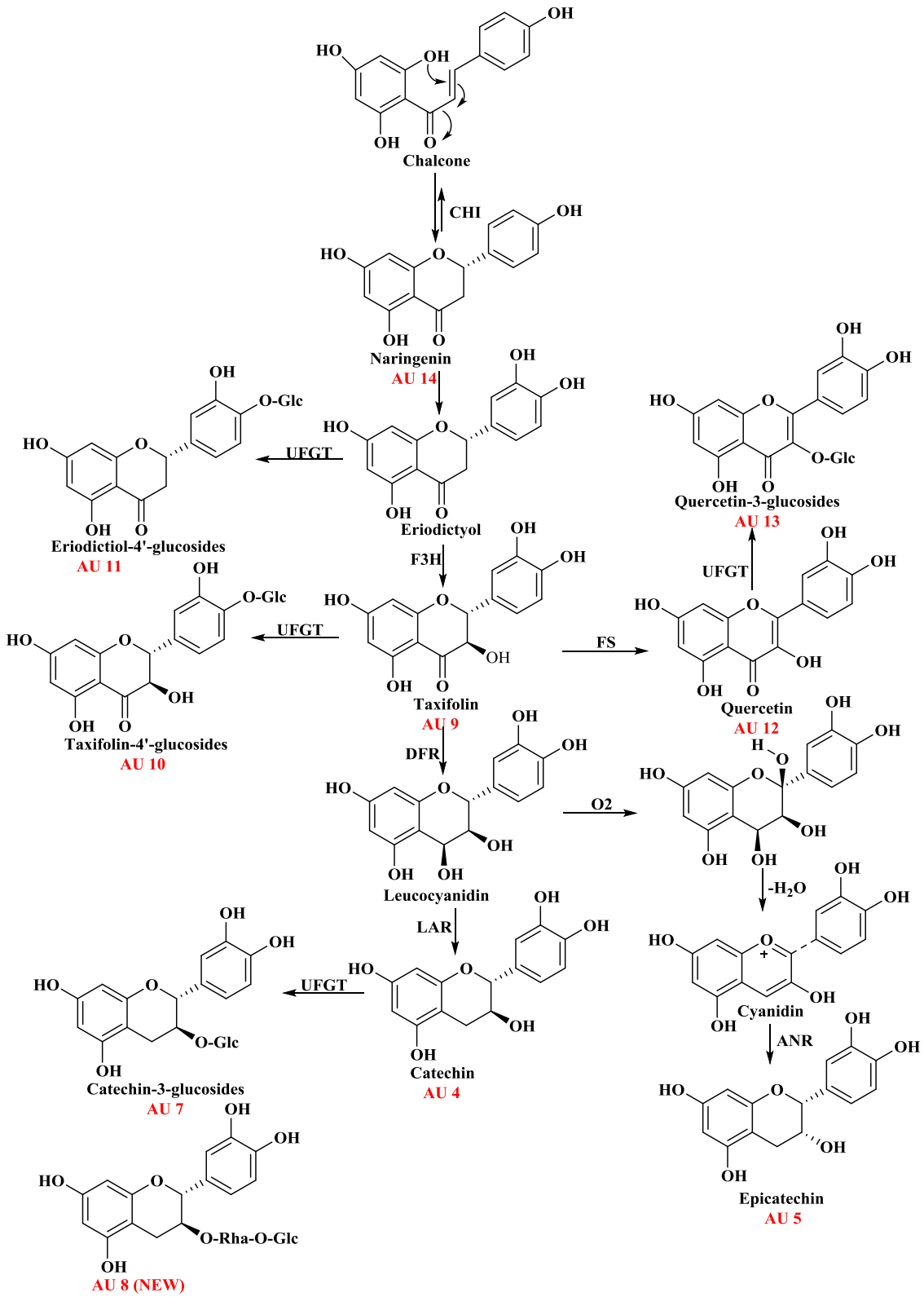

Abbreviations for enzymes catalysing key reactions: CHI, chlcone flavanone isomerase; F3H, flavanone 3β-hydroxylase; O2, 2-oxoglutarate; LAR, leucoanthocyanidin reductase; ANR, anthocyanidin reductase; UFGT, flavonoids-glycosyltransferase; DFR, dihydroflavanol-4-reductase

5.2.1 Biosynthesis of flavonoids

The biosynthetic pathways of flavonoids compounds in plants begins with the formation of a central C-15 intermediate known as chalcone (Fig. 5.1 and 5.4). The main role of chalcones in flavonoids biosynthesis has been discussed in many reviews (Harbone, 1993; Heller and Forkmann, 1988; Koes et al., 1994; Shirley, 2002). The formation of chalcone is catalysed by chalcone synthase (CHS), which is one of the key enzyme in flavonoid biosynthesis. The precursors for chalcone formation are malonyl-CoA and p-coumaroyl-CoA (hydroxycinnamic acid CoA ester) (Fig. 5.4). These chalcone precursors are derived from carbohydrates. The malonyl-CoA is synthesized from the glycolysis intermediate acetyl-CoA and carbon dioxides, the reaction is catalysed by acetyl-CoA carboxylase. The synthesis of p-coumaroyl-CoA is complex (Fig 5.3), it involves the shikimate pathway which is the main path to phenylalanine formation. This synthesis involved the use of three key enzymes, phenylalanine ammonia-iyase (PAL), cinnamic acid 4-hydroxylase (C4H) and 4-coumarate-CoA ligase (CHS) (Koes et al., 1994b). The biosynthesis of shikimic acid begins with the condensation of D-erythrose-4-phosphate and phosphoenolpyruvic acid (Fig 5.2).

The control of these enzymatic activity seems to be a key factor in regulating this pathway. This control can be done either endogenously during development differentiation or regulated by exogenous factors such as light, temperature and wounding (Bennet and Wallsgrove, 1994; Dixon and Paiva, 1995; Strack, 1997). The presence of these flavonoids in *Trichilia emetica* is in good agreement with the biosynthesis. The biosynthetic pathways of flavonoids compounds in plants are catalysed by several membrane-associated multienzyme complexes as shown in (Figure 5.1).

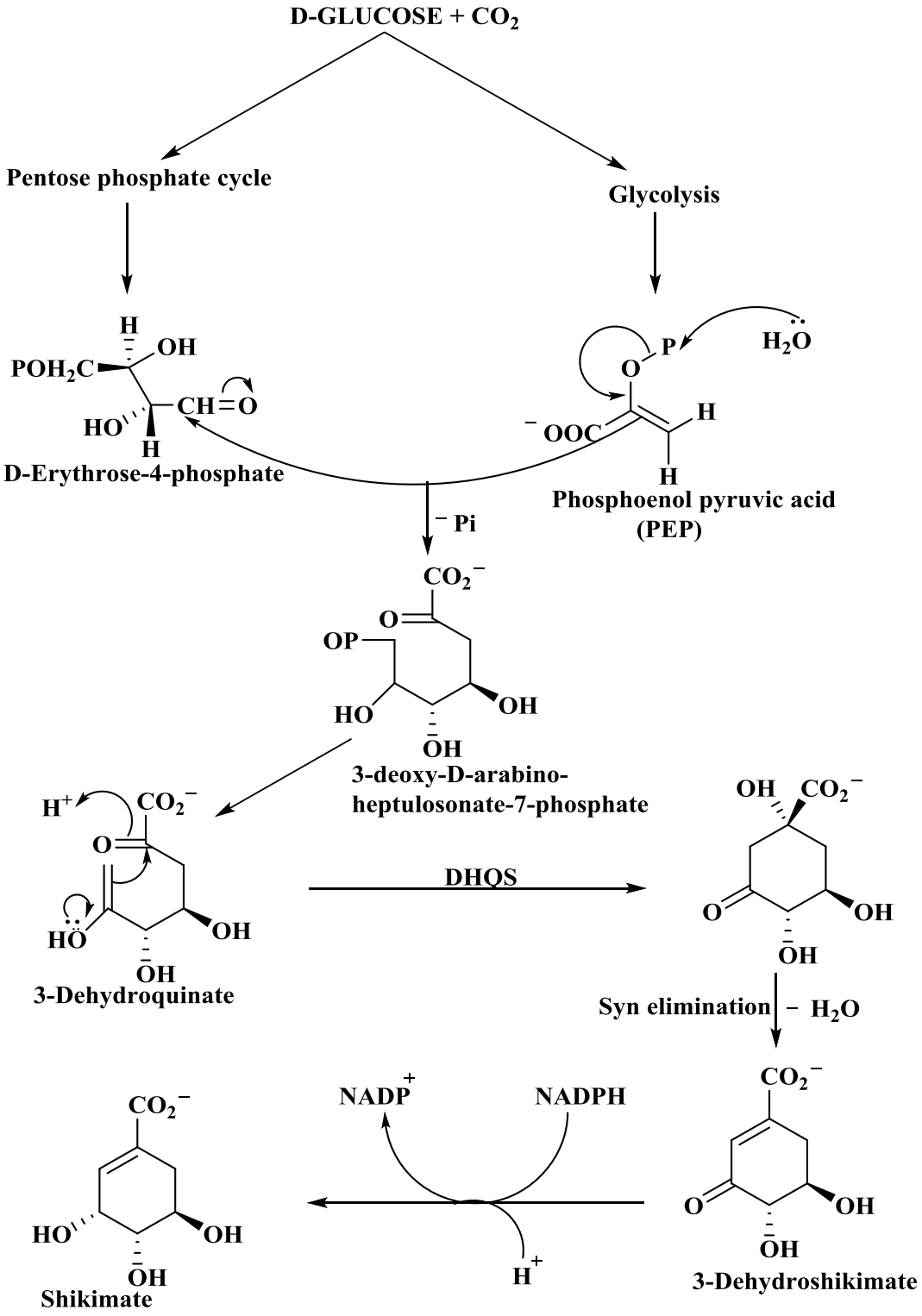

Fig. 5.2. Biosynthesis of Shikimate

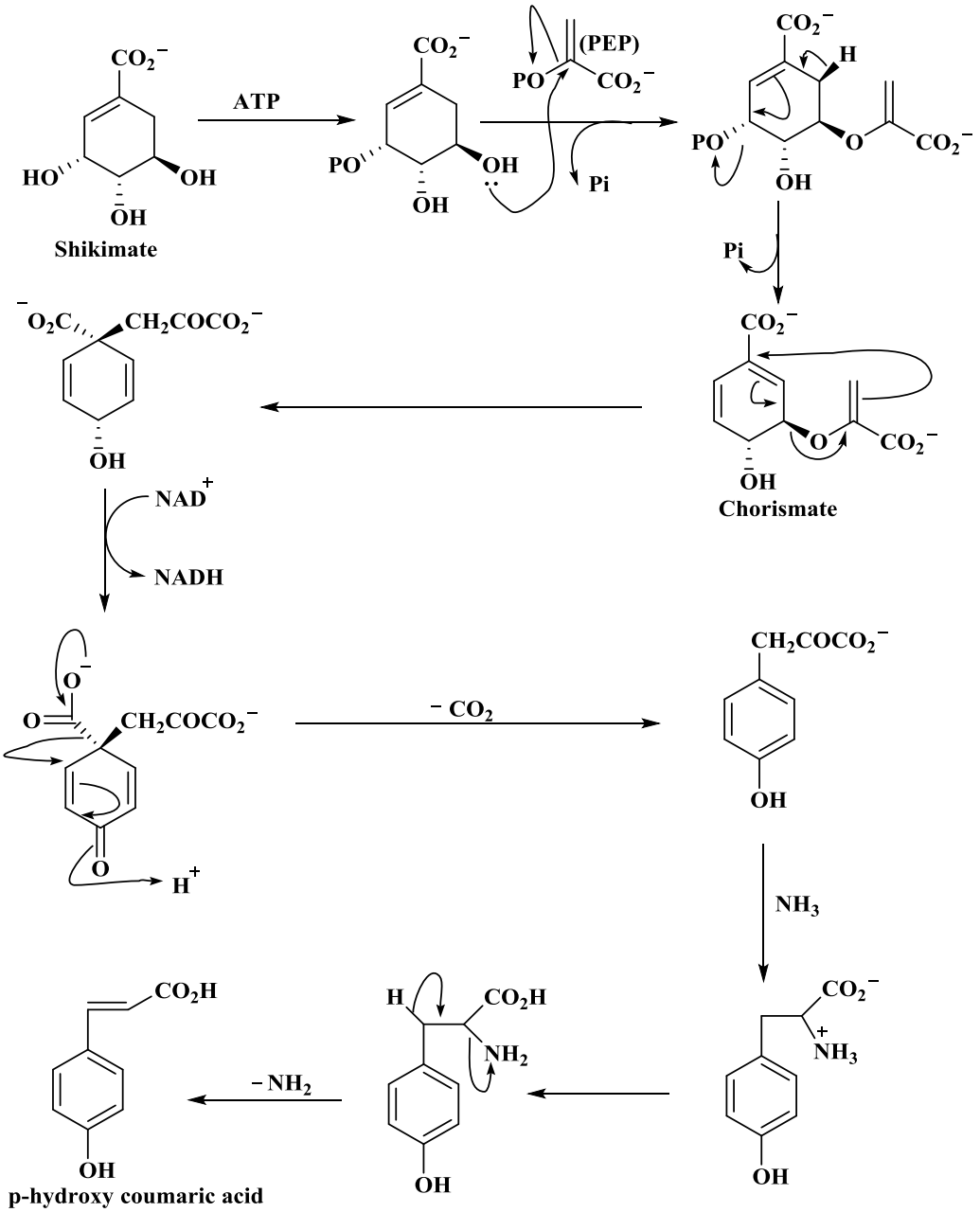

Fig. 5.3. Biosynthesis of p-coumaric acid

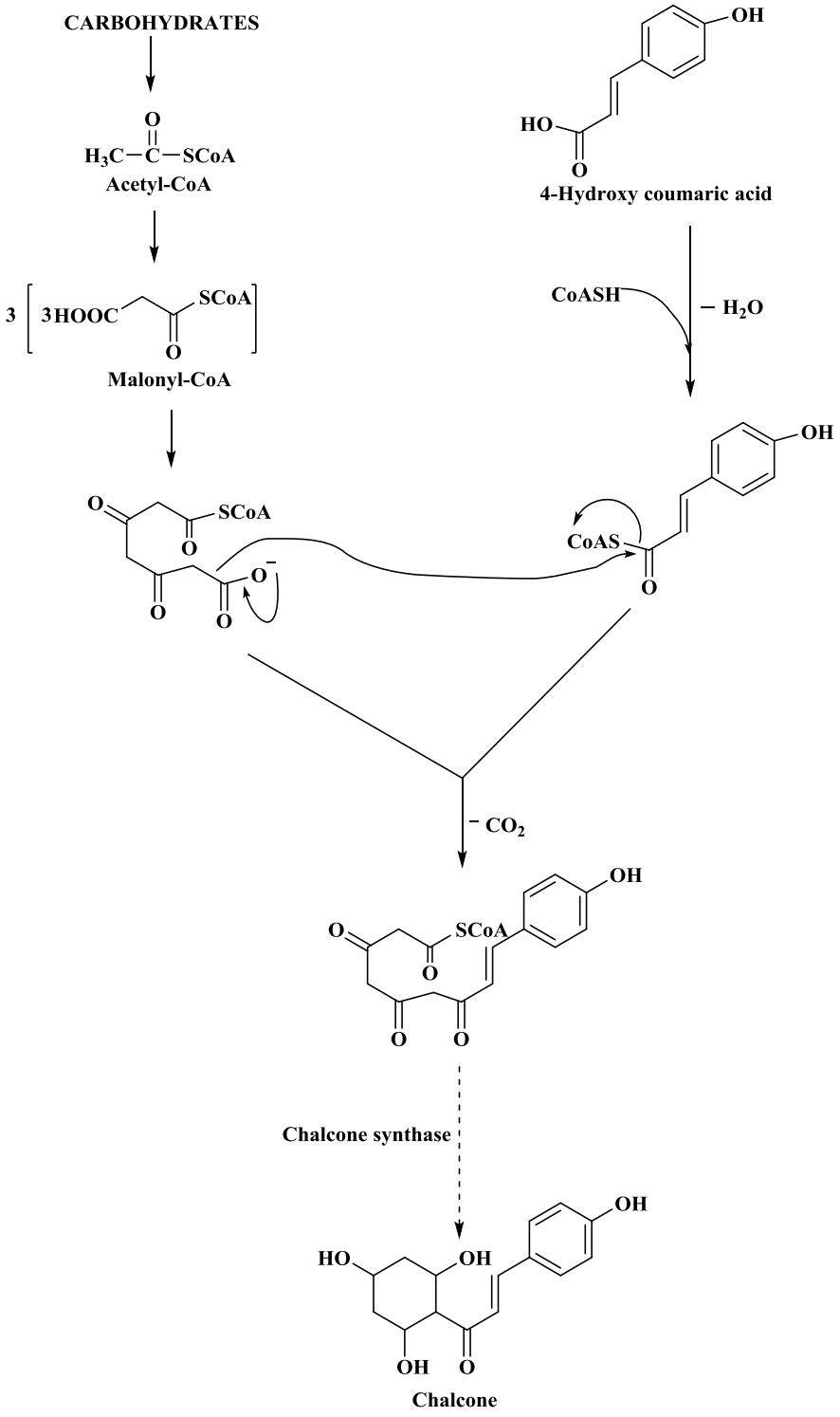

Fig. 5.4. Biosynthesis of chalcone

5.2.2 Relationship of compounds from *Trichilia emetica*

Naringenin (AU 14) a flavanones is formed from chalcones by intra-molecular cyclization (isomerization) (Fig. 5.5). There are reliable evidence about the in vitro and in vivo existence of equilibrium between naringenin and the corresponding chalcones, the intercoversion between naringenin and chalcones is catalysed by an enzyme known as chalcone isomerase (Koes et al., 1994, 1990; Monitto, 1981). Naringenin was further hydrolysed using an enzyme flavanone 3β-hydroxylase (F3H) to produce eriodictyol (Spribille and Forkmann, 1982) and was converted to glycosides (AU 11) using flavonoids-glycosyltransferase (UFGT) (Pfeiffer et al., 2006).

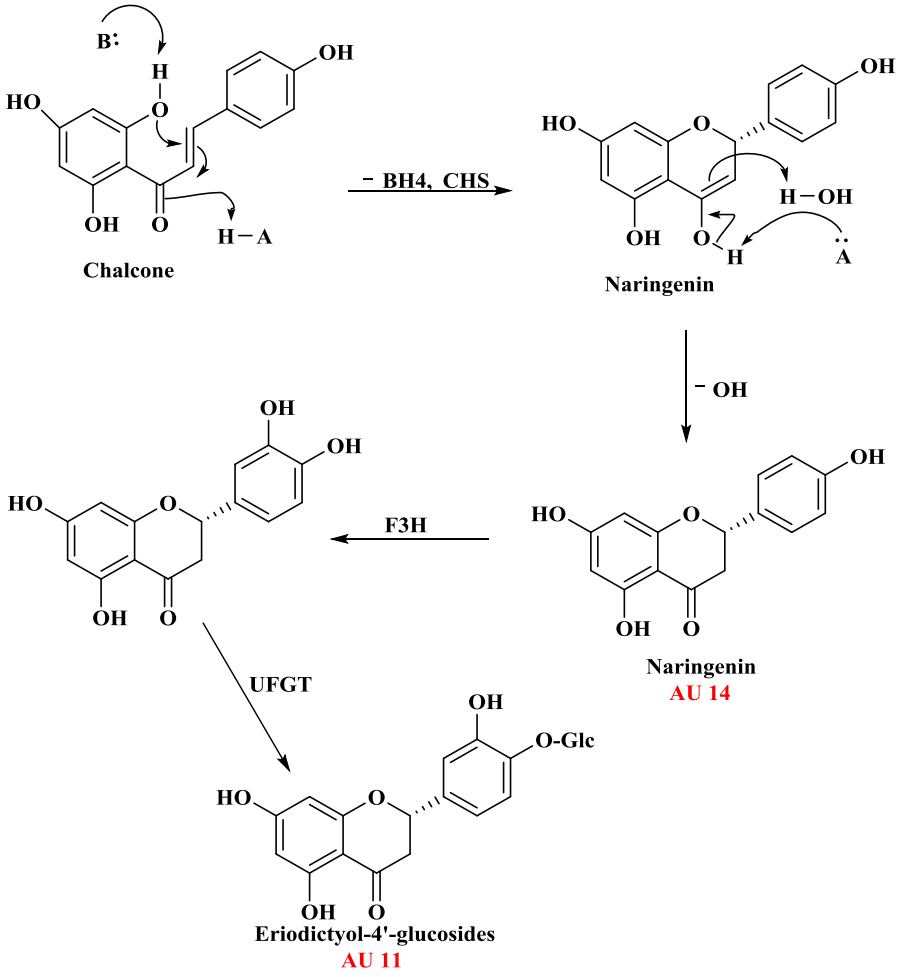

Fig. 5.5. Biosynthesis of flavanone

The conversion of eriodictyol to a taxifolin (AU 9) a dihydroflavonols is catalysed by soluble 2-oxoglutarate dependent oxygenase (Fig. 5.6). Similarly, a further enzymatic conversion of dihydroflavonols to flavonols was first observed with enzymes prepared from parsley cell suspension cultures and was also catalysed using soluble 2-oxoglutarate dependent oxygenase (Monitto, 1981). The flavonol synthesized proceeds through a 2-hydroxy intermediates with subsequent dehydration, giving rise to the respective flavonols and further conversion with UFGT yielded a glucoside (AU 13) (Koes et al., 1994; Pfeiffer et al., 2006).

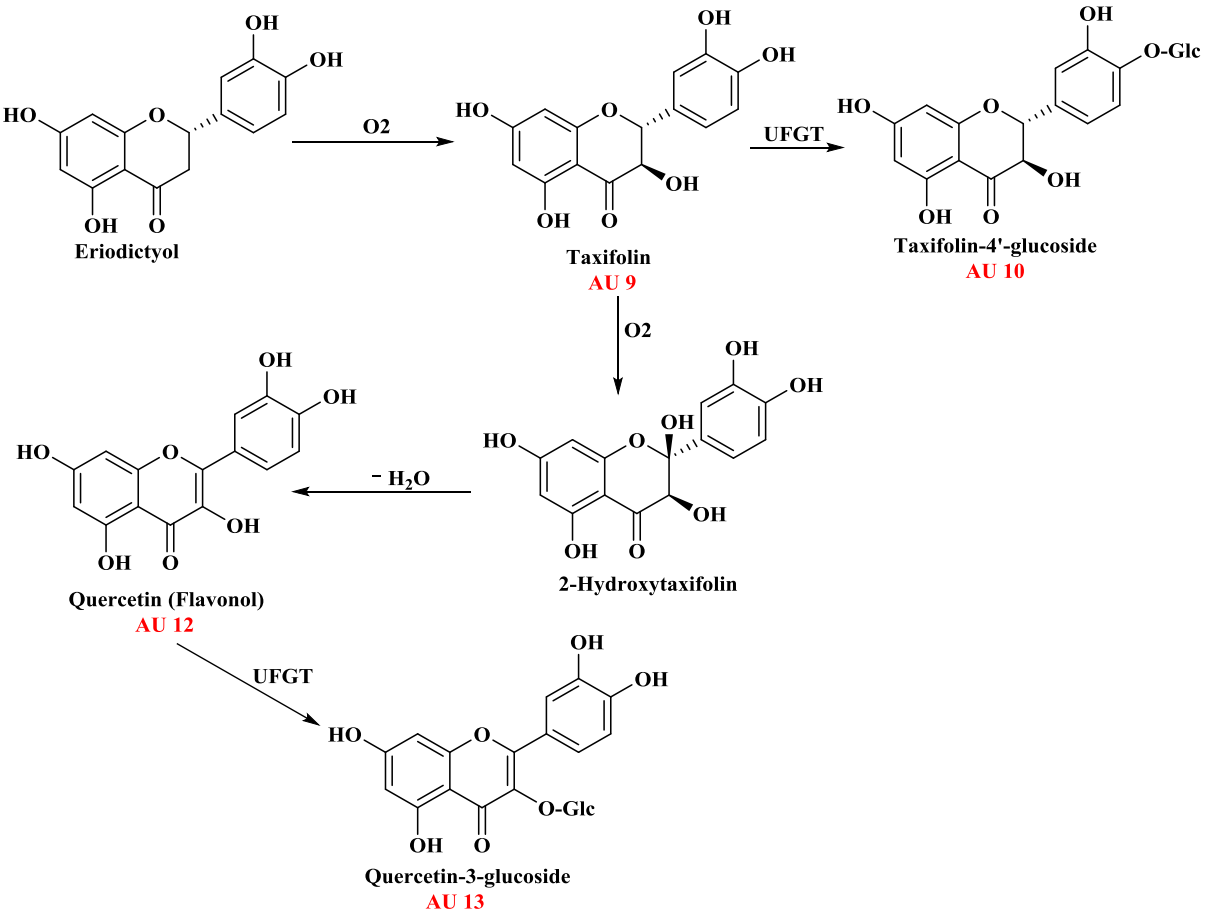

Fig. 5.6. Biosynthesis of flavonol

The reduction of a dihydroflavonols to flavanols is catalysed by dihydroflavonol 4-reductase (DFR) yielding leucocyanidin, which was then converted to catechin (AU 4) using leucocyanidin reductase (LAR). Flavonoids glycosyltransferase (UFGT) converted catechin to catechin-3-O-β-D-glucopyranoside (AU 7) and catechin-3-O-α-L-rhamnopyranosyl (1→4) β-D-glucopyranoside (AU 8). Similarly, leucocyanidin was converted to 2,4-dihydroxyflavanols

using an enzymes 2-oxoglutarate, followed by the elimination of water through a dehydratase to form cyanidin which become converted to Epicatechin (AU 5) using anthocyanidin reductase (ANR) (Fig. 5.7) (Harborne and Mabry, 1982; Pfeiffer et al., 2006; Shirley, 2002).

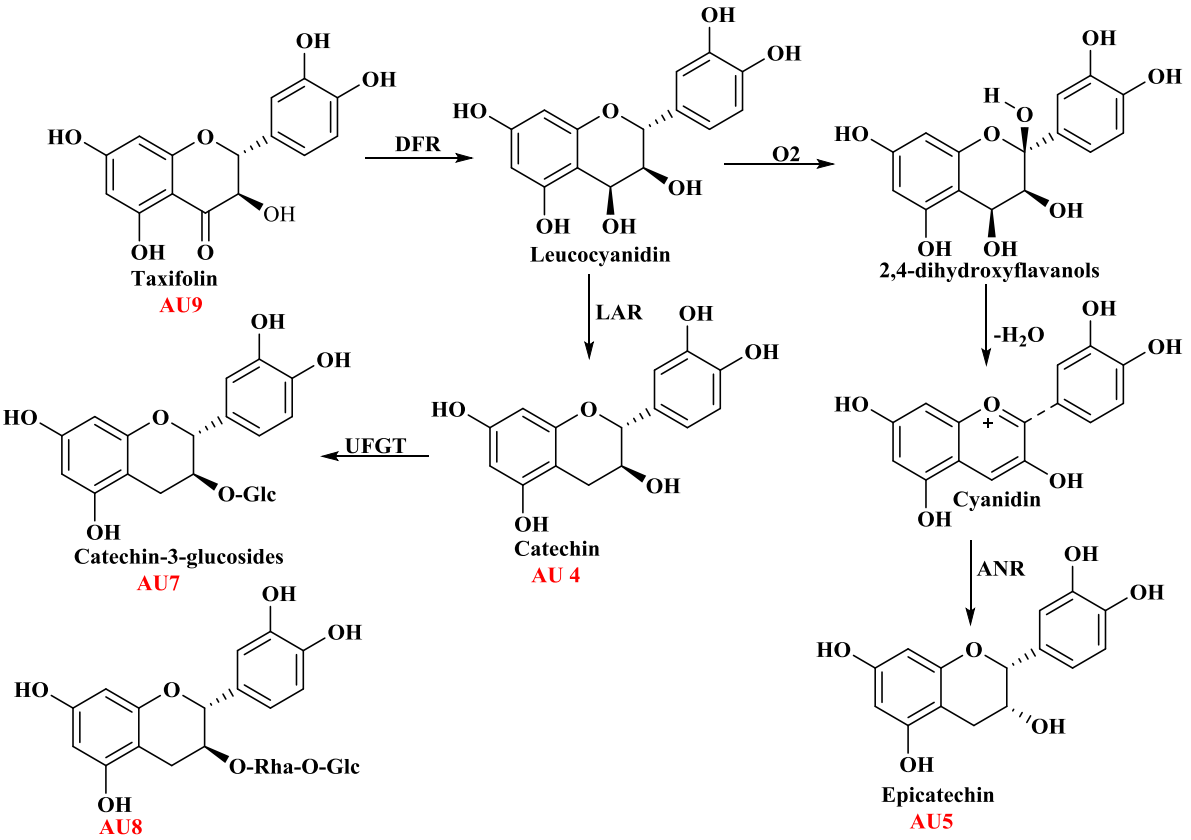

Fig. 5.7. Biosynthesis of Flavanols

5.2.3 Biosynthesis of sterols

The phytosterols are products of the isoprenoid or mevalonate biosynthetic pathway. The sole carbon feed stock of the pathway is acetyl-CoA (Fig. 5.8). The first step involves the condensation of two acetyl-CoA molecules to yield acetoacetyl-CoA. This is followed by a further condensation to form 3-hydroxymethyl-3-glutaryl-CoA (HMG-CoA). The reduction of HMG-CoA to mevalonate is catalysed by HMG-CoA reductase requiring Nicotinamide adenine dinucleotide phosphate (NADPH) as co-factor.The mevalonate is then directed into sterol pathway by squalene synthase (SS). This pathway has more than 30 enzyme-catalysed reactions and it occurs in plant cytoplasm(Miziorko, 2011; Piironen et al., 2000). The conversion of cycloartenol to β-sitosterol and stigmasterol involves two methylation steps; the

first is the gene which encodes a cycloartenol C-24 methyl transferase (SMT1) and the second is SAM-24-methylene lophenol-C-24'-methyl transferase (SMT2) which is responsible for the ability of plants to synthesise 24-ethyl sterols. These genes where characterised from the experiment on *Oriza sativa* (BuvierNave et al., 1998; Piironen et al., 2000).

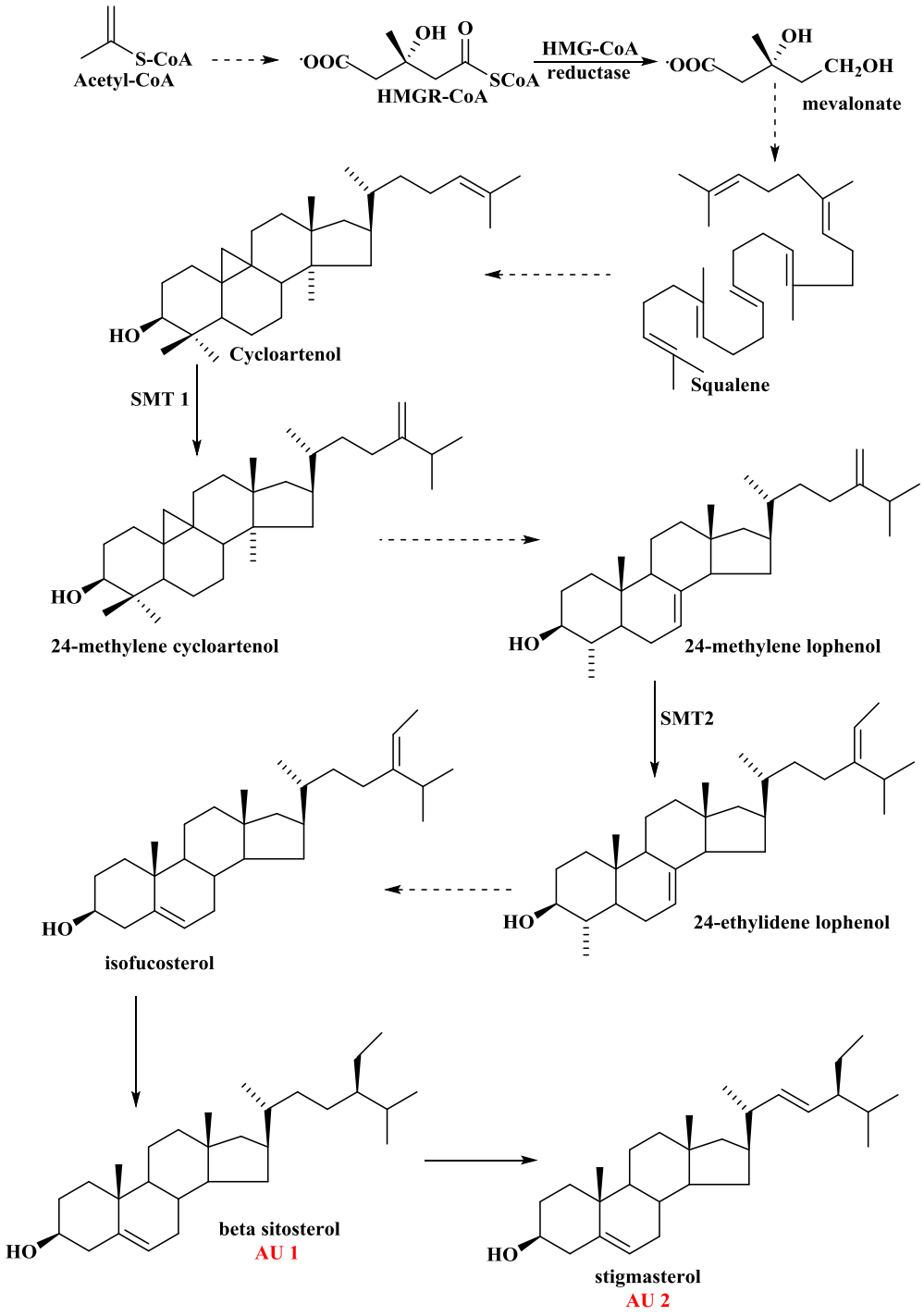

Fig. 5.8. Hypothetic biosynthetic scheme leading to compounds AU 1 and 2

5.3 Compounds from *Azadirachta indica* and *Millettia pinnata*

A. indica, is a tree in the mahogany family Meliaceae, which has been under intensive research in the past half a century. In this study, *A. indica* seed from Nigeria was used as a model to check if the methods used in the several failed attempt to isolate a limonoids from the seeds of *Trichilia emetic*a were workable or not. These resulted in the isolation of two known limonoids (tetranortriterpenes); nimbin (AU 18) and azadirachtin (AU 19). Although, several phytochemicals have been reported from this plant, the most popular and important is azadirachtin which has been proven to have antifeedant properties against insect pest (Kraus et al., 1981; Kumar et al., 1996; Ley et al., 1993).

A. indica seed oil bought from an open market in Bangladash was also studied. All effort to isolate limonoids from this oil sample proved abortive, instead furanoflavonoids compounds; karanjin (AU 15), pongapin (AU 16) and lanceolatin (AU 17) were isolated which are typical of *M. pinnata* seed oil (Chopade et al., 2008; Li et al., 2006; Tanaka et al., 1992; Yadav et al., 2004). A trace of limonoids was not found in this oil sample, the possibility of contamination or adulteration is rule out. I hypothesized that this oil sample is *M. pinnata* seed oil. To the best of the author's knowledge there are no reorts on the biosynthesis of furanoflavonoids.

5.3.1 The biosynthesis of neem terpenoids

The biosynthesis of neem terpenoids involves very complex enzymatic, oxidation, and cyclization reactions (Fig. 5.9). The biosynthetic precursors are derived from isoprenoid or mevalonate biosynthetic pathway (5.2.3). The cyclization of squalene results into chiral tetracyclic ions, euphane/tirucallane and this is catalysed by terpene synthase (TS). Allylic isomerization of euphane/tirucallane give rise to butyrospermol, which is then oxidized and rearranges through a Wagner-Meerwein reaction by 1,2 methyl shift to form another chiral compound apoeuphane/apotirucallane. Cleavage reactions of four terminal carbons on the side chain give rise to furan ring which is finally oxidized to form azadirone and azadiradione. Further oxidation and cyclization of azadirone and azadiradione result in the formation of azadirachtin and nimbin, respectively. This final steps are catalysed by cytochrome P450s (CYPs) (Kumar et al., 2014; Miziorko, 2011).

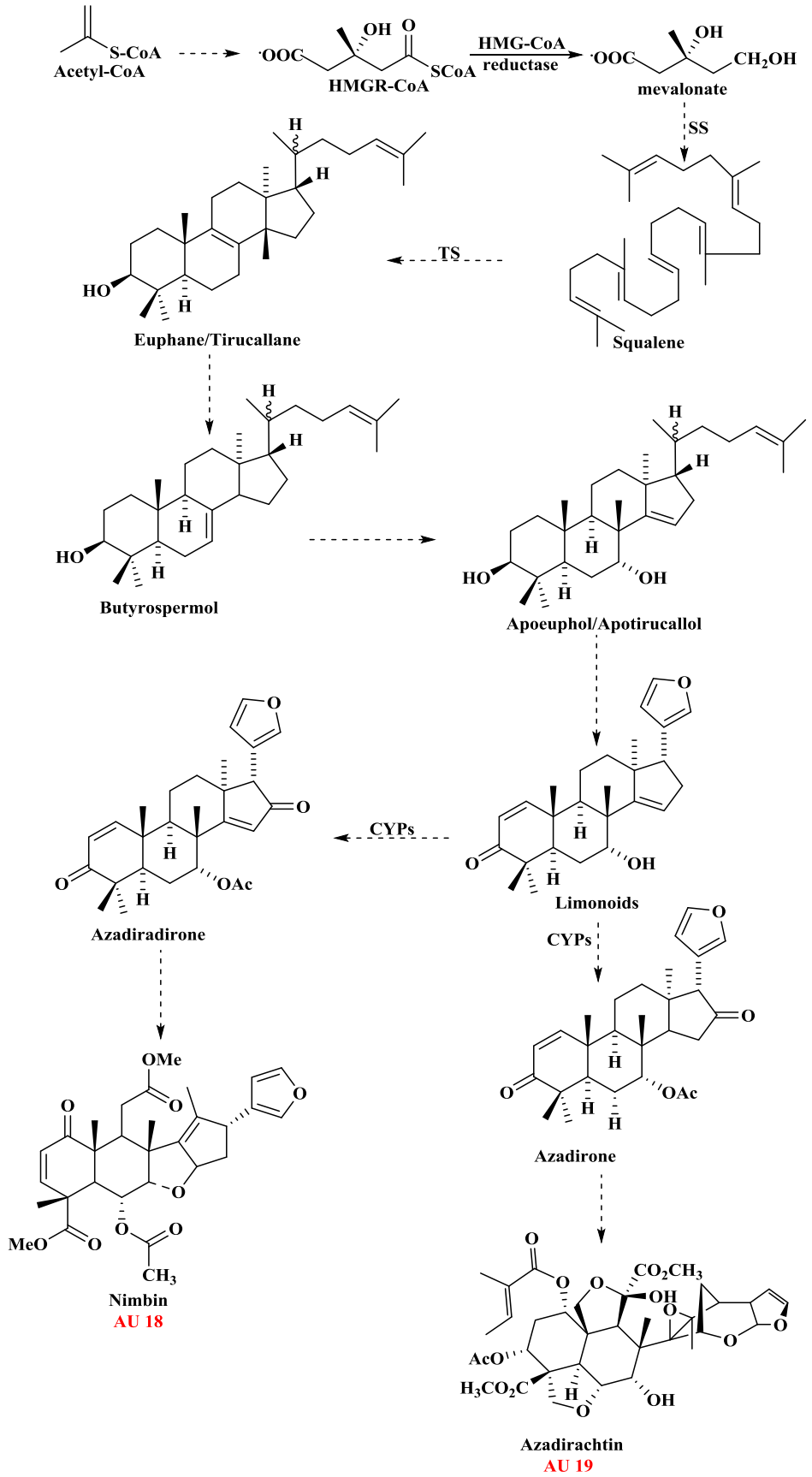

Fig. 5.9. Hypothetic biosynthetic scheme leading to compounds AU 18 and 19.

5.4 Recommendations

T. emetica seed oil is currently used for domestic and industrial purposes in Eastern and Southern Africa. In West Africa, *T. emetica* seed is treated as a waste product, this is because of the bitter nature of the seed oil and the processes involved in the oil extraction and the removal of the bitterness. With the dwindling reserve of mineral oil and the desire for eco-friendly and renewable energy, there is need for the examination of these seed oil samples which could serve as an alternative feedstock for biodiesel production. The preliminary examination should be an assay of the oil under standardised test conditions for pour-points, cloud-point and cold filter plugging point.

Crushed *T. emetica* seeds is used in protecting cowpea seed from storage pest (Van der Vossen and Mkamilo, 2007). This study revealed that the water extract of this seed sample is a reach source of flavonoids and could be used as a source of powerful anti-oxidant, free radical scavengers, repellent, toxin or preserving agents, but could not be used for human consumption because of the presence of alkaloids. Some *Citrus* flavonoids are used directly as repellents or toxins or in plant improvement programs to obtained more resistant crop which themselves may have a repellent or selectively toxic effect (Benavente-Garcia et al., 1997). Since the chemical constituent of this water extract is known, I wish to recommend that it should be investigated against some insect pests so as to evaluate whether if the extract has any activity on them. The extract should also be tested against non-target species so as assess it impact on them. The shelf life of this water extract should also be assessed.

CHAPTER 6

6.0 Experimental

6.1 Instruments and Chemicals

Solvents were supplied by Fisher Scientific. Melting points were determined by a Stuart instrument and are uncorrected. Optical rotations were measured in methanol solution on a ADP 440+ polarimeter. Infrared samples were prepared as thin films, solutions or as KBr discs using sodium chloride plates and the spectra recorded on a Perkin Elmer 100 FT-IR spectrometer. NMR spectra were recorded on a Bruker Avance (400 or 500 MHz) spectrometer with internal references of δ_H 7.27 and 77.0 ppm for $CDCl_3$ and δ_C 3.31 and δ_C 49.0 ppm for CD_3OD. HPLC analysis was carried out on Ultimate 3000 auto sampler HPLC, fitted with an ultimate 3000 RS variable UV detector and a Spherisil ODS3 RP-C18 (250 × 4.6 mm, id, 5µm) column, using a linear gradient of solvents Water with either Acetonitrile or methanol each containing 0.1 % formic acid. All chromatograms were recorded and processed by Chromeleon version 7.1. Reveleris^{TM} Flash System fitted with Grace Reveleris® C18 column with silica flash cartridges of 12 g (82 mm × 22 mm) using ELSD (Evaporation Light Scattering Detection) and 2 selected UV-VIS wavelength detector using a linear gradient of either CH_3CN or MeOH / H_2O (containing 0.1 % formic acid) was used for the purification of polar compounds or $CHCl_3$-CH_3CN (3:1) isocratic gradient for the non- polar compounds on normal phase silica. Flash column chromatography was perform on Fluorochem silica gel 60A. Thin layer chromatography (TLC) and Preparative thin layer chromatography (PTLC) was conducted on precoated E. Merck TLC silica gel 60 F_{254} glass plates. The compounds were visualised using phosphomolybdic acid, bromocresol green stains, Dragendorff's reagent (A. bismuth nitrate 0.17 g) dissolved in H_2O/AcOH (4:1, 10 ml) B. KI (4 g) dissolved in H_2O/AcOH (2:1, 30 ml). Solution A and B mixed together and diluted to 100 ml with H_2O, vanillin sulphuric acid or under UV light. Concentration and dehydration of samples in vials was accomplish using Techne Dri-Block DB 3 Sample Concentrator. Thermo Scientific 1300 GC Chromatograph equipped with a TRIPLUS RSH autosampler, ITQ 900 MS detector and Rxi®-ms (length = 30 m, i.d = 0.25 mm, film thickness = 0.25 µm) column was used for identification of sugars in glycosides and Omega Wax-DB5 capillary column (length = 30 m, i.d = 0.25 mm, film thickness = 0.25 µm) was used for fatty acid analysis. Mass spectrometry were carried on a Bruker MICRO-TOF, Dionex Ultimate 3000-ThermoScientific Exactive HPLC system and Thermo Instruments HPLC system mass spectrometer with an ESI source.

6.2 Plant Materials

The stems and seeds of *T. emetica* were identified and supplied by a botanist Martin A Akoh from KNUST botanical garden in Kumasi, Ghana. *T. emetica* seed was also supplied from Mozambique by Dr Radek Messias Braganca and the voucher specimen TBG-2014-1 was deposited at the herbarium of Treborth botanical garden. Neem seeds (*Azadirachta indica*) were collected from Shabu-Lafia, Nigeria in August 2014, and were identified by Professor Bala Sidi and a voucher specimen No. 173 was deposited at the herbarium of Ahmadu Bello University Zaria, Nigeria. *M. pinnata* seed oil supplied by Dr Mohammed Nur Alam was bought in an open market in Bangladash as *Azadirachta indica* seed oil.

6.3 Extraction of lipids/fats

The lipids were extracted following the procedure of (Mariod et al., 2010). Flaked *T. emetica* shell (50 g) and seeds (100 g) were extracted with hexane (100 ml × 7) and (200 ml × 7) at room temperature. The combined extracts were concentrated to give 11.3 and 59.6 g yellow golden brown lipids of *T. emetica* shell and seeds. The lipids obtained were stored at room temperature until further analysis.

6.4. Physico-chemical Characteristics of *T. emetica* Oils

6.4.1 Trans-esterification of the Oils

The method of (Thoss et al., 2012) was used with modification. *Trichilia emetica* seeds oil (5 g) was dissolved in sodium methoxide (0.5 M, 40 ml) and heated under reflux for 30 minutes to produce fatty acid methyl esters (FAMEs). Deionised water (100 ml) was then added, and the solution extracted with n- hexane (100 ml × 3). The hexane fractions were combined, dried over $MgSO_4$, filtered under gravity and the solvent removed using rotary evaporator at 40^{o} C. The trans-esterified samples were diluted (1:1000) with hexane and analysed by GC- MS.

6.4.2 Peroxide Value

The peroxide value was determined following the procedure of (AOAC, 1990). Seeds (2.0 g) were dissolved in 25 ml of a glacial acetic acid and chloroform (3:2) mixture. The mixture was thoroughly shaken and 13% potassium iodide (1 ml) was added and incubated for 1 minute. 35 ml of water was added and titrated with 0.01 M sodium thiosulphate solution using 1 ml of starch as indicator. The sample was run in triplicate and the average end point used. Simultaneously, a blank solution was prepared in a similar manner.

The perioxide value was calculated using equation 1.

Perioxide value = 1000M (V2-V1)/ W eq.1

Where,

Volume of sodium thiosulphate used in the test = V2

Volume of sodium thiosulphate used in the blank = V1

Molarity of sodium thiosulphate = M

Weight of sample = W

6.4.3 Iodine Value

Iodine value was determined following the method of (James, 1998). *T. emetica* oil (0.2 g) was dissolved in carbon tetrachloride (10. 0 ml) and Wij's solution (25 ml) was added. The mixture was shaken for 1 minute and incubated for 30 minutes. 20 ml of 10% potassium iodide solution was added, followed by 100 ml of water.The mixture was titrated with 0.25 M sodium thiosulphate solution until the color turned pale yellow, then 3 ml of starch was added and the titration continue to the colourless end point. The sample was run in triplicate and the average end point used. Blank titration was also run.

The iodine value was calculared using equation 2.

$$\text{Iodine value g } I_2 / 100\text{g} = \frac{(B - T) \times 0.03175}{W} \times 100 \quad \text{eq. 2}$$

Where,

Volume of sodium thiosulphate used in the test = T

Volume of sodium thiosulphate used in the blank = B

Weight of sample = W

1 ml of 0.25 M sodium thiosulphate solution = 0.03175

6.4.4 Acid Value

Titrimetric method was used to determine the acid value following the procedure of (AOAC, 1990). *T. emetica* oils (2.0 g) was dissolved in methanol (50 ml) and heated under reflux for 20 minutes. The solution was titrated against potassium hydroxide (0.2 M × 25 ml), using phenolphthalein as indicator. The end point was obtained by the restoration of pink color. The procedure was repeated thrice and average end point used. The acid value was computed using equation 3.

$$\text{Acid value mg KOH / g of sample} = \frac{56.1 \times M \times V}{W} \quad \text{eq. 3}$$

Where, V = Volume of KOH

M = Molarity of KOH

W = Weight of sample

56.1 = Molecular weight of KOH

6.4.5 Saponification Number

The (AOAC, 1990) method was used. *T. emetica* oil (5.0 g) was dissolved in 100 ml of ethanolic potassium hydroxide (0.5 M) and refluxed for 2 hours. On cooling, three drops of phenolphthalein were added to the mixture and titrated with 1 M hydrochloric acid until the pink color disappeared. The sample was run in triplicate and average end point used. Blank titration was also run. The saponification value of the samples were calculated using equation 4:

Saponification number = $56.1M (V_2 - V_1) / W$ eq. 4

Where, Molarity of hydrochloric acid = M

Volume of hydrochloric acid used in test = V1

Volume of hydrochloric acid used in the blank = V2

Mass in gram of oil/fat weighed used in the test = W

Molecular weight of KOH (g/mole) =56.1

6.4.6 Determination of Percentage Unsaponifiable Matter

The method of (Cañabate-Díaz et al., 2007) was used with modification. *Trichilia emetica* oil (5.0 g) was dissolved in 100 ml of ethanolic potassium hydroxide (0.5 M) and refluxed for 2 hours, with constant stirring. After cooling at room temperature, the mixture was diluted with 100 ml deionised water and transferred to a separating funnel. The unsaponifiables were extracted with diethyl ether (100 ml × 5). The diethyl ether extract was washed with (0.5 M) potassium hydroxide (100 ml × 2) to remove any residual free fatty acid. The ether extract was further washed with deionised water (100 ml × 7). The ether extracts was dried over $MgSO_4$, filtered under gravity and the solvent removed under vacuum at 40 ^{O}C.

The percentage of unsaponifiables matter in all the oil samples were determined using the equation 5:

Percentage of unsaponifiables matter (%) = $K / K_0 \times 100$ eq. 5

Where

Weight of unsaponifiables matter = K

Weight of oil = K_0

6.4.7 Isolation of sterols from unsaponifiable matter

The seperation of unsaponifiable matter (4.1 g) was carried out by flash column chromatography. The column was run using a gradient mixture of hexane and chloroform (100:0 to 0:100), and chloroform and methanol (100:0 to 90:10). Fifty three (53) eluates were collected (50 ml each) and the eluted fractions were monitored by TLC. Fractions were pooled based on their TLC profile to give five primary fractions (A1-A5, Table 6.1).

Table 6.1. Fractions obtained from unsaponifiables matter.

Fraction	Weight (g)	Physical characteristic
A1	1.21	pale yellow
A2	0.32	Pale yellow
A3	0.71	Pale yellow
A4*	0.29	Pale yellow
A5	0.91	Pale yellow

* TLC profiles of these fractions showed major spots after treated with PMA and on heating at 100 ^{O}C. Thus was further investigated.

Fraction A4 (0.29 g) obtained on elution with 2% methanol in chloroform was further purified by CC using a step gradient mixture of chloroform and ethyl acetate (100:0 to 60:40). A total 31 fractions were collected and pooled based on their TLC profile to give six primary fractions (B1-B6, Table 6.2).

Table 6.2. Fractions combinations from fraction A4.

Fraction	Weight (mg)	Physical characteristic
B1	38.06	Pale yellow viscous liquid
B2	103.12	Pale yellow viscous liquid
B3*	27.42	Pale yellow viscous liquid
B4*	19.11	Pale yellow viscous liquid
B5*	43.25	Pale yellow viscous liquid
B6	49.43	Pale yellow viscous liquid

* TLC profiles of these fractions showed some spots after treated with PMA and on heating at 100 ^{O}C. Thus was further investigated

Fraction B3 (27.42 mg) was obtained on elution with 8% EtOAc in $CHCl_3$ and was purified by PTLC using ethyl acetate-hexane (7:3) as developing solvent to give AU 2 (6 mg, white powder).

Fractions B4 and B5 (62.31 mg) were combined and seperated by PTLC using ethyl acetate-hexane (9:1) as the mobile phase yielding AU 1 (17 mg, white powder).

6.5. Chemical investigation of the *T. emetica* seeds

All the fractions were assessed using TLC, HPLC, and ^{1}H NMR spectroscopy.

6.5.1 Extraction and isolation of metabolites

Seeds (100 g) were refluxed in water (500 ml) for 30 minutes and filtered. The filtrate was concentrated to dryness to give 14.23 g dark gummy extract, which was suspended in water. The aqueous extract was sequentially extracted with chloroform and ethyl acetate at different pH values (pH 10, pH 3 and pH 7), and the pH was adjusted by the addition of 2 M NaOH and 2 M HCl. The TLC profiles of these fractions were assessed; the EtOAc fractions showed major spots under UV and their ^{1}H NMR spectra showed aromatic proton signals. Hence, the EtOAc fractions were combine (1.58 g) and investigated further while chloroform and aqueous fractions showed poor TLC and proton NMR profiles.

6.5.2 Chemical investigation of ethyl acetate extract.

Purification of the ethyl acetate extract (1.58 g) was carried out by flash column chromatography in a polarity gradient manner. Hexane – EtOAc was used as the eluent at the gradient mixtures of 100:0 to 0:100 and finally 100% methanol. The fractions were pooled based on their TLC profile to give five primary fractions, designated as (C1 to C5, Table 6.3).

Table 6.3. Fractions obtained from ethyl acetate extract.

Fraction	Weight (mg)	Physical characteristic
C1	66.09	Yellow viscous liquid
C2	175.48	Yellow viscous liquid
C3	323.21	Yellow viscous liquid
C4*	191.11	Yellow viscous liquid
C5	437.25	Dark viscous liquid

* This fraction showed two major spots under uv light and was further investigated

Fraction C4 (191.11 mg) obtained with 40% hexane in EtOAc was purified by PTLC using [Hexane – EtOAc – MeOH (5:4:1), 12 runs] yielding AU4 (27 mg).

6.5.3 Chemical investigation of strong (3 hours) decocted seeds extract.

Seeds (20.0 g) were refluxed in water (100 ml) for 3 hours and filtered. The filtrate was concentrated to dryness to give 1.23 g dark viscous extract. The TLC profiles of this extract was evaluated and it showed one major spot under UV. Similarly, the ^{1}H NMR spectra showed an impure glycoside. This compound was purified by PTLC with mixed solvent systems; $CHCl_3$ and MeOH (97:3) yielding AU 7 (43 mg).

6.5.4 Chemical investigation of 20 minutes decocted seeds extract.

T. emetica seeds 1.0 kg was boiled in water (2.0 l × 3) for 20 minutes each time. The combined filtrate was concentrated to dryness to give 72.14 g dark viscous residue. This residue (72.14 g) was dissolved in water (300 ml) and partitioned with organic solvents to yield chloroform extract (31.02 g), ethyl acetate extract (26.50 g) and water extract (11.93 g) respectively. The TLC profiles of these fractions were assessed; the EtOAc fractions showed major spots under UV and their ^{1}H NMR spectra showed aromatic proton signals. Hence, the EtOAc fractions (26.50 g) was investigated further while chloroform and water fractions showed poor TLC and ^{1}H NMR profiles, hence discarded.

6.5.5 Chemical investigation of ethyl acetate extract (20 minutes decoction)

Isolation of the minor component in ethyl acetate fraction (26.50 g) (Figure 6.1) was carried out by flash column chromatography using gradient mixture of hexane and chloroform (100:0 and 50:50) and chloroform and methanol (100:0 to 0:100). A total of 79 fractions were collected, and on the basis of their TLC profiles and their retention time in the HPLC chromatogram, similar fractions were combined to give six primary fractions, designated as (D1-D6, Table 6.4).

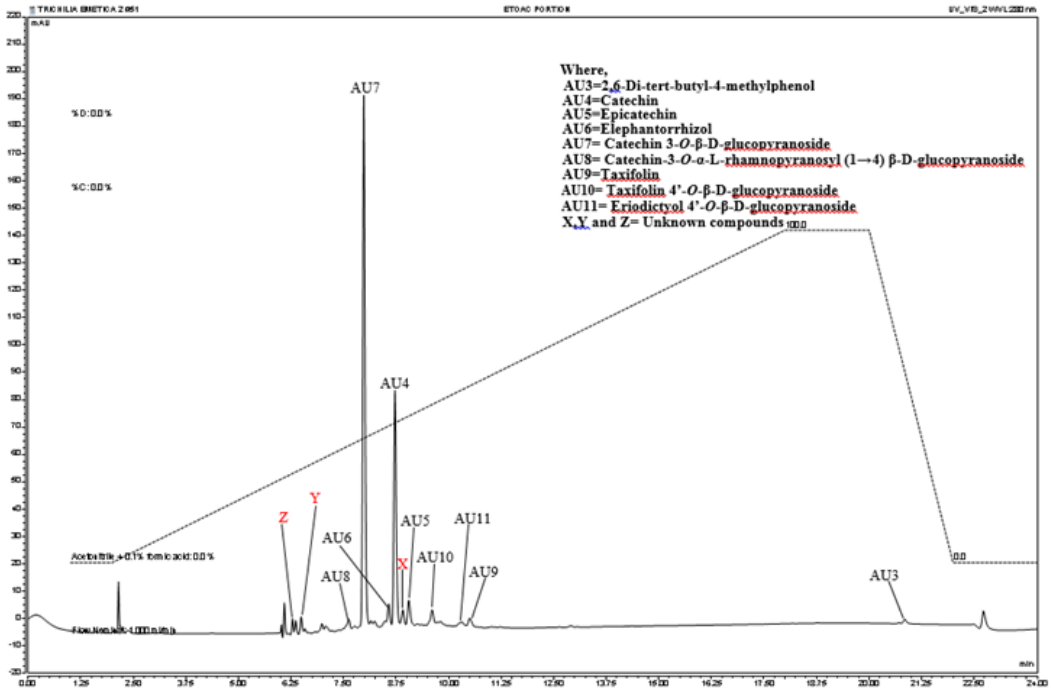

Fig. 6.1. HPLC chromatogram of EtOAc portion of decocted T. emetica seed extract.

Table 6.4. Fractions obtained from ethyl acetate extract. (20 minutes decoct.).

Fraction combination	Weight (g)	Physical characteristic
D1*	1.32	Pale yellow needle
D2[a]	2.09	Yellow viscous liquid
D3*	4.74	Yellow viscous liquid
D4*	4.22	Yellow viscous liquid
D5*	5.90	Yellow viscous liquid
D6*	3.20	Dark viscous liquid

***** These fractions were further investigated based on their TLC and ^{1}H NMR signals. [a] is a fat, discarded

Fraction D1 gave AU 3 (1.32 g)

Fraction D3 (4.74 g) obtained on elution with 3 % methanol in chloroform was further purified by column chromatography using a step gradient of chloroform and methanol. The fractions were pooled based on their TLC characteristics and retention time in the HPLC chromatogram to give four primary fractions, designated as (E1 – E4, Table 6.5).

Table 6.5. Fractions obtained from D3.

Fractions combination	Weight (g)	Physical characteristic
E1	1.94	Yellow viscous liquid
E2*	0.04	Yellow viscous liquid
E3*	0.24	Yellow viscous liquid
E4*	32.12	Yellow viscous liquid

*These fractions were further investigated based on their TLC and ^{1}H NMR signals

Fraction E2 was purified with 50 % methanol in FC yielding **AU 4 (3.0 mg)**, **AU 9 (4.0 mg).**

Fraction 43 (51 mg) of E3 was purified with by PTLC using hexane: EtOAc (1:4, 10 runs) as the developing solvent yielding **AU 7 (16 mg)**.

Fraction E4 (32.12 mg) was subjected to CC using a gradient mixture of hexane / EtOAc (1:7) to give 7 fractions F1 – F7, (Table 6.6).

Table 6.6. Fractions obtained from E4.

Fractions combination	Weight (mg)	Physical characteristic
F1	4	Yellow viscous liquid
F2	2	Yellow viscous liquid
F3	3	Yellow viscous liquid
F4*	6	Yellow viscous liquid
F5*	5	Yellow viscous liquid
F6	3	Yellow viscous liquid
F7	3	Yellow viscous liquid

*These fractions were further investigated based on their TLC and ^{1}H NMR signals

Fraction F4 and F5 were combined (11 mg) and purified with Grace C18 cartridge using 100 % methanol yielding **AU 11 (2.7 mg)**.

Fraction D4 (4.20 g) was purified by flash column chromatography and the column was eluted with a gradient mixture of chloroform-methanol (10:0 to 0:10). 40 fractions were collected (150 ml each) and all the eluted fractions were monitored by thin layer chromatography. Fractions were pooled based on their retention time in the HPLC chromatogram to give six primary fractions, designated as G1- G6, (Table 6.7).

Table 6.7. Fractions obtained from D4.

Fractions combination	Weight (mg)	Physical characteristic
G1	1020.0	Yellow viscous liquid
G2*	20.0	Yellow viscous liquid
G3*	41.0	Yellow viscous liquid
G4*	73.0	Yellow viscous liquid
G5	1000.0	Yellow viscous liquid
G6*	60.0	Yellow viscous liquid

* These fractions were further investigated based on their TLC and ^{1}H NMR signals.

Fractions G2, G3 and G4 were further purified in Grace C18 cartridge using 50 % acetonitriles in H_2O.

Fractions combinations G2 yielded **AU 4 (2.4 mg)**, G3 gave **AU 5 (4.0 mg)**, **AU 9 (4.3 mg)** and **AU 10 (4.1 mg)**, G4 also yielded **AU 4 (3 mg)**, **AU 6 (1.6 mg)** (^{1}H NMR only) and **AU 9** (4 mg).

Fraction G6 was also purified in Grace C18 cartridge using with 100 % acetonitrile yielding **AU 7 (6 mg)**.

Fraction D5 (5.90 g) was also purified by flash column chromatography and the column was eluted with a gradient mixture of chloroform-methanol (10:0 to 0:10). 40 fractions were collected (250 ml each) and all the eluted fractions were monitored by thin layer chromatography. Fractions were pooled based on their retention time in the HPLC chromatogram to give five primary fractions, designated as H1-H5, (Table 6.8).

Table 6.8. Fractions obtained from D5.

Fractions combination	Weight (mg)	Physical characteristic
H1	170.0	Yellow viscous liquid
H2*	51.4	Yellow viscous liquid
H3	120.0	Yellow viscous liquid
H4*	1140.0	Yellow viscous liquid
H5*	2040.0	Dark viscous liquid

* These fractions were further investigated based on their TLC and ^{1}H NMR signals.

Fractions H2 (51.43 mg) was purified by PLC using hexane/ EtOAc / MeOH (5:4:1) as the developing solvent to give **AU 4 (19 mg).**

Fraction H4 (1140 mg) was further purified by CC and the column was eluted with gradient of hexane and EtOAc to give 32 fractions. Similar fractions were pooled to give 6 fractions (I1-I6, Table 6.9).

Table 6.9. Fractions obtained from H4.

Fractions combination	Weight (mg)	Physical characteristic
I1	31	Yellow viscous liquid
I2	17	Yellow viscous liquid
I3*	49	Yellow viscous liquid
I4	54	Yellow viscous liquid
I5	107	Yellow viscous liquid
I6	491	Dark viscous liquid

*Fraction was further investigated

Fraction I3 (49 mg) was separated with C18 cartridge using 10-50% MeOH yielding **AU 6 (1.1 mg)** and **AU 9 (14.2 mg)**.

Fraction H5 (2040.0 mg) was further purified using column chromatography with a gradient mixture of chloroform-methanol to give 50 fractions. Fractions were pool based on their TLC profiles and retention time in the HPLC chromatogram to give five primary fractions, designated as (J1-J5, Table 6.10).

Table 6.10. Fractions obtained from H5.

Fraction	Weight (mg)	Physical characteristic
J1	19	Yellow viscous liquid
J2	63	Yellow viscous liquid
J3*	46	Yellow viscous liquid
J4	72	Yellow viscous liquid
J5	51	Dark viscous liquid

* This fraction was further investigated.

Fractions J3 was purified with Grace C18 cartridge using (10-35% MeOH) to give **AU 8 (5 mg)**.

Fraction D6 (3.21 g) was purified by flash column chromatography and the column was eluted with a gradient mixture of chloroform-methanol to give 31 fractions. Fraction 3 and Fractions combination 18-31 were further purified

Fraction 3 (29 mg) was purified with Grace C18 cartridge using (100 % MeOH) to give **Unknown compound (X, 5 mg).**

Fractions combination 18-31 was separated using CC and the column was eluted with gradient mixture of $CHCl_3$/MeOH to give 26 fractions. Fraction 2 was purified with (100 % MeOH) yielding **Unknown compound (Y, 8 mg)**.

Figure 6.2. Extraction and isolation scheme from *T emetica* boiled seeds.

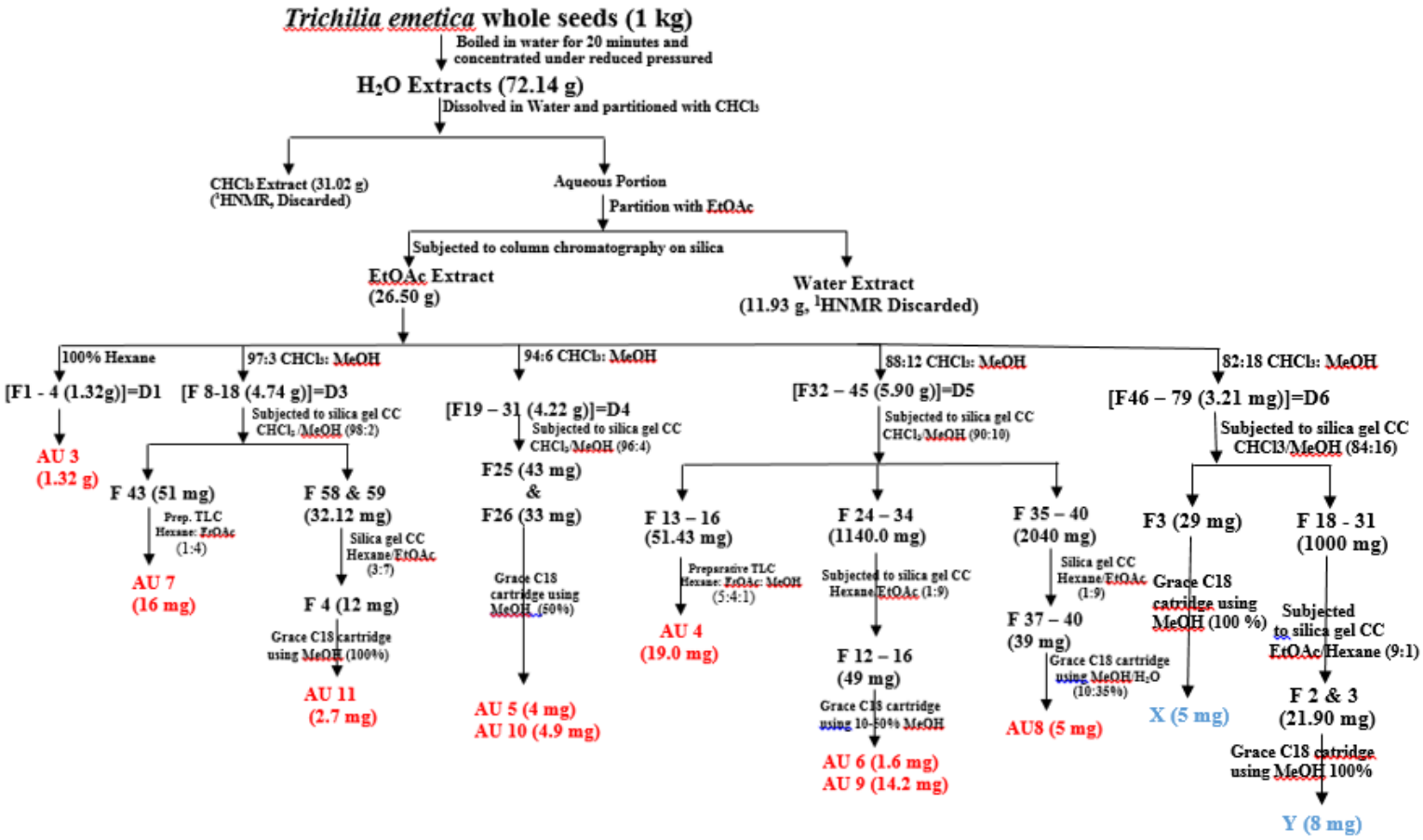

6.5.6 Chemical investigation of methanol extract of *T. emetica* seeds

Seeds (50 g) were soaked in methanol for 48 hours at room temperature. The mixture was filtered under gravity and the filtrate concentrated to dryness to give 3.42 g residue. The TLC characteristics of these extract showed major spots under UV and their proton NMR spectra showed aromatic proton signals. Column chromatography was conducted to separate these spots. The column was then eluted with gradient mixture of chloroform-methanol (10:0-0:10). A total of 42 fractions were collected (100 ml each). All the eluted fractions were monitored by thin layer chromatography. Five major fractions were pooled based on their TLC profiles, designated B, C, D, E and F, Table 6.11.

Table 6.11. Fractions obtained from methanol extract.

Fractions combination	Weight (g)	Physical characteristic
B	0.25	Yellow viscous liquid
C	1.13	Yellow viscous liquid
D*	1.06	Yellow viscous liquid
E*	0.45	Yellow viscous liquid
F	0.51	Yellow viscous liquid

* These fractions were further investigated based on their TLC and ^{1}H NMR signals.

Fraction D and E (1.51 g) were combined and was further purified by column chromatography using a step gradient of chloroform and methanol to give 6 fractions (K1-K6, Table 6.12).

Table 6.12. Fractions obtained from combinations D and E.

Fractions combination	Weight (mg)	Physical characteristic
K1	61.2	Yellow viscous liquid
K2	242.0	Yellow viscous liquid
K3*	154.1	Yellow viscous liquid
K4*	270.5	Yellow viscous liquid
K5	183.1	Yellow viscous liquid
K6	421.5	Dark viscous liquid

* This fraction was further investigated based on their TLC and ^{1}H NMR signals

Fraction K3 (154.06 mg) was further purified by PTLC with mixed solvent systems; ethyl acetate-hexane-methanol (5:3:2, 10 runs) yielding **AU4 (11 mg) and Unknown compound (Z, 19 mg)**.

Fraction K4 (270.45 mg) was separated by PTLC using chloroform-methanol (94:6, 6 runs) as the developing solvent to give **AU 9 (7 mg)**.

6.6 Isolation of limonoids from the seeds of *T. emetica*. First approach.

T. emetica oil (100 ml) was dissolved in 150 ml of hexane and partitioned with 95% MeOH and H_2O (4 × 150 ml). The combined extracts were concentrated to dryness to give (10.53 g) yellowish brown gum. The extract was dissolved in 50 % MeOH (100 ml) and extracted with EtOAc (4 × 100 ml). The proton NMR signals of these extracts; EtOAc (**A1**, 4.63 g) and aqueous MeOH (**A2**, 5.41 g) did not show any limonoids signals at δ 7.3, 7.12, and 6.22 assigned to β-furan ring moiety, but the TLC characteristics of EtOAc extract showed some spots under UV light.

6.6.1 Chemical investigation of soluble ethyl acetate extract

Purification of ethyl acetate extract (4.60 g) was done by column chromatography. The column was then eluted with dichloromethane: acetone at the gradient mixture of 100:0 to 0:100. These fractions were monitor using TLC. A total of 29 fractions were collected each in 250 ml conical flask. The fractions were pooled based on their TLC profile to give four fractions (A to D, Table 6.13).

Table 6.13. Fractions obtained from ethyl acetate extracts.

Fractions combination	Weight (g)	Physical characteristic
A	0.25	Yellow viscous liquid
B	1.19	Yellow viscous liquid
C	0.52	Yellow viscous liquid
D	2.31	Dark viscous liquid

The TLC profiles of these fractions were check using bromocresol green stains, the appearance of yellow spot on blue background give an indication of fat and this was confirmed by the ^{1}H NMR signals (**A3**) of these combinations. See appendix III for ^{1}H NMR spectra for A1, A2 and A3.

6.6.2 Isolation of limonoids from the seeds of *T. emetica*. Second approach.

Flaked *T. emetica* seeds (500 g) was extracted by hot percolation at 50 ^{O}C with hexane (3 × 700 ml) for 3 hours each time. The solvent was evaporated to give a dark brown oil (239 ml). This was diluted to 600 ml with hexane and extracted with 95% methanol (4 × 200 ml). Each of these methanol extracts were re-extracted with hexane (4 × 200 ml) to give a 4 × 4 partition. In addition, the extracts was checked using a TLC. The first two methanol extracts have the same TLC profiles and were pooled together and evaporated to give a yellowish brown gum (4.47g). The extracts was then purified using column chromatography.

6.6.3 Chemical investigation of aqueous methanol extract

The separation of methanol extract (4.40 g) was achieved by column chromatography using hexane and ethyl acetate in a polarity gradient manner to give 40 fractions.
Based on their TLC profiles, similar fractions were pooled together to give 5 primary fractions (J – N, Table 6.14).

Table 6.14. Fractions obtained from methanol extracts.

Fractions combination	Weight (g)	Physical characteristic
J	0.09	Yellow viscous liquid
K	1.23	Yellow viscous liquid
L	1.02	Yellow viscous liquid
M	0.28	Yellow viscous liquid
N	1.62	Dark viscous liquid

This fractions combinations were also checked using bromocresol green stains, it also show to be fat and this was confirmed by their ^{1}H NMR signals. See appendix III, for ^{1}H NMR spectra of J, L and N.

6.6.4 Isolation of limonoids from the seeds of *T. emetica*. Third approach.

T. emetica seed oil (200 ml) was dissolved in 500 ml of n-hexane and refluxed at 100 ^{O}C for 2 hours. The extract was cooled to room temperature and extracted with 95% methanol (5 × 300 ml). The extracts were re-extracted with n-hexane (5 × 300 ml) to give a 5 × 5 partition. All the extracts were monitored by thin layer chromatography. The first two fractions were combined and dried down giving 0.2479 g while fraction 3 and 4 was also dried down to give

0.31 and 0.71g respectively. The ^{1}H NMR of these extracts were conducted and did not show any limonoid signals (Fig Bi, Bii and Biii). See appendix III.

6.6.5 Isolation of limonoids from the seeds of *T. emetica*. Fourth approach.

T. emetica seeds defatted flour (50 g) were extracted with methanol (200 ml × 7) at room temperature. The combined extract were dried down under a vacuum at 40 ^{O}C to give 4.15 g (8.3% w/w) methanol extract. The extract was suspended in water and partitioned against organic solvents to yield chloroform extract 1.12 g (26.99 % w/w), ethyl acetate extract 0.28 g (6.75% w/w), n butanol extract 0.58 g (13.98% w/w) and water extract 1.27 g (30.60 % w/w). The ^{1}H NMR spectra of these extracts; n-butanol (Fig. C1) and EtOAc (Fig. C2) showed good profile, while that of chloroform (Fig. C3) and water (Fig. C4) indicate fats and sugars, hence discarded.

6.6.5.1 Chromatographic separation of n-butanol extract

The purification of butanol extract (0.58 g) was done by column chromatography using chloroform and methanol (10:0 to 0:10) in a polarity gradient manner. All the eluted fractions were monitored by TLC and similar fractions were combined to give 7 fractions (A – G, Table 6.15).

Table 6.15. Fractions obtained from n butanol extracts.

Fractions combination	Weight (mg)	Physical characteristic
A	33.9	Brown viscous liquid
B	91.3	Brown viscous liquid
C	104.6	Brown viscous liquid
D	110.2	Brown viscous liquid
E	63.6	Brown viscous liquid
F	102.3	Brown viscous liquid
G	42.9	Dark viscous liquid

These fractions combinations gave poor ^{1}H NMR signals; A (Fig. AA), and G (Fig. GA), see appendix III.

6.6.5.2 Chromatographic separation of ethyl acetate extract

The ethyl acetate extract 0.28 g was purified by column chromatography and the column was eluted with a gradient mixture of chloroform and methanol. On the basis of their TLC profiles, similar fractions were pooled to give 4 major fractions (A – D, Table 6.16).

Table 6.16. Fractions obtained from ethyl acetate extract.

Fraction	Weight (mg)	Physical characteristic
A	91.4	Yellow viscous liquid
B	67.6	Yellow viscous liquid
C	39.1	Yellow viscous liquid
D	54.0	Dark viscous liquid

These fractions combinations were fat based on the observation of the bromocresol green stains and this was confirmed by their ^{1}H NMR signals. ^{1}H NMR spectrum Fr A-D, see appendix III.

The above protocols were used at different concentrations (150 g, 500 g and 2.0 kg) to isolate limonoids, but without success (Fig. 6.3).

Fig. 6.3. The extraction and isolation of limonoids from *T. emetica* seeds. 4th approach

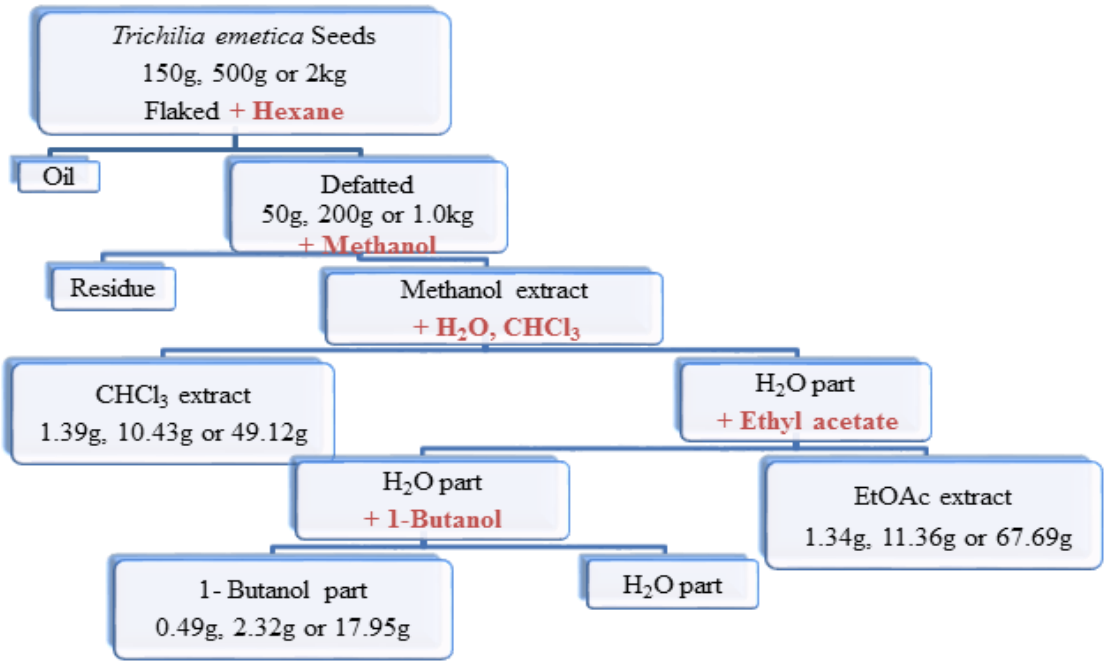

6.6.6 Isolation of limonoids from the seeds of *T. emetica.* Fifth approach.

Flaked *T. emetica* seeds (700 g) were extracted with hexane (7 × 1200 ml) at room temperature. The combined extracts were concentrated to give (385.57 ml) brown yellowish oil and the defatted flour was dried down to give (310.63 g) residue. The defatted flour (300 g) was extracted with 95 % ethanol (6 × 600 ml). The combined extract were concentrated to dryness to give 62.61 g of residue. The ethanolic extract was dissolved in 95 % aqueous methanol (200 ml) and then subjected to partitioning with petroleum ether (6 × 100 ml). The aqueous methanol and the combined petroleum ether extracts were dried down in vacuum to give 19.51 and 41.11 g of residue, respectively. The 95% aqueous methanol extract (19.51 g) was dissolved in water (100 ml) and partitioned with ethyl acetate (6 × 50 ml). The water extract and the combined ethyl acetate extract was also concentrated to yield 4.48 and 14.14 g of residue, respectively. The ethyl acetate extract 14.14 g was vacuum filtered through a plug of silica gel in a glass column using ethyl acetate as the eluent and the filtrate is concentrated to give (10.05 g) (Scheme 6.4). The ^{1}H NMR spectrum (EF) of this extracts was poor but the TLC profile show some UV active compounds. See appendix III for ^{1}H NMR spectrum of EF.

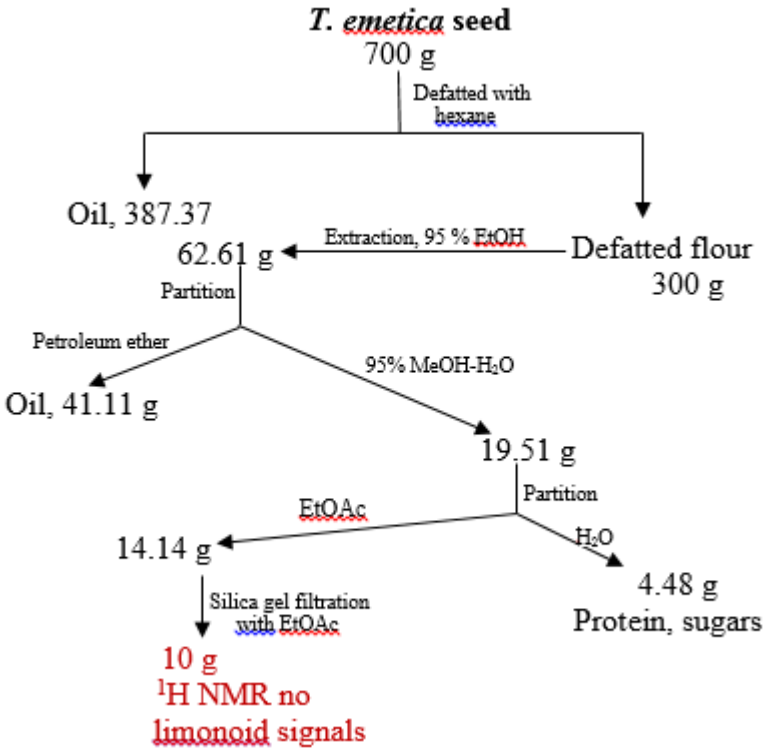

Fig. 6.4. Flow chart for the isolation of limonoids from the seeds of *T. emetica*. 5TH approach

6.6.6.1 Chromatographic separation of ethyl acetate extracts.

The separation of the ethyl acetate extract (10.52 g) was conducted by column chromatography using a gradient mixture of hexane: ethyl acetate (10:0 - 0:10) and methanol: EtOAc (1:99 – 4:96). All the eluted fractions (55) were screened with bromocresol green stains, yellow spots on a light blue background were observed indicating the presence of fatty acid. Some of these fractions were checked using ^{1}H NMR spectroscopy, see appendix III for spectra of E3 and E50.

6.7. Chemical investigation of *T. emetica* stems.

Air-dried stems of *T. emetica* (1.8 kg) were chopped into smaller pieces and extracted with methanol (3.5 L) at room temperature for two weeks, and the resulting extract was concentrated to give (137.97 g) dark gummy extract. This extract was suspended in water and extracted with chloroform and ethyl acetate. Each extract was concentrated in vacuum to give chloroform-soluble fraction (49.94 g), ethyl acetate-soluble fraction (52.30 g) and water fraction (31.92 g) respectively. The ^{1}H NMR spectra showed chloroform fraction to be fats, water fraction to be sugars while ethyl acetate fraction to be made up aromatic signals.

6.7.1 Chromatographic separation of stem ethyl acetate extracts.

The ethyl acetate soluble part of methanolic extract of *T. emetica* was subjected to column chromatography on silica gel using a step gradient of chloroform and methanol to give 4 fractions (S1 – S4, Table 6.17).

Table 6.17. Fractions obtained from stem ethyl acetate extract.

Fractions combination	Weight (g)	Physical characteristic
S1	10.24	Brown viscous liquid
S2*	4.69	Brown viscous liquid
S3	6.58	Brown viscous liquid
S4*	5.13	Dark viscous liquid

*Fractions were further investigated

The combined S2 (4.69 g) was further purified by CC using chloroform and methanol in a polarity gradient manner. All the eluted 24 fractions were monitored by thin layer chromatography. Fraction 4 (49 mg) was purified with Grace C18 cartridge using (50% MeOH) to give AU 14 (8 mg) and ZA (4 mg).

The combination S4 (5.13 g) was also purified by CC and the column was eluted with gradient mixture of chloroform and methanol. Fractions 5, 6 and 7 were combined and purified with Grace C18 cartridge using (10 - 50% MeOH) to give AU 12 (5 mg) and AU 13 (11 mg). Three pure compounds were isolated and purified as shown in Figure 6.5.

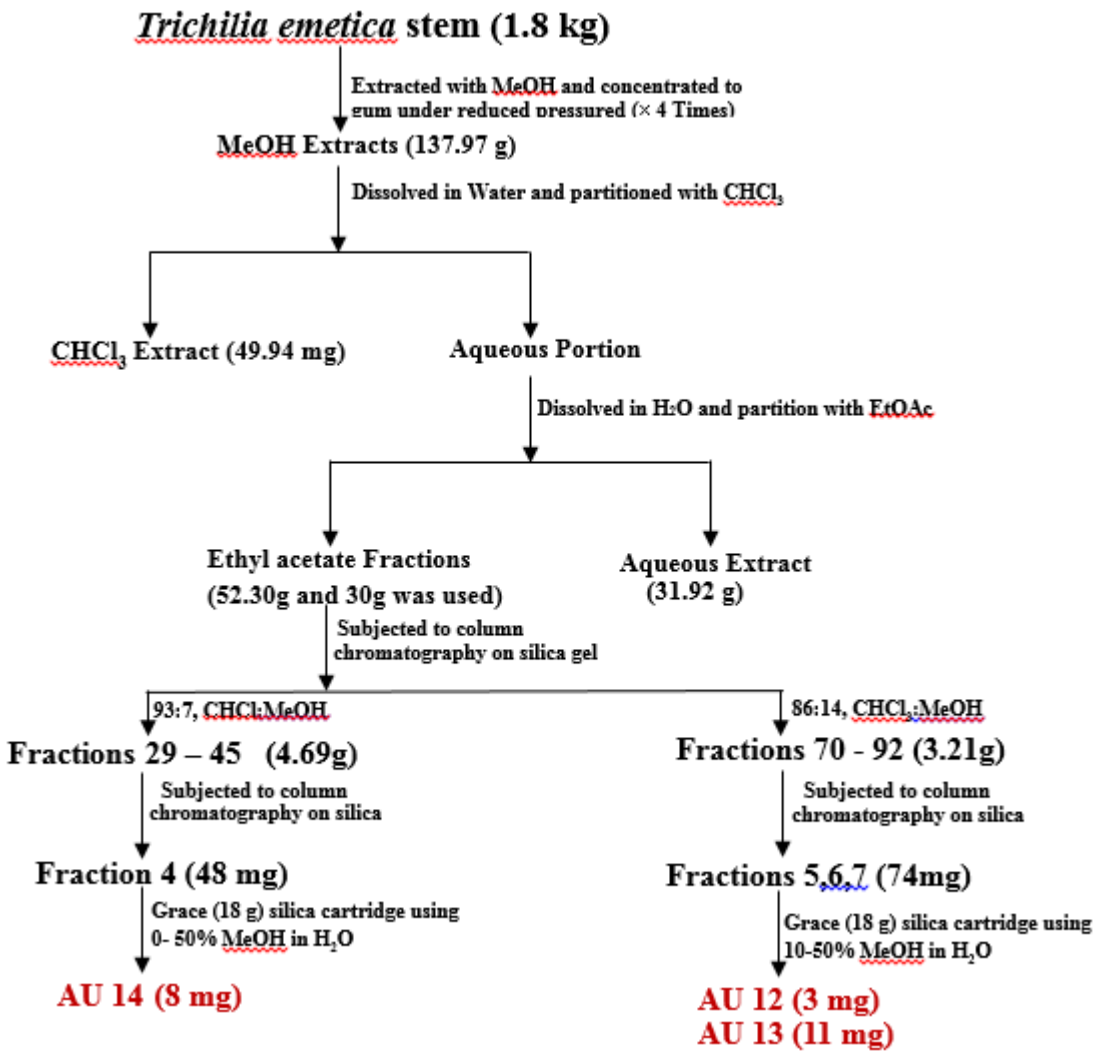

Fig. 6.5. Extraction and isolation scheme from the stem of *Trichilia emetica*

6.8. Chemical investigation of Karanjin seeds (*M. pinnata*) oil.

Karanjin seeds oil (100 ml) was diluted to 300 ml with hexane and extracted with 95% methanol (4 × 150 ml). Each of these methanol extracts were re-extracted with hexane (4 × 150 ml) to give a 4 × 4 partition, and the extracts were checked using a TLC. The first two methanol extracts had the same TLC profiles and were pooled together and evaporated to give a brown gum (3.72 g).

6.8.1 Chromatographic separation of *M. pinnata* methanol extracts.

The separation of methanol extract (3.70 g) was achieved by column chromatography using hexane and ethyl acetate in a polarity gradient manner to give 43 fractions. Fractions 17, 18 and 21 obtained on elution with hexane: EtOAc (1:1) yielded white crystals, which crystallized from methanol. Fractions 17 and 18 were combined based on their TLC characteristic to yield AU 27 (15 mg) while fraction 21 gave AU 16 (9 mg). Similarly, fraction 24 gave AU 17 (11 mg).

6.9 Chemical investigation of Nigerian neem seeds (*Azadirachta indica*) oil.

Neem seeds (1.80 kg) were extracted with hexane (4 × 3.00 L) at room temperature. The filtrates were combined and concentrated in vacuum to give a brownish oil (316.77 ml) and a residue (1482.18 g). This oil extract (100 ml) was diluted to 250 ml with n-hexane and extracted with 95% methanol (4 × 150 ml). These methanol extracts were re-extracted with hexane (4 × 150 ml) to give a 4 × 4 partition. On the basis of their TLC profiles, the first two methanol extracts were pooled together and evaporated to give a brown gum (5.32 g).

6.9.1 Chromatographic separation of neem methanol extracts.

The purification of methanol extract (5.30 g) was carried out by column chromatography using a step gradient of hexane and ethyl acetate to give 32 fractions. Fraction 17 obtained on elution with hexane: EtOAc (1:1) yielded white crystals, which crystallized from methanol to yield **AU 18 (41 mg)**.

6.9.2 Chemical investigation of neem (*Azadirachta indica*) defatted seeds flour

Neem seeds defatted flour (1 kg) were extracted with 95% ethanol (5 × 600 ml). The combine extract was concentrated to dryness to give 81.79 g of residue. The ethanolic extract was dissolved in 95% aqueous methanol (300 ml) and then subjected to partitioning with petroleum ether (5 × 200 ml). The aqueous methanol and the combined petroleum ether extracts were dried down in vacuum to give 35.63 and 13.29 g of residue respectively. The 95% aqueous methanol extract (35.63 g) was dissolved in water (300 ml) and partitioned with ethyl acetate (5 × 100 ml). The water extract and the combined ethyl acetate extract was also concentrated to yield 25.07 and 8.53 g of residue. The ethyl acetate extract 8.53 g was vacuum filtered through a plug of silica gel in a glass column using ethyl acetate as the eluent and the filtrate was concentrated to give (5.60 g).

This filtrate was further purified isocratically using hexane-ethyl acetate (1:3) to give 15 fractions. On the basis of their TLC characteristics, similar fractions were pooled to give 4 fractions (W-Z, Table 6.18).

Table 6.18. Fractions obtained from neem ethyl acetate extract.

Fraction	Weight (g)	Physical characteristic
W	2.17	Yellow viscous liquid
X	1.51	Yellow viscous liquid
Y*	1.09	Yellow viscous liquid
Z	0.59	Yellow viscous liquid

*This fraction is further investigated

Crystallization of fraction Y (1.09 g) from CCl_4 gave a white crystalline material (55.08 mg). This material was subjected to flash chromatography isocratically using $CHCl_3$-MeCN, 3:1 as the mobile phase to give 13 sub-fractions. This sub-fractions were evaporated and subjected to NMR analysis. The ^1H NMR of sub-fraction 8 (2.3 mg) corresponding to AU 19. This isolation procedure is illustrated in the scheme below (Fig. 6.6).

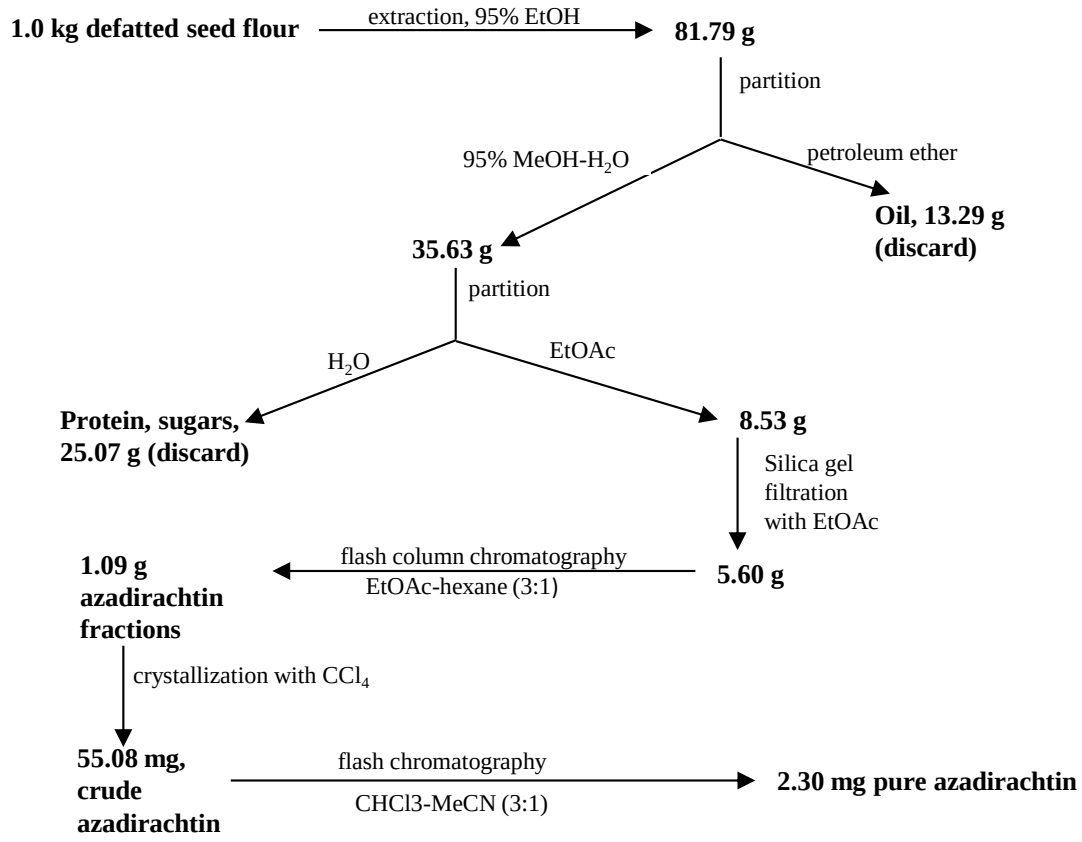

Fig. 6.6. Flow chart for the isolation of limonoids (azadirachtin) from the seeds of *Azadirachta indica.*

6.10 Acid hydrolysis.

The nature of sugars present in these glycosides (Catechin 3-*O*-β-D-glucopyranoside, Taxifolin 4'-*O*-β-D-glucopyranoside, Eriodictyol 4'-*O*-β-D-glucopyranoside, Quercetin 3-*O*-β-D-glucopyranoside, catechin-3-*O*-α-L-rhamnopyranosyl (1→4) β-D-glucopyranoside) were confirmed by hydrolysis. Each glycoside (2.0 mg) was dissolved in methanol (2.5 ml) and 2 M HCl (2.5 ml). The mixture was heated in a water bath at 100 ^{O}C under reflux for 60 minutes. On cooling, the methanol was evaporated under vacuum and the H_2O washed with EtOAc (4 × 5 ml). The aqueous portion was examined for sugars by direct comparism on silica gel TLC with authentic glucose, galactose, mannose and rhamnose using (CH_2Cl_2/MeOH/H_2O, 17:6:1). For further confirmation, the H_2O portion was evaporated to dryness under reduced pressure at 40 ^{O}C. The dried H_2O extract was silylated by reacting 0.5 mg of the extract with $NH_2OH.HCl$ (0.1 ml) in dry pyridine (0.1 ml) and heated at 60 ^{O}C for 40 minutes. The mixture was allowed to cool and BSTFA: TMCS (99:1, 0.1 ml) was added and allowed to react at room temperature

for 30 minutes. Hexane (0.5 ml) and H_2O (0.3 ml) was added and vortexed for 1 minute. The silylated product was then analysed by GC.

The silylated derivatives of sugars standards (glucose, galactose, mannose and rhamnose) prepared in the same manner were used as references.

A Thermo Scientific 1300 gas chromatograph equipped with a TRIPLUS RSH autosampler and an ITQ 900 MS detector was used for the analysis of the silylated sugars. The conditions of the GC were as follows: column, Rxi®-ms (length: 30 m, ID: 0.25 mm, df: 0.25 μm). Inlet temperature 250 ^{o}C, split flow 30 ml/min, split ratio 20 and carrier flow rate 1.5 ml/min. The temperature program start at 172 ^{o}C, hold for 1 min, then increased at 10 ^{o}C/min up to 210 ^{o}C, hold for 1 min then 20 ^{o}C/min up to 220 ^{o}C, hold for 1 min, then a final ramp of 10 ^{o}C/min to 280 ^{o}C and hold for 1.5 min. Total run time of 15 min.

The retention times of standards were as follows: rhamnose; 3.99 min, D-glucose; 5.49 min and galactose; 5.40 min.

6.11 Biological assays

6.11.1 Alamar blue assay to determine drug sensitivity of African trypanosomes in vitro

The antitrypanosomal activity of the flavonoids were tested against the blood stream form of the Trypanosoma brucei (S427) using a modification of the microplate Alamar blue assay. The compounds were prepared as 10 mg/ml stock solutions in 100% DMSO. The 200 μg/ml test solution was prepared by adding 4 μl of (10 mg/ml) stock solution to 196 μl HM1-9 medium (%10 FCS). Hundred microliters of the test solution were pipetted in duplicate into the first column of a 96-well microplates and the serial 1:1 dilutions was carried out from column 2 to 11. DMSO at a concentration range of 0.001–1% and suramin over a concentration range of 0.008–1 μM were included as negative and positive controls. A sterility check was conducted by using 90μl of the diluted bacterial inoculum to all the assay plates with the exception of well A1. The microplates were incubated at 37 ºC in a humidified 5% CO_2 atmosphere for 48 hours. Thereafter, 10% alamar blue™ was added to each well and the microplates were incubated for a further 20 hours. Fluorescence was determined using a microplat fluorometer at an excitation wavelength of 560 nm and an emission wavelength of 590 nm. Percentages of control values were calculated and the MIC was determined as the lowest compound concentration with <5 % of the control values.

6.11.2 Antimicrobial assay - M. marinum ATCC.BAA535

A modification of the microplate Alamar blue method for susceptibility testing of fast growing species of *Mycobacterium* was used. *Mycobacterium marinum* ATCC.BAA535 from the thawed stock cryoculture was streaked onto Columbia (5% horse blood) agar slopes and incubated at 31 ^{o}C for 5 days. A loopful of the culture was then transferred into 10 mL of sterile 0.9% NaCl containing glass beads. The suspension was mixed and allowed to settle. 1 mL of the supernatant was added to 10 mL sterile MHB (Mueller Hinton broth) saline that had been used to zero the turbidity meter. The turbidity of the solution was adjusted to be the same as a 0.5 McFarland standard. A few drops of Tween 80 0.02% were filter sterilized and added to homogenise the suspension. This was then shaken and the inoculum diluted 1 in 10 with Mueller Hinton Broth for use in the assay. Samples were dissolved in a sufficient quantity of DMSO to reach a concentration of 10 mg/mL or 1 mg/100 µL. For the initial screen, the 10 mg/mL stock solutions of the samples were diluted to 1000 µg/mL using MHB. Twenty microlitres of each extract were placed in each well and 80 µL of MHB was added. DMSO was added as the negative control at a concentration range of 1 to 0.002% and gentamycin as positive control at a range of 100 to 0.78 µg/mL. One hundred microlitres of the bacterial suspension were added to the wells. The plates were sealed and incubated at 31 ^{o}C for 5 days before the addition of 10 µl of Alamar blue. The plates were again sealed and incubated at the same temperature for 24 hours after which fluorescence was determined using the Wallac Victor microplate reader in fluorescence mode (Excitation 530 nm; Emission 590 nm). The results were calculated as percentages.

The same method was used for *Klebsiella pneumonia* (strains ATCC 13883 and BAA 2146) and *Methicillin resistant staphylococcus aureus* (strains 16 and 106) except that a loopful of each bacterial strain was streaked on to individual Columbia / 5% horse blood agar slopes and were incubated at 37 ^{o}C for 20 hours.

6.11.3 Antimicrobial screening of selected Gram positive and Gram negative bacterials

Antimicrobial screens were performed using a high-throughput, 96 well plate method. The four bacterial species used in the screen were *Escherichia coli* K12, *Bacillus cereus* ATCC 14579, *Staphyloccocus aureus* RN42420, and *Pseudomonas aeruginosa* PA01. The extracts were screened, with triplicate repeats against each bacterial species per 96 well plate. The working stock solutions were prepared by adding 10 µL of an overnight culture to 190 µL of nutrient broth (Lab M) under sterile conditions in each well. And 10 µL of each extract was added to

each well as per the 'Rapid Screen Plan' attached, with triplicate negative and positive growth controls used, in addition to antimicrobial controls using rifampacin at a concentration of 10 mg/mL. The 96 well plate was then analysed using a Hidex Sense plate reader set at 37°C on a continuous orbital shake of 150 rpm. The optical density readings at 600 nm, were taken in every 20 minutes for 24 hours, and the result extracted into Microsoft Excel. The first optical density reading was subtracted from every subsequent reading for each well. After which, 10 was added to each optical density reading and a Log10 transformation completed. Triplicate readings were then combined and standard deviations calculated and plotted alongside mean optical density readings.

6.11.4 Antifungal assay

Five strains of *C. albicans* harbouring a range of *ERG3* and *ERG11* mutations (Table 6.19), and representing different anti-fungal resistance spectra were selected to analyse the potential toxic properties of these compounds. The 5 strains were SC514 (wild type), CA12, CA488, CA490 and CA1008. A description of the mutations present in each strain is detailed in Table 1. All *C. albicans* strains were cultured on YPD (1% yeast extract, 2% peptone, and 1% dextrose) agar plates at 30°C. For routine growth, yeast strains were grown with rotary shaking at 37°C in RPMI-1640 + 2% glucose media.

Table 6.19. *Candida albicans* strains.

Strain	*ERG3* Mutation	*ERG11* Mutation
SC514	-	-
CA12	W332R	-
CA488	H243N; T330A; A351V	D225G; E266D; E391G; V488I
CA490	D147G; T330A; A351V	F72S; T229A; E266D; N440S; V488I; R523G
CA1008	K97E; L193P; V237A; A351V; A353T	E266D

The plated cultures of *C. albicans* were grown for 24 hours at 30°C. Isolated colonies were then selected from this plated culture, transferred to 0.85% Saline and cell density determined by haemocytometer counts. Cell suspensions at a density of 1.5×10^3 cells/mL were prepared in RPMI-1640 media, and 100µL of inoculate transferred to each well of 96 well flat-bottomed plate. Working stocks of the compounds were prepared in RPMI-1640 media at concentrations of 40 µg/mL and 80 µg/mL and 100 uL added to each of triplicate wells to give final

concentrations of 20 µg/mL and 40 g/ml, respectively. Thus, each plate consisted of a specific yeast strain with each compound assessed in triplicate. Plates were incubated with shaking at 37 °C for 24 hours and then the cell growth assessed by microscopy with a 10x objective. The experiments were performed in duplicate.

References

Abayeh, O., Okoughae, O., 1998. Oil content and oil quality characteristics of some Nigerian oils seeds. J. pure Appl. Sci. 1, 17–23.

Aggarwal, B.B., Sundaram, C., Malani, N., Ichikawa, H., 2007. Curcumin: The Indian sold gold, in: The Molecular Targets and Therapeutic Uses of Curcumin in Health and Disease. Springer US, Boston, MA, pp. 1–75.

Ahmad, M., Khan, M.A., Marwat, K.S., Zafar, M., Khan, A.., Hassan, U.T., Sultana, S., 2009. Useful Medicinal Flora Enlisted in Holy Quran and Ahadith. Am. J. Agric. Environ. Sci., 1, 126–140.

Ahn, J.H., Kim, E.S., Lee, C., Kim, S., Cho, S.-H., Hwang, B.Y., Lee, M.K., 2013. Chemical constituents from *Nelumbo nucifera* leaves and their anti-obesity effects. Bioorg. Med. Chem. Lett. 23, 3604–3608.

Akhtar, Y., Yeoung, Y.-R., Isman, M.B., 2007. Comparative bioactivity of selected extracts from Meliaceae and some commercial botanical insecticides against two noctuid caterpillars, *Trichoplusia ni* and *Pseudaletia unipuncta*. Phytochem. Rev. 7, 77–88.

Anyasor, G.N., Ogunwenmo, K.O., Oyelana, O.A., Ajayi, D., Dangona, J., 2009. Anyasor AV.pdf. Pakistani J. Nutr. 3, 269–272.

AOAC, 1990. Official methods of analysis, 15th ed.: Association of Official Analytical Chemists: Washington DC.

Araujo, C., Sousa, M.J., Ferreira, M.F., Leao, C., 2003. Activity of essential oils from Mediterranean *Lamiaceae species* against food spoilage yeast. J. Food Prot. 66, 625–632.

Arnason, J.T., Philogene, B.J.R., Donskov, N., Kubo, I., 1987. Limonoids from Meliaceae and Rutaceae reduce feeding growth and development of *Ostrinia nubilalis*. Entomol Exp Appl 43, 221–226.

Atindehou, K.., Schmid, C., Brun, R., Koné, M.., Traore, D., 2004. Antitrypanosomal and antiplasmodial activity of medicinal plants from Côte d'Ivoire. J. Ethnopharmacol. 90, 221–227.

Atindehou, K.K., Schmid, C., Brun, R., Kone, M. w., Traore, D., 2004. Antitrypanosomal and antiplasmodial activity of medicinal plants from Cote d'Ivoire. J. Ethnopharmacol. 90, 221–227.

Bae, Y.-S., Burger, J.F.W., Steynberg, J.P., Ferreira, D., Hemingway, R.W., 1994. Flavan and procyanidin glycosides from the bark of blackjack oak. Phytochemistry 35, 473–478.

Bah, B., Jager, A.K., Adsersen, A., Diallo, D., Smestad-Paulsen, B., 2007. Antiplasmodial and GABA-benzodiazepine receptor binding acitivities of five plants used in traditional medicine in Mali, West Africa. J. Ethnopharmacol. 110, 451–457.

Balasundram, N., Sundram, K., Samman, S., 2006. Phenolic compounds in plants and agri-industrial by-products: Antioxidant activity, occurrence, and potential uses. Food Chem. 99, 191–203.

Beerhues, L., Forkmann, G., Schopker, H., Stotz, G., Wiermann, R., 1989. Flavanone 3-hydroxylase and dihydroflavonol oxygenase activities in anthers of Tulipa. The significance of the tapetum fraction in flavonoid metabolism. J. Plant Physiol. 133, 743–746.

Beggs, C.J., Stolzer-Jehle, A., Wellman, E., 1985. Isoflavonoid formation as an indicator of UV stress in bean (*Phaseolus vulgaris* L.) leaves: The significance of photo-repair in assessing potential damage by increased solar UV-B radiation. Plant Physiol. Plant Physiol. 79, 630–634.

Benavente-Garcia, O., Castillo, J., Marin, R.F., Ortuno, A., Rio, D.A.J., 1997. Uses and properties of *Citrus* flavonoids. J. Agric. Food Chem. 45, 4505–4515.

Benjamin, B.M., Raaen, V.F., Hagaman, E. w., Brown, L.L., 1978. Some Unusual Oxidation Products of 2,6-Di-tert-butyl-4-methylphenol. Am. Chem. Soc. 43, 2986–2991.

Bennet, R., Wallsgrove, R., 1994. Secondary metabolites in plant defence mechanisms. Tansley Review No. 72. New Phytol 127, 617–633.

Bero, J., Ganfon, H., Jonville, M.-C., Frédérich, M., Gbaguidi, F., DeMol, P., Moudachirou, M., Quetin-Leclercq, J., 2009. In vitro antiplasmodial activity of plants used in Benin in traditional medicine to treat malaria. J. Ethnopharmacol. 122, 439–444.

Bieza, K., Lois, R., 2001. An Arabidopsis mutant tolerant to lethal ultraviolet-B levels shows constitutively elevated accumulation of flavonoids and other phenolics. Plant Physiol. 126, 1105–1115.

Britton, G., 1983. The Biochemistry of natural pigments. Cambridge Univ. Press., Cambridge, UK.

Bryant, D.A., Frigaard, N.-U., 2006. Prokaryotic photosynthesis and phototrophy illuminated. Trends Microbiol. 14, 488–496.

Butler, M.S., 2004. The role of natural product chemistry in drug discovery. J. Nat. Prod. 67, 2141–2153.

BuvierNave, P., Husselstein, T., Beneviste, P., 1998. Two families of sterol methyltransferases are involved in the first and the second methylation steps of plant sterol biosynthesis. Eur. J Biochem 256, 88–96.

Cañabate-Díaz, B., Segura Carretero, A., Fernández-Gutiérrez, A., Belmonte Vega, A., Garrido Frenich, A., Martínez Vidal, J.L., Duran Martos, J., 2007. Separation and determination of sterols in olive oil by HPLC-MS. Food Chem. 102, 593–598.

Capasso, L., 1998. 5300 Years ago, the Ice Man used Natural Laxatives and antibiotics. Lancet 9143, 1864.

Carini, J.P., Leitao, G.G., Schneider, P.H., Santos, C.C., Costa, F.N., Holzschuh, M.H., Klamt, F., Bassani, V.L., 2015. Isolation of achyrobichalcone from Achyrocline satureioides by high-speed counter current chromatography. Pharm. Biotechnol. 16, 66–71.

Chan, K., Kan, Y.W., 1999. Nrf2 is essential for protection against acute pulmonary injury in mice. Proc. Natl. Acad. Sci. 96, 12731–12736.

Chander, M.P., Kumar, K.V., Shriram, A.N., Vijayachari, P., 2015. Anti-leptospiral activities of an endemic plant *Glyptopetalum calocarpum* (Kurz.) prain used as medicinal plant by Nicobarese of Andaman and Nicobar Island. Nat. Prod. Res. 29, 1575–1577.

Chaturvedula, V.S.P., Prakash, I., 2012. Isolation of Stigmasterol and β-Sitosterol from the dichloromethane extract of *Rubus suavissimus*. Int. Curr. Pharm. J. 1, 239–242.

Chopade, V., Tankar, A., Pande, V., Tekade, A., Gowekar, N., Bhandari, S., Khandake, S., 2008. *Pongamia pinnata*: Phytochemical constituents, traditional uses and pharmacological properties: A review. Int. J. Green Pharm. 2, 72.

Coates-Palgrave, K., 1972. Trees of Southern Africa. Stuik Publishers, Cape Town.

Collier, H.O.J., 1984. In Discoveries in Pharmacology. Elsevier Science Publishers, New York.

Conqueiro, A., Regasini, O.L., Skrzek, G.C.S., Queiroz, F.M.M., Silva, S.H.D., Bolzani, V., 2013. Free radical scavenging activity of *Kielmeyera variabilis* (Clusiaceae). Molecules 18, 2376–2385.

Copping, G.L., Menn, J.J., 2000. Biopesticides: A review of their action, applications and efficacy. Pest Manag. 56, 651–676.

Cowan, M.M., 1999. Plant products as antimicrobial agents. Clin. Microbiol. Rev. 4, 564–582.

Cunningham, A.B.H.A.S.A.H.L.G., 1996. Zulu Medicinal Plants. University of Natal Press, Pietermaritzburg., KwaZulu-Natal.

Dacre, J., 1961. The metabolism of 3: 5-ditert.-4-hydroxybenzoic acid in the rabbit. Biochem. J. 4, 758–766.

Dalluge, J.J., Nelson, B.C., 2000. Determination of tea catechins. J. Chromatogr. 881, 411–424.

Dharmananda, S., 2003. Myrrh and frankincense, spiritual significance. Internet J. 2, 1–6.

Diallo, D., Paulsen, B.S., Liljeback, T.H.A., Michaelsen, T.E., 2003. The malian medicinal plant *Trichilia emetica*; studies on polysaccharides with complement fixing ability. J. Ethnopharmacol. 84, 279–287.

Dixon, R., Paiva, N., 1995. Stress-induced phenylpropanoid metabolism. Plant Cell 7, 1085–1097.

Ekpa, O.., Epka, U.., 1996. Comparison of the charateristic parameters and deterioration properties of oils from the Tenera and Dura variety of the oil palm. Niger. J. Chem. Res. 1, 26–33.

El Tahir, A., Satti, G.M.H., Khalid, S.M., 1999. Antiplasmodial activity of selected Sudanese medicinal plants with emphasis on *Maytenus senegalensis* (Lam.) Exell. J. Ethnopharmacol. 64, 227–233.

Engelter, C., Wehmeyer, a S., 1957. Fatty acid composition of oils of some edible seeds of wild plants. J. Agric. Food Chem. 18, 25–26.

Eromosele, C.O., Paschal, N.H., 2003. Characterization and viscosity parameters of seed oils from wild plants. Bioresour. Technol. 86, 203–205.

Evans, B.E., Rittle, K.E., Bock, M.G., Dipardo, R.M., Freidinger, R.M., Whitter, W.L., Lundell, G.F., Veber, D.F., Anderson, P.S., Chang, R.S.L., Lotti, V.J., Cerino, D.J., Chen, T., Kling, P.J., Kunkel, K.A., Springer, J.P., Hirshfied, J., 1988. Methods for drug discovery: development of potent , selective, orally effective *cholecystokinin antagonist*. J. Med. Chem. 31, 2235–2246.

Fabricant, D.S., Farnsworth, N.R., 2001. The value of plants used in traditional medicine for drug discovery. Environ. Heal. Perspect. 109, 69–75.

Fan, P., Lou, H., Yu, W., Ren, D., Ma, B., Ji, M., 2004. Novel flavanol derivatives from grape seeds. Tetrahedron Lett. 45, 3163–3166.

FAO/WHO, 1994. Fats and oils in human nutrition, Report of expert committee, Food and Nutrition Paper No. 57, FAO. Rome, Italy.

Fernando, C., Akujobi, E., 1987. Chemical Analysis of Selected Vegetable Oils and Fats of Sokoto State of Nigeria. J. Basic Appl. Sci. 1.

Fisher, R.F., Long, R.S., 1992. Rhizobium-plant signals exchange. Nature 357, 655–660.

Foo, L.Y., Karchesy, J.J., 1989. Polyphenolic glycosides from *Douglas fir* inner bark. Phytochemistry 28, 1237–1240.

Frum, Y., Viljoen, A.M., 2006. In vitro 5-lipoxygenase and anti-oxidant activities of South African medicinal plants commonly used topically for skin diseases. Pharmacol. Physiol. 19, 329–335.

Fupi, P.C., Mork, W.K., 1982. Mafura Nut Oil and Meal : Processing and Purification. JAOCS 59, 94–98.

Gadow, A.V., Joubert, E., Hansmann, C.F., 1997. Comparison of the antioxidant activity of rooibos tea (*Aspalathus linearis*) with green, oolong and black tea. Food Chem. 60, 73–77.

Garcez, R.F., Scramin, S., Nascimento, D.C.M., Mors, B.W., 1988. Prenylated flavonoids as evolutionary indicators in the Genus dahlstedtia. Phytochemistry 27, 1079–1083.

Gasparetto, J.C., Martinsa, C.A.F., Hayashia, S.S., Otuky, M.F., Pontaroloa, R., 2011. Ethnobotanical and scientific aspects of *Malva sylvestris* L.: a millennial herbal medicine. Parmacy Pharmacol. 64, 172–189.

Germanò, M.P., D'Angelo, V., Biasini, T., Sanogo, R., De Pasquale, R., Catania, S., 2006. Evaluation of the antioxidant properties and bioavailability of free and bound phenolic acids from Trichilia emetica Vahl. J. Ethnopharmacol. 105, 368–373.

Germanò, M.P., D'Angelo, V., Sanogo, R., Catania, S., Alma, R., Pasquale, R. De, Bisignano, G., 2005. Hepatoprotective and antibacterial effects of extracts from *Trichilia emetica* Vahl. (Meliaceae). J. Ethnopharmacol. 96, 227–232.

Geyid, A., Abebe, D., Debella, A., Makonnen, Z., Aberra, F., Teka, F., Kebede, T., Urga, K., Yersaw, K., Biza, T., Mariam, B.H., Guta, M., 2005. Screening of some medicinal plants of Ethiopia for their anti-microbial properties and chemical profiles. J. Ethnopharmacol. 97, 421–427.

Gimmel, M., 2008. Reading Medicine In The Codex De La Cruz Badiano. J. Hist. ideas 2, 169–192.

Govindanchari, R.T., Narasimhan, S.N., Suresh, G., Partho, D.P., Gopalakrishnan, G., 1996. Insect antifeedant and growth-regulating activities of salannin and other C-seco limonoids from neem oil in relation to azadirachtin. J. Chem. Ecol. 22, 1453–1462.

Grundy, I.M., Campbell, B.M., 1993. Potential production and utilisation of oil from *Trichilia SPP*. (Meliaceae). Econ. Bot. 47, 148–153.

Gunatilaka, A.A.L., Bolzani, V.S., Dagne, E., Hofmann, G.A., Johnson, R.K., Mccabe, F.L., Mattern, M.R., Kingston, D.G.I., 1998. Limonoids Showing Selective Toxicity to DNA Repaire-Deficient Yeast and Other Constituents of *Trichilia emetica*. J. Nat. Prod. 61, 179–184.

Gunawan, S., Darmawan, R., Nanda, M., Setiawan, A.D., Fansuri, H., 2013. Proximate composition of *Xylocarpus moluccensis* seeds and their oils. Ind. Crops Prod. 41, 107–112.

Han, H.X., Hong, S.S., Hwang, S.J., Lee, K.M., Hwang, Y.B., Ro, S.J., 2007. Monoamine oxidase inhibitory components from *Cayratia japonica*. Arch Pharm Res 30, 13–17.

Harbone, J.B., 1993. Introduction to Ecological Biochemistry. Academic Press, London UK.

Harborne, J.B., Baxter, H., Moss, G.P., 1999. Phytochemical dictionary: Handbook of bioactive compounds from plants, 2nd ed. Taylor and Francis, London.

Harborne, J.B., Mabry, T.J., 1982. The flavonoids. Chapman and Hall, London.

Heinrich, M., Barnes, J., Gibbons, S., Williamson, E.M., 2004. Fundamentals of Pharmacognosy and Phytotherapy. Churchhill Livinstone, London UK.

Heller, W., Forkmann, G., 1988. Biosynthesis. In the flavonoids, J.B. Harbo. ed. Chapman and Hall, London.

Herrmann, K., 1988. On the occurence of flavonol and flavone glycosides in vegetables: a review. Z Leb. Forsch 186, 1–5.

Herrmann, K., 1976. Flavonols and flavones in food plants: a review. J. Food Technol 11, 433–448.

Hidalgo, F.J., Zamora, R., 2003. Edible oil analysis by high-resolution nuclear magnetic resonance spectroscopy: recent advances and future perspectives. Trends Food Sci. Technol. 14, 499–506.

Hilbert, G., Temsamani, H., Bordenave, L., Pedrot, E., Chaher, N., Cluzet, S., Delaunay, J.-C., Ollat, N., Delrot, S., Mérillon, J.-M., Gomès, E., Richard, T., 2015. Flavonol profiles in berries of wild Vitis accessions using liquid chromatography coupled to mass spectrometry and nuclear magnetic resonance spectrometry. Food Chem. 169, 49–58.

Hill, A.F., 1989. Economic botany: A Text Book of Useful Plants and Plant Products., Second. ed. Mc Graw Hill Book Company, New York.

Hilton, J.W., 1989. Antioxidants: function, types and necessity of inclusion in pet foods. Can Vet J 30, 682–684.

Hoet, S., Opperdoes, F., Brun, R., Adjakidje, V., Quetin-Leclercq, J., 2004. In vitro antitrypanosomal activity of ethno pharmacoligically selected Beninese plants. J. Ethnopharmacol. 91, 37–42.

Hollman, P.C.H., Katan, M.B., 1999. Dietary flavonoids: intake, health effects and bioavailability. Food Chem. Taxicology 37, 937–942.

Huffman, M.A., Seifu, M., 1989. Observation on the illness and consumption of a possibly medicinal plant *Vernomia amygdalina* (DEL.), by a wild chimpanzee in the Mahale Mountains National Park, Tanzania. Primate 30, 51–63.

Hummel, H.E., Langner, S.S., Leithold, G., Schmutterer, H., 2014. Neem: Unususally versatile plant genus azadirachta with many useful and so far insufficiently exploited properties for agriculture, medicine and industry. Commun agric appl biol sci 79, 211–228.

Hwang, T., Kashiwada, Y., Nonaka, G., Nishioka, I., 1989. Flavan-3-ol and proanthocyanidin allosides from *Davallia divaricata*. Phytochemistry 28, 891–1989.

Hye, M.A., Taher, M.A., Ali, M.Y., Ali, M.U., Zaman, S., 2009. Isolation of (+)-Catechin from *Acacia catechu* (Cutch tree) by a convenient method. J. Sci. Res. 2, 300–305.

Ibrahim, M., Ambreen, S., Hussain, A., Hussan, N., Imran, M., Ali, B., Sumrra, S.H., Yousuf, M., Rehmani, F.S., 2014. Phytochemical Investigation on *Eucalyptus globulus* Labill. Asian J. Chem. 26, 1011–1014.

Ishimaru, K., Nonaka, G., Nishioka, I., 1987. Flavan-3-ol and procyanidin glycosides from *Quercus miyagii*. Phytochemistry 26, 1167–1170.

Isman, B.M., 2006. Botanical Insecticides, Deterrents, and Repellents in Modern Agriculture and An Increasing Regulated World. Annu. Rev. Entomol. 51, 45–66.

Isman, M.B., 1997. Neem and other botanical insecticides: barriers to commercialization. Phytoparasitica 25, 339–344.

Iwu, M.M., 2014. Handbook of African Medicinal Plants, 2 edition. ed. CRC Press, NW, USA.

James, C.S., 1998. Analytical Chemistry of Foods. Chapman and Hall, London.

Jie, M.S., Mustafa, J., 1997. High-resolution nuclear magnetic resonance spectroscopy--applications to fatty acids and triacylglycerols. Lipids 32, 1019–1034.

Johnson, S., Morgan, E.D., 1997. Comparison of chromatographic systems for triterpenoids from Neem (*Azadirachta indica*) seeds. J. Chromatogr. A. 761, 53–63.

Kamboj, V.P., 2000. Herbal medicine. Curr. Sci. 78, 35–39.

Kang, W., Wang, J., Cao, N., 2012. Inhibitory activity of *Euphorbia humifusa* for alpha glucosidase in vitro and in vivo. Chem. Nat. Compd. 48, 886–888.

Katekhaye, S.D., Kale, M.S., Laddha, K.S., 2012. A simple and improved method for isolation of karanjin from *Pongamia pinnata* Linn. seed oil. Indian J. Nat. Prod. Resour. 1, 131–134.

Khallouki, F., Haubner, R., Hull, E.W., Erben, G., Spiegelhalder, B., Bartsch, H., Owen, W.R., 2007. Isolation, purification and identification of ellagic acid derivatives, catechins, and procyanidins from the root bark of *Anisophyllea dichostyla* R. Br. Food Chem. Toxicol. 45, 472–485.

Khumalo, L.W., Majoko, L., Read, J.S., Ncube, I., 2002. Characterisation of some underutilised vegetable oils and their evaluation as starting materials for lipase-catalysed production of cocoa butter equivalents. Ind. Crops Prod. 16, 237–244.

Kim, S.M., Kang, K., Jho, E.H., Jung, Y.J., Nho, C.W., Um, B.H., Pan, C.H., 2011. Hepatoprotective effect of flavonoid glycosides from *Lespedeza cuneata* against oxidative stress induced by tert-butyl hyperoxide. Phyther. Res. 25, 1011–1017.

Kingston, D.G.I., 2000. Recent Advances in the Chemistry of Taxol. J. Nat. Prod. 63, 726–734.

Koes, R.E., Quattrocchio, F., Joseph, N.M.M., 1994a. The flavonoids biosynthetic pathway in plants: Function and Evolution. BioEssays 16, 123–132.

Koes, R.E., Quattrocchio, F., Mol, J.N.M., 1994b. The flavonoid biosynthetic pathway in plants: Function and evolution. BioEssays 16, 123–132.

Koes, R.E., Van Blokland, R., Quattrocchio, F., Van Tumen, A.J., Mol, J.N.M., 1990. Chalcone synthase promoters in petunia are active in pigmented and unpigmented cell types. Plant Cell 2, 379–392.

Kolaczkowski, M., Kolaczkowska, A., Środa, K., Ramalhete, C., Michalak, K., Mulhovo, S., Ferreira, M.J.U., 2010. Substrates and modulators of the multidrug transporter Cdr1p of *Candida albicans* in antifungal extracts of medicinal plants. Mycoses 53, 305–310.

Komane, B.M., Olivier, E.I., Viljoen, A.M., 2011. *Trichilia emetica* (Meliaceae) - A review of traditional uses, biological activities and phytochemistry. Phytochem. Lett. 4, 1–9.

Kondo, T., Yoshida, K., Nakagawa, A., Kawai, T., Hirotoshi, T., Goto, T., 1992. Structural basis of blue color development in flower petals of *Commelina communis*. Nature 358, 515–518.

Kraus, W., 2002. Azadirachntin and other triterpenoids. In: Schmutterer H (ed) *Azadirachta indica* A Juss and Meliaceous plants: sources of unique natural products for integrated pest management, medicine, industry and other purposes, 2nd edn. Neem Foundation, Mumba.

Kraus, W., Cramer, R., Sawitzki, G., 1981. Tetranortriterpenoids from the seeds of *Azadirachta indica*. Phytochemistry 20, 117–120.

Kumar, C.S.S., Srinivas, M., Yakkundi, S., 1996. Limonoids from the seeds of *Azadirachta indica*. Phytochemistry 43, 451–455.

Kumar, D., Poornima, M., Kushwaha, R.N., Won, T.-J., Ahn, C., Ganesh Kumar, C., Jang, K., Shin, D.-S., 2015. Antimicrobial and docking studies of (−)-catechin derivatives. J. Korean Soc. Appl. Biol. Chem. 58, 581–585.

Kumar, S.S.A., Bose, C.S.K., Kumar, P.S.T.V.K., Raghavan, S., Murali, M.P., 2014. Terpenoids and Its Commercial Utility from Neem: The Nature's Own Pharmacy. Asian J. Chem. 26, 4940–4948.

Kwom, D.-J., Bae, Y.-S., 2011. Chemical constituents from the stem bark of *Acer barbinerve*. Chem. Nat. Compd. 47, 636–638.

Lanigan, R., Yamarik, T., 2002. Final report on the safety assessment of BHT (1). Int. J. Toxicol. 21, 19–94.

Lee, Y.R., Morehead, A.T., 1995. A new route for the synthesis of furanoflavone and furanochalcone natural products. Tetrahedron 51, 4909–4922.

Ley, S.V., Denholm, A.A., Wood, A., 1993. The chemistry of Azadirachtin.

Li, L., Li, X., Shi, C., Deng, Z., Fu, H., Proksch, P., Lin, W., 2006. Pongamone A–E, five flavonoids from the stems of a mangrove plant, *Pongamia pinnata*. Phytochemistry 67, 1347–1352.

Lie Ken Jie, M.S.., Lam, C.., 1995. 13C-NMR studies of polyunsaturated triacylglycerols of type AAA and mixed triacylglycerols containing saturated, acetylenic and ethylenic acyl groups. Chem. Phys. Lipids 78, 1–13.

Lin, H.Y., Kuo, Y.H., Lin, Y.L., Chiang, W., 2009. Antioxidative effect and active components from leaves of lotus (*Nelumbo nucifera*). J. Agric. Food Chem. 57, 6623–6629.

Loudon, I., 2002. Western Medicine: An Illustrated History. Oxford University Press.

Magalhaes, A.F., Tozzi, A.M.A., Magalhaes, E.G., Nogueira, M.A., Queiroz, S.C.N., 2000. Flavonoids from *Lonchocarpus latifolius* root. Phytochemistry 55, 787–792.

Mannina, L., Luchinat, C., Emanuele, M.C., Segre, A., 1999. Acyl positional distribution of glycerol tri-esters in vegetable oils: A 13C NMR study. Chem. Phys. Lipids 103, 47–55.

Mannina, L., Luchinat, C., Patumi, M., Emanuele, M.C., Rossi, E., Segre, A., 2000. Concentration dependence of 13C NMR spectra of triglycerides: implications for the NMR analysis of olive oils. Magn. Reson. Chem. 38, 886–890.

Mariod, A., Matthäus, B., Eichner, K., 2004. Fatty acid, tocopherol and sterol composition as well as oxidative stability of three unusual sudanese oils. J. Food Lipids 11, 179–189.

Mariod, A.A., Elkheir, S., Ahmed, Y.M., Matthäus, B., 2010. *Annona squamosa* and *Catunaregam nilotica* Seeds, the effect of the extraction method on the oil composition. JAOCS, J. Am. Oil Chem. Soc. 87, 763–769.

Marshall, S., 2004. Myrrh: Magic, medicine and mortality. Pharm. J. 273, 919–920.

Martin, C., Gerats, T., 1993. The control of pigment biosynthesis during petal development. Plant Cell 5, 1253–1264.

Mashungwa, G.N., Mmolotsi, R.M., 2007. *Trichilia emetica* Vahl. PROTA (Plant Resources of Tropical Africa/Resources vegetales d l' Afrique tropicale). [WWW Document]. http://www.prota4u.org/search.asp.

Mason, J.S., Morize, I., Menard, P.R., Cheney, D.L., Hulme, C., Labaudiniere, R.F., 1999. New 4-point pharmacophore method for molecular similarity and diversity applications: overview of the method and application, including a novel approach to the design of combinatorial libraries containing privileged substructures. J. Med. Chem. 42, 3251–3264.

Matu, E.M., van Staden, J., 2003. Antibacterial and anti-inflammatory activities of some plants used for medicinal purposes in Kenya. J. Ethnopharmacol. 87, 35–41.

Mazumdar, P., Borugadda, V.B., Goud, V. V., Sahoo, L., 2012. Physico-chemical characteristics of *Jatropha curcas* L. of North East India for exploration of biodiesel. Biomass and Bioenergy 46, 546–554.

Mbafor, J.T., ATCHADE, A.T., NKENGFACK, A.E., FOMUM, Z.T., STERNER, O., 1995. Furanoflavones from root bark of *Millettia sanagana*. Phytochemistry 40, 949–952.

McGaw, L.J., Jager, A.K., van Staden, J., 1997. Prostaglandin synthesis inhibitory activity in Zulu, Xhosa and Sotho medicinal plants. J. Phytother. Res. 11, 113–117.

McLerffaty, W.F., 1959. Mass spectrometric analysis, molecular rearrangements. Anal. Chem. 31, 82–87.

Merken, H.M., Beecher, G.R., 2000. Measurement of food flavonoids by high-performance liquid chromatography: a review. J. Agric. Food Chem. 48, 577–599.

Meshnick, R.S., Dobson, J.M., 2001. Antimalarial chemotheray. Springer US.

Mikolajczak, K.L., Reed, D.K., 1987. Extractives of seeds of the Meliaceae: Effect on *Spodoptera frugiperda* (J.E. Smith), *Acalymma vittatum* (F) and *Artemia salina* Leach. J. Chem. Ecol. 13, 99–111.

Mikolajczak, K.L., Zilkowski, B.W., Bartelt, R.J., 1989. Effects of meliaceous seed extracts on growth and survival of *Spodoptera frugiperda* (J.E. Smith). J. Chem. Ecol. 15, 121–128.

Miller, L.H., Su, X., 2011. Artemisinin: Discovery from the Chinese Herbal Garden. Cell 146, 855–858.

Minakawa, T., Toume, K., Ahmed, F., Sadhu, K.S., Ohtsuki, T., Arai, A.M., Ishibashi, M., 2010. Constituents of *Pongamia pinnata* isolated in a screening for activity to overcome tumor necrosis factor-related apoptosis-inducing ligand resistance. Chem. Pharm. Bull 11, 1549–1551.

Miziorko, H., 2011. Enzymes of the mevalonate pathway of isoprenoid biosynthesis. Arch Biochem Biophys 505, 131–143.

Mo, Y., Nagel, C., Taylor, L.P., 1992. Biochemical complementation of chalcone synthase mutants defines a role for flavonols in functional pollen. Proc Natl Acad Sci USA 89, 7213–7217.

Monga, J., Aggarwal, V., Suthar, S.K., Monika, M., Nongalleima, K., Sharma, M., 2014. Topical (+)-catechin emulsified gel prevents DMBA/TPA-induced squamous cell carcinoma of the skin by modulating antioxidants and inflammatory biomarkers in BALB/c mice. Food Funct. 5, 3197–3207.

Monitto, P., 1981. Biosynthesis of natural products. Ellis Harwood Limited, John Willey and Sons, New York.

Mordue, J.A., Nisbet, J.A., 2000. Azadirachtin from the neem tree *Azadirachta indica*: its action against insects. An. Soc. Entomol. Bras. 4, 615–632.

Mori, A., Nishino, C., Enoki, N., Tawata, S., 1987. Antibacterial activity and mode of action of plant flavonoids against *Proteus vulgaris* and *Staphylococcus aureus*. Phytochemistry 26, 2231–2234.

Moyo, F., Gashe, B. a., Majinda, R.R.T., 1999. A new flavan from *Elephantorrhiza goetzei*. Fitoterapia 70, 412–416.

Mukerjee, S.K., Sarkar, S.C., Seshadri, T.R., 1969. The structure and synthesis of pongachrome, a new component of *Pongamia glabra*. Tetrahedron 23, 1063–1069.

Muller, J.L., 1998. "Love portions and the ointment of witches: historical aspects of the nightshade alkaloids." J. Toxicol. Clin Toxicol, 6, 617–627.

Nakatani, M., James, J.C., Nakanishi, K., 1985. Structure of Limonoid Antifeedant from *Trichilia roka*. Phytochemistry 24, 195–196.

Nakatani, M., James, J.C., Nakanishi, K., 1981. Isolation and structures of Trichilins, Antifeedants against the Southern Army Worms. J. Am. Chem. Soc. 103, 1228–1230.

Narasimhan, S., Mohankumar, R., Santhanakrishnan, V.P., Radhakrishnan, V., 2011. Acid Catalysed Isomerization of Nimbin to Isonimbin. Am. J. Org. Chem. 1, 6–9.

Ndamba, J., Nyazema, N., Makaza, N., Anderson, C., Kaondera, K.C., 1994. Traditional herbal remedies used for the treatment of urinary schistosomiasis in Zimbabwe. J. Ethnopharmacol. 42, 125–132.

Newman, D.J., 2008. Natural products as leads to potential drugs: An old process or the new hope for drug discovery? J. Med. Chem. 51, 2589–2599.

Newman, D.J., Cragg, G.M., 2012. Natural Products As Sources of New Drugs over the 30 Years from 1981 to 2010. J. Nat. Prod. 75, 311–335.

Ng, S., Gee, P.T., 2001. Determination of iodine value of palm and palmkernel oil by carbon-13 nuclear magnetic resonance spectroscopy. Eur J Lipid Sci Technol 103, 223–227.

Ngassapa, F., Othman, O., 2001. Physicochemical characteristics of some locally manufactured edible vegetable oils marketed in Dar es Salaam. Tanzania J. Sci. 27.

Nyam, K.L., Tan, C.P., Lai, O.M., Long, K., Che Man, Y.B., 2009. Physicochemical properties and bioactive compounds of selected seed oils. LWT - Food Sci. Technol. 42, 1396–1403.

Nyila, M.A., Leonard, C.M., Hussein, A.A., Lall, N., 2012. Activity of South African medicinal plants against Listeria monocytogenes biofilms, and isolation of active compounds from *Acacia karroo*. South African J. Bot. 78, 220–227.

O'Neill, T.M., Mansfiel, J.W., 1982. Antifungal activity of hydroxyflavans and other flavonoids. Trans. Br. mycol. Soc. 79, 229–237.

Ogbobe, O., 1992. *Sclerocarya birrea*. Plant Foods Hum. Nutr. 201–206.

Oh, M.H., Park, K.H., Kim, M.H., Kim, H.H., Park, K.J., Heo, J.H., Lee, M.W., 2014. Anti-oxidative and anti-inflammatory effects of phenolic compounds from the stems of Quercus acuta Thunberg. Asian J. Chem. 26, 4582–4586.

Olsen, H.T., Stafford, G.I., van Staden, J., Christensen, S.B., Jäger, A.K., 2008. Isolation of the MAO-inhibitor naringenin from *Mentha aquatica* L. J. Ethnopharmacol. 117, 500–502.

Orwa, C., Mutua, A., Kindt, R., J., R., Simons, A., 2009. *Trichilia emetica*. Agroforestree database: a tree reference and selection guide version 4.0. Available at http://www.worldagroforestry.org/af/treedb/. [WWW Document].

Palmer, E., Pitman, N., 1972. Trees of Southern Africa. New Holland Publishers, Cape Town.

Pennington, P.D., Styles, B.T., 1975. A generic monograph of the Meliaceae. Blumea 22, 419–540.

Perkins, E.G., 1992. Effect of lipid oxidation on oil and food quality in deep frying: Angelo AJS (ed) Lipid oxidation in food. Am. Chem. Soc. ACS Sympos, 310–321.

Pfeiffer, J., Kühnel, C., Brandt, J., Duy, D., Punyasiri, P.A.N., Forkmann, G., Fischer, T.C., 2006. Biosynthesis of flavan 3-ols by leucoanthocyanidin 4-reductases and anthocyanidin reductases in leaves of grape (*Vitis vinifera* L.), apple (*Malus x domestica* Borkh.) and other crops. Plant Physiol. Biochem. 44, 323–334.

Pietta, P.G., 2000. Flavonoids as antioxidants. J. Nat. Prod. 63, 1035–1042.

Piironen, V., Lindsay, G.D., Miettinen, A.T., Toivo, J., Lampi, A.M., 2000. Review: biosynthesis, biological function and their importance to human nutrition. J. Sci. Food Agric. 80, 939–966.

Pizzolatti, M.G., Venson, A.F., Smânia Júnior, A., Smânia, E.D.F. a, Braz-Filho, R., 2002. Two epimeric flavalignans from *Trichilia catigua* (Meliaceae) with antimicrobial activity. Zeitschrift fur Naturforsch. - Sect. C J. Biosci. 57, 483–488.

Pliev, T.N., 1970. NMR spectra of alkyl phenols. Zhurnal Prikl. Spektrosk. 13, 124–141.

Puupponen-Pimia, R., Nohynek, L., Meier, C., Kahkonen, M., Heinonen, M., Hopia, A., Oksman-Caldentey, K.M., 2001. Antimicrobial properties of phenolic compounds from berries. J. Appl. Microbiol. 90, 494–507.

Raab, T., Barron, D., Arce Vera, F., Crespy, V., Oliveira, M., Williamson, G., 2010. Catechin Glucosides: Occurrence, synthesis, and stability. J. Agric. Food Chem. 58, 2138–2149.

Ranga Rao, R., Tiwari, A.K., Prabhakar Reddy, P., Suresh Babu, K., Ali, A.Z., Madhusudana, K., Madhusudana Rao, J., 2009. New furanoflavanoids, intestinal α-glucosidase inhibitory and free-radical (DPPH) scavenging, activity from antihyperglycemic root extract of *Derris indica* (Lam.). Bioorg. Med. Chem. 17, 5170–5175.

Rauha, J.P., Remes, S., Heinonen, M., Hopia, A., Kähkönen, M., Kujala, T., Pihlaja, K., Vuorela, H., Vuorela, P., 2000. Antimicrobial effects of Finnish plant extracts containing flavonoids and other phenolic compounds. Int. J. Food Microbiol. 56, 3–12.

Ryan, K.G., Swinny, E.E., Markham, K.R., Winefield, C., 2002. Flavonoid gene expression and UV photoprotection in transgenic and mutant Petunia leaves. Phytochemistry 59, 23–32.

Ryan, K.G., Swinny, E.E., Winefield, C., Markham, K.R., 2001. Flavonoid and uv photoprotection in Arabidopsis mutants. Z Naturforsch 56c, 745–754.

Sacchi, R., Patumi, M., Fontanazza, G., Barone, P., Fiordiponti, P., Mannina, L., Rossi, E., Segre, A.L., 1996. A high-field 1H nuclear magnetic resonance study of the minor components in virgin olive oils. JAOCS, J. Am. Oil Chem. Soc. 23, 747–758.

Saka, J.D.., Msonthi, J.D., 1994. Nutritional value of edible fruits of indigenous wild trees in Malawi. For. Ecol. Manage. 64, 245–248.

Schlaman, H.R.M., Okker, R.J.H., Lugtenberg, B.J.J., 1992. Regulation of modulation gene expression by NodD in Rhizobia. J. Bacteriol 174, 5177–5182.

Schmutterer, H., 1990. Properties and potential of natural pesticides from the neem tree, *Azadiracta indica*. Annu. Rev. Entomol. 35, 271–97.

Seeram, N., Nair, M., 2002. Inhibition of lipid peroxidation and structure-activity related studies of the dietary constituents anthocyanins, anthocyanidins, and catechins. J. Agric. Food Chem. 50, 5308–5312.

Sen, A., Dhavan, P., Shukla, K.K., Singh, S., Tejovathi, G., 2012. Analysis of IR , NMR and Antimicrobial Activity of β-Sitosterol Isolated from *Momordica charantia*. Sci. Secur. J. Biotechnol. 1, 9–13.

Seto, R., Nakamura, H., Nanjo, F., Hara, Y., 1997. Preparation of epimers of tea catechins by heat treatment. Biosci. Biotech. Biochem. 9, 1434–1439.

Shai, L.J., McGaw, L.J., Masoko, P., Eloff, J.N., 2008. Antifungal and antibacterial activity of seven traditionally used South African plant species active against *Candida albicans*. South African J. Bot. 74, 677–684.

Shen, D., Wu, Q., Wang, M., Yang, Y., Lavoie, E.J., Simon, J.E., 2006. Determination of the Predominant Catechins in *Acacia catechu* by Liquid Chromatography/Electrospray Ionization−Mass Spectrometry. J. Agric. Food Chem. 54, 3219–3224.

Shirley, W.B., 2002. Biosynthesis of flavonoids and effects of stress. Curr. Opin. Plant Biol. 5, 218–223.

Si, W., Gong, J., Tsao, R., Kalab, M., Yin, Y., 2006. Bioassay-guided purification and identification of antimicrobial components in Chinese green tea extract. J. Chromatogr. 1125, 204–210.

Silva, T.C.J., Jham, N.G., Oliveira, D.R., Brown, L., 2007. Purification of the seven tetranortriterpenoids in neem (*Azadirachta indica*) seed by counter-current chromatography sequentioally followed by isocratic preparative reversed-phase high performance liquid chromatography. J. Chromatogr. A. 1151, 203–210.

Simova, S., Ivanova, G., Spassov, S.L., 2003. Alternative NMR method for quantitative determination of acyl positional distribution in triacylglycerols and related compounds. Chem. Phys. Lipids 126, 167–176.

Sindiga, I., 1994. Indigenous (medical) Knowledge of the Maasai. Indigenous Knowledge and Development Monitor. Indig. Knowl. Dev. Monit. 2, 16–18.

Solecki, R.S., 1975. Shanidar IV, a Neanderthal Flower Burial in Northern Iraq. Science (80-.). 190, 880–881.

Sparg, S.G., van Staden, J., Jager, A.K., 2000. Efficiency of traditionally used South Africa plants against schistosomiasis. J. Ethnopharmacol. 73, 209–214.

Spribille, R., Forkmann, G., 1982. Chalcone synthesis and hydroxylation of flavonoids in 3'-position with enzyme preparations from flowers of *Dianthus caryophyllus* L. (carnation). Planta 155, 176–182.

Strack, D., 1997. Phenolic metabolism. In: Dey PM, Harborne JB, eds. Plant Biochemistry.

Sumner, J., 2000a. The Natural History of Medicinal Plants. Timber Press.

Sumner, J., 2000b. The Natural History of Medicinal Plants. Timber Press.

Sun, J., Jiang, Y., Wei, X., Shi, J., You, Y., Liu, H., Kakuda, Y., Zhao, M., 2006. Identification of (-) - epicatechin as the direct substrare for polyphenol oxidase isolated from litchi pericarp. Food Rrsearch Int. 39, 864–870.

Takahama, U., Yamauchi, R., Hirota, S., 2013. Isolation and characterization of a cyanidin-catechin pigment from adzuki bean (*Vigna angularis*). Food Chem. 141, 282–288.

Tanaka, T., Iinuma, M., Yuki, K., Fujii, Y., Mizuno, M., 1992. Flavonoids in root bark of *Pongamia pinnata*. Phytochemistry 31, 993–998.

Tariq, M., Ali, S., Ahmad, F., Ahmad, M., Zafar, M., Khalid, N., Khan, M.A., 2011. Identification, FT-IR, NMR (1H and 13C) and GC/MS studies of fatty acid methyl esters in biodiesel from rocket seed oil. Fuel Process. Technol. 92, 336–341.

Tasdemir, D., Kaiser, M., Brun, R., Yardley, V., Schmidt, T.J., Tosun, F., Ruedi, P., 2006. Antitrypanosomal and antileishmanial activities of flavonoids and their analogues: In vitro, in vivo, structure-activity relationship, and quantitative structure-activity relationship studies. Antimicrob. Agents Chemother. 50, 1352–1364.

Thacker, J.M.R., 2002. An Introduction to Arthropod Pest Control. Cambridge Univ. Press., Cambridge, UK.

Thoss, V., Murphy, P.J., Marriott, R., Wilson, T., 2012. Triacylglycerol composition of British bluebell (*Hyacinthoides non-scripta*) seed oil. RSC Adv. 2, 5314.

Toda, M., Okubo, S., Hara, Y., Shimamura, T., 1991. Antibacterial and bactericidal activities of of tea extract and catechins against methicillin resistant *Staphylococcus aureus*. Japanese J. Bacteriol. 46, 839–845.

Traore, M., Zhai, L., Chen, M., Olsen, C.E., Odile, N., Pierre, G.I., Bosco, O.J., Robert, G.T., Christensen, S.B., 2007. Cytotoxic kurubasch aldehyde from *Trichilia emetica*. Nat. Prod. Res. 21, 13–17.

Tredgold, M.H., 1986. Food plants of Zimbabwe. Mambo, GWERU.

Tsuchiya, H., Sato, M., Miyazaki, T., Fujiwara, S., Tanigaki, S., Ohyama, M., Tanaka, T., Iinuma, M., 1996. Comparative study on the antibacterial activity of phytochemical flavanones against methicillin-resistant *Staphylococcus aureus*. J. Ethnopharmacol. 50, 27–34.

"Turmeric," 2012. (http://tamilnadu.com/herbs/turmeric.html) [WWW Document].

Van Acker, S.A.B.E., van den Berg, D.-J., Tromp, M.N.J.L., Griffioen, D.H., van Bennekom, W.P., van der Vijgh, W.J.F., 1996. Structural aspects of antioxidant activity of flavonoids. Free Radic. Biol. Med. 20, 331–342.

Van der Meer, I.M., Stam, M., Van Tumen, A.J., Mol, J.N.M., Stuitje, A.R., 1992. Antisense inhibition of flavonoidn biosynthesis in Petunia anthers result in male sterility. Plant Cell 4, 253–262.

Van der Vossen, H.A.., Mkamilo, G.S., 2007. Vegetable oils of tropical Africa, conclusion and recommendations based on PROTA 14: "Vegetable oils". Available on: PROTA (Plant Resources of Tropical Africa/Resources vegetales de I'Afrique tropicale), Wageningen, Netherlands http://www.prota.co.ke/en/p. PROTA.

Van Wyk, B., van Wyk, P., van Wyke, B.E., 2000. Photographic Guide to Trees of South Africa. Stuik Publishers, Pretoria.

Vermaak, I., Kamatou, G.P.P., Komane-Mofokeng, B., Viljoen, a. M., Beckett, K., 2011. African seed oils of commercial importance - Cosmetic applications. South African J. Bot. 77, 920–933.

Verschaeve, L., Van Staden, J., 2008. Mutagenic and antimutagenic properties of extracts from South African traditional medicinal plants. J. Ethnopharmacol. 119, 575–587.

Vismaya, Sapna Eipeson, W., Manjunatha, J.R., Srinivas, P., Sindhu Kanya, T.C., 2010. Extraction and recovery of karanjin: A value addition to karanja (*Pongamia pinnata*) seed oil. Ind. Crops Prod. 32, 118–122.

Vlahov, G., Kiprono Chepkwony, P., Ndalut, P.K., 2002. 13C NMR characterization of triacylglycerols of *Moringa oleifera* seed oil: An "oleic-vaccenic acid" oil. J. Agric. Food Chem. 50, 970–975.

Vlahov, G., Schiavone, C., Simone, N., 2001. Quantitative 13 C NMR method using the DEPT pulse sequence for the determination of the geographical origin (DOP) of olive oils 35, 689–695.

Vogt, T., Pollak, P., Tarlyn, N., Taylor, L., 1994. Pollination or wound induced kaempferol accumulation in *petunia stigmas* enhances seed production. Plant Cell 6, 11–23.

Waage, S.K., Hedin, P.A., 1985. Quercetin 3-O-galactocyl-(1->6)-glucoside, a compound from narrowleaf vetch with antibacterial activity. Phytochemistry 24, 243–245.

Wang, L., Li, X., Zhang, S., Lu, W., Liao, S., Liu, X., Shan, L., Shen, X., Jiang, H., Zhang, W., Huang, J., Li, H., 2012. Natural products as a gold mine for selective matrix metalloproteinases inhibitors. Bioorganic Med. Chem. 20, 4164–4171.

Wei, X.H., Yang, S.J., Liang, N., Hu, D.Y., Jin, L.H., Xue, W., Yang, S., 2013. Chemical constituents of *Caesalpinia decapetala* (Roth) alston. Molecules 18, 1325–1336.

Wheeler, A.D., Isman, M.B., Sanchez-Vindas, E.P., Arnason, J.T., 2001. Screening of Costa Rican *Trichilia* species for biological activity against the larvae of *Spodoptera litura* (Lepidoptera: Noctuidae). Biochem. Syst. Ecol. 29, 347–358.

Wiley, R.A., Rich, D.H., 1993. Peptidomimetics derived from natural products. Med. Res. Rev. 13, 327–3884.

Williamson, J., 1974. Useful plants of Malawi,. University of Malawi, Zomba.

Wink, M., 2003. Evolution of secondary metabolites from an ecological and molecular phylogenetic perspective. Phytochemistry 64, 3–19.

Wink, M., 1993. The plant vacuole: A multifunctional compartment. J. Exp. Bot. 44, 231–246.

Wink, M., 1988. Plant breeding: Importance of plants secondary metabolites for protection against pathogens and herbivores. Genet. Theor. Appl. 75, 225–233.

Wink, M., Mohamed, G.I.A., 2003. Evolution of chemical defense traits in the Leguminosae: mapping of distribution patterns of secondary metabolites on a molecular phylogeny inferred from nucleotide sequences of the rbcL gene. Biochem. Syst. Ecol. 31, 897–917.

Wu, J.-N., 2005. An Illustrated Chinese Materia Medica. Oxford University Press.

Wu, Q., Wang, M., Simon, J.E., 2003. Determination of proanthocyanidins in grape products by liquid chromatography/mass spectrometric detection under low collision energy. Anal. Chem. 75, 2440–2444.

Xie, Y.S., Isman, M.B., Gunning, P., Mackinnon, S., Arnason, J.T., Taylor, D.R., Sanchez, P., Hasbun, C., Towers, G.H.N., 1994. Biological activity of extracts of *Trichilia* species and the limonoids hirtin against lepidopteran larvae. Biochem. Syst. Ecol. 22, 129–136.

Xu, X., Xie, H., Hao, J., Jiang, Y., Wei, X., 2011. Flavonoid glycosides from the seeds of *litchi chinensis*. J. Agric. Food Chem. 59, 1205–1209.

Yadav, P.P., Ahmad, G., Maurya, R., 2004. Furanoflavonoids from *Pongamia pinnata* fruits. Phytochemistry 65, 439–443.

Yahaya, M.A.A., Yaacob, W.A., Nazlina, I., 2011. Isolation of chemical constituent from rhizomes of *Etlingera sphaerochala* Var. grandiflora. Malaysian J. Anal. Sci. 15, 22–26.

Yang, W.C., Canter Cremers, H.C.J., Hogendijk, P., Katinakis, P., Wijffelman, C.A., Franssen, H., Van Kammen, A., Bisseling, T., 1992. In situ localization of chalcone synthase mRNA in pea root nodule development. Plant Cell 2, 143–151.

Yao, H., Liao, Z., Wu, Q., Lei, G., Liu, Z., Chen, D., Chen, J., Zhou, T., 2006. Antioxidative flavanone glycosides from the branches and leaves of *Viscum coloratum*. Chem. Pharm. Bull 54, 133–135.

Yehye, W.A., Rahman, N.A., Ariffin, A., Abd Hamid, S.B., Alhadi, A.A., Kadir, F.A., Yaeghoobi, M., 2015. Understanding the chemistry behind the antioxidant activities of butylated hydroxytoluene (BHT): A review. Eur. J. Med. Chem. 101, 295–312.

APPENDICES

Appendix I: **Page number**

Appendix II:

APPENDIX 1

Infrared Spectrum of Compound AU 1

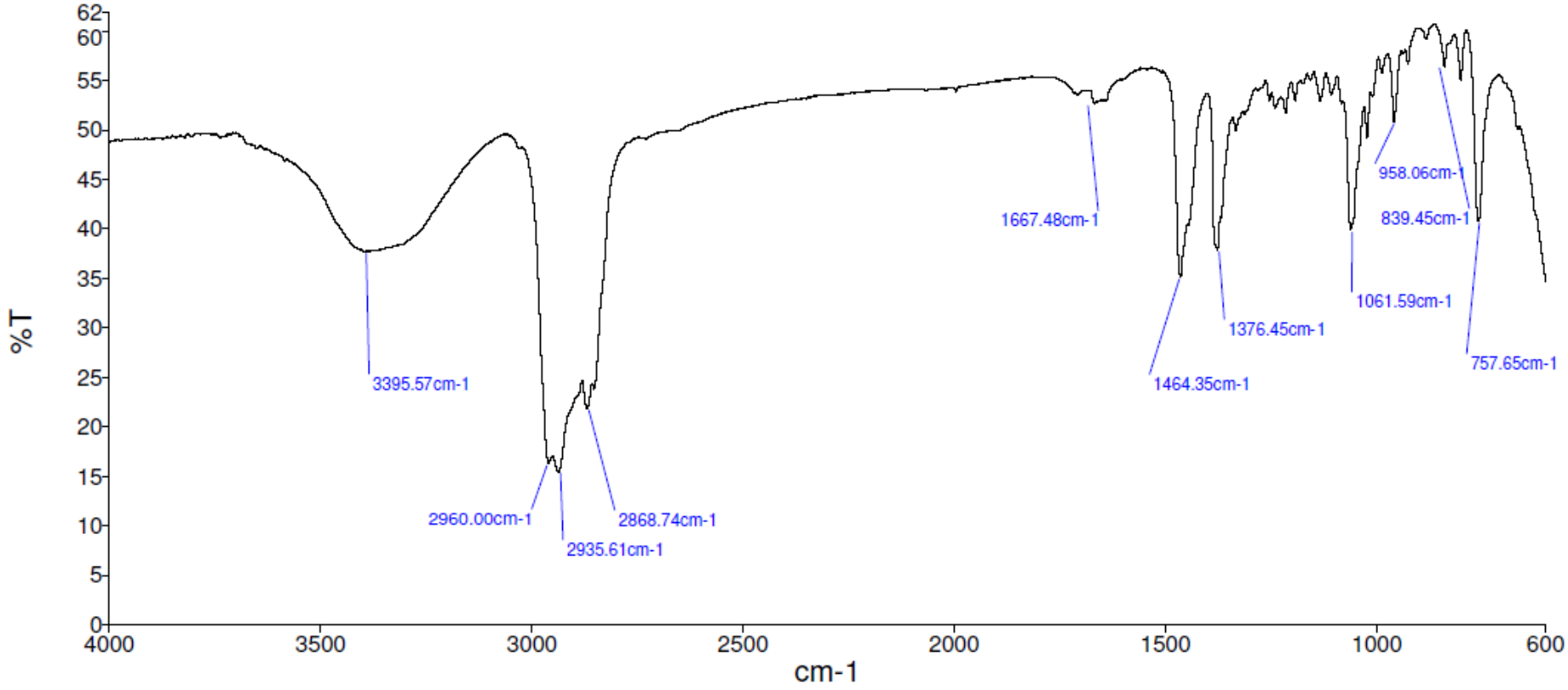

Infrared spectrum of Compound AU 2

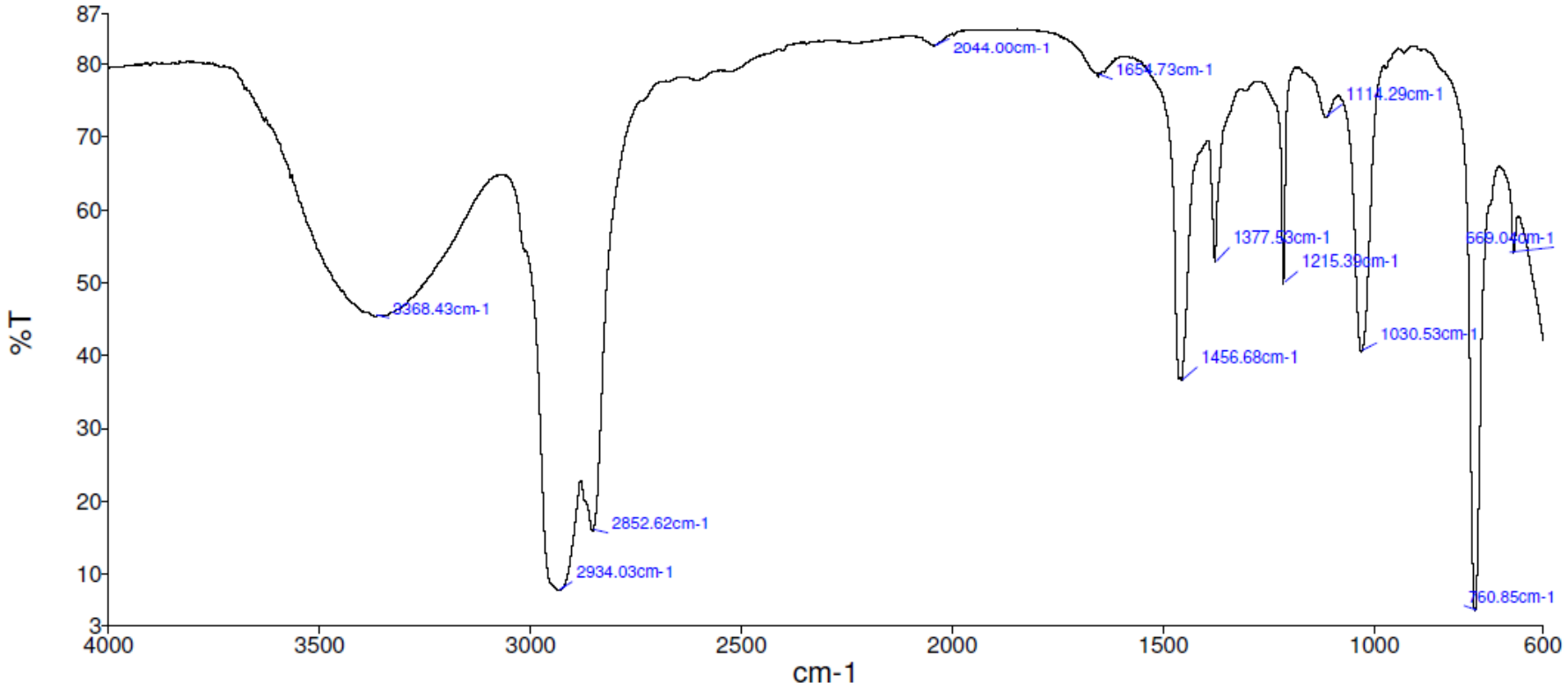

Infrared spectrum of Compound AU 3

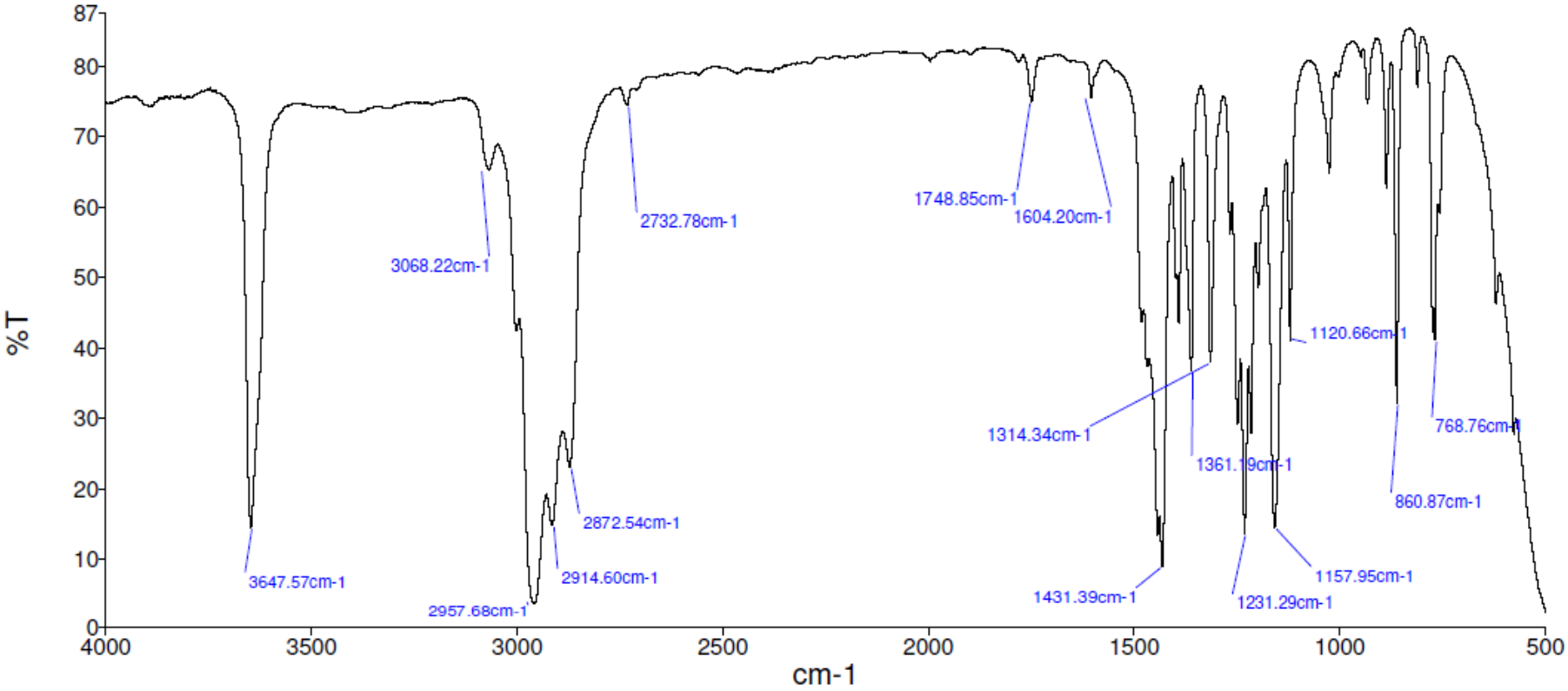

Infrared spectrum of Compound AU 4

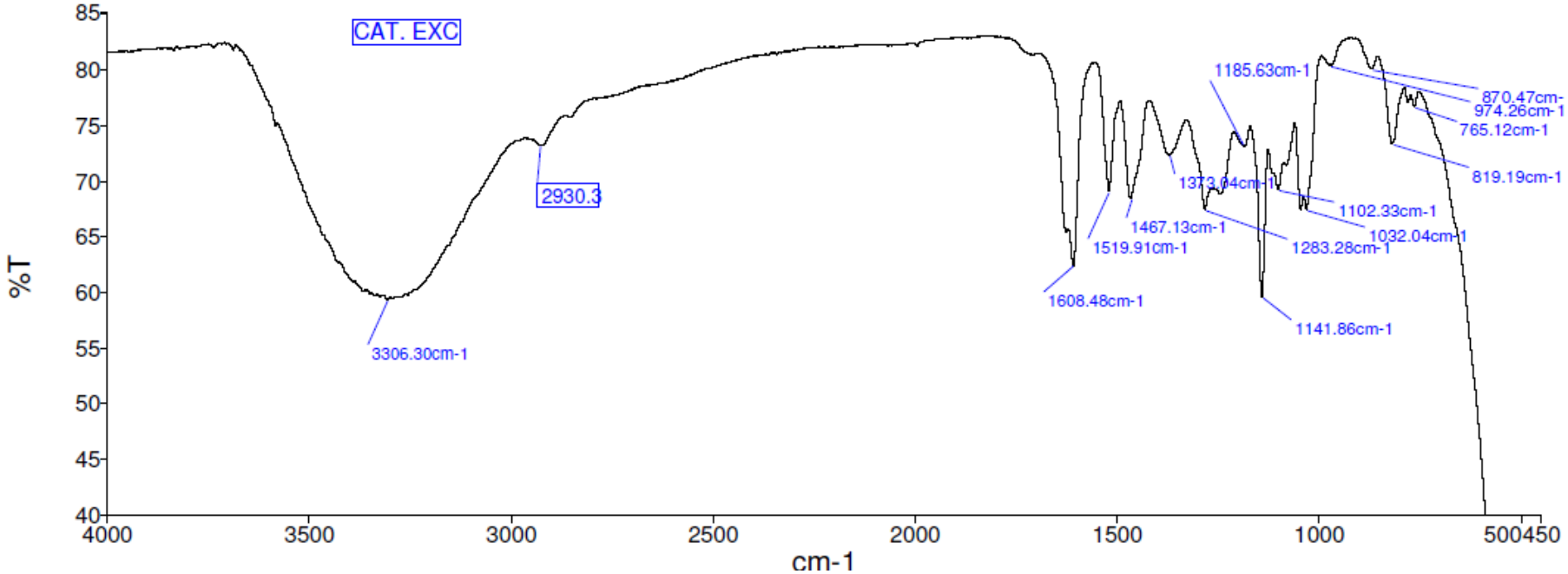

Infrared spectrum of Compound AU 5

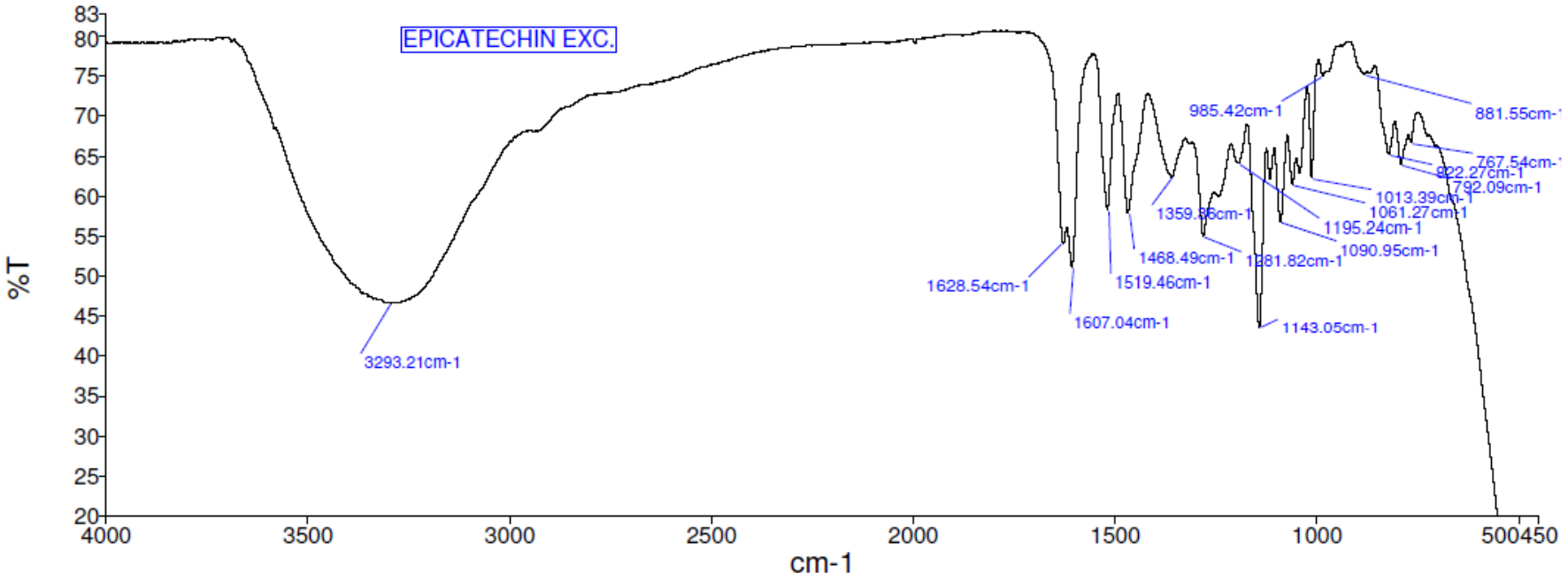

Infrared spectrum of Compound AU 6

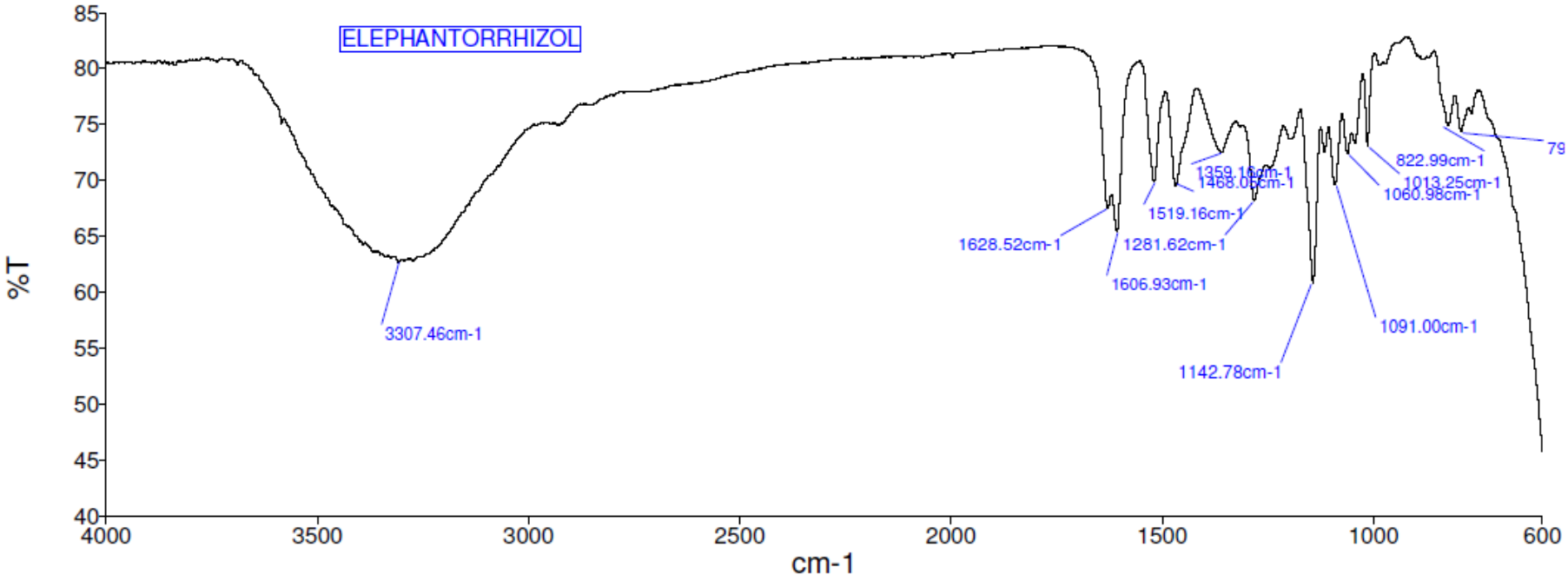

Infrared spectrum of Compound AU 7

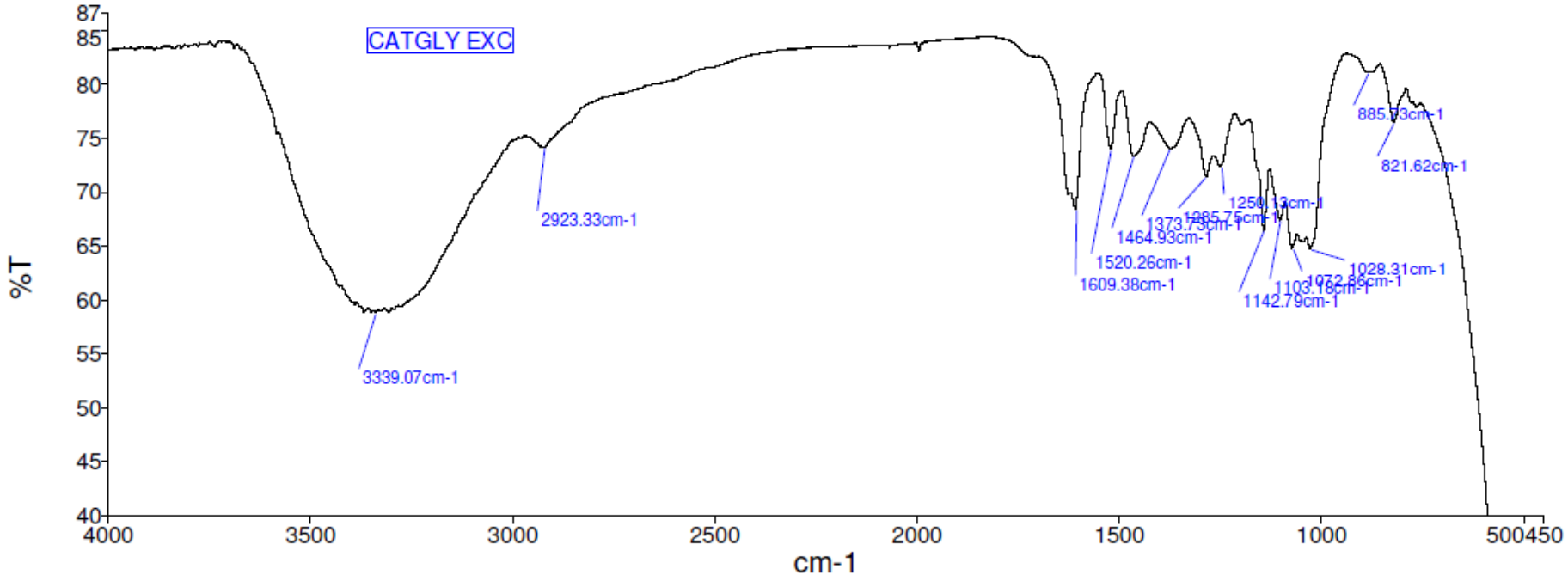

Infrared spectrum of Compound AU 8

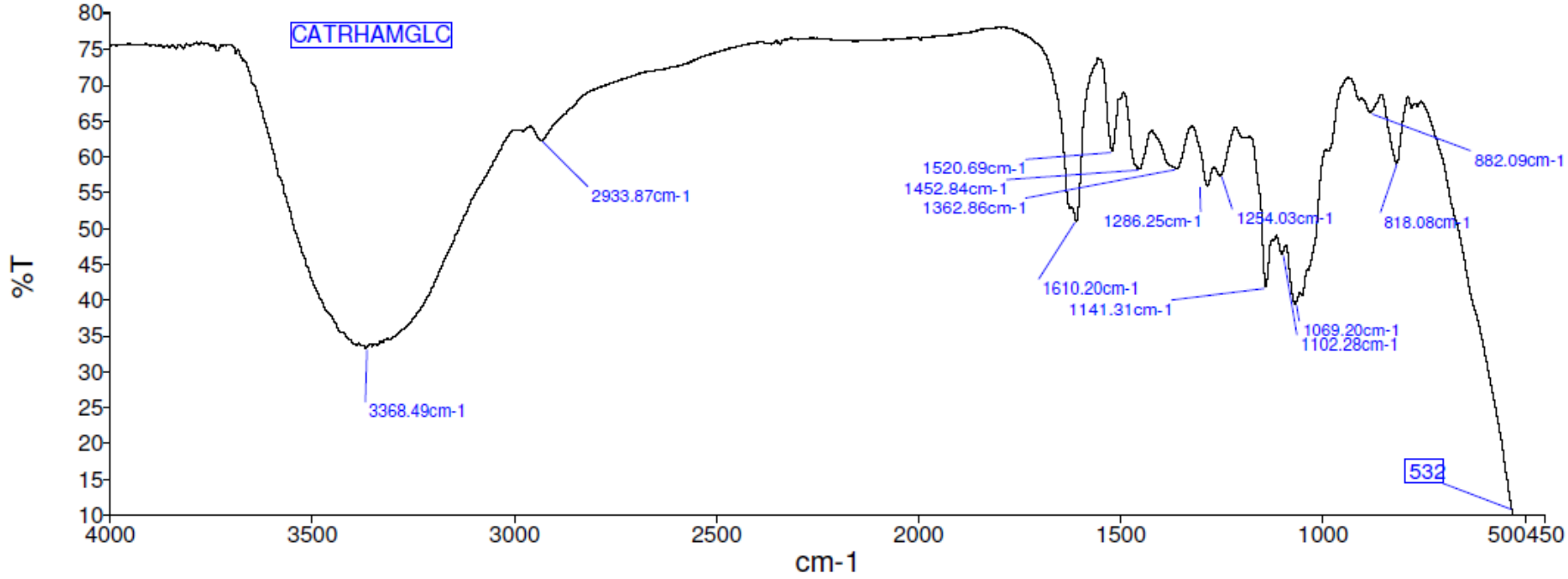

Infrared spectrum of Compound AU 9

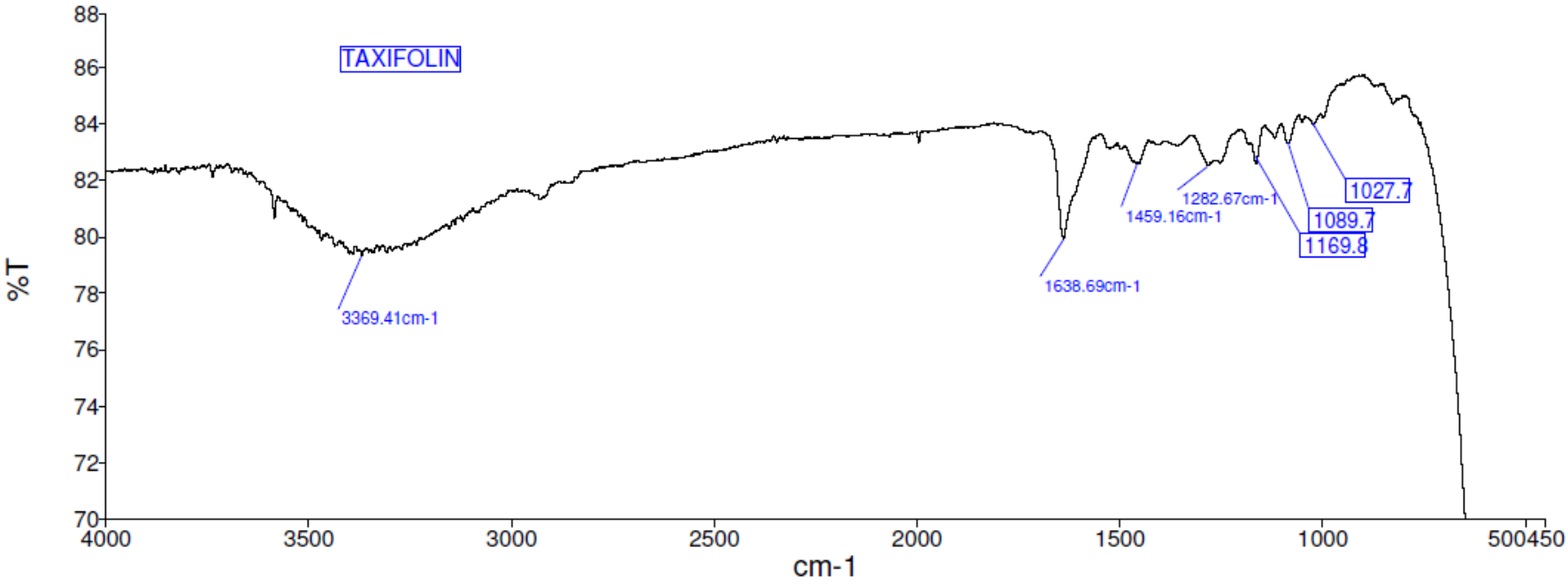

Infrared spectrum of Compound AU 10

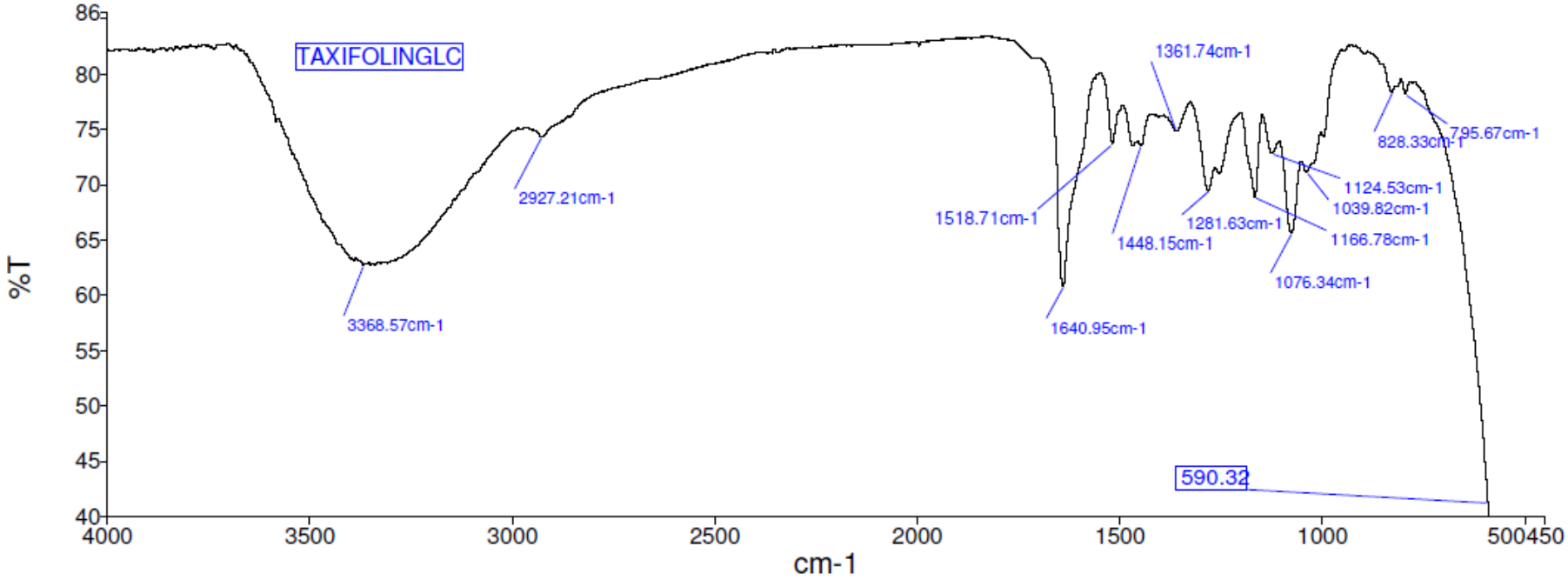

Infrared spectrum of Compound AU 11

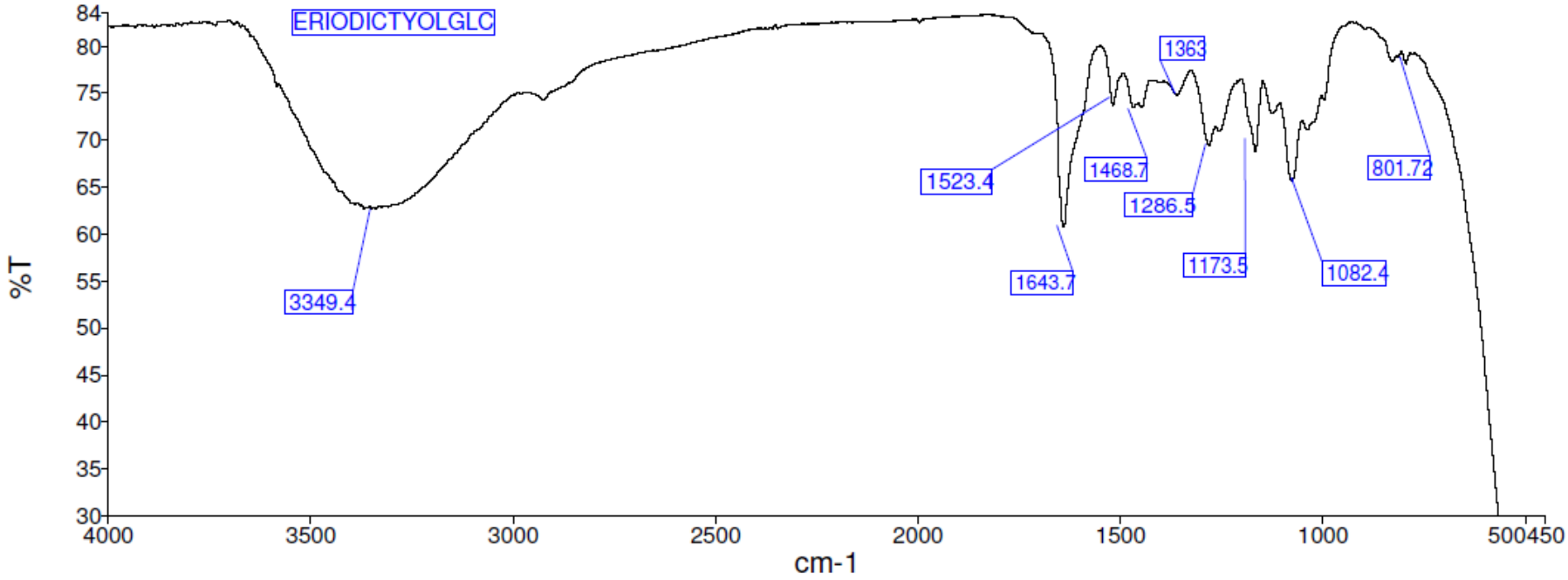

Infrared spectrum of Compound AU 12

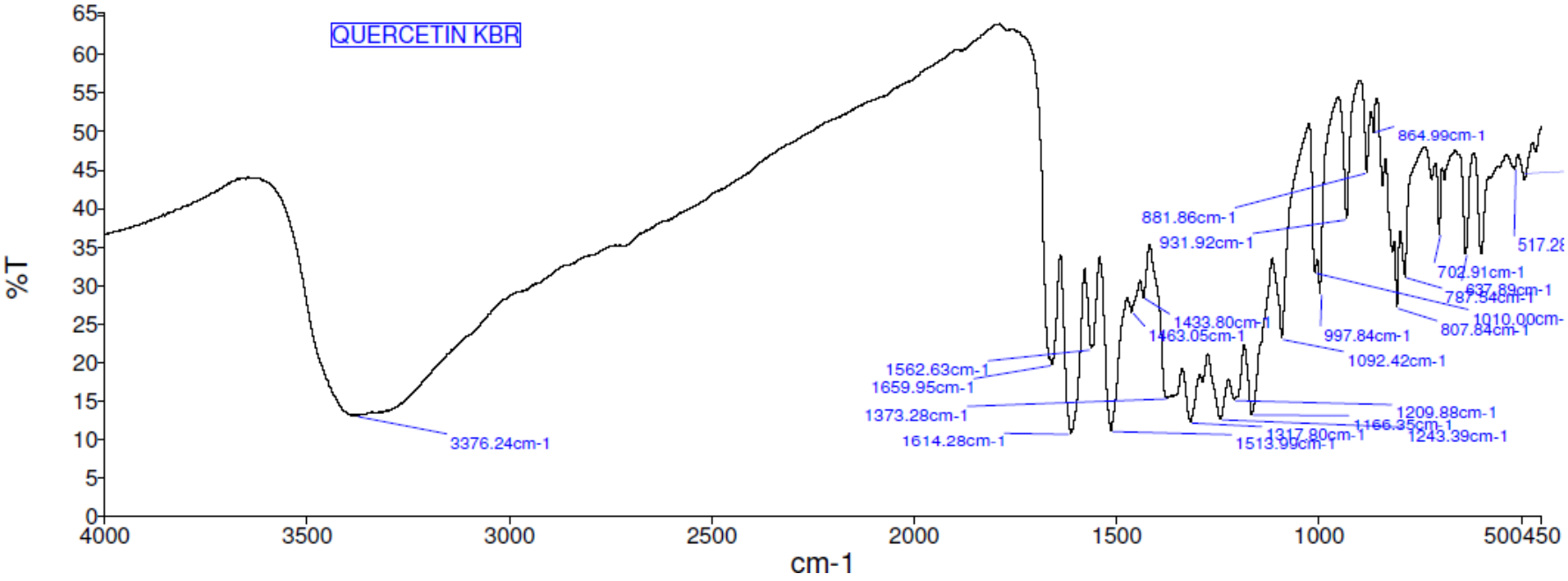

Infrared spectrum of Compound AU 13

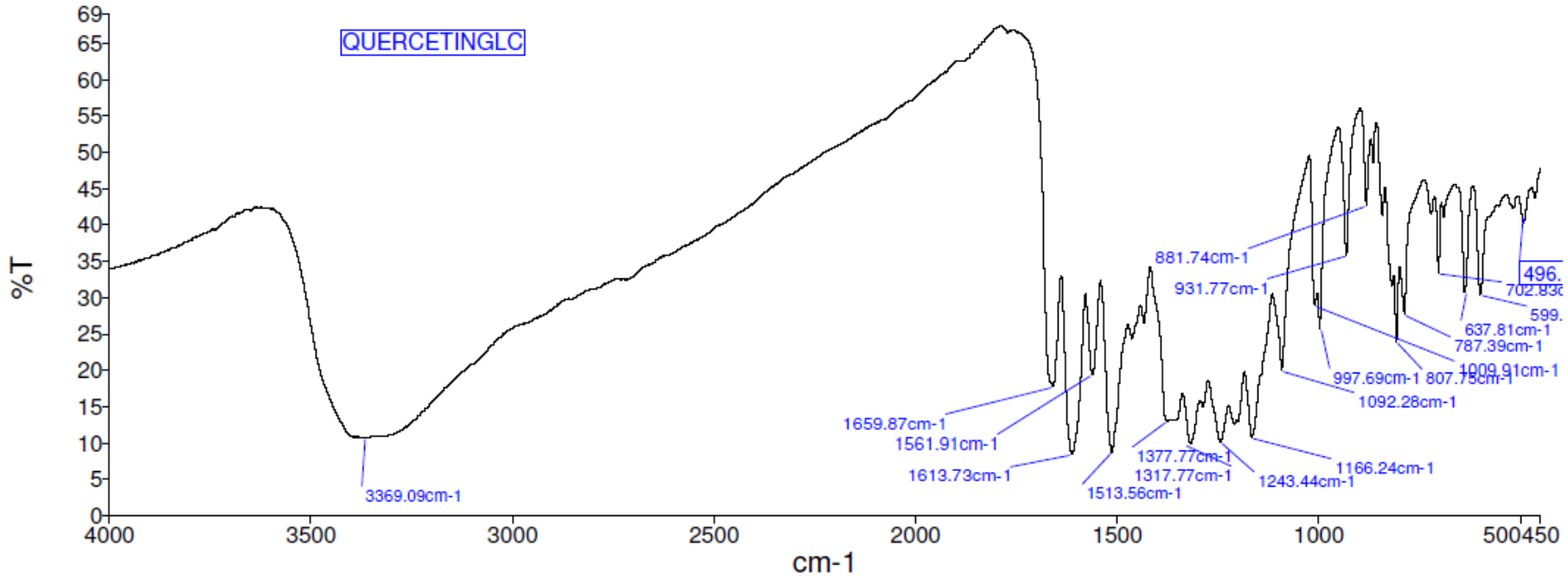

Infrared spectrum of Compound AU 14

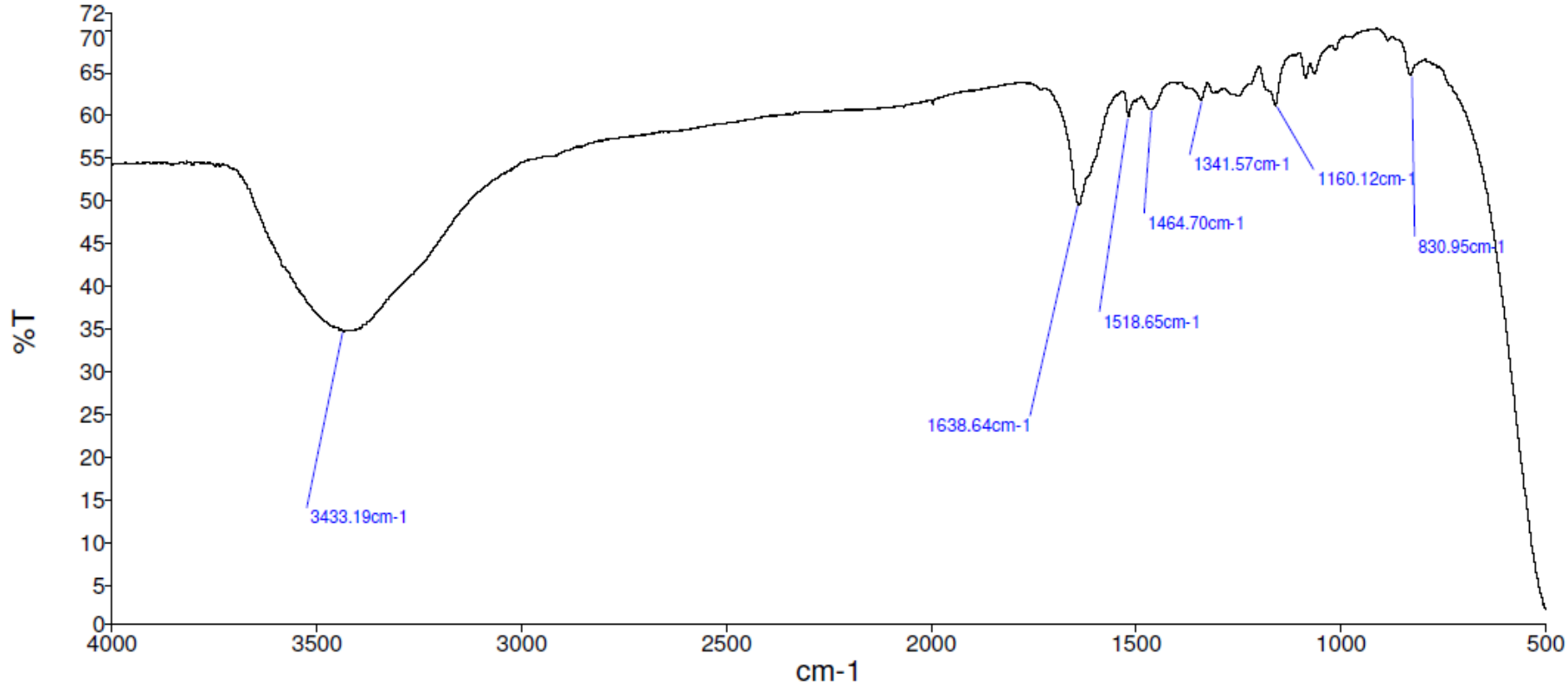

Infrared spectrum of Compound AU 15

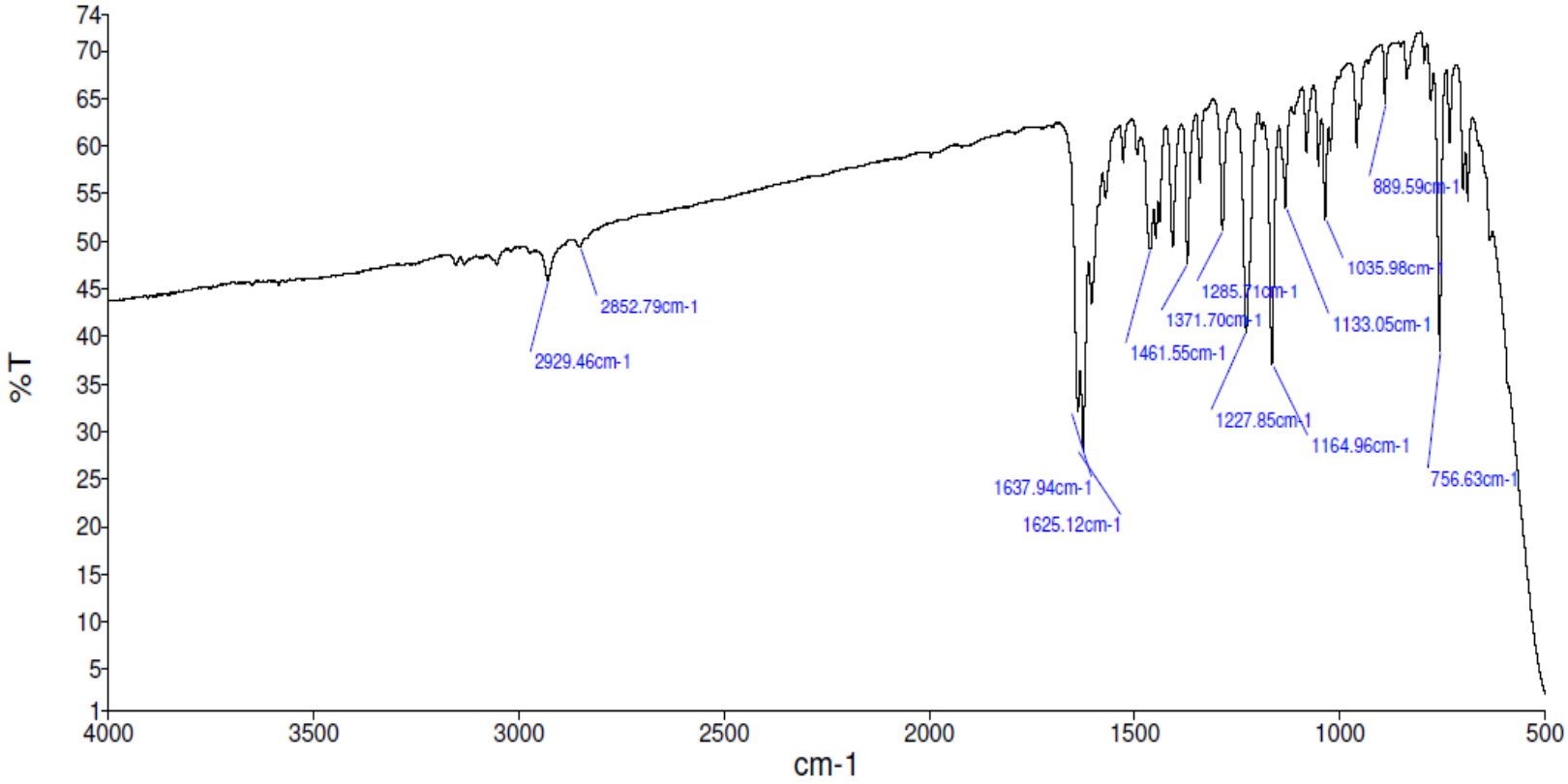

Infrared spectrum of Compound AU 16

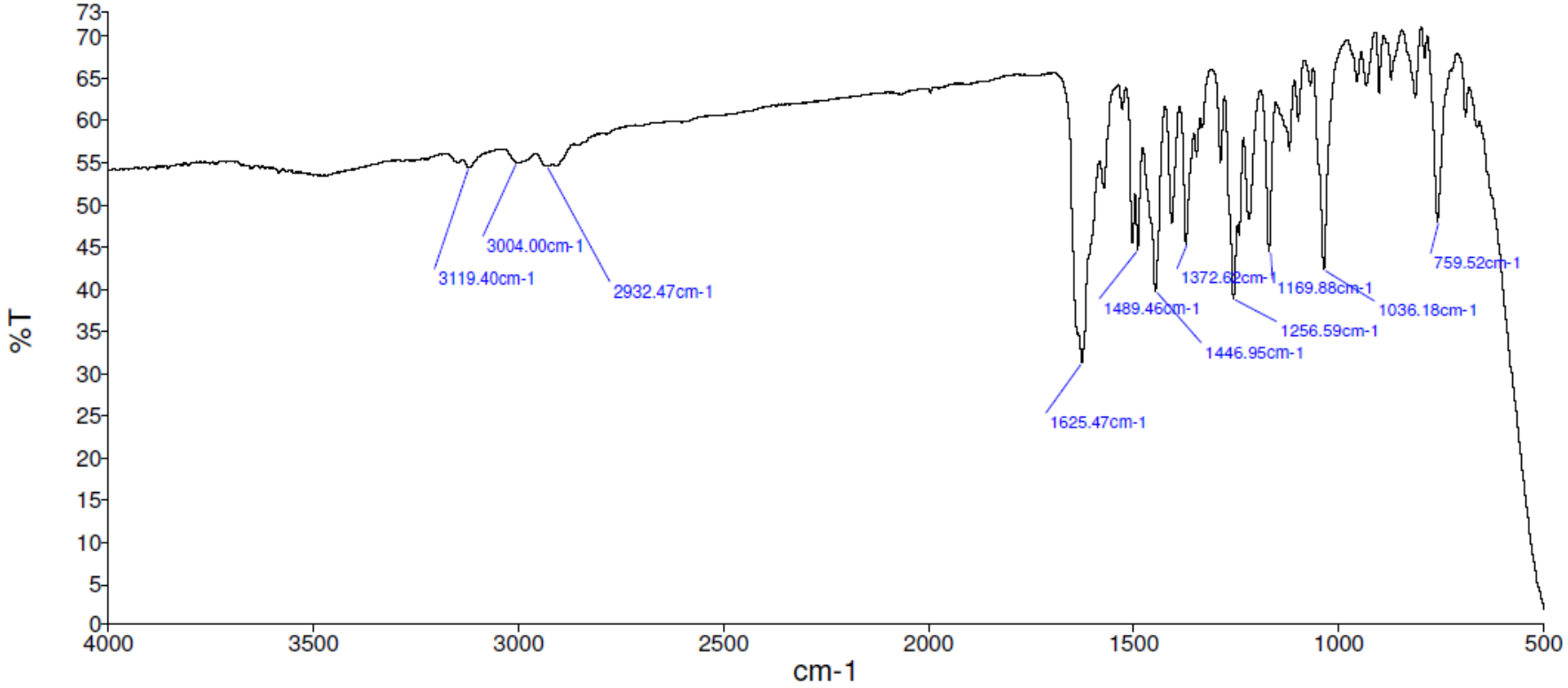

Infrared spectrum of Compound AU 17

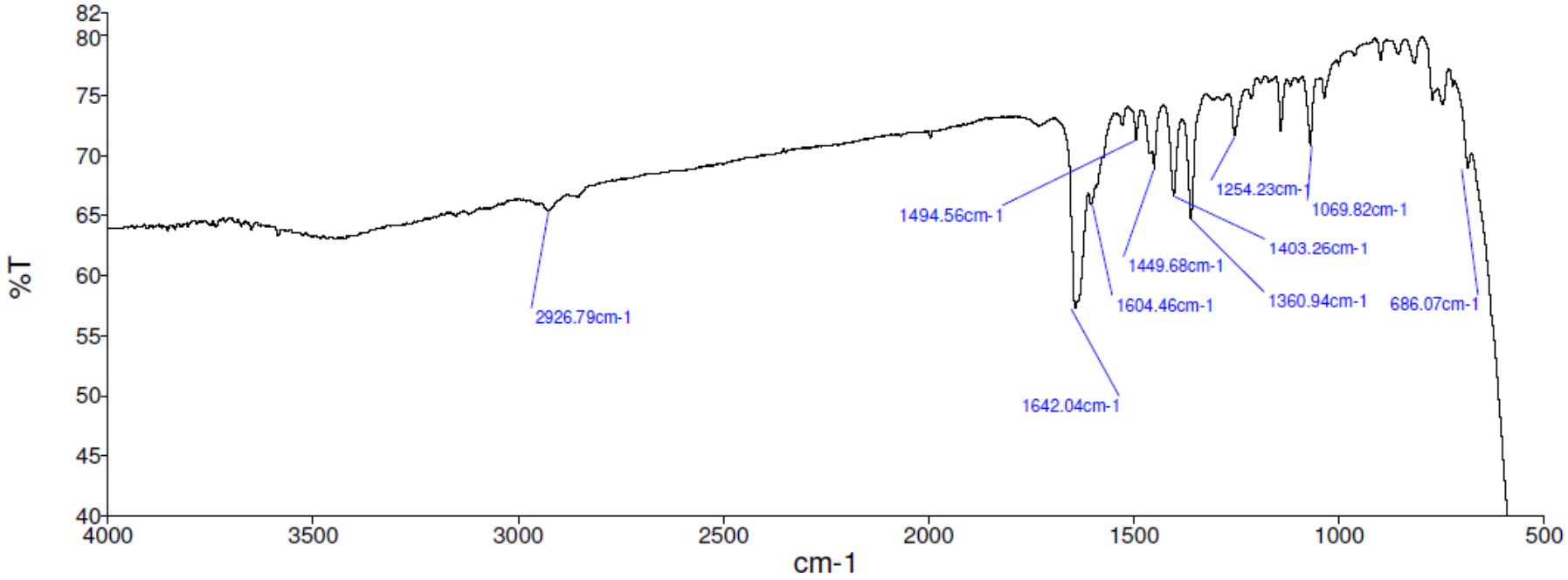

Infrared spectrum of Compound AU 18

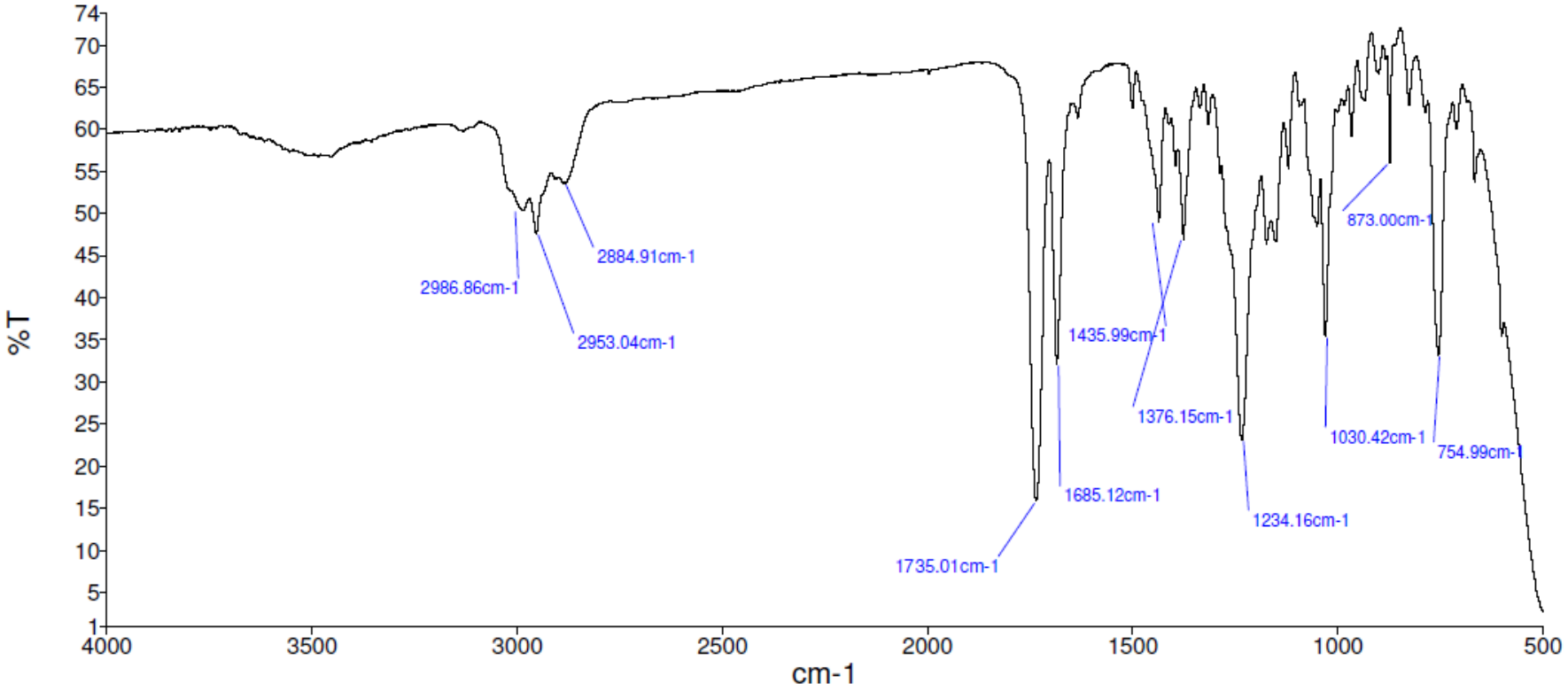

APPENDIX II

Compound X

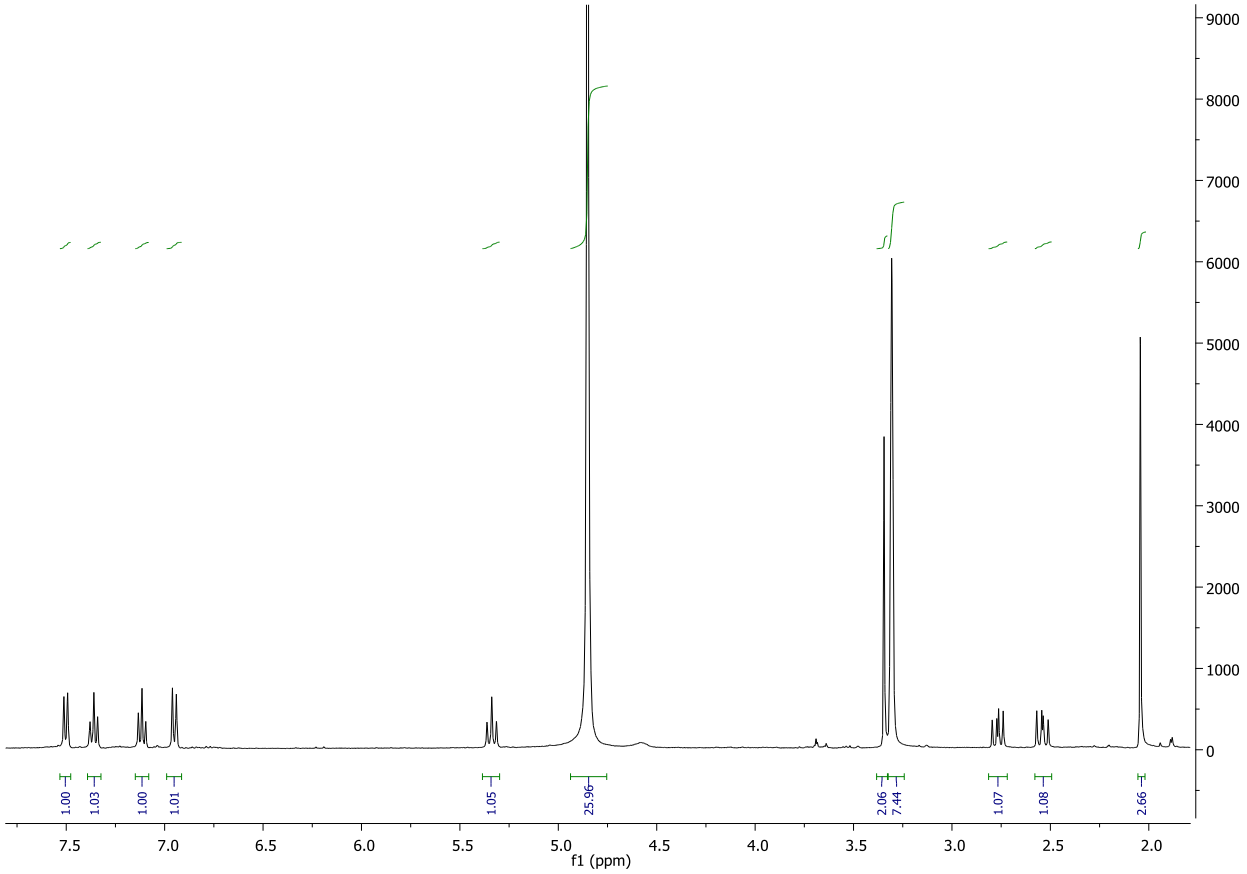

^{1}H NMR spectrum of compound X

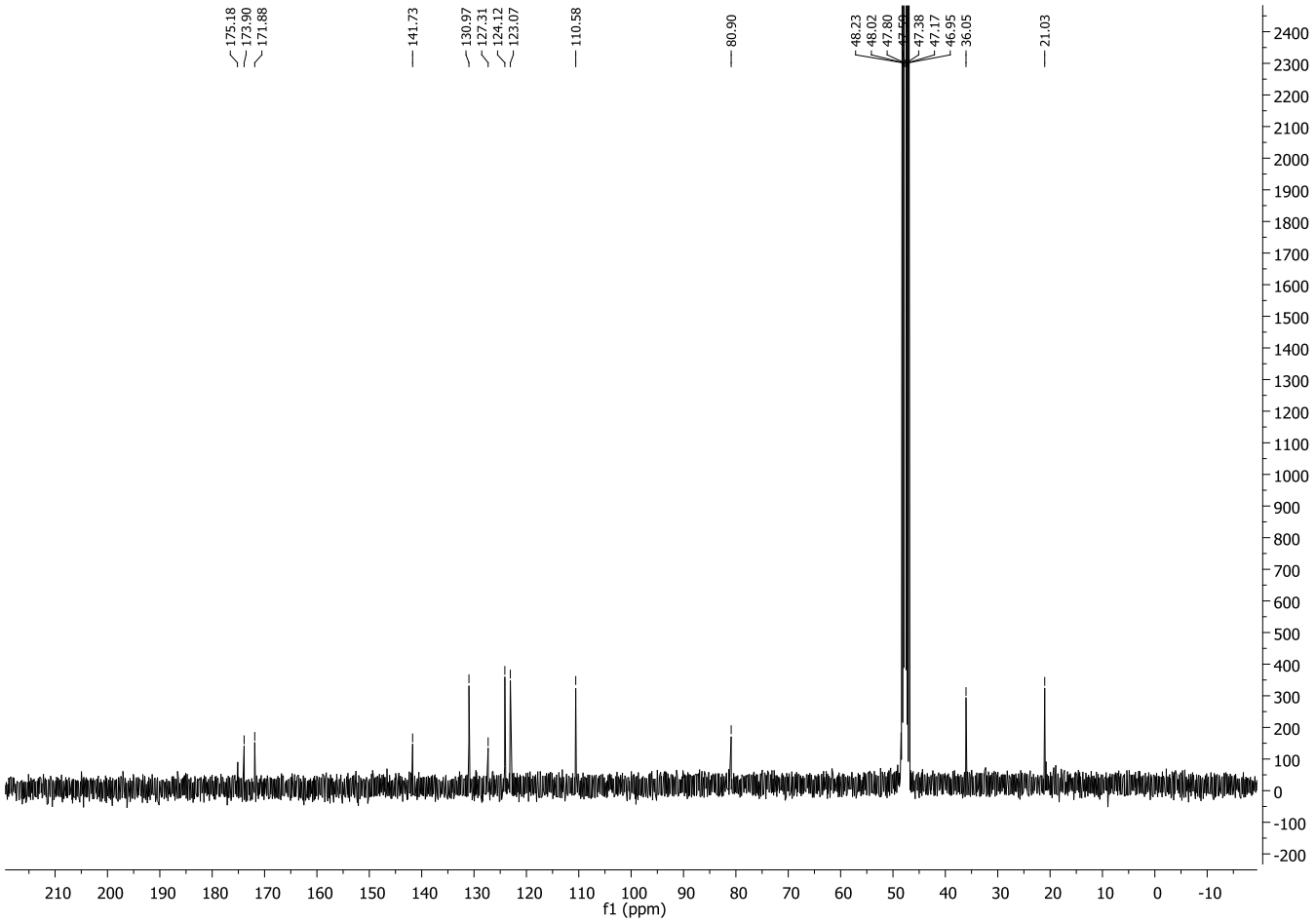

^{13}C NMR spectrum of compound X

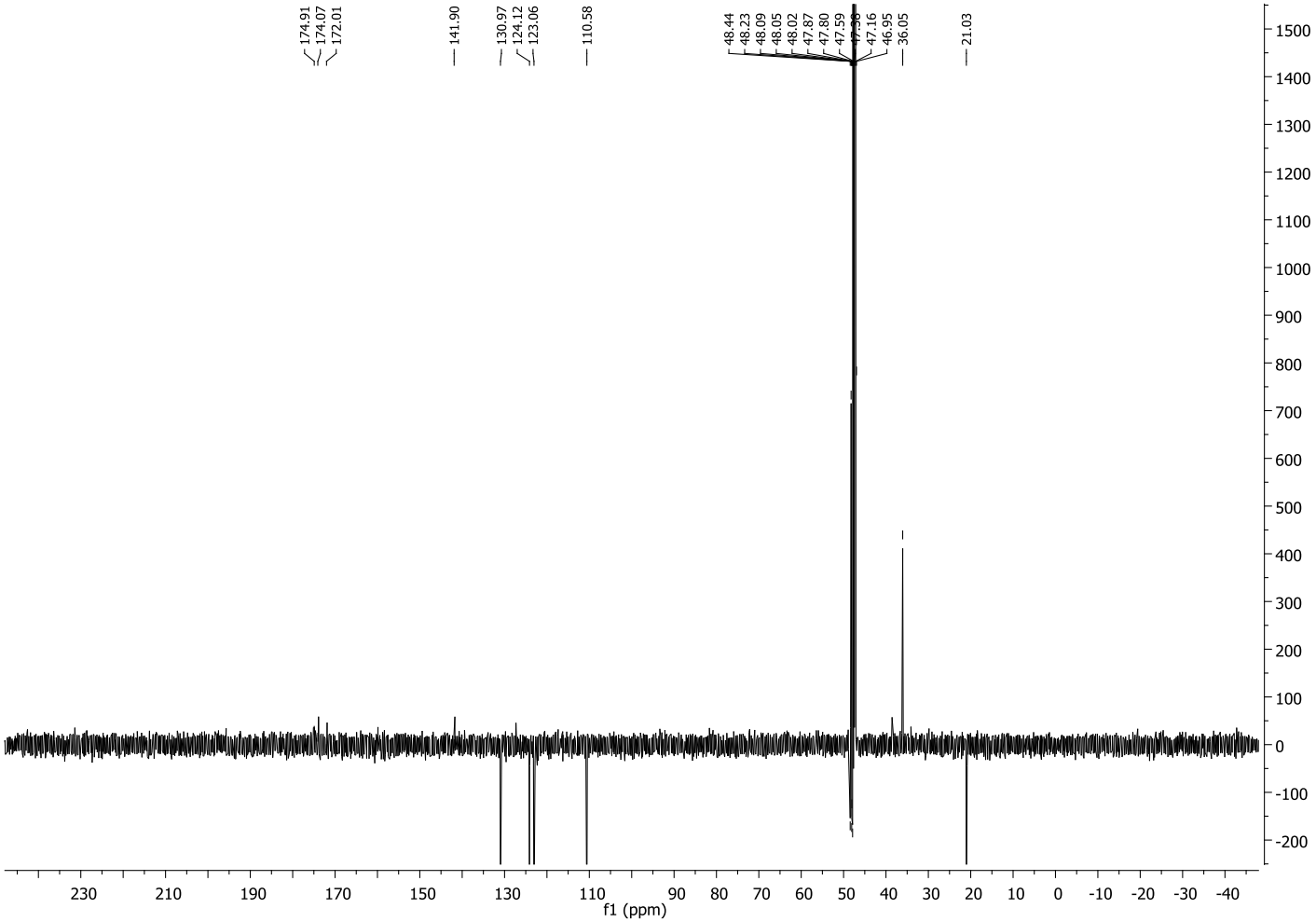

DEPT spectrum of compound X

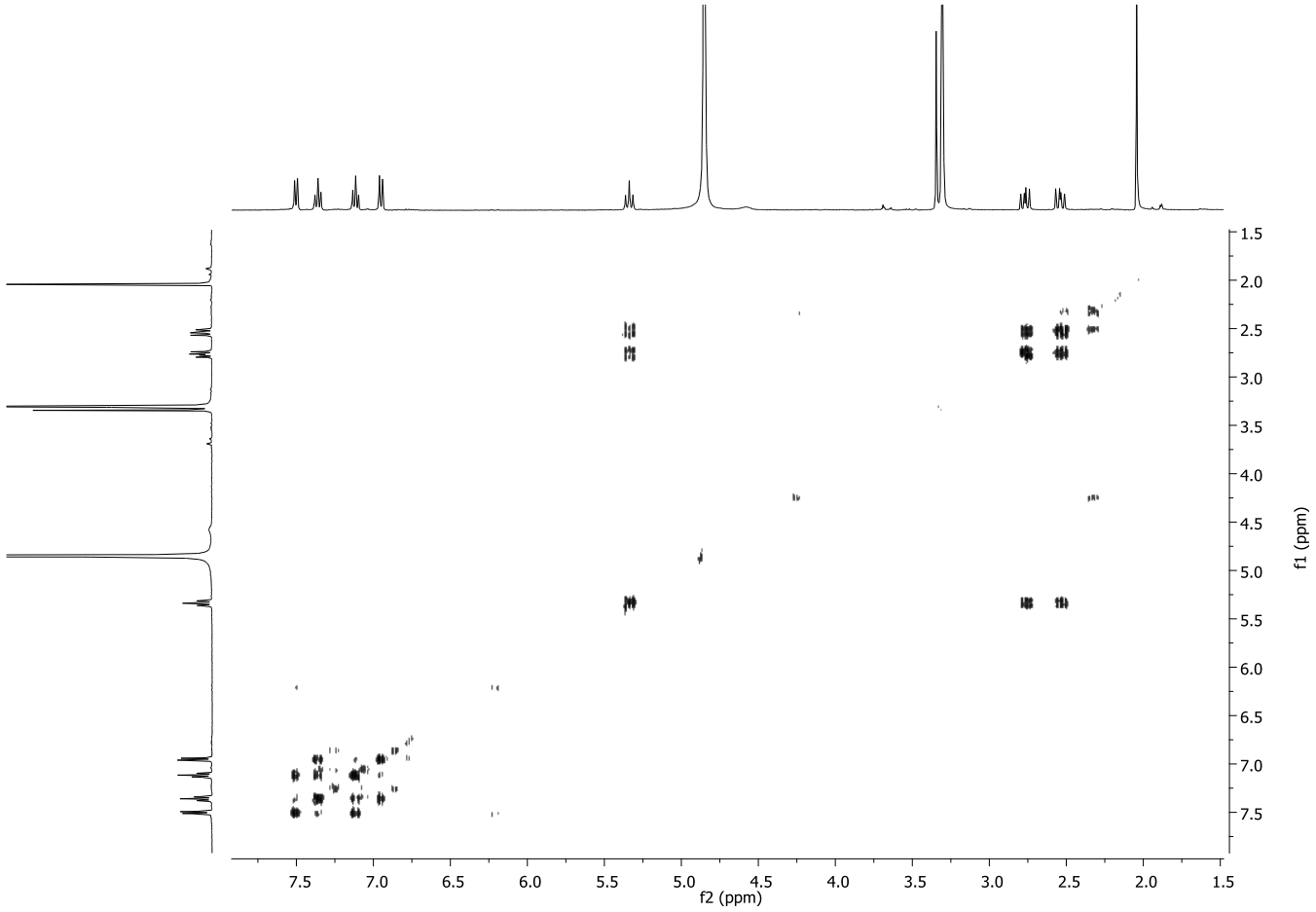

COSY spectrum of compound X

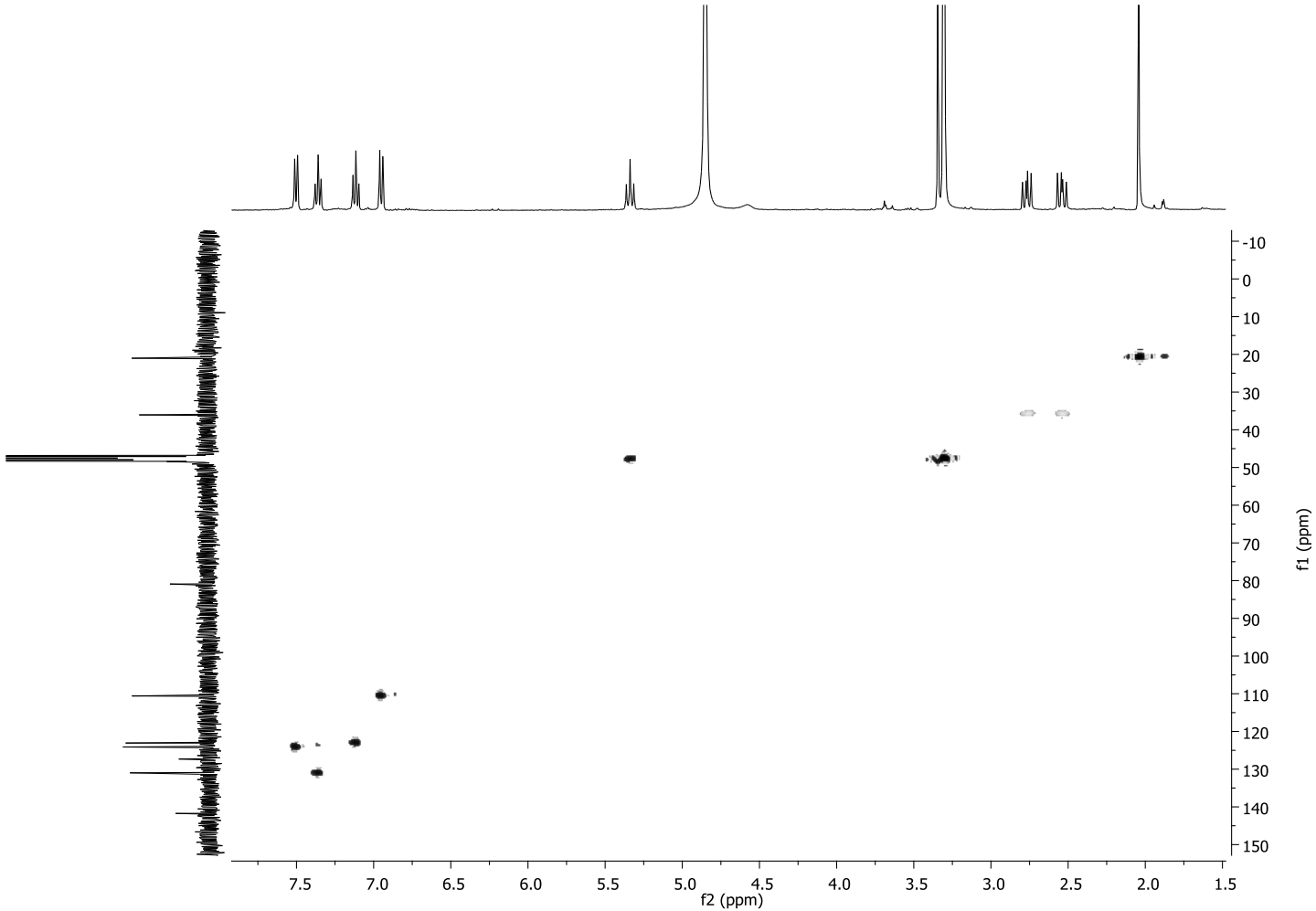

HSQC spectrum of compound X

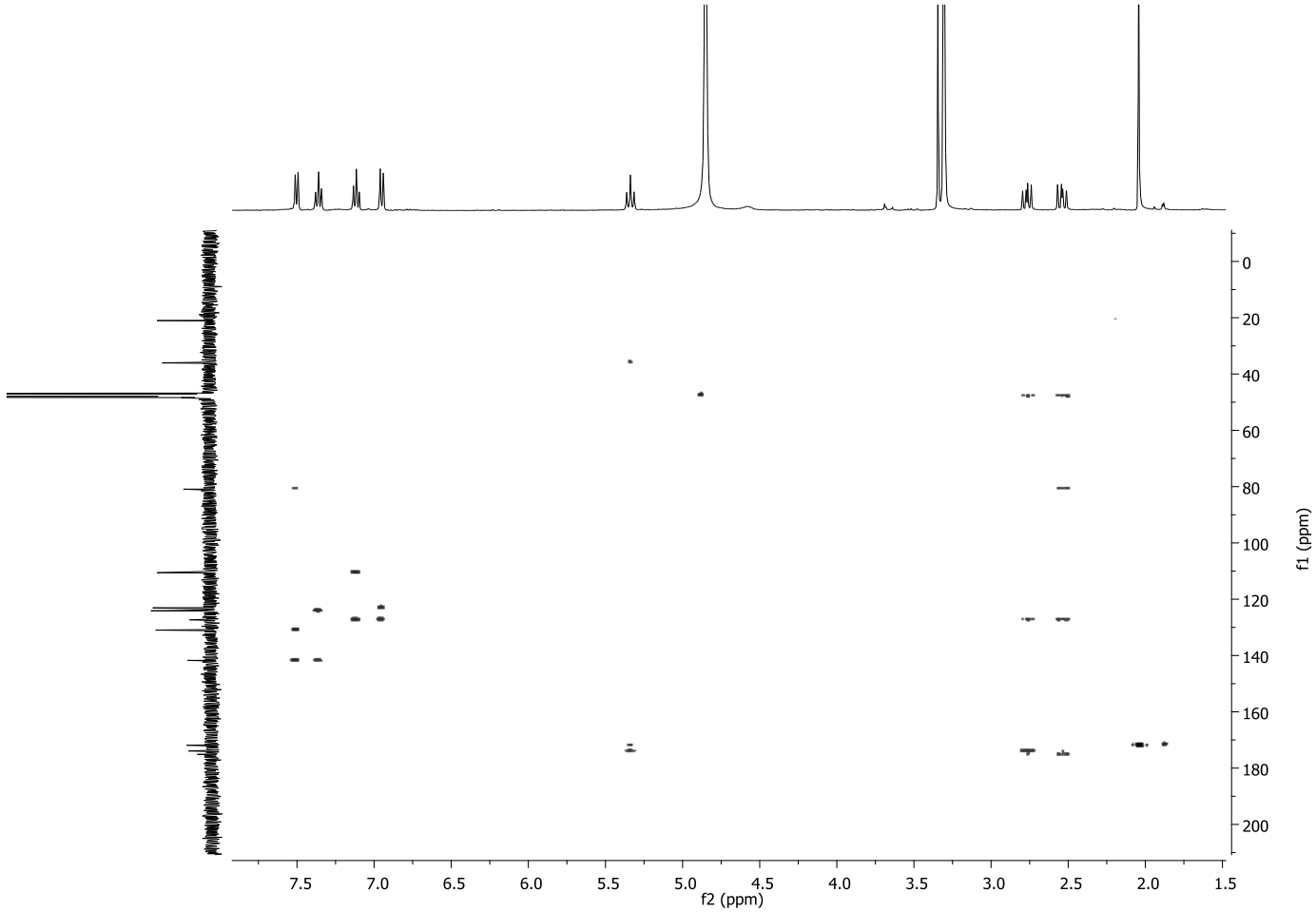

HMBC spectrum of compound X

Compound Y

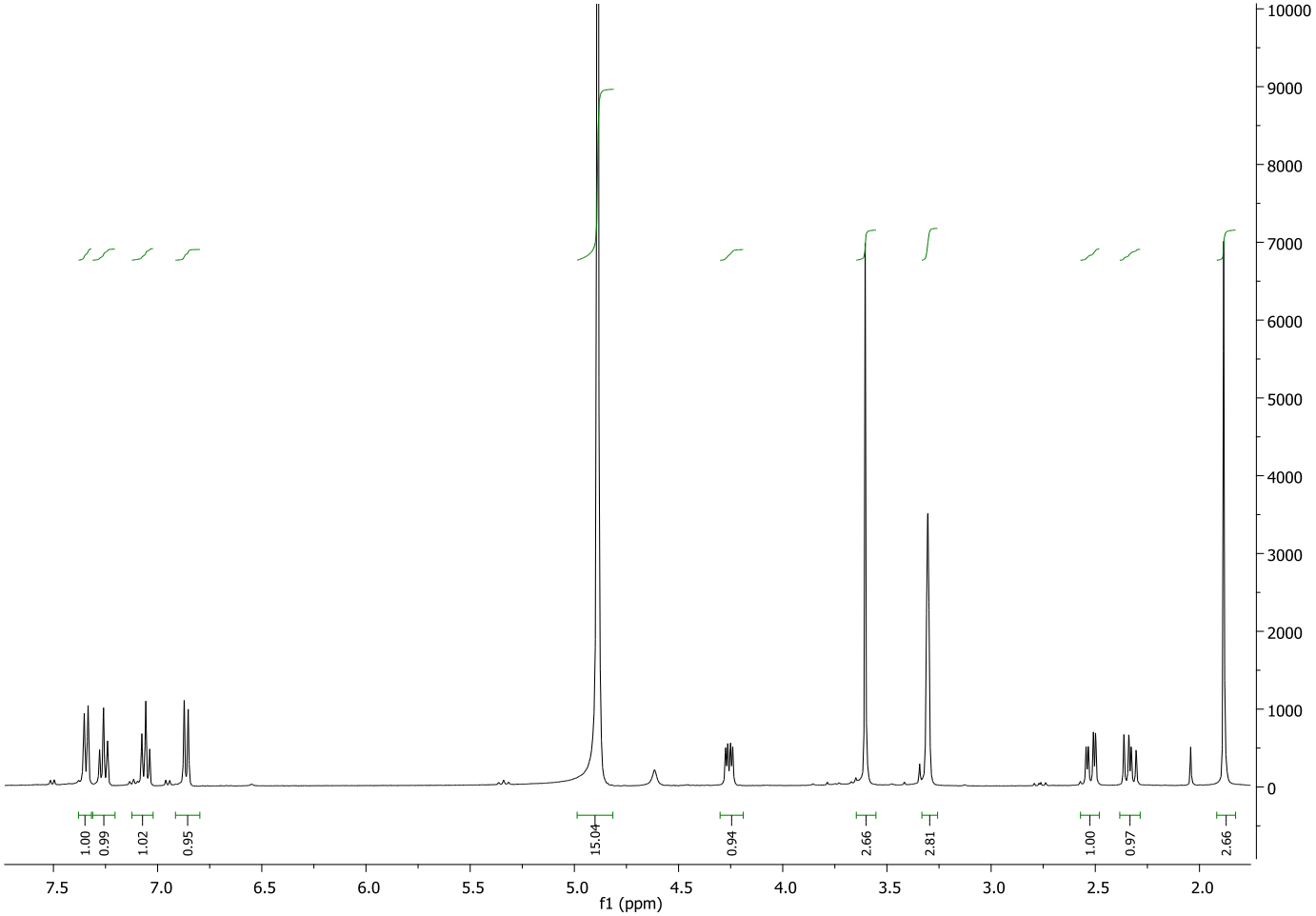

^{1}H NMR spectrum of compound Y

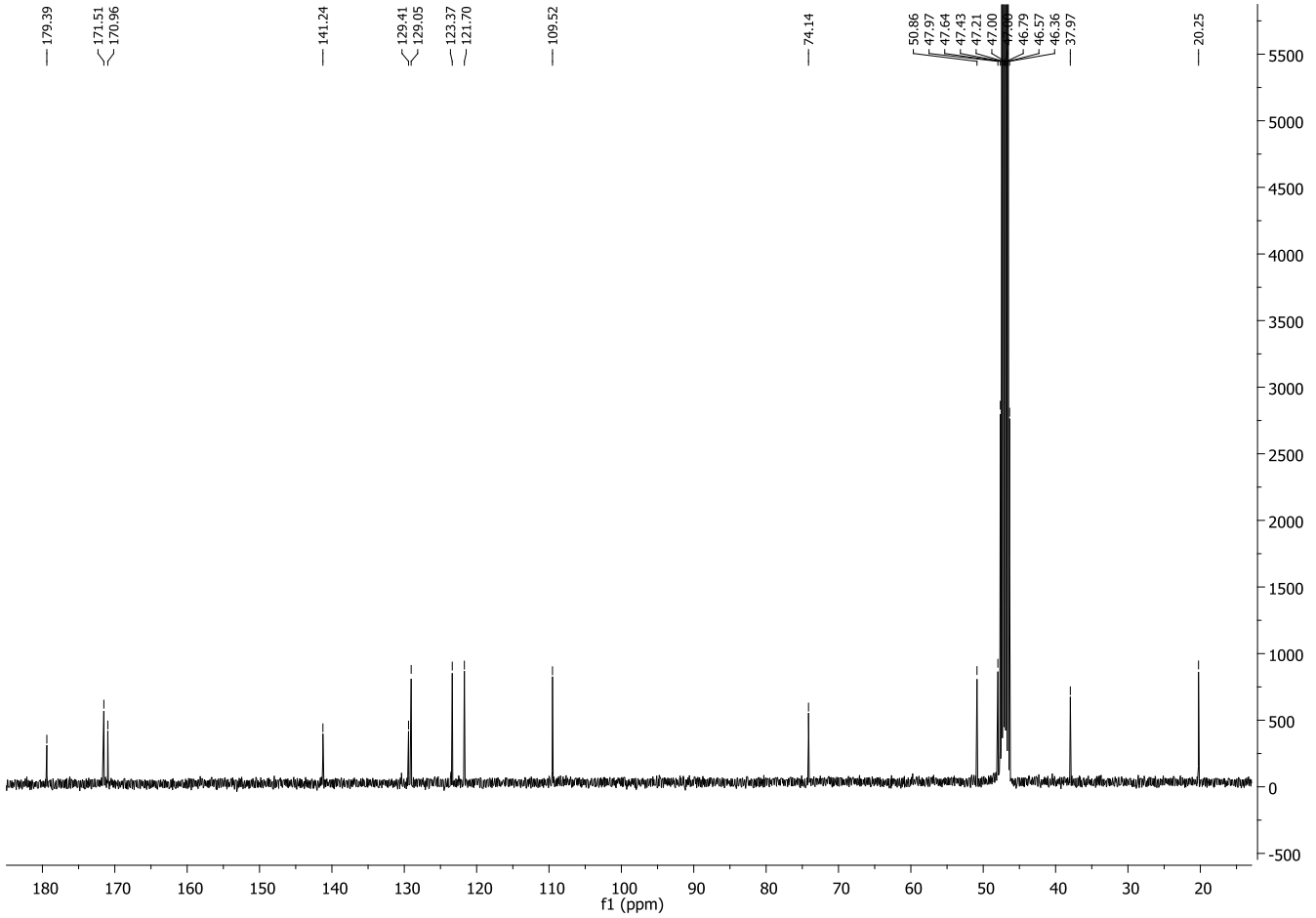

^{13}C NMR spectrum of compound Y

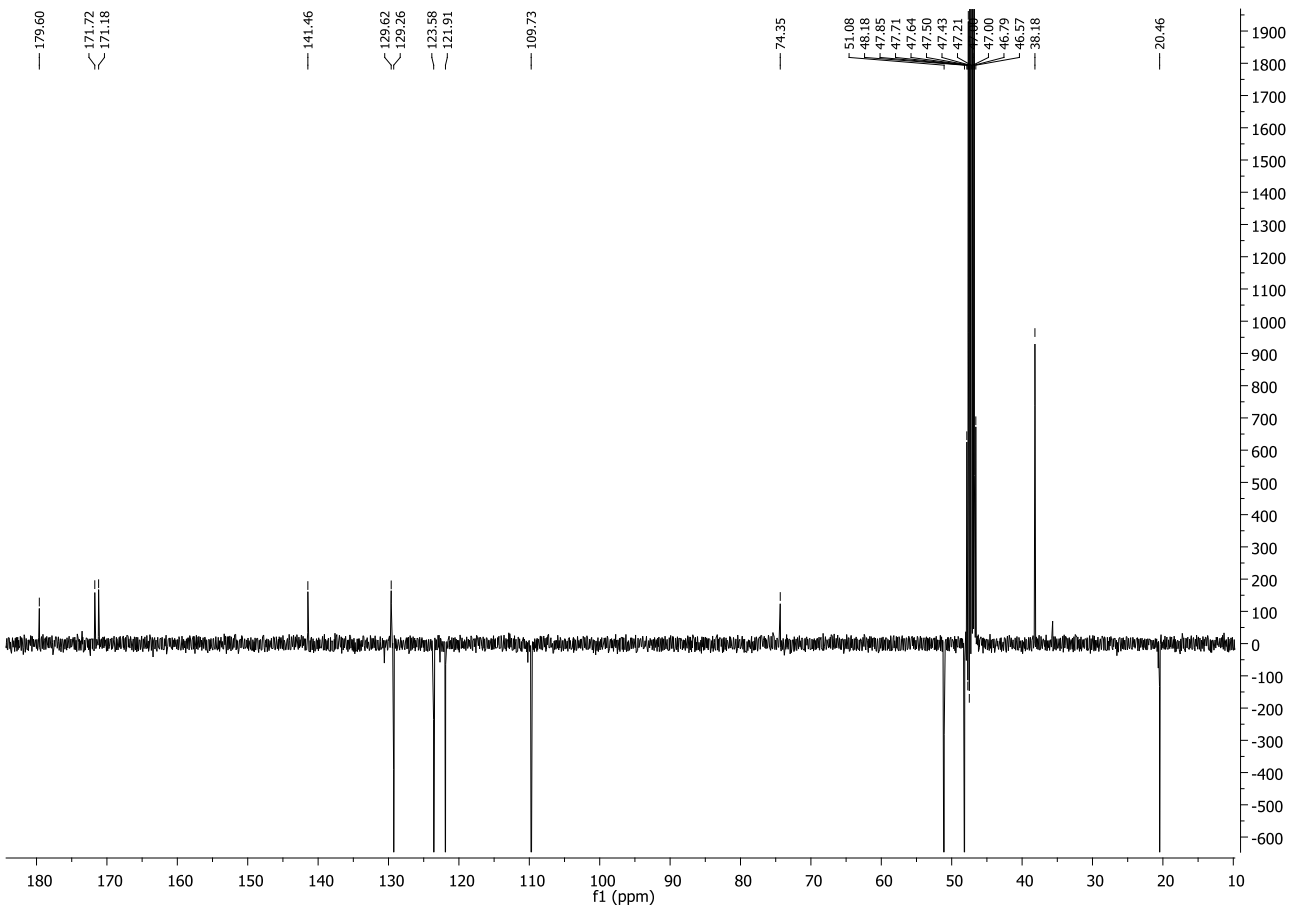

DEPT spectrum of compound Y

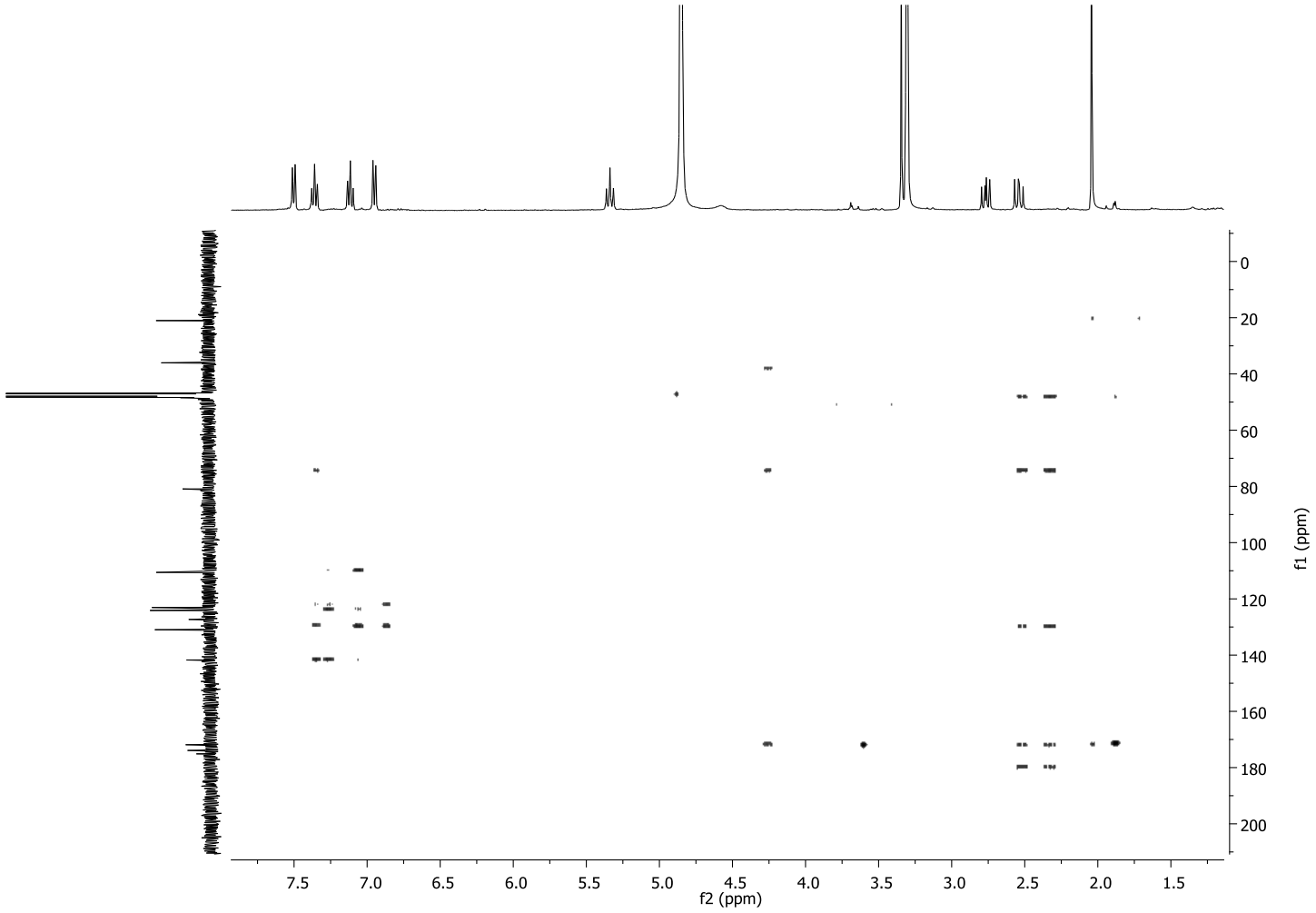

HMBC spectrum of compound Y

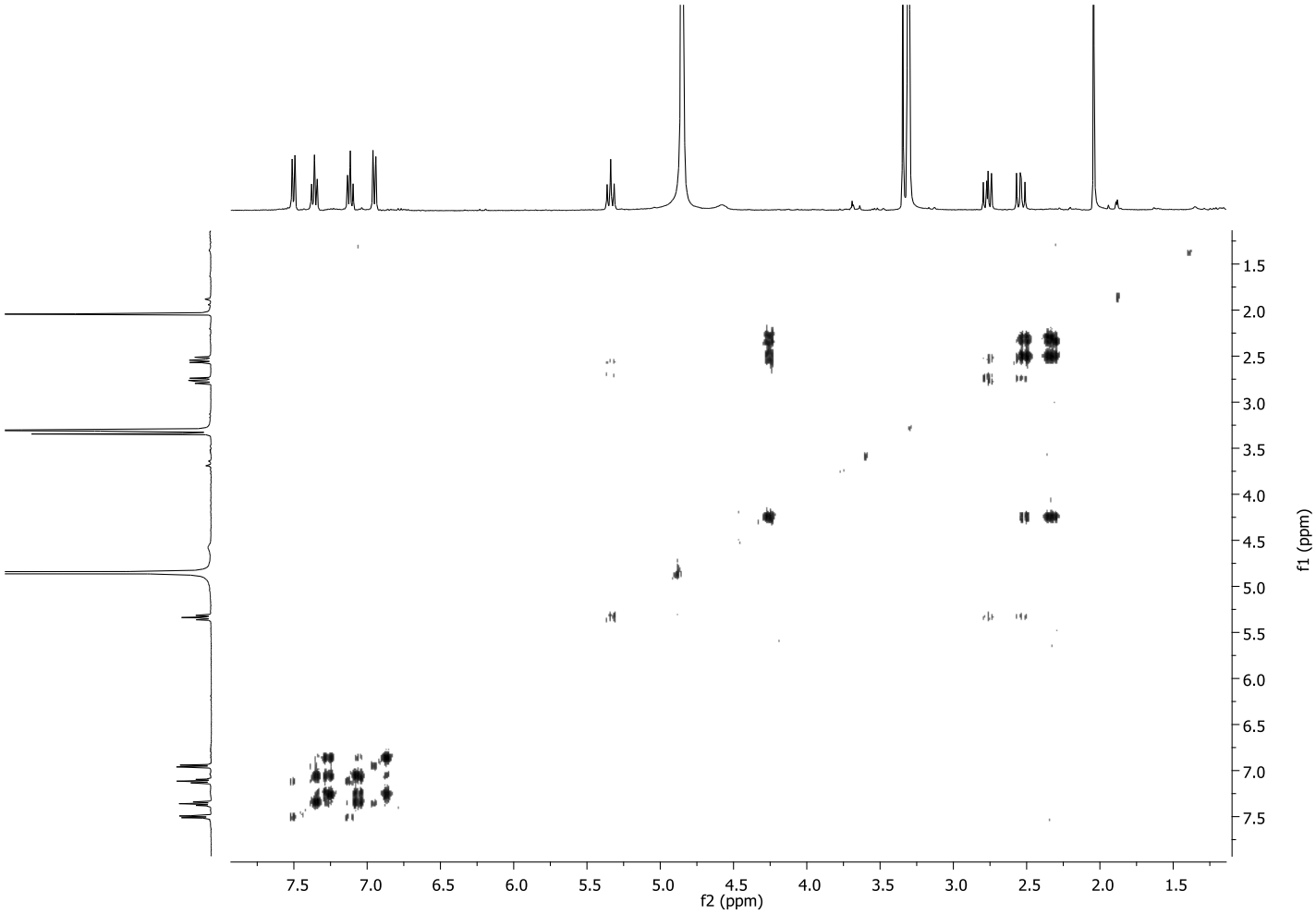

COSY spectrum of compound Y

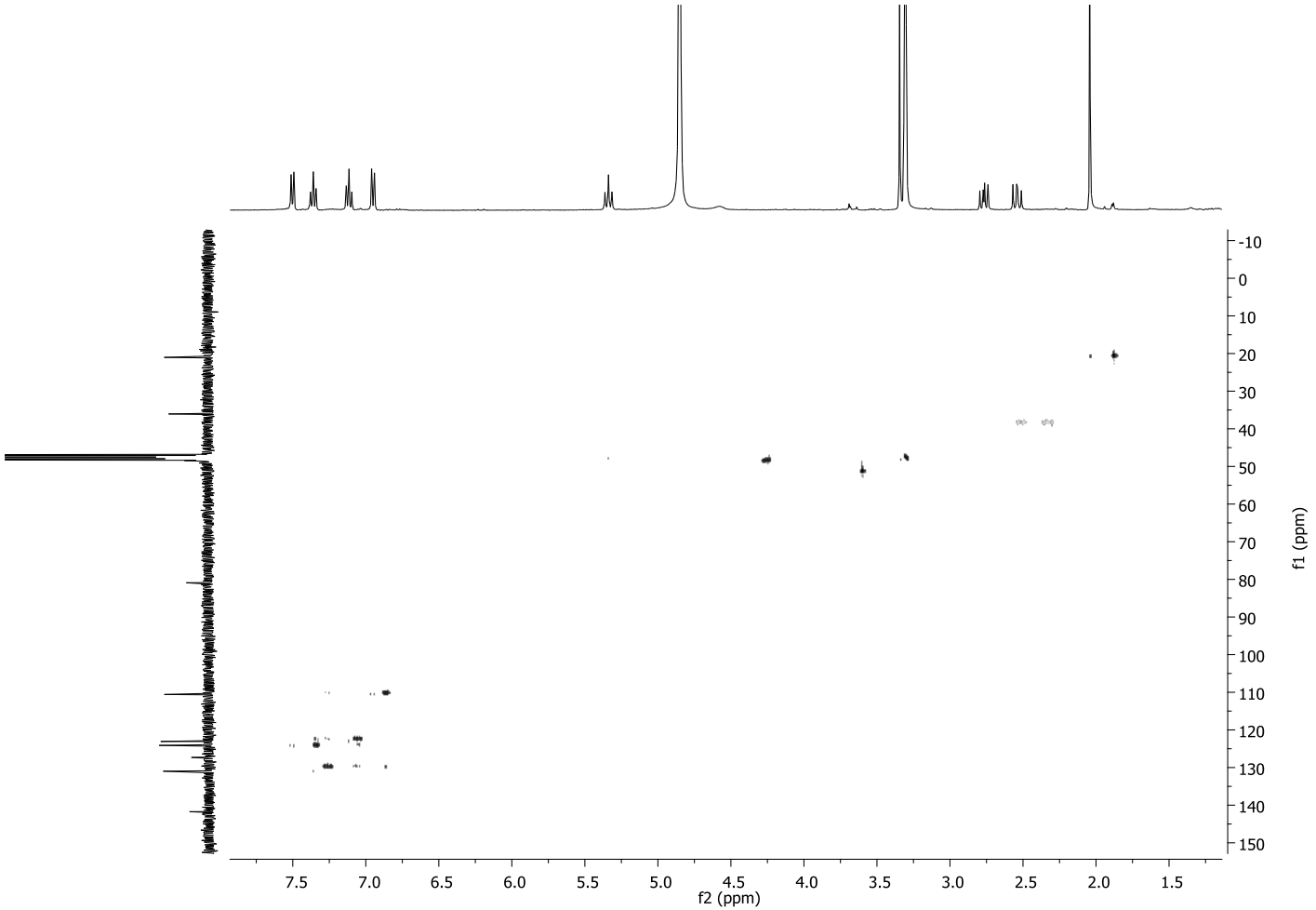

HSQC spectrum of compound Y

Compound Z

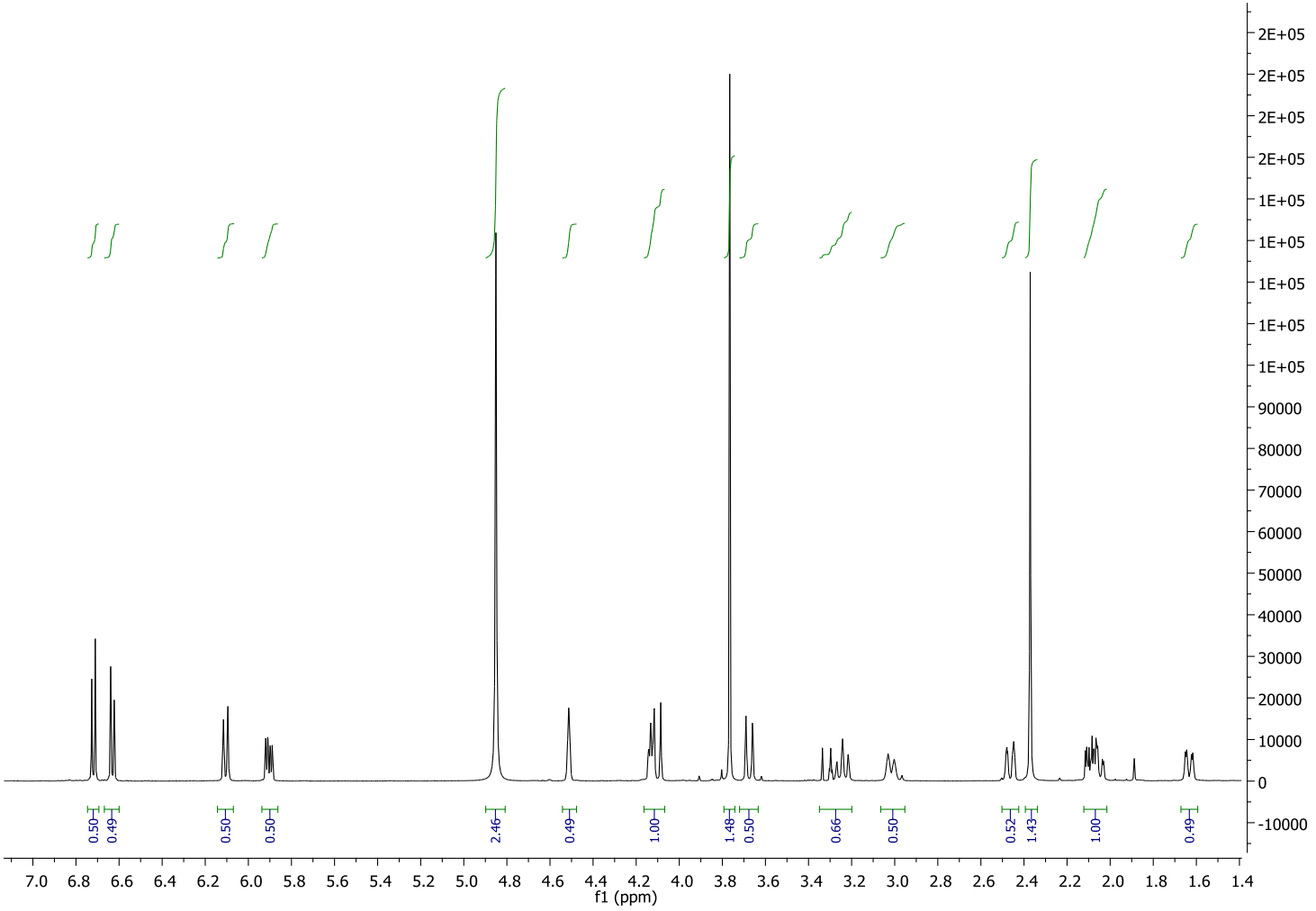

^{1}H NMR spectrum of compound Z

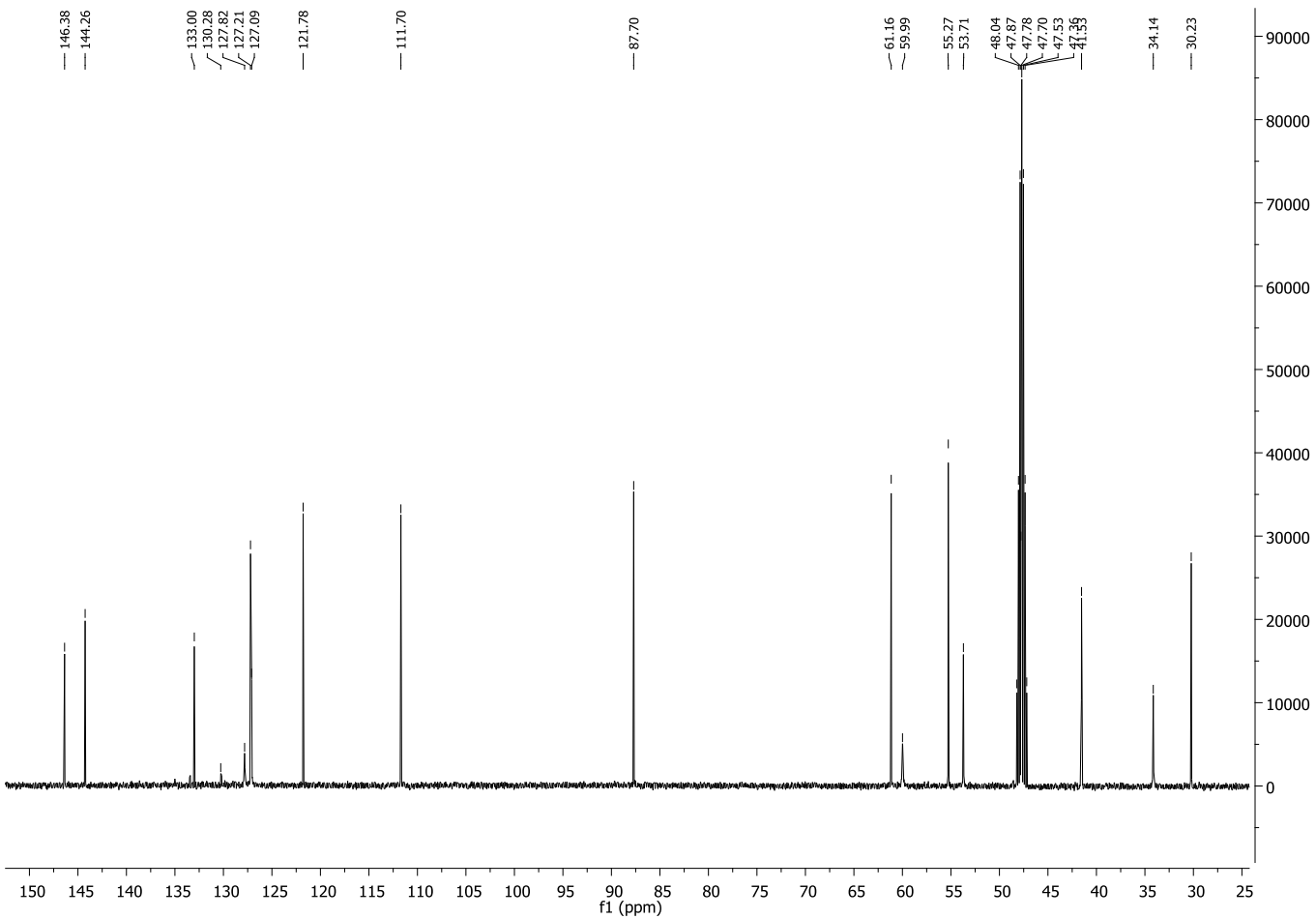

^{13}C NMR spectrum of compound Z

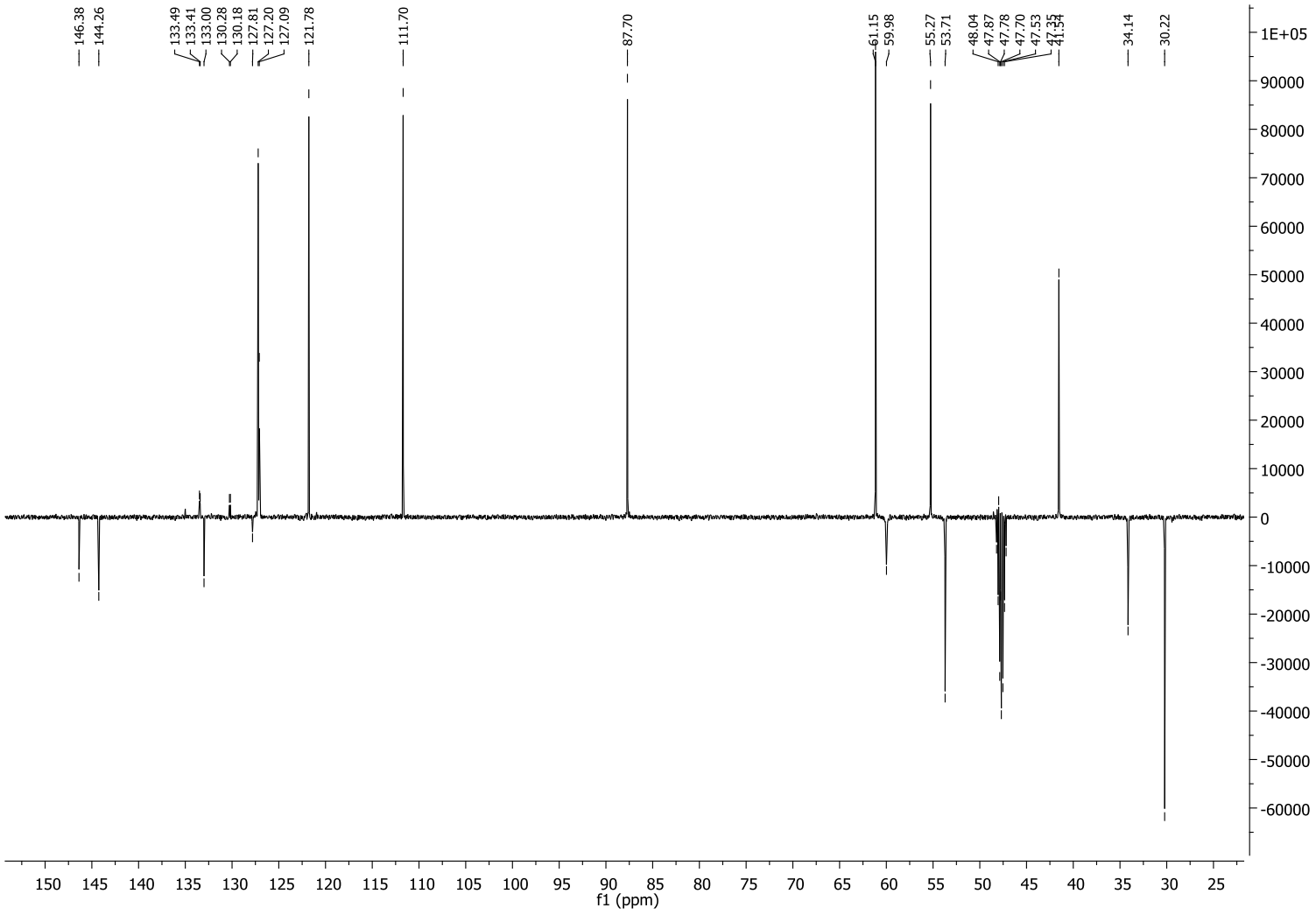

DEPT spectrum of compound Z

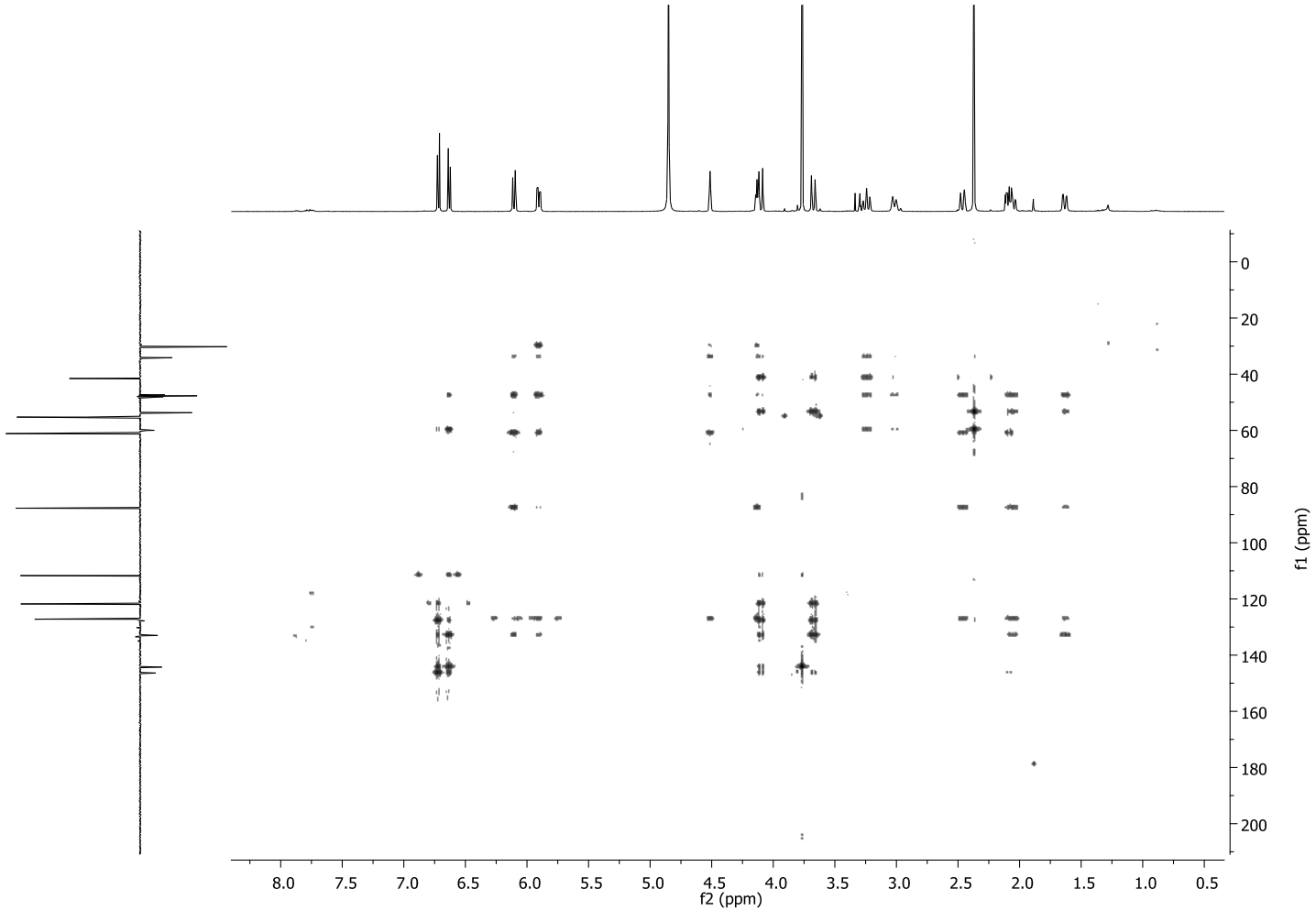

HMBC spectrum of compound Z

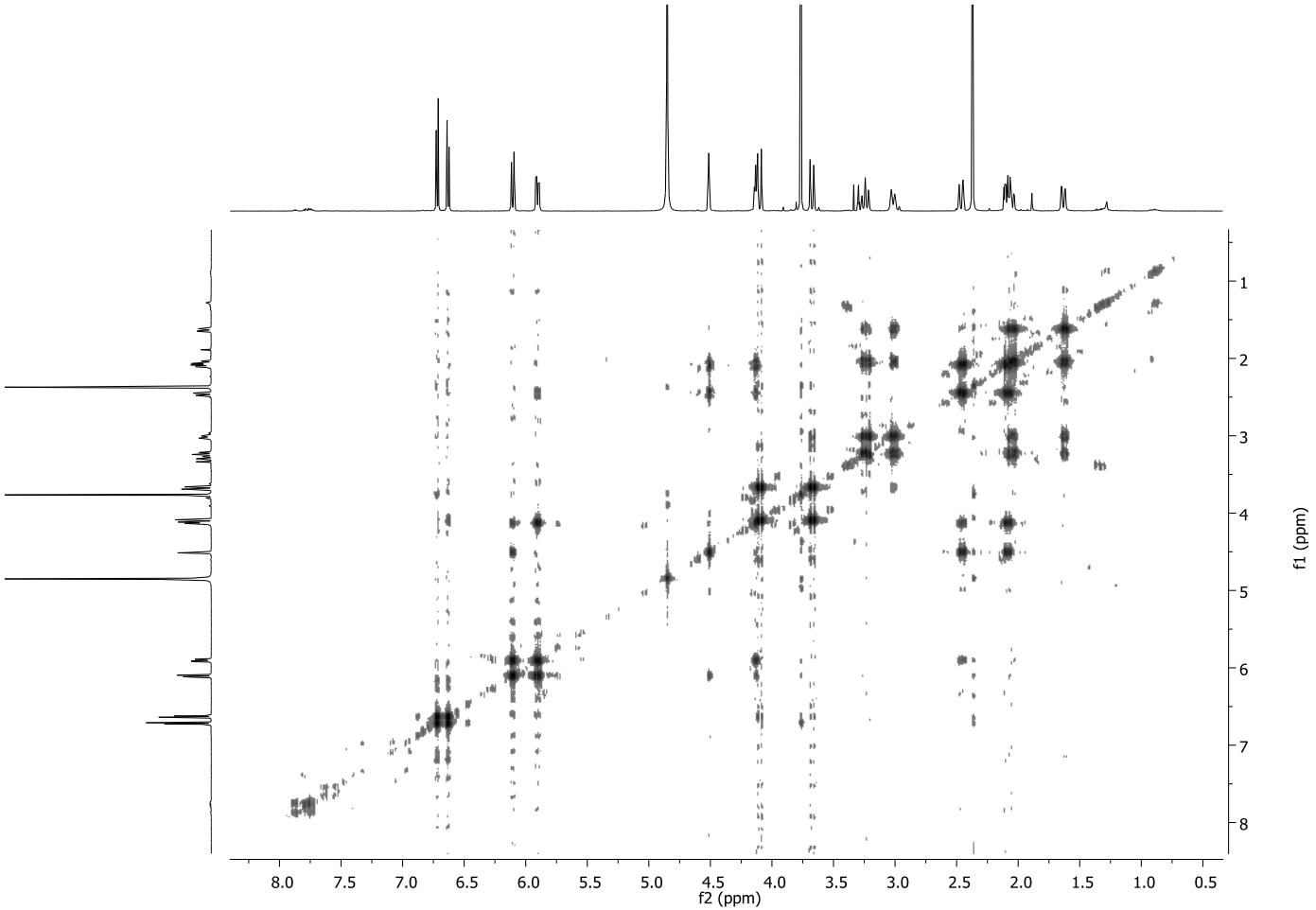

COSY spectrum of compound Z

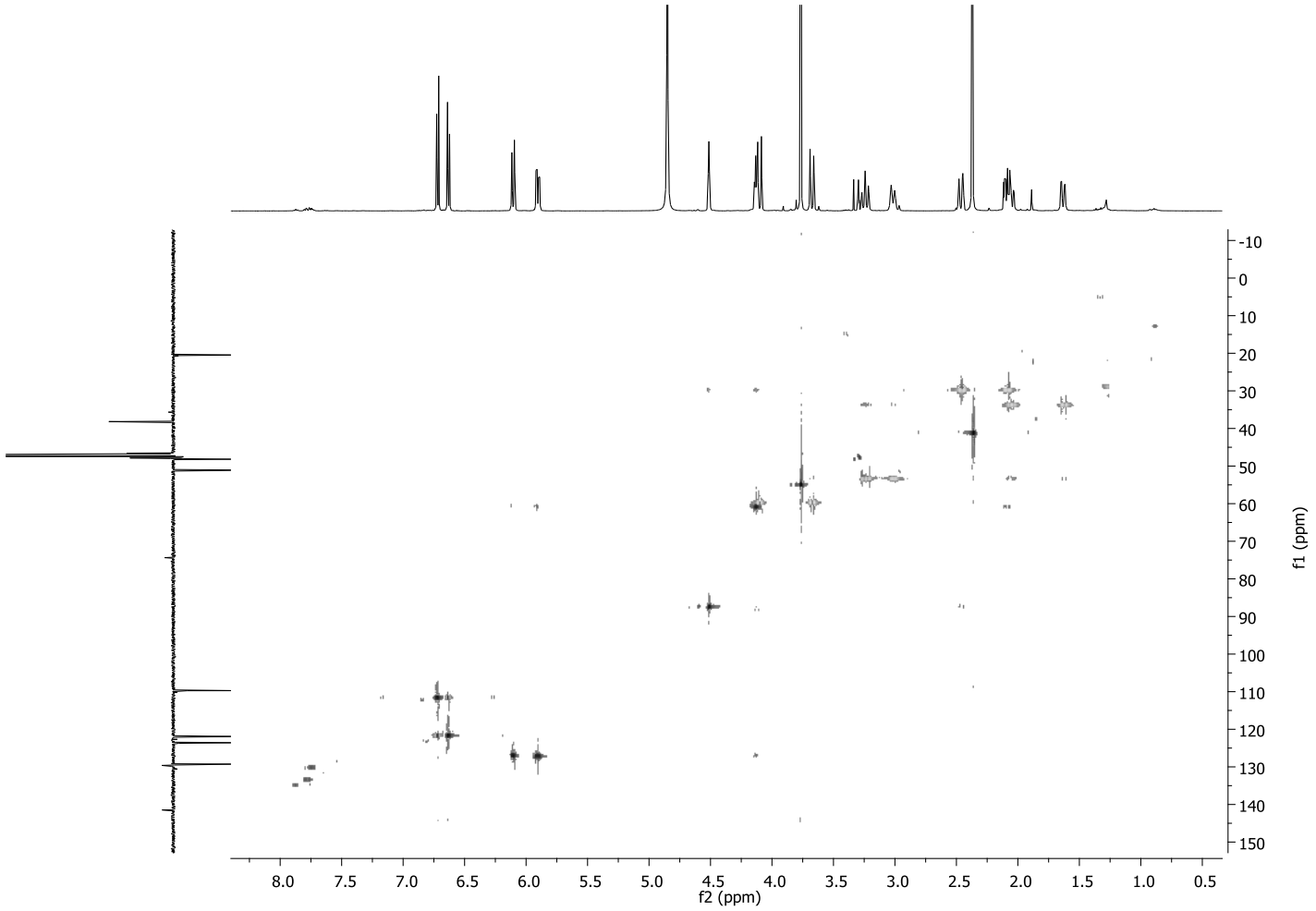

HSQC spectrum of compound Z

Compound ZA

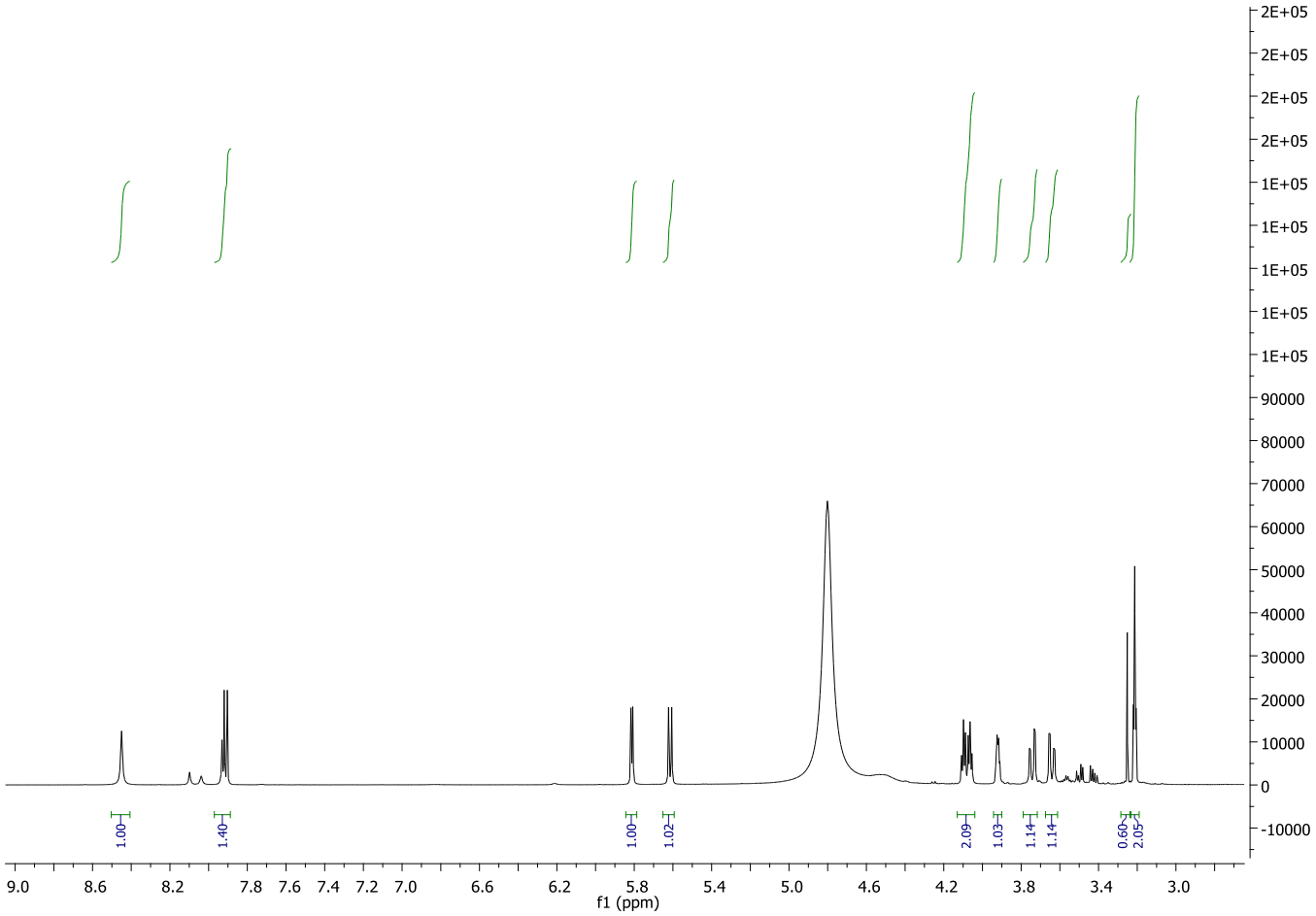

^{1}H NMR spectrum of compound ZA

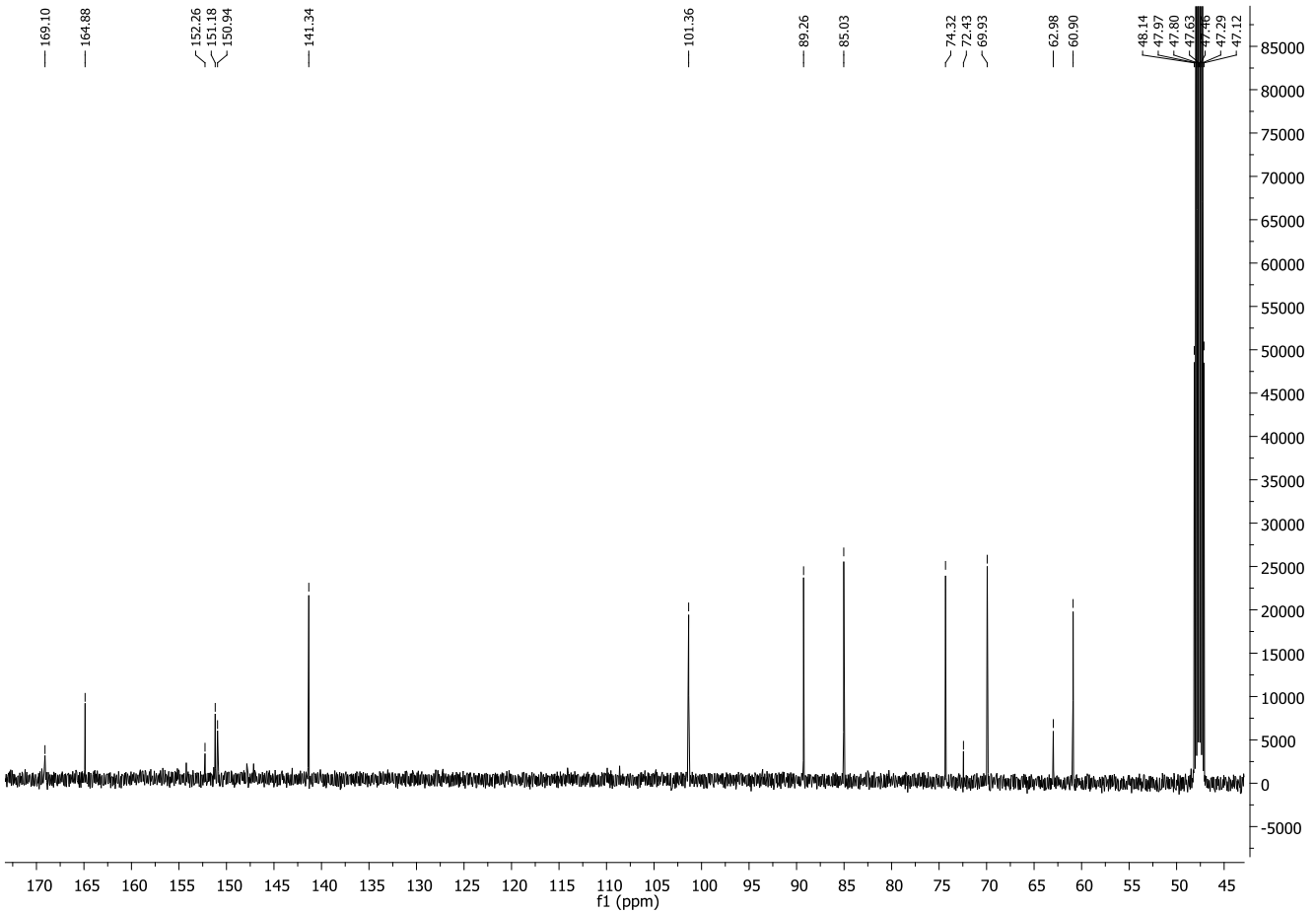

^{13}C NMR spectrum of compound ZA

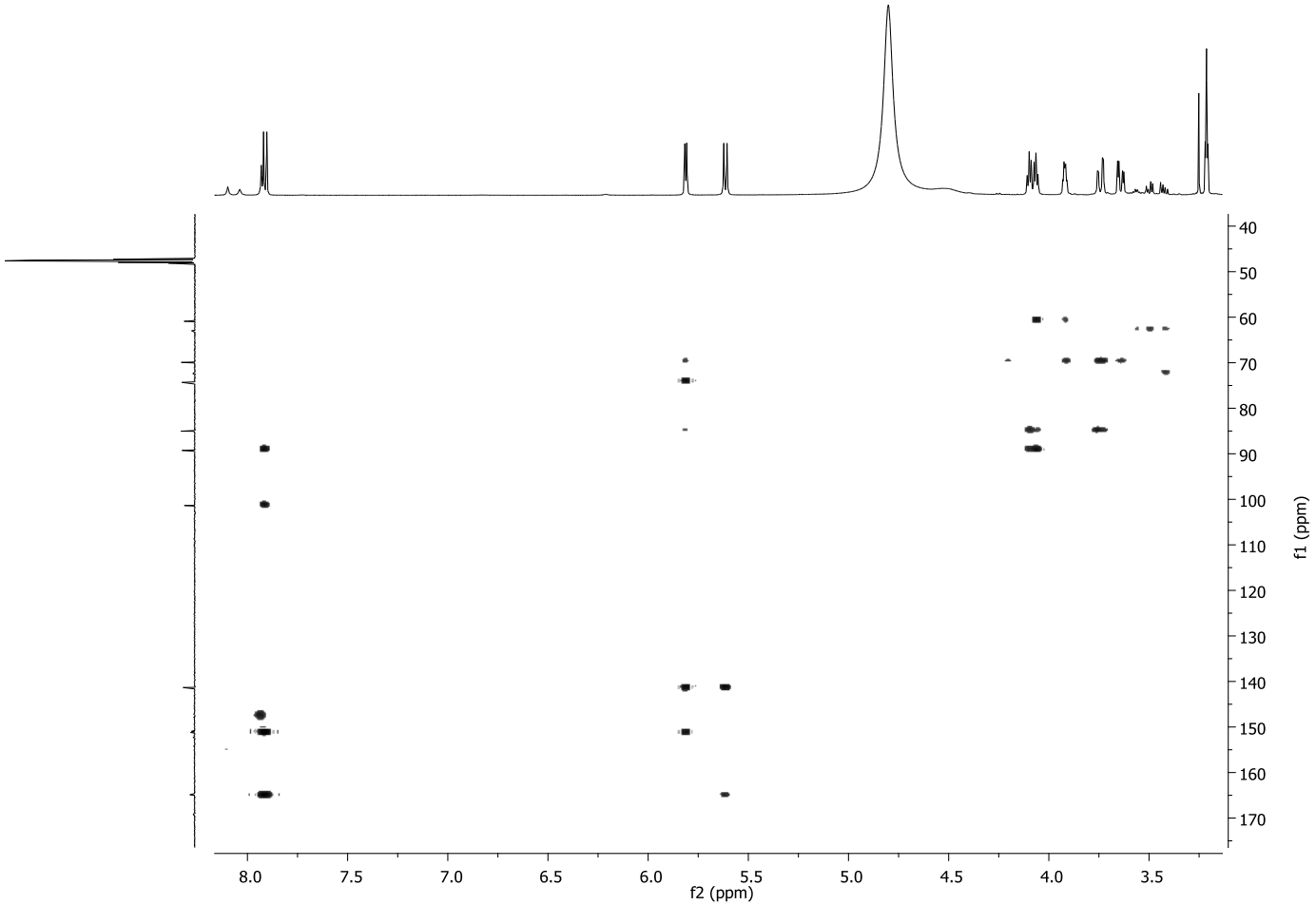

HMBC spectrum of compound ZA

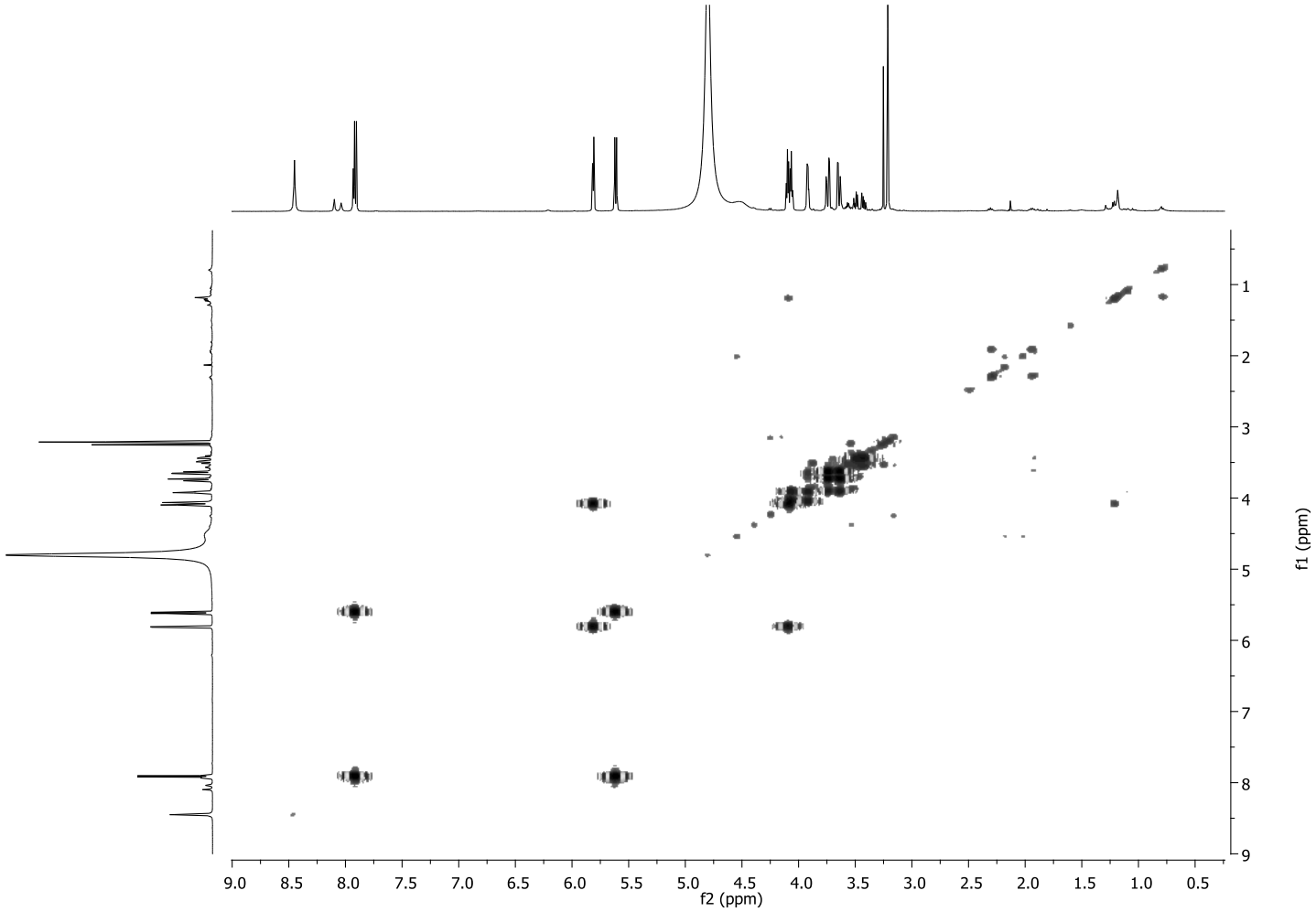

COSY spectrum of compound ZA

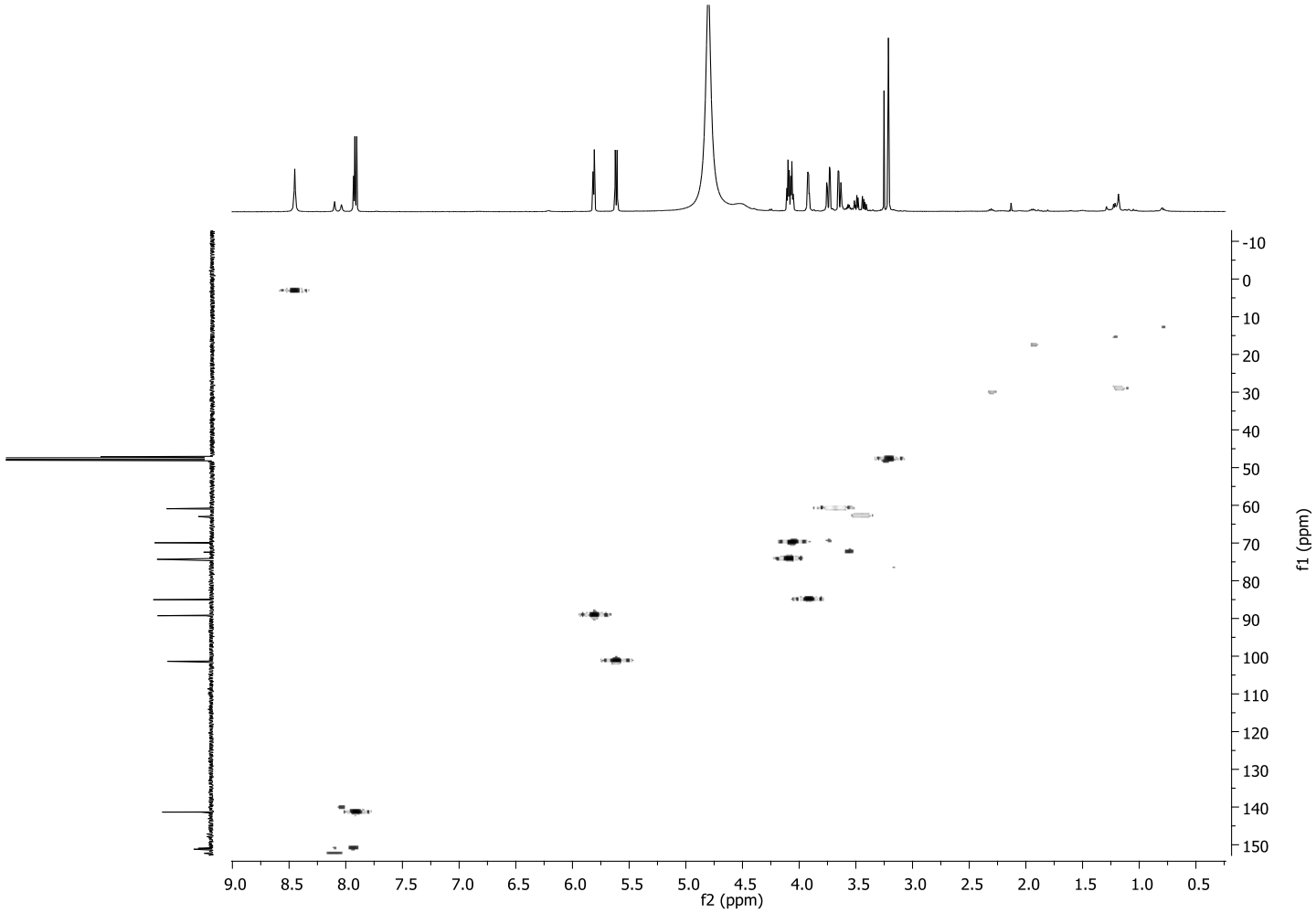

HSQC spectrum of compound ZA

APPENDIX III

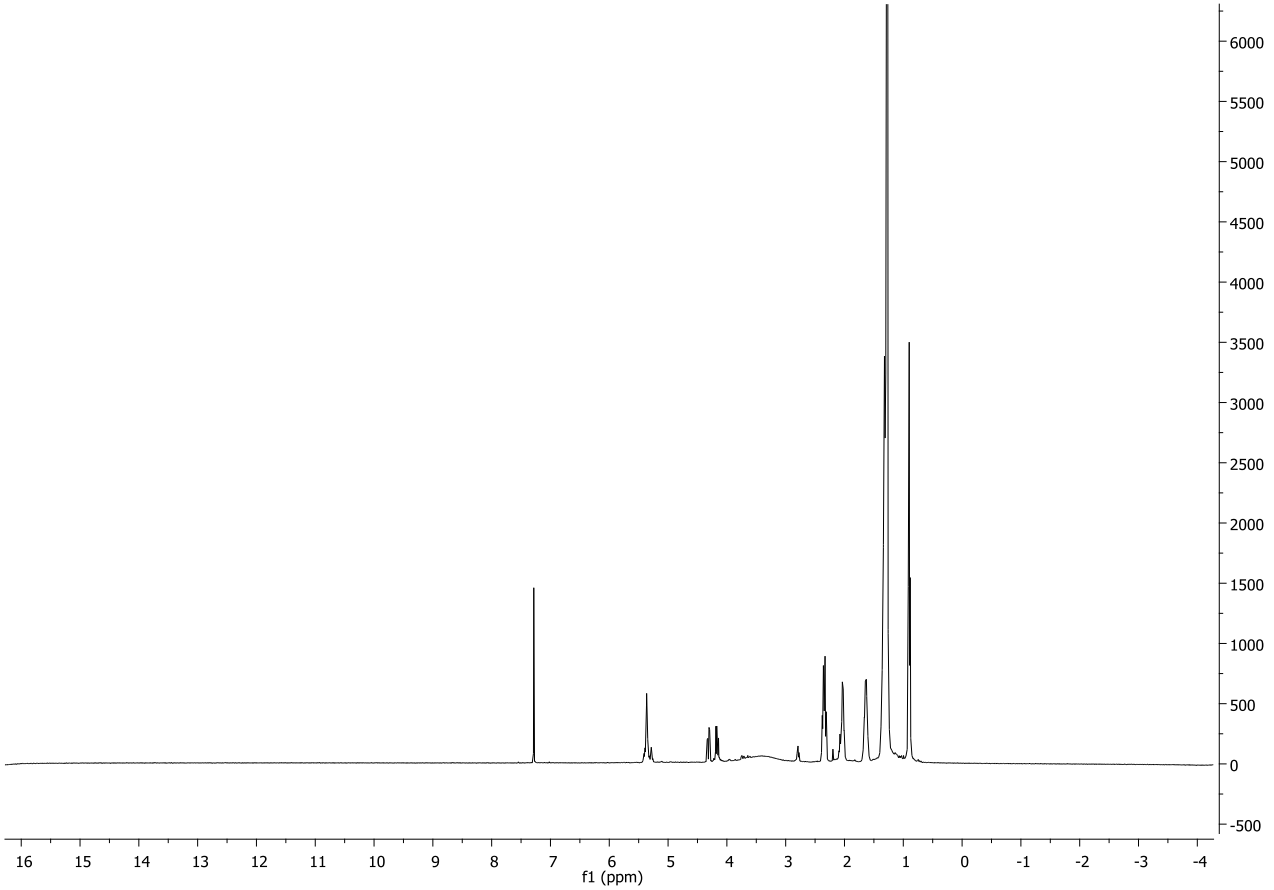

First approach. ^{1}H NMR spectrum A1

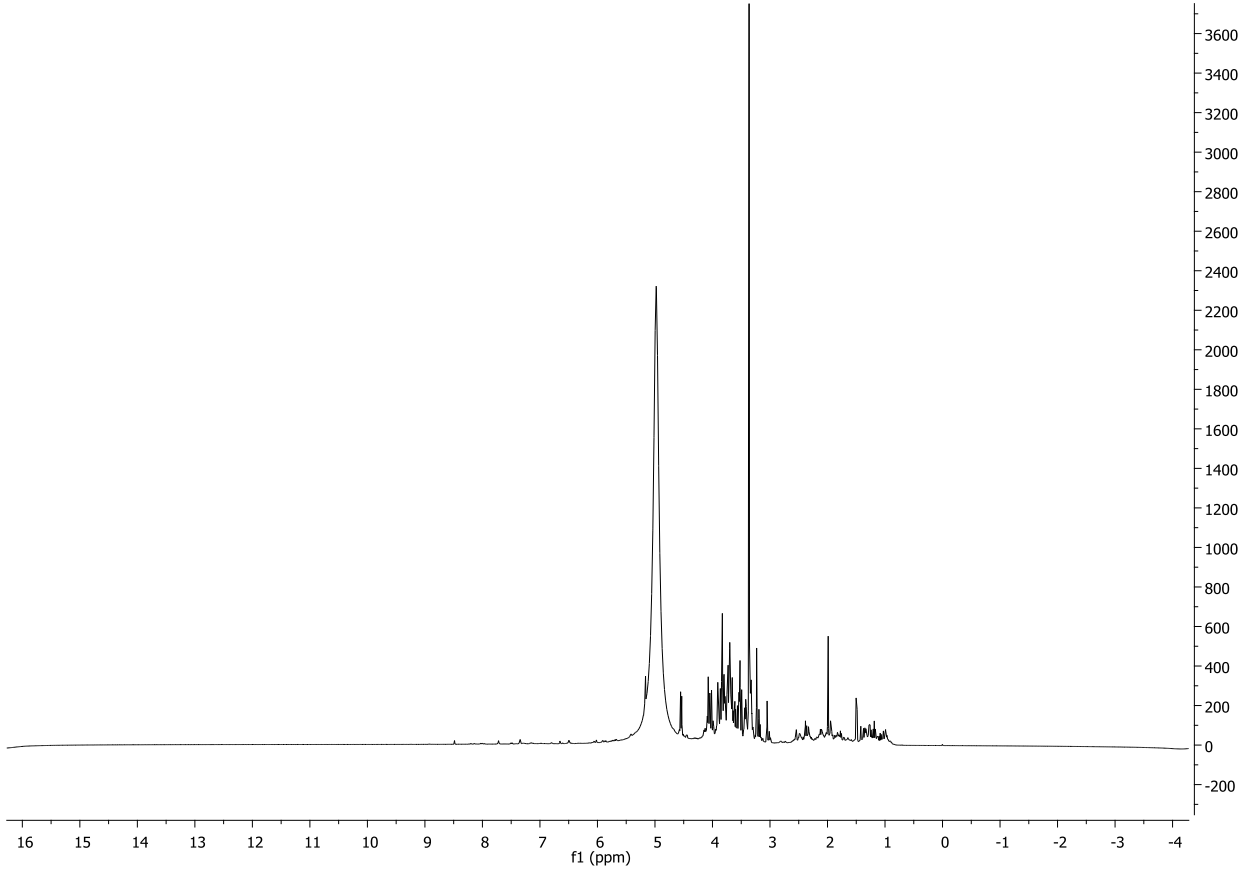

First approach. ^{1}H NMR spectrum A2

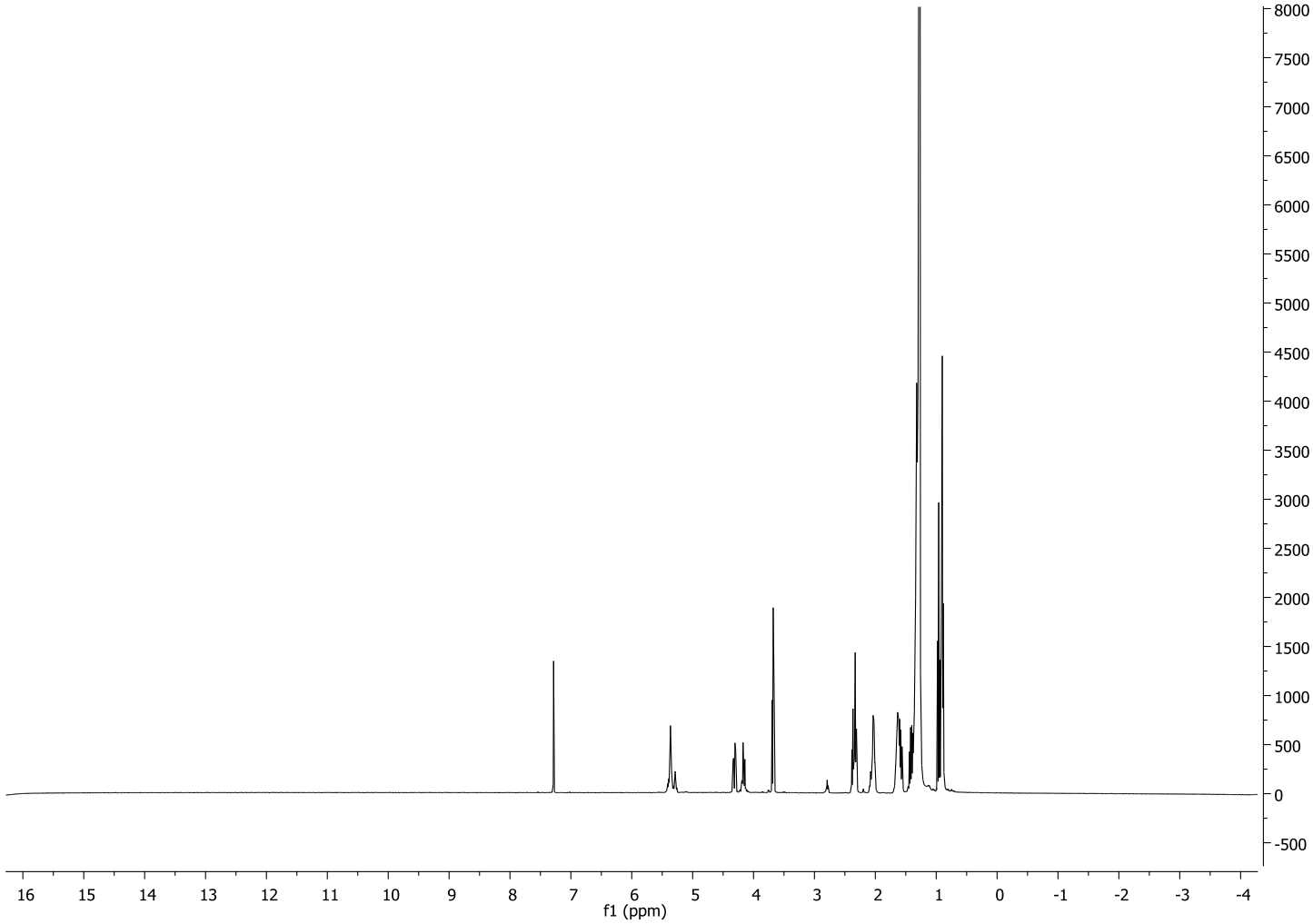

First approach. ^{1}H NMR spectrum A3

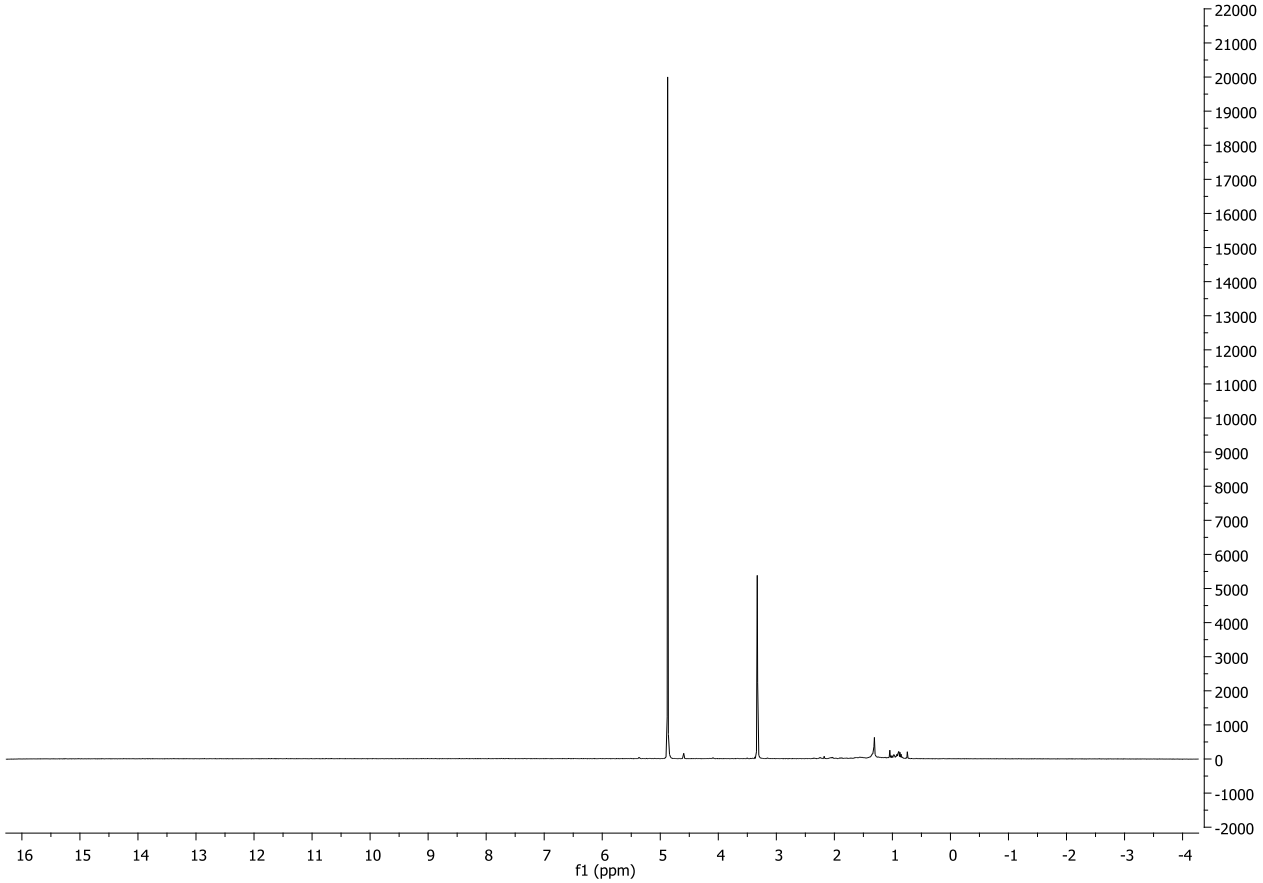

Second approach. ^{1}H NMR spectrum of J

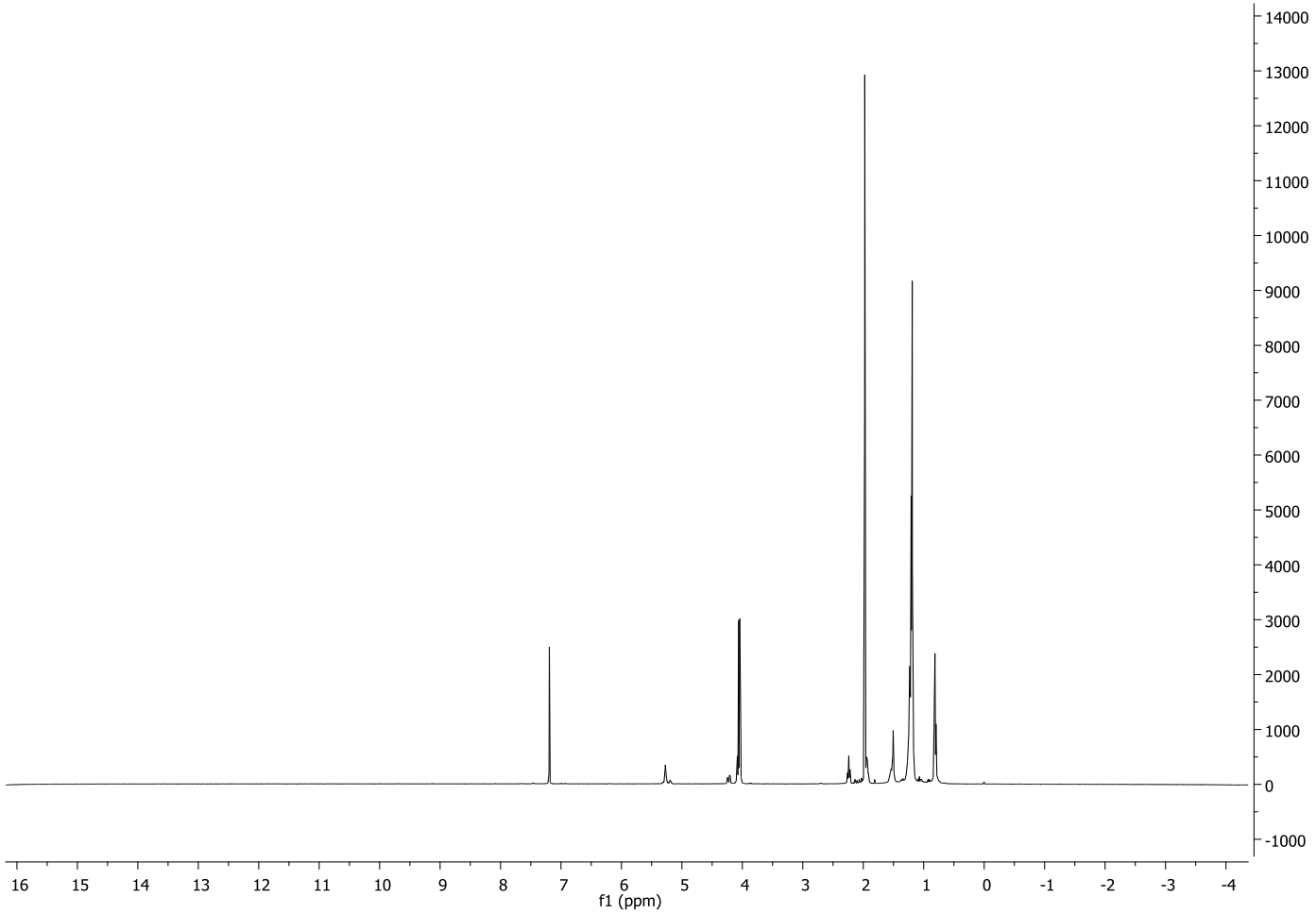

Second approach. ^{1}H NMR spectrum of L

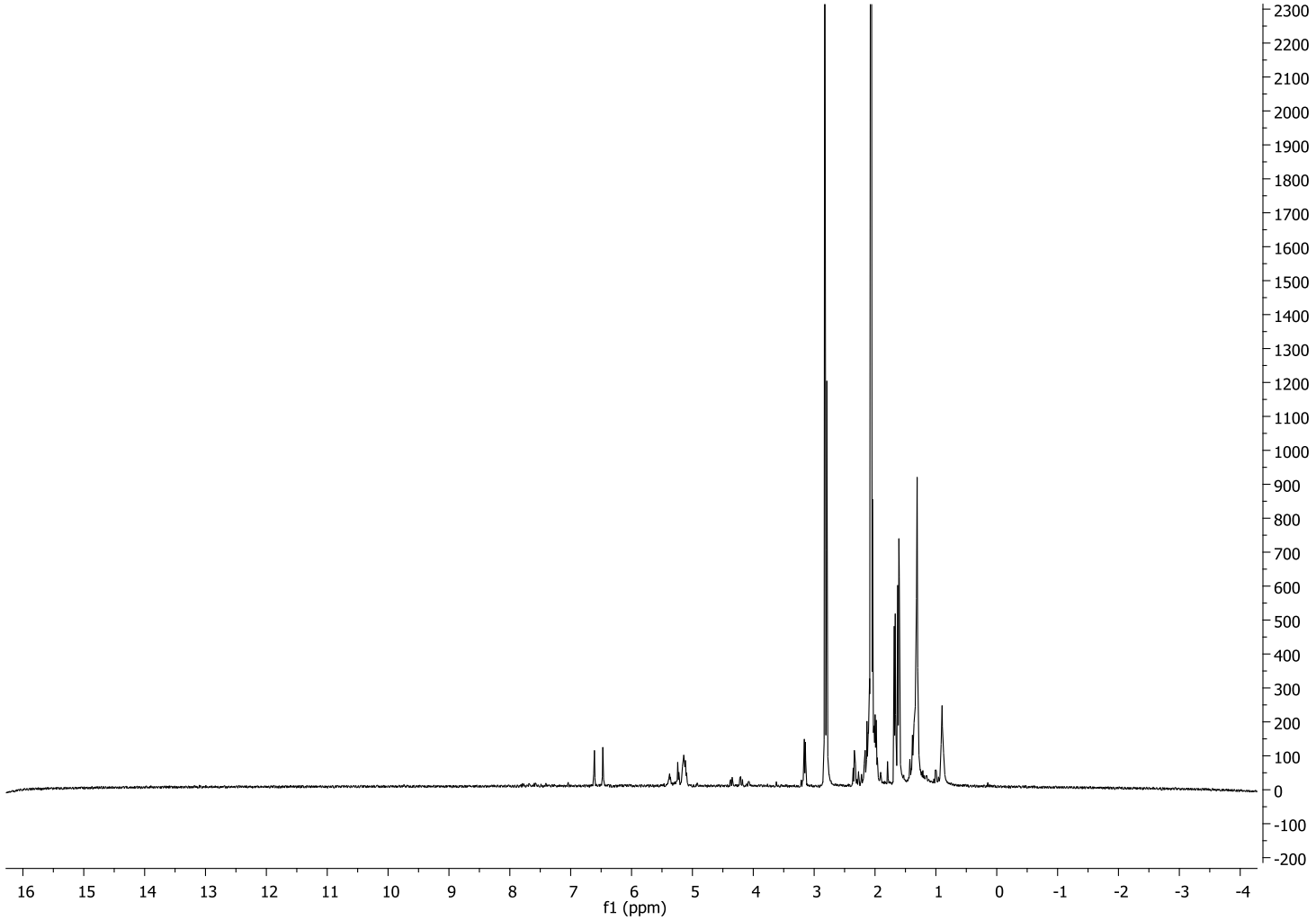

Second approach. ^{1}H NMR spectrum of N

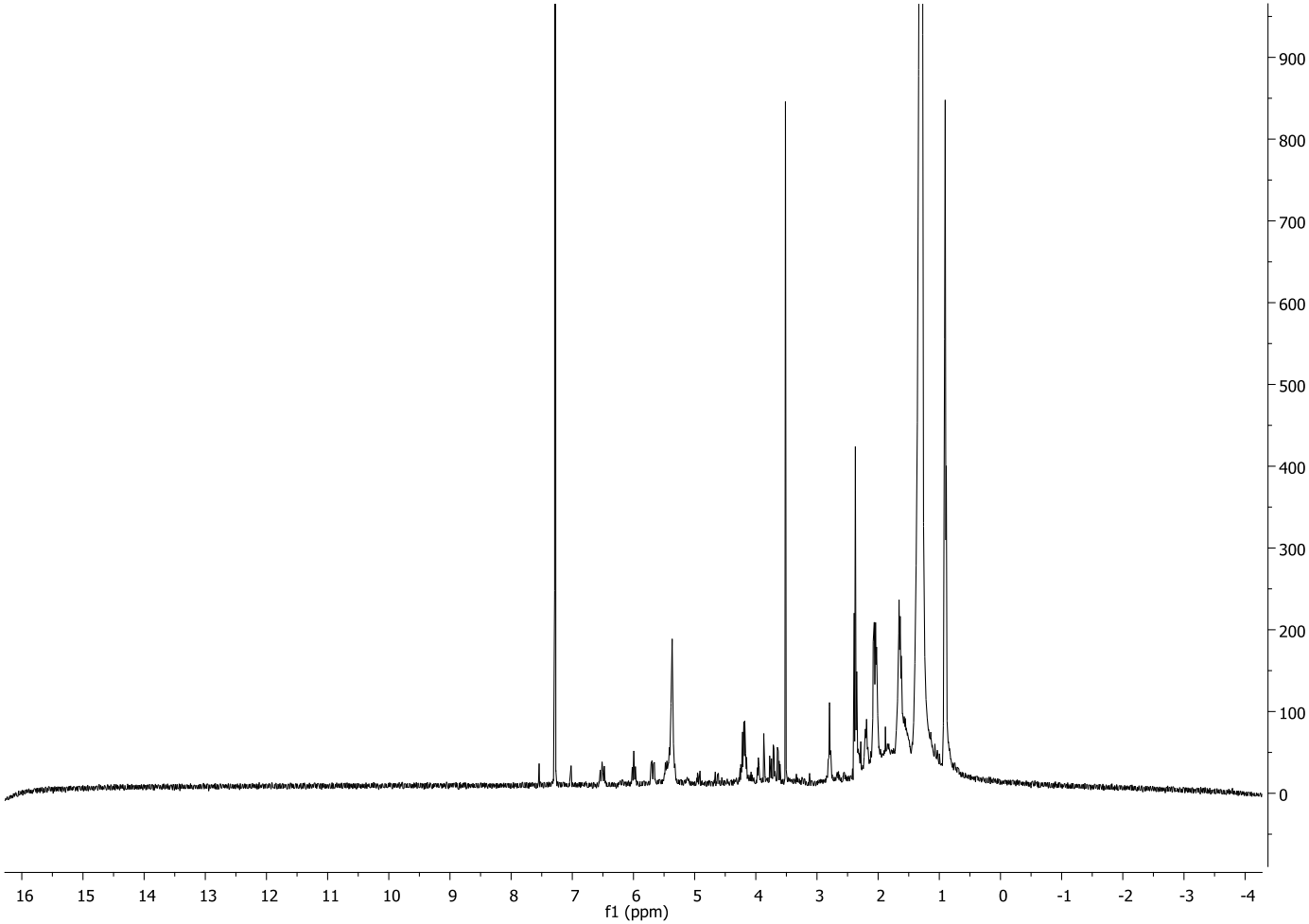

Third approach. ^{1}H NMR spectrum of Bi

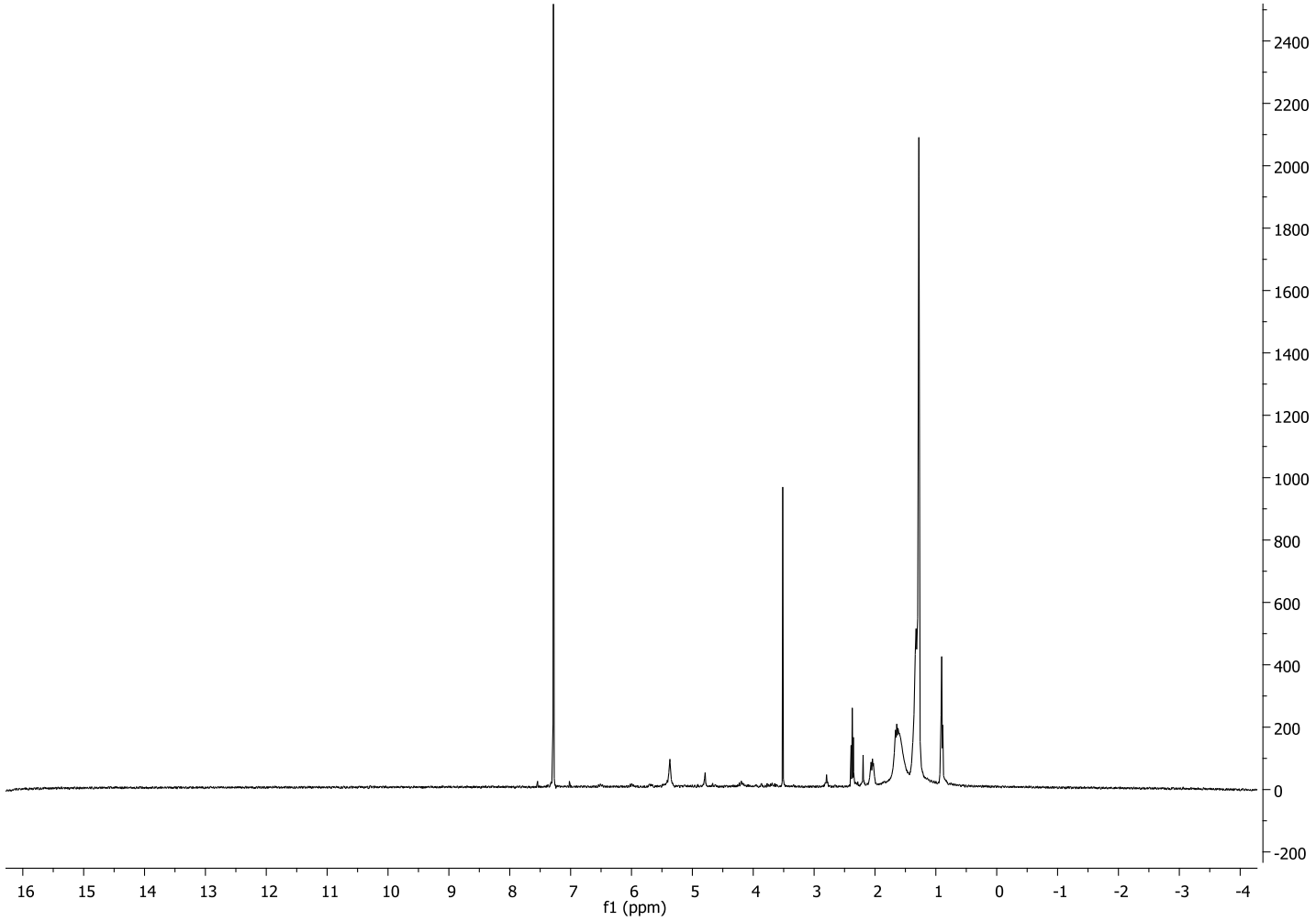

Third approach. ^{1}H NMR spectrum of Bii

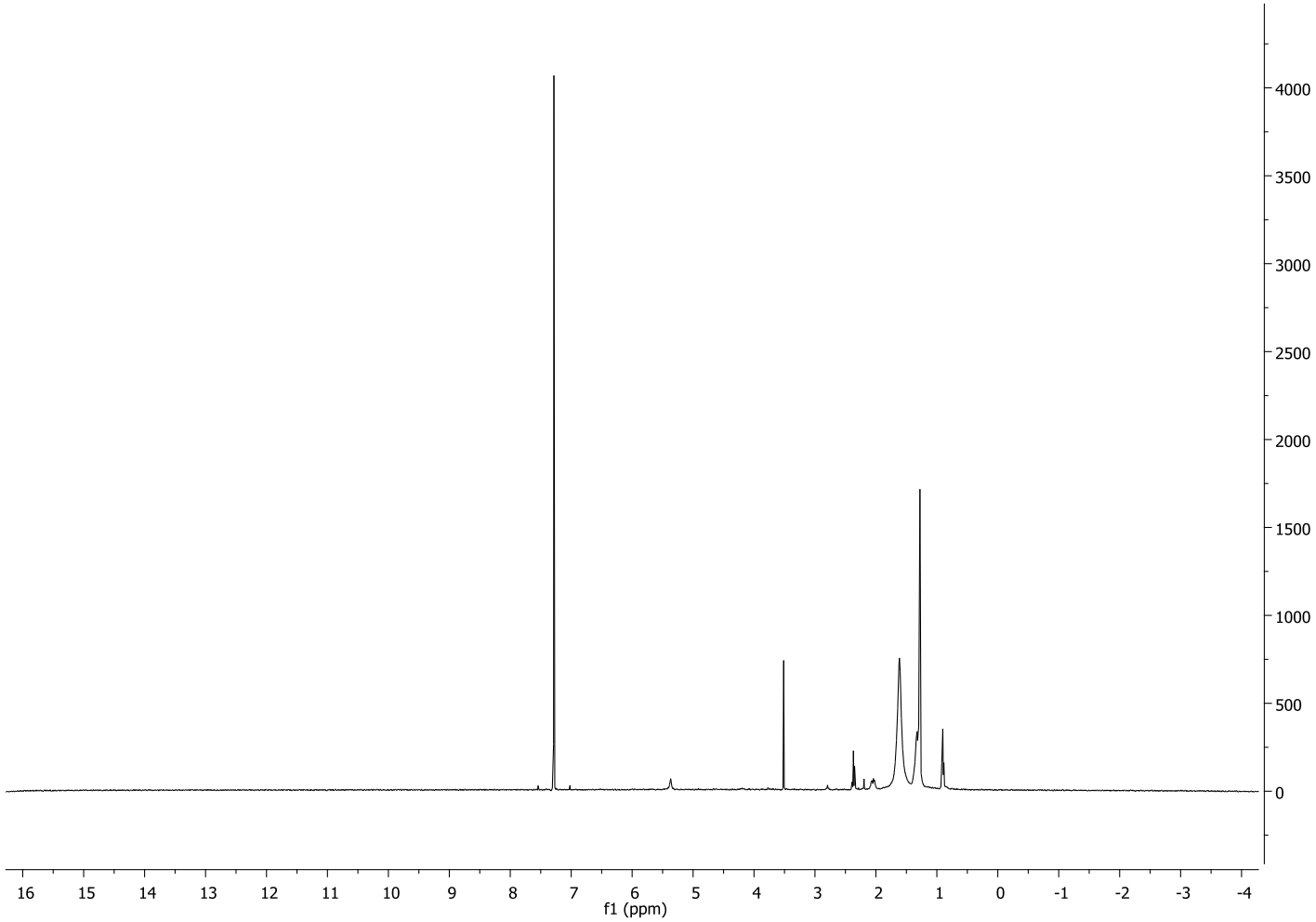

Third approach. ^{1}H NMR spectrum of Biii

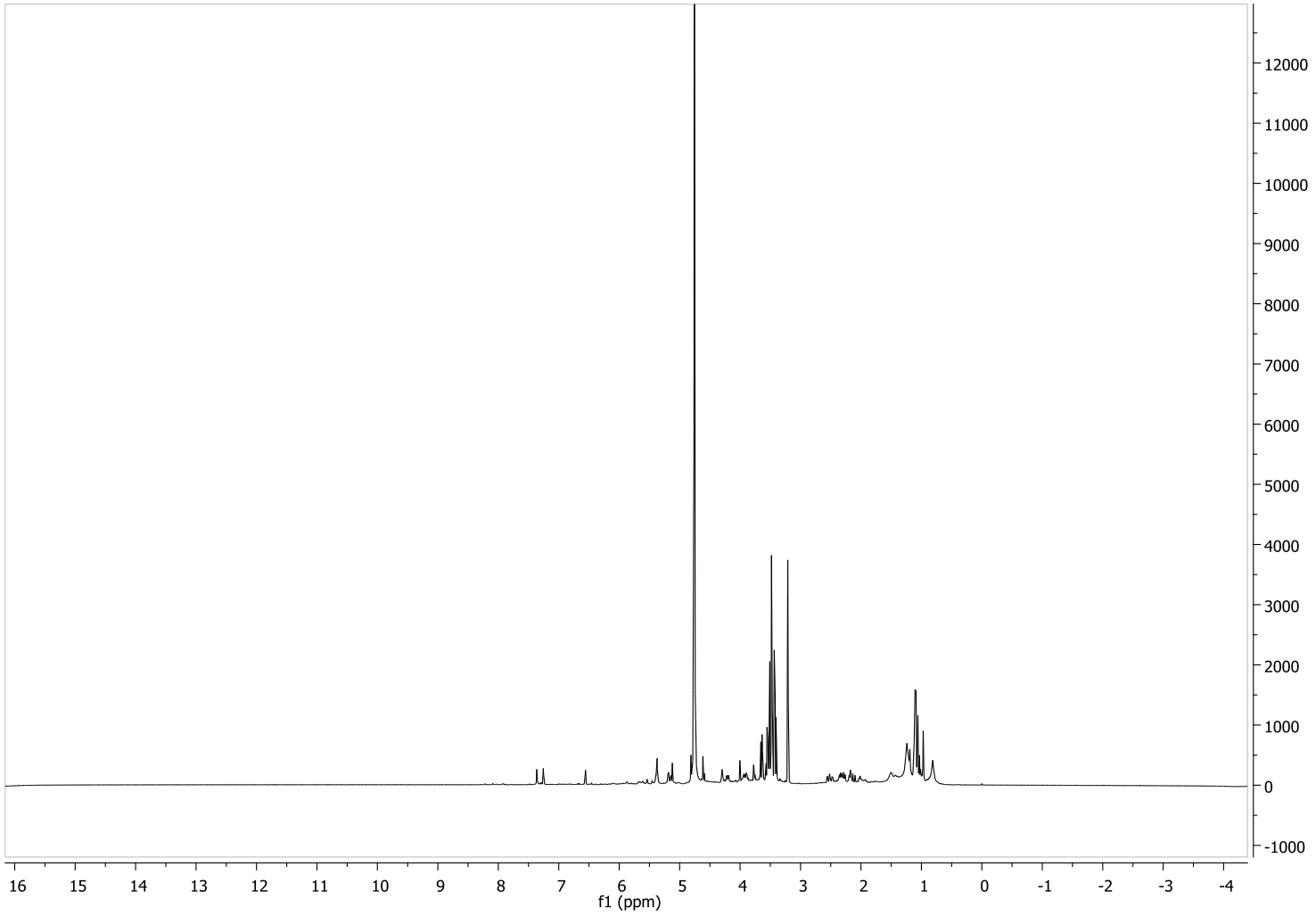

Fourth approach. ^{1}H NMR spectrum of C1

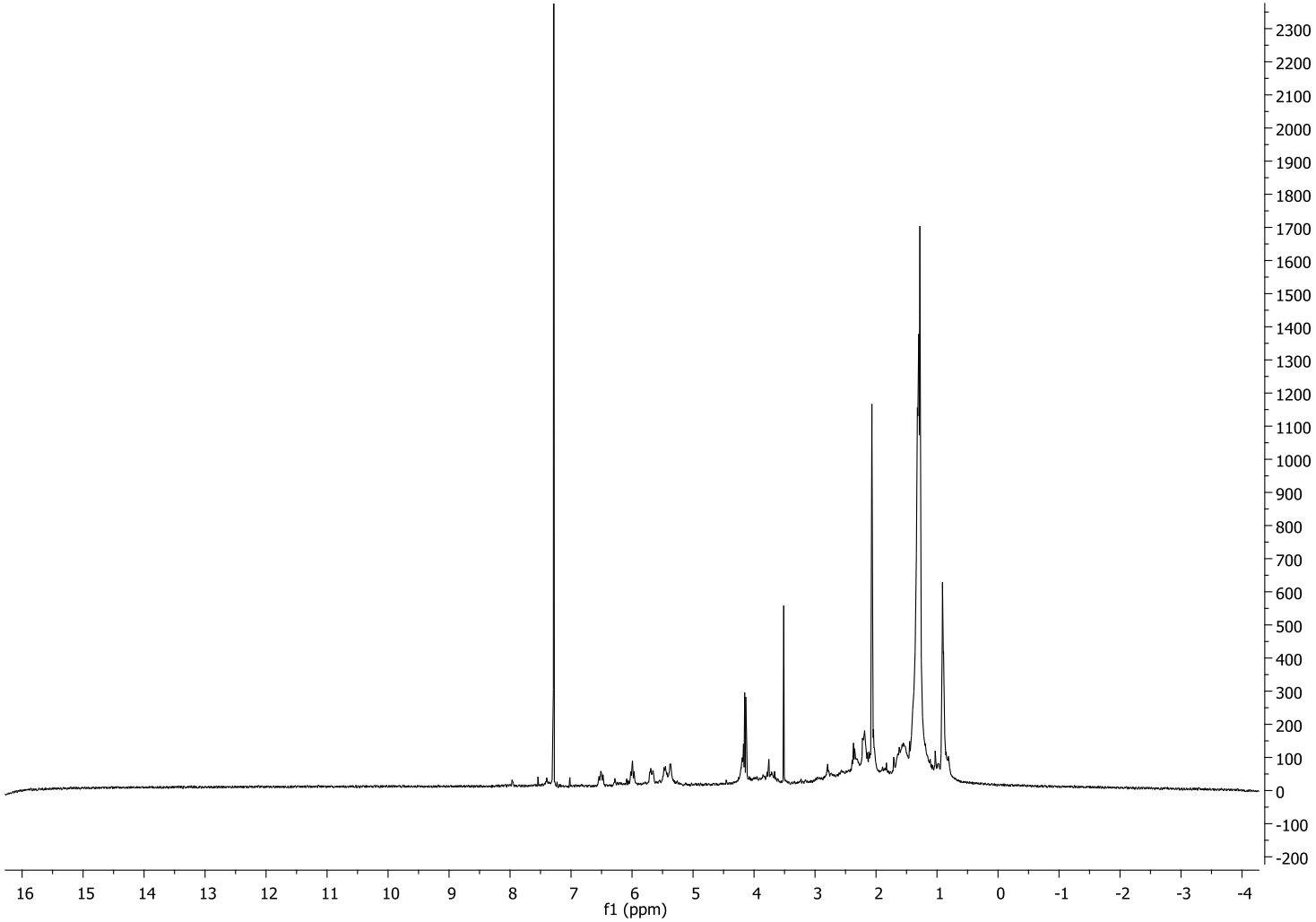

Fourth approach. ^{1}H NMR spectrum of C2

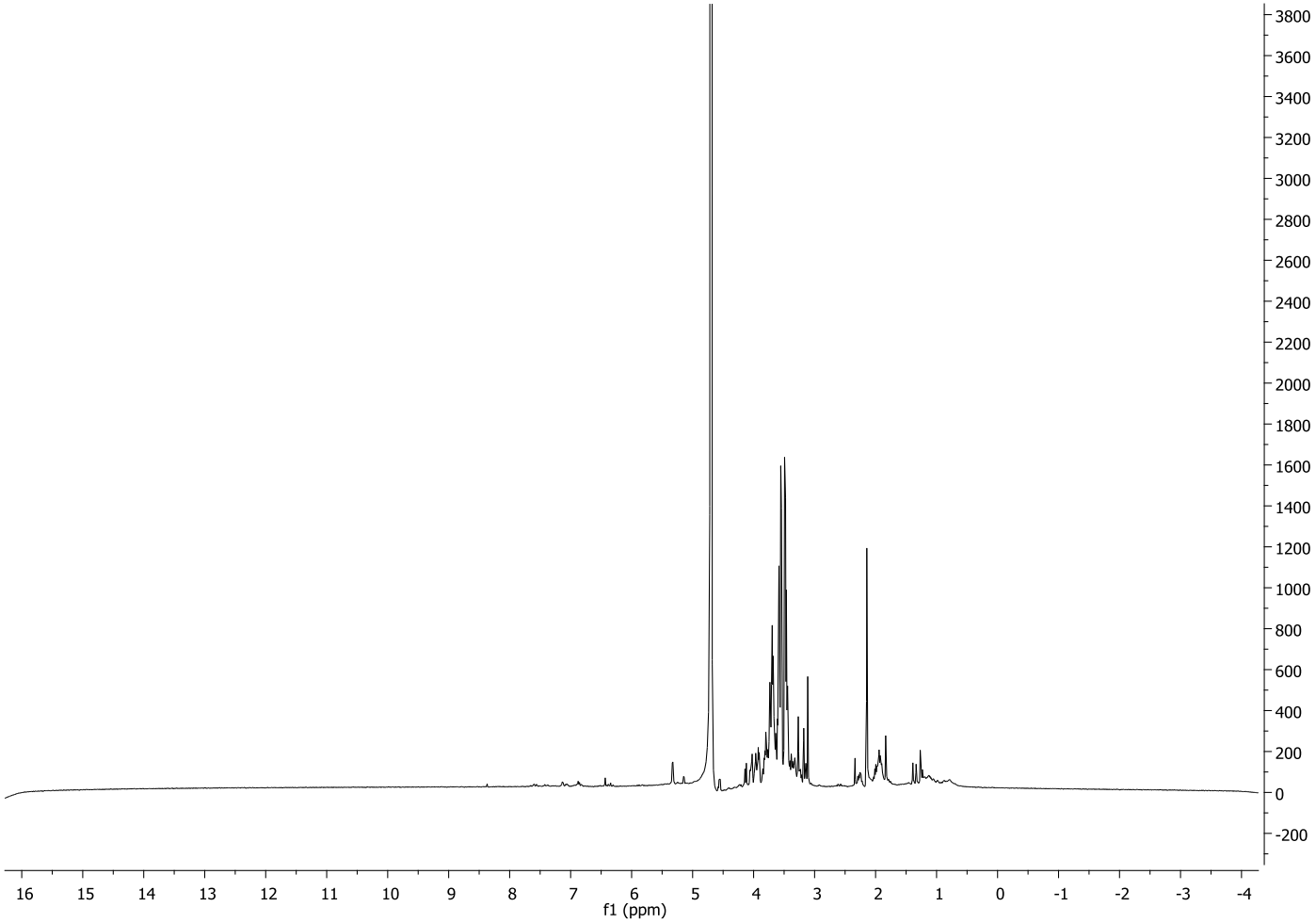

Fourth approach. ^{1}H NMR spectrum of C3

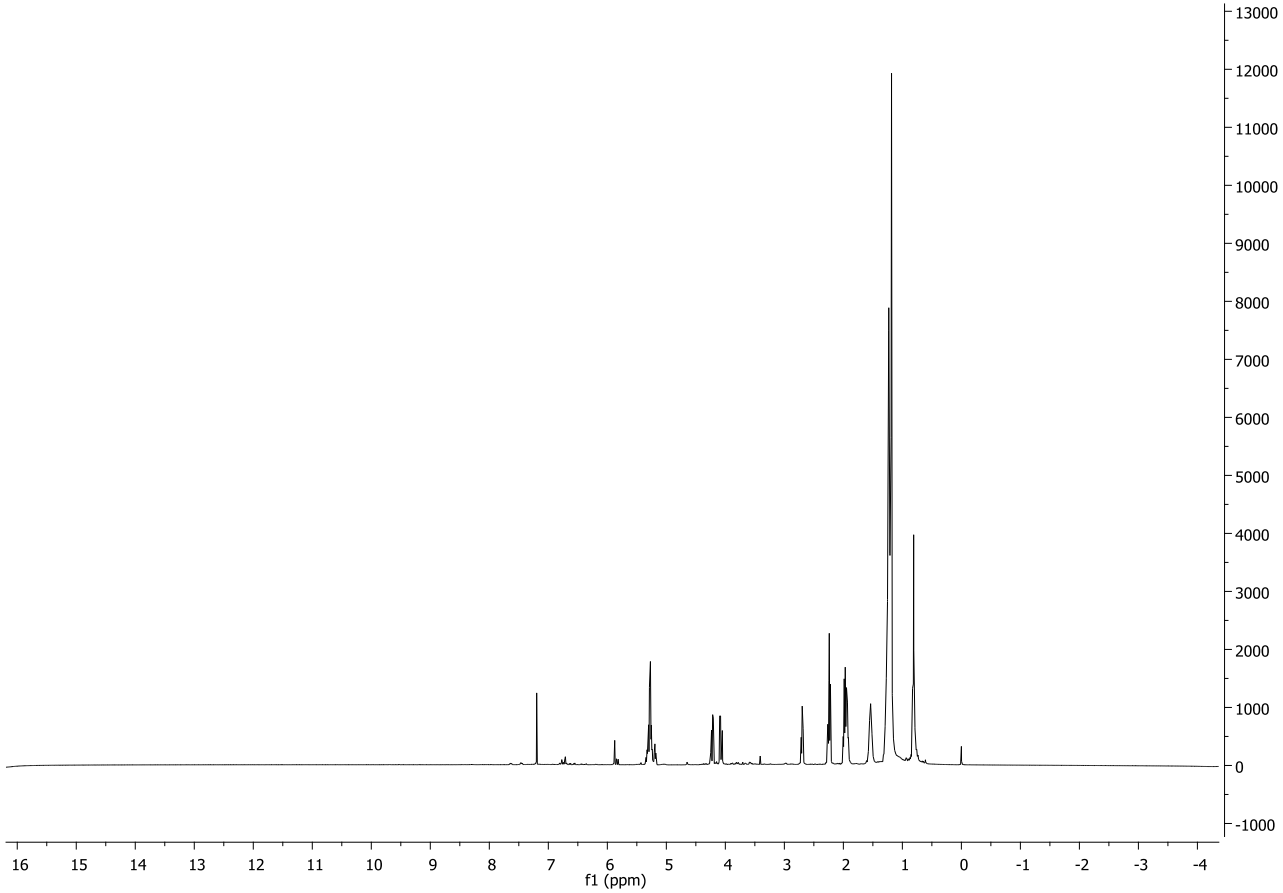

Fourth approach. ^{1}H NMR spectrum of C4

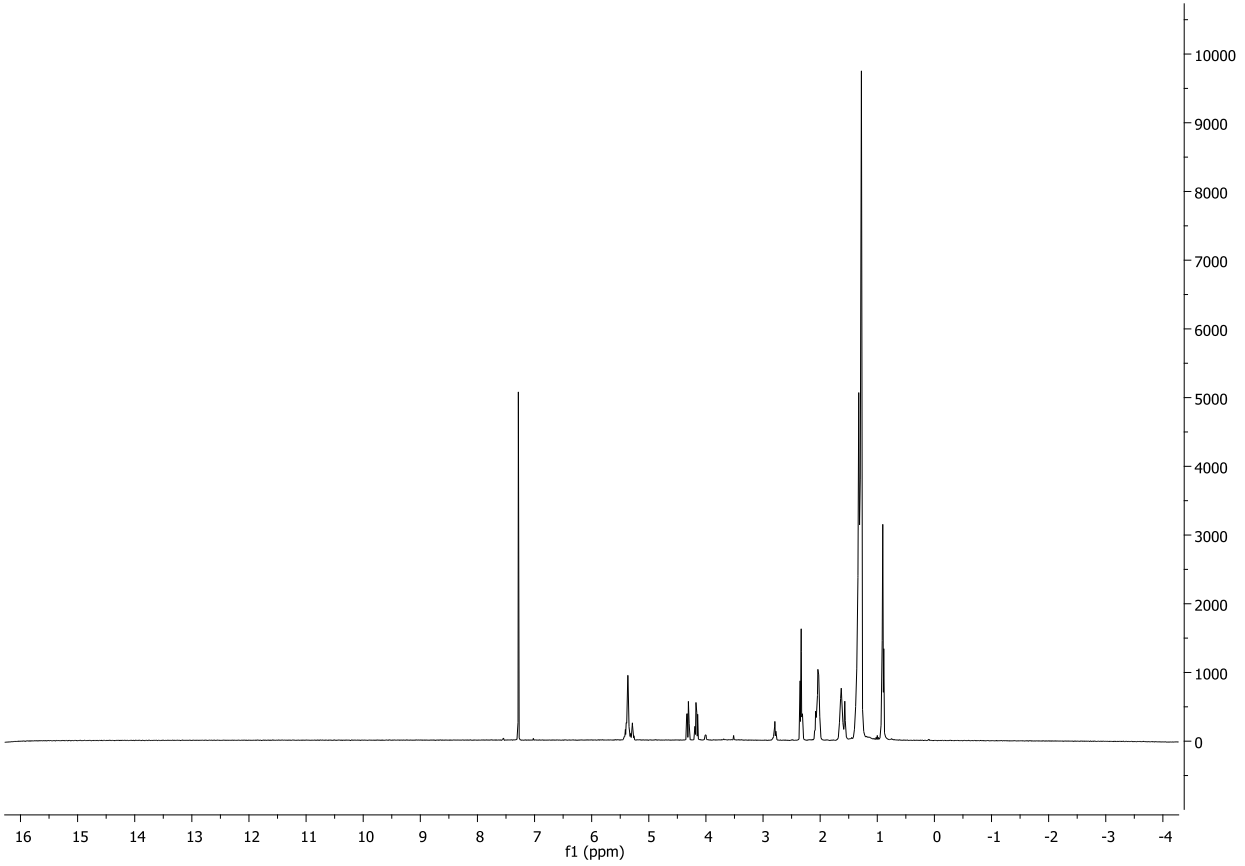

Fourth approach. ^{1}H NMR spectrum of AA

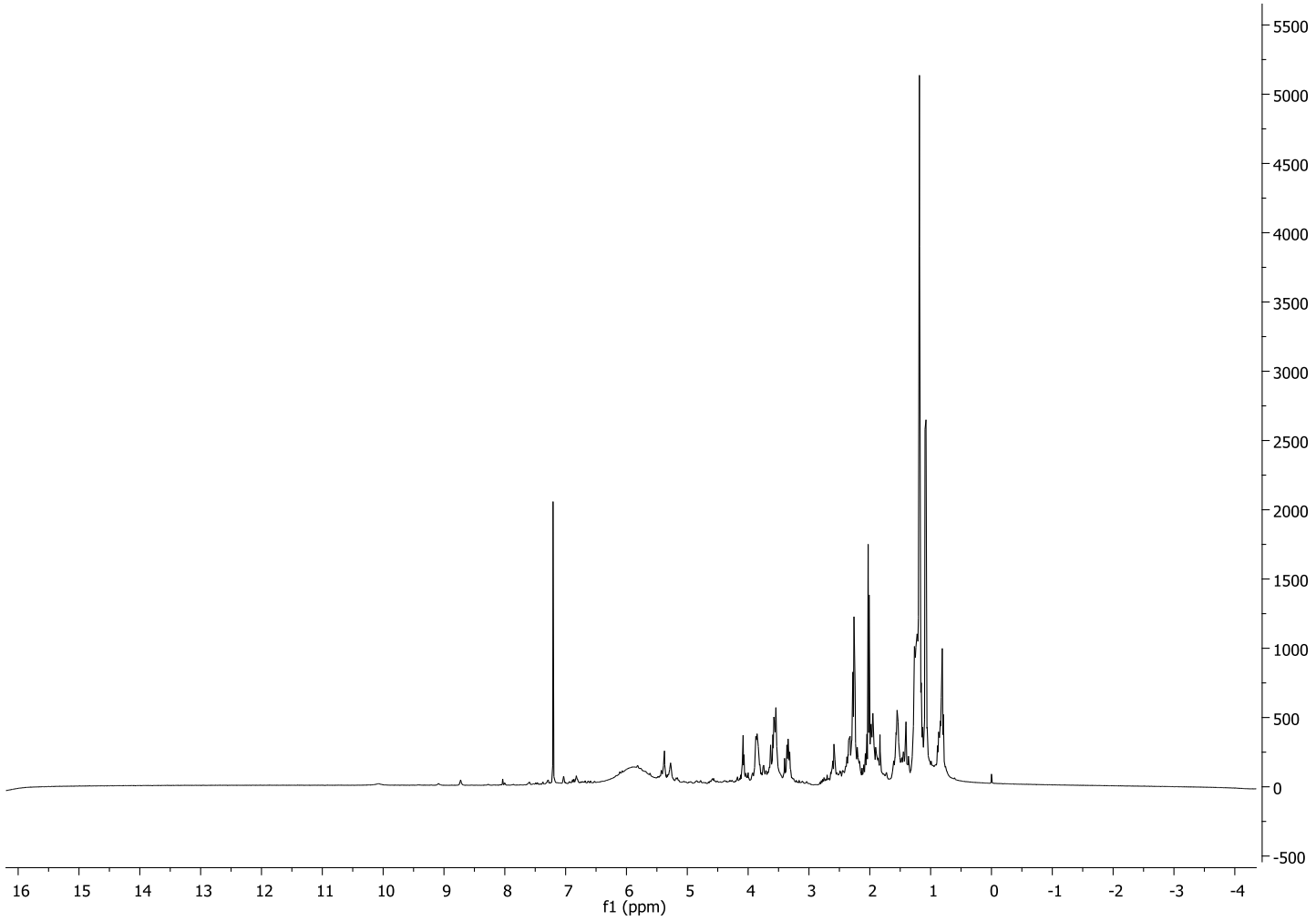

Fourth approach. ^{1}H NMR spectrum of GA

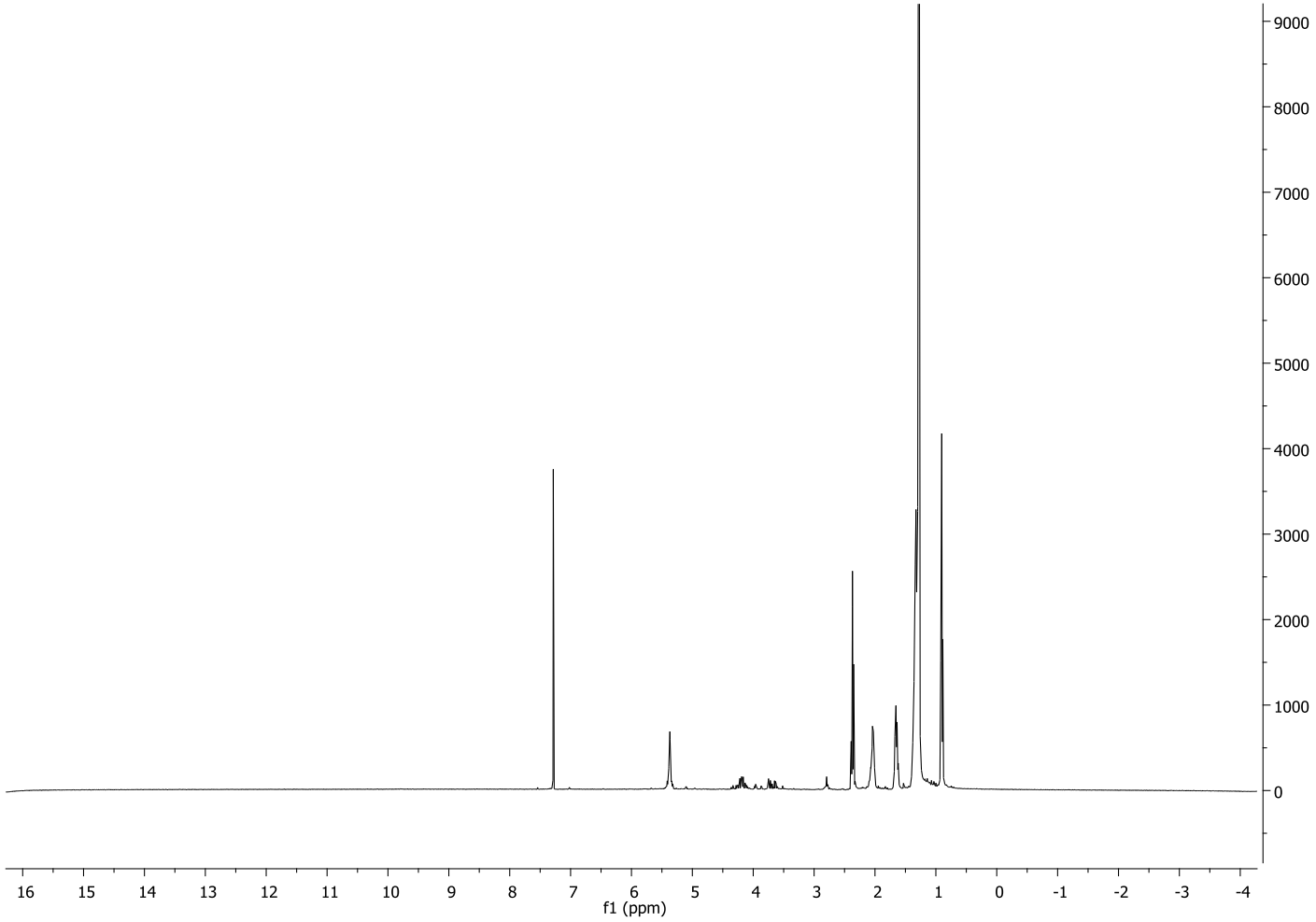

Fourth approach. ^{1}H NMR spectrum of Fr A

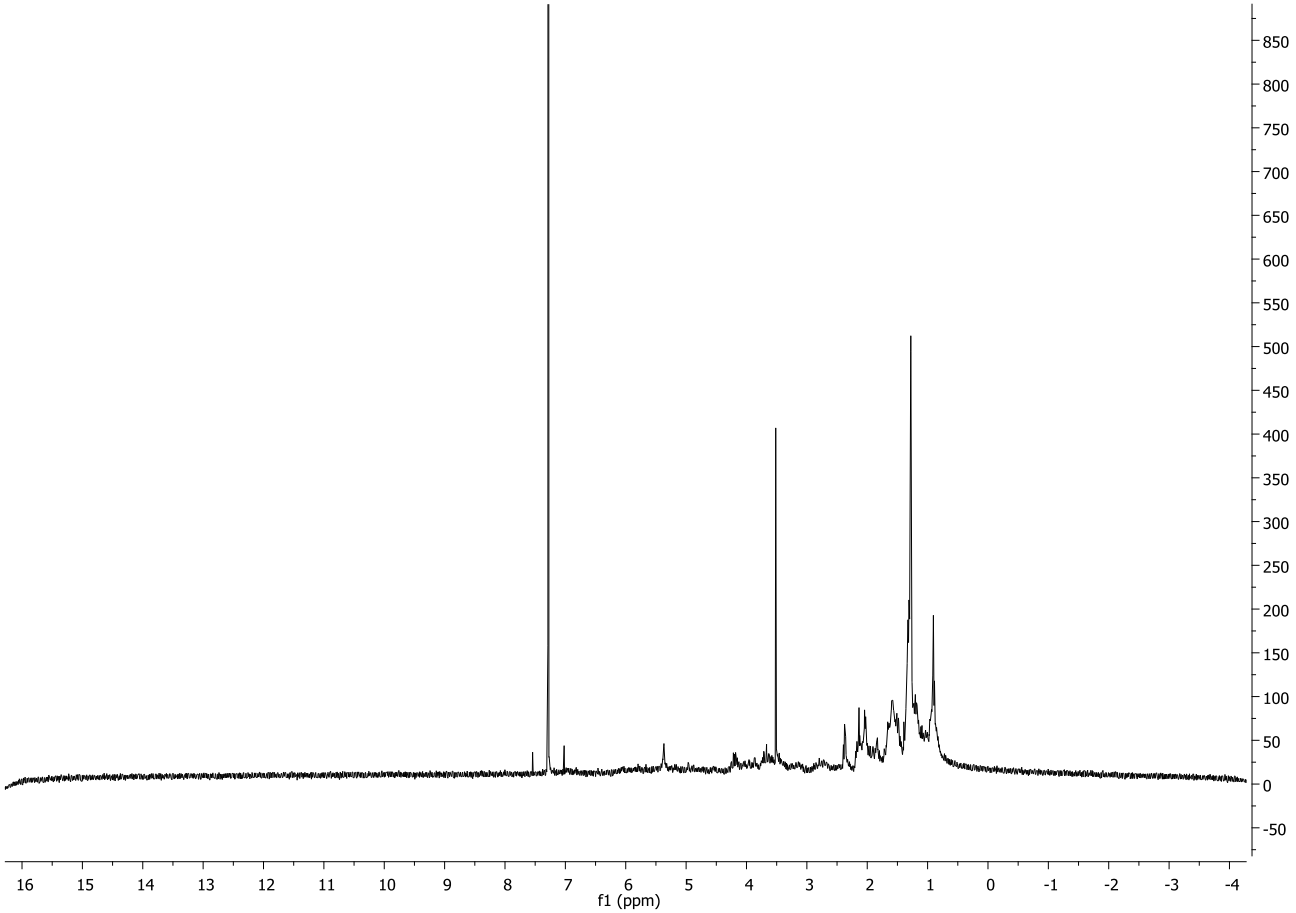

Fourth approach. ^{1}H NMR spectrum of Fr B

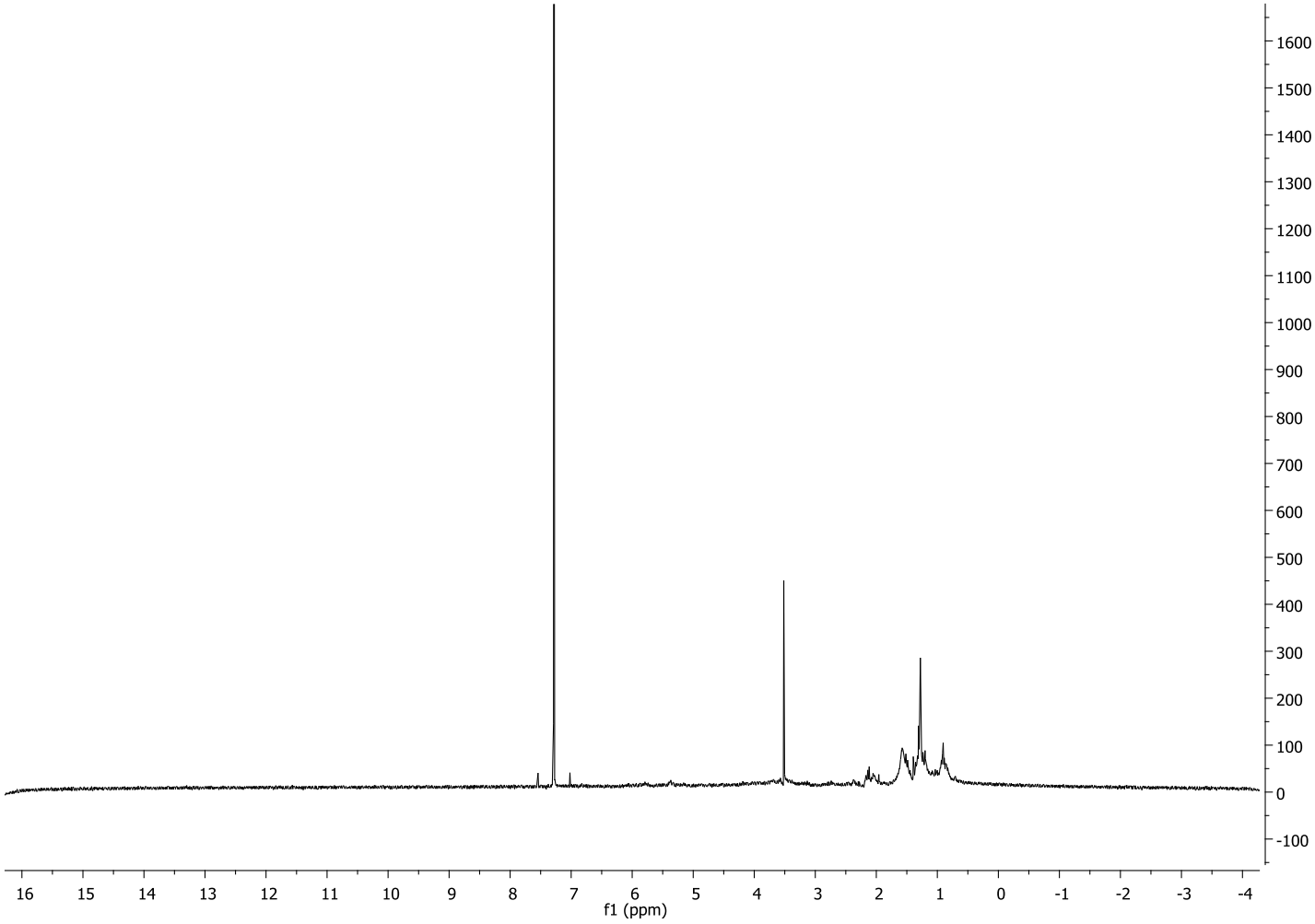

Fourth approach. ^{1}H NMR spectrum of Fr C

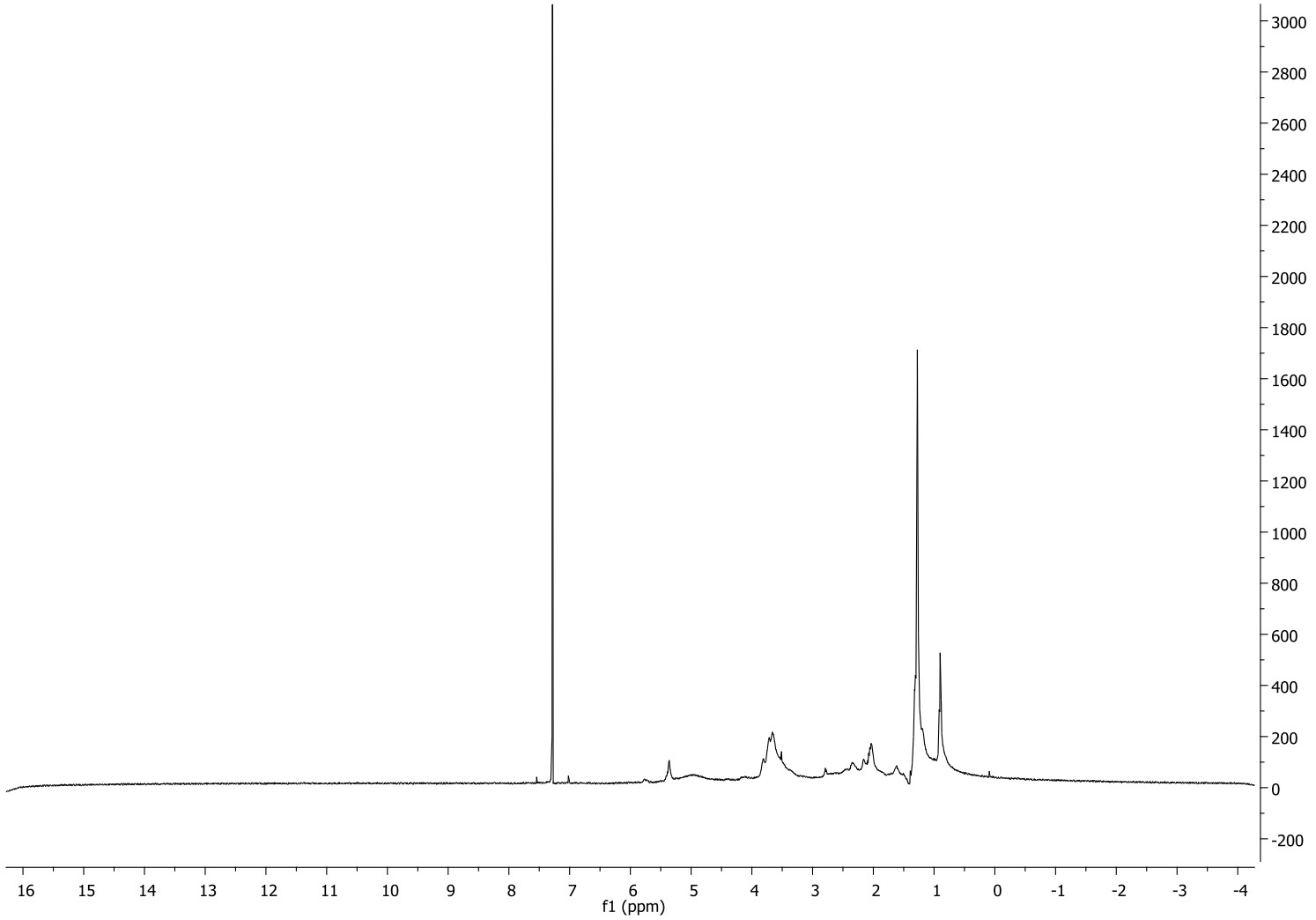

Fourth approach. ^{1}H NMR spectrum of Fr D

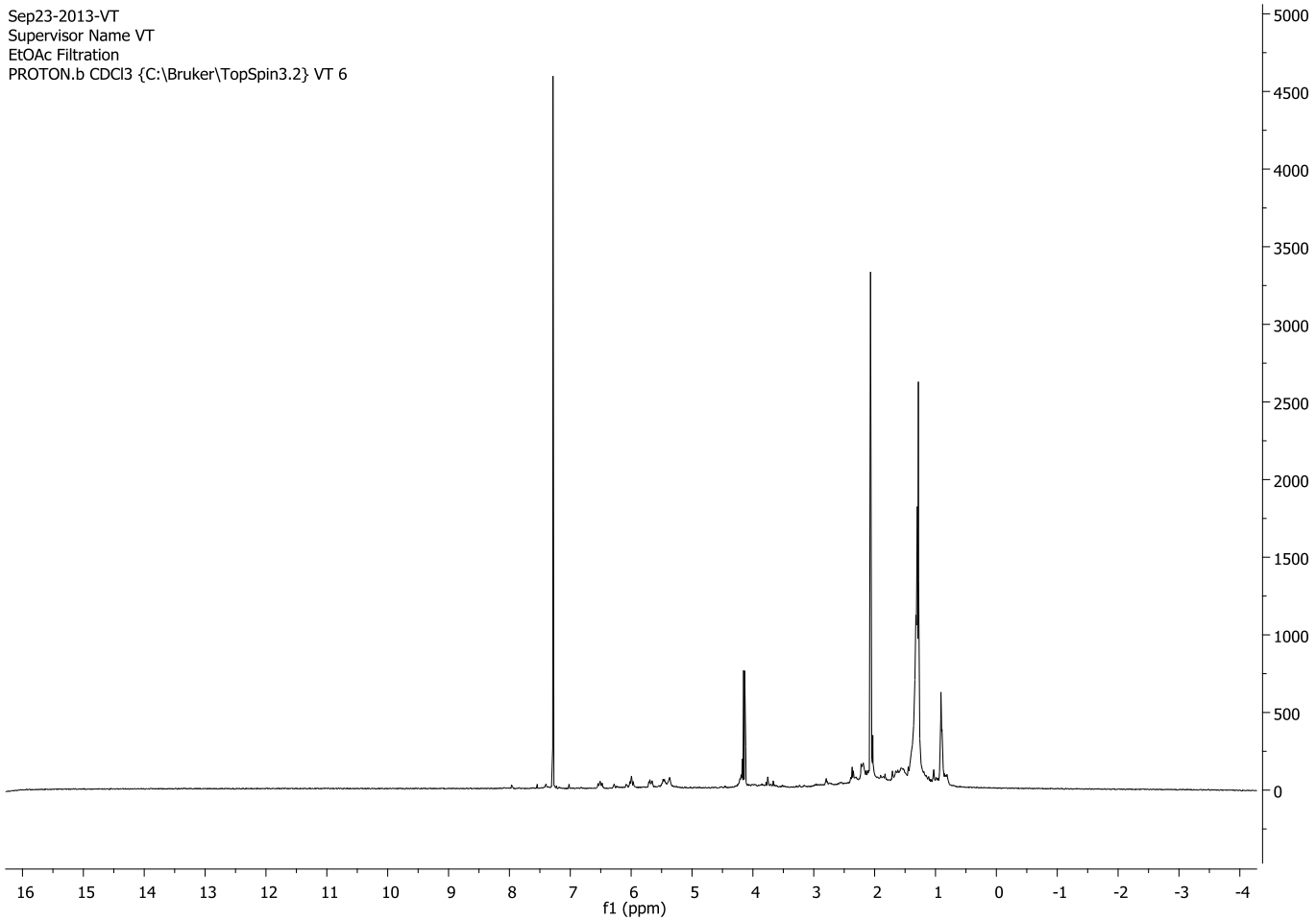

Fifth approach. ^{1}H NMR spectrum of Fr EF

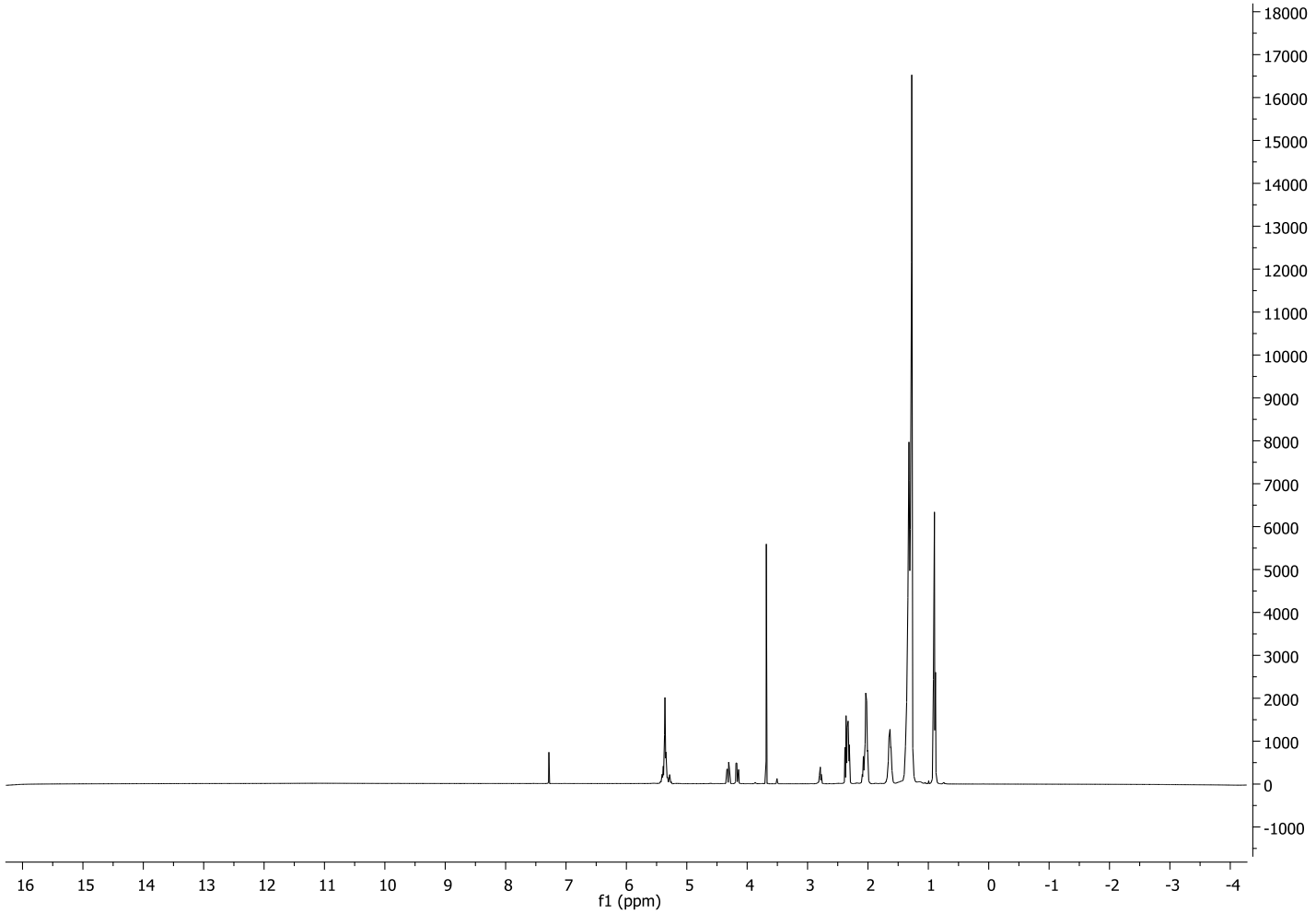

Fifth approach. ^{1}H NMR spectrum of Fr E3

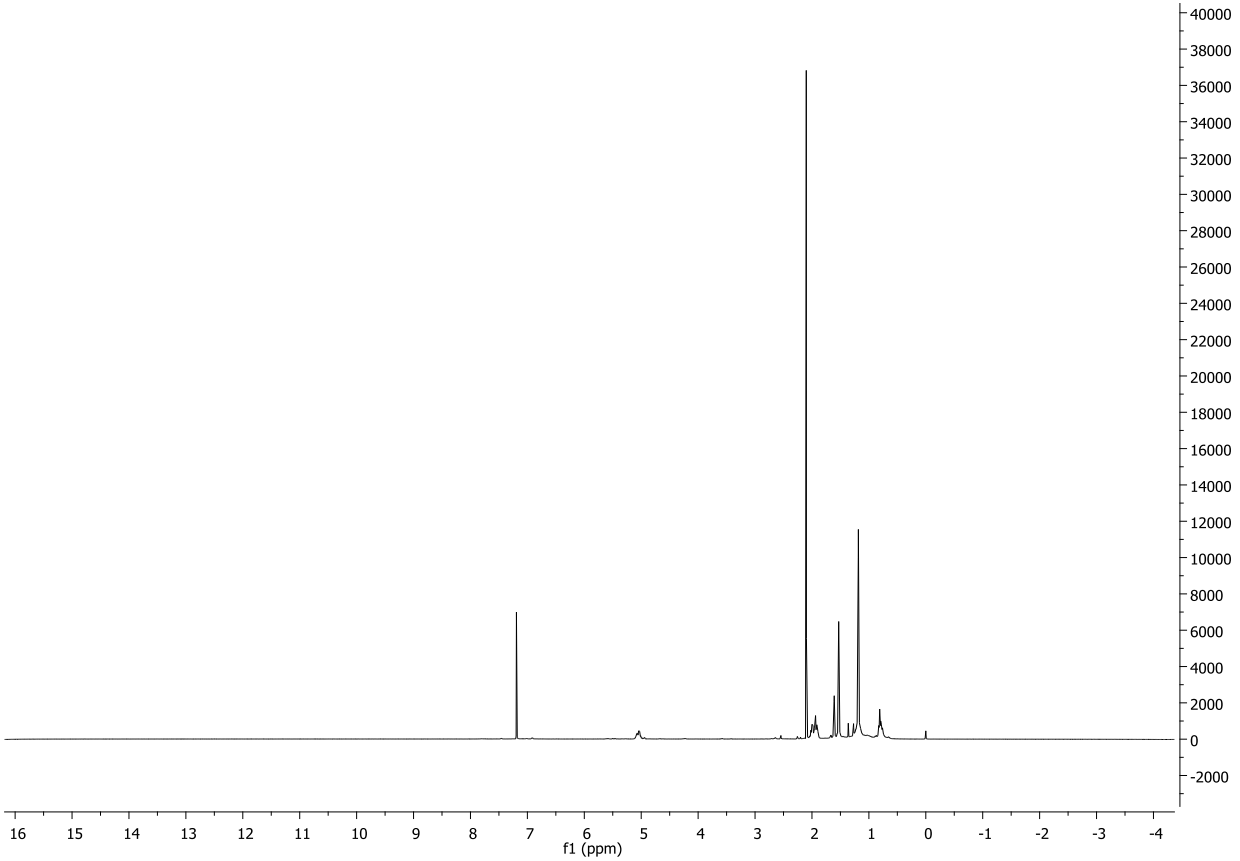

Fifth approach. ^{1}H NMR spectrum of Fr E50

APPENDIX IV

ncs | UK National Crystallography Service

A**Table 1.** Crystal data and structure refinement details.

Identification code	**2015ncs0159dlsza**	
Empirical formula	$C_{19}H_{12}O_6$	
Formula weight	336.29	
Temperature	30(2) K	
Wavelength	0.6889 Å	
Crystal system	Orthorhombic	
Space group	*Pna*21	
Unit cell dimensions	*a* = **18.4606(12) Å**	α = **90°**
	b = **4.9823(3) Å**	β = **90°**
	c = **15.4367(9) Å**	γ = **90°**
Volume	1419.81(15) Å^3	
Z	4	
Density (calculated)	1.573 Mg / m^3	
Absorption coefficient	0.111 mm^{-1}	
F(000)	696	
Crystal	Plate; colourless	
Crystal size	0.06 × 0.04 × 0.01 mm^3	
θ range for data collection	2.139 – 26.570°	
Index ranges	$-23 \le h \le 23$, $-6 \le k \le 6$, $-20 \le l \le 19$	
Reflections collected	12686	
Independent reflections	3061 [R_{int} = 0.1303]	
Completeness to θ = 24.415°	99.9 %	
Absorption correction	Semi–empirical from equivalents	
Max. and min. transmission	1.00000 and 0.40576	
Refinement method	Full-matrix least-squares on F^2	
Data / restraints / parameters	3061 / 1 / 227	

Goodness-of-fit on F^2	1.012
Final R indices [$F^2 > 2\sigma(F^2)$]	$R1$ = 0.0661, $wR2$ = 0.1572
R indices (all data)	$R1$ = 0.1173, $wR2$ = 0.1888
Absolute structure parameter	−0.3(10)
Extinction coefficient	n/a
Largest diff. peak and hole	0.261 and −0.311 e Å^{-3}

Diffractometer: Beamline I19 situated on an undulator insertion device with a combination of double crystal monochromator, vertical and horizontal focussing mirrors and a series of beam slits (primary white beam and either side of the focussing mirrors). The experimental hutch (EH1) is equipped with a Crystal Logic 4-circle kappa geometry goniometer with a Rigaku Saturn 724 CCD detector and an Oxford Cryosystems Cryostream plus cryostat (80-500K). For conventional service crystallography the beamline operates at a typical energy of 18 keV (Zr K absorption edge) and a Rigaku ACTOR robotic sample changing system is available. **Cell determination and data collection**: *CrystalClear-SM Expert 2.0 r5* (Rigaku, 2010). **Data reduction, cell refinement and absorption correction**: *CrysAlisPro 1.171.37.35* (Agilent, 2014). **Structure solution**: *SHELXT-2014* (Sheldrick, G.M. (2015). Acta Cryst. A71, 3-8). **Structure refinement**: *SHELXL-2014* (Sheldrick, G.M. (2015). Acta Cryst. C71, 3-8). **Graphics:** *OLEX2* (Dolomanov, O. V., Bourhis, L. J., Gildea, R. J., Howard, J. A. K. & Puschmann, H. (2009). J. Appl. Cryst. 42, 339-341).

Special details:

Table 2. Atomic coordinates [$\times 10^4$], equivalent isotropic displacement parameters [$Å^2 \times 10^3$] and site occupancy factors. U_{eq} is defined as one third of the trace of the orthogonalized U^{ij} tensor.

Atom	*x*	*y*	*z*	U_{eq}	*S.o.f.*
O1	6930(2)	7091(9)	4981(3)	28(1)	1
O2	8507(3)	14105(10)	4549(4)	40(1)	1
O3	6098(3)	7530(9)	2555(3)	36(1)	1
O4	5448(2)	4300(9)	3754(3)	31(1)	1
O5	4937(3)	−1798(9)	6097(3)	32(1)	1
O6	5456(3)	−1115(9)	7445(3)	33(1)	1
C1	7194(3)	8946(13)	4422(4)	27(1)	1
C2	7739(3)	10654(13)	4725(4)	29(1)	1
C3	8098(4)	11090(15)	5528(5)	38(2)	1
C4	8548(4)	13172(16)	5388(5)	40(2)	1
C5	7998(3)	12538(12)	4152(5)	30(2)	1
C6	7779(4)	12803(14)	3301(5)	37(2)	1
C7	7240(3)	11123(12)	3016(5)	30(1)	1
C8	6933(3)	9170(12)	3578(4)	26(1)	1
C9	6344(3)	7491(13)	3300(4)	28(1)	1
C10	6052(3)	5746(12)	3965(4)	26(1)	1
C11	6350(3)	5535(12)	4767(4)	24(1)	1
C12	6130(3)	3801(13)	5477(4)	25(1)	1
C13	5618(3)	1764(13)	5352(4)	27(1)	1
C14	5435(3)	264(12)	6060(4)	24(1)	1
C15	4876(4)	−2486(14)	7007(4)	31(1)	1
C16	5738(4)	676(13)	6874(4)	28(1)	1
C17	6233(4)	2639(13)	7006(5)	29(1)	1
C18	6435(3)	4198(13)	6289(4)	28(2)	1
C19	4783(4)	5750(14)	3916(5)	36(2)	1

Table 3. Bond lengths [Å] and angles [°].

O1–C1	1.355(8)	C15–H15A	0.9900
O1–C11	1.361(7)	C15–H15B	0.9900
O2–C4	1.377(9)	C16–C17	1.354(9)
O2–C5	1.367(8)	C17–H17	0.9500
O3–C9	1.237(8)	C17–C18	1.402(10)
O4–C10	1.366(8)	C18–H18	0.9500
O4–C19	1.447(8)	C19–H19A	0.9800
O5–C14	1.379(7)	C19–H19B	0.9800
O5–C15	1.449(8)	C19–H19C	0.9800
O6–C15	1.438(8)		
O6–C16	1.358(8)	C1–O1–C11	121.2(5)
C1–C2	1.397(9)	C5–O2–C4	105.5(6)
C1–C8	1.394(9)	C10–O4–C19	112.8(5)
C2–C3	1.422(10)	C14–O5–C15	105.5(5)
C2–C5	1.377(9)	C16–O6–C15	106.9(5)
C3–H3	0.9500	O1–C1–C2	117.5(6)
C3–C4	1.346(11)	O1–C1–C8	121.7(6)
C4–H4	0.9500	C8–C1–C2	120.9(6)
C5–C6	1.380(10)	C1–C2–C3	136.1(7)
C6–H6	0.9500	C5–C2–C1	116.8(6)
C6–C7	1.374(9)	C5–C2–C3	107.1(6)
C7–H7	0.9500	C2–C3–H3	127.3
C7–C8	1.421(9)	C4–C3–C2	105.4(7)
C8–C9	1.438(9)	C4–C3–H3	127.3
C9–C10	1.450(9)	O2–C4–H4	123.9
C10–C11	1.360(9)	C3–C4–O2	112.1(6)
C11–C12	1.453(9)	C3–C4–H4	123.9
C12–C13	1.400(9)	O2–C5–C2	109.8(7)
C12–C18	1.388(9)	O2–C5–C6	125.0(6)
C13–H13	0.9500	C2–C5–C6	125.1(6)
C13–C14	1.368(9)	C5–C6–H6	121.3
C14–C16	1.390(9)	C7–C6–C5	117.3(7)

C7–C6–H6	121.3	C17–C16–C14	121.0(6)
C6–C7–H7	119.6	C16–C17–H17	121.3
C6–C7–C8	120.7(7)	C16–C17–C18	117.4(6)
C8–C7–H7	119.6	C18–C17–H17	121.3
C1–C8–C7	119.2(6)	C12–C18–C17	121.7(6)
C1–C8–C9	119.6(6)	C12–C18–H18	119.1
C7–C8–C9	121.1(6)	C17–C18–H18	119.1
O3–C9–C8	123.1(6)	O4–C19–H19A	109.5
O3–C9–C10	122.1(6)	O4–C19–H19B	109.5
C8–C9–C10	114.8(6)	O4–C19–H19C	109.5
O4–C10–C9	116.8(5)	H19A–C19–H19B	109.5
C11–C10–O4	120.5(5)	H19A–C19–H19C	109.5
C11–C10–C9	122.7(6)	H19B–C19–H19C	109.5
O1–C11–C12	112.1(5)		
C10–C11–O1	119.7(5)		
C10–C11–C12	128.2(6)		
C13–C12–C11	121.1(6)		
C18–C12–C11	118.8(6)		
C18–C12–C13	120.1(6)		
C12–C13–H13	121.5		
C14–C13–C12	117.0(6)		
C14–C13–H13	121.5		
O5–C14–C16	109.9(5)		
C13–C14–O5	127.3(6)		
C13–C14–C16	122.8(6)		
O5–C15–H15A	110.4		
O5–C15–H15B	110.4		
O6–C15–O5	106.6(5)		
O6–C15–H15A	110.4		
O6–C15–H15B	110.4		
H15A–C15–H15B	108.6		
O6–C16–C14	109.6(6)		
C17–C16–O6	129.5(6)		

Symmetry transformations used to generate equivalent atoms:

Table 4. Anisotropic displacement parameters [Å$^2\times 10^3$]. The anisotropic displacement factor exponent takes the form: $-2\pi^2[h^2a^{*2}U^{11} + \cdots + 2\ h\ k\ a^*\ b^*\ U^{12}\ ]$.

Atom	U^{11}	U^{22}	U^{33}	U^{23}	U^{13}	U^{12}
O1	33(2)	24(2)	28(2)	1(2)	1(2)	−1(2)
O2	35(3)	29(3)	57(4)	−11(2)	8(2)	−7(2)
O3	55(3)	31(2)	21(3)	2(2)	1(2)	−5(2)
O4	42(3)	28(2)	24(2)	2(2)	1(2)	−3(2)
O5	46(3)	28(2)	21(2)	0(2)	1(2)	−6(2)
O6	47(3)	27(2)	25(2)	2(2)	−2(2)	−4(2)
C1	30(3)	19(3)	31(4)	1(3)	6(2)	−1(3)
C2	33(3)	22(3)	32(4)	−6(3)	2(3)	1(3)
C3	43(4)	36(4)	34(4)	−4(3)	4(3)	3(3)
C4	35(4)	39(4)	44(5)	−17(4)	−3(3)	0(3)
C5	29(3)	21(3)	41(4)	−5(3)	6(3)	−4(3)
C6	39(4)	24(4)	47(5)	−2(3)	13(3)	1(3)
C7	39(3)	24(3)	25(3)	−3(3)	8(3)	−5(3)
C8	33(3)	21(3)	24(3)	−3(3)	3(3)	−2(3)
C9	35(3)	27(3)	22(4)	0(3)	5(3)	0(3)
C10	37(3)	20(3)	21(3)	0(2)	2(2)	−6(3)
C11	27(3)	20(3)	25(3)	−5(2)	2(2)	−1(2)
C12	25(3)	23(3)	28(4)	−1(3)	2(2)	1(3)
C13	31(3)	27(3)	23(4)	−5(3)	1(2)	−1(3)
C14	32(3)	16(3)	23(3)	1(2)	2(3)	−1(3)
C15	45(4)	27(3)	21(3)	3(3)	−2(3)	2(3)
C16	37(3)	23(3)	25(4)	3(3)	4(3)	4(3)
C17	36(3)	24(3)	27(3)	0(3)	−5(3)	2(3)
C18	42(4)	22(3)	21(3)	0(3)	−3(3)	3(3)
C19	46(4)	32(4)	29(4)	2(3)	−1(3)	−3(3)

Table 5. Hydrogen coordinates [$\times 10^4$] and isotropic displacement parameters [$Å^2 \times 10^3$].

Atom	*x*	*y*	*z*	U_{eq}	*S.o.f.*
H3	8034	10118	6052	46	1
H4	8858	13911	5817	48	1
H6	7993	14095	2928	44	1
H7	7069	11268	2437	36	1
H13	5408	1439	4800	32	1
H15A	4402	–1901	7238	37	1
H15B	4921	–4450	7087	37	1
H17	6436	2949	7562	35	1
H18	6789	5562	6361	34	1
H19A	4767	7358	3551	53	1
H19B	4762	6277	4528	53	1
H19C	4368	4597	3780	53	1

Table 6. Torsion angles [°].

O1–C1–C2–C3	–3.4(11)
O1–C1–C2–C5	–179.6(6)
O1–C1–C8–C7	–179.0(6)
O1–C1–C8–C9	3.2(9)
O1–C11–C12–C13	–170.2(5)
O1–C11–C12–C18	9.9(8)
O2–C5–C6–C7	–177.5(6)
O3–C9–C10–O4	–5.5(10)
O3–C9–C10–C11	175.0(6)
O4–C10–C11–O1	–176.7(5)
O4–C10–C11–C12	3.0(10)
O5–C14–C16–O6	0.9(7)
O5–C14–C16–C17	–178.7(6)
O6–C16–C17–C18	179.4(6)
C1–O1–C11–C10	3.2(9)
C1–O1–C11–C12	–176.6(5)
C1–C2–C3–C4	–176.7(7)
C1–C2–C5–O2	178.0(5)
C1–C2–C5–C6	–2.2(10)
C1–C8–C9–O3	–178.0(6)
C1–C8–C9–C10	2.5(9)
C2–C1–C8–C7	1.5(9)
C2–C1–C8–C9	–176.4(6)
C2–C3–C4–O2	–0.3(8)
C2–C5–C6–C7	2.7(10)
C3–C2–C5–O2	0.8(8)
C3–C2–C5–C6	–179.4(6)
C4–O2–C5–C2	–0.9(7)
C4–O2–C5–C6	179.2(6)
C5–O2–C4–C3	0.8(8)
C5–C2–C3–C4	–0.3(8)
C5–C6–C7–C8	–1.1(9)
C6–C7–C8–C1	–0.9(9)

C6–C7–C8–C9	176.9(6)
C7–C8–C9–O3	4.2(10)
C7–C8–C9–C10	–175.3(6)
C8–C1–C2–C3	176.1(8)
C8–C1–C2–C5	0.0(9)
C8–C9–C10–O4	174.1(5)
C8–C9–C10–C11	–5.5(9)
C9–C10–C11–O1	2.9(9)
C9–C10–C11–C12	–177.4(6)
C10–C11–C12–C13	10.0(10)
C10–C11–C12–C18	–169.9(6)
C11–O1–C1–C2	173.3(5)
C11–O1–C1–C8	–6.3(9)
C11–C12–C13–C14	–178.9(6)
C11–C12–C18–C17	178.4(6)
C12–C13–C14–O5	178.7(6)
C12–C13–C14–C16	–0.6(9)
C13–C12–C18–C17	–1.4(9)
C13–C14–C16–O6	–179.6(6)
C13–C14–C16–C17	0.7(10)
C14–O5–C15–O6	–11.1(6)
C14–C16–C17–C18	–1.1(10)
C15–O5–C14–C13	–172.9(6)
C15–O5–C14–C16	6.5(6)
C15–O6–C16–C14	–8.0(7)
C15–O6–C16–C17	171.5(7)
C16–O6–C15–O5	11.8(6)
C16–C17–C18–C12	1.5(10)
C18–C12–C13–C14	1.0(9)
C19–O4–C10–C9	–87.5(7)
C19–O4–C10–C11	92.1(7)

Symmetry transformations used to generate equivalent atoms:

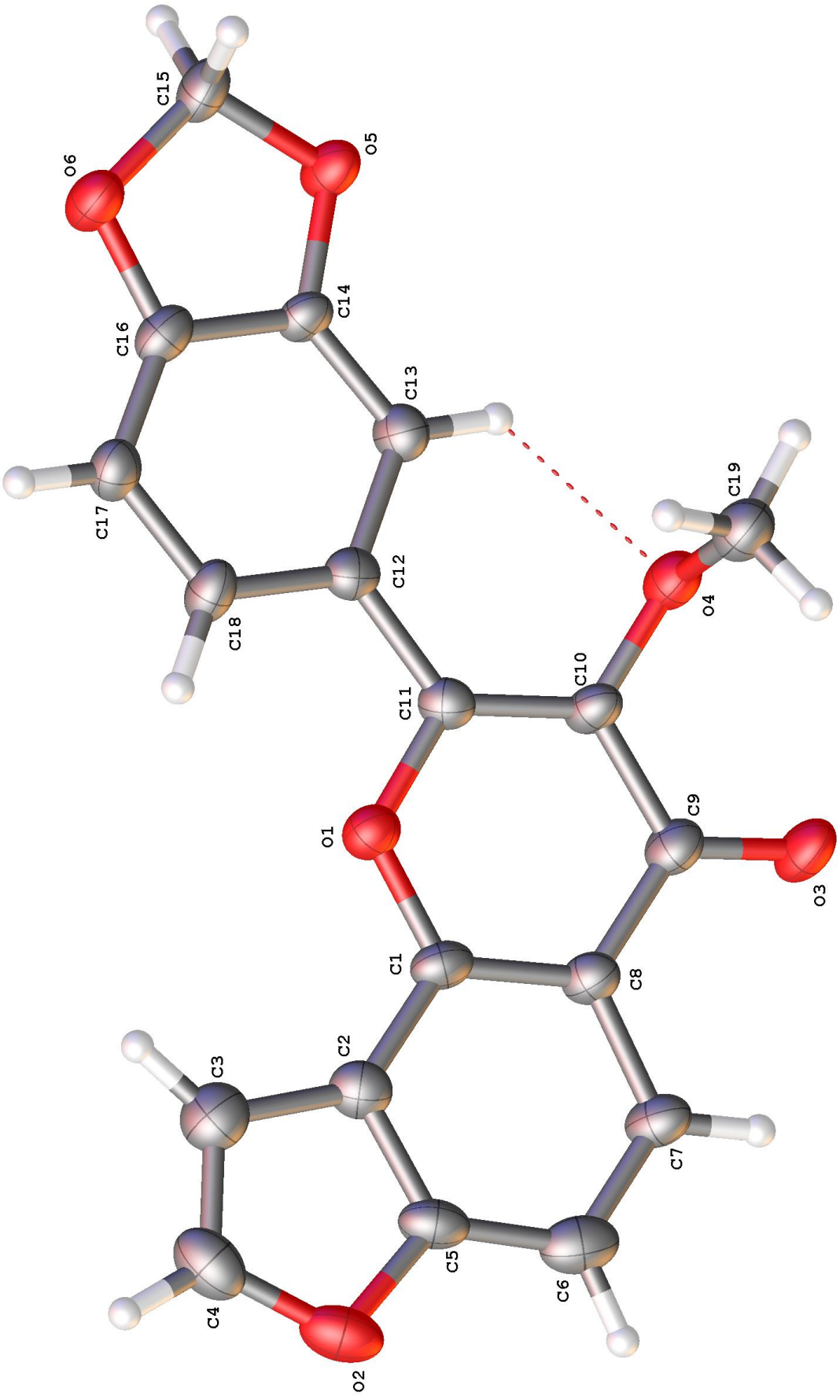
C15
O6
O5
C14
C16
C13
C17
C19
C12
O4
C18
C10
C11
C9
O1
O3
C1
C8
C2
C3
C7
C5
C6
C4
O2